

Quantum Mechanical Vistas on the Road to Quantum Gravity

Thesis by
Ashmeet Singh

In Partial Fulfillment of the Requirements for the
Degree of
Doctor of Philosophy

The logo for the California Institute of Technology (Caltech), featuring the word "Caltech" in a bold, orange, sans-serif font.

CALIFORNIA INSTITUTE OF TECHNOLOGY
Pasadena, California

2020
Defended May 11, 2020

© 2020

Ashmeet Singh

ORCID: 0000-0002-4404-1416

All rights reserved

ACKNOWLEDGEMENTS

My journey as a PhD student at Caltech over the last five years has been a rather unique one. It has been formative in ways more than one taking me through highs and lows spanning the spectrum, and I feel I am a more holistic person for it. I owe my gratitude to all those people who have made this journey, and this thesis, possible, and because of whom my experience of working toward a doctoral degree has been one that I will cherish. I am grateful to the Almighty (a concept I have now begun to more closely associate with the creative power in Nature) for the gift of good health and ascending spirits, which made working on this thesis enriching, both academically and otherwise.

Let me begin with the academic facet of my PhD life. My most intellectually valuable take-away from my research life at Caltech is the profound research direction I got to be a part of – an effort to understand quantum gravity from minimal elements in quantum mechanics. I am very thankful to our research group at Caltech for letting me be part of this bold and stimulating endeavor.

First and foremost, my strongest gratitude to my advisor, Sean Carroll. Ever since I wandered into his office during my first month at Caltech, wanting to discuss ideas in foundational quantum mechanics, Sean has not just been a mentor to me, but rather an inspiration. I feel the biggest thing I learned from him is the ability to think big, think independent, and not be tamed by conventional boundaries. Sean allowed me the freedom to explore bold and risky ideas on my own, while always having my back when my steps faltered. It never ceases to amaze me how Sean connects big picture ideas spanning across various fields in physics, and has such great intuition for seemingly far-fetched, convoluted concepts. Every discussion with him made me push my boundaries, and appreciate the subtle ideas better. His diverse interests, captivating communication style which makes the densest topics seem lucid, and not to mention being a physicist par excellence are an inspiration – something I hope to emulate in my own journey.

I would like to thank my collaborators, Ning Bao, Charles Cao, Aidan Chatwin-Davies, Sean Carroll, Oleg Kabernik and Jason Pollack, with whom I had the privilege of discussing physics and working on exciting problems together. Our Quantum Spacetime Reading Group, lovingly called as the “CosmoQM” group, was instrumental in ushering a lot of interesting interactions, discussions and col-

laborations during my first few years. Being the youngest in the group, I got to learn a lot from the group's senior student members: Anthony Bartolotta, Jason Pollack, Grant Remmen, Charles Cao, and Aidan Chatwin-Davies.

Another pillar which defined me and my time at Caltech was my engagement with teaching of the undergraduate core physics curriculum. While for most graduate students around me, the academic experience revolved primarily around research, I got a chance to witness the “best of both worlds.” What usually gets labeled as “due to lack of funding in theoretical physics” for most, my reasons to be a teaching assistant and instructor found their roots in a deeper connection and passion for teaching. I was very fortunate to have the opportunity to engage in full lecture-style and recitation teaching for over 4 years spanning Classical Mechanics, Electrodynamics, Special Relativity, Vibrations and Waves, Quantum Mechanics and Statistical Mechanics and Thermodynamics. Teaching those very courses in the very places Richard Feynman taught back in the day is an experience in itself, and I want to thank all my students who made the experience so memorable and unique, often putting up with my random tangents and silly jokes in class. I want to thank Prof. Steve Frautschi – chatting with him and seeing his dedication to teaching and his students continues to be a source of inspiration for me. A special mention for Prof. Frank Porter with whom I taught two terms of Ph2a: Vibrations and Waves. Frank has been incredibly supportive of all my teaching endeavors, one of which culminated in our course being offered as an online course on YouTube. Witnessing his commitment to teaching up-close is a delight, and it has been an absolute pleasure and privilege teaching with him. I would also like to thank Freddy Mora, Meagan Heirwegh and Sofie Leon for their administrative support during my teaching years. Also, thanks to Cassandra Horii and Jenn Weaver at Caltech's Center for Teaching, Learning and Outreach (CTLO) for their encouragement and involvement in many of my teaching endeavors.

The time I spent in my office, 414 Downs-Lauritsen, would have been somewhat monotonous had it not been for my office mates. Matt Heydeman during my first three years, and Nabha Shah for my final year with whom the endless conversations about physics, politics, academia, and more, were a lot of fun.

A warm thank you to Carol Silbertstein, our administrator for the High Energy Physics Theory group. It still amazes me how efficiently and smoothly Carol man-

aged the group, and I have fond memories of long, interesting chats with her in the office.

I would also like to thank members of my PhD Thesis Committee, Profs. Fernando Brandao, Sean Carroll, David Hsieh, and John Preskill, for their time and input at my PhD Candidacy Meeting and my PhD defense.

A PhD in Theoretical Physics is not all academics, by far. On a personal note, I would like to thank my mother, Sdn. Harneet Kaur and father, S. Arvinder Pal Singh, and my grandparents, S. Surjit Singh and Sdn. Surinder Kaur. They have been my constant support, both in exciting times as well as the inevitable dull stretches one faces in research. A special shout out to my mother, who is now well versed in concepts of Hilbert space, Hamiltonians and diffeomorphisms, despite having no background in physics, as she took keen interest in my progress and weathered with me through my struggles. Their blessings and unceasing support have helped me come far and strong this way.

A few friends I would like to take special notice of – friends who were instrumental in shaping the last five years of my life. Let me first mention Aditya Pandey (aka Pandey) and Sudepto Gangopadhyay (aka Dada). They have been privy to the closest details of my life, academic and otherwise, and their unwavering presence and the constant conversation they keep alive have been strong pillars in my life – something for which I am very grateful for. From spending late work nights at Au Coquolet café during Pandey’s Berkeley days (where I would end up driving almost every other week) to the countless road trips and hikes; the endless brainstorming and our mutual admiration for sleep, Pandey has been with me through it all. I am also proud to call him an academic collaborator – we combined Pandey’s background in statistics and civil engineering with mine in physics (which begs for a “Civil Engineer and a Physicist walk into a bar...” joke) to work on using field theoretic techniques to earthquake engineering and it is been an absolute pleasure. Dada is someone whom I got introduced to in the most unexpected way, and ever since that first evening we met, we have found a shared bond in our penchant for late work nights in cafes (which would almost always culminate in long conversations in the parking lot), racquetball, road trips, late night walks (to Dada’s almost constant chagrin), and the constant ribbing of Pandey. Dada is one of the most fun-loving, caring people I have met, and his largess in life never ceases to fascinate me!

I would be remiss if I did not mention Garima Singh, in whom I found a friend and sister I could invariably depend on. She has been my partner-in-crime, brought together by our mutual love for road trips, telescopes, and the shimmering night sky. My thanks to Swati Chaudhary who has always been there with her kindness, be it talking about my bizarre physics ideas, having me over for dinner ever so often (a blessing for someone whose towering culinary feat is scrambled eggs), to always being ready for a quick trip to Namaste for some evening pakoras.

My group of friends at Caltech – Charles Cao, Aidan Chatwin-Davies, Zander Moss, Alec Ridgway, and James St. Germaine-Fuller – y’all made my time at Caltech better with all the support and fun. Long rants and laughs with Alec, discussions with Charles, the renewed energy Zander brought to the group, and barging into James’ office unannounced, it’s all been a lot of fun! Charles Cao and Aidan Chatwin-Davies were my academic brothers, of whom I was comfortable asking any and every silly physics question I had, be it in the office or on a back-country camping trip to White Sands National Monument. I would also like to thank Rajashik Tarafder and Jagannadh Kumar. Rajashik’s multi-dimensional view of life and Jag’s positive vibe made my last year at Caltech much more exciting (though you both still have a lot to learn from me in the racquetball court!)

A special thanks to the Sikh community of Southern California – I found emotional and spiritual stability through the many Gurudwaras (Sikh House of Worship) around Los Angeles. I found home away from home here. I am grateful to Manjit Singh and family, along with Rupinder Kaur Walia and her family, who welcomed me in their lives like their own son.

I am deeply grateful to my wonderful friends who have stood by me, come-what-may, through the last n years, with $n \gg 5$. Be it long discussions on the meaning of life with Satwik, spending the day at Six Flags with Megh Shah the day before my PhD Candidacy Exam, or those endless engaging discussions with Naveen, Aiman Khan, Himanshu Khanchandani, Arnab Dhani, Parth Kapoor and Pranay Sumbly – thanks for always being there. You folks make life fun!

Given that my work as a theoretical physicist primarily involves me thinking for long, uninterrupted stretches of time while staring at a bunch of cool looking math (something which never gets old!), I found very close-knit and conducive work environments in Pasadena’s coffee shops. They became my “second office” (Hey! Where is Ashmeet? Umm, it’s 7:30pm, must be in Peets.) where I found the perfect balance of solitude and an upbeat setting. I spent countless hours in

Einstein Bros. Bagels, Peets Coffee, the Sidewalk Cafe, and Winchell's Donuts – becoming an almost permanent evening fixture there, scratching my old pencil on an endless supply of yellow legal writing pads. The aroma of coffee, bagels just an order away, the lively ambiance, and not to forget, the fun conversation with the occasional stranger (some of whom ended up becoming friends) who would want to know why I was reading a book on Quantum Mechanics!

To sum it, I would like to raise a toast to Nature's creative expression found in Physics and Mathematics. Be it the shimmering Milky Way or the equation of quantum mechanics, I am in continual awe of the infinite beauty in our cosmos – a feeling that drives a bubbling wish in me to understand the very heart and soul of how Nature works.

The material compiled in this thesis is based upon work supported by the U.S. Department of Energy, Office of Science, Office of High Energy Physics, under Award Number DE-SC0011632, as well as by the Walter Burke Institute for Theoretical Physics at Caltech and the Foundational Questions Institute.

ABSTRACT

In this thesis, we lay out the goal, and a broad outline, for a program that takes quantum mechanics in its minimal form to be the fundamental ontology of the universe. Everything else, including features like space-time, matter and gravity associated with classical reality, are emergent from these minimal quantum elements. We argue that the Hilbert space of quantum gravity is locally finite-dimensional, in sharp contrast to that of conventional field theory, which could have observable consequences for gravity. We also treat time and space on an equal footing in Hilbert space in a reparametrization invariant setting and show how symmetry transformations, both global and local, can be treated as unitary basis changes.

Motivated by the finite-dimensional context, we use Generalized Pauli Operators as finite-dimensional conjugate variables and define a purely Hilbert space notion of locality based on the spread induced by conjugate operators which we call “Operator Collimation.” We study deviations in the spectrum of physical theories, particularly the quantum harmonic oscillator, induced by finite-dimensional effects, and show that by including a black hole-based bound in a lattice field theory, the quantum contribution to the vacuum energy can be suppressed by multiple orders of magnitude.

We then show how one can recover subsystem structure in Hilbert space which exhibits emergent quasi-classical dynamics. We explicitly connect classical features (such as pointer states of the system being relatively robust to entanglement production under environmental monitoring and the existence of approximately classical trajectories) with features of the Hamiltonian. We develop an in-principle algorithm based on extremization of an entropic quantity that can sift through different factorizations of Hilbert space to pick out the one with manifest classical dynamics. This discussion is then extended to include direct sum decompositions and their compatibility with Hamiltonian evolution.

Following this, we study quantum coarse-graining and state-reduction maps in a broad context. In addition to developing a first-principle quantum coarse-graining algorithm based on principle component analysis, we construct more general state-reduction maps specified by a restricted set of observables which do not span the full algebra (as could be the case of limited access in a laboratory or in various situations in quantum gravity). We also present a general, not inherently numeric,

algorithm for finding irreducible representations of matrix algebras.

Throughout the thesis, we discuss implications of our work in the broader goal of understanding quantum gravity from minimal elements in quantum mechanics.

PUBLISHED CONTENT AND CONTRIBUTIONS

The following articles constitute Chapters 2 - 10 of this thesis. I was a major contributing author for all of these articles and participated in the writing process for each of these papers.

- [1] S. M. Carroll and A. Singh, *Mad-Dog Everettianism: Quantum mechanics at its most minimal*, pp. 95–104. Springer International Publishing, 2019.
https://doi.org/10.1007/978-3-030-11301-8_10.
- [2] N. Bao, S. M. Carroll, and A. Singh, “The Hilbert space of quantum gravity is locally finite-dimensional,” *Int. J. Mod. Phys. D* **26** no. 12, 1743013, [arXiv:1704.00066](https://arxiv.org/abs/1704.00066) [hep-th].
- [3] A. Singh, “Quantum space, quantum time, and relativistic quantum mechanics,” [arXiv:2004.09139](https://arxiv.org/abs/2004.09139) [quant-ph].
- [4] A. Singh and S. M. Carroll, “Modeling position and momentum in finite-dimensional Hilbert spaces via generalized Pauli operators,” [arXiv:1806.10134](https://arxiv.org/abs/1806.10134) [quant-ph].
- [5] C. Cao, A. Chatwin-Davies, and A. Singh, “How low can vacuum energy go when your fields are finite-dimensional?,” *Int. J. Mod. Phys. D* **28** no. 14, (2019) 1944006, [arXiv:1905.11199](https://arxiv.org/abs/1905.11199) [hep-th].
- [6] S. M. Carroll and A. Singh, “Quantum Mereology: Factorizing Hilbert space into subsystems with quasi-classical dynamics,” [arXiv:2005.12938](https://arxiv.org/abs/2005.12938) [quant-ph].
- [7] J. Pollack and A. Singh, “Towards space from Hilbert space: Finding lattice structure in finite-dimensional quantum systems,” *Quant. Stud. Math. Found.* **6** no. 2, (2019) 181–200, [arXiv:1801.10168](https://arxiv.org/abs/1801.10168) [quant-ph].
- [8] A. Singh and S. M. Carroll, “Quantum decimation in Hilbert space: Coarse-graining without structure,” *Phys. Rev. A* **97** no. 3, (2018) 032111, [arXiv:1709.01066](https://arxiv.org/abs/1709.01066) [quant-ph].
- [9] O. Kabernik, J. Pollack, and A. Singh, “Quantum state reduction: Generalized bipartitions from algebras of observables,” *Phys. Rev. A* **101** no. 3, (2020) 032303, [arXiv:1909.12851](https://arxiv.org/abs/1909.12851) [quant-ph].

TABLE OF CONTENTS

Acknowledgements	iii
Abstract	viii
Published Content and Contributions	x
Bibliography	x
Table of Contents	x
List of Illustrations	xiv
List of Tables	xx
Chapter I: Prologue	1
I On a Quantum Footing	10
Chapter II: Mad-Dog Everettianism: Quantum Mechanics at Its Most Minimal	11
2.1 Taking Quantum Mechanics Seriously	11
2.2 The Role of Classical Variables	12
2.3 The Role of Emergence	13
2.4 Local Finite-Dimensionality	14
2.5 Spacetime from Hilbert Space	15
2.6 Emergent Classicality	16
2.7 Gravitation from Entanglement	18
2.8 The Problem(s) of Time	19
2.9 Prospects and Puzzles	20
Chapter III: The Hilbert Space of Quantum Gravity is Locally Finite-Dimensional	22
Chapter IV: Quantum Space, Quantum Time, and Relativistic Quantum Mechanics	27
4.1 Introduction	27
4.2 Time, Space, and Spin in Hilbert Space	31
4.3 Hamiltonian and Momentum Constraints	35
4.4 Symmetry transformations as Basis Changes	43
4.5 Discussion	48
II (In)Finiteness and Beyond	52
Chapter V: Modeling Position and Momentum in Finite-Dimensional Hilbert Spaces via Generalized Pauli Operators	53
5.1 Introduction	53
5.2 Finite-Dimensional Conjugate Variables from the Generalized Pauli Operators	56
5.3 Operator Collimation: The Conjugate Spread of Operators	65
5.4 Finite-Dimensional Quantum Mechanics	70

5.5 Discussion	76
Chapter VI: How Low can Vacuum Energy go when your Fields are Finite-Dimensional	78
6.1 Introduction: Gravity and Quantum Field Theory	78
6.2 Finite-Dimensional Effective Field Theory	79
6.3 Conclusion: Hilbert Space and Holography	82
III Structure in Hilbert Space	85
Chapter VII: Quantum Mereology: Factorizing Hilbert Space into Subsystems with Quasi-Classical Dynamics	86
7.1 Introduction	86
7.2 Factorization and Classicality	89
7.3 Robustness and Entanglement	91
7.4 Predictability and Classical Dynamics	96
7.5 The Quantum Mereology Algorithm	106
7.6 Discussion	116
7.7 Appendix: Bases and Factorizations	117
7.8 Appendix: Evolution of the Linear Entropy	120
7.9 Appendix: Generalized Pauli Operators	123
7.10 Appendix: Generic Evolution of Reduced Density Operators	127
Chapter VIII: Towards Space from Hilbert Space: Finding Lattice Structures in Finite-Dimensional Quantum Systems	131
8.1 Introduction	131
8.2 The Non-Genericity of Lattice Hilbert Spaces	134
8.3 Direct-Sum Hilbert Spaces	136
8.4 Direct-Sum Locality and Robustness	140
8.5 A Worked Example: The Double-Well Potential	144
8.6 Towards Field Theory	151
8.7 Conclusion	152
8.8 Appendix: A Primer on Generalized Clifford Algebra	153
IV Quantum State-Reduction	159
Chapter IX: Quantum Decimation in Hilbert Space: Coarse-Graining without Structure	160
9.1 Introduction	160
9.2 Constructing the Principle Component Basis	162
9.3 Coarse-Graining via Decimation	171
9.4 Epilogue and Conclusion	180
Chapter X: Quantum State Reduction: Generalized Bipartitions from Algebras of Observables	183
10.1 Introduction and Motivation	184
10.2 Preliminaries	196
10.3 Operational Approach to Decoherence	208

10.4 Irrep Decomposition of Matrix Algebras by Scattering of Projections	213
10.5 Examples of State Reduction via Irrep Decomposition of Operational Constraints	239
10.6 Beyond Matrix Algebras: Partial Bipartitions	247
10.7 Classicality from Coarse-Grainings using Partial Bipartitions: Variational Approach	256
10.8 Example of the Variational Approach: Coarse-Graining the Ising Model as a Partial Bipartition	264
10.9 Applications and Future Work	275
V Bibliography	281
Bibliography	282

LIST OF ILLUSTRATIONS

<i>Number</i>	<i>Page</i>
1.1 A succinct representation of the challenges one might face in a quantum-first approach to quantum gravity. (Picture credit: Abstruse Goose https://abstrusegoose.com/111)	2
3.1 On the left, the Hilbert space of quantum gravity is portrayed as a tensor product, $\mathcal{H}_{\text{QG}} = \mathcal{H}_{\text{sys}} \otimes \mathcal{H}_{\text{env}}$, and two decohered branches $ \Psi_a\rangle_{\text{sys}} \otimes \Psi_a\rangle_{\text{env}}$ are shown. Under the map Φ , the system factors of these states map to regions Σ_a of a semiclassical spacetime background, on which are defined a spatial metric and its conjugate momentum as well as the quantum state of an effective field theory.	24
5.1 Plot showing $\hat{\phi}$ -shift profiles of various powers of $\hat{\pi}$. The quadratic operator $\hat{\pi}^2$ is seen to have the most collimated profile, implying that this operator does the least to spread the state in the conjugate direction. Also plotted is the profile for a random hermitian operator, for which the spread is approximately uniform.	69
5.2 ϕ -collimation of various powers of $\hat{\pi}$. Even powers are seen to have systematically larger values of operator collimation. Also plotted for comparison is a line marking the ϕ -collimation of a random Hermitian operator.	70
5.3 Eigenspectrum (normalized by Ω) for a $\dim \mathcal{H} = 401$ ($l = 200$) finite-dimensional oscillator for different values of Ω . Depending on the value of Ω , the spectrum deviates from the vanilla spectrum of the infinite-dimensional oscillator, which has also been plotted for comparison.	74
5.4 Plot of the maximum eigenvalue (normalized by Ω) of the finite-oscillator as a function of dimension $\dim \mathcal{H} = 2l + 1$ for different values of Ω . A linear trend is observed.	75
5.5 Plot of the minimum eigenvalue (normalized by Ω) of the finite-oscillator as a function of dimension $\dim \mathcal{H} = 2l + 1$ for different values of Ω . A gradual build-up is noticed, with more suppression for larger Ω for a given \mathcal{H} , which saturates to the vanilla, infinite-dimensional result of $\lambda_{\min}/\Omega = 0.5$	76

6.1	Minimum energy eigenvalue for a finite-dimensional field mode, normalized by Ω/L , as a function of the dimension d and for several values of Ω	83
7.1	Plot showing $\hat{\phi}$ -shift profiles of various powers of $\hat{\pi}$. The quadratic operator $\hat{\pi}^2$ has the most collimated profile, implying that this operator does the least to spread the state in the conjugate direction. Also plotted is the profile for a random Hermitian operator, for which the spread is approximately uniform.	101
7.2	ϕ -collimation of various powers of $\hat{\pi}$. Even powers are seen to have systematically larger values of ϕ -collimation. Also plotted for comparison is a line marking the ϕ -collimation of a random Hermitian operator.	102
7.3	Plot showing correlation between rate of change of variance of the pointer observable $d(\Delta^2 \hat{O}_A)/dt$ and collimation $C_\phi(\hat{H}_A)$ of the self-Hamiltonian \hat{H}_A . More collimated self terms do not spread states much in the conjugate directions and correspondingly induce a small change in the variance of the consistent pointer observable that depends on one of these conjugate variables. In this example, we kept \hat{O}_A fixed at $\hat{O}_A \equiv \hat{\phi}_A$ and changed the self-Hamiltonian \hat{H}_A and computed the correlation for a peaked state in $\hat{\phi}_A$ eigenspace in a Hilbert space of $\dim \mathcal{A} = 27$	104
7.4	Plot showing correlation, in the Quantum Measurement Limit (QML), between pointer entropy $\check{S}_{pointer}(0)$ and the rate of change of variance of the pointer observable for a peaked state in pointer eigenspace. For peaked states in pointer eigenspace, low rate of change of variance implies a small spread in the pointer entropy and is characterized by self-Hamiltonians that are highly collimated in the conjugate direction picked out by the pointer observable. In this example, similar to fig. 7.3, we kept \hat{O}_A fixed at $\hat{O}_A \equiv \hat{\phi}_A$ and changed the self-Hamiltonian \hat{H}_A and computed the correlation for a peaked state in $\hat{\phi}_A$ eigenspace in a Hilbert space of $\dim \mathcal{A} = 27$	111

7.5	Quantum Mereology Algorithm: sifting through different factorizations of Hilbert space to recover the QC factorization by minimization of the Schwinger entropy. In the QC factorization, the quantum system is described by two harmonic oscillators coupled by their positions. The quasi-classical factorization (the first factorization we begin with) is marked by a red square. Details in the text.	114
7.6	Quantum Mereology Algorithm: a run similar to figure 7.5 sifting through different factorizations of Hilbert space but this time with larger, successive perturbations away from the identity operator to generate the unitary transformation Λ . In the QC factorization, which minimizes the Schwinger entropy, the quantum system is described by two harmonic oscillators coupled by their positions. Factorizations away from QC quickly saturate to generic, large values of Schwinger entropy. The quasi-classical factorization (the first factorization we begin with) is marked by a red square. Details in the text.	115
8.1	Histogram of $\Omega(n)$ for $2^{64} - 5000 < n < 2^{64} + 5000$. The mean is 4.85, the standard deviation is 2.21.	135
8.2	Histogram of $\Omega(n)$ for $2^{64} - 15000 < n < 2^{64} - 5000$. The mean is 4.84, the standard deviation is 2.13.	136
8.3	Histogram of $\Omega(n)$ for $2^{64} + 5000 < n < 2^{64} + 15000$. The mean is 4.84, the standard deviation is 2.13.	137
8.4	The $\hat{\phi}$ -representation of the double-well potential $\hat{V}(\hat{\phi})$ for a Hilbert space of dimension $N = 301$ is plotted. Along with it, we show the lowest two energy eigenstates and one of the highest ones ($n = 298$) for a Hilbert space corresponding to $N = 301$. We have added +1 by hand to the wave function of the $n = 298$ state to cleanly separate it from the low-lying one and demonstrate how higher energy states are delocalized across the two wells. Eigenstates $n = 299, 300, 301$ are very high energy states localized near the barriers of the potential as a result of the the finite-dimensional, cyclic structure of $\hat{\phi}$, as can be seen in Fig. 8.5. The state $n = 299$ is peaked around the central barrier, and $n = 300, 301$ are peaked at the edges.	145

- 8.5 Energy spectrum of the double-well Hamiltonian of Eq. (8.35).
 One can easily notice the (approximate) double degeneracy in the low-lying eigenvalues (corresponding to the two symmetric wells). The last three (the highest two are indistinguishable on the plot) highly-energetic eigenstates are an artifact of working in a finite-dimensional space with a relatively small N with the algebra of conjugate variables having a cyclic structure. They cause spurious features in other plots, but have no bearing on our physical results. . . . 146
- 8.6 The trace of the square of the tunneling term in the Hamiltonian $\text{Tr} \left(\hat{H}_{\text{tunnel}(\sigma)}^2 \right)$ for different decompositions building up from the canonical, ordered $(-l, -l + 1, \dots, -1) \cup (0, 1, 2, \dots, l)$ decomposition. This quantity acts as a measure of the strength of the tunneling term for the choice $\hat{O} \equiv \hat{\phi}$ and quantifies the scrambling of the decomposition as discussed in the text. 148
- 8.7 Plot showing the dependence of Tunneling Spread $\mathbb{T}(|\psi\rangle, A_\sigma, D_\oplus)$ on energy eigenstates (represented by their eigenvalues E_n) of the double-well Hamiltonian expressed in different direct-sum decompositions $D_\oplus(\hat{\phi}, \sigma, m = l)$ of \mathcal{H}_{DW} . There exists a preferred decomposition into direct sum subspaces (the canonical, ordered $(-l, -l + 1, \dots, -1) \cup (0, 1, 2, \dots, l)$ one) in which low-lying energy states have very small tunneling spreads and hence represent robust, localized states in the direct-sum subspace. Other decompositions are near-generic where there is no manifestation of direct-sum locality. Notice the log scale on the y-axis representing the tunneling spread. The very-high energy behavior is a consequence of the three largest energy eigenstates, which are artifacts of finite-dimensional, cyclic constructions and do not bear any physical significance for our results. 149
- 8.8 Plot showing correlation between E_n and $(E_n)_{A_\sigma}$ for different choices of scramblings $D_\oplus = \{\hat{\phi}, \sigma, m\}$ in the double-well toy model. Only in the canonical, preferred decomposition do the low-lying eigenstates of \hat{H} serve as low energy states which can be localized within a given direct-sum subspace. The very-high energy behavior is a consequence of the three largest energy eigenstates, which are artifacts of finite-dimensional, cyclic constructions and do not bear any physical significance for our results. 150

9.1	Plot of von Neumann entanglement entropy of a constituent qubit of a state as a function of the number of PCA components retained in reconstructing the state.	178
10.1	Update rules for reflection relations after scattering. The red (dashed) edges represent unknown reflection relations, black (solid) edges represent properly-reflecting pairs, absent edges represent orthogonal pairs. One-sided edges stand for the reflection relations with other projections in the rest of the network. (a) In the generic case where each $\Pi_{i=1,2}$ breaks down into $\{\Pi_i^{(\lambda_k)}\}$, the result is a series of properly reflecting pairs (for $\lambda = 0$ the pair is orthogonal) as described in Lemma 10.4.4. All the external edges are inherited by $\{\Pi_i^{(\lambda_k)}\}$ from Π_i with the black (solid) edges being reset to red (dashed). (b) In the special case where Π_1 did not break down under scattering, we know $\Pi_1 \equiv \Pi_1^{(\lambda_1)}$. In this case, Π_2 may break down to at most two projections (if it also did not break down, then Π_1, Π_2 should just be relabeled as reflecting) such that $\Pi_1^{(\lambda_1)}, \Pi_2^{(\lambda_1)}$ are properly reflecting and $\Pi_2^{(0)}$ is orthogonal to both. In (b) the update rule of external edges differs from the generic case (a) in that for unbroken projection $\Pi_1^{(\lambda_1)}$, the black (solid) edges are not reset to red (dashed).	221
10.2	Evolution of the reflection network of the toy model during two scattering iterations. The red (dashed) edges represent unknown reflection relations, black (solid) edges represent properly reflecting pairs, absent edges represent orthogonal pairs. (a) is the initial improper reflection network. (b) is the intermediate network after one scattering iteration. (c) is the final proper reflection network after two scatterings.	223
10.3	Completion of a reflection network lacking an MSMP (a), to the one that has an MSMP (b).	231
10.4	Plot of average entanglement growth rate Q_{BPT} over different BPTs (different row arrangements) for $N = 3$ spins with the compatible collective observable $M_c = \sum_{\mu=1}^3 \sigma_z^{(\mu)}$ corresponding to a value of $g = 0.5 < g_{\text{crit}}$	270

- 10.5 Transition structure of the Hamiltonian in the tensor product basis of $M_c = \sum_{\mu=1}^3 \sigma_z^{(\mu)}$ for $N = 3$ spins. It should be noted that this is not a BPT representation, but only illustrates the transition structure of the Hamiltonian in the chosen basis. 271
- 10.6 (color online) The 6 selected, quasi-classical BPTs which maximize Q_{BPT} as a measure of dynamical coherence for $N = 3$ spins corresponding to the compatible collective observable $M_c = \sum_{\mu=1}^3 \sigma_z^{(\mu)}$. Allowed transitions by the Hamiltonian flip single bits in the $\{|0\rangle, |1\rangle\}$ basis. States in the middle two columns not connected by Hamiltonian transitions are shown by the same color. 271
- 10.7 One instance of the class of selected quasi-classical BPTs for $N = 4$ spins corresponding to the compatible collective observable $M_c = \sum_{\mu=1}^3 \sigma_z^{(\mu)}$. Allowed transitions by the Hamiltonian flip single bits in the $\{|0\rangle, |1\rangle\}$ basis. 272
- 10.8 Plot of average entanglement growth rate Q_{BPT} over different BPTs (different row arrangements) for $N = 4$ spins with the compatible collective observable $M_c = \sum_{\mu=1}^3 \sigma_z^{(\mu)}$ corresponding to a value of $g = 0.6 < g_{\text{crit}}$. The inset shows the first few classes of BPTs with lowest values of Q_{BPT} 272
- 10.9 The selected, unique quasi-classical BPTs with minimum entanglement growth rate for $N = 3$ spins corresponding to the compatible collective observable $M_c = \sum_{\mu=1}^3 \sigma_x^{(\mu)}$. Allowed transitions by the Hamiltonian flip two adjacent bits in the $\{|+\rangle, |-\rangle\}$ basis which induce the superselection sectors. 273

LIST OF TABLES

<i>Number</i>		<i>Page</i>
9.1	List of Important Notation Used	164
10.1	Tensor Product Eigenstates for $M_c = \sum_{\mu=1}^3 \sigma_z^{(\mu)}$ for $N = 3$ spins, arranged in columns labeled by distinct eigenvalues. Note that this is <i>not</i> a BPT, just an enumeration of the eigenstates arranged by the column structure governed by the compatible M_c	269

Chapter 1

PROLOGUE

Quantum mechanics, our most fundamental theory of the universe has been tremendously successful in making quantitative predictions for experiments; however we have not been as successful in understanding what it really means, and how it connects with underlying reality. Part of the disconnect can be attributed to the fact that we tend to think in terms of classical ideas such as “space,” “particles,” and “fields.” Such constructions may not have a place in the fundamental ontology of quantum mechanics which, at its heart, simply describes the evolution of a state vector in an abstract Hilbert space. We typically start with some classical theory and then “quantize” it. Presumably Nature works the other way around: it is quantum-mechanical from the start, and a classical limit emerges in the right circumstances.

The situation becomes particularly acute when we think about a quantum theory of gravity, which should allow for intrinsically quantum-mechanical spacetimes (characterized by features such as the possibility of superpositions of different spacetimes, for instance) and which should not rely on any a priori choice of spacetime background. While background-dependent approaches, such as string theory and related conjectures such as the AdS/CFT correspondence [1] teach us a great deal about interesting features of quantum gravity, considerations above motivate studying quantum gravity from the perspective of finding gravity within basic quantum mechanics. In other words, one should try “gravitizing” quantum mechanics instead of quantizing classical gravity.

In this thesis, we take such a quantum-first approach. Our focus is to explore topics in quantum mechanics with an eye toward their applicability in broader questions in quantum gravity. In such an approach, we work in a paradigm involving only minimal elements in quantum mechanics. We do not rely on, or presuppose any classical structure and we study its emergence from more ontologically fundamental elements in quantum mechanics. The title of this thesis is a reflection on this approach. It involves giving up our most cherished classical notions, such as space, subsystems and locality, to mention a few; and while it is a tall order as Figure 1 depicts, we feel it can shed some light on interesting aspects of quantum gravity.

The first part of this thesis titled “On a Quantum Footing” is a collection of papers

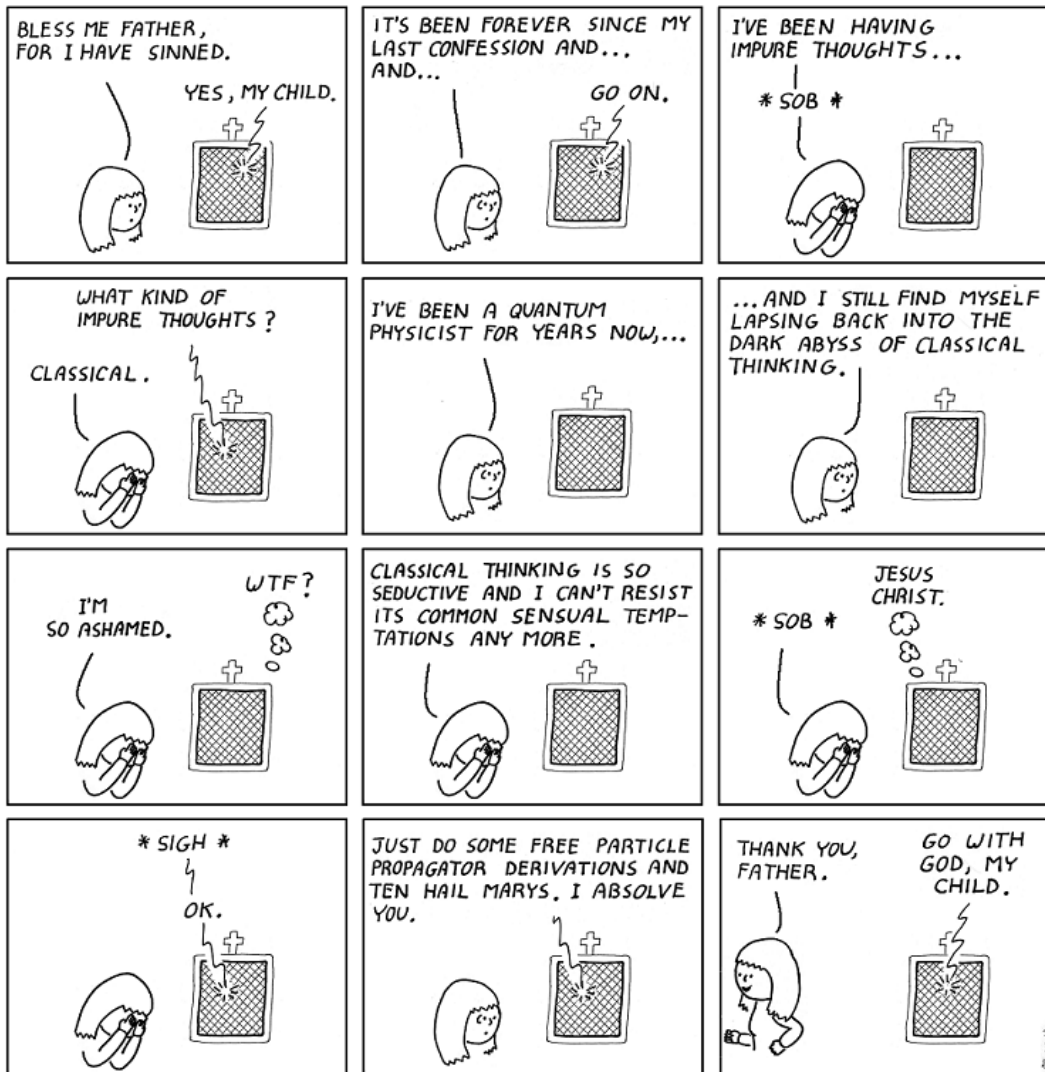


Figure 1.1: A succinct representation of the challenges one might face in a quantum-first approach to quantum gravity. (Picture credit: Abstruse Goose <https://abstrusegoose.com/111>)

which lay out the quantum mechanical framework, the motivation for our work, and some big picture musings. In Chapter 2, we raise the question how far we can take the idea that the world is fundamentally quantum, with a minimal plausible ontology: a Hilbert space, \mathcal{H} , a vector $|\psi\rangle$ within it, and a Hamiltonian \hat{H} governing the evolution of that vector over time. Such an approach, which we call “Mad-Dog Everettianism” is characterized by abstract elements in Hilbert space, without a preferred algebra of observables, and without necessarily representing Hilbert space as a set of wavefunctions over some classical variables. All of the additional elements familiar in physical theories, are required to be emergent from the state vector in

Hilbert space, which by itself, is a rather featureless construct. We outline the broad goal of the program and discuss a possible road-map to emerge the rich features of the classical world we live in – including space, matter and gravity – from minimal elements in quantum mechanics. As we work towards a quantum theory of gravity from a quantum-first perspective, it is important to understand the structure of its Hilbert space. In Chapter 3, motivated by the Bekenstein bound, the Holographic principle, and its applicability to horizons such as the de Sitter patch of the universe we live in, we argue in a model independent way that the Hilbert space of quantum gravity is locally finite-dimensional. We discuss ensuing implications, including for how basic quantum mechanical data can get mapped to the richness of quantum field theory (QFT) on curved backgrounds. Chief among these implications is that on separable Hilbert spaces (of which finite-dimensional spaces are a special case), the Stone-von Neumann theorem [2] guarantees us uniqueness of the irreducible representation of the algebra of the canonical commutation relations (CCRs), upto unitary equivalence. This connects back into the heart of the Mad-Dog Everettianism program – it implies that all Hilbert spaces of a given finite dimension are isomorphic, and the algebra of observables is simply that of “all Hermitian operators,” and any further structure on it must be emergent in an appropriate limit. This is in stark contrast to the Hilbert space structure of conventional quantum field theory where one transits from a finite to an infinite number of degrees of freedom and hence an un-countably infinite-dimensional Hilbert space (which is non-separable). In this case of QFT, there can be unitarily inequivalent representations of the CCRs¹ and one might therefore conclude that specification of additional data (such as the inequivalent, cyclic representation of the algebra) is also an important ingredient in defining a quantum theory, over and above the Hamiltonian, weakening the notion of emergence from minimal quantum elements.

We then go on to focus on another interesting aspect of quantum gravity, the famous “problem of time;” reconciling how time enters as an independent, absolute, classical parameter in quantum mechanics, whereas in relativity, time has a relative connotation depending on the observer and distribution of mass-energy. More generally, theories with reparametrization invariance such as classical general relativity, which has general (local) coordinate invariance, have a formulation in terms of constraints. Physical states in Hilbert space in the theory are the ones that are annihilated by these constraints. In particular, this is reflected in the Wheeler-DeWitt

¹In Algebraic Quantum Field Theory, this is described by Haag’s theorem [3].

equation [4], which represents a Hamiltonian constraint of the form $\hat{H}|\psi\rangle = 0$ in the context of quantizing general relativity. In such a setup, there is no external time parameter with respect to which states evolve. Rather, time evolution is deemed as an emergent feature. In this context, the Page-Wootters formulation (and extensions thereof) [5–8] is one of the most famous constructions of emergent time, where time is treated as an internal quantum degree of freedom and not as an external classical parameter. The global quantum state is static and the apparent “flow” of time is due to the entanglement and correlations between the temporal degree of freedom with the rest of Hilbert space. We generalize this construction in Chapter 4 by treating space and time on an equal footing in Hilbert space (in the context of relativistic quantum mechanics of particles). We base our construction on using both Hamiltonian and momentum constraints which are explicitly linear and first order in conjugate momenta, and their joint kernel as defining the set of physical states *i.e.* the ones annihilated by the constraints. For such physical states, spatial and temporal translation features emerge as a consequence of entanglement and correlations between different factors of the global Hilbert space \mathcal{H} . By applying dispersion relations to eigenvalues appearing in these constraints, and not treating them as operator-valued equations, we show that Klein-Gordon and Dirac equations in relativistic quantum mechanics can be treated with a uniform approach (unlike the conventional textbook approach). We show symmetry transformations to be implemented by unitary basis changes in Hilbert space. Global symmetries, such as Lorentz transformations, modify the decomposition of Hilbert space; and local symmetries, such as $U(1)$ gauge symmetry are diagonal in coordinate basis and do not alter the decomposition of Hilbert space. Such a construction where space and time are treated as quantum degrees of freedom offers a natural paradigm to study interaction of spacetime with matter in the context of gravitational back-reaction which could help us better understand the quantum nature of the universal coupling of gravity to mass-energy.

Motivated by the argument that the Hilbert space of quantum gravity is locally finite-dimensional, a common thread in this thesis is the emphasis on finite-dimensional Hilbert spaces and how it maps onto conventional field theory, which is infinite dimensional. In Part II of the thesis, we transition to discuss features and implications of finite-dimensional quantum mechanics with an eye towards quantum gravity. Chapter 5 studies the role of generalized Pauli operators (which derive their algebraic structure from the generalized Clifford algebra [9]) as a natural paradigm

for studying finite-dimensional conjugate variables and the role they can play in modifying a theory's spectrum from the usual infinite-dimensional case. We define a purely Hilbert space, pre-geometric notion of "locality" called *Operator Collimation*, based on the spread induced by finite-dimensional conjugate variables, from which one can try to understand more conventional notions of geometric and graph locality. Such ab-initio finite-dimensional effects can also introduce non-trivial modifications to the structure of canonical commutation relations, Feynman diagrams and uncertainty principles and could be important imprints of the quantum mechanical structure of gravity. We study modifications to the spectrum of the classic harmonic oscillator Hamiltonian due to effects of a finite-dimensional Hilbert space. In particular, we show that the zero-point energy of a harmonic oscillator with frequency ω depends both on the Hilbert space dimension and the frequency ω of the oscillator – in sharp deviation from its conventional (infinite-dimensional) counterpart, $E_0 = \omega/2$ (in units with $\hbar = 1$). Chapter 6 puts these finite-dimensional conjugate operators to use in the context of the quantum contribution to vacuum energy in quantum field theory. We explore the viewpoint that quantum field theory may emerge from an underlying theory that is locally finite-dimensional, and we construct a locally finite-dimensional version of a Klein-Gordon scalar field using generalized Pauli operators. We model gravitational effects in our theory by demanding that the effective field theory should cut off below any excitations that would collapse into black holes. We therefore impose the condition that the largest energy eigenvalue for each Klein-Gordon mode should not exceed the Schwarzschild energy of the box. Using bounds on the largest eigenvalue of a finite-dimensional harmonic oscillator, we constrain the Hilbert space dimension of each Klein-Gordon mode based on our black hole condition, with high energy modes therefore getting lower dimension of Hilbert space, and vice versa. Due to this energy dependence in the Hilbert space dimension, we then show that the net zero point energy of these Klein-Gordon modes which contributes to the quantum contribution to the vacuum energy undergoes a massive suppression as compared to the conventional textbook calculation. Thus, taking finite-dimensionality and holography together seriously can possibly have important predictive consequences for gravity.

We then go on, in Part III, to focus on a central theme of the Mad-Dog Everettianism program: the emergence of structure in an otherwise featureless Hilbert space. Chapter 7 focuses on understanding what governs the non-trivial subsystem structure we associate classical reality with. What dictates the split between system and

environment in the decoherence paradigm? (This question is sometimes referred to as the “Set Selection” or the “generalized preferred basis” problem in the quantum foundations literature.) In the presence of gravity, locality and subsystem structure are more subtle than in traditional laboratory settings, and therefore it is an interesting direction to investigate them as emergent phenomena from first-principles. We argue that a quasi-classical factorization of Hilbert space has the following features:

1. **Robustness:** There exist preferred pointer states of the system (and associated pointer observables) that, if initially unentangled with the environment, typically remain unentangled under evolution by the Hamiltonian.
2. **Predictability:** For states with near definite value of the pointer observable, it will serve as a predictable quasi-classical variable, with minimal spreading under Hamiltonian evolution.

Based on this, we establish an (in principle) algorithm, based on entanglement and entropic structures, that distinguishes quasi-classical tensor factorizations of Hilbert space from arbitrary ones. We explicitly connect these characteristics of classical factorizations with features of the Hamiltonian such as existence of (approximate) low entropy eigenstates which are robust to entanglement production, and high operator collimation (as introduced in our work in Ref. [10]) and locality.

We then go on in Chapter 8 to generalize this discussion to direct sum decompositions of Hilbert space where, with an eye towards understanding how lattice structures can emerge in Hilbert space. We point out that the vast majority of finite-dimensional Hilbert spaces cannot be isomorphic to the tensor product of Hilbert-space subfactors that describes a lattice theory. A generic Hilbert space can only be split into a direct sum corresponding to a basis of state vectors spanning the Hilbert space and we studied a toy model (the finite-dimensional discretization of the quantum-mechanical double-well potential) where geometric states evolve locally within each such direct sum factor. We define a notion of “direct-sum locality” which characterizes states and decompositions compatible with Hamiltonian time evolution, and show that such decompositions are highly non-generic.

In addition to emergent classicality and lattice structures, extension of our work on preferred decompositions of Hilbert space can segue into understanding important questions in theories with duals such as AdS/CFT (which represent different factorizations of the same underlying Hilbert space); horizon complementarity and the information paradox; and the emergence of spacetime and matter from basic

quantum elements.

Moving on to Part IV, we study quantum coarse-graining and state-reduction maps in a broad context which can offer a natural paradigm for emergence of various phenomenon in quantum gravity. Access to limited information/degrees of freedom is what makes quantum mechanics so rich and exciting. Important concepts such as entanglement, decoherence, emergent time in the Page-Wootters construction, and even localized quantum information in a region of space, all hinge on the existence of appropriate state-reduction maps. In the words of Landsman [11],

The essence of a “measurement,” “fact” or “event” in quantum mechanics lies in the non-observation, or irrelevance, of a certain part of the system in question. (...) A world without parts declared or forced to be irrelevant is a world without facts.

In Chapter 9, we describe a coarse-graining technique for a set of specified states in a finite-dimensional Hilbert space without relying on any preferred structure of locality or preferred set of observables. We use principle component analysis (PCA) to define the state reduction map, and the resulting coarse-grained quantum states live in a lower dimensional Hilbert space whose basis is defined using the underlying (isometric embedding) transformation of the set of fine-grained states we wish to coarse-grain. We show that the transformation can be interpreted an “entanglement coarse-graining” scheme that retains most of the global, useful entanglement structure of each state, while needing fewer degrees of freedom for its reconstruction. Such a first-principles coarse-graining technique is motivated from, and fits well, with the Mad-Dog Everettianism program where we are working with minimal elements in quantum mechanics and often don’t have any a priori notion of coarse-graining based on subsystem structure, locality, and the likes.

The most common state-reduction map in quantum mechanics is the partial trace map based on a tensor product factorization of Hilbert space. While it is the keystone construction on which decoherence is based, and has ubiquitous use in quantum information, one can notice that most coarse-grainings and state reduction maps cannot be described with the partial trace map. For example, most observables do not take the simple form of acting on a single tensor factor, even when such a factorization of the Hilbert space exists. In particular, the sorts of collective observables which correspond to the averaged, macroscopic properties featured in statistical mechanics do not take this form. That is, we do not expect, even

approximately, a factorization of the form $\mathcal{H} \cong \mathcal{H}_{\text{collective}} \otimes \mathcal{H}_{\text{other}}$ for the sorts of collective observables we might measure in a laboratory.

A similar situation arises in field theories, in which we often wish to construct some notion of a state restricted to a finite spatial region. It is well known [12, 13] that even in the simplest field theories we cannot simply apply the naive partial-trace map to construct the reduced state as discussed above. When the theory has a gauge symmetry, the physical Hilbert space is restricted to states which obey global constraints like a Gauss law, and we cannot consistently restrict to subregions in a gauge-invariant way. Given that many natural coarse-grainings of quantum systems cannot be captured by the partial-trace map, it is natural to consider more general state-reduction maps, which is our focus in Chapter 10. We investigate the general problem of identifying how the quantum state reduces given a restriction on the observables which do not span the full algebra of observables. For example, in an experimental setting, the set of observables that can actually be measured is usually modest (compared to the set of all possible observables) and their resolution is limited. We show that in such situations, the appropriate state-reduction map can be defined via a *generalized bipartition*, which is associated with the structure of irreducible representations of the algebra generated by the restricted set of observables. One of our main technical results is a general, not inherently numeric, algorithm for finding irreducible representations of matrix algebras. The main application of the algorithm that we will focus on is the idea that operational constraints lead to state reductions which generalize the prototypical system-environment split in the context of the decoherence program.

We further define more general ways of decomposing Hilbert space than tensor products and direct sums which we call *partial bipartitions*. In particular, such partial bipartitions describe reductions specified by a discrete set of observables which do not make up a subalgebra either. Using this machinery, we can capture very general coarse-grainings of Hilbert space, since in most cases, the coarse-grained space which will preserve some relevant information will not correspond to a tensor factor of Hilbert space. A particular interesting case which we consider is to look for coarse-graining of a collection of N underlying degrees of freedom (such as N particles) based on a collective or average feature of these degrees of freedom while tracing out the internal features. Using the Ising Model in 1D as an example, we outline an algorithm that can vary over different partial bipartitions of Hilbert space to find the one which represents the most quasi-classical dynamics in the reduced space which preserves the collective information of the degrees of freedom. We

also discuss the relevance our results might have for quantum information, bulk reconstruction in holography, and quantum gravity. Such partial partitions of Hilbert space can have consequences for our understanding of questions such as the localization of quantum information in spatial regions in the presence of gravity. Partitions and coarse-graining could also be important in understanding how spacetime, just as the phases of a thermodynamic system emerges from the underlying quantum degrees of freedom.

The quantum nature of space and time forms a core question in our understanding of quantum gravity. We propound the viewpoint that re-examining crucial first principle ideas in quantum mechanics can be an important direction of inquiry toward our understanding of quantum gravity. As part of our program to emerge the richness of the classical world we live in – including space, matter and gravity – from minimal elements in quantum mechanics, this thesis is a glimpse into some interesting results and avenues in this direction.

Part I

On a Quantum Footing

*Chapter 2***MAD-DOG EVERETTIANISM: QUANTUM MECHANICS AT ITS MOST MINIMAL**

To the best of our current understanding, quantum mechanics is part of the most fundamental picture of the universe. It is natural to ask how pure and minimal this fundamental quantum description can be. The simplest quantum ontology is that of the Everett or Many-Worlds interpretation, based on a vector in Hilbert space and a Hamiltonian. Typically one also relies on some classical structure, such as space and local configuration variables within it, which then gets promoted to an algebra of preferred observables. We argue that even such an algebra is unnecessary, and the most basic description of the world is given by the spectrum of the Hamiltonian (a list of energy eigenvalues) and the components of some particular vector in Hilbert space. Everything else – including space and fields propagating on it – is emergent from these minimal elements.

This chapter is based on the following reference:

S. M. Carroll and A. Singh, *Mad-Dog Everettianism: Quantum mechanics at its most minimal*, pp. 95–104. Springer International Publishing, 2019. https://doi.org/10.1007/978-3-030-11301-8_10

2.1 Taking Quantum Mechanics Seriously

The advent of modern quantum mechanics marked a profound shift in how we view the fundamental laws of nature: it was not just a new theory, but a new *kind* of theory, a dramatic shift from the prevailing Newtonian paradigm. Over nine decades later, physicists have been extremely successful at applying the quantum rules to make predictions about what happens in experiments, but much less successful at deciding what quantum mechanics actually *is* – its fundamental ontology and indeed its relation to underlying reality, if any.

One obstacle is that, notwithstanding the enormous empirical success of quantum theory, we human beings still tend to think in classical terms. Quantum theory describes the evolution of a state vector in a complex Hilbert space, but we populate our theories with ideas like “spacetime,” “particles,” and “fields.” We typically con-

struct quantum theories by starting with some classical theory and then “quantizing” it. Presumably Nature works the other way around: it is quantum-mechanical from the start, and a classical limit emerges in the right circumstances.

In this chapter we ask how far we can take the idea that the world is fundamentally quantum, with a minimal plausible ontology: a Hilbert space \mathcal{H} , a vector $|\psi\rangle$ within it, and a Hamiltonian \hat{H} governing the evolution of that vector over time. This is a version of the Everettian (Many-Worlds) approach to quantum mechanics, in which the quantum state is the only variable and it smoothly evolves according to the Schrödinger equation with a given Hamiltonian,

$$\hat{H}|\psi(t)\rangle = i\partial_t|\psi(t)\rangle. \quad (2.1)$$

Our approach is distinguished by thinking of that state as a vector in Hilbert space, without any preferred algebra of observables, and without necessarily representing Hilbert space as a set of wave functions over some classical variables. All of the additional elements familiar in physical theories, we will argue, can be emergent from the state vector (cf. [15]). We call this approach “Mad-Dog Everettianism,” to emphasize that it is as far as we can imagine taking the program of stripping down quantum mechanics to its most pure, minimal elements.¹

2.2 The Role of Classical Variables

The traditional way to construct a quantum theory is to posit some classical configuration space \mathbf{X} (which could be momentum space or some other polarization of phase space), then considering the space of all complex-valued functions on that space. With an appropriate inner product $\langle \cdot, \cdot \rangle$, the subset of square-integrable functions forms a Hilbert space:

$$\mathcal{H} = \{\psi : \mathbf{X} \rightarrow \mathbb{C} \mid \langle \psi, \psi \rangle < \infty\}. \quad (2.2)$$

This gives us a *representation* of \mathcal{H} , but the Hilbert space itself is simply a complete, normed, complex-valued vector space. That gives us very little structure to work with: all Hilbert spaces of the same finite dimensionality are isomorphic, as are infinite-dimensional ones that are separable (possessing a countable dense subset, which implies a countable orthonormal basis). We may therefore ask, once \mathcal{H} is constructed, is there any remnant of the original classical space \mathbf{X} left in the theory?

¹The name is inspired by philosopher Owen Flanagan’s description of his colleague Alex Rosenberg’s philosophy as “Mad-Dog Naturalism.”

The answer is “not fundamentally, no.” A given representation might be useful for purposes of intuition or calculational convenience, but it is not necessary for the fundamental definition of the theory. Representations are very far from unique, even if we limit our attention to representations corresponding to sensible physical theories.

One lesson of dualities in quantum field theories is that a single quantum theory can be thought of as describing completely different classical variables. The fundamental nature of the “stuff” being described by a theory can change under such dualities, as in that between the sine-Gordon boson in 1+1 dimensions and the theory of a massive Thirring fermion [16]. Even the dimensionality of space can change, as is well-appreciated in the context of the AdS/CFT correspondence, where a single quantum theory can be interpreted as either a conformal field theory in a fixed d -dimensional Minkowski background or a gravitational theory in a dynamical $(d+1)$ -dimensional spacetime with asymptotically anti-de Sitter boundary conditions [1].

The lesson we draw from this is that Nature at its most fundamental is simply described by a vector in Hilbert space. Classical concepts must emerge from this structure in an appropriate limit. The problem is that Hilbert space is relatively featureless; given that Hilbert spaces of fixed finite or countable dimension D are all isomorphic, it is a challenge to see precisely how a rich classical world is supposed to emerge.

Ultimately, all we have to work with is the Hamiltonian and the specific vector describing the universe. In the absence of any preferred basis, the Hamiltonian is fixed by its spectrum, the list of energy eigenvalues:

$$\{E_0, E_1, E_2, \dots\}, \quad \hat{H}|n\rangle = E_n|n\rangle, \quad (2.3)$$

and the state is specified by its components in the energy eigenbasis,

$$\{\psi_0, \psi_1, \psi_2, \dots\}, \quad |\psi\rangle = \sum_n \psi_n |n\rangle. \quad (2.4)$$

The question becomes: how do we go from such austere lists of numbers to the fullness of the world around us?

2.3 The Role of Emergence

One might ask why, if the fundamental theory of everything is fixed by the spectrum of some Hamiltonian, we don't simply imagine writing the state of the universe in the energy eigenbasis, where its evolution is trivial? The answer is the one that

applies to any example of emergence: there might be other descriptions of the same situation that provide useful insight or computational simplification.

Consider the classical theory of N particles moving under the influence of some multi-particle potential in 3 dimensions of space. The corresponding phase space is $6N$ -dimensional, and we *could* simply think of the theory as that of one point moving in a $6N$ -dimensional structure. But by thinking of it as N particles moving in a 3-dimensional space of allowed particle positions, we gain enormous intuition; for example, it could become clear that particles influence each other when they are nearby in space, which in turn suggests a natural way to coarse-grain the theory. Similarly, writing an abstract vector in Hilbert space as a wave function over some classical variables can provide crucial insight into the most efficient and insightful way to think of what is happening to the system.

2.4 Local Finite-Dimensionality

The Hilbert spaces considered by physicists are often infinite-dimensional, from a simple harmonic oscillator to quantum field theories. For separable Hilbert spaces (finite-dimensional or infinite-dimensional countable), the Stone-von Neumann theorem guarantees us uniqueness of the irreducible representation of the algebra of the canonical commutation relations (CCRs), up to unitary equivalence. In non-separable Hilbert spaces, however, there can be unitarily inequivalent representations of the CCRs, implying that the physical subspaces spanned by eigenstates of operators in a particular representation will be different. In Algebraic Quantum Field Theory, this is described by Haag’s theorem [3]. Then different choices of states (a unit-normed, positive linear functional) on the algebra specify different inequivalent (cyclic) representations. One might therefore conclude that specification of the algebra state is also an important ingredient in defining a quantum theory, over and above the Hamiltonian.

However, there are good reasons from quantum gravity to think that the true Hilbert space of the universe is “locally finite-dimensional” [17]. That is, we can decompose \mathcal{H} into a (possibly infinite) tensor product of finite-dimensional factors,

$$\mathcal{H} = \bigotimes_{\alpha} \mathcal{H}_{\alpha}, \quad (2.5)$$

where for each α we have $\dim(\mathcal{H}_{\alpha}) < \infty$. If we have factored the Hilbert space into the smallest possible pieces, we will call these “micro-factors.” The idea is that if we specify some region of space and ask how many states could possibly occupy the

region inside, the answer is finite, since eventually the energy associated with would-be states becomes large enough to create a black hole the size of the region [18]. Similarly, our universe seems to be evolving toward a de Sitter phase dominated by vacuum energy; a horizon-sized patch of such a spacetime is a maximum-entropy thermal state [19] with a finite entropy and a corresponding finite number of degrees of freedom [20, 21].

There are subtleties involved with trying to map collections of factors in (2.5) directly to regions of space, including the fact that “a region of space” \mathcal{R} might not be well-defined across different branches of the quantum-gravitational wave function. All that matters for us, however, is the existence of a decomposition of this form, and the idea that everything happening in one particular region of space on a particular branch is described by a finite-dimensional factor of Hilbert space $\mathcal{H}_{\mathcal{R}}$ that can be constructed as a finite tensor product of micro-factors \mathcal{H}_{α} . Given some overall pure state $|\psi\rangle \in \mathcal{H}$, physics within this region is described by the reduced density operator

$$\rho_{\mathcal{R}} = \text{Tr}_{\bar{\mathcal{R}}} |\psi\rangle\langle\psi|. \quad (2.6)$$

In that case, there is no issue of specifying the correct algebra of observables: the algebra is simply “all Hermitian operators acting on $\mathcal{H}_{\mathcal{R}}$.” Any further structure must emerge from the spectrum of the Hamiltonian and the quantum state.

2.5 Spacetime from Hilbert Space

Fortunately, we are guided in our quest by the fact that we know a great deal about what an appropriate emergent description should look like – a local effective field theory defined on a semiclassical four-dimensional dynamical spacetime. The first step is to choose a decomposition of the Hilbert space $\mathcal{H}_{\mathcal{R}}$ (representing, for example, the interior of our cosmic horizon) into finite-dimensional micro-factors. We can say that the Hamiltonian is “local” with respect to such a decomposition if, for some small integer k , the Hamiltonian connects any specific factor H_{α_*} to no more than k other factors; intuitively, this corresponds to the idea that degrees of freedom at one location only interact with other degrees of freedom nearby.

It turns out that a generic Hamiltonian will not be local with respect to *any* decomposition, and for the special Hamiltonians that can be written in a local form, the decomposition in which that works is essentially unique [22]. In other words, for the right kind of Hamiltonian, there is a natural decomposition of Hilbert space in which physics looks local, which is fixed by the spectrum alone. From the empirical suc-

cess of local quantum field theory, we will henceforth assume that the Hamiltonian of the world is of this type, at least for low-lying states near the vacuum.

This preferred local decomposition naturally defines a graph structure on the space of Hilbert-space factors, where each node corresponds to a factor and two nodes are connected by an edge if they have a nonzero interaction in the Hamiltonian. To go from this topological structure to a geometric one, we need to look beyond the Hamiltonian to the specifics of an individual low-lying state. Given any factor of Hilbert space constructed from a collection of smaller factors, $\mathcal{H}_A = \otimes_{\alpha \in A} \mathcal{H}_\alpha \subset \mathcal{H}_\mathcal{R}$, and its relative complement $\mathcal{H}_{\bar{A}} = \mathcal{H}_\mathcal{R} \setminus \mathcal{H}_A$, we can construct its density matrix and entropy,

$$\rho_A = \text{Tr}_{\bar{A}} \rho_\mathcal{R}, \quad S_A = -\text{Tr} \rho_A \log \rho_A, \quad (2.7)$$

and given any two such factors \mathcal{H}_A and \mathcal{H}_B , we can define their mutual information

$$I(A : B) = S_A + S_B - S_{AB}. \quad (2.8)$$

Guided again by what we know about quantum field theory, we consider “redundancy-constrained” states, which capture the notion that nearby degrees of freedom are highly entangled, while faraway ones are unentangled. In that case, the entropy of ρ_A can be written as the sum of mutual informations between micro-factors inside and outside \mathcal{H}_A ,

$$S_A = \frac{1}{2} \sum_{\alpha \in A, \beta \in \bar{A}} I(\alpha : \beta). \quad (2.9)$$

The mutual information allows us to assign weights to the various edges in our Hilbert-space-factor graph. With an appropriate choice of weighting, these weights can be interpreted as distances, with large mutual information corresponding to short distances [23]. That gives our graph an emergent spatial geometry, from which we can find a best-fit smooth manifold using multidimensional scaling. (Alternatively, the entropy across a surface can be associated with the surface’s area, and the emergent geometry defined using a Radon transform [24].) As the quantum state evolves with time according to the Schrödinger equation, the spatial geometry does as well; interpreting these surfaces as spacelike slices with zero extrinsic curvature yields an entire spacetime with a well-defined geometry.

2.6 Emergent Classicality

A factorization of Hilbert space into local micro-factors is not quite the entire story. To make contact with the classical world as part of an emergent description, we need

to further factorize the degrees of freedom within some region into macroscopic “systems” and a surrounding “environment,” and define a preferred basis of “pointer states” for each system. This procedure is crucial to the Everettian program, where the interaction of systems with their environment leads to decoherence and branching of the wave function. To describe quantum measurement, one typically considers a quantum object \mathcal{H}_q , an apparatus \mathcal{H}_a , and an environment \mathcal{H}_e . Branching occurs when an initially unentangled state evolves first to entangle the object with the apparatus (measurement), and then the apparatus with orthogonal environment states (decoherence), for example:

$$|\psi\rangle = (\alpha|+\rangle_q + \beta|-\rangle_q) \otimes |0\rangle_a \otimes |0\rangle_e \quad (2.10)$$

$$\rightarrow (\alpha|+\rangle_q|+\rangle_a + \beta|-\rangle_q|-\rangle_a) \otimes |0\rangle_e \quad (2.11)$$

$$\rightarrow \alpha|+\rangle_q|+\rangle_a|+\rangle_e + \beta|-\rangle_q|-\rangle_a|-\rangle_e. \quad (2.12)$$

The Born Rule for probabilities, $p(i) = |\psi_i|^2$, is not assumed as part of the theory; it can be derived using techniques such as decision theory [25] or self-locating uncertainty [26].

Two things do get assumed: an initially unentangled state and a particular factorization into object/apparatus/environment. The former condition is ultimately cosmological – the universe started in a low-entropy state, which we will not discuss here. The factorization, on the other hand, should be based on local dynamics. While this factorization is usually done based on our quasi-classical intuition, there exists an infinite unitary freedom in the choice of our system and environment. We seek an algorithm for choosing this factorization that leads to approximately classical behavior on individual branches of the wave function.

This question remains murky at the present time, but substantial progress is being made. The essential observation is that, if quantum behavior is distinguished from classical behavior by the presence of entanglement, classical behavior may be said to arise when entanglement is relatively unimportant. In the case of pointer states, this criterion is operationalized by the idea that such states are the ones that remain robust under being monitored by the environment [27]. For a planet orbiting the Sun in the solar system, for example, such states are highly localized around classical trajectories with definite positions and momenta.

A similar criterion may be used to define the system/environment split in the first place [28, 29]. Consider a fixed Hamiltonian and some Hilbert-space factorization into subsystems A and B . Generically, if we start with an unentangled (tensor-

product) state in that factorization, the amount of entanglement will grow very rapidly. However, we can seek the factorization in which there exist low-entropy states for which entanglement grows at a minimum rate. That will be the factorization in which it is useful to define robust pointer states in one of the subsystems, while treating the other as the environment.

This kind of procedure for factorizing Hilbert space is, in large measure, the origin of our notion of preferred classical variables. Given a quantum system in a finite-dimensional part of Hilbert space, in principle we are able to treat any Hermitian operator as representing an observable. But given the overall Hamiltonian, there will be certain specific interaction terms that define what is being measured when some other system interacts with our original system. We think of quantum systems as representing objects with positions and momenta because those are the operators that are most readily measured by real devices, given the actual Hamiltonian of the universe. We think of ourselves as living in position space, rather than in momentum space, because those are the variables in terms of which the Hamiltonian appears local.

2.7 Gravitation from Entanglement

We have argued that the geometry of spacetime can be thought of as arising from the entanglement structure of the quantum state in an appropriate factorization. To match our empirical experience of the world, this emergent spacetime should respond to emergent energy-momentum through Einstein's equation of general relativity. While we cannot do full justice to this problem in this chapter, we can mention that there are indications that such behavior is quite natural.

The basic insight is Jacobson's notion of "entanglement equilibrium" [30], extended to the case where spacetime itself is emergent rather than postulated [24]. Consider a subsystem in Hilbert space, in a situation where the overall quantum state is in the vacuum. It is then reasonable to imagine that the subsystem is in entanglement equilibrium: a small perturbation leaves the entropy of the region unchanged to first order. If we divide the entanglement into a small-scale ultraviolet term that determines the spacetime geometry and a longer-scale infrared term characterizing matter fields propagating within that geometry, the change in one kind of entropy must be compensated for by a corresponding change in the other,

$$\delta S_{UV} = -\delta S_{IR}. \quad (2.13)$$

Here, the left-hand side represents a change in geometry, and can be related directly

to the spacetime curvature. The right-hand side represents a matter perturbation, which can be related to the modular Hamiltonian of an emergent effective field theory on the background. At the linearized level (the weak-field limit), it can be shown that this relation turns into the 00 component of Einstein's equation in the synchronous gauge,

$$\delta G_{00} = 8\pi G \delta T_{00}. \quad (2.14)$$

If the overall dynamics are approximately Lorentz invariant (which they must be for this program to work, although it is unclear how to achieve this at this time), demanding that this equation hold in any frame implies the full linearized Einstein's equation, $\delta G_{\mu\nu} = 8\pi G \delta T_{\mu\nu}$.

There are a number of assumptions at work here, but it seems plausible that the spacetime dynamics familiar from general relativity can arise in an emergent spacetime purely from generic features of the entanglement structure of the quantum state. Following our quantum-first philosophy, this would be an example of finding gravity within quantum mechanics, rather than quantizing a classical model for gravitation.

2.8 The Problem(s) of Time

Given our ambition to find the most minimal fundamental description of reality, it is natural to ask whether time as well as space could be emergent from the wave function. The Wheeler-deWitt equation of canonical quantum gravity takes the form

$$\hat{H}|\psi\rangle = 0, \quad (2.15)$$

for some particular form of \hat{H} in a particular set of variables. In this case, time dependence is absent, but one may hope to recover an emergent notion of time by factorizing Hilbert space into a “clock” subsystem and the rest of the universe,

$$\mathcal{H} = \mathcal{H}_U \otimes \mathcal{H}_C, \quad (2.16)$$

then constructing an effective Hamiltonian describing evolution of the universe with respect to the clock.

Given our discussion thus far, the problem with such a procedure should be clear: what determines the decomposition (2.16)? In the Schrödinger case we can have data in the form of the spectrum of the Hamiltonian, but in the Wheeler-deWitt case the universe is in a single eigenstate; no other features of the Hamiltonian, including its other energy eigenvalues, can be relevant. This problem has been dubbed the “clock ambiguity” [31].

One potential escape would be to imagine that the fundamental state of the universe is described not by a vector in Hilbert space, but by a density operator acting on it. Then we have an alternative set of data to appeal to: the eigenvalues of that density matrix. These can be used to compute a modular Hamiltonian (given by the negative of the logarithm of the density operator), which in turn can yield an effective notion of time evolution, a proposal known as the “thermal time hypothesis” [32]. Thus it is conceivable that time as well as space could be emergent, at the cost of positing a fundamental density operator describing the state of the universe.²

2.9 Prospects and Puzzles

The program outlined here is both ambitious and highly speculative. We find it attractive as a way of deriving most of the familiar structure of the world from a minimal set of truly quantum ingredients. In particular, we derive rather than postulate such notions as space, fields, and particles. The fact that our Hilbert space is locally finite-dimensional suggests an escape from the famous problems of ultraviolet divergences in quantum field theory, and the emergence of spacetime geometry from quantum entanglement is an interesting angle on the perennial problems of quantum gravity.

Numerous questions remain; we will highlight just two. One is the emergence of local Lorentz-invariant dynamics. There are no unitary representations of the Lorentz group on a finite-dimensional factor of Hilbert space. This might seem to imply that Lorentz symmetry would be at best approximate, a possibility that is experimentally intriguing but already highly constrained. It would be interesting to understand how numerically large any deviations from perfect Lorentz invariance would have to be in this framework, and indeed if they have to exist at all.

The other issue is the emergence of an effective field theory in curved spacetime that could describe matter fields in our geometric background. We have posited that a field theory might be identified with infrared degrees of freedom while the geometry is determined by ultraviolet degrees of freedom, but there is much to be done to make this suggestion more concrete. A promising idea is to invoke the idea of a quantum error-correcting code [24, 34]. Such codes imagine identifying a “code subspace” within the larger physical Hilbert space, such that the quantum

²If time is fundamental rather than emergent, there is a very good reason to believe that the entirety of Hilbert space is infinite-dimensional, even if the factor describing our local region is finite-dimensional; otherwise the dynamics would be subject to recurrences and Boltzmann-brain fluctuations [33].

information in the code can be redundantly stored in the physical Hilbert space. There is a natural way to associate the code subspace with the infrared degrees of freedom of the matter fields, with the rest of the physical Hilbert space providing the ultraviolet entanglement that defines the emergent geometry. Once again, this is a highly speculative but a promising line of investigation.

We are optimistic that this minimal approach to the ontology of quantum mechanics is sufficient, given an appropriate Hamiltonian and quantum state, to recover all of the richness of the world as we know it. It would be a profound realization to ultimately conclude that what is fundamental does not directly involve spacetime or propagating quantum fields, but simply a vector moving smoothly through a very large-dimensional Hilbert space. Further investigation will be needed to determine whether such optimism is warranted, or whether we have just gone mad.

Chapter 3

THE HILBERT SPACE OF QUANTUM GRAVITY IS LOCALLY
FINITE-DIMENSIONAL

We argue in a model-independent way that the Hilbert space of quantum gravity is locally finite-dimensional. In other words, the density operator describing the state corresponding to a small region of space, when such a notion makes sense, is defined on a finite-dimensional factor of a larger Hilbert space. Because quantum gravity potentially describes superpositions of different geometries, it is crucial that we associate Hilbert-space factors with spatial regions only on individual decohered branches of the universal wave function. We discuss some implications of this claim, including the fact that quantum field theory cannot be a fundamental description of Nature.

This chapter is based on the following reference:

N. Bao, S. M. Carroll, and A. Singh, “The Hilbert space of quantum gravity is locally finite-dimensional,” *Int. J. Mod. Phys. D* **26** no. 12, (2017) 1743013, [arXiv:1704.00066](https://arxiv.org/abs/1704.00066) [hep-th]

In quantum field theory, the von Neumann entropy of a compact region of space R is infinite, because an infinite number of degrees of freedom in the region are entangled with an infinite number outside. In a theory with gravity, however, if we try to excite these degrees of freedom, many states collapse to black holes with finite entropy $S = A/4G$, where A is the horizon area [18, 35]. It is conceivable that there are degrees of freedom within a black hole that do not contribute to the entropy. However, if such states were low-energy, the entropy of the black hole could increase via entanglement, violating the Bekenstein bound. If they are sufficiently high-energy that they do not become entangled, exciting them would increase the size of the black hole, taking it out of the “local region” with which it was associated.

The finiteness of black hole entropy therefore upper bounds the number of degrees of freedom that can be excited within R , and therefore on the dimensionality of \mathcal{H}_R , the factor of Hilbert space associated with R (as the dimensionality of Hilbert space is roughly the exponential of the number of degrees of freedom). Similarly, a patch of de Sitter space, which arguably represents an equilibrium configuration

of spacetime, has a finite entropy proportional to its horizon area, indicative of a finite-dimensional Hilbert space [19, 36–39].

The most straightforward interpretation of this situation is that in the true theory of nature, which includes gravity, any local region is characterized by a finite-dimensional factor of Hilbert space. Some take this statement as well-established, while others find it obviously wrong. Here, we argue that the straightforward interpretation is most likely correct, even if the current state of the art prevents us from drawing definitive conclusions.

This discussion begs an important question: what is “the Hilbert space associated with a region”? Quantum theories describe states in Hilbert space, and notions like “space” and “locality” should emerge from that fundamental level [22, 23, 40]. Our burden is therefore to understand what might be meant by the Hilbert space of a local region, and whether that notion is well-defined in quantum gravity.

We imagine that the fundamental quantum theory of nature describes a density operator ρ acting on a Hilbert space \mathcal{H}_{QG} . The entanglement structure of near-vacuum states in spacetime is very specific, so generic states in \mathcal{H}_{QG} will not look like spacetime at all [22, 23]. Rather, in phenomenologically relevant, far-from-equilibrium states ρ , there will be macroscopic pointer states representing semiclassical geometries. To that end, we imagine a decomposition

$$\mathcal{H}_{\text{QG}} = \mathcal{H}_{\text{sys}} \otimes \mathcal{H}_{\text{env}}, \quad (3.1)$$

where the system factor \mathcal{H}_{sys} will describe a region of space and its associated long-wavelength fields, and the environment factor \mathcal{H}_{env} is traced over to obtain our system density matrix, $\rho_{\text{sys}} = \text{Tr}_{\text{env}} \rho$. The environment might include microscopic degrees of freedom that are either irrelevant or spatially distant. Then decoherence approximately diagonalizes the system density matrix in the pointer basis,

$$|\Psi_a\rangle \in \mathcal{H}_{\text{sys}}, \quad \rho_{\text{sys}} = \sum_a p_a |\Psi_a\rangle \langle \Psi_a|. \quad (3.2)$$

An emergence map Φ associates decohered branches of the quantum-gravity wave function with states of an effective field theory defined on a semiclassical background spacetime. In a space+time decomposition, the emergent theory describes spatial manifolds Σ with 3-metric γ_{ij} and conjugate momentum π_{ij} , along with a Hilbert space $\mathcal{H}_{\text{EFT}}^{(\Sigma)}$ of quantum fields on Σ ,

$$\Phi : |\Psi_a\rangle \rightarrow \left\{ \Sigma_a, g_{ij}^{(a)}, \pi_{ij}^{(a)}, |\phi^{(a)}\rangle \right\}, \quad (3.3)$$

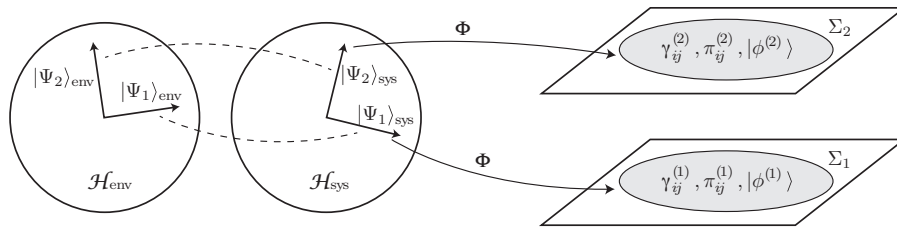


Figure 3.1: On the left, the Hilbert space of quantum gravity is portrayed as a tensor product, $\mathcal{H}_{\text{QG}} = \mathcal{H}_{\text{sys}} \otimes \mathcal{H}_{\text{env}}$, and two decohered branches $|\Psi_a\rangle_{\text{sys}} \otimes |\Psi_a\rangle_{\text{env}}$ are shown. Under the map Φ , the system factors of these states map to regions Σ_a of a semiclassical spacetime background, on which are defined a spatial metric and its conjugate momentum as well as the quantum state of an effective field theory.

where $|\phi^{(a)}\rangle \in \mathcal{H}_{\text{EFT}}^{(\Sigma_a)}$. We do not insist that Σ_a be a boundaryless surface; it may simply be a finite region of space (e.g., the interior of a de Sitter horizon). Horizon complementarity [41] suggests that there could be a limit on the extent of Σ_a , perhaps in the form of an entropy bound à la Bousso [42].

Now imagine that, in some emergent geometry, we divide Σ into a closed region R and its exterior \bar{R} . The proposition “a region of space is described by a finite-dimensional factor of Hilbert space” should be interpreted as the claim that we can decompose the system Hilbert space in the fundamental theory as $\mathcal{H}_{\text{sys}} = \mathcal{H}_R \otimes \mathcal{H}_{\bar{R}}$, representing factors describing physics inside and outside R , such that $\dim \mathcal{H}_R$ is finite. (As is standard with emergent theories, the map $\mathcal{H}_R \otimes \mathcal{H}_{\bar{R}} \rightarrow \mathcal{H}_R^{(\Sigma)} \otimes \mathcal{H}_{\bar{R}}^{(\Sigma)}$ represents an approximation. In particular, our ability to divide space into two sets of degrees of freedom does not imply that we can continue to subdivide it into many small regions simultaneously.)

Such a decomposition is familiar in the case of quantum field theories on a fixed spacetime background. (There may be subtleties due to gauge invariance on the boundary, e.g. [43, 44].) This is necessitated by the success of locality as an underlying principle of everyday physics. If a single degree of freedom were accessible both in R and \bar{R} , a unitary operator localized within R could change the state elsewhere – not in the sense of branching the wave function, but in the sense of direct superluminal information transfer, as the reduced density matrix $\rho_{\bar{R}} = \text{Tr}_R \rho_{\text{sys}}$ would change instantly. Indeed, the notion that we can sensibly talk about the entropy of a black hole implicitly assumes this kind of locality.

A complication could arise due to the fact that gravity is a long-range force coupled to a conserved charge (mass-energy) that is always positive [15, 45–47]. Any

operator with nonzero energy or other conserved Poincaré charges is “dressed” by a gravitational field stretching out to infinity, representing an apparent obstacle to localization. In particular, diffeomorphism-invariant operators are considered from the start.

A locally-finite theory, however, need not give rise *directly* to a diffeomorphism-invariant description of gravity. The fundamental description could correspond to a particular gauge, in which the symmetries of the theory were not manifest, even though they could be restored once the effective theory had emerged. It is dangerous to start with symmetries of the sought-after continuum theory, defined in the context of an infinite-dimensional Hilbert space, and demand that they be present at the discrete level; all that we should require is that crucial physical properties ultimately emerge (e.g. [48]).

From our perspective, gravitational dressing is not inconsistent with localizing a finite number of degrees of freedom within a region of space. (Even the notion of “at infinity” is unlikely to be well-defined as a statement about \mathcal{H}_{QG} , but we will not rely on that loophole.) Rather, there are superselection sectors corresponding to total gauge charges, including energy, operators that change the total energy connect one quantum-gravity pointer state to a state with a different energy. Such operators are not necessary for describing the local dynamics, which can be captured entirely by operators that commute with global charges; physical changes in the local state of a system are not instantaneously communicated to infinity. Equivalently, there is no obstacle to decomposing the Hamiltonian into a term acting only within R , one acting only within \bar{R} , and an interaction defined by a sum of tensor products of such local operators. When working in any one such sector, then, we are allowed to factorize our system Hilbert space as $\mathcal{H}_{\text{sys}} = \mathcal{H}_R \otimes \mathcal{H}_{\bar{R}}$.

Given the validity of this factorization, the finite dimensionality of \mathcal{H}_R follows from the black-hole arguments above, with one consideration: when we attempt to excite degrees of freedom until we reach a black hole, we should not consider operators that change the Poincaré charges at infinity. This is no problem; it is easy enough to imagine creating black holes simply by moving around existing mass/energy within the state (as actually happens in the real world when black holes are created). The upper bound from black-hole entropy on the number of ways this could happen implies an upper bound on the effective degrees of freedom, and therefore on $\dim \mathcal{H}_{\text{sys}}$.

We therefore conclude that it is sensible to associate factors of Hilbert space with

regions of space, at the level of individual branches representing semiclassical spacetimes, and that such factors have finite dimensionality. There are well-known obstacles to constructing phenomenologically acceptable theories with finite-dimensional Hilbert spaces, including a lack of exact Lorentz invariance. It is therefore imperative to investigate whether such features can arise in an approximate fashion without violating experimental bounds [49].

Locally finite-dimensional Hilbert spaces entail a number of consequences. This perspective suggests new tools for investigating the behavior of quantum spacetime, such as the quantum-circuit approach [50]. It also implies an attitude toward ultraviolet divergences in quantum gravity: there are no such divergences, as there are only finitely many degrees of freedom locally. The cosmological constant problem becomes the question of why the factor associated with our de Sitter patch has its particular large, finite dimensionality, $\exp(10^{122})$ [36]; perhaps other fine-tuning questions, such as the hierarchy problem, can be similarly recast.

*Chapter 4***QUANTUM SPACE, QUANTUM TIME, AND RELATIVISTIC
QUANTUM MECHANICS**

We treat space and time as bona fide quantum degrees of freedom on an equal footing in Hilbert space. Motivated by considerations in quantum gravity, we focus on a paradigm dealing with linear, first-order Hamiltonian and momentum constraints that lead to emergent features of temporal and spatial translations. Unlike the conventional treatment, we show that Klein-Gordon and Dirac equations in relativistic quantum mechanics can be unified in our paradigm by applying relativistic dispersion relations to eigenvalues rather than treating them as operator-valued equations. With time and space being treated on an equal footing in Hilbert space, we show symmetry transformations to be implemented by unitary basis changes in Hilbert space, giving them a stronger quantum mechanical footing. Global symmetries, such as Lorentz transformations, modify the decomposition of Hilbert space; and local symmetries, such as $U(1)$ gauge symmetry are diagonal in coordinate basis and do not alter the decomposition of Hilbert space. We briefly discuss extensions of this paradigm to quantum field theory and quantum gravity.

This chapter is based on the following reference:

A. Singh, “Quantum space, quantum time, and relativistic quantum mechanics,”
[arXiv:2004.09139](https://arxiv.org/abs/2004.09139) [quant-ph]

4.1 Introduction

Quantum mechanics, in the conventional paradigm, treats time and space on a vastly different footing. Time enters the Schrödinger equation as an external, classical parameter that flows independent of the quantum mechanical system. Space, on the other hand, is often elevated to have a genuine quantum mechanical status with corresponding position/momentum operators, unitary transformations, eigenstates, etc. While such an approach works well, both conceptually and mathematically in non-relativistic physics, one would like to treat time and space on an equal footing in relativistic quantum mechanics. Attempts to promote time to an operator have been conventionally argued against, citing the Stone-von Neumann theorem [2] due

to which the Hamiltonian (with a spectrum bounded from below) and time cannot be bona fide conjugate observables. One then goes on to work with quantum field theory, where time and space are treated as mere labels on a background manifold, and matter is treated quantum mechanically living on this background spacetime.

In relativistic quantum mechanics of particles¹, while one tries to use relativistic dispersion relations to treat time and space symmetrically from an algebraic perspective, their quantum nature is still treated vastly differently as is evident in the Schrödinger equation. Efforts to use first order expressions in both the Hamiltonian and momentum lead to rather disparate approaches dealing with Klein-Gordon (spin-0 particles) and Dirac (spin-1/2 particles) equations. In the case of Klein-Gordon equation, one typically promotes the relativistic dispersion relation $E = \sqrt{|\vec{p}|^2 + m^2}$ for a particle to an operator-valued equation, $\hat{H} = \sqrt{|\hat{\vec{p}}|^2 + m^2}$ to use in the Schrödinger equation $\hat{H} |\psi(t)\rangle = i\partial_t |\psi(t)\rangle$. Expanding the “square root” Hamiltonian operator gives a series in all positive even powers of momentum which makes it far from being first-order and leads to issues with non-locality, probabilistic interpretation of the wavefunction, etc., as can be found in detail in many advanced undergraduate level texts [52–54] dealing with relativistic quantum mechanics. The Dirac equation, on the other hand, is able to circumvent this issue by explicitly involving the spin of the particle that makes the Hamiltonian first-order in momentum by using the spinor gamma matrices of the Clifford algebra. In addition to this, the status of Lorentz transformations from a Hilbert space perspective is often left somewhat ambiguous since time and space are treated rather differently, and hence symmetry transformations are implemented at a classical level. Can these disparities be traced back to, and remedied, by better understanding the quantum mechanical status of space and time? In this paper, we answer this question in the affirmative by treating time and space on an equal footing in Hilbert space.

While quantum theory, in particular its formulation as quantum field theory, has been spectacularly successful in predicting outcomes for scattering experiments etc., our primary motivation here is to better understand aspects of quantum gravity where it is important to examine the status of space and time in the context of quantum mechanics. Approaches to quantum gravity are often plagued by the “problem of time” [55–58]: reconciling how time enters as an independent, absolute, clas-

¹Often referred to as first quantization, though we will refrain from using this terminology in this paper.

sical parameter in quantum mechanics; whereas in relativity, time has a relative connotation depending on the observer and distribution of mass-energy. More generally, theories with reparametrization invariance [59–61] such as classical general relativity, which has general (local) coordinate invariance, have a formulation in terms of *constraints* [62, 63]. Physical states in the theory are the ones that are annihilated by these constraints, and therefore represent the kernel of the constraint operators. In general relativity, Hamiltonian and momentum constraints demand the total energy and momentum to be zero and this is used to identify the physical states. In particular, this is reflected in the Wheeler-DeWitt [64] equation, which represents a Hamiltonian constraint of the form $\hat{H} |\Psi\rangle = 0$. In this setup, physical states of the theory do not evolve with respect to an external time. Time evolution, in such a setup would therefore be an emergent feature.

The author and collaborators have argued for a “quantum-first” approach [65] to quantum gravity where we begin with minimal elements in quantum mechanics in Hilbert space and from it, derive higher-level structures such as space, locality, matter, and eventually, gravity. Similar quantum-first approaches have been advocated by other authors too [66, 67]. With this motivation in mind, we take a small step in this paper toward understanding the quantum mechanical status of space and time in the context of relativistic quantum mechanics, in a way to lay out groundwork to treat quantum field theory and eventually, gravity in a similar paradigm, appropriately extended. We will treat space and time on an equal footing in Hilbert space, and to this end, we will work with a Hilbert space decomposition of the form,

$$\mathcal{H} \simeq \mathcal{H}_t \otimes \mathcal{H}_{\vec{x}} \otimes \mathcal{H}_{\text{spin}} , \quad (4.1)$$

where we have a factor of Hilbert space, \mathcal{H}_t for a temporal degree of freedom, a factor, $\mathcal{H}_{\vec{x}}$ for a spatial degree of freedom and $\mathcal{H}_{\text{spin}}$ corresponding to the spinorial degree of freedom of the particle. Global states in this Hilbert space will neither evolve relative to an external time nor will they have a notion of spatial translations relative to any external coordinate system. With both a Hamiltonian constraint $\hat{\mathbb{J}}_H$ and momentum constraints $\hat{\mathbb{J}}_{\vec{p}}$ as central structures in this construction, spatial and temporal translations will be emergent features for physical states. The constraints will be explicitly linear and first order in conjugate momenta, and their joint kernel will define the set of physical states *i.e.* the ones annihilated by the constraints. For such physical states, spatial and temporal translation features emerge as a consequence of entanglement and correlations between different factors of the global

Hilbert space \mathcal{H} . Since we are working with a relativistic setup, the compatibility $[\hat{H}, \hat{P}] = 0$ of the Hamiltonian and momentum, two of the generators of the Poincaré group will restrict the kinds of theories we can write down and we will discuss this point in some detail. Using these first-order constraints, we will show that Klein-Gordon and Dirac equations in relativistic quantum mechanics can be treated with a uniform approach. This will be done by applying dispersion relations to eigenvalues which appear in constraints, and not treat them as operator-valued equations. With such an approach, the “square root” Hamiltonian in Klein-Gordon theory is handled naturally at par with the Dirac equation. Along the way, we will also discuss differences of our setup compared to the usual constructions and how one can attempt to bridge the gap. Treating time and space on an equal footing in Hilbert space, we show symmetry transformations to be implemented by unitary basis changes in Hilbert space. Global symmetries, such as Lorentz transformations, modify the decomposition of Hilbert space; and local symmetries, such as $U(1)$ gauge symmetry are diagonal in coordinate basis and do not alter the decomposition of Hilbert space.

Our focus in this paper is to simplistically evaluate the quantum mechanical status of space and time with an eye toward relativistic quantum mechanics: recasting the basics of quantum mechanics in a way that can be made amenable to the study of quantum gravity from first principles. The paper is organized as follows. In section 4.2, we first introduce the concept of internal time treated as a quantum degree of freedom (à la Page-Wootters), and then use it as our motivation to lay out the Hilbert space structure treating space and time on an equal footing. Once we have our vector spaces in place, we will then go on to talk about Hamiltonian and momentum constraints in section 4.3 and apply it to Klein-Gordon and the Dirac equations. In section 4.4, we will use the power of our Hilbert space construction to identify the status of symmetry transformations in relativistic quantum mechanics as implementing basis changes in Hilbert space. Lorentz transformations will be seen as global changes of factorization of Hilbert space and $U(1)$ gauge symmetry will be enacted as a local basis change while treating time and space symmetrically. We will conclude in section 4.5, discussing implications and extensions of our construction to quantum field theory and quantum gravity.

4.2 Time, Space, and Spin in Hilbert Space

Inspiration: Time as an Internal Quantum Degree of Freedom

We begin by reviewing (an extension of) the Page-Wootters construction [5–7] which is one of the most famous and elegant approaches to emergent time in quantum mechanics. We will closely follow the work in Ref. [8] for this quick review. This will serve as motivation for us to generalize its features to treat space and time on an equal footing in Hilbert space in the context of the quantum mechanics of a relativistic particle. The Page-Wootters formulation is one of internal time, where time is treated as an internal quantum degree of freedom and not as an external classical parameter. The global quantum state is static and the apparent “flow” of time is due to the entanglement and correlations between the temporal degree of freedom with the rest of Hilbert space.

The global Hilbert space \mathcal{H} is factorized into a temporal degree of freedom \mathcal{H}_t , often called as the “clock,” and the system \mathcal{H}_S (what we typically describe in conventional quantum mechanics) (we have used \simeq to denote Hilbert space isomorphisms throughout the paper),

$$\mathcal{H} \simeq \mathcal{H}_t \otimes \mathcal{H}_S . \quad (4.2)$$

As we will see, correlations between \mathcal{H}_t and \mathcal{H}_S will lead to effective time evolution for states in \mathcal{H}_S governed by a Hamiltonian. The temporal Hilbert space \mathcal{H}_t is taken isomorphic to $\mathbb{L}_2(\mathbb{R})$ (akin to the Hilbert space of a single particle on a 1D line in conventional non-relativistic quantum mechanics) and on the space of linear operators $\mathcal{L}(\mathcal{H}_t)$, we associate conjugate variables: the “time” \hat{t} and its conjugate momentum \hat{p}_t that satisfy Heisenberg canonical commutation relation (CCR), in units with $\hbar = 1$,

$$[\hat{t}, \hat{p}_t] = i . \quad (4.3)$$

A priori, the conjugate momentum \hat{p}_t to the time operator \hat{t} should not be tied in any way to the Hamiltonian. At this stage, we have just specified a standard pair of conjugate operators on the Hilbert space \mathcal{H}_t . Eigenstates of the time operator \hat{t} are defined by $\hat{t}|t\rangle = t|t\rangle \forall t \in \mathbb{R}$ and these eigenstates follow Dirac orthonormality $\langle t'|t\rangle = \delta(t - t')$. The Page-Wootters internal time construction then can be written in terms of a constraint operator $\hat{\mathbb{J}}$ in the linear space of operators $\mathcal{L}(\mathcal{H})$,

$$\hat{\mathbb{J}} = \hat{p}_t \otimes \hat{\mathbb{I}}_S + \hat{\mathbb{I}}_t \otimes \hat{H}_S , \quad (4.4)$$

where $\hat{\mathbb{I}}_t$ and $\hat{\mathbb{I}}_S$ are identity operators on \mathcal{H}_t and \mathcal{H}_S , respectively, and \hat{H}_S is the conventional Hamiltonian for the system. Physical states $|\Psi\rangle\rangle$ in the global Hilbert

space \mathcal{H} are identified to be the ones annihilated by the constraint operator $\hat{\mathbb{J}}$,

$$\hat{\mathbb{J}} \approx 0 \implies \hat{\mathbb{J}} |\Psi\rangle\rangle = 0. \quad (4.5)$$

We use the double-ket notation $|\Psi\rangle\rangle$ to stress the fact that the state is defined on the global Hilbert space $\mathcal{H}_t \otimes \mathcal{H}_S$. Such a technique of quantization based on constraints can be attributed to Dirac [62, 63], and also represents the constraint feature of the Wheeler-DeWitt equation. These physical states, which are eigenstates of the constraint operator $\hat{\mathbb{J}}$ with eigenvalue zero, are globally static, but encode an apparent flow of time from the perspective of \mathcal{H}_S . Such physical states annihilated by a global constraint are therefore consistent with the Wheeler-DeWitt equation. Conventional time-dependent states of the system are obtained by conditioning the global, physical state $|\Psi\rangle\rangle$ with the eigenvector $|t\rangle$ of the time operator \hat{t} ,

$$|\psi(t)\rangle = \langle t | \Psi \rangle\rangle \in \mathcal{H}_S, \quad (4.6)$$

which obeys the conventional Schrödinger equation governed by the Hamiltonian \hat{H}_S ,

$$\langle t | \hat{\mathbb{J}} | \Psi \rangle\rangle = \langle t | \hat{p}_t \otimes \hat{\mathbb{I}}_S | \Psi \rangle\rangle + \hat{H}_S |\psi(t)\rangle = 0. \quad (4.7)$$

Inserting a complete set of states on \mathcal{H}_t given by $\int dt |t\rangle \langle t| = \hat{\mathbb{I}}_t$, and remembering that the matrix elements of the conjugate momenta are $\langle t | \hat{p}_t | t' \rangle = -i \frac{\partial}{\partial t} \delta(t - t')$, we get the time evolution equation for states $|\psi(t)\rangle$ of the system,

$$\hat{H}_S |\psi(t)\rangle = i \frac{\partial}{\partial t} |\psi(t)\rangle, \quad (4.8)$$

which is indeed the Schrödinger equation for $|\psi(t)\rangle \in \mathcal{H}_S$. Thus, we see that effective time evolution for states in the subfactor \mathcal{H}_S of the global Hilbert space, governed by a Hamiltonian \hat{H}_S can be recovered from a constraint operator.

Such a construction is succinct and elegant since it gives a strong quantum mechanical notion of a temporal degree of freedom in Hilbert space. It also overcomes Dirac's criticism on treating time as an operator: following the Schrödinger equation, one might wish to establish a conjugate relationship between the Hamiltonian and the time operator as canonically conjugate variables, but this is not allowed due to the Stone-von Neumann theorem. The theorem demands a set of conjugate operators satisfying the Heisenberg CCR to have their eigenvalue spectra unbounded from below; but for physical theories, the Hamiltonian has a ground state with an energy bounded from below. In the Page-Wootters construction, the time operator \hat{t}

and the system Hamiltonian \hat{H}_S are not conjugates since they act on different Hilbert spaces. There is a bona fide pair of conjugate operators on \mathcal{H}_t , the time operator \hat{t} and its conjugate \hat{p}_t which satisfy the Heisenberg CCR. It is only for the physical states which are annihilated by the constraint $\hat{\mathbb{J}}$ that leads to a Schrödinger evolution for these states.

While elegant and succinct, the Page-Wootters formulation of internal time treats time as a special, distinguished variable on a vastly different footing than space as is evident from the construction. The nature of the system Hilbert space \mathcal{H}_S is left open-ended on purpose and has the potential of representing a variety of degrees of freedom, or combinations thereof, including but not limited to space and spin. While one might choose a position or momentum basis for \mathcal{H}_S in certain examples, it does not have any explicit and universal connection to a spatial degree of freedom as is evident by the lack of a corresponding momentum constraint (just like we have a Hamiltonian constraint associated with the temporal degree of freedom). It therefore, in its current form, is not very amenable to understanding relativistic quantum mechanics and the status of symmetry transformations such as Lorentz transformations etc. in Hilbert space. In an effort to formulate a quantum-first approach to quantum gravity, we would like to be able to treat space and time coordinates on an equal footing in a reparametrization invariant way. Motivated by the Page-Wootters construction, we now move on to developing the basic framework to treat time and space on an equal footing in Hilbert space with a corresponding Hamiltonian and momentum constraints. The interested reader who would like to delve more into the problem of time in quantum gravity more broadly, the Page-Wootters mechanism, conditional probability approach to time, and allied topics is referred to [68–72] (and references therein).

Hilbert Space Structure

Our focus in this paper is the quantum mechanics of a relativistic particle in a 3+1 d spacetime, *i.e.* three spatial dimensions and one temporal dimension. Let us begin by introducing the formal Hilbert space structure of the theory, as a modification to the Hilbert space decomposition of Eq. (4.2) in the Page-Wootters construction above. For a similar Hilbert space construction applied to relativistic ideas of time dilation, please see Ref. [73]. Instead of having a system Hilbert space \mathcal{H}_S , we will treat space on an equal footing with time by assigning it as a factor in the Hilbert

space decomposition in addition to accounting for the spin of the particle,

$$\mathcal{H} \simeq \mathcal{H}_t \otimes \mathcal{H}_{\vec{x}} \otimes \mathcal{H}_{\text{spin}} , \quad (4.9)$$

where \mathcal{H}_t is the Hilbert space associated with a temporal degree of freedom, $\mathcal{H}_{\vec{x}}$ with a spatial degree of freedom, and $\mathcal{H}_{\text{spin}}$ corresponds to the spinorial degree of freedom. The temporal Hilbert space \mathcal{H}_t is again taken isomorphic to $\mathbb{L}_2(\mathbb{R})$ (akin to the Hilbert space of a single particle on a 1D line in conventional non-relativistic quantum mechanics) similar to the Page-Wootters case, and on the space of linear operators $\mathcal{L}(\mathcal{H}_t)$, we associate conjugate variables: the ‘‘time’’ coordinate operator \hat{t} and its conjugate momentum \hat{p}_t , which satisfy Heisenberg canonical commutation relation (CCR), in units with $\hbar = 1$,

$$[\hat{t}, \hat{p}_t] = i . \quad (4.10)$$

Similar to the Page-Wootters construction, the conjugate momentum \hat{p}_t to the time operator \hat{t} a priori should not be tied to the Hamiltonian in any way. The eigenstates of the time operators are defined in the usual way $\hat{t} |t\rangle = t |t\rangle \forall t \in \mathbb{R}$ satisfying Dirac orthonormality $\langle t|t'\rangle = \delta(t - t')$ and the conjugate momentum \hat{p}_t generates translations of the $|t\rangle$ eigenstates, $\exp(-i\hat{p}_t \Delta t) |t\rangle = |t + \Delta t\rangle$.

For the spatial factors of Hilbert space, since we are working in 3 spatial dimensions, we associate a factor isomorphic to $\mathbb{L}_2(\mathbb{R})$ for each orthogonal direction which we choose to label by Cartesian directions x , y , and z ,

$$\mathcal{H}_{\vec{x}} \simeq \mathcal{H}_x \otimes \mathcal{H}_y \otimes \mathcal{H}_z , \quad (4.11)$$

and for each of these factors, we associate conjugate variables satisfying Heisenberg CCR,

$$[\hat{j}, \hat{p}_j] = i, \text{ for } j = x, y, z . \quad (4.12)$$

Throughout the paper, we use Latin index j to run over the spatial coordinates $j = x, y, z$ and Greek indices $\mu, \nu = 0, 1, 2, 3$ to run over spacetime coordinates. We also define 4-operators \hat{X}^μ and \hat{P}_μ for $\mu = 0, 1, 2, 3$ living in $\mathcal{L}(\mathcal{H})$, the set of linear operators on the full Hilbert space, akin to 4-vectors in special relativity in anticipation of making the formulation covariant,

$$\hat{X}^\mu \equiv (\hat{X}^0, \hat{X}^1, \hat{X}^2, \hat{X}^3) \in \mathcal{L}(\mathcal{H}_t \otimes \mathcal{H}_{\vec{x}}) , \quad (4.13)$$

where \hat{X}^0 is to be interpreted as $\hat{X}^0 = \hat{t} \otimes \hat{\mathbb{1}}_{\vec{x}}$, $\hat{X}^1 = \hat{t} \otimes \hat{x} \otimes \hat{\mathbb{1}}_y \otimes \hat{\mathbb{1}}_z$, etc., and similarly its conjugate momentum,

$$\hat{P}_\mu = (\hat{P}_0, \hat{P}_1, \hat{P}_2, \hat{P}_3) \in \mathcal{L}(\mathcal{H}_t \otimes \mathcal{H}_{\vec{x}}) , \quad (4.14)$$

where $\hat{P}_0 = \hat{p}_t \otimes \hat{\mathbb{1}}_{\vec{x}}$, $\hat{P}_1 = \hat{\mathbb{1}}_t \otimes \hat{p}_x \otimes \hat{\mathbb{1}}_y \otimes \hat{\mathbb{1}}_z$, etc. and these conjugate operators satisfy Heisenberg CCR, $[\hat{X}^\mu, \hat{P}_\nu] = i\delta_\nu^\mu$, where δ_ν^μ is the Kronecker delta function.

The spinorial factor of Hilbert space $\mathcal{H}_{\text{spin}}$ will encode information about spin of the particle, and will typically be spanned by the corresponding spinorial matrices. In particular, a spin-0 particle will have $\dim \mathcal{H}_{\text{spin}} = 1$ and a spin-1/2 particle will correspond to $\dim \mathcal{H}_{\text{spin}} = 4$ (as with the spinor gamma matrices in the Dirac equation that describes both the particle and its antiparticle).

We would like to emphasize that in this setup, there is no notion of an external, classical time parameter, and consequently, no Schrödinger evolution for states (or evolution of operators in the Heisenberg picture). Time is treated on an equal footing with the spatial degree of freedom of a particle and any notion of spatial or temporal translations should be emergent features as we will see in the next section.

4.3 Hamiltonian and Momentum Constraints

With our motivation from quantum gravity to deal with theories with reparametrization invariance such as those with coordinate invariance, we focus on their characteristic signature of being represented in a constraint-based formulation. We too would like to formulate our construction in terms of linear, first-order constraints while treating time and space on an equal quantum-mechanical footing. We thus have a formulation in terms of Hamiltonian and momentum constraints, which assert that the total energy and momentum are zero and these constraints identify physical states to be the ones that are annihilated by them.

At variance with the Page-Wootters construction outlined in section 4.2 that treats time as a distinguished quantum degree of freedom and hence deals only with a Hamiltonian constraint, we are attempting to treat both space and time on an equal footing and this will have us using both Hamiltonian and momentum constraints to identify physical states. Since we are dealing with relativistic quantum mechanics, we require the constraints to commute with each other (since the Hamiltonian and momentum of a relativistic system commute). As a consequence of this setup being applied to relativistic particles (or as some would say, first quantization), we use a collection of constraints parametrized by $\vec{k} \in \mathbb{R}^3$ and the corresponding dispersion relation of the particle. We discuss extensions of this construction to field theory in section 4.5 where we can deal with single Hamiltonian and momentum constraints that commute with each other.

Klein-Gordon Equation (Spin-0)

We first analyze the case of relativistic quantum mechanics of a spin-0 particle with rest mass m , which obeys the Klein-Gordon equation. The energy-momentum dispersion relation for the Klein-Gordon free particle is

$$E(\vec{k}) = \sqrt{|\vec{k}|^2 + m^2}, \quad (4.15)$$

for a momentum $\vec{k} \in \mathbb{R}^3$ carried by the particle. In the usual construction dealing with the Klein-Gordon equation, one typically promotes the relativistic dispersion relation of the particle to an operator-valued equation, $\hat{H} = \sqrt{|\hat{p}|^2 + m^2}$ that is then used in the Schrödinger equation $\hat{H} |\Psi\rangle = i\partial_t |\Psi\rangle$. Expanding the “square-root” Hamiltonian operator gives a series in all even powers of momentum that is far from being first-order, and leads to a slew of issues, from non-locality (due to the higher powers of momentum) in the theory, to not having a consistent probabilistic interpretation of the wavefunction. These issues are brought to light in a standard undergraduate-level quantum mechanical text [52–54] and we do not reproduce these arguments in detail there. Instead, we will recast the physics of the Klein-Gordon equation in the language of linear, first-order Hamiltonian and momentum constraints, and see how it can help us deal with some of these issues.

The spinorial Hilbert space in this case will have $\dim \mathcal{H}_{\text{spin}} = 1$ since the particle does not have any spin. Hence, each energy/momentum configuration can be labelled by the spatial momentum \vec{k} of the particle. The Hamiltonian constraint of the system, for a given \vec{k} , can be written as,

$$\hat{\mathbb{J}}_H(\vec{k}) = \hat{p}_t \otimes \hat{\mathbb{1}}_{\vec{x}} \otimes \hat{\mathbb{1}}_{\text{spin}} + \hat{\mathbb{1}}_t \otimes \hat{\mathbb{1}}_{\vec{x}} \otimes \left(E(\vec{k}) \hat{\mathbb{1}}_{\text{spin}} \right), \quad (4.16)$$

where we have formally written down the energy $E(\vec{k})$ in the one-dimensional spinorial Hilbert space $\mathcal{H}_{\text{spin}}$ with the identity element $\hat{\mathbb{1}}_{\text{spin}} = 1$. The momentum constraints, one for each orthogonal direction, parametrized by $\vec{k} \equiv (k_x, k_y, k_z)$, is

$$\hat{\mathbb{J}}_{P_j}(\vec{k}) = \hat{\mathbb{1}}_t \otimes \hat{p}_j \otimes \hat{\mathbb{1}}_{\text{spin}} - \hat{\mathbb{1}}_t \otimes \hat{\mathbb{1}}_{\vec{x}} \otimes \left(k_j \hat{\mathbb{1}}_{\text{spin}} \right) \text{ for } j = x, y, z. \quad (4.17)$$

Physical states $|\psi_{\vec{k}}\rangle\rangle$ in Hilbert space \mathcal{H} are identified to be the ones that are annihilated by the constraints,

$$\hat{\mathbb{J}}_H(\vec{k}) \approx 0 \implies \left(\hat{p}_t \otimes \hat{\mathbb{1}}_{\vec{x}} \otimes \hat{\mathbb{1}}_{\text{spin}} + \hat{\mathbb{1}}_t \otimes \hat{\mathbb{1}}_{\vec{x}} \otimes \left(E(\vec{k}) \hat{\mathbb{1}}_{\text{spin}} \right) \right) |\psi_{\vec{k}}\rangle\rangle = 0, \quad (4.18)$$

$$\hat{\mathbb{J}}_{P_j}(\vec{k}) \approx 0 \implies \left(\hat{\mathbb{1}}_t \otimes \hat{p}_j \otimes \hat{\mathbb{1}}_{\text{spin}} - \hat{\mathbb{1}}_t \otimes \hat{\mathbb{1}}_{\vec{x}} \otimes \left(k_j \hat{\mathbb{1}}_{\text{spin}} \right) \right) |\psi_{\vec{k}}\rangle\rangle = 0 \text{ for } j = x, y, z. \quad (4.19)$$

Again, we have used the double-ket notation to explicitly reflect that these states are defined on the full Hilbert space \mathcal{H} . Since the Hamiltonian and momentum constraint operators commute, $[\hat{\mathbb{J}}_H, \hat{\mathbb{J}}_{P_j}] = 0$ as one would expect for a relativistic theory (where the generators \hat{H} and \hat{P} of the Poincaré group commute). We can write down the physical states $|\psi_{\vec{k}}\rangle\rangle$ as simultaneous eigenstates of $\hat{\mathbb{J}}_H$ and $\hat{\mathbb{J}}_{P_j}$ with zero eigenvalue (from the constraints Eqs. (4.18) and (4.19)),

$$|\psi_{\vec{k}}\rangle\rangle = |p_t = -E(\vec{k})\rangle \otimes |p_x = k_x\rangle \otimes |p_y = k_y\rangle \otimes |p_z = k_z\rangle, \quad (4.20)$$

where $|p_t = -E(\vec{k})\rangle$ is the eigenstate of \hat{p}_t with eigenvalue $(-E(\vec{k}))$ and similarly $|p_j = k_j\rangle$ is an eigenstate of \hat{p}_j with eigenvalue k_j . The physical eigenstate $|\psi_{\vec{k}}\rangle\rangle$ of the constraints have a tensor product form in the momentum basis since each term in a given constraint operator commutes with each other. Written in the coordinate basis, these physical eigenstates can be expressed as,

$$|\psi_{\vec{k}}\rangle\rangle = \frac{1}{\sqrt{2\pi}} \int dt e^{-iE(\vec{k})t} |t\rangle \otimes \frac{1}{(2\pi)^{3/2}} \int d^3x e^{i\vec{k}\cdot\vec{x}} |\vec{x}\rangle, \quad (4.21)$$

where $|\vec{x}\rangle \equiv |x\rangle \otimes |y\rangle \otimes |z\rangle$. We can now obtain the wavefunction of the particle by conditioning a global physical state $|\Psi\rangle\rangle \in \mathcal{H}$ on a tensor product basis element $|t\rangle \otimes |\vec{x}\rangle$. The conditioned state lives in $\mathcal{H}_{\text{spin}}$, the spinorial Hilbert space and since in this case, the particle is spinless, $\mathcal{H}_{\text{spin}}$ is one-dimensional, and hence we get the wavefunction of the particle,

$$\Psi(t, \vec{x}) \equiv \left(\langle t| \otimes \langle \vec{x}| \right) |\Psi\rangle\rangle. \quad (4.22)$$

We can similarly condition the constraint equations, Eqs. (4.18) and (4.19) and get governing evolution equations in space and time for the wavefunction. Let us first do this for the Hamiltonian constraint,

$$\left(\langle t| \hat{p}_t \otimes \langle x| \right) |\psi_{\vec{k}}\rangle\rangle + \left(\sqrt{|\vec{k}|^2 + m^2} \right) \psi_{\vec{k}}(t, \vec{x}) = 0. \quad (4.23)$$

Inserting a complete set of states on \mathcal{H}_t given by $\int dt' |t'\rangle \langle t'| = \hat{\mathbb{1}}_t$ and remembering that the matrix elements of the conjugate momenta go as $\langle t| \hat{p}_t |t'\rangle = -i \frac{\partial}{\partial t} \delta(t - t')$, we get the time evolution equation for the wavefunction $\psi_{\vec{k}}(t, \vec{x})$ corresponding to the physical state $|\psi_{\vec{k}}\rangle\rangle$,

$$i \frac{\partial}{\partial t} \psi_{\vec{k}}(t, \vec{x}) = \left(\sqrt{|\vec{k}|^2 + m^2} \right) \psi_{\vec{k}}(t, \vec{x}), \quad (4.24)$$

which represents the analogue of Schrödinger equation governing the time evolution of the wavefunction dictated by the ‘‘Hamiltonian,’’ in this case the energy of the particular \vec{k} mode.

One can similarly get an equation that governs the spatial translations of the wavefunction from the momentum constraint of Eq. (4.19),

$$-i\vec{\nabla}\psi_{\vec{k}}(t,\vec{x}) = \vec{k}\psi_{\vec{k}}(t,\vec{x}). \quad (4.25)$$

The wavefunction solution corresponding to the physical eigenstate $|\psi_{\vec{k}}\rangle\rangle$ satisfying Eqs. (4.18) and (4.19) can be found from Eq. (4.21),

$$\psi_{\vec{k}}(t,\vec{x}) \sim \exp\left(-iE(\vec{k})t + i\vec{k}\cdot\vec{x}\right), \quad (4.26)$$

which, as expected, yields plane wave solutions (we use a \sim , and not an exact equality here since individual plane wave solutions are non-normalizable). For completeness, we mention that one can also have a negative sign with $E(\vec{k})$, interpreted as a negative frequency, in the Hamiltonian constraint, $\hat{\mathbb{J}}_H(\vec{k}) = \hat{p}_t \otimes \hat{\mathbb{1}}_{\vec{x}} \otimes \hat{\mathbb{1}}_{\text{spin}} + \hat{\mathbb{1}}_t \otimes \hat{\mathbb{1}}_{\vec{x}} \otimes (-E(\vec{k})\hat{\mathbb{1}}_{\text{spin}}) \approx 0$, and by including this, one can recover both positive and negative frequency solutions of the Klein-Gordon equation. Formally, however, we always keep a positive sign between the \hat{p}_t term and the frequency term in the Hamiltonian constraint (similar to Eq. 4.4 in the Page-Wootters construction).

We can construct a generic, normalizable state by taking a superposition of these plane wave solutions obtained from the physical eigenstates, each of which obeys their corresponding Hamiltonian and momentum constraints,

$$|\Psi\rangle\rangle = \int d^3k c(\vec{k}) |\psi_{\vec{k}}\rangle\rangle, \quad (4.27)$$

which, written in the coordinate basis, will be a correlated or entangled state between the temporal and spatial degrees of freedom²,

$$|\Psi\rangle\rangle = \int d^3k \int dt d^3x c(\vec{k}) \exp\left(-iE(\vec{k})t + i\vec{k}\cdot\vec{x}\right) |t\rangle \otimes |\vec{x}\rangle. \quad (4.28)$$

Thus, time evolution and spatial translations can be interpreted in terms of entanglement between the spatial and temporal degrees of freedom in the global physical states $|\Psi\rangle\rangle \in \mathcal{H}$. The corresponding wavefunction $\Psi(t,\vec{x})$ of the generic state $|\Psi\rangle\rangle$ can then be found by conditioning with a coordinate basis element $|t\rangle \otimes |\vec{x}\rangle$,

$$\Psi(t,\vec{x}) \equiv \left(\langle t| \otimes \langle \vec{x}| \right) |\Psi\rangle\rangle = \int d^3k c(\vec{k}) \exp\left(-iE(\vec{k})t + i\vec{k}\cdot\vec{x}\right), \quad (4.29)$$

²A similar entangled state $|\Psi\rangle\rangle$ can be written in the Page-Wootters formulation too with entanglement between states in \mathcal{H}_t and \mathcal{H}_S [8].

which we recognize as the generic solution of the Klein-Gordon equation in the relativistic quantum mechanics of a particle. Issues regarding normalizability, particularly with respect to the temporal degree of freedom, and the use of continuous functional spaces and rigged Hilbert spaces in such a paradigm have been discussed elsewhere and the interested reader is encouraged to look at Refs. [8, 74] (and references therein). We would, however, like to point out that normalization in the temporal coordinate is a subtle issue and is treated rather distinctly from normalization over space. We feel this is an interesting point that warrants further investigation in future work to help understand it better.

Thus, the physical Hilbert space $\mathcal{H}_{\text{phys}}$ can be defined to be the span of physical eigenstates $|\psi_{\vec{k}}\rangle\rangle$ that satisfy the Hamiltonian and momentum constraint equations,

$$\mathcal{H}_{\text{phys}} \simeq \text{span} \left\{ |\psi_{\vec{k}}\rangle\rangle : \hat{\mathbb{J}}_H(\vec{k}) |\psi_{\vec{k}}\rangle\rangle = \hat{\mathbb{J}}_{P_j}(\vec{k}) |\psi_{\vec{k}}\rangle\rangle = 0 \quad \forall \vec{k} \in \mathbb{R}^3, j = x, y, z \right\}. \quad (4.30)$$

We can also recover the Klein-Gordon equation explicitly by combining the Hamiltonian and momentum constraints of Eqs. (4.18) and (4.19),

$$\left[\left(\hat{p}_t \otimes \hat{\mathbb{I}}_{\vec{x}} \otimes \hat{\mathbb{I}}_{\text{spin}} \right)^2 - \sum_{j=x,y,z} \left(\hat{\mathbb{I}}_t \otimes \hat{p}_j \otimes \hat{\mathbb{I}}_{\text{spin}} \right)^2 \right] |\psi_{\vec{k}}\rangle\rangle = m^2 |\psi_{\vec{k}}\rangle\rangle. \quad (4.31)$$

Once we have the Klein-Gordon equation for a single physical eigenstate $|\psi_{\vec{k}}\rangle\rangle$ in the form of Eq. (4.31), we can superpose appropriately and write a similar equation for an arbitrary physical state $|\Psi\rangle\rangle$ of Eq. (4.28),

$$\left[\left(\hat{p}_t \otimes \hat{\mathbb{I}}_{\vec{x}} \otimes \hat{\mathbb{I}}_{\text{spin}} \right)^2 - \sum_{j=x,y,z} \left(\hat{\mathbb{I}}_t \otimes \hat{p}_j \otimes \hat{\mathbb{I}}_{\text{spin}} \right)^2 \right] |\Psi\rangle\rangle = m^2 |\Psi\rangle\rangle. \quad (4.32)$$

We can now use the relativistically covariant notation of Eq. (4.14) and use the Minkowski flat metric $\eta^{\mu\nu} = \text{diag}(+1, -1, -1, -1)$ to give the Klein-Gordon equation a much more familiar form,

$$\left(\hat{P}^\mu \hat{P}_\mu \otimes \hat{\mathbb{I}}_{\text{spin}} - m^2 \hat{\mathbb{I}}_{\mathcal{H}} \right) \approx 0 \implies \left(\hat{P}^\mu \hat{P}_\mu \otimes \hat{\mathbb{I}}_{\text{spin}} - m^2 \hat{\mathbb{I}}_{\mathcal{H}} \right) |\Psi\rangle\rangle = 0, \quad (4.33)$$

where the repeated index μ is summed over. Thus, we see that we can recover the quantum mechanics of a spinless relativistic particle obeying the Klein-Gordon equation without having to deal with the ‘‘square-root’’ Hamiltonian operator explicitly, but rather by working with a collection of *linear, first-order* Hamiltonian and momentum constraints in a setup that deals with time and space on an equal footing

in Hilbert space. It is important to note that relativistic dispersion relations were applied to eigenvalues featuring in the constraints, and not be used as operator-values equations. While we obtain a collection of physical eigenstates $|\psi_{\vec{k}}\rangle\rangle$ for each spatial momentum \vec{k} from the constraints, we are able to recover the full Klein-Gordon equation for generic physical states $|\Psi\rangle\rangle \in \mathcal{H}$.

While relativistically consistent interactions between multiple particles can be added in this scheme, interaction of a single particle with a background field are typically not relativistically compatible since they break either time or space translational symmetry that leads to the energy and/or momentum of the particle not being conserved. Hence, we do not add interaction with a background field in the constraint equations above since they would not be consistent with the commuting compatibility $[\hat{\mathbb{J}}_H, \hat{\mathbb{J}}_{P_j}] = 0$ of the constraints. It is therefore instructive to investigate the non-relativistic limit of the Klein-Gordon setup and see how one can restore interactions to recover the non-relativistic Schrödinger equation in the conventional form. For Eq. (4.18), we can take the non-relativistic limit ($|\vec{k}| \ll m$) by expanding $E(\vec{k})$ in powers of $|\vec{k}|^2$ and retaining the leading order \vec{k} -dependent piece along with dropping the constant rest mass energy m contribution,

$$\left(\hat{p}_t \otimes \hat{\mathbb{I}}_{\vec{x}} \otimes 1 + \hat{\mathbb{I}}_t \otimes \hat{\mathbb{I}}_{\vec{x}} \otimes \frac{|\vec{k}|^2}{2m} \right) |\psi_{\vec{k}}\rangle\rangle_{\text{NR}} = 0, \quad (4.34)$$

where $|\psi_{\vec{k}}\rangle\rangle_{\text{NR}}$ is the non-relativistic physical eigenstate. Combining with the momentum constraint of Eq. (4.19), this yields the Schrödinger equation for a given non-relativistic physical eigenstate in the full Hilbert space \mathcal{H} ,

$$\left(\hat{p}_t \otimes \hat{\mathbb{I}}_{\vec{x}} \otimes 1 \right) |\psi_{\vec{k}}\rangle\rangle_{\text{NR}} = - \left[\sum_{j=x,y,z} \frac{\left(\hat{\mathbb{I}}_t \otimes \hat{p}_j \right)^2}{2m} \right] |\psi_{\vec{k}}\rangle\rangle_{\text{NR}}. \quad (4.35)$$

We can now construct a general state by superposition of different physical eigenstates as in Eq. (4.27) that gives us the Schrödinger equation for a non-relativistic free particle. At this stage, since we are no longer working to keep our constraints relativistically compatible, we can also add by hand an ‘‘interaction term’’ $V(t, \vec{x})$ to model interactions of the non-relativistic particle with a background field,

$$\left(\hat{p}_t \otimes \hat{\mathbb{I}}_{\vec{x}} \otimes 1 \right) |\Psi\rangle\rangle_{\text{NR}} = - \left[\sum_{j=x,y,z} \frac{\left(\hat{\mathbb{I}}_t \otimes \hat{p}_j \right)^2}{2m} + V \left(\hat{t} \otimes \hat{\mathbb{I}}_{\vec{x}}, \hat{\mathbb{I}}_t \otimes \hat{\vec{x}} \right) \right] |\Psi\rangle\rangle_{\text{NR}}, \quad (4.36)$$

which, when written in terms of the wavefunction, gives us

$$i \frac{\partial}{\partial t} \Psi_{\text{NR}}(t, \vec{x}) = \left(-\frac{1}{2m} \vec{\nabla}^2 + V(t, \vec{x}) \right) \Psi_{\text{NR}}(t, \vec{x}) . \quad (4.37)$$

We would again like to emphasize here that interactions could only be added in the non-relativistic limit where the Hamiltonian and momentum need not commute. We briefly remark on this aspect about interactions and its connection with quantum field theory in section 4.5.

Dirac Equation (Spin-1/2)

Now that we have showed a constraint-based approach to Klein-Gordon equation of a single relativistic particle of spin-0, let us focus on the Dirac equation which describes fermionic particles with spin-1/2. Since one can find an instructive treatment of the Dirac equation in most advanced undergraduate quantum mechanics texts, we will not reproduce that discussion here. Instead, we will jump right in to describe using Hamiltonian and momentum constraints to work out the Dirac equation. One key thing to remember is that even in the usual textbook construction, the Dirac equation – at variance with the standard treatment of the Klein-Gordon equation – is a linear, first-order equation in both energy and momentum (or one may say, first-order in its treatment of time and space).

For relativistic quantum mechanics of a spin-1/2 particle, we know that the dimension of the spinorial Hilbert space $\mathcal{H}_{\text{spin}}$ is $\dim \mathcal{H}_{\text{spin}} = 4$ since it is used to describe both the particle and its antiparticle (which could be the same as the particle itself, as in the case of Majorana fermions). Following the usual construction, we use gamma matrices γ^μ of spinors which satisfy the anti-commutation relations of Clifford algebra, $\{\gamma^\mu, \gamma^\nu\} = 2\eta^{\mu\nu} \hat{\mathbb{I}}_{\text{spin}}$, where $\{A, B\} = AB + BA$ is the anti-commutator of A and B , and we have used the metric signature $\eta^{\mu\nu} = \text{diag}(+1, -1, -1, -1)$. Depending on the representation of the gamma matrices, we can describe both Dirac fermions (particles having distinct antiparticles) and Majorana fermions (particles which are their own antiparticles) [75]. Let us define,

$$\beta \equiv \gamma^0 \quad , \quad \alpha_j \equiv \gamma^0 \gamma^j \quad , \quad j = x, y, z \quad , \quad (4.38)$$

which satisfy $\alpha_j^2 = \hat{\mathbb{I}}_{\text{spin}} \forall j$, $\beta^2 = \hat{\mathbb{I}}_{\text{spin}}$, $\{\alpha_j, \alpha_{j'}\} = 0 \forall j \neq j'$ and $\{\alpha_j, \beta\} = 0 \forall j$. As before, the Hamiltonian and momentum constraints will be parametrized by a vector $\vec{k} \in \mathbb{R}^3$. The Hamiltonian constraint is given by,

$$\hat{\mathbb{J}}_H(\vec{k}) = \hat{p}_t \otimes \hat{\mathbb{I}}_{\vec{x}} \otimes \hat{\mathbb{I}}_{\text{spin}} + \hat{\mathbb{I}}_t \otimes \hat{\mathbb{I}}_{\vec{x}} \otimes \left(\sum_{j=x,y,z} k_j \alpha_j + m\beta \right) \quad , \quad (4.39)$$

and the momentum constraint by,

$$\hat{\mathbb{J}}_{P_j}(\vec{k}) = \hat{\mathbb{I}}_t \otimes \hat{p}_j \otimes \hat{\mathbb{I}}_{\text{spin}} - \hat{\mathbb{I}}_t \otimes \hat{\mathbb{I}}_{\vec{x}} \otimes (k_j \hat{\mathbb{I}}_{\text{spin}}) \quad \text{for } j = x, y, z. \quad (4.40)$$

Notice, in the constraint equations above, the values of energy and momentum eigenvalues are associated explicitly with operators that act on $\mathcal{H}_{\text{spin}}$, just how we did in the Klein-Gordon case (though it was a trivial association there). The spinorial term in the Hamiltonian constraint can be identified as the matrix square root of the Klein-Gordon energy-momentum dispersion relation,

$$\left(\sum_{j=x,y,z} k_j \alpha_j + m\beta \right)^2 = (|\vec{k}|^2 + m^2) \hat{\mathbb{I}}_{\text{spin}}. \quad (4.41)$$

This is expected, since the Dirac equation, even in the standard construction, is understood as a “square-root” of the Klein-Gordon equation and doing so necessarily relies on the spin of the particle. Physical eigenstates $|\psi_{\vec{k}}\rangle\rangle$ are identified to be the ones that are annihilated by the constraints,

$$\hat{\mathbb{J}}_H(\vec{k}) \approx 0 \implies \hat{\mathbb{J}}_H(\vec{k}) |\psi_{\vec{k}}\rangle\rangle = 0, \quad (4.42)$$

$$\hat{\mathbb{J}}_{P_j}(\vec{k}) \approx 0 \implies \hat{\mathbb{J}}_{P_j}(\vec{k}) |\psi_{\vec{k}}\rangle\rangle = 0 \quad \text{for } j = x, y, z. \quad (4.43)$$

One can now combine the Hamiltonian and momentum constraints of Eqs. (4.42) and (4.43) to eliminate the explicit \vec{k} dependence,

$$\hat{p}_t \otimes \hat{\mathbb{I}}_{\vec{x}} \otimes \hat{\mathbb{I}}_{\text{spin}} + \sum_{j=x,y,z} \left(\hat{\mathbb{I}}_t \otimes \hat{p}_j \otimes \alpha_j \right) + \left(\hat{\mathbb{I}}_t \otimes \hat{\mathbb{I}}_{\vec{x}} \otimes m\beta \right) \approx 0, \quad (4.44)$$

which is precisely the Schrödinger equation for a spin-1/2 particle, which in the conventional form is written as,

$$i \frac{\partial}{\partial t} \psi = \left(\vec{\alpha} \cdot \hat{\vec{p}} + m\beta \right) \psi. \quad (4.45)$$

We can also recover the Dirac equation by pre-multiplying Eq. (4.44) with $\left(\hat{\mathbb{I}}_t \otimes \hat{\mathbb{I}}_{\vec{x}} \otimes \beta \right)$,

$$\left(\hat{p}_t \otimes \hat{\mathbb{I}}_{\vec{x}} \otimes \beta \right) + \sum_{j=x,y,z} \left(\hat{\mathbb{I}}_t \otimes \hat{p}_j \otimes \beta \alpha_j \right) + m \left(\hat{\mathbb{I}}_t \otimes \hat{\mathbb{I}}_{\vec{x}} \otimes \hat{\mathbb{I}}_{\text{spin}} \right) \approx 0. \quad (4.46)$$

Switching back to the gamma matrix notation,

$$\gamma^0 \equiv \beta \quad , \quad \gamma^j \equiv \beta \alpha_j \quad , \quad j = x, y, z, \quad (4.47)$$

and this gives us the Dirac equation,

$$\left(\hat{p}_t \otimes \hat{\mathbb{I}}_{\vec{x}} \otimes \gamma^0\right) + \sum_{j=x,y,z} \left(\hat{\mathbb{I}}_t \otimes \hat{p}_j \otimes \gamma^j\right) + m \hat{\mathbb{I}}_{\mathcal{H}} \approx 0. \quad (4.48)$$

We can now write this equation in the relativistically covariant notation of Eq. (4.14),

$$\hat{P}_\mu \otimes \gamma^\mu + m \hat{\mathbb{I}}_{\mathcal{H}} \approx 0. \quad (4.49)$$

where the repeated index μ is summed over. One can introduce interactions with a background electromagnetic field $A_\mu(t, \vec{x})$ by adding it as an effective term at the level of the Dirac equation of Eq. (4.49). Adding such an interaction with a background field directly in the constraint equations of Eqs. (4.39) and (4.40) will be inconsistent since it will break spatial/temporal translation symmetry for the relativistic particle whose physics we are focusing on. One can envision assigning Hilbert spaces to the background field as quantum degrees of freedom and then adding relativistic compatible interactions with other fields. We will briefly discuss this point from a field-theoretic point of view in section 4.5.

Thus, we see that we are able to treat both Klein-Gordon and Dirac equations with a common approach based on linear, first-order constraints by treating space and time on an equal footing in Hilbert space and applying dispersion relations to eigenvalues instead of an operator-valued equation in $\mathcal{H}_{\vec{x}}$.

4.4 Symmetry transformations as Basis Changes

Treating space and time on an equal footing as quantum degrees of freedom in Hilbert space can help us analyse symmetry transformations using unitary basis changes in Hilbert space. This gives a stronger quantum mechanical ground for symmetry transformations, especially in relativistic quantum mechanics where transformations of temporal degrees of freedom are often handled in an ad-hoc, often classical way compared to the spatial degrees of freedom. It also lets us tie together global and local symmetry transformations into one framework and in this section, we will focus on two important symmetry transformations: Lorentz transformations and $U(1)$ gauge symmetry. Global symmetries, such as Lorentz transformations, will affect decomposition changes in Hilbert space, whereas local symmetries, such as $U(1)$, will correspond to basis changes in Hilbert space while leaving the decomposition invariant.

Lorentz Transformations

Lorentz transformations are global transformations that mix space and time components of 4-vectors while preserving the speed of light, the causal structure, and the form of laws of physics in each inertial reference frame. In Hilbert space, we will implement a Lorentz transformation as a decomposition change of $\mathcal{H}_t \otimes \mathcal{H}_{\vec{x}}$. Thus, it is an overall basis change that alters the factorization between the temporal and spatial degrees of freedom in Hilbert space. We will implement a Lorentz transformation Λ by a unitary transformation $\hat{U}(\Lambda)$ that changes the decomposition,

$$\hat{U}(\Lambda) : \mathcal{H}_t \otimes \mathcal{H}_{\vec{x}} \rightarrow \mathcal{H}_t' \otimes \mathcal{H}_{\vec{x}}'. \quad (4.50)$$

Such a decomposition change manifests itself by mixing conjugate operators in \mathcal{H}_t and $\mathcal{H}_{\vec{x}}$ under the following transformation,

$$\hat{X}^{\mu'} = \hat{U}^\dagger(\Lambda) \hat{X}^\mu \hat{U}(\Lambda) = \Lambda_\nu^\mu \hat{X}^\nu, \quad (4.51)$$

$$\hat{P}'_\mu = \hat{U}^\dagger(\Lambda) \hat{P}_\mu \hat{U}(\Lambda) = \Lambda_\mu^\nu \hat{P}_\nu. \quad (4.52)$$

It is important to note that $\hat{X}^{\mu'}$ and \hat{P}'_μ are “separable” operators, *i.e.*, they have a tensor product structure in the transformed space $\mathcal{H}_t' \otimes \mathcal{H}_{\vec{x}}'$. For example, the components of $\hat{X}^{\mu'} \in \mathcal{L}(\mathcal{H}_t' \otimes \mathcal{H}_{\vec{x}}')$ written explicitly are,

$$\hat{X}^{0'} \equiv \hat{t}' \otimes \hat{\mathbb{1}}_{\vec{x}}', \quad \hat{X}^{1'} \equiv \hat{\mathbb{1}}_t \otimes \hat{x}' \otimes \hat{\mathbb{1}}_y' \otimes \hat{\mathbb{1}}_z', \quad (4.53)$$

$$\hat{X}^{2'} \equiv \hat{\mathbb{1}}_t \otimes \hat{\mathbb{1}}_x' \otimes \hat{y}' \otimes \hat{\mathbb{1}}_z', \quad \hat{X}^{3'} \equiv \hat{\mathbb{1}}_t \otimes \hat{\mathbb{1}}_x' \otimes \hat{\mathbb{1}}_y' \otimes \hat{z}', \quad (4.54)$$

and therefore, each of these transformed operators is a linear combination of separable operators in $\mathcal{H}_t \otimes \mathcal{H}_{\vec{x}}$ as governed by Eq. (4.51) (and hence, $\hat{X}^{\mu'}$ and \hat{P}'_μ themselves are not separable in $\mathcal{H}_t \otimes \mathcal{H}_{\vec{x}}$).

Let us look at this in more detail with an example of the Klein-Gordon equation as treated in section 4.3 to study how the Hamiltonian and momentum constraints transform under a Lorentz transformation and its implications. For concreteness and simplicity, let us focus on a Lorentz boost with a boost parameter v (the relative speed of the two inertial frames in units with $c = 1$) along the x -direction. We define $\Gamma = (1 - v^2)^{-1/2}$, and with this, the Lorentz transformation matrix Λ takes the form,

$$\Lambda_\nu^\mu = \begin{bmatrix} \Gamma & -\Gamma v & 0 & 0 \\ -\Gamma v & \Gamma & 0 & 0 \\ 0 & 0 & 0 & 0 \\ 0 & 0 & 0 & 0 \end{bmatrix}. \quad (4.55)$$

In this case, the unitary transform $\hat{U}(\Lambda)$ changes the decomposition of $\mathcal{H}_t \otimes \mathcal{H}_x$ to $\mathcal{H}'_t \otimes \mathcal{H}'_x$ and leaves $\mathcal{H}_y \otimes \mathcal{H}_z$ untransformed, such that,

$$\hat{\mathbb{I}}_t \otimes \hat{\mathbb{I}}_x \otimes \hat{p}_y \otimes \hat{\mathbb{I}}_z \mapsto \hat{\mathbb{I}}'_t \otimes \hat{\mathbb{I}}'_x \otimes \hat{p}'_y \otimes \hat{\mathbb{I}}'_z = \hat{\mathbb{I}}_t \otimes \hat{\mathbb{I}}_x \otimes \hat{p}_y \otimes \hat{\mathbb{I}}_z, \quad (4.56)$$

$$\hat{\mathbb{I}}_t \otimes \hat{\mathbb{I}}_x \otimes \hat{\mathbb{I}}_y \otimes \hat{p}_z \mapsto \hat{\mathbb{I}}'_t \otimes \hat{\mathbb{I}}'_x \otimes \hat{\mathbb{I}}_y \otimes \hat{p}'_z = \hat{\mathbb{I}}_t \otimes \hat{\mathbb{I}}_x \otimes \hat{\mathbb{I}}_y \otimes \hat{p}_z, \quad (4.57)$$

$$\hat{p}_t \otimes \hat{\mathbb{I}}_x \mapsto \hat{p}'_t \otimes \hat{\mathbb{I}}'_x = \Gamma(\hat{p}'_t \otimes \hat{\mathbb{I}}'_x) - \Gamma_V(\hat{\mathbb{I}}'_t \otimes \hat{p}'_x \otimes \hat{\mathbb{I}}_y \otimes \hat{\mathbb{I}}_z) \quad (4.58)$$

$$\hat{\mathbb{I}}_t \otimes \hat{p}_x \otimes \hat{\mathbb{I}}_y \otimes \hat{\mathbb{I}}_z \mapsto \hat{\mathbb{I}}'_t \otimes \hat{p}'_x \otimes \hat{\mathbb{I}}_y \otimes \hat{\mathbb{I}}_z = \Gamma(\hat{\mathbb{I}}'_t \otimes \hat{p}'_x \otimes \hat{\mathbb{I}}_y \otimes \hat{\mathbb{I}}_z) - \Gamma_V(\hat{p}'_t \otimes \hat{\mathbb{I}}'_x \otimes \hat{\mathbb{I}}_y \otimes \hat{\mathbb{I}}_z). \quad (4.59)$$

We can now see from the above equations that a Lorentz transformation changes the decomposition of Hilbert space. Under this transformation, the Hamiltonian constraint of Eq. (4.16) transforms as,

$$\hat{\mathbb{J}}_H'(\vec{k}) = \Gamma(\hat{p}'_t \otimes \hat{\mathbb{I}}'_x \otimes 1) - \Gamma_V(\hat{\mathbb{I}}'_t \otimes \hat{p}'_x \otimes \hat{\mathbb{I}}_y \otimes \hat{\mathbb{I}}_z \otimes 1) + (\hat{\mathbb{I}}'_t \otimes \hat{\mathbb{I}}'_x \otimes E(\vec{k})) \approx 0, \quad (4.60)$$

and the x -momentum constraint takes the form,

$$\begin{aligned} \hat{\mathbb{J}}_{P_x}'(\vec{k}) &= \Gamma(\hat{\mathbb{I}}'_t \otimes \hat{p}'_x \otimes \hat{\mathbb{I}}_y \otimes \hat{\mathbb{I}}_z \otimes 1) - \Gamma_V(\hat{p}'_t \otimes \hat{\mathbb{I}}'_x \otimes \hat{\mathbb{I}}_y \otimes \hat{\mathbb{I}}_z \otimes 1) \\ &\quad - (\hat{\mathbb{I}}'_t \otimes \hat{\mathbb{I}}'_x \otimes k_x) \approx 0. \end{aligned} \quad (4.61)$$

The y and z -momentum constraints remain unchanged since the Lorentz transformation only mixes $\mathcal{H}_t \otimes \mathcal{H}_x$. As expected, the Hamiltonian and momentum constraints of Eqs. (4.60) and (4.61) have mixed terms, but we can decouple them by substitution of one equation into the other. The transformed Hamiltonian constraint then becomes,

$$\hat{\mathbb{J}}_H'(\vec{k}) = (\hat{p}'_t \otimes \hat{\mathbb{I}}'_x \otimes 1) + (\hat{\mathbb{I}}'_t \otimes \hat{\mathbb{I}}'_x \otimes (\Gamma E(\vec{k}) - \Gamma_V k_x)) \approx 0, \quad (4.62)$$

which, as expected, represents a Hamiltonian constraint with the Lorentz transformed energy $E' = (\Gamma E(\vec{k}) - \Gamma_V k_x)$. The momentum constraint similarly transforms to reflect the Lorentz transformed momentum $k'_x = (\Gamma k_x - \Gamma_V E(k))$,

$$\hat{\mathbb{J}}_{P_x}'(\vec{k}) = (\hat{\mathbb{I}}'_t \otimes \hat{p}'_x \otimes \hat{\mathbb{I}}_y \otimes \hat{\mathbb{I}}_z \otimes 1) - (\hat{\mathbb{I}}'_t \otimes \hat{\mathbb{I}}'_x \otimes (\Gamma k_x - \Gamma_V E(k))) \approx 0. \quad (4.63)$$

Thus, we see that Lorentz transformations that are global symmetry transformations are implemented as global basis changes in Hilbert space altering the factorization between the temporal and spatial factors of Hilbert space. One can perform a similar Lorentz transformation for the Dirac equation as discussed in section 4.3, though we avoid repeating a similar analysis here.

U(1) Symmetry

Let us now look at $U(1)$ gauge symmetry through the lens of unitary basis changes in Hilbert space. The $U(1)$ gauge symmetry is a local transformation that lets the wavefunction pick up a local phase,

$$\Psi(t, \vec{x}) \mapsto \Psi'(t, \vec{x}) = e^{i\lambda(t, \vec{x})} \psi(t, \vec{x}), \quad (4.64)$$

for a gauge function³ $\lambda(t, \vec{x})$. The usual story of the $U(1)$ transformation is told in the presence of a gauge field $A_\mu(X)$ to which the particle couples. Under the gauge transformation of Eq. (4.64), we require the gauge field A_μ to transform accordingly,

$$\vec{A}(t, \vec{x}) \longrightarrow \vec{A}(t, \vec{x}) - \vec{\nabla}\lambda(t, \vec{x}), \quad (4.65)$$

$$A_0(t, \vec{x}) \longrightarrow A_0(t, \vec{x}) + \frac{\partial}{\partial t}\lambda(t, \vec{x}), \quad (4.66)$$

to keep the Schrödinger equation invariant. One of the outcomes of this transformation A_μ is to effectively shift the conjugate momentum operator,

$$\hat{p} \longrightarrow \hat{p} - \vec{\nabla}\lambda(t, \vec{x}) \implies -i\vec{\nabla} \longrightarrow -i\vec{\nabla} - \vec{\nabla}\lambda(t, \vec{x}). \quad (4.67)$$

On the other hand, due to lack of a conjugate temporal momentum in the textbook construction, the time derivative operator $i\partial_t$ (which equates itself to the Hamiltonian in the Schrödinger equation for physical states) therefore transforms as,

$$i\frac{\partial}{\partial t} \longrightarrow i\frac{\partial}{\partial t} + \frac{\partial}{\partial t}\lambda(t, \vec{x}). \quad (4.68)$$

We now show, that in our construction which treats space and time on an equal footing in Hilbert space using linear, first-order constraints, $U(1)$ gauge transform is a local unitary transformation in the spatio-temporal Hilbert space $\mathcal{H}_t \otimes \mathcal{H}_{\vec{x}}$. Transformations, both in the temporal and spatial components, emerge naturally as a consequence of this unitary transformation. While one can couple the particle to an external/background field A_μ , reference to this gauge field (which defines the field strength that is invariant under $U(1)$) is not explicitly required to affect the symmetry transformation. Spatial and temporal quantum degrees of freedom transform under a common mechanism, unlike as done in Eqs. (4.67) and (4.68).

The unitary transformation $\hat{U}_1 \in \mathcal{L}(\mathcal{H}_t \otimes \mathcal{H}_{\vec{x}})$ that affects this $U(1)$ symmetry is not a global decomposition change in $\mathcal{H}_t \otimes \mathcal{H}_{\vec{x}}$, but rather a local basis change as one would expect from a gauge transformation, and hence does not alter the decomposition of

³The function $\lambda(t, \vec{x})$ is typically taken to be continuous and sufficiently differentiable in its variables and dies off rapidly enough as $\vec{x} \rightarrow \pm\infty$.

Hilbert space. The local nature of the unitary basis change operator is reflected in being diagonal in the coordinate basis $\{|t\rangle \otimes |\vec{x}\rangle \equiv |t, \vec{x}\rangle\}$ (we are considering a spinless particle for this analysis here),

$$\hat{U}_1 = \left(\int dt d^3x e^{-i\lambda(t, \vec{x})} |t, \vec{x}\rangle \langle \langle t, \vec{x}| \right) \otimes \hat{\mathbb{1}}_{\text{spin}} = \exp \left(-i\lambda(\hat{t} \otimes \hat{\mathbb{1}}_{\vec{x}}, \hat{\mathbb{1}}_t \otimes \hat{\vec{x}}) \right) \otimes \hat{\mathbb{1}}_{\text{spin}}. \quad (4.69)$$

Under this unitary transformation, the state $|\Psi\rangle \in \mathcal{H}_t \otimes \mathcal{H}_{\vec{x}}$ transforms as follows,

$$|\Psi'\rangle = \hat{U}_1^\dagger |\Psi\rangle, \quad (4.70)$$

which transforms the wavefunction as required for a $U(1)$ transformation by picking up a local phase,

$$\Psi'(t, \vec{x}) \equiv \left(\langle t| \otimes \langle \vec{x}| \right) |\Psi'\rangle = \left(\langle t| \otimes \langle \vec{x}| \right) \hat{U}_1^\dagger |\Psi\rangle = e^{i\lambda(t, \vec{x})} \Psi(t, \vec{x}). \quad (4.71)$$

The \hat{U}_1 transformation also transforms operators in a way consistent with a local gauge transformation. In this case, when time and space are treated on an equal footing in Hilbert space, we do not need to explicitly rely on the existence of a gauge field A_μ since the unitary transformation directly leads to transformation of the conjugate momenta in both \mathcal{H}_t and $\mathcal{H}_{\vec{x}}$. Whereas in the textbook story, time is treated as an external parameter and not as a quantum degree of freedom, and hence there is no momenta conjugate to a time coordinate. Because of this, we have to impose transformations on the gauge field A_μ of Eqs. (4.65) and (4.66) to keep evolution equations invariant. Here, we treat space and time on an equal footing, and it is reflected in the unitary transformation of the conjugate momenta as follows,

$$\hat{P}_\mu' = \hat{U}_1^\dagger \hat{P}_\mu \hat{U}_1 = \exp(i\lambda(\hat{X})) \hat{P}_\mu \exp(-i\lambda(\hat{X})), \quad (4.72)$$

where $\lambda(\hat{X})$ is to denote that the function λ depends on the coordinate operators \hat{X}^μ of Eq. (4.13). We can use Baker-Campbell-Hausdorff lemma to further write,

$$\hat{P}_\mu' = \hat{P}_\mu + i[\lambda(\hat{X}), \hat{P}_\mu] - \frac{1}{2}[\lambda(\hat{X}), [\lambda(\hat{X}), \hat{P}_\mu]] + \dots \quad (4.73)$$

Recalling that $[\lambda(\hat{X}), \hat{P}_\mu] = i\partial_\mu\lambda(\hat{X})$, we can further simplify the above equation to yield,

$$\hat{P}_\mu' = \hat{P}_\mu - \partial_\mu\lambda(\hat{X}), \quad (4.74)$$

since two-point and higher nested commutators in Eq. (4.73) all vanish because $\lambda(\hat{X})$ and its derivatives $\partial_\mu\lambda(\hat{X})$ are only functions of \hat{X}_μ . Thus, both spatial and temporal conjugate momenta get modified, in particular,

$$\hat{p}_t' \otimes \hat{\mathbb{1}}_{\vec{x}} = \hat{p}_t \otimes \hat{\mathbb{1}}_{\vec{x}} - \frac{\partial}{\partial t}\lambda(\hat{t} \otimes \hat{\mathbb{1}}_{\vec{x}}, \hat{\mathbb{1}}_t \otimes \hat{\vec{x}}), \quad (4.75)$$

and,

$$\hat{\mathbb{I}}_t \otimes \hat{p}' = \hat{\mathbb{I}}_t \otimes \hat{p} - \vec{\nabla} \lambda \left(\hat{t} \otimes \hat{\mathbb{I}}_{\vec{x}}, \hat{\mathbb{I}}_t \otimes \hat{x} \right). \quad (4.76)$$

The coordinate operators \hat{X}^μ themselves do not transform since they commute with the local function $\lambda(\hat{X})$ and it should also be pointed out that by virtue of \hat{U}_1 being unitary, the CCR between the conjugate operators is left unmodified under the transformation.

We can see how the Hamiltonian and momentum constraints transform under the $U(1)$ gauge transformation. Using Eqs. (4.16) and (4.75), the transformed Hamiltonian constraint operator looks like,

$$\hat{\mathbb{J}}_H'(\vec{k}) = \hat{p}_t \otimes \hat{\mathbb{I}}_{\vec{x}} \otimes \hat{\mathbb{I}}_{\text{spin}} + \left(\hat{\mathbb{I}}_t \otimes \hat{\mathbb{I}}_{\vec{x}} \otimes \left(E(\vec{k}) \hat{\mathbb{I}}_{\text{spin}} \right) - \frac{\partial}{\partial t} \lambda \left(\hat{t} \otimes \hat{\mathbb{I}}_{\vec{x}}, \hat{\mathbb{I}}_t \otimes \hat{x} \right) \right), \quad (4.77)$$

which is the equivalent of the transformation of Eq. (4.68), but now arrived at by directly transforming the temporal conjugate momentum. The transformed momentum constraint operator, using Eqs. (4.17) and (4.75) becomes,

$$\hat{\mathbb{J}}_{P_j}'(\vec{k}) = \hat{\mathbb{I}}_t \otimes \hat{p}_j \otimes \hat{\mathbb{I}}_{\text{spin}} - \left(\hat{\mathbb{I}}_t \otimes \hat{\mathbb{I}}_{\vec{x}} \otimes \left(k_j \hat{\mathbb{I}}_{\text{spin}} \right) + \vec{\nabla} \lambda \left(\hat{t} \otimes \hat{\mathbb{I}}_{\vec{x}}, \hat{\mathbb{I}}_t \otimes \hat{x} \right) \right) \approx 0 \text{ for } j = x, y, z, \quad (4.78)$$

which is the equivalent of the transformation of Eq. (4.67), but now arrived at by directly transforming the spatial conjugate momentum by a unitary transformation on an equal footing with its temporal component. Thus, the evolution equations (both spatial and temporal) are transformed in accordance with a $U(1)$ unitary transformation on an equal footing. The sign difference between the space and time components of Eqs. (4.65) and (4.66) are therefore traced back to the difference in the corresponding sign between the Hamiltonian and momentum constraints and not in the unitary transformation of the conjugate momenta. The transformed constraint operators still commute and the constraint equations are satisfied for the transformed state $|\Psi'\rangle\rangle$ by the transformed operators, *i.e.* $\hat{\mathbb{J}}_H'(\vec{k}) |\Psi'\rangle\rangle = 0 = \hat{\mathbb{J}}_{P_j}'(\vec{k}) |\Psi'\rangle\rangle$, which is the statement that the evolution equations are left invariant under the $U(1)$ gauge transformation as expected.

4.5 Discussion

The quantum nature of space and time forms a core question in our understanding of quantum gravity. Motivated by considerations in a quantum-first approach to quantum gravity, we attempted to treat space and time on an equal footing in Hilbert space and focus on a paradigm dealing with linear, first-order constraints. Using both

Hamiltonian and momentum constraints that annihilate physical states in Hilbert space, we can get emergent features like spatial and temporal translations. Using these constraints, we analysed Klein-Gordon and Dirac equations and showed that our analysis treats both equations with a uniform approach, arguing that dispersion relations should apply to eigenvalues and not be used as operator-valued equations. With such an approach, the “square root” Hamiltonian in the Klein-Gordon theory is handled naturally on a common footing with the Dirac equation. Treating both time and space as quantum degrees of freedom in Hilbert space, the quantum mechanical status of Lorentz transformations and $U(1)$ symmetry is seen as change of basis or decomposition of Hilbert space. Our construction in this chapter keeps space, time, and spin on an equal footing in Hilbert space as given by Eq. (4.9), and this gives a homogeneous use of the same underlying algebra operating in each of the Hilbert space factors. The Generalized Clifford Algebra [9, 10, 76] can be seen to provide this common algebraic structure for conjugate operators in \mathcal{H}_t , $\mathcal{H}_{\vec{x}}$ and $\mathcal{H}_{\text{spin}}$. In both \mathcal{H}_t and $\mathcal{H}_{\vec{x}}$, it provides the conjugate algebra through Weyl’s form of the CCR [77] that approaches the Heisenberg CCR in the infinite-dimensional limit, and for $\mathcal{H}_{\text{spin}}$, it furnishes the spinor matrices obeying Clifford algebra (for instance, the Pauli matrices are the algebra obtained by a Generalized Clifford Algebra with two generators in two-dimensions). In addition, due to the Bekenstein bound [18] and holographic principle [78, 79], the Hilbert space of quantum gravity may be locally finite-dimensional [17, 20, 21]. In such a finite-dimensional scenario, the Generalized Clifford Algebra also offers a finite-dimensional version of conjugate operators obeying Weyl’s exponential form of the CCR.

Such a program can be extended into various future directions, some of which we would like to point out here and discuss their implications. One of the most natural and interesting generalizations of this approach is to formulate quantum field theory in this language. To this extent, we can imagine a Hilbert space decomposition, as an extension of Eq. (4.9),

$$\mathcal{H} \simeq \mathcal{H}_t \otimes \mathcal{H}_{\vec{x}} \otimes \mathcal{H}_{\text{matter}} , \quad (4.79)$$

which could describe quantum-mechanical matter $\mathcal{H}_{\text{matter}}$ living on a background spacetime described by quantum degrees of freedom $\mathcal{H}_t \otimes \mathcal{H}_{\vec{x}}$. The structure of the spacetime Hilbert space and its interplay with the matter Hilbert space in the context of field theory warrants further investigation. In the conventional field theory paradigm, one colloquially associates a Hilbert space at each point in space, and

states in this space evolve unitarily through time. While the analysis in this chapter focussed on Hamiltonian and momentum constraints parametrized by $\vec{k} \in \mathbb{R}^3$, as in Eqs. (4.18) and (4.19), an extension to a field theory-like setup would allow writing single Hamiltonian and momentum constraints using the generators of the Poincaré group,

$$\hat{\mathbb{J}}_H = \hat{p}_t \otimes \hat{\mathbb{I}}_{\vec{x}} \otimes \hat{\mathbb{I}}_{\text{matter}} + \hat{\mathbb{I}}_t \otimes \hat{\mathbb{I}}_{\vec{x}} \otimes \hat{H} \approx 0, \quad (4.80)$$

$$\hat{\mathbb{J}}_{\vec{p}} = \hat{\mathbb{I}}_t \otimes \hat{p} \otimes \hat{\mathbb{I}}_{\text{matter}} - \hat{\mathbb{I}}_t \otimes \hat{\mathbb{I}}_{\vec{x}} \otimes \hat{P} \approx 0, \quad (4.81)$$

where \hat{H} and \hat{P} are the Hamiltonian and momentum of the matter field, respectively. In a relativistically covariant theory, these generators commute and physical states would therefore be simultaneous eigenstates of the constraints. While interactions with a background field were not possible in the analysis of section 4.3 since they break time and/or space translation symmetry, we can treat interacting theories naturally in the context of the field theoretic generalization of Eq. (4.79).

An interesting feature to note in the constraints we have discussed so far is the exclusive use of operators that do not couple different subfactors of \mathcal{H} . They have a decoupled form, *i.e.*, they are a collection of terms, each of which acts non-trivially only on a particular Hilbert space factor. Adding interaction terms that couple the spacetime Hilbert space $\mathcal{H}_t \otimes \mathcal{H}_{\vec{x}}$ to matter $\mathcal{H}_{\text{matter}}$ could be useful in understanding effects like gravitational coupling and back-reaction. For example, interactions between the temporal degree of freedom and the system in the context of the Page-Wootters internal time (as described in section 4.2) has been explored in Ref. [74]. We saw in section 4.4 how different decompositions of the spacetime Hilbert space implemented by global basis changes can describe Lorentz transformations. More generally, we can expect a broad class of unitary basis choices implementing different decompositions of Hilbert space to correspond to different choices of coordinate systems. The apparent freedom in the choice of decomposition of Hilbert space \mathcal{H} of Eq. (4.2) to choose a different clock/temporal degree of freedom \mathcal{H}_t , and therefore different emergent dynamics for the system \mathcal{H}_S (in the context of the Page-Wootters formulation of section 4.2), is often referred to as the ‘‘Clock Ambiguity’’ [31, 80, 81]. While the decoupled form of the constraints are rather special in their own right (such as Ref. [82] where it is argued that a decoupled form of the constraint can help ease the Clock Ambiguity) and some unitary transformations will preserve it (for instance, the global basis changes in section 4.4 to implement Lorentz transformations are such examples), not all unitary transformations will preserve this decoupled form. Investigating generic unitary basis changes for constraints

containing interacting terms could shed light upon the nature of coordinates in the context of a quantum field theoretic setup for spacetime and matter, and will be taken up in future work. Not all decompositions may be allowed and some may be preferred over others in determining which degrees of freedom in \mathcal{H} make up the background spacetime and which make up the matter degrees of freedom. While definitely an interesting question that could have implications for the Hilbert space structure of quantum gravity, it is beyond the scope of this work and is left for future investigation. The interested reader is encouraged to look into a rich literature [83–87] (and references therein) available on quantum frames of reference and its connections with Hamiltonian constraints.

We would also like to emphasize that while we have attempted to treat space and time on an equal footing in Hilbert space in the context of relativistic quantum mechanics, there are important and crucial differences between the nature of time and space. For instance, relativistic light cone structures demand causal influence in timelike directions and not spacelike, and the nature of time, more conventionally interpreted, seems to be inseparably intertwined with thermodynamics and the arrow of time [32, 88]. The interplay between space, time, and quantum mechanics can be better understood by re-examining crucial first principle ideas, which we believe to be an important direction of inquiry toward our understanding of quantum gravity.

Part II

(In)Finitude and Beyond

*Chapter 5***MODELING POSITION AND MOMENTUM IN
FINITE-DIMENSIONAL HILBERT SPACES VIA
GENERALIZED PAULI OPERATORS**

The finite entropy of black holes suggests that local regions of spacetime are described by finite-dimensional factors of Hilbert space, in contrast with the infinite-dimensional Hilbert spaces of quantum field theory. With this in mind, we explore how to cast finite-dimensional quantum mechanics in a form that matches naturally onto the smooth case, especially the recovery of conjugate position/momentum variables, in the limit of large Hilbert-space dimension. A natural tool for this task are the Generalized Pauli operators (GPO). Based on an exponential form of Heisenberg’s canonical commutation relation, the GPO offers a finite-dimensional generalization of conjugate variables without relying on any *a priori* structure on Hilbert space. We highlight some features of the GPO, its importance in studying concepts such as spread induced by operators, and point out departures from infinite-dimensional results (possibly with a cutoff) that might play a crucial role in our understanding of quantum gravity. We introduce the concept of “Operator Collimation,” which characterizes how the action of an operator spreads a quantum state along conjugate directions. We illustrate these concepts with a worked example of a finite-dimensional harmonic oscillator, demonstrating how the energy spectrum deviates from the familiar infinite-dimensional case.

This chapter is based on the following reference:

A. Singh and S. M. Carroll, “Modeling position and momentum in finite-dimensional Hilbert spaces via generalized Pauli operators,” [arXiv:1806.10134](https://arxiv.org/abs/1806.10134) [quant-ph]

5.1 Introduction

The Hilbert space of a quantum field theory is infinite-dimensional for three different reasons: wavelengths can be arbitrarily large, and they can be arbitrarily small, and at any one wavelength, the occupation number of bosonic modes can be arbitrarily high. Once we include gravity, however, all of these reasons come into question.

In the presence of a positive vacuum energy, the de Sitter radius provides a natural infrared cutoff at long wavelengths; the Planck scale provides a natural ultraviolet cutoff at short wavelengths; and the Bekenstein bound [18, 35, 89] (or more generally, black hole formation and its consequent finite entropy) provides an energy cutoff. It therefore becomes natural to consider theories where Hilbert space, or at least the factor of Hilbert space describing our observable region of the cosmos, is finite-dimensional [17, 19–21, 36–39, 65].

Our interest here is in how structures such as fields and spatial locality emerge in a locally finite-dimensional context. Hilbert space is featureless: all Hilbert spaces of a specified finite dimension are isomorphic, and the algebra of observables is simply “all Hermitian operators.” Higher-level structures must therefore emerge from whatever additional data we are given, typically eigenstates and eigenvalues of the Hamiltonian and perhaps the amplitudes of a particular quantum state. (For work in this direction see [15, 22, 65, 67].) One aspect of this emergence is the role of conjugate variables, generalizations of position and momentum. To begin an exploration of how spacetime and locality can emerge from a Hamiltonian acting on states in a finite-dimensional Hilbert space, in this chapter we consider the role of conjugate variables in a finite-dimensional context.

In the familiar (countably) infinite-dimensional case, such as non-relativistic quantum mechanics of a single particle, classical conjugate variables such as position (q) and momentum (p) are promoted to linear operators on Hilbert space obeying the Heisenberg canonical commutation relations (CCR),

$$[\hat{q}, \hat{p}] = i, \tag{5.1}$$

where throughout this chapter, we take $\hbar = 1$. In field theory, one takes the field and its conjugate momentum as operators labelled by spacetime points and generalizes the CCR to take a continuous form labelled by spacetime locations. ¹

The Stone-von Neumann theorem guarantees that there is a unique irreducible representation (up to unitary equivalence) of the CCR on infinite-dimensional Hilbert

¹In making the transition to field theory, one transits from a finite to an infinite number of degrees of freedom and hence an uncountably infinite-dimensional Hilbert space (which is non-separable). In this case, there can be unitarily inequivalent representations of the CCRs, implying that the physical subspaces spanned by eigenstates of operators in a particular representation will be different. In Algebraic Quantum Field Theory, this is described by Haag’s theorem[3]. Then different choices of states (a unit-normed, positive linear functional) on the algebra specify different inequivalent (cyclic) representations.

spaces that are *separable* (possessing a countable dense subset), but also that the operators \hat{q}, \hat{p} must be unbounded. There are therefore no such representations on finite-dimensional spaces.

There is, however, a tool that works in finite-dimensional Hilbert spaces and maps onto conjugate variables in the infinite-dimensional limit: the Generalized Pauli operators (GPO). As we shall see, the GPO is generated by a pair of normalized operators \hat{A} and \hat{B} – sometimes written as “clock” and “shift” matrices – that commute up to a dimension-dependent phase,

$$\hat{A}\hat{B} = \omega^{-1}\hat{B}\hat{A}, \quad (5.2)$$

where $\omega = \exp(2\pi i/N)$ is a primitive root of unity. Any linear operator can be written as a sum of products of these generators. Appropriate logarithms of these operators reduce, in the infinite-dimensional limit, to conjugate operators obeying the CCR. The GPO therefore serves as a starting point for analyzing the quantum mechanics of finite-dimensional Hilbert spaces in a way that matches naturally onto the infinite-dimensional limit.

We will follow a series of papers by Jagannathan, Santhanam, Tekumalla, and Vasudevan [76, 90, 91] from the 1970-80’s, which developed the subject of finite-dimensional quantum mechanics, motivated by the Weyl’s exponential form of the CCR. These were introduced first by Sylvester [92] and then applied to quantum mechanics by von Neumann [93], Weyl [77], and Schwinger [94, 95], and since have been discussed by many others in various contexts. Some representative papers include [96, 97, 97–109] (and references therein). This paradigm of the Generalized Pauli operators has also been referred in the vast literature on this subject as the discrete Heisenberg group or the finite Weyl-Heisenberg group and also has been called Schwinger bases, Weyl operators [110], and generalized spin [111], among others. From an algebraic point of view, this structure corresponds to a generalized Clifford algebra (GCA) [9] with two generators that follow an ordered commutation relation.² The basic mathematical constructions worked out in this chapter are not new; our goal here is to distill the features of the GPO that are useful in the study of locally finite-dimensional Hilbert spaces in quantum gravity, especially the emergence of a classical limit.

²In general, a GCA can be defined with more generators and their braiding relations. For instance, the Clifford algebra of the “gamma” matrices used in spinor QFT and the Dirac equation is a particular GCA with 4 generators [9].

The chapter is organized as follows. In Section 5.2, we motivate the need for an intrinsic finite-dimensional construction by pointing out the incompatibility of conventional textbook quantum mechanics and QFT with a finite-dimensional Hilbert space, and follow it up by introducing and using the GPO to construct a finite-dimensional generalization of conjugate variables. In Section 5.3, we introduce the concept of Operator Collimation as a means to quantify and study the spread induced by operators along the conjugate variables. Section 5.4 deals with understanding equations of motion for conjugate variables in a finite-dimensional context and how they map to Hamilton's equations in the large dimension limit, and we explore features of the finite-dimensional quantum mechanical oscillator.

5.2 Finite-Dimensional Conjugate Variables from the Generalized Pauli Operators

Prelude

Consider the problem of adapting the Heisenberg CCR (5.1) to finite-dimensional Hilbert spaces. One way of noticing an immediate obstacle is to take the trace of both sides; the left-hand side vanishes, while the right-hand side does not. To remedy this, Weyl [77] gave an equivalent version of Heisenberg's CCR in exponential form,

$$e^{i\eta\hat{p}} e^{i\zeta\hat{q}} = e^{i\eta\zeta} e^{i\zeta\hat{q}} e^{i\eta\hat{p}}, \quad (5.3)$$

for some real parameters η and ζ . This does indeed admit a finite-dimensional representation (which is unique, up to unitary equivalence, as guaranteed by the Stone-von Neumann theorem which works for separable Hilbert spaces (hence, finite-dimensional and countable infinite-dimensional) [2]). One can interpret this to be a statement of how the conjugate operators \hat{q} and \hat{p} fail to commute, although the commutation relation $[\hat{q}, \hat{p}]$ will now no longer have the simple form of a c-number (5.1).

The GPO offers a natural implementation of Weyl's relation (5.3) to define a set of intrinsically finite-dimensional conjugate operators. In this section, we will follow the construction laid out in references [76, 90, 91] in developing finite-dimensional quantum mechanics based on Weyl's exponential form of the CCR.

The Generalized Pauli Operators

Consider a finite-dimensional Hilbert space \mathcal{H} of dimension

$$\dim \mathcal{H} = N, \quad (5.4)$$

with $N < \infty$. Let us associate Generalized Pauli operators (GPO) by equipping the space $\mathcal{L}(\mathcal{H})$ of linear operators acting on \mathcal{H} with two unitary operators as generators of the group, call them \hat{A} and \hat{B} , which satisfy the following commutation relation,

$$\hat{A}\hat{B} = \omega^{-1}\hat{B}\hat{A}, \quad (5.5)$$

where $\omega = \exp(2\pi i/N)$ is a primitive root of unity. This is also known as the Weyl Braiding relation in the physics literature, and is the basic commutation relation obeyed by the generators. In addition to being unitary, the generators also satisfy the following toroidal property,

$$\hat{A}^N = \hat{B}^N = \hat{\mathbb{I}}, \quad (5.6)$$

where $\hat{\mathbb{I}}$ is the identity operator on \mathcal{H} . The spectrum of the operators is identical for both GPO generators \hat{A} and \hat{B} ,

$$\text{spec}(\hat{A}) = \text{spec}(\hat{B}) = \{1, \omega^1, \dots, \omega^2, \dots, \omega^{N-1}\}. \quad (5.7)$$

Thus, in line with our Hilbert-space perspective, specifying just the dimension N of Hilbert space is sufficient to construct the group, which determines the spectrum of the generators and the basic commutation relations.

The GPO can be constructed for both even and odd values of N and both cases are important and useful in different contexts. In this section, let us specialize to the case of odd $N \equiv 2l + 1$ for some $l \in \mathbb{Z}^+$, which will be useful in constructing conjugate variables whose eigenvalues can be thought of labelling lattice sites centered around 0. In the case of even dimensions $N = 2m$ for some $m \in \mathbb{Z}^+$, one will be able to define conjugate on a lattice labelled from $\{0, 1, 2, \dots, N-1\}$ and not on a lattice centered around 0. For the case of $N = 2$, we recover the Pauli matrices, corresponding to $A = \sigma_x$ and $B = \sigma_z$. Operators on qubits can be seen as a special $N = 2$ case of the GPO. While the subsequent construction can be done in a basis-independent way, we choose a hybrid route, switching between an explicit representation of the GPO and abstract vector space relations, to explicitly point out the properties of the group.

Let us follow the convention that all indices used in this section (for the case of odd $N = 2l + 1$) for labelling states or matrix elements of an operator in some basis will run over

$$i, j, k \in -l, (-l+1), \dots, -1, 0, 1, \dots, l-1, l. \quad (5.8)$$

The eigenspectrum of both GPO generators \hat{A} and \hat{B} can be relabelled as,

$$\text{spec}(\hat{A}) = \text{spec}(\hat{B}) = \{\omega^{-l}, \omega^{-l+1}, \dots, \omega^{-1}, 1, \omega^1, \dots, \omega^{l-1}, \omega^l\}. \quad (5.9)$$

There exists a unique irreducible representation (up to unitary equivalence) [9] of the generators of the GPO defined via Eqs. (5.2) and (5.6) in terms of $N \times N$ matrices

$$A = \begin{bmatrix} 0 & 0 & 0 & \cdots & 1 \\ 1 & 0 & 0 & \cdots & 0 \\ 0 & 1 & 0 & \cdots & 0 \\ \cdot & \cdot & \cdots & \cdot & \cdot \\ \cdot & \cdot & \cdots & \cdot & \cdot \\ 0 & 0 & \cdots & 1 & 0 \end{bmatrix}_{N \times N}, \quad B = \begin{bmatrix} \omega^{-l} & 0 & 0 & \cdots & 0 \\ 0 & \omega^{-l+1} & 0 & \cdots & 0 \\ \cdot & \cdot & \cdots & \cdot & \cdot \\ \cdot & \cdot & \cdots & \cdot & \cdot \\ 0 & 0 & 0 & \cdots & \omega^l \end{bmatrix}_{N \times N}. \quad (5.10)$$

The $\hat{\cdot}$ has been removed to stress that these matrices are representations of the operators \hat{A} and \hat{B} in a particular basis, in this case, the eigenbasis of \hat{B} (so that B is diagonal). More compactly, the matrix elements of operators \hat{A} and \hat{B} in this basis are,

$$[A]_{jk} \equiv \langle b_j | \hat{A} | b_k \rangle = \delta_{j,k+1}, \quad [B]_{jk} \equiv \langle b_j | \hat{B} | b_k \rangle = \omega^j \delta_{j,k}, \quad (5.11)$$

with the indices j and k running from $-l, \dots, 0, \dots, l$ and δ_{jk} is the Kronecker delta function. The generators obey the following trace condition,

$$\text{Tr}(\hat{A}^j) = \text{Tr}(\hat{B}^j) = N \delta_{j,0}. \quad (5.12)$$

Let us now further understand the properties of the eigenvectors of \hat{A} and \hat{B} and the action of the group elements on them. Consider the set $\{|b_j\rangle\}$ of eigenstates of \hat{B} ,

$$\hat{B} |b_j\rangle = \omega^j |b_j\rangle. \quad (5.13)$$

As can be seen in the matrix representation of \hat{A} in Eq. (5.10), the operator \hat{A} acts to generate cyclic shifts for the eigenstates of \hat{B} , mapping an eigenstate to the next,

$$\hat{A} |b_j\rangle = |b_{j+1}\rangle. \quad (5.14)$$

The unitary nature of these generators implies a cyclic structure in which one identifies $|b_{l+1}\rangle \equiv |b_{-l}\rangle$, so that $\hat{A} |b_l\rangle = |b_{-l}\rangle$.

The operators \hat{A} and \hat{B} have the same relative action on the eigenstates of one another, as there is nothing in the group structure which distinguishes between the two. The operator \hat{B} generates unit shifts in eigenstates of \hat{A} ,

$$\hat{B} |a_k\rangle = |a_{k+1}\rangle, \quad (5.15)$$

with cyclic identification $|a_{l+1}\rangle \equiv |a_{-l}\rangle$. Hence we have a set of operators that generate shifts in the eigenstates of the other, which is precisely the way in which conjugate variables act and which is why the GPO provides a natural structure to define conjugate variables on Hilbert space. While we should think of these eigenstates of \hat{A} and \hat{B} to be marked by their eigenvalues on a lattice, there is no notion of a scale or physical distance at this point, just a lattice of states labelled by their eigenvalues in a finite-dimensional construction along with a pair of operators which translate each other's states by unit shifts, respectively. It should be mentioned at this stage that even though this construction lacks the notion of a physical scale, there still exists a *symplectic structure* [112, 113] (and references therein). This is a rich topic with a lot of interesting details which we will not discuss here, and the interested reader is encouraged to look into the references mentioned above.

To further reinforce this conjugacy relation between \hat{A} and \hat{B} , we see that they are connected to each other under a discrete Fourier transformation implemented by Sylvester's matrix S , which is an $N \times N$ unitary matrix connecting A and B via $SAS^{-1} = B$. Sylvester's matrix in the $\{|b_j\rangle\}$ basis has the form $[S]_{jk} = \omega^{jk} / \sqrt{N}$. The GPO generators \hat{A} and \hat{B} have been studied in various contexts in quantum mechanics and are often referred to as "clock and shift" matrices. They offer a higher dimensional, non-hermitian generalization of the Pauli matrices.

The set of N^2 linearly independent unitary matrices, $\{B^b A^a | b, a = -l, (-l+1), \dots, 0, \dots, (l-1), l\}$, which includes the identity for $a = b = 0$, form a unitary basis for $\mathcal{L}(\mathcal{H})$. Schwinger [94] studied the role of such unitary basis, hence this operator basis is often called Schwinger unitary basis. Any operator $\hat{M} \in \mathcal{L}(\mathcal{H})$ can be expanded in this basis,

$$\hat{M} = \sum_{b,a=-l}^l m_{ba} \hat{B}^b \hat{A}^a. \quad (5.16)$$

Since from the structure of the GPO we have $\text{Tr} \left[\left(\hat{B}^{b'} \hat{A}^{a'} \right)^\dagger \left(\hat{B}^b \hat{A}^a \right) \right] = N \delta_{b,b'} \delta_{a,a'}$, we can invert Eq. (7.23) to get the coefficients m_{ba} as,

$$m_{ba} = \frac{1}{N} \text{Tr} \left[\hat{A}^{-a} \hat{B}^{-b} \hat{M} \right]. \quad (5.17)$$

Thus, in addition to playing the role of conjugate variables in a finite-dimensional construction, the GPO fits in naturally with the program of minimal quantum mechanics in Hilbert space [65, 67]. By being able to define a notion of conjugate variables, one is able to classify and use any other operator on this space, including the Hamiltonian that governs the dynamics. This notion will be important to us when we define the idea of conjugate spread of operators, the so-called ‘‘Operator Collimation,’’ in Section 5.3.

Finite-Dimensional Conjugate Variables

We are now prepared to define a notion of conjugate variables on a finite-dimensional Hilbert space. The defining notion for a pair of conjugate variables is identifying two self-adjoint operators that each generate translations in the eigenstates of the other. For instance, in textbook quantum mechanics, the momentum operator \hat{p} generates translations in the eigenstates of its conjugate variable, the position operator \hat{q} , and vice-versa. Taking this as our defining criterion, we would like to define a pair of conjugate operators acting on a finite-dimensional Hilbert space, each of which is the generator of translations in the eigenstates of its conjugate.

We define a pair $\hat{\phi}$ and $\hat{\pi}$ to be conjugate operators by making the following identification,

$$\hat{A} \equiv \exp(-i\alpha\hat{\pi}), \quad \hat{B} \equiv \exp(i\beta\hat{\phi}), \quad (5.18)$$

where α and β are non-zero real parameters which set the scale of the eigenspectrum of the operators $\hat{\phi}$ and $\hat{\pi}$. These are bounded operators on \mathcal{H} , and due to the virtue of the GPO generators \hat{A} and \hat{B} being unitary, the conjugate operators $\hat{\phi}$ and $\hat{\pi}$ are self-adjoint, satisfying $\hat{\phi}^\dagger = \hat{\phi}$ and $\hat{\pi}^\dagger = \hat{\pi}$. The operator $\hat{\pi}$ is the generator of translations of $\hat{\phi}$ and vice-versa. The apparent asymmetry in the sign in the exponential in Eq. (5.18) when identifying $\hat{\phi}$ and $\hat{\pi}$ is to ensure that the j -th column (with $j = -l, -l+1, \dots, 0, \dots, l-1, l$) of Sylvester’s matrix S that diagonalizes A is an eigenstate of $\hat{\pi}$ with eigenvalue proportional to j , and hence on an ordered lattice. Of course, $\hat{\phi}$ has common eigenstates with those of \hat{B} and $\hat{\pi}$ shares eigenstates with \hat{A} . Let us label the eigenstates of $\hat{\phi}$ as $|\phi_j\rangle$ and those of $\hat{\pi}$ as $|\pi_j\rangle$ with the index j running from $-l, \dots, 0, \dots, l$. The corresponding eigenvalue equations for $\hat{\phi}$ and $\hat{\pi}$ can be easily deduced using Eqs. (5.18) and (5.7),

$$\hat{\phi}|\phi_j\rangle = j \left(\frac{2\pi}{(2l+1)\beta} \right) |\phi_j\rangle, \quad \hat{\pi}|\pi_j\rangle = j \left(\frac{2\pi}{(2l+1)\alpha} \right) |\pi_j\rangle. \quad (5.19)$$

Let us now solve for the conjugate operators $\hat{\phi}$ and $\hat{\pi}$ explicitly by finding their

matrix representations in the $|\phi_j\rangle$ basis. By virtue of being diagonal, the principle logarithm of B is

$$\log B = (\log \omega) \text{diag} (-l, -l+1, \dots, 0, \dots, l-1, l) . \quad (5.20)$$

Hence we have the matrix representation of $\hat{\phi}$,

$$\langle \phi_j | \hat{\phi} | \phi_{j'} \rangle = j \left(\frac{2\pi}{(2l+1)\beta} \right) \delta_{jj'} , \quad (5.21)$$

which is diagonal in the $|\phi_j\rangle$ basis as expected. To find a representation of $\hat{\pi}$ in this basis, we notice that \hat{A} is diagonalized by Sylvester's matrix, hence we can get its principle logarithm as $\log A = S^{-1} (\log B) S$. In the case of odd dimension $N = 2l + 1$, the principle logarithms of A and B are well-defined, and we are able to find explicit matrix representations for operators $\hat{\phi}$ and $\hat{\pi}$ as above. The conjugate operators $\hat{\phi}$ and $\hat{\pi}$ are connected through Sylvester's operator,

$$\hat{\pi} = \left(\frac{-\beta}{\alpha} \right) \hat{S}^{-1} \hat{\phi} \hat{S} , \quad \hat{\phi} = \left(\frac{-\alpha}{\beta} \right) \hat{S} \hat{\pi} \hat{S}^{-1} . \quad (5.22)$$

The following parity relations are obeyed, since S^2 is the parity operator, $[S^2]_{jk} = \delta_{j,-k}$,

$$\hat{S}^4 = \hat{\mathbb{I}} , \quad \hat{S}^2 \hat{\phi} \hat{S}^{-2} = -\hat{\phi} , \quad \hat{S}^2 \hat{\pi} \hat{S}^{-2} = -\hat{\pi} . \quad (5.23)$$

These relations have the same form as in infinite-dimensional quantum mechanics.

Using the expression $\log A = S^{-1} (\log B) S$, the matrix representation for $\hat{\pi}$ in the $|\phi_j\rangle$ basis is,

$$\begin{aligned} \langle \phi_j | \hat{\pi} | \phi_{j'} \rangle &= \left(\frac{2\pi}{(2l+1)^2 \alpha} \right) \sum_{n=-l}^l n \exp \left(\frac{2\pi i (j-j') n}{2l+1} \right) \\ &= \begin{cases} 0 , & \text{if } j = j' \\ \left(\frac{i\pi}{(2l+1)\alpha} \right) \text{cosec} \left(\frac{2\pi l (j-j')}{2l+1} \right) , & \text{if } j \neq j' . \end{cases} \end{aligned} \quad (5.24)$$

The eigenstates of both $\hat{\phi}$ and $\hat{\pi}$ each individually are orthonormal bases for the Hilbert space \mathcal{H} ,

$$\langle \phi_j | \phi_{j'} \rangle = \delta_{j,j'} , \quad \sum_{j=-l}^l |\phi_j\rangle \langle \phi_j| = \hat{\mathbb{I}} , \quad \langle \pi_j | \pi_{j'} \rangle = \delta_{j,j'} , \quad \sum_{j=-l}^l |\pi_j\rangle \langle \pi_j| = \hat{\mathbb{I}} . \quad (5.25)$$

Thus, using the generators of the GPO, we are able to naturally identify a notion of conjugate operators, each of which is the generator of translations for the eigenstates of the other as seen by Eqs. (5.18), (5.14) and (5.15). While the GPO provides us with a notion of dimensionless conjugate variables that have familiar “position/-momentum” properties, there is no notion of a physical length scale as yet. The operators we will ultimately identify as classical position and momentum operators depend on a non-generic decomposition of Hilbert space into subsystems that makes emergent classicality manifest. This is the so-called quantum factorization problem [28, 29, 114], sometimes referred to as the set selection problem [115].

The Commutator

In this section, we will work out the commutation relation between conjugate operators $\hat{\phi}$ and $\hat{\pi}$ as defined from the GPO in a finite-dimensional Hilbert space, and understand how they deviate from the usual Heisenberg CCR and converge to it in the large dimension limit. In the infinite limit, the conjugate operators $\hat{\phi}$ and $\hat{\pi}$ obey Heisenberg’s form of the CCR $[\hat{\phi}, \hat{\pi}] = i$, while our conjugate variables based on Eq. (5.18) satisfy the GPO commutation relation,

$$\exp(-i\alpha\hat{\pi}) \exp(i\beta\hat{\phi}) = \exp\left(-\frac{2\pi i}{2l+1}\right) \exp(i\beta\hat{\phi}) \exp(-i\alpha\hat{\pi}). \quad (5.26)$$

On expanding the left-hand side of the GPO braiding relation Eq. (5.26) and using the Baker-Campbell-Hausdorff Lemma, we obtain,

$$\begin{aligned} \exp\left(i\beta\hat{\phi} + [-i\alpha\hat{\pi}, i\beta\hat{\phi}] + \frac{1}{2!}[-i\alpha\hat{\pi}, [-i\alpha\hat{\pi}, i\beta\hat{\phi}]] + \dots\right) \exp(-i\alpha\hat{\pi}) \\ = \exp\left(\frac{2\pi i}{2l+1}\right) \exp(i\beta\hat{\phi}) \exp(-i\alpha\hat{\pi}). \end{aligned} \quad (5.27)$$

While this holds for arbitrary real, non-zero α and β for any dimension $N = 2l + 1$, let us focus on the infinite limit when $\hat{\phi}$ and $\hat{\pi}$ should satisfy Heisenberg’s CCR of Eq. (5.1). Substituting this in Eq. (5.27), we obtain,

$$\exp(i\beta\hat{\phi} - i\alpha\beta) \exp(-i\alpha\hat{\pi}) = \exp\left(-\frac{2\pi i}{2l+1}\right) \exp(i\beta\hat{\phi}) \exp(-i\alpha\hat{\pi}), \quad (5.28)$$

which immediately gives us a constraint on the parameters α and β ,

$$\alpha\beta = \frac{2\pi}{2l+1}, \quad (5.29)$$

such that the commutation relation in the infinite-dimensional limit maps onto the Weyl form of the CCR, Eq. (5.26). Thus, when Eq. (5.29) is satisfied, the commutator of $\hat{\phi}$ and $\hat{\pi}$ will obey Heisenberg’s CCR in the infinite-dimensional limit.

We will show this explicitly later in this section, but before that, let us first compute the commutator of $\hat{\phi}$ and $\hat{\pi}$ in finite dimensions. The matrix representation of $[\hat{\phi}, \hat{\pi}]$ in the $\{|\phi_j\rangle\}$ basis is,

$$\begin{aligned} \langle \phi_j | [\hat{\phi}, \hat{\pi}] | \phi_{j'} \rangle &= \frac{4\pi^2(j-j')}{(2l+1)^3\alpha\beta} \sum_{n=-l}^l n \exp\left(\frac{2\pi i(j-j')n}{2l+1}\right) \\ &= \frac{2\pi(j-j')}{(2l+1)^2} \sum_{n=-l}^l n \exp\left(\frac{2\pi i(j-j')n}{2l+1}\right). \end{aligned} \quad (5.30)$$

Imposing $\alpha\beta(2l+1) = 2\pi$ and performing the sum, the commutator becomes

$$\langle \phi_j | [\hat{\phi}, \hat{\pi}] | \phi_{j'} \rangle = \begin{cases} 0, & \text{if } j = j' \\ \frac{i\pi(j-j')}{(2l+1)} \operatorname{cosec}\left(\frac{2\pi l(j-j')}{2l+1}\right), & \text{if } j \neq j'. \end{cases} \quad (5.31)$$

Under the constraint of Eq. (5.29), the matrix elements of $\hat{\phi}$ and $\hat{\pi}$ become

$$\langle \phi_j | \hat{\phi} | \phi_{j'} \rangle = j\alpha\delta_{j,j'}, \quad \langle \phi_j | \hat{\pi} | \phi_{j'} \rangle = \left(\frac{\beta}{2l+1}\right) \sum_{n=-l}^l n \exp\left(\frac{2\pi i(j-j')n}{2l+1}\right). \quad (5.32)$$

While we need α and β to satisfy Eq. (5.29) to obtain the correct limit of Heisenberg's CCR in infinite dimensions, there is still freedom to choose one of the two parameters independently. One possibility is that their values are determined by the eigenvalues and functional dependence of the Hamiltonian on these conjugate operators. (Since powers of $\hat{\phi}$ and $\hat{\pi}$ generate the Schwinger unitary basis of Eq. (7.23), any operator can be expressed as a function of these conjugate operators.) Alternatively, since there is no sense of scale at this level of construction and the conjugate operators are dimensionless and symmetric, one could by fiat impose $\alpha = \beta = \sqrt{2\pi/(2l+1)}$ and, accordingly, change the explicit functional form of the Hamiltonian, which should have no bearing on the physics.

The most important feature of the finite-dimensional commutator is its non-centrality, departing from being a commuting c-number (as it is in infinite dimensions). Many characteristic features of quantum mechanics and quantum field theory hinge on this property of a central commutator of conjugate operators. It is expected that the presence of a non-central commutator will induce characteristic changes in familiar results, such as computing the zero-point energy. Non-centrality allows for a richer structure in quantum mechanical models, as we will discuss in Section 5.4. Let

us write down the finite-dimensional commutator as $[\hat{\phi}, \hat{\pi}] = i\hat{Z}$, where \hat{Z} is a hermitian operator whose matrix elements in the $\hat{\phi}$ -basis can be read off from Eq. (5.31). The matrix Z (i.e. the matrix elements of \hat{Z} in the $\hat{\phi}$ basis) is a real, traceless (null entries on the diagonal), symmetric Toeplitz matrix. Such structure can be exploited to better understand deviations of the commutator in finite dimensions as compared to the usual infinite-dimensional results.

We now turn to recovering conventional notions associated with conjugate variables in quantum mechanics based on an infinite-dimensional Hilbert space. In the infinite-dimensional case of continuum quantum mechanics, we take $l \rightarrow \infty$ and at the same time make the spectral differences of $\hat{\phi}$ and $\hat{\pi}$ infinitesimally small so that they are now labelled by continuous indices on the real line \mathbb{R} , while at the same time respecting the constraint $\alpha\beta(2l + 1) = 2\pi$. While finite-dimensional Hilbert spaces in the $N \rightarrow \infty$ limit are not isomorphic to infinite-dimensional ones (even with countably finite dimensions), there is a way in which we can recover Heisenberg's CCR as $N \rightarrow \infty$.

In the expression for the commutator in Eq. (5.30), replace $n/(2l + 1)$ with a continuous variable $x \in \mathbb{R}$ and replace the sum with an integral with $dx \equiv 1/(2l + 1)$ playing the role of the integration measure,

$$\langle \phi_j | [\hat{\phi}, \hat{\pi}] | \phi_{j'} \rangle = 2\pi(j - j') \int_{-\infty}^{\infty} dx x \exp(2\pi i(j - j')x). \quad (5.33)$$

Since the labels j and j' are continuous, we can re-write the integral above as,

$$\langle \phi_j | [\hat{\phi}, \hat{\pi}] | \phi_{j'} \rangle = 2\pi(j - j') \frac{1}{2\pi i} \frac{d}{d(j - j')} \int_{-\infty}^{\infty} dx \exp(2\pi i(j - j')x), \quad (5.34)$$

$$= -i(j - j') \frac{d}{d(j - j')} \delta(j - j'), \quad (5.35)$$

$$= i\delta(j - j'), \quad (5.36)$$

where we have used $y\delta'(y) = -\delta(y)$. Thus, we are able to recover Heisenberg's CCR as the infinite-dimensional limit of the Weyl braiding relation. It can be shown on similar lines that in the infinite-dimensional limit, $\hat{\pi}$ has the familiar representation of $-id/d\phi$ in the $\hat{\phi}$ basis. Hence, finite-dimensional quantum mechanics based on the GPO reduces to known results in the infinite-dimensional limit, while at the same time offering more flexibility to tackle finite-dimensional problems, as might be the case for local spatial regions in quantum gravity. As we will discuss in Sections 5.4 and 5.5, infinite-dimensional quantum mechanics with cutoffs is very different from an intrinsic finite-dimensional theory; these difference could

affect our understanding of fine-tuning problems due to radiative corrections, such as the hierarchy and cosmological-constant problems. Also, finite-dimensional constructions can offer new features in the spectrum of possible Hamiltonians, as we discuss in Section (5.4).

5.3 Operator Collimation: The Conjugate Spread of Operators

The concept of locality manifests itself in different ways in conventional physics. In field theory, commutators of spacelike-separated fields vanish, the Hamiltonian can be written as a spatial integral of a Hamiltonian density $\hat{H} = \int d^3x \hat{\mathbf{H}}(\vec{x})$, and Lagrangians typically contain local interaction terms and kinetic terms constructed from low powers of the conjugate momenta. Higher powers of the conjugate momenta are interpreted as non-local effects and are expected to be suppressed. Haag’s formulation of algebraic QFT [3, 116] is also based on an understanding of locality.³

From a quantum information perspective, when we think about sub-systems in quantum mechanics as a tensor product structure in Hilbert space $\mathcal{H} = \bigotimes_j \mathcal{H}_j$, the interaction Hamiltonian is taking to be k -local on the graph [22], thereby connecting only k -tensor factors for some small integer k , thus reinforcing the local character of physical interactions. Typically, given a pair of conjugate variables, a dynamics worthy of the label “local” should have the feature that a state localized around a given position should not instantly evolve into a delocalized state. For example, the Hamiltonian for a single non-relativistic particle typically takes the special form $\hat{H} \sim \hat{p}^2/2 + \hat{V}(\hat{x})$ for classical conjugate variables of position \vec{x} and momentum \vec{p} . Both the quadratic nature of the kinetic term and fact that the Hamiltonian is additively separable in the conjugate variables serve to enforce this kind of locality by not allowing arbitrarily large spread of localized position states.

In a theory with gravity, the role of locality is more subtle. On general grounds, considering the metric as a quantum operator (or as a field to be summed over in a path integral) makes it impossible to define local observables, since there is no unique way to associate given coordinate values with “the same” points of spacetime. In the context of the black-hole information puzzle, the principles of holography (the number of degrees of freedom within a black hole scales as the area of the horizon)

³Localized states and their properties form an interesting set of ideas in quantum field theory (for example, see [117]) and have been debated on for a long time now. They connect to various important constructions and theorems such as Newton-Wigner [118, 119] localization and the Reeh-Schlieder theorem [120, 121] in field theory. Such ideas will not be discussed here since our motivation is trying to understand emergence of structures such as spacetime, causality, and classicality from basic quantum mechanics, without presupposing any such structure.

and horizon complementarity (infalling observers see degrees of freedom spread out according to principles of local quantum field theory, while external observers see them as scrambled across the horizon) strongly suggest that the fundamental degrees of freedom in quantum gravity are not locally distributed in any simple way [78, 79, 122, 123].

En route to understanding how spacetime emerges from quantum mechanics, we would like to understand these features better in a finite-dimensional construction without imposing additional structure or implicit assumptions of a preferred decomposition of Hilbert space, preferred observables, or conventional locality. With this motivation in mind, we can consider an even more primitive notion of “locality”. The following notion of “locality”, which we will call Operator Collimation, is a purely Hilbert-space construction and does not depend or refer to any underlying causal structure, relativistic or otherwise. Within our framework of conjugate variables, this primitive kind of locality can be understood by studying how operators in general (and the Hamiltonian in particular) act to spread eigenstates of conjugate variables in Hilbert space.

In this section, we develop a notion of the conjugate spread of an operator. This quantity helps characterize the support of an operator along the two conjugate directions. While this notion is not intrinsically tied to any time evolution generated by a Hamiltonian, and rather discusses the how different operators have support with respect to the two conjugate variables, it can be adapted to connect with more conventional notions of locality once relevant structures such as space, preferred observables, classicality etc. have been emerged under the right conditions.

As discussed in Section 5.2, the Schwinger unitary basis $\{B^b A^a | b, a = -l, (-l + 1), \dots, 0, \dots, (l - 1), l\}$ offers a complete basis for linear operators in $\mathcal{L}(\mathcal{H})$. The GPO generator \hat{A} corresponds to a unit shift in the eigenstates of $\hat{\phi}$, and \hat{B} generates unit shifts in the eigenstates of $\hat{\pi}$; hence, a basis element $B^b A^a$ generates a units of shift in eigenstates of $\hat{\phi}$ and b units in eigenstates of $\hat{\pi}$, respectively (up to overall phase factors).

For more general operators, the shifts implemented by the GPO generators turn into spreading of the state. Consider a self-adjoint operator $\hat{M} \in \mathcal{L}(\mathcal{H})$ expanded in terms of GPO generators,

$$\hat{M} = \sum_{b,a=-l}^l m_{b,a} \hat{B}^b \hat{A}^a . \quad (5.37)$$

Since \hat{M} is self-adjoint $\hat{M}^\dagger = \hat{M}$, we get a constraint on the expansion coefficients, $\omega^{-ba} m_{-b,-a}^* = m_{b,a}$, which implies $|m_{b,a}| = |m_{-b,-a}|$ since $\omega = \exp(2\pi i/(2l+1))$ is a primitive root of unity. The coefficients $m_{b,a}$ are a set of basis-independent numbers that quantify the spread induced by the operator \hat{M} along each of the conjugate variables $\hat{\phi}$ and $\hat{\pi}$. To be precise, $|m_{b,a}|$ represents the amplitude of b shifts along $\hat{\pi}$ for an eigenstate of $\hat{\pi}$ and a shifts along $\hat{\phi}$ for an eigenstate of $\hat{\phi}$. The indices of $m_{b,a}$ run from $-l, \dots, 0, \dots, l$ along both conjugate variables and thus, characterize shifts in both increasing (a or $b > 0$) and decreasing (a or $b < 0$) eigenvalues on the cyclic lattice. The action of \hat{M} on a state depends on details of the state, and in general will lead to a superposition in the eigenstates of the chosen conjugate variable as our basis states, but the set of numbers $m_{b,a}$ quantify the spread along conjugate directions by the operator \hat{M} independent of the choice of state. The coefficient m_{00} accompanies the identity $\hat{1}$, and hence corresponds to no shift in either of the conjugate variables.

From $m_{b,a}$, which encodes amplitudes of shifts in both $\hat{\phi}$ and $\hat{\pi}$ eigenstates, we would like to extract profiles which illustrate the spreading features of \hat{M} in each conjugate variable separately. Since the coefficients $m_{b,a}$ depend on details of \hat{M} , in particular its norm, we define normalized amplitudes $\tilde{m}_{b,a}$ for these shifts,

$$\tilde{m}_{b,a} = \frac{m_{b,a}}{\sum_{b',a'=-l}^l |m_{b',a'}|}. \quad (5.38)$$

Then we define the $\hat{\phi}$ -shift profile of \hat{M} by marginalizing over all possible shifts in $\hat{\pi}$,

$$m_a^{(\phi)} = \sum_{b=-l}^l |\tilde{m}_{b,a}| = \frac{\sum_{b=-l}^l |m_{b,a}|}{\sum_{b',a'=-l}^l |m_{b',a'}|}, \quad (5.39)$$

which is a set of $(2l+1)$ positive numbers characterizing the relative importance of \hat{M} spreading the $\hat{\phi}$ variable by a units, $a = -l, \dots, 0, \dots, l$. Thus, \hat{M} acting on an eigenstate of $\hat{\phi}$, say $|\phi = j\rangle$, will, in general, result in a superposition over the support of the basis of the $\hat{\phi}$ eigenstates $\{|\phi = j + a \pmod{l}\rangle\} \forall a$, such that the relative importance (absolute value of the coefficients in the superposition) of each such term is upper bounded by $m_a^{(\phi)}$.

Let us now quantify this spread by defining *operator collimations* for each conjugate variable. Consider the ϕ -shift profile first. Operators with a large $m_a^{(\phi)}$ for small $|a|$ will have small spread in the $\hat{\phi}$ -direction, while those with larger $m_a^{(\phi)}$ for larger $|a|$ can be thought of connecting states further out on the lattice for each eigenstate.

Following this motivation, we define the ϕ -collimation C_ϕ of the operator \hat{M} as,

$$C_\phi(\hat{M}) = \sum_{a=-l}^l m_a^{(\phi)} \exp\left(-\frac{|a|}{2l+1}\right). \quad (5.40)$$

The exponential function suppresses the contribution of large shifts in our definition of collimation. There is some freedom in our choice of the decay function in our definition of operator collimation, and using an exponential function as in Eq. (7.27) is one such choice. Thus, an operator with a larger C_ϕ is highly collimated in the $\hat{\phi}$ -direction and does not spread out eigenstates with support on a large number of basis states on the lattice.

On similar lines, one can define the π -shift profile for \hat{M} as,

$$m_b^{(\pi)} = \sum_{a=-l}^l |\tilde{m}_{b,a}| = \frac{\sum_{a=-l}^l |m_{b,a}|}{\sum_{b',a'=-l}^l |m_{b',a'}|}, \quad (5.41)$$

and a corresponding π -collimation C_π with a similar interpretation as the $\hat{\phi}$ -case,

$$C_\pi(\hat{M}) = \sum_{b=-l}^l m_b^{(\pi)} \exp\left(-\frac{|b|}{2l+1}\right). \quad (5.42)$$

Operators such as $\hat{M}(\hat{\pi})$ that depend on only one of the conjugate variables will only induce spread in the $\hat{\phi}$ direction since they have $m_{b,a} = m_{0,a}\delta_{b,0}$, hence they possess maximum π -collimation, $C_\pi(\hat{M}) = 1$, as they do not spread eigenstates of $\hat{\pi}$ at all. Having a large contribution from terms such as $m_{0,0}, m_{b,0}, m_{0,a}$ will ensure larger operator collimation, since there are conjugate direction(s) where the operator has trivial action and does not spread the relevant eigenstates.

In general, we expect that operators which are additively separable in their arguments, $\hat{M}(\hat{\phi}, \hat{\pi}) = \hat{M}_\phi(\hat{\pi}) + \hat{M}_\pi(\hat{\phi})$, will have higher operator collimation as compared to a generic non-separable \hat{M} . Let us focus on operators depending only on one conjugate variable, say $\hat{M} \equiv \hat{M}(\hat{\pi})$. While the maximum value of $C_\pi(\hat{M}(\hat{\pi}))$ can be at most unity, one can easily see that the hermitian operator,

$$\hat{M}(\hat{\pi}) = \frac{A + A^\dagger}{2} = \frac{\exp(-i\alpha\hat{\pi}) + \exp(i\alpha\hat{\pi})}{2} = \cos(\alpha\hat{\pi}) = \hat{\mathbb{1}} - \frac{\alpha^2\hat{\pi}^2}{2} + \frac{\alpha^4\hat{\pi}^4}{4} - \dots, \quad (5.43)$$

has the least non-zero spread along the $\hat{\phi}$ direction: it connects only ± 1 shifts along eigenstates of $\hat{\phi}$ and hence has highest (non-unity) ϕ -collimation $C_\phi(\hat{M})$. Thus, one can expect that operators which are quadratic in conjugate variables are highly

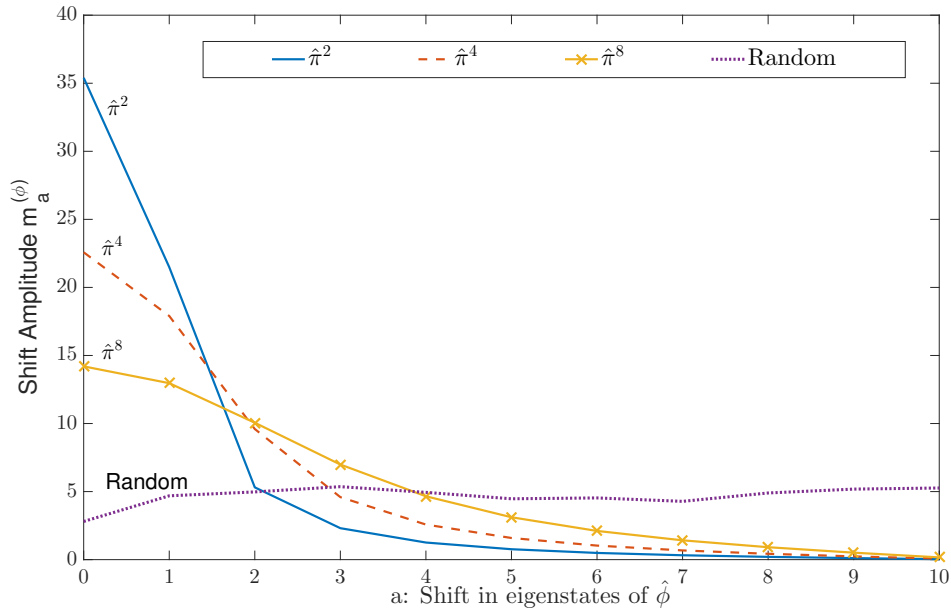


Figure 5.1: Plot showing $\hat{\phi}$ -shift profiles of various powers of $\hat{\pi}$. The quadratic operator $\hat{\pi}^2$ is seen to have the most collimated profile, implying that this operator does the least to spread the state in the conjugate direction. Also plotted is the profile for a random hermitian operator, for which the spread is approximately uniform.

collimated. We see that the fact that real-world Hamiltonians include terms that are quadratic in the momentum variables (but typically not higher powers) helps explain the emergence of classicality: it is Hamiltonians of that form that have high operator collimation, and therefore induce minimal spread in the position variable.

Let us follow this idea further. The quadratic operator $\hat{\pi}^2$ has higher ϕ -collimation than any other integer power $\hat{\pi}^n$, $n \geq 1$, $n \neq 2$. There is a difference between odd and even powers of $\hat{\pi}$, with even powers systematically having larger operator collimation than the odd powers. This is because odd powers of $\hat{\pi}$ do not have support on the identity $\hat{\mathbb{I}}$ term in the Schwinger unitary basis expansion (and hence have $m_{00} = 0$), and having an identity contribution boosts collimation since it contributes to the highest weight in C_ϕ by virtue of causing no shifts. In Figure (7.1), we plot the ϕ -shift profiles for a few powers of $\hat{\pi}$ and it is explicitly seen that quadratic $\hat{\pi}^2$ has the least spreading and hence is most $\hat{\phi}$ -collimated, values which are plotted in Figure (7.2). Note that due to the symmetry $|m_{b,a}| = |m_{-b,-a}|$, we only needed to plot the positive half for $a > 0$, which captures all the information about the spread. Also, for comparison, we also plot the ϕ -spread and its $\hat{\phi}$ -collimation of a “random”

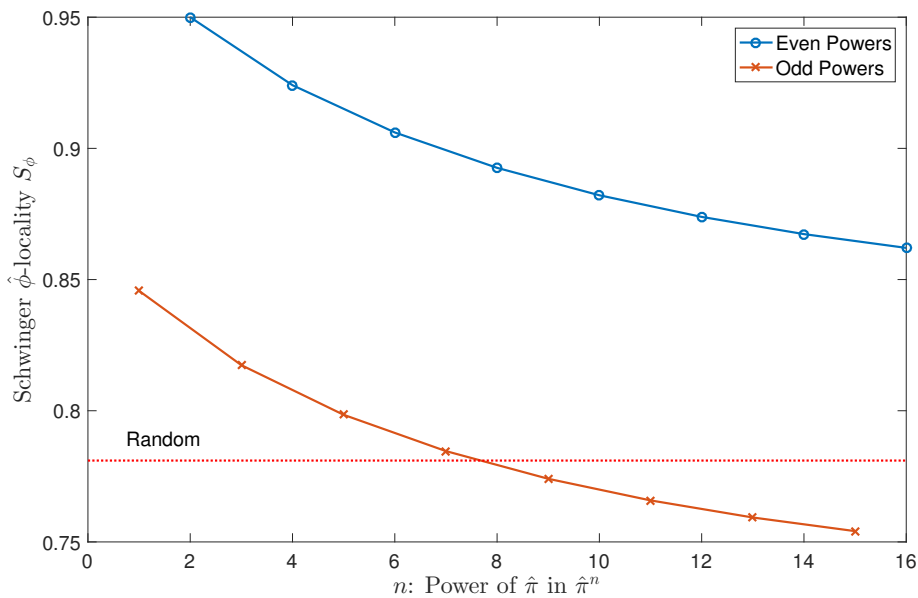


Figure 5.2: ϕ -collimation of various powers of $\hat{\pi}$. Even powers are seen to have systematically larger values of operator collimation. Also plotted for comparison is a line marking the ϕ -collimation of a random Hermitian operator.

Hermitian operator (one whose matrix elements in the $\hat{\phi}$ basis are chosen randomly from a normal distribution); such operators spread states almost evenly and thus have low values of operator collimation. These constructions will be used to study locality properties of Hamiltonians and other observables in our upcoming work on studying emergent classical structure on Hilbert space [29].

5.4 Finite-Dimensional Quantum Mechanics

Equations of Motion for Conjugate Variables

We would next like to understand equations of motion of conjugate variables defined by the GPO in a finite-dimensional Hilbert space evolving under a given Hamiltonian (and a continuous time parameter). In the large-dimension limit, and when appropriate classical structure has been identified on Hilbert space, conjugate variables $\hat{\phi}$ and $\hat{\pi}$ can be identified as position and momenta which satisfy Hamilton's equations of motion. As we will see, the structure of Hamilton's equations of motion is seen to emerge from basic algebraic constructions of the GPO when accompanied by an evolution by the Hamiltonian. Note that using the GPO, one can work with finite-dimensional phase space constructions, such as the discrete Wigner-Weyl construction, Gibbons-Hoffman-Wootters construction [124, 125], and further dis-

cussed by various other authors [107, 126–132] (and references therein). We will not discuss such finite-dimensional phase space ideas here, but rather focus on understanding the equations of motion for conjugate variables and how they connect to Hamilton’s equations.

Consider a Hamiltonian operator $\hat{H}^\dagger = \hat{H}$ on \mathcal{H} which acts as the generator of time translations. We wish to construct operators corresponding to “ $\partial H/\partial\phi$ ” and “ $\partial H/\partial\pi$,” and be able to connect them with time derivatives of $\hat{\phi}$ and $\hat{\pi}$. We saw that the operator \hat{A} from the GPO generates translations in the eigenstates of $\hat{\phi}$, and \hat{B} generates translations in eigenstates of $\hat{\pi}$. Notice that one can define a change in the ϕ variable as a finite central difference (we have used constraint $\alpha\beta = 2\pi(2l+1)$ from Eq. (5.29) which gives the eigenvalues of $\hat{\phi}$ from Eq. (5.32)),

$$\delta_\phi \hat{\phi} \equiv \left(\hat{A}^\dagger \hat{\phi} \hat{A} - \hat{A} \hat{\phi} \hat{A}^\dagger \right) \implies \langle \phi_j | \delta_\phi \hat{\phi} | \phi_{j'} \rangle = 2j\alpha \delta_{j,j'}, \quad (5.44)$$

up to “edge” terms in the matrix where the finite-difference scheme will not act in the usual way as it does on a lattice due to the cyclic structure of the GPO eigenstates. Following this, we can write the change in \hat{H} due to a change in the ϕ variable (translation in $\hat{\phi}$) as a central difference given by,

$$\delta_\phi \hat{H} \equiv \left(\hat{A}^\dagger \hat{H} \hat{A} - \hat{A} \hat{H} \hat{A}^\dagger \right). \quad (5.45)$$

This allows us to define an operator corresponding to $\partial H/\partial\phi$ based on these finite central difference constructions,

$$\left(\frac{\partial \hat{H}}{\partial \phi} \right) = \frac{1}{2\alpha} \left(\hat{A}^\dagger \hat{H} \hat{A} - \hat{A} \hat{H} \hat{A}^\dagger \right), \quad (5.46)$$

and similarly, for the change with respect to the other conjugate variable $\hat{\pi}$,

$$\left(\frac{\partial \hat{H}}{\partial \pi} \right) = \frac{1}{2\beta} \left(\hat{B}^\dagger \hat{H} \hat{B} - \hat{B} \hat{H} \hat{B}^\dagger \right). \quad (5.47)$$

The central difference is one possible construction of the finite derivative on a discrete lattice. One could use other finite difference schemes, but in the large-dimension limit, as we approach a continuous spectrum, any well-defined choice will converge to its continuum counterpart.

With this basic construction, let us now make contact with equations of motion (EOM) for the set of conjugate variables $\hat{\phi}$ and $\hat{\pi}$. We will work in the Heisenberg picture, where operators rather than states are time-dependent, even though we do

not explicitly label our operators with a time argument. The Heisenberg equation of motion for an operator $\hat{\mathcal{O}}$ that is explicitly time-independent ($\partial_t \hat{\mathcal{O}} = 0$) is,

$$\frac{d}{dt} \hat{\mathcal{O}} = i [\hat{H}, \hat{\mathcal{O}}] . \quad (5.48)$$

In particular, for the time evolution of $\hat{\pi}$, we expand the right hand side of Eq. (5.46) using the Baker-Campbell-Hausdorff formula, and isolate the commutator $i [\hat{H}, \hat{\pi}]$ that will be the time rate of change of $\hat{\pi}$. One can easily show that,

$$\frac{d}{dt} \hat{\pi} = i [\hat{H}, \hat{\pi}] = - \left(\frac{\partial H}{\partial \phi} \right)_{op} + \sum_{n=3}^{\text{odd}} \frac{i^n}{n!} \alpha^{n-1} [\hat{\pi}, \hat{H}]_n , \quad (5.49)$$

where we have defined $[\hat{\pi}, \hat{H}]_n$ as the n -point nested commutator in $\hat{\pi}$,

$$[\hat{\pi}, \hat{H}]_n = [\hat{\pi}, [\hat{\pi}, [\hat{\pi} \cdots (n \text{ times}), \hat{H}] \cdots]] . \quad (5.50)$$

The corresponding equation for $\hat{\phi}$ is likewise

$$\frac{d}{dt} \hat{\phi} = i [\hat{H}, \hat{\phi}] = \left(\frac{\partial H}{\partial \pi} \right)_{op} + \sum_{n=3}^{\text{odd}} \frac{i^n}{n!} \beta^{n-1} [\hat{\phi}, \hat{H}]_n . \quad (5.51)$$

In the infinite-dimensional limit, we take $l \rightarrow \infty$, and α and β are taken to be infinitesimal but obeying $\alpha\beta(2l + 1) = 2\pi$ to recover the Heisenberg CCR. As expected, the equations of motion simplify to resemble Hamilton's equations of motion from classical mechanics,

$$\frac{d}{dt} \hat{\pi} = i [\hat{H}, \hat{\pi}] = - \left(\frac{\partial H}{\partial \phi} \right)_{op} , \quad (5.52)$$

and

$$\frac{d}{dt} \hat{\phi} = i [\hat{H}, \hat{\phi}] = \left(\frac{\partial H}{\partial \pi} \right)_{op} . \quad (5.53)$$

These are intrinsically quantum equations for a set of conjugate variables from the GPO. They resemble the form of the classical equations of motion, but they do not necessarily describe quasiclassical dynamics. The emergence of quasiclassicality and identification of $\hat{\phi}$ and $\hat{\pi}$ with the classical conjugate variables of position and momentum is possible only in special cases when the substructure in Hilbert space allows for decoherence and robustness in the conjugate variables chosen. This is the concern of the quantum factorization problem of our upcoming work [29].

The Finite-Dimensional Quantum Harmonic Oscillator

With this technology of conjugate variables from the GPO, we can revisit some important models in quantum mechanics from a finite-dimensional perspective to compare the results with the usual infinite-dimensional results on $\mathbb{L}_2(\mathbb{R})$. All such results from finite-dimensional models will converge to the conventional infinite-dimensional ones when we take the limit $\dim \mathcal{H} \rightarrow \infty$.

We will focus on a finite-dimensional version of the harmonic oscillator. Consider the following Hamiltonian \hat{H} operator for an oscillator with “frequency” Ω on a finite-dimensional Hilbert space \mathcal{H} with $\dim \mathcal{H} = 2l + 1$, and let $\hat{\phi}$ and $\hat{\pi}$ be conjugate operators from the GPO,

$$\hat{H} = \frac{1}{2}\hat{\pi}^2 + \frac{1}{2}\Omega^2\hat{\phi}^2 = \Omega \left(\hat{a}^\dagger \hat{a} + \frac{1}{2} [\hat{a}, \hat{a}^\dagger] \right). \quad (5.54)$$

At this stage, $\hat{\phi}$ and $\hat{\pi}$ are dimensionless operators, and Ω is a dimensionless parameter, so the Hamiltonian is also dimensionless. One can define a change of variables,

$$\hat{a} = \sqrt{\frac{\Omega}{2}}\hat{\phi} + \frac{i}{\sqrt{2\Omega}}\hat{\pi}, \quad \hat{a}^\dagger = \sqrt{\frac{\Omega}{2}}\hat{\phi} - \frac{i}{\sqrt{2\Omega}}\hat{\pi}, \quad (5.55)$$

but as we will see, these will *not* serve as ladder or annihilation/creation operators in the finite-dimensional case, since the non-central nature of the commutator carries through, $[\hat{\phi}, \hat{\pi}] = i [\hat{a}, \hat{a}^\dagger] = i\hat{Z}$.

Due to finite-dimensionality of Hilbert space and finite separation between eigenvalues of the conjugate variables, standard textbook results such as a uniformly spaced eigenspectrum will no longer hold. Depending on the interplay of eigenvalues of $\hat{\pi}$ and $\Omega\hat{\phi}$, there is an effective separation of scales, and correspondingly, the eigenvalue spectrum will have different features to reflect this. In the infinite-dimensional case, for any finite Ω , the spectra of $\hat{\pi}$ and $\Omega\hat{\phi}$ match, since the conjugate operators have continuous, unbounded eigenvalues (the reals \mathbb{R}). In this sense, there is more room for non-trivial features in the finite-dimensional oscillator as compared to the infinite case.

In the eigenbasis of $\hat{\phi}$, the matrix elements of the Hamiltonian are,

$$[\hat{H}]_{jj'} = \begin{cases} \sum_{n \neq j} \frac{\pi}{4(2l+1)} \csc^2 \left(\frac{2\pi l}{2l+1} (j-n) \right) + \frac{\Omega^2 \pi}{2l+1} j^2, & \text{if } j = j' \\ \sum_{n \neq j, n \neq j'} \frac{\pi}{4(2l+1)} \csc \left(\frac{2\pi l}{2l+1} (j-n) \right) \csc \left(\frac{2\pi l}{2l+1} (n-j') \right), & \text{if } j \neq j' \end{cases} \quad (5.56)$$

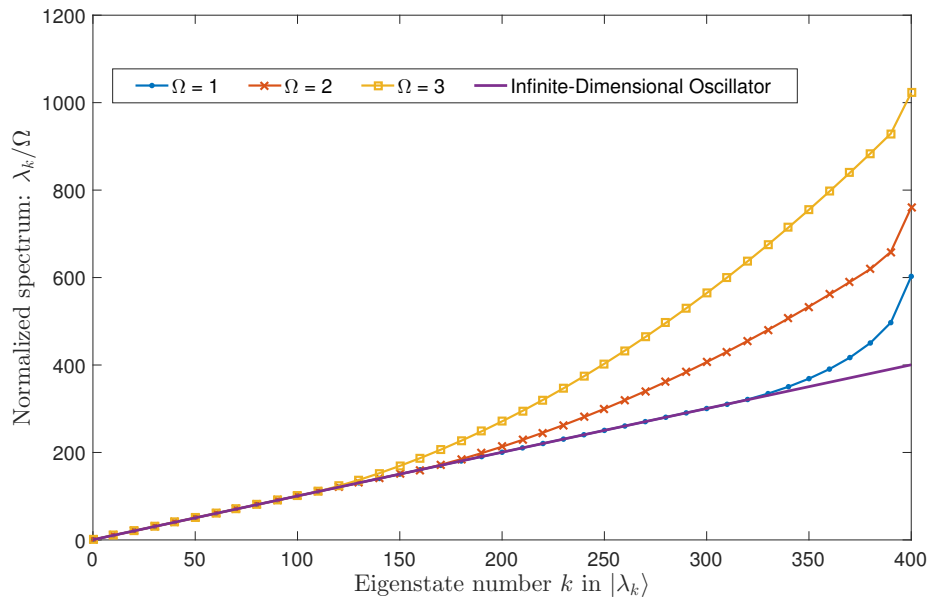


Figure 5.3: Eigenspectrum (normalized by Ω) for a $\dim \mathcal{H} = 401$ ($l = 200$) finite-dimensional oscillator for different values of Ω . Depending on the value of Ω , the spectrum deviates from the vanilla spectrum of the infinite-dimensional oscillator, which has also been plotted for comparison.

where we have used the constraint $\alpha = \beta = \sqrt{2\pi/2l + 1}$ as described in Section (5.2), and all sums and indices run from $-l, \dots, 0, \dots, l$. In the infinite-dimensional case, one can solve for the spectrum of the harmonic oscillator and obtain equispaced eigenvalues, which we refer to as the “vanilla” spectrum,

$$\lambda_n^{(\text{vanilla})} = \left(n + \frac{1}{2}\right) \Omega, n = 0, 1, 2, \dots \quad (5.57)$$

The finite-dimensional case is more involved and we were unable to find an analytic, closed form for the spectrum $\{\lambda_k\}$ in terms of l and Ω . We can solve for the spectrum numerically for different values of l and Ω , and here we point out a few important features.

First, consider the spectra of various oscillators with different Ω and how they compare with the vanilla, infinite-dimensional spectrum. In Figure (5.3), we plot the spectrum for a $\dim \mathcal{H} = 401$ ($l = 200$) finite-dimensional oscillator for different values of Ω . Depending on how much Ω breaks the symmetry between eigenstates of $\hat{\pi}$ and $\Omega\hat{\phi}$ (corresponding to $\max(\Omega, 1/\Omega)$), the spectrum of the finite oscillator deviates from the vanilla, infinite-dimensional case and is no longer uniformly spaced. For the lower eigenvalues (what constitutes “lower” depends on Ω), both

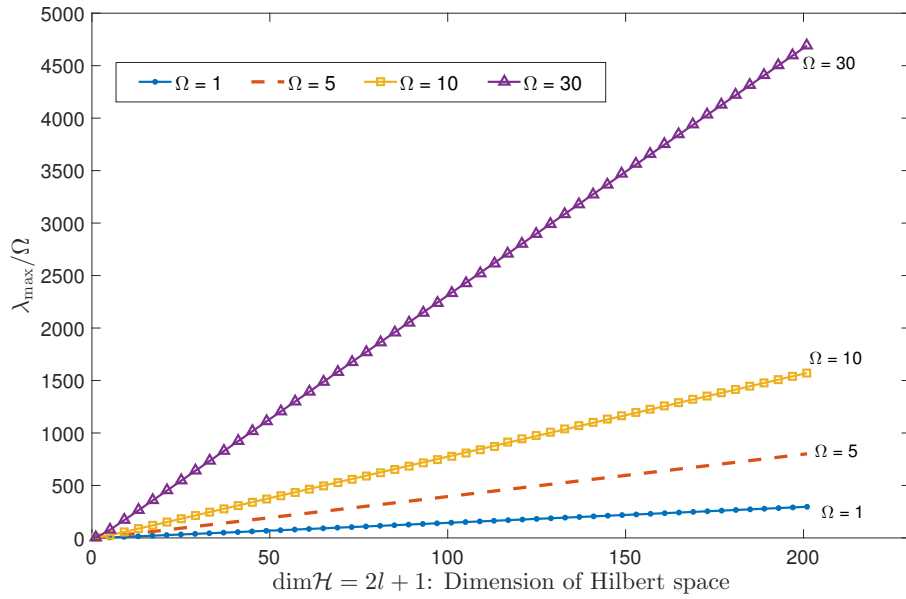


Figure 5.4: Plot of the maximum eigenvalue (normalized by Ω) of the finite-oscillator as a function of dimension $\dim \mathcal{H} = 2l + 1$ for different values of Ω . A linear trend is observed.

spectra match, and for larger eigenvalues, the finite-dimensional oscillator is seen to have larger values as compared to the vanilla case. On the same figure, we have also plotted part of the equispaced vanilla spectrum (which holds in infinite dimensions) for comparison. Another important feature to consider is the maximum eigenvalue of \hat{H} , λ_{\max} . While there is no maximum eigenvalue in the infinite-dimensional case, we find that λ_{\max} has almost linear behavior in the dimension $\dim \mathcal{H}$ of Hilbert space, as plotted in Figure (5.4).

A bound for λ_{\max} can easily be given,

$$\lambda_{\max} \leq \frac{1}{2} (1 + \Omega^2) (l\alpha)^2 = \frac{\pi l^2}{2l + 1} (1 + \Omega^2), \quad (5.58)$$

where we have used the fact that for Hermitian matrices P, Q , and R such that $P = Q + R$, the maximum eigenvalue of P is at most the sum of maximum eigenvalues of Q and R .

At the other end, while the minimum eigenvalue, normalized by Ω , has a constant $1/2$ value for the vanilla, infinite-dimensional oscillator, we find a richer structure for the minimum eigenvalue of the finite oscillator, plotted in Figure (5.5). This is itself a reflection of the non-centrality of the commutator $[\hat{a}, \hat{a}^\dagger] \neq 1$, and we see how the

lowest eigenvalue normalized by Ω is suppressed for larger values of Ω for a given Hilbert space. These features of the finite-dimensional oscillator spectrum could

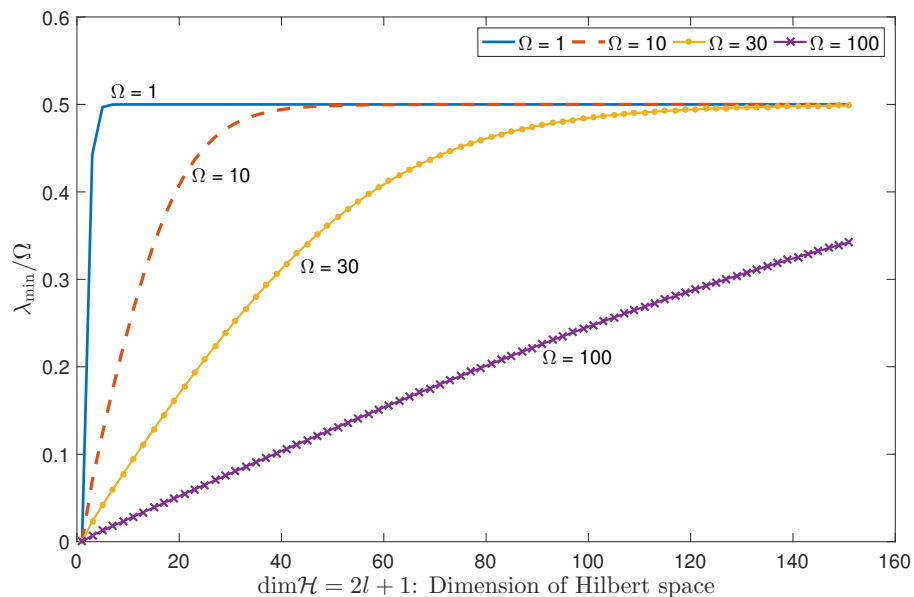


Figure 5.5: Plot of the minimum eigenvalue (normalized by Ω) of the finite-oscillator as a function of dimension $\dim \mathcal{H} = 2l + 1$ for different values of Ω . A gradual build-up is noticed, with more suppression for larger Ω for a given \mathcal{H} , which saturates to the vanilla, infinite-dimensional result of $\lambda_{\min}/\Omega = 0.5$.

play a crucial role in the physics of locally finite-dimensional models of quantum gravity.

5.5 Discussion

Quantum-mechanical models have been extensively studied in both finite- and infinite-dimensional Hilbert spaces; the connection between the two contexts is less well-understood, and has been our focus in this paper. Infinite-dimensional models are often constructed by quantizing classical systems that have a description in terms of phase space and conjugate variables. We have therefore studied the Generalized Pauli operators as a tool for adapting a form of conjugate variables to the finite-dimensional case, including the appropriate generalization of the Heisenberg canonical commutation relations.

An advantage of the GPO is that it is completely general, not relying on any pre-existing structure or preferred algebra of observables. This makes it a useful tool for investigating situations where we might not know ahead of time what such observ-

ables should be, such as in quantum gravity. We have investigated the development of position/momentum variables, and an associated notion of operator collimation, within this framework. This analysis revealed hints concerning the special nature of the true Hamiltonian of the world, especially the distinction between position and momentum and the emergence of local interactions (and therefore of space itself).

As we have seen, features of a theory based on an intrinsic finite-dimensional Hilbert space can be very different than one based on naive truncation of an infinite-dimensional one. This is particularly seen in the example of the finite-dimensional quantum harmonic oscillator discussed in Section 5.4, where the spectrum of the oscillator differs from a simple truncation of the vanilla spectrum based on the infinite-dimensional oscillator. A consistent finite-dimensional construction applied to field theory could have important consequences for issues such as the hierarchy problem, the cosmological constant problem, and Lorentz violation, and may lead to corrections in Feynman diagrams for given scattering problems. In addition to its possible role in field theory, modifications to the commutation relation of conjugate variables (departure from it being a commuting number) can further lead to modifications to uncertainty relations. It has been shown [133–136] (and references therein) that taking into account gravitational effects will lead to modified commutation relations, and the GPOs can provide a natural way to understand these in terms of the local dimension of Hilbert space in a theory with gravity. The GPO can also play an important role in our understanding of emergent classicality in a finite-dimensional setting, where in some preferred factorization of Hilbert space into sub-systems, the conjugate variables can be identified as classical conjugates such as positions and momenta.

Constructions based on the GPO have also been shown to be important in quantum error correction and fault tolerance [137], where one can further try and quantify robustness of different operators based on a notion of operator collimation. Once dynamics is added to the problem, one can study the operator collimation of operators as a function of time, understanding how their support on Hilbert space evolves, and this can be connected with ideas in quantum chaos and out-of-time-ordered-correlators (OTOCs) [138].

In future work, we plan to further explore the emergence of spacetime and quantum field theory in a locally finite-dimensional context.

*Chapter 6***HOW LOW CAN VACUUM ENERGY GO WHEN YOUR FIELDS ARE FINITE-DIMENSIONAL**

According to the holographic bound, there is only a finite density of degrees of freedom in space when gravity is taken into account. Conventional quantum field theory does not conform to this bound, since in this framework, infinitely many degrees of freedom may be localized to any given region of space. In this chapter, we explore the viewpoint that quantum field theory may emerge from an underlying theory that is locally finite-dimensional, and we construct a locally finite-dimensional version of a Klein-Gordon scalar field using generalized Clifford algebras. Demanding that the finite-dimensional field operators obey a suitable version of the canonical commutation relations makes this construction essentially unique. We then find that enforcing local finite dimensionality in a holographically consistent way leads to a huge suppression of the quantum contribution to vacuum energy, to the point that the theoretical prediction becomes plausibly consistent with observations.

This chapter is based on the following reference:

C. Cao, A. Chatwin-Davies, and A. Singh, “How low can vacuum energy go when your fields are finite-dimensional?,” *Int. J. Mod. Phys. D* **28** no. 14, (2019) 1944006, [arXiv:1905.11199](https://arxiv.org/abs/1905.11199) [hep-th]

6.1 Introduction: Gravity and Quantum Field Theory

A quantum field theory has infinitely many degrees of freedom in any given region of space. In the presence of gravity, when we try to excite such degrees of freedom that are supported on a compact region, many of the resulting states would collapse the region into a black hole. Recall that a black hole has a finite amount of entropy which scales as the area of its horizon. Therefore, any attempts to increase the region’s entropy by creating further excitations would only increase the size of the resulting black hole, and hence also the size of its supporting region. Such considerations suggest that the amount of entropy that can be localized in a compact region of space is finite [17, 20, 21, 36–39, 65]. This idea is succinctly expressed through the holographic bound [78, 79], which says that the amount of entropy in a spacelike

region \mathcal{R} is bounded by the area of its boundary in Planck units,

$$S(\mathcal{R}) \leq \frac{|\partial\mathcal{R}|}{4\ell_{\text{Pl}}^2}. \quad (6.1)$$

If we turn it around, the holographic bound, as well as its covariant generalizations [42], says that only finitely many degrees of freedom could have been localized to a compact region of space in the first place. The von Neumann entropy of a maximally mixed state in a Hilbert space of dimension $\exp(|\partial\mathcal{R}|/4\ell_{\text{Pl}}^2)$ is enough to saturate the holographic bound, and so the degrees of freedom localized to \mathcal{R} can have at most this number of orthogonal microstates. In other words, the Hilbert space of a gravitating system is locally finite-dimensional.

At a first glance, it would therefore seem that quantum field theory is in conflict with the local finite dimensionality implied by gravity. One way of addressing this conflict is to work within the framework of quantum field theory and introduce regulators so that it has effective finite dimension, e.g., through suitable infrared (IR) and ultraviolet (UV) cutoffs. Another approach is to view the effective low energy behavior of quantum field theory as something that must emerge from a theory that is intrinsically locally finite-dimensional.

We will explore the latter stance in this essay and construct a finite-dimensional version of an effective scalar field theory, in particular for which each mode cannot carry arbitrarily many excitations. We will see that an automatic consequence of intrinsic finite dimensionality and the holographic bound is a tremendous suppression of the quantum contribution to vacuum energy compared to the prediction of conventional field theory. Many authors before us have argued for observable consequences of holography in gravity, including corrections to vacuum energy [140–143]; this chapter offers a fresh perspective on this line of reasoning through intrinsic finite dimensionality.

6.2 Finite-Dimensional Effective Field Theory

Finite-Dimensional Field Operators

In a conventional infinite-dimensional setting, such as the non-relativistic quantum mechanics of a single particle, classical conjugate variables ϕ and π are promoted to linear Hilbert space operators which obey the Heisenberg canonical commutation relation (CCR)

$$[\hat{\phi}, \hat{\pi}] = i, \quad (6.2)$$

where we have set $\hbar = 1$. In a quantum field theory, the field and its conjugate momentum are operator-valued functions on spacetime which obey a continuous version of the CCR, labelled by spacetime points.

The Stone-von Neumann theorem guarantees that there is an irreducible representation of Eq. (6.2), which is unique up to unitary equivalence, on any infinite-dimensional Hilbert space that is separable (i.e., that possesses a countable dense subset) [2]. However, in this case, the theorem also implies that the operators $\hat{\phi}$ and $\hat{\pi}$ must be unbounded. There are therefore no irreducible representations of Eq. (6.2) on finite-dimensional Hilbert spaces.

Instead, consider the following commutation relation due to Weyl [77] on a finite-dimensional Hilbert space of dimension d :

$$e^{-i\alpha\hat{\pi}} e^{i\beta\hat{\phi}} = e^{-i\alpha\beta} e^{i\beta\hat{\phi}} e^{-i\alpha\hat{\pi}}. \quad (6.3)$$

This is an exponentiated form of Heisenberg's CCR in the sense that, if the real parameters α and β are chosen such that $\alpha\beta = 2\pi/d$, then Eq. (6.3) is equivalent to Eq. (6.2) in the limit as $d \rightarrow \infty$. The operators $\hat{\phi}$ and $\hat{\pi}$ defined through Weyl's CCR do admit an irreducible representation on a Hilbert space with finite dimension d . Moreover, the representation is still unique up to unitary equivalence via the Stone-von Neumann theorem, since a finite-dimensional Hilbert space is separable.

The generalized Clifford algebra (GCA) [9, 10, 76, 90, 91] provides a simple way to write down the operators $\hat{\phi}$ and $\hat{\pi}$. For example, let the dimension of Hilbert space be $d = 2l + 1$ for some non-negative integer l . (The construction works when the dimension is even too, but we focus on odd values to streamline the notation.) The GCA is generated by two unitary matrices

$$\hat{A} = \begin{pmatrix} 0 & 0 & 0 & \cdots & 0 & 1 \\ 1 & 0 & 0 & \cdots & 0 & 0 \\ 0 & 1 & 0 & \cdots & 0 & 0 \\ \vdots & \vdots & \vdots & \ddots & \vdots & \vdots \\ 0 & 0 & 0 & \cdots & 0 & 0 \\ 0 & 0 & 0 & \cdots & 1 & 0 \end{pmatrix} \quad \hat{B} = \begin{pmatrix} \omega^{-l} & 0 & \cdots & 0 \\ 0 & \omega^{-l+1} & \cdots & 0 \\ \vdots & \vdots & \ddots & \vdots \\ 0 & 0 & \cdots & \omega^l \end{pmatrix}, \quad (6.4)$$

which satisfy the commutation relation $\hat{A}\hat{B} = \omega^{-1}\hat{B}\hat{A}$ and multiplicative closure $\hat{A}^d = \hat{B}^d = \mathbb{I}_d$, where $\omega = \exp(2\pi i/d)$. The identification $\hat{A} \equiv \exp(-i\alpha\hat{\pi})$ and $\hat{B} \equiv \exp(i\beta\hat{\phi})$ then realizes Eq. (6.3). These conjugate operators $\hat{\phi}$ and $\hat{\pi}$ from the GCA each have a bounded, linearly-spaced, discrete spectrum of dimensionless

eigenvalues. In the infinite-dimensional limit, they reduce to the usual conjugate operators with unbounded spectra and obey the Heisenberg CCR.

Vacuum Energy

Let us now use these finite-dimensional conjugate operators to construct a finite-dimensional version of a scalar field theory. Consider first a scalar field in a three-dimensional box of side length L with the usual Klein-Gordon Hamiltonian, which we can decompose in terms of its Fourier modes,

$$\hat{H} = \sum_{\vec{k}} \hat{H}_{\vec{k}} = \frac{1}{L} \sum_{\vec{k}} \left(\frac{1}{2} \hat{\pi}_{\vec{k}}^2 + \frac{1}{2} \Omega_k^2 \hat{\phi}_{\vec{k}}^2 \right). \quad (6.5)$$

This Hamiltonian describes a number of decoupled quantum harmonic oscillators, one for each mode \vec{k} with natural frequency Ω_k . We have pulled out a factor of $1/L$ in the equation above so that the $\hat{\phi}_{\vec{k}}$'s and $\hat{\pi}_{\vec{k}}$'s are dimensionless. Similarly, each $\Omega_k \equiv kL$ is a dimensionless frequency, where $k \equiv |\vec{k}|$. Since we have cast the Hamiltonian in terms of dimensionless operators, we can obtain a finite-dimensional theory by simply replacing the $\hat{\phi}_{\vec{k}}$'s and $\hat{\pi}_{\vec{k}}$'s with the (dimensionless) finite-dimensional operators described above. Letting the Hilbert space dimension d_k of each mode go to infinity restores the original Klein-Gordon theory. For finite dimension d_k , however, the spectrum of each $\hat{H}_{\vec{k}}$ is not linearly spaced and possesses both maximum and minimum eigenvalues which depend on the values of Ω_k as well as d_k [10].

To fix the d_k 's, we come back to the question of creating black holes. A gravitationally-acquainted effective field theory should cut off below any excitations that would collapse into black holes. Therefore, it is natural to impose that the largest energy eigenvalue for each mode k should not exceed the Schwarzschild energy of the box. The largest energy eigenvalue is fixed according to the finite-dimensional construction of conjugate variables introduced in the previous section. As is discussed in Ref. [10], the largest eigenvalue of each finite-dimensional conjugate operator, $\hat{\phi}_{\vec{k}}$ and $\hat{\pi}_{\vec{k}}$, is $l\sqrt{2\pi/(2l+1)}$. Then, from Horn's inequalities [144, 145], one can consequently show that the largest eigenvalue of \hat{H}_k is tightly bounded by

$$E_{\max}(k) \leq \frac{\pi\Omega_k^2 d_k}{4L}. \quad (6.6)$$

By demanding that $E_{\max}(k)$ be less than $\sim Lm_{pl}^2/4$, we arrive at

$$d_k \lesssim \frac{L^2 M_{pl}^2}{\pi\Omega_k^2}. \quad (6.7)$$

In particular, this bound suppresses the dimension of high-frequency modes and defines a smallest mode residing at $k = m_{\text{Pl}}/\sqrt{\pi}$, for which $d_k = 1$. Note that this construction is inherently different from simply truncating every Klein-Gordon mode's usual spectrum, each of which is that of an infinite-dimensional harmonic oscillator.

Let us now examine the minimum energy eigenvalue of each mode. $E_{\min}(k)$ is always bounded above by $k/2$, the zero point energy of an infinite dimensional oscillator, and lowering the value of d_k lowers the value of $E_{\min}(k)$; this is illustrated in Fig. 6.1. Therefore, the bound (6.7) also suppresses $E_{\min}(k)$, with the suppression becoming increasingly severe at higher frequencies.

In summary, we find that imposing a finite dimension that prevents each mode from exceeding the box's Schwarzschild energy reduces the ground state energy of each field mode. The quantum contribution to total vacuum energy density will consequently be lowered as well, even when summing over modes all the way to the Planck scale. While our finite-dimensional field-in-a-box is not a precise cosmological model, we can get a sense for what the size of the effect might be for our Hubble patch by taking the box size L to be the current Hubble radius. The resulting vacuum energy density that we compute is

$$\begin{aligned} \rho_0^{GCA} &= \frac{1}{L^3} \sum_{\vec{k}} E_{\min}(k) \\ &\approx \frac{1}{L^3} \int_{L^{-1}}^{m_{\text{Pl}}/\sqrt{\pi}} dk 4\pi k^2 \left(\frac{L}{\pi}\right)^3 E_{\min}(k) \lesssim (10^4 \text{ GeV})^4. \end{aligned} \quad (6.8)$$

This is 60 orders of magnitude lower than the naïve counting of vacuum energy density contribution from a free Klein-Gordon field,

$$\begin{aligned} \rho_0^{KG} &= \frac{1}{L^3} \sum_{\vec{k}} \frac{k}{2} \\ &\approx \frac{1}{L^3} \int_{L^{-1}}^{m_{\text{Pl}}} dk 4\pi k^2 \left(\frac{L}{\pi}\right)^3 \frac{k}{2} \sim (10^{19} \text{ GeV})^4. \end{aligned} \quad (6.9)$$

6.3 Conclusion: Hilbert Space and Holography

While an intrinsically finite-dimensional version of a scalar field results in a vastly smaller vacuum energy compared to the original infinite-dimensional theory, it is still many orders of magnitude above the observed value, $\rho_0 \lesssim (10^{-11} \text{ GeV})^4$ [146, 147]. However, this is because our simple estimate still counts many more

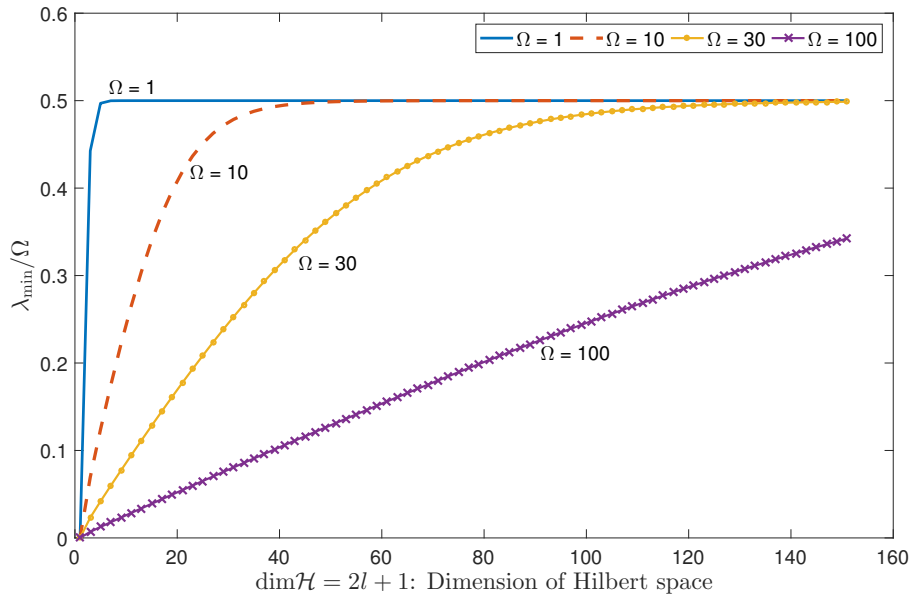


Figure 6.1: Minimum energy eigenvalue for a finite-dimensional field mode, normalized by Ω/L , as a function of the dimension d and for several values of Ω .

states than allowed by the holographic bound. This can be seen by setting d_k equal to the bound (6.7) and computing the dimension, D , of the total Hilbert space:

$$\log D = \sum_{\bar{k}} \log d_k \approx \int_{L^{-1}}^{m_{\text{Pl}}/\sqrt{\pi}} dk 4\pi k^2 \left(\frac{L}{\pi}\right)^3 \log d_k \sim (Lm_{\text{Pl}})^3 + \mathcal{O}(\log(Lm_{\text{Pl}})). \quad (6.10)$$

According to the holographic bound, this should be no more than $S \sim (Lm_{\text{Pl}})^2$.

Local finite dimension according to Eq. (6.7) alone is therefore not the end of the story. There will also be a holographic depletion of states, which should be strongest in the UV [148, 149]. This can be understood heuristically by noting that the density of field theoretic degrees of freedom is observed to scale extensively in the IR, and also that many otherwise-valid states would collapse to form black holes in the UV. For example, exciting every Klein-Gordon mode up to $k \sim 1$ meV is already enough to reach the Schwarzschild energy of our universe-sized box.

In a crude attempt to model this holographic depletion of states, we can try modifying the density of modes $g(k) dk = 4\pi k^2 dk$ by setting

$$\tilde{g}(k) = \begin{cases} 4\pi k^2 & L^{-1} < k < k_* \\ 2\pi k & k_* < k < m_{\text{Pl}}/\sqrt{\pi} \end{cases}. \quad (6.11)$$

Taking the crossover to lie at $k_* \sim 1$ meV, we find that the vacuum energy is reduced to $\rho_0^{GCA} \lesssim (10^{-10} \text{ GeV})^4$, which is consistent with the observed value of vacuum energy to within an order of magnitude. This result should be taken with a grain of salt, however, due to the delicate interplay between the finite oscillator dimensions d_k and the density of modes $\tilde{g}(k)$, which we have yet to investigate in detail. Nevertheless, the calculation discussed here for vacuum energy illustrates that taking finite dimensionality and holography together seriously can have important predictive consequences for gravity.

Part III

Structure in Hilbert Space

Chapter 7

QUANTUM MEREOLGY: FACTORIZING HILBERT SPACE INTO SUBSYSTEMS WITH QUASI-CLASSICAL DYNAMICS

We study the question of how to decompose Hilbert space into a preferred tensor-product factorization without any pre-existing structure other than a Hamiltonian operator, in particular the case of a bipartite decomposition into “system” and “environment.” Such a decomposition can be defined by looking for subsystems that exhibit quasi-classical behavior. The correct decomposition is one in which pointer states of the system are relatively robust against environmental monitoring (their entanglement with the environment does not continually and dramatically increase) and remain localized around approximately-classical trajectories. We present an in-principle algorithm for finding such a decomposition by minimizing a combination of entanglement growth and internal spreading of the system. Both of these properties are related to locality in different ways. This formalism could be relevant to the emergence of spacetime from quantum entanglement.

This chapter is based on the following reference:

S. M. Carroll and A. Singh, “Quantum Mereology: Factorizing Hilbert Space into Subsystems with Quasi-Classical Dynamics,” [arXiv:2005.12938](https://arxiv.org/abs/2005.12938) [quant-ph]

7.1 Introduction

If someone hands you two qubits A and B , there is a well-understood procedure for constructing the quantum description of the composite system constructed from the two of them. If the individual Hilbert spaces are $\mathcal{H}_A \simeq \mathbb{C}^2$ and $\mathcal{H}_B \simeq \mathbb{C}^2$, the composite Hilbert space is given by the tensor product, $\mathcal{H} \simeq \mathcal{H}_A \otimes \mathcal{H}_B \simeq \mathbb{C}^4$, where \simeq represents isomorphism. The total Hamiltonian is the sum of the two self-Hamiltonians, \hat{H}_A and \hat{H}_B , acting on \mathcal{H}_A and \mathcal{H}_B , respectively, plus an appropriate interaction term, \hat{H}_{int} , coupling the two factors.

What about the other way around? If someone hands you a four-dimensional Hilbert space and a Hamiltonian, is there a procedure by which we can factorize the system into the tensor product of two qubits? In general there will be an infinite number of

possible factorizations, each defined by a bijection of the form

$$\lambda : \mathcal{H} \rightarrow \mathcal{H}_A \otimes \mathcal{H}_B. \quad (7.1)$$

Unitary transformations \hat{U} can be used to define different bijections,

$$\tilde{\lambda} = \lambda \circ \hat{U} : \mathcal{H} \rightarrow \mathcal{H}_A \otimes \mathcal{H}_B. \quad (7.2)$$

While some unitaries will simply induce rotations within the factors \mathcal{H}_A and \mathcal{H}_B , generically the factorization defined by $\tilde{\lambda}$ will not be equivalent to that defined by λ . Is there some notion of the “right” factorization for a given physical situation?

In almost all applications, these questions are begged rather than addressed. When someone hands us two spin-1/2 particles, it seems obvious how to assign Hilbert spaces to each and form the relevant tensor product. But there are circumstances, perhaps including quantum gravity, when we might know nothing more than the total Hilbert space and the Hamiltonian (and perhaps a specified initial state), and want to use that information to reverse-engineer a sensible notion of what physical system is being described, including what its individual parts are [65]. This is the subject of “Quantum Mereology,” where “mereology” is the study of how parts relate to the whole. It is especially important in the context of finite-dimensional Hilbert spaces, where any Hermitian operator defines an observable, and there is no notion of preferred observables that can be used to define a corresponding factorization.

In this paper we seek to address this problem in a systematic way. Given nothing more than a Hilbert space of some dimensionality, the Hamiltonian, and an initial state, what is the best way to factorize Hilbert space into subsystems? Since we are not given a preferred factorization to begin with, there is no preferred basis other than the eigenstates of the Hamiltonian. The Hamiltonian itself is therefore specified by its spectrum (the set of energy eigenvalues), and the initial state by its components in the energy eigenbasis. Our task is to use this meager data to find the most useful way of decomposing Hilbert space into tensor factors.

The key here is “useful,” and we interpret this as meaning “allows for a quasi-classical description of the dynamics within the subsystems (or one subsystem coupled to an environment).” A well-understood feature of conventional quantum dynamics is the selection of pointer states of a system that is being monitored by an environment. In general the reduced density matrix of the system can always be diagonalized in some basis, but for systems that can exhibit quasi-classical behavior, the pointer states define a basis in which the system’s density matrix will rapidly approach

a diagonal form. These pointer states then obey quasi-classical dynamics. This implies in particular that a system in a pointer state remains relatively unentangled with the environment, and that we can define pointer observables that approximately obey classical equations of motion. This suggests a criterion for determining the proper system/environment factorization: choose the tensor-product decomposition in which the system has a pointer basis that most closely adheres to these properties. As we will see, generic Hamiltonians will have no such decomposition available, so quasi-classical behavior is non-generic.

In this paper we develop an algorithm for making this criterion precise. For any given decomposition, we start with an unentangled state, and calculate the growth of entanglement. Since our interest is in finite-dimensional Hilbert spaces [17, 20, 21], we use Generalized Pauli Operators (which have their algebraic roots in generalized Clifford algebra) to define conjugate operators \hat{q} and \hat{p} ; in the infinite-dimensional limit, these obey the Heisenberg canonical commutation relations. The position operator \hat{q} is the one that appears in the interaction Hamiltonian. We can then calculate the rate of spread of the uncertainty in the position variable. Both the entanglement between system and environment and the spread of the system's position can be characterized by an entropy. Our criterion is that the correct decomposition minimizes the maximum of these two entropies, for initially localized and unentangled states.

While this question has not frequently been addressed in the literature on quantum foundations and emergence of classicality, a few works have highlighted its importance and made attempts to understand it better. Brun and Hartle [150] studied the emergence of preferred coarse-grained classical variables in a chain of quantum harmonic oscillators. Efforts to address the closely related question of identifying classical set of histories (also known as the "Set Selection" problem) in the Decoherent Histories formalism [115, 151–155] have also been undertaken. Tegmark [28] has approached the problem from the perspective of information processing ability of subsystems and Piazza [114] focuses on emergence of spatially local subsystem structure in a field theoretic context. Hamiltonian induced factorization of Hilbert space which exhibit k -local dynamics has also been studied by Cotler *et al* [22]). The idea that tensor product structures and virtual subsystems can be identified with algebras of observables was originally introduced by Zanardi *et al* in [156, 157] and was further extended in Kabernik, Pollack and Singh [158] to induce more general structures in Hilbert space. In a series of papers (e.g. [159–162]; see also [163])

Castagnino, Lombardi, and collaborators have developed the self-induced decoherence (SID) program, which conceptualizes decoherence as a dynamical process which identifies the classical variables by inspection of the Hamiltonian, without the need to explicitly identify a set of environment degrees of freedom. Similar physical motivations but different mathematical methods have led Kofler and Brukner [164] to study the emergence of classicality under restriction to coarse-grained measurements.

The paper is organized as follows. Section 7.2 describes the important features of a quasi-classical factorization, settling on two important features: “robustness,” referring to slow growth of entanglement between pointer states and the environment, and “predictability,” meaning that pointer observables approximately obey classical equations with low variance. We emphasize how these features will not be manifest in any arbitrary factorization and use a bipartite example to demonstrate these characteristics. We then examine these two features in turn. Section 7.3 considers robustness, showing that it is non-generic, and investigating what kinds of decompositions will minimize the growth of entanglement. Section 7.4 we derive conditions for the existence of classical behavior of the system interacting with its environment. These include the “collimation” of the self-Hamiltonian, needed to ensure that initially peaked states remain relatively peaked, and the pointer observables approximately obeying classical equations of motion. In section 7.5, we will outline an algorithm to sift through different decompositions of Hilbert space, given a Hamiltonian to pick out the one with manifest quasi-classicality. We will define an entropy-based quantity that we call *Schwinger Entropy* whose minimization ensures the existence of low entropy states that are both resistant to entanglement production and have a pointer observable that evolves quasi-classically. We close with a worked example and some discussion.

7.2 Factorization and Classicality

There is a great deal of freedom in the choice of factorization of Hilbert space corresponding to different subsystems. In principle any factorization can be used, or none; for purposes of unitary dynamics, one is free to express the quantum state however one chooses. For purposes of pinpointing quasi-classical behavior, however, choosing the right factorization into system \mathcal{S} and environment \mathcal{E} is crucial. Similar considerations will apply to further factorization of the system into subsystems. Let us therefore review what is meant by “quasi-classical behavior.”

Consider a bipartite split of a finite-dimensional Hilbert space $\mathcal{H} \equiv (\mathcal{A} \otimes \mathcal{B})_{\{\theta\}}$ into subsystems \mathcal{A} and \mathcal{B} in a factorization labeled by $\{\theta\}$ relative to some arbitrary chosen one. (In Appendix 7.7 we establish some notation and formulae relevant to factorizations and transformations between them.) The dimension of \mathcal{A} is $\dim \mathcal{A} = d_A$ and $\dim \mathcal{B} = d_B$, with $\dim \mathcal{H} = D = d_A d_B$. The Hamiltonian \hat{H} in this decomposition can be written as a sum of self terms and an interaction term, following Eq. (7.64),

$$\hat{H} = \hat{H}_A \otimes \hat{\mathbb{1}}_B + \hat{\mathbb{1}}_A \otimes \hat{H}_B + \hat{H}_{\text{int}} . \quad (7.3)$$

We only consider traceless Hamiltonians, so there is no need for a trace term $h_0 = \text{Tr} \hat{H}/D$. Under factorization changes, even though $\text{Tr} \hat{H}$ is preserved, there would be an ambiguity in assigning the trace terms to either of the self-Hamiltonians of \mathcal{A} or \mathcal{B} . Also, since we are not considering gravity as an external field, subtracting off a constant from \hat{H} is physically trivial.

The form of the Hamiltonian is dependent on the choice of the decomposition $\{\theta\}$. The interaction term can be expanded in the $SU(d_A) \otimes SU(d_B)$ operator basis as following Eq. (7.66),

$$\hat{H}_{\text{int}} = \sum_{a=1}^{d_A^2-1} \sum_{b=1}^{d_B^2-1} h_{ab} \left(\hat{\Lambda}_a^{(A)} \otimes \hat{\Lambda}_b^{(B)} \right) . \quad (7.4)$$

One can rewrite \hat{H}_{int} in a diagonal form,

$$\hat{H}_{\text{int}} = \sum_{\alpha=1}^{n_{\text{int}}} \lambda_{\alpha} \left(\hat{A}_{\alpha} \otimes \hat{B}_{\alpha} \right) , \quad (7.5)$$

where \hat{A}_{α} and \hat{B}_{α} are combinations of the Hermitian generators¹ in Eq. (7.4) and the total number of terms will generically be $n_{\text{int}} = (d_A^2 - 1)(d_B^2 - 1)$. The coefficients λ_{α} characterize the strength of each contribution in the interaction Hamiltonian, which we ensure by absorbing any normalization of operators \hat{A}_{α} and \hat{B}_{α} in λ_{α} such that $\|\hat{A}_{\alpha}\| = \|\hat{B}_{\alpha}\| = 1$ under a suitable choice of operator norm $\|\cdot\|$. While there appear to be a large number of terms in the expansion in Eq. (7.5), we will see later how in the preferred, quasi-classical decomposition, most of these terms condense into familiar local operators that serve as pointer observables.

¹While in a general diagonal decomposition of the interaction Hamiltonian, the operators \hat{A}_{α} and \hat{B}_{α} can be unitary but not necessarily Hermitian, but our form of Eq. (7.5) is obtained by re-labeling/recollecting terms in an expansion with Hermitian terms of Eq. (7.4), hence \hat{A}_{α} and \hat{B}_{α} will be Hermitian. This will also help us make easy contact with talking about observables being monitored by subsystems.

A quasi-classical (QC) factorization of \mathcal{H} that we will denote by $\{\theta\}_{QC}$ can be associated with the following features:

1. **Robustness:** There exist preferred pointer states of the system (and associated pointer observables) that, if initially unentangled with the environment, typically remain unentangled under evolution by \hat{H} .
2. **Predictability:** For states with near definite value of the pointer observable, it will serve as a predictable quasi-classical variable, with minimal spreading under Hamiltonian evolution.

Informally, these two criteria correspond to the conventional notions that “wave function branchings are rare” and “expectation values of observables remain peaked around classical trajectories in the appropriate regime.” We can now examine in detail how these features can be characterized quantitatively.

7.3 Robustness and Entanglement

It is a feature of the universe (albeit as-yet imperfectly explained) that entropy was low at early times, and has been subsequently increasing [165, 166]. In the quantum context, this corresponds to relatively small amounts of initial entanglement between subsystems, and between macroscopic systems and their environment. Here we are imagining a bipartite split

$$\mathcal{H} = \mathcal{S} \otimes \mathcal{E} \tag{7.6}$$

into \mathcal{S} , which corresponds to “system” degrees of freedom we wish to track, and an environment \mathcal{E} , which is the part we are not interested in or do not have control over. In Everettian quantum mechanics [167], this feature underlies the fact that the wave function branches as time moves toward the future, not the past. Our interest is therefore in initially low-entropy situations, where the system is unentangled with its environment.

With a generic Hamiltonian in a generic factorization, we would expect any initially-unentangled system state to quickly become highly entangled with its environment, on timescales typical of the overall Hamiltonian. By “highly entangled” we mean that the entropy of the system’s reduced density matrix would approach $\log(\dim \mathcal{H}_{\mathcal{S}})$. In Everettian language, that would correspond to splitting into a number of branches of order $\dim \mathcal{H}_{\mathcal{S}}$. This is not what we expect from robust quasi-classical behavior; to a good approximation, Schrödinger’s cat splits into two branches, not into the exponential of Avogadro’s number of branches.

We will therefore ask, given some Hamiltonian \hat{H} , how we can factorize \mathcal{H} into $\mathcal{S} \otimes \mathcal{E}$ such that the entanglement growth rate of certain initially-unentangled states is minimized. We will explicitly work to $\mathcal{O}(t^2)$, which we will see is the lowest non-trivial contribution to the entanglement growth. This will help us quantify robustness and quasi-classicality for small times. (Factorizations that are not quasi-classical for small times will not be quasi-classical for later times either.)

Decoherence Is Non-Generic

It is well-known that wave functions tend to “collapse” (or branch) into certain preferred pointer states, depending on what observable is being measured. The decoherence paradigm outlines how in an appropriate factorization, we search for a pointer observable $\hat{O}_S \in \mathcal{L}(\mathcal{S})$ such that eigenstates $\{|s_j\rangle \mid j = 1, 2, \dots, d_S\}$ of \hat{O}_S serve as pointer states [27], which are robust to entanglement production with states of the environment. Thus, there exist special product states $|s_j\rangle \otimes |E\rangle$ that do not entangle (or stay approximately unentangled) under the evolution by the total Hamiltonian \hat{H} . This feature allows suppression of interference between superpositions of different pointer states, and in the eigenbasis of \hat{O}_S , the reduced density operator for \mathcal{S} given by $\hat{\rho}_S(t)$ evolves toward a diagonal form, since the conditional environmental states corresponding to different pointer states of the system become dynamically orthogonal $\langle E(s_j)|E(s_k)\rangle \rightarrow \delta_{jk}$ relatively fast in time.

In particular in the Quantum Measurement Limit (QML) [168], when the Hamiltonian is dominated by interactions \hat{H}_{int} (when the spectral frequencies available in \hat{H}_{int} are much larger than those of the self term \hat{H}_{self}), the pointer observable satisfies Zurek’s commutativity criterion [27],

$$[\hat{H}_{\text{int}}, \hat{O}_S] \approx 0 \implies [\hat{H}_{\text{int}}, \hat{O}_S \otimes \hat{\mathbb{I}}_E] \approx 0. \quad (7.7)$$

This is interpreted as saying that the environment \mathcal{E} robustly monitors [169] a certain observable \hat{O}_S of the system (typically a “local” one, such as position) that is compatible with the interaction Hamiltonian \hat{H}_{int} and selects this to serve as the pointer observable. This commutativity criterion of Eq. (7.7) further implies that generically all terms \hat{A}_α occurring with $\lambda_\alpha \neq 0$ will individually satisfy

$$[\hat{A}_\alpha, \hat{O}_S] \approx 0 \quad \forall \alpha. \quad (7.8)$$

The discussion can be extended to the quantum limit of decoherence [168], where the self term \hat{H}_{self} dominates over \hat{H}_{int} and selects eigenstates of the self-Hamiltonian

for the system \hat{H}_S to be the pointer states. In general, Zurek's "predictability sieve" [170] sifts through different states in the system's Hilbert space \mathcal{S} to search for states that are robust to entanglement production under evolution by the full Hamiltonian \hat{H} . In this paper, we primarily focus on the quantum measurement limit (QML) since a broad class of physical models exhibit this feature where interactions play a dominant and crucial role in the emergence of classicality.

Decoherence and the existence of low-entropy states in \mathcal{H} that do not get entangled under the action of \hat{H} depend sensitively on the Hamiltonian and factorization $\mathcal{H} = \mathcal{A} \otimes \mathcal{B}$ taking a particular, non-generic form. In the quasi-classical factorization, we will identify subsystem \mathcal{A} as the "system" \mathcal{S} , and the subsystem \mathcal{B} as the "environment" \mathcal{E} . In general, as we saw in Eq. (7.4) and particularly in the diagonal decomposition Eq. (7.5), the interaction term has a slew of non-commuting terms \hat{A}_α in the summand. Searching for a "pointer observable" is equivalent to finding an operator compatible with \hat{H}_{int} , and hence satisfying $[\hat{H}_{\text{int}}, \hat{O}] \approx 0$. Due to the presence of large number of non-commuting terms in \hat{H}_{int} , the eigenstates of \hat{O} will be highly entangled and not be low entropy states that can be resilient to entropy production.

Said differently, the "pointer observable" \hat{O} will not be of a separable form $\hat{O} \neq \hat{O}_A \otimes \hat{O}_B$, and only specific factorizations for Hamiltonians can allow decoherence, where many terms of \hat{H}_{int} in Eq. (7.5) conspire together to collect into a few local and compatible terms allowing for consistent monitoring of the system by the environment. (To emphasize, by "decoherence" here we mean not simply "becoming entangled with the environment," but the existence of a preferred set of pointer states that define a basis in which the reduced density matrix dynamically diagonalizes.) As we saw, the existence of initial low entropy states $\hat{\rho}(0) = \hat{\rho}_A(0) \otimes \hat{\rho}_B(0)$ that are robust under evolution to entanglement production is highly constrained and only in particular cases when many of the λ_α strengths vanish or terms conspire to condense into a few local terms will they exist to serve as the pointer states for subsystems being robustly monitored by the environment (other subsystems). This can be further understood by considering the constraint counting discussed in Section 7.3 below.

In Appendix 7.10 we detail this behavior more explicitly.

Minimizing Entropy Growth

In an arbitrary decomposition $\mathcal{H} \equiv (\mathcal{A} \otimes \mathcal{B})_{\{\theta\}}$, let us begin with an initial ($t = 0$) pure state of zero entropy for the factors, which we take to be a product state,

$$\hat{\rho}(0) \equiv |\psi(0)\rangle \langle\psi(0)| = \hat{\rho}_A(0) \otimes \hat{\rho}_B(0) \equiv |\psi_A(0)\rangle \langle\psi_A(0)| \otimes |\psi_B(0)\rangle \langle\psi_B(0)| . \quad (7.9)$$

At this stage, the decomposition $\{\theta\}$ is completely general and has no notion of preferred observables or classical behavior. Let us work with a traceless Hamiltonian of Eq. (7.3) even though the calculation below holds for $\text{Tr} \hat{H} \neq 0$ since this will only be an overall phase in the unitary evolution of density matrices and hence, cancels out. Time evolution of states is implemented using a unitary operator $\hat{U}(t) \equiv \exp(-i\hat{H}t)$, where we are working in units with $\hbar = 1$, and the time evolved state is $|\psi(t)\rangle = \hat{U}(t) |\psi(0)\rangle$. Let us write $\hat{U}(t)$ in a more suggestive form working explicitly to order $\mathcal{O}(t^2)$.

In Appendix 7.8, we compute the linear entanglement entropy² $S_{lin}(\hat{\rho}_A(t)) = (1 - \text{Tr} \hat{\rho}_A^2(t))$ for the reduced density matrix of \mathcal{A} given by Eq. (7.74), which corresponds to starting with an unentangled (and hence, zero entropy) state $\hat{\rho}(0)$. Putting these together in Eq. (7.82), we obtain,

$$\begin{aligned} S_{lin}(\hat{\rho}_A(t)) = t^2 \sum_{\alpha,\beta} \lambda_\alpha \lambda_\beta & \left(\langle \hat{A}_\alpha \hat{A}_\beta \rangle_0 \langle \hat{B}_\alpha \hat{B}_\beta \rangle_0 + \langle \hat{A}_\beta \hat{A}_\alpha \rangle_0 \langle \hat{B}_\beta \hat{B}_\alpha \rangle_0 \right. \\ & - \langle \hat{A}_\alpha \rangle_0 \langle \hat{A}_\beta \rangle_0 \left(\langle \{ \hat{B}_\alpha, \hat{B}_\beta \}_+ \rangle_0 - \langle \hat{B}_\alpha \rangle_0 \langle \hat{B}_\beta \rangle_0 \right) \\ & \left. - \langle \hat{B}_\alpha \rangle_0 \langle \hat{B}_\beta \rangle_0 \left(\langle \{ \hat{A}_\alpha, \hat{A}_\beta \}_+ \rangle_0 - \langle \hat{A}_\alpha \rangle_0 \langle \hat{A}_\beta \rangle_0 \right) \right) + \mathcal{O}(t^3) . \end{aligned} \quad (7.10)$$

For condensed notation, let us write $S_{lin}(\hat{\rho}_A(t)) = \ddot{S}_{lin}(0) t^2 + \mathcal{O}(t^3)$. The quantity \ddot{S}_{lin} will play an important role in quantifying the quasi-classicality of different factorizations of Hilbert space. In particular, for the important case when the interaction Hamiltonian takes the simple form $\hat{H}_{int} = \lambda (\hat{A} \otimes \hat{B})$, we notice that the expression for S_{lin} simplifies to,

$$S_{lin}(\hat{\rho}_A(t)) = 2\lambda^2 t^2 \left(\langle \hat{A}^2 \rangle_0 - \langle \hat{A} \rangle_0^2 \right) \left(\langle \hat{B}^2 \rangle_0 - \langle \hat{B} \rangle_0^2 \right) . \quad (7.11)$$

Let us note a few key features of the entropy growth Eq. (7.10). We are working in the context of unentangled (low entropy) states. As we have seen, the entanglement

²A common entanglement measure used is the von-Neumann entanglement entropy $S_{vN}(\hat{\rho}) = -\text{Tr}(\hat{\rho} \log \hat{\rho})$ for a given density matrix $\hat{\rho}$. However, the presence of the logarithm makes the entropy hard to analytically compute and give expressions for, hence we will focus on its leading order contribution, the Linear Entropy (which is the Tsallis second order entropy measure), $S_{lin}(\hat{\rho}) = (1 - \text{Tr} \hat{\rho}^2)$.

growth rate depends on the interaction strengths λ_α ; stronger interactions would entangle subsystems more quickly. One might be tempted to conclude that finding a decomposition where the interaction Hamiltonian has the minimum strength would ensure least entanglement production, but we must take note of the important role played by the initial (unentangled) state in determining the rate of entanglement generation³. In particular, we notice from Eqs. (7.11) and (7.10) the presence of variance-like terms of the interaction Hamiltonian in the initial state. States that are more spread relative to terms in the interaction Hamiltonian (hence more variance) allow for more ways for the two subsystems to entangle and such features will play an important role in distinguishing the QC factorization. Interestingly, the self-Hamiltonian plays no role in entanglement production for initially unentangled states to $O(t^2)$. As we will see later, the self term is nevertheless important in determining the collimation of pointer observables under evolution, and will serve as an important feature of the QC factorization.

Not all unentangled states will allow for $\ddot{S}_{lin}(0) = 0$, even approximately, and only a special class of states for a given factorization will be robust to entanglement production. For an arbitrary factorization, there will not exist such entanglement-resilient states that do not get entangled (to $O(t^2)$) under evolution. When $\ddot{S}_{lin}(0) = 0$, for an arbitrary factorization where all n_{int} terms are present in the interaction Hamiltonian without any constraints or relationship amongst different terms, each individual summand in Eq. (7.10) will typically have to vanish separately, giving us $(n_{int})(n_{int} + 1)/2$ equations in the variables that make up the initial unentangled state $|\psi(0)\rangle_A \otimes |\psi(0)\rangle_B$. A generic unentangled state of this form has $(2d_A - 2)(2d_B - 2) \ll (n_{int})(n_{int} + 1)/2$ real, free parameters (twice the dimension accounting for real coefficients; reduce two degrees of freedom, one due to normalization and one for the overall phase), hence forming an overdetermined set of equations. Only in very special cases, where quasi-classicality will be manifest will we see that many terms in \hat{H}_{int} will vanish having $\lambda_\alpha = 0$ or will conspire together to reduce/condense into familiar classical observables being monitored by other subsystems for there to exist robust, unentangled states that are resilient to entanglement production (and will serve as the pointer basis of the system). Such states will also be important for allowing decoherence to be an effective mechanism to suppress interference between

³This is in line with Tegmark's [28] "Hamiltonian Diagonality Theorem," which proves that the Hamiltonian is maximally separable (with minimum norm of the interaction Hamiltonian) in the energy eigenbasis. Tegmark further argues that this factorization corresponding to the energy eigenbasis is not the quasi-classical one despite maximum separability due to a crucial role played by the state.

superpositions of such pointer states.

7.4 Predictability and Classical Dynamics

Pointer Observables and Predictable Diagonal-Sliding

The mere existence of a pointer observable consistently monitored by other subsystems is not enough for classical evolution of states starting with a peaked value of the observable. In addition to slow entanglement growth of initially unentangled pointer states, we must ensure that such states define a predictable variable that evolves classically. A possible measure for the predictability of an operator under evolution is the change in variance of the observable under an initial state with almost definitive value of the observable. Let us compute the time rate of change in variance of an observable $\hat{O}_A \in \mathcal{L}(\mathcal{A})$ under the evolution by \hat{H} . Here we will see how the self-Hamiltonian \hat{H}_A becomes important in determining the how quickly the observable spreads.

The variance of \hat{O}_A as a function of time is defined as,

$$\Delta^2 \hat{O}_A(t) = \text{Tr} \left(\hat{\rho}_A(t) \hat{O}_A^2 \right) - \text{Tr}^2 \left(\hat{\rho}_A(t) \hat{O}_A \right). \quad (7.12)$$

We will use the expression for $\hat{\rho}_A(t)$ to $\mathcal{O}(t)$ from Eq. (7.76) since this is the lowest non-trivial order at which the effect of the Hamiltonian can be seen,

$$\hat{\rho}_A(t) = \hat{\sigma}_A(t) - it \sum_{\alpha} \lambda_{\alpha} \langle \hat{B}_{\alpha} \rangle_0 [\hat{A}_{\alpha}, \hat{\rho}_A(0)] + \mathcal{O}(t^2), \quad (7.13)$$

which gives us,

$$\begin{aligned} \text{Tr} \left(\hat{\rho}_A(t) \hat{O}_A^2 \right) &= \langle \hat{O}_A^2 \rangle_t^{\text{self}} - it \sum_{\alpha} \lambda_{\alpha} \langle \hat{B}_{\alpha} \rangle_0 \text{Tr} \left([\hat{A}_{\alpha}, \hat{\rho}_A(0)] \hat{O}_A^2 \right) + \mathcal{O}(t^2) \\ &= \langle \hat{O}_A^2 \rangle_t^{\text{self}} - it \sum_{\alpha} \lambda_{\alpha} \langle \hat{B}_{\alpha} \rangle_0 \langle [\hat{O}_A^2, \hat{A}_{\alpha}] \rangle_0 + \mathcal{O}(t^2), \end{aligned} \quad (7.14)$$

and similarly,

$$\text{Tr} \left(\hat{\rho}_A(t) \hat{O}_A \right) = \langle \hat{O}_A \rangle_t^{\text{self}} - it \sum_{\alpha} \lambda_{\alpha} \langle \hat{B}_{\alpha} \rangle_0 \langle [\hat{O}_A, \hat{A}_{\alpha}] \rangle_0 + \mathcal{O}(t^2), \quad (7.15)$$

where the self-evolved variance $\left(\Delta^2 \hat{O}_A \right)^{\text{self}}$ is found similarly, depending on the self-Hamiltonian \hat{H}_A ,

$$\begin{aligned} \left(\Delta^2 \hat{O}_A \right)^{\text{self}}(t) &= \text{Tr} \left(\hat{\sigma}_A(t) \hat{O}_A^2 \right) - \text{Tr}^2 \left(\hat{\sigma}_A(t) \hat{O}_A \right) + \mathcal{O}(t^2) \\ &= \left(\Delta^2 \hat{O}_A \right)_0 - it \left(\langle [\hat{O}_A^2, \hat{H}_A] \rangle_0 - 2 \langle [\hat{O}_A, \hat{H}_A] \rangle_0 \langle \hat{O}_A \rangle_0 \right) + \mathcal{O}(t^2). \end{aligned} \quad (7.16)$$

We can now put everything together to get the variance $\Delta^2 \hat{O}_A(t)$ to $\mathcal{O}(t)$,

$$\Delta^2 \hat{O}_A(t) = \left(\Delta^2 \hat{O}_A \right)_0^{\text{self}} - it \sum_{\alpha} \lambda_{\alpha} \langle \hat{B}_{\alpha} \rangle_0 \left(\langle [\hat{O}_A^2, \hat{A}_{\alpha}] \rangle_0 - 2 \langle [\hat{O}_A, \hat{A}_{\alpha}] \rangle_0 \langle \hat{O}_A \rangle_0 \right) + \mathcal{O}(t^2). \quad (7.17)$$

We can now obtain the leading order contribution to the time derivative of the variance that captures the contribution to various terms in the Hamiltonian,

$$\begin{aligned} \frac{d}{dt} \Delta^2 \hat{O}_A(t) = & \left(\langle i [\hat{H}_A, \hat{O}_A^2] \rangle_0 - 2 \langle i [\hat{H}_A, \hat{O}_A] \rangle_0 \langle \hat{O}_A \rangle_0 \right) + \\ & \left(\left\langle i \left[\sum_{\alpha} \lambda_{\alpha} \langle \hat{B}_{\alpha} \rangle_0 \hat{A}_{\alpha}, \hat{O}_A^2 \right] \right\rangle_0 - 2 \left\langle i \left[\sum_{\alpha} \lambda_{\alpha} \langle \hat{B}_{\alpha} \rangle_0 \hat{A}_{\alpha}, \hat{O}_A \right] \right\rangle_0 \langle \hat{O}_A \rangle_0 \right) + \mathcal{O}(t). \end{aligned} \quad (7.18)$$

The spreading of the variance depends on terms which resemble those in the Heisenberg equation of motion of the observable \hat{O}_A (and its square) under evolution by both the self-Hamiltonian \hat{H}_A and relevant terms in \hat{H}_{int} .

Let us now analyze this variance change for the case where the interaction Hamiltonian \hat{H}_{int} in the chosen factorization admits a consistent pointer observable (in the QML) satisfying Eq. (7.7), in which case $[\hat{f}(\hat{O}_A), \hat{A}_{\alpha}] \approx 0 \forall \alpha$ for any function $\hat{f}(\hat{O}_A)$ depending only on \hat{O}_A . For such a pointer observable, the time derivative of the variance from Eq. (7.18) simplifies and depends only on self-dynamics governed by \hat{H}_A ,

$$\frac{d}{dt} \Delta^2 \hat{O}_A(t) = \langle i [\hat{H}_A, \hat{O}_A^2] \rangle_0 - 2 \langle i [\hat{H}_A, \hat{O}_A] \rangle_0 \langle \hat{O}_A \rangle_0 + \mathcal{O}(t) \quad \text{for } [\hat{O}_A, \hat{A}_{\alpha}] \approx 0. \quad (7.19)$$

For the pointer observable \hat{O}_A to offer a predictable variable, it should obey $\frac{d}{dt} \Delta^2 \hat{O}_A(t) \ll 1$ for initial states that are peaked around some eigenvalue of \hat{O}_A . Having states as peaked superpositions of the pointer states instead of exact eigenstates fits in well with the idea of ‘‘predictability sieve’’ à la Zurek [170]: while the pointer observable is chosen using the compatibility criterion with \hat{H}_{int} as seen in Eq. (7.7), the most robust states (under the full Hamiltonian \hat{H}) will have a small width instead of being exact eigenstates due to the effects of the (systematically smaller) self-Hamiltonian (in the QML). Such peaked states, for a predictable \hat{O}_A , will not spread much, and offer candidates for classical states that evolve primarily under the action of the self-Hamiltonian \hat{H}_A .

The reduced density matrix of \mathcal{A} in such a pointer basis will be mostly diagonal (due to decoherence, as discussed in Section 7.3), and a peaked state of \hat{O}_A will

slide along the diagonal under self-dynamics [28]. This “diagonal sliding” feature can also be seen from the expression for $\dot{\hat{\rho}}_A(t)$ from Eq. (7.110), where the diagonal entries of the decoherence term $\mathcal{D}(\hat{\rho}_A(t))$ of Eq. (7.111) in the pointer basis $\{|s_j\rangle\}$ vanish identically, and the diagonal entries in $\dot{\hat{\rho}}_A(t)$ in the pointer basis evolve as,

$$\left[\frac{d}{dt} \hat{\rho}_A(t) \right]_{jj} = \left(-i [\hat{H}_A(t), \hat{\rho}_A(t)]_{jj} \right) + \mathcal{O}(t^2), \quad (7.20)$$

since even the interaction pieces from the effective self-Hamiltonian also vanish in the pointer basis (see Appendix 7.10 for details), $\langle a_j | [\hat{A}_\alpha, \hat{\rho}_A(t)] | a_j \rangle \equiv [\hat{A}_\alpha, \hat{\rho}_A(t)]_{jj} = 0$. Thus, these diagonal terms evolve under the action of the self-Hamiltonian and dictate the diagonal sliding of the density matrix in the pointer basis once it has decohered.

We will now make contact with dimensional conjugate variables, using which we will connect properties of the self-Hamiltonian with the rate of change of variance of the pointer observable.

Finite-Dimensional Conjugate Variables

Classical mechanics is formulated in phase space, with conjugate position and momentum variables. For quantum mechanics in infinite-dimensional Hilbert spaces, we can define corresponding quantum operators, subject to the Heisenberg canonical commutation relations (CCR). Since we are explicitly focusing on finite-dimensional Hilbert spaces, we will use the Generalized Pauli Operators (which find their algebraic roots in the generalized Clifford algebra) to provide us with finite-dimensional conjugate variables that obey the CCR in the infinite-dimensional limit. We will then use these to define the “collimation” of an operator, an important notion that characterizes how the action of an operator on a state induces a spread in eigenspace.

We explain the basics of generalized Pauli operators (GPOs) in Appendix 7.9. The essential point is that we can construct Hermitian conjugate operators \hat{q} and \hat{p} that match onto position- and momentum-like operators in the infinite-dimensional limit. To do this we introduce two unitary operators \hat{A} and \hat{B} that will generate the GPO algebra. On a Hilbert space of dimension $d < \infty$, they obey the Weyl braiding relation,

$$\hat{A}\hat{B} = \omega^{-1}\hat{B}\hat{A}, \quad (7.21)$$

where $\omega = \exp(2\pi i/d)$ is the d -th primitive root of unity, and are sometimes referred to as “Clock” and “Shift” operators in the literature. Then the conjugate variables

are defined via

$$\hat{A} \equiv \exp(-i\alpha\hat{\pi}), \quad \hat{B} = \exp(i\beta\hat{\phi}), \quad (7.22)$$

where α and β are non-zero real parameters that set the scale of the eigenspectrum of the operators $\hat{\phi}$ and $\hat{\pi}$ with a cyclic structure. For concreteness, we take the dimension to be an odd integer, $d = 2l + 1$ for some $l \in \mathbb{Z}^+$.

The set of N^2 linearly independent unitary matrices,

$\{B^b A^a | b, a = -l, (-l+1), \dots, 0, \dots, (l-1), l\}$, which includes the identity for $a = b = 0$, form a unitary basis for $\mathcal{L}(\mathcal{H})$. Schwinger [94] studied the role of such unitary basis, hence this operator basis is often called Schwinger's unitary basis. Any operator $\hat{M} \in \mathcal{L}(\mathcal{H})$ can be expanded in this basis,

$$\hat{M} = \sum_{b,a=-l}^l m_{ba} \hat{B}^b \hat{A}^a. \quad (7.23)$$

Since from the structure of the GPO algebra we have $\text{Tr} \left[\left(\hat{B}^{b'} \hat{A}^{a'} \right)^\dagger \left(\hat{B}^b \hat{A}^a \right) \right] = d \delta_{b,b'} \delta_{a,a'}$, we can invert Eq. (7.23) to get the coefficients m_{ba} as,

$$m_{ba} = \frac{1}{d} \text{Tr} \left[\hat{A}^{-a} \hat{B}^{-b} \hat{M} \right]. \quad (7.24)$$

The GPO generator \hat{A} corresponds to a unit shift in the eigenstates of $\hat{\phi}$, and \hat{B} generates unit shifts in the eigenstates of $\hat{\pi}$; hence, a basis element $B^b A^a$ generates a units of shift in eigenstates of $\hat{\phi}$ and b units in eigenstates of $\hat{\pi}$, respectively (up to overall phase factors).

For an operator \hat{M} that is Hermitian $\hat{M}^\dagger = \hat{M}$, we get a constraint on the expansion coefficients, $\omega^{-ba} m_{-b,-a}^* = m_{ba}$, which implies $|m_{ba}| = |m_{-b,-a}|$ since $\omega = \exp(2\pi i/(2l+1))$ is a primitive root of unity. The coefficients m_{ba} are a set of basis-independent numbers that quantify the spread induced by the operator \hat{M} along each of the conjugate variables $\hat{\phi}$ and $\hat{\pi}$. To be precise, $|m_{b,a}|$ represents the amplitude of b shifts along $\hat{\pi}$ for an eigenstate of $\hat{\pi}$ and a shifts along $\hat{\phi}$ for an eigenstate of $\hat{\phi}$. The indices of m_{ba} run from $-l, \dots, 0, \dots, l$ along both conjugate variables and thus, characterize shifts in both increasing (a or $b > 0$) and decreasing (a or $b < 0$) eigenvalues on the cyclic lattice. The action of \hat{M} on a state depends on details of the state, and in general will lead to a superposition in the eigenstates of the chosen conjugate variable as our basis states, but the set of numbers m_{ba} quantify the spread along conjugate directions by the operator \hat{M} independent of the choice of state. The coefficient m_{00} accompanies the identity $\hat{\mathbb{1}}$, and hence corresponds to no shift in either of the conjugate variables.

From m_{ba} , which encodes amplitudes of shifts in both $\hat{\phi}$ and $\hat{\pi}$ eigenstates, we would like to extract profiles which illustrate the spreading features of \hat{M} in each conjugate variable separately. Since the coefficients m_{ba} depend on details of \hat{M} , in particular its norm, we define normalized amplitudes \tilde{m}_{ba} for these shifts,

$$\tilde{m}_{ba} = \frac{m_{ba}}{\sum_{b',a'=-l}^l |m_{b'a'}|}. \quad (7.25)$$

Then we define the $\hat{\phi}$ -shift profile of \hat{M} by marginalizing over all possible shifts in $\hat{\pi}$,

$$m_a^{(\phi)} = \sum_{b=-l}^l |\tilde{m}_{ba}| = \frac{\sum_{b=-l}^l |m_{ba}|}{\sum_{b',a'=-l}^l |m_{b'a'}|}, \quad (7.26)$$

which is a set of $(2l + 1)$ positive numbers, normalized under $\sum_{a=-l}^l m_a^{(\phi)} = 1$, characterizing the relative importance of \hat{M} spreading the $\hat{\phi}$ variable by a units, $a = -l, \dots, 0, \dots, l$. Thus, \hat{M} acting on an eigenstate of $\hat{\phi}$, say $|\phi = j\rangle$, will in general, result in a superposition over the support of the basis of the $\hat{\phi}$ eigenstates $\{|\phi = j + a \pmod{l}\rangle\} \forall a$, such that the relative importance (absolute value of the coefficients in the superposition) of each such term is upper bounded by $m_a^{(\phi)}$.

Let us now quantify this spread by defining the collimation for each conjugate variable. Consider the ϕ -shift profile first. Operators with a large $m_a^{(\phi)}$ for small $|a|$ will have small spread in the $\hat{\phi}$ -direction, while those with larger $m_a^{(\phi)}$ for larger $|a|$ can be thought of connecting states further out on the lattice for each eigenstate. Following this motivation, we define the ϕ -collimation C_ϕ of the operator \hat{M} as,

$$C_\phi(\hat{M}) = \sum_{a=-l}^l m_a^{(\phi)} \exp\left(-\frac{|a|}{2l+1}\right). \quad (7.27)$$

The exponential function suppresses the contribution of large shifts in our definition of collimation. There is some freedom in our choice of the decay function in our definition of collimation, and using an exponential function as in Eq. (7.27) is one such choice. Thus, an operator with a larger C_ϕ is highly collimated in the $\hat{\phi}$ -direction and does not spread out eigenstates with support on a large number of basis states on the lattice.

On similar lines, one can define the π -shift profile for \hat{M} as,

$$m_b^{(\pi)} = \sum_{a=-l}^l |\tilde{m}_{ba}| = \frac{\sum_{a=-l}^l |m_{ba}|}{\sum_{b',a'=-l}^l |m_{b'a'}|}, \quad (7.28)$$

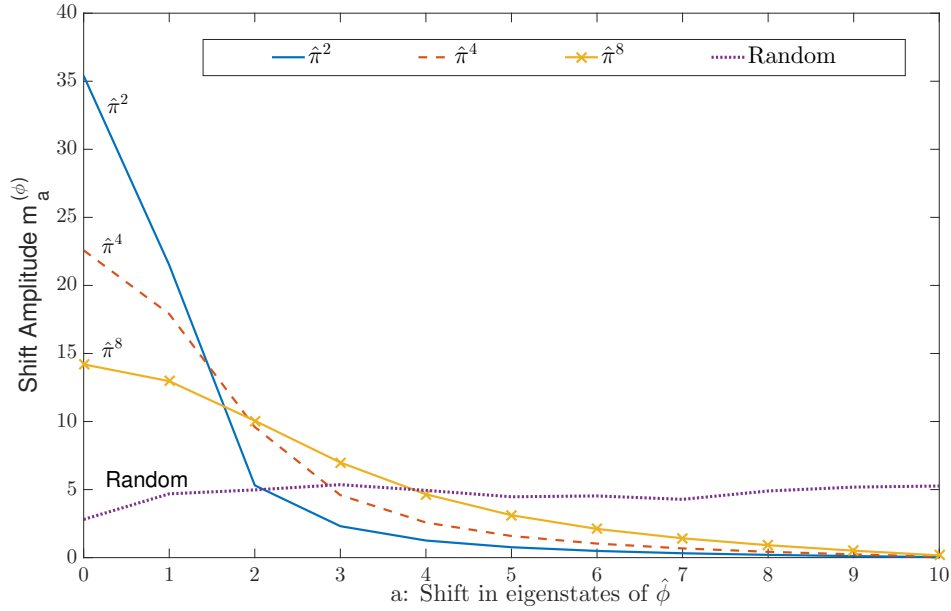


Figure 7.1: Plot showing $\hat{\phi}$ -shift profiles of various powers of $\hat{\pi}$. The quadratic operator $\hat{\pi}^2$ has the most collimated profile, implying that this operator does the least to spread the state in the conjugate direction. Also plotted is the profile for a random Hermitian operator, for which the spread is approximately uniform.

and a corresponding π -collimation C_π with a similar interpretation as the $\hat{\phi}$ -case,

$$C_\pi(\hat{M}) = \sum_{b=-l}^l m_b^{(\pi)} \exp\left(-\frac{|b|}{2l+1}\right). \quad (7.29)$$

Operators such as $\hat{M} \equiv \hat{M}(\hat{\pi})$ that depend on only one of the conjugate variables will only induce spread in the $\hat{\phi}$ direction, since they have $m_{b,a} = m_{0,a}\delta_{b,0}$, hence they possess maximum π -collimation, $C_\pi(\hat{M}) = 1$, as they do not spread eigenstates of $\hat{\pi}$ at all.

While the maximum value of $C_\pi(\hat{M}(\hat{\pi}))$ can be at most unity, one can easily see that the Hermitian operator,

$$\hat{M}(\hat{\pi}) = \frac{A + A^\dagger}{2} = \frac{\exp(-i\alpha\hat{\pi}) + \exp(i\alpha\hat{\pi})}{2} = \cos(\alpha\hat{\pi}) = \hat{\mathbb{1}} - \frac{\alpha^2\hat{\pi}^2}{2} + \frac{\alpha^4\hat{\pi}^4}{4} - \dots, \quad (7.30)$$

has the least non-zero spread along the $\hat{\phi}$ direction: it connects only ± 1 shifts along eigenstates of $\hat{\phi}$ and hence has highest (non-unity) ϕ -collimation $C_\phi(\hat{M})$. Thus, one can expect operators which are quadratic in conjugate variables are highly collimated. This will connect to the fact that real-world Hamiltonians include terms

that are quadratic in the momentum variables (but typically not higher powers) and will help explain the emergence of classicality: it is Hamiltonians of that form that have high position collimation, and therefore induce minimal spread in the position variable.

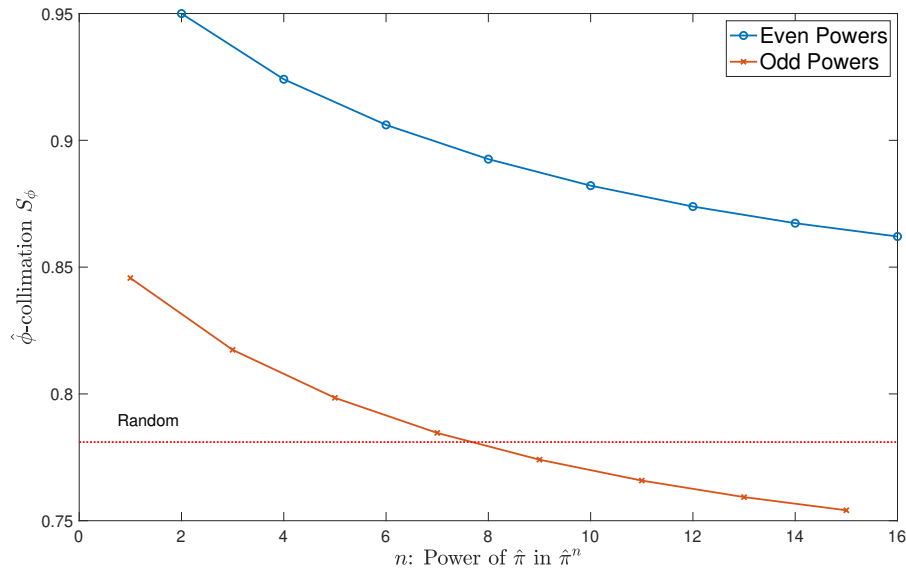


Figure 7.2: ϕ -collimation of various powers of $\hat{\pi}$. Even powers are seen to have systematically larger values of ϕ -collimation. Also plotted for comparison is a line marking the ϕ -collimation of a random Hermitian operator.

The quadratic operator $\hat{\pi}^2$ has higher ϕ -collimation than any other integer⁴ power $\hat{\pi}^n$, $n \geq 1$, $n \neq 2$. In Figure (7.1), we plot the ϕ -shift profiles for a few powers of $\hat{\pi}$ and it is explicitly seen that quadratic $\hat{\pi}^2$ has the least spreading and hence is most $\hat{\phi}$ -collimated, values for which are plotted in Figure (7.2). Note that due to the symmetry $|m_{b,a}| = |m_{-b,-a}|$, we only needed to plot the positive half for $a > 0$, which captures all the information about the spread. Also, for comparison, we also plot the ϕ -spread and the $\hat{\phi}$ -collimation of a random Hermitian operator (with random matrix elements in the $\hat{\phi}$ basis); such operators spread states almost evenly and thus have low values of collimation.

⁴There is a difference between odd and even powers of $\hat{\pi}$, with even powers systematically having larger collimations than the odd powers. This is because odd powers of $\hat{\pi}$ do not have support of the identity $\hat{1}$ term in the Schwinger unitary basis expansion (and hence have $m_{00} = 0$), and having an identity contribution boosts collimation since it contributes to the highest weight in C_ϕ by virtue of causing no shifts.

Operator Collimation, Locality, and the Self-Hamiltonian

Typically, one begins with a notion of classical subsystems, then defines the Hamiltonian for these systems based on classical energy functions, and proceeds to quantize. In non-relativistic quantum mechanics, the self terms usually go as $\hat{p}^2/2m + \hat{V}(\hat{q})$ for canonically conjugate operators \hat{p} and \hat{q} . Interaction terms usually depend on one of the conjugate variables, usually the position of each subsystem.

For each subsystem one can associate a set of finite-dimensional conjugate operators from the Generalized Pauli Operators. For our bipartite split $\mathcal{H} = \mathcal{A} \otimes \mathcal{B}$, we have conjugate operators $\{\hat{\phi}_A, \hat{\pi}_A\} \in \mathcal{L}(\mathcal{A})$ and $\{\hat{\phi}_B, \hat{\pi}_B\} \in \mathcal{L}(\mathcal{B})$. For arbitrary factorizations, these GPO-based conjugate variables will not correspond to physical position and momentum variables; only in a quasi-classical decomposition would the identification $\hat{\pi} \equiv \hat{p}$ and $\hat{\phi} \equiv \hat{q}$ be appropriate.

The conjugate variables can be used to define the Schwinger Unitary Basis [94], and hence we can write self terms in the Hamiltonian \hat{H} from (7.3) in terms of these conjugates,

$$\hat{H}_A \equiv \hat{H}_A(\hat{\pi}_A, \hat{\phi}_A) \quad \hat{H}_B \equiv \hat{H}_B(\hat{\pi}_B, \hat{\phi}_B) , \quad (7.31)$$

and the interaction term can be written as,

$$\hat{H}_{\text{int}} \equiv \hat{H}_{\text{int}}(\hat{\pi}_A, \hat{\phi}_A, \hat{\pi}_B, \hat{\phi}_B) = \sum_{\alpha} \lambda_{\alpha} \left(\hat{A}_{\alpha}(\hat{\pi}_A, \hat{\phi}_A) \otimes \hat{B}_{\alpha}(\hat{\pi}_B, \hat{\phi}_B) \right) . \quad (7.32)$$

Before we explicitly discuss the idea of collimation and the role it plays in emergent quasi-classicality, let us comment on the functional form of \hat{H}_{int} for there to exist a robust pointer observable as described in the previous Section 7.2. Since $\hat{\phi}_A$ and $\hat{\pi}_A$ do not commute, for there to exist a compatible pointer observable monitored consistently by other subsystems, we would demand that interaction terms \hat{A}_{α} depend only on one such conjugate variable, say $\hat{\phi}_A$. In many physical cases, the interaction term is the position of the subsystem under consideration, as that is the quantity that is monitored by the environment, since interactions are local in space. Under these conditions, the pointer observable can be identified as $\hat{O}_A \equiv \hat{O}_A(\hat{\phi}_A)$, depending only on one conjugate variable.

Let us see how the idea of predictability connects with features of the self-Hamiltonian. From Eq. (7.19), we see that the rate of change of variance of the pointer observable depends, in addition to the state at $t = 0$, on the Heisenberg equation of motion for $\hat{O}_A(\hat{\phi}_A)$ under the self-Hamiltonian \hat{H}_A . Thus, it can be expected that self terms \hat{H}_A that are collimated in the $\hat{\phi}_A$ variable will spread states less rapidly under time

evolution and keep the change of variance of \hat{O}_A small. They therefore offer a predictable interpretation to \hat{O}_A .

This can be seen in the following example. We keep fixed the pointer observable $\hat{O}_A \equiv \hat{\phi}_A$ and vary the self-Hamiltonian, and for each choice of the self-Hamiltonian we compute the time derivative of $\Delta^2 \hat{O}_A$ from Eq. (7.19) for an initial state that is a peaked Gaussian profile in $\hat{\phi}_A$ states, representing a peaked wavepacket. In Figure (7.3), we plot these results and see that high ϕ -collimation $C_\phi(\hat{H}_A)$ inversely correlates with the variance change of the pointer observable. Therefore, evolving under a highly ϕ -collimated self-Hamiltonian, peaked states in pointer space have a smaller rate of change of variance of the pointer observable \hat{O}_A .

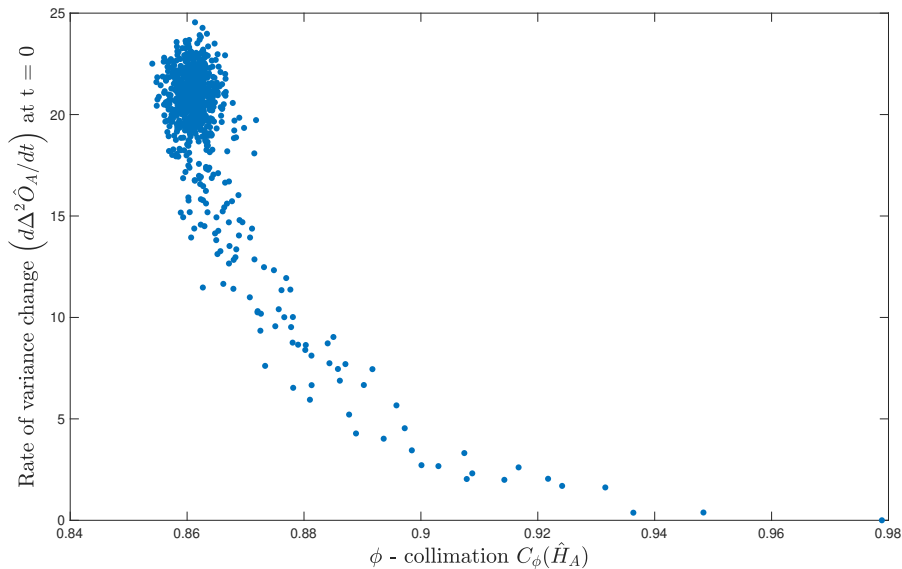


Figure 7.3: Plot showing correlation between rate of change of variance of the pointer observable $d(\Delta^2 \hat{O}_A)/dt$ and collimation $C_\phi(\hat{H}_A)$ of the self-Hamiltonian \hat{H}_A . More collimated self terms do not spread states much in the conjugate directions and correspondingly induce a small change in the variance of the consistent pointer observable that depends on one of these conjugate variables. In this example, we kept \hat{O}_A fixed at $\hat{O}_A \equiv \hat{\phi}_A$ and changed the self-Hamiltonian \hat{H}_A and computed the correlation for a peaked state in $\hat{\phi}_A$ eigenspace in a Hilbert space of $\dim \mathcal{A} = 27$.

Note the different roles played by collimation and locality. In quantum field theories or lattice theories, we can factor Hilbert space into sets of degrees of freedom located in small regions of space. Spatial locality then implies that the interaction

Hamiltonian takes a k -local form, where each factor interacts directly with only its neighboring factors; cf. Eq. (7.65). For our purposes we can turn this around, looking for factorizations in which interactions are k -local, which is a necessary requirement for the emergence of spatial locality [22]. Collimation, by contrast, is an important feature of the self-Hamiltonian. In order to recover familiar classical behavior, we require that pointer observables evolve in relatively predictable ways, rather than being instantly spread out over a wide range of values.

Classical Dynamics

Besides the existence of predictable pointer observables, the other feature we require for quasi-classical behavior is that conjugate “position” and “momentum” operators, or some generalization thereof, approximately obey the corresponding classical Heisenberg equations of motion.

As was shown in Ref [10], and this argument can be easily extended for multi-partite systems, the equations of motion for the conjugate operators $\hat{\phi}_A$ and $\hat{\pi}_A$ for some subsystem \mathcal{A} can be found to be,

$$\frac{d}{dt}\hat{\pi} = i [\hat{H}, \hat{\pi}_A] = -\left(\overline{\frac{\partial H}{\partial \phi_A}}\right) + \sum_{n=3}^{odd} \frac{i^n}{n!} \alpha^{n-1} \left[\hat{\pi}_A, \hat{H}\right]_n, \quad (7.33)$$

where we have defined $\left[\hat{\pi}_A, \hat{H}\right]_n$ as the n -point nested commutator in $\hat{\pi}_A$,

$$\left[\hat{\pi}_A, \hat{H}\right]_n = \left[\hat{\pi}_A, \left[\hat{\pi}_A, \left[\hat{\pi}_A, \dots (n \text{ times}), \hat{H}\right] \dots\right]\right]. \quad (7.34)$$

The corresponding equation for $\hat{\phi}_A$ can be found on similar lines,

$$\frac{d}{dt}\hat{\phi}_A = i [\hat{H}, \hat{\phi}_A] = \left(\overline{\frac{\partial H}{\partial \pi_A}}\right) + \sum_{n=3}^{odd} \frac{i^n}{n!} \beta^{n-1} \left[\hat{\phi}_A, \hat{H}\right]_n. \quad (7.35)$$

In the infinite-dimensional limit we take $l \rightarrow \infty$, and α and β are taken to be infinitesimal but obeying $\alpha\beta d = 2\pi$ to recover the Heisenberg CCR. In this limit, as one expects, the equations of motion simplify to resemble Hamilton’s equations,

$$\frac{d}{dt}\hat{\pi}_A = i [\hat{H}, \hat{\pi}_A] = -\left(\overline{\frac{\partial H}{\partial \phi_A}}\right), \quad (7.36)$$

and,

$$\frac{d}{dt}\hat{\phi}_A = i [\hat{H}, \hat{\phi}_A] = \left(\overline{\frac{\partial H}{\partial \pi_A}}\right), \quad (7.37)$$

where \hat{H} is the Hamiltonian for the entire Hilbert space. Even though in the large-dimension limit these resemble classical equations of motion, they are inherently quantum mechanical equations for operators in $\mathcal{L}(\mathcal{H})$. Additional features have to be imposed for the conjugate variables $\hat{\phi}_A$ and $\hat{\pi}_A$ to serve as classical conjugate variables.

These equations serve as classical evolution equations when we consider peaked states of the pointer observable \hat{O}_A that would depend on only one of the conjugate variables, say $\hat{O}_A \equiv \hat{O}_A(\hat{\phi}_A)$. Peaked states in \hat{O}_A eigenspace can be candidates for classical evolution since they can obey the Ehrenfest theorem when one takes expectation value of Eqs. (7.36) and (7.37) by pulling in the expectation into the Hamiltonian, for example,

$$\left\langle \left(\frac{\partial \overline{H}}{\partial \pi_A} \right) \right\rangle \rightarrow \left(\frac{\partial \langle \hat{H} \rangle}{\partial \pi_A} \right) \text{ for peaked states in pointer observable space.} \quad (7.38)$$

The condition for persistence of such classical states obeying classical equation of motion will be to have low spreading of the variance of such a peaked state, which as we saw corresponds to a highly collimated self-Hamiltonian. Thus, under the criterion of there existing a predictable and consistent pointer observable (from \hat{H}_{int} in the Quantum Measurement Limit) that depends on one of the conjugate variables and a collimated self-Hamiltonian, we would be able to identify the conjugate variables $\hat{\phi}_A$ and $\hat{\pi}_A$ (from the GPO algebra) with classical conjugate variables. While one can always define conjugates, the existence of classical ones corresponding to our familiar notion of position and momenta are highly non-generic and connect to predictability features in the Hamiltonian.

7.5 The Quantum Mereology Algorithm

Given a Hilbert space and a Hamiltonian, how does one sift through Hilbert space factorizations and pick out the one corresponding to the QC decomposition? This section aims to use the features described in Section 7.2 as pointers to outline an algorithm that quantifies the quasi-classicality of each factorization and uses this to pick out the one in which the QC features are most manifestly seen. We will do this for the bipartite case we have focused on in this paper. As we have seen, features like existence of low entropy states and robustness against entanglement production, non-generic decoherence and predictability of pointer observables are highly special and particular to the QC factorization and will not be seen in other, arbitrary factorizations. Hence, for an algorithm that sifts through Hilbert space factorizations,

we need to identify a homogeneously defined quantity for each factorization that would be extremized for the QC factorization. We will use the S_{lin} computation from Section 7.3 and predictability of the pointer observable from Section 7.4 to identify such a quantity.

Candidate Pointer Observables

As we have seen, low entropy states obtained as eigenstates of a consistent pointer observable that are resilient to entanglement production ($\ddot{S}_{lin} = 0$ to $\mathcal{O}(t^2)$ in our calculation) are highly non-generic; they are a special feature of the QC factorization. To belabor this point a little more, consistent pointer observables of the form $\hat{O}_A \otimes \hat{O}_B$ with $[\hat{H}_{int}, \hat{O}_A \otimes \hat{O}_B] \approx 0$ do not exist generically. This motivates us to define a *Candidate Pointer Observable* (CPO) for an arbitrary factorization $\{\theta\}$ that can serve as a proxy for the pointer observable by being the closest observable consistently monitored by the environment. Of course, for the QC decomposition $\{\theta\}_{QC}$, the CPO coincides with the pointer observable, and for other factorizations away from the QC, the CPO will introduce a “penalty” term in our measure of predictability and robustness of classical states in the factorization.

Let the CPO \hat{O}_{CPO} have a particular, consistent form,

$$\hat{O}_{CPO} \equiv \hat{O}_A \otimes \hat{O}_B, \quad (7.39)$$

for some operators $\hat{O}_A \in \mathcal{A}$ and $\hat{O}_B \in \mathcal{B}$, found by the following extremization,

$$\hat{O}_{CPO} = \hat{O}_A \otimes \hat{O}_B \text{ such that } \|\hat{H}_{int}, \hat{O}_{CPO}\|_2 \text{ is minimized.} \quad (7.40)$$

Thus, \hat{O}_{CPO} serves as the closest (with regards to the norm measure) product operator to \hat{H}_{int} as can therefore serve as a proxy/best possible notion of a consistent pointer observable, and in the QC factorization, \hat{O}_{CPO} will coincide with an actual pointer observable which is consistently monitored by the environment. In case more than one such \hat{O}_{CPO} satisfying criterion of Eq. (7.40), then one can pick the one corresponding to the minimum norm $\|\hat{O}_{CPO}\|_2$ since it would typically lead to lower entropy production rate. This can be implemented using the Pitsianis-Van Loan algorithm [171], which computationally finds the nearest tensor product approximation to a given matrix. The algorithm preserves structure in the sense that both \hat{O}_A and \hat{O}_B will be hermitian since \hat{H}_{int} is hermitian.

The next thing to focus on is the kind of state we will be using to quantify the quasi-classicality of a given factorization $\{\theta\}$. As we have seen, peaked states of a

consistent pointer observable can serve as good candidates for studying predictability, and in the correct limit be identified as classically predictable states. Following this motivation, we can construct states that represent peaked states of the CPO \hat{O}_A on \mathcal{A} ,

$$|\psi_j(0)\rangle_{CPO} = |\tilde{\psi}(0)\rangle_A \otimes |\tilde{\psi}(0)\rangle_B. \quad (7.41)$$

They represent an initially predictable state for our subsystem \mathcal{A} having a definite value of the candidate pointer observable. One possible prescription for the state $\{|\tilde{\psi}_j(0)\rangle_A\}$ is to construct a peaked state around an eigenstate of \hat{O}_A , and take the state on \mathcal{B} to be a uniform superposition of all eigenstates of \hat{O}_B to represent a ready state for the candidate environment \mathcal{B} .

One can now compute \check{S}_{lin} for the state $|\psi(0)\rangle_{CPO}$ using Eq. (7.10), which will serve as a measure of the entanglement resilience of low entropy states in the decomposition $\{\theta\}$. For the particular case of the QC factorization $\{\theta\}_{QC}$, we will find \check{S}_{lin} for $|\psi(0)\rangle_{CPO}$ to vanish (or even approximately so) since the state will correspond to one constructed out of a consistent pointer observable that is robust to entanglement production under evolution. For other factorizations $\check{S}_{lin} \neq 0$ will serve as a penalty quantifier, with higher the value of \check{S}_{lin} , the more non classical the factorization.

Pointer Entropy

The other part of the story comes from peaked states of a pointer observable being predictable under evolution. This corresponds to small spread in the variance of such states by a highly collimated self-Hamiltonian as discussed in Section 7.4. One can compute $d(\Delta^2 \hat{O}_A)/dt$ from Eq. (7.19) as a measure of the predictability of the pointer observable, but such a quantity will not be a good homogeneous measure on the same footing as a dimensionless entropy like S_{lin} . This is because from the point of view of constructing an algorithm, we want to take into account both low entanglement growth and predictability of pointer observables to determine the QC factorization.

To discuss an entropy measure that captures essentially the same physics as $d(\Delta^2 \hat{O}_A)/dt$, we define a *Pointer Entropy* as the second order ($q = 2$) Tsallis entropy of the probability distribution given by $\hat{\rho}_A(t)$ in the candidate pointer basis of the eigenstates of \hat{O}_A ,

$$S_{pointer}(t) = 1 - \sum_{j=1}^{d_A} p_j^2(t), \quad (7.42)$$

where $p_j(t)$ is the probability distribution defined by,

$$p_j(t) = \text{Tr}_A \left(\hat{\rho}_A(t) |a_j\rangle \langle a_j| \right) \equiv \text{Tr}_A \left(\hat{\rho}_A(t) \hat{O}_j \right) = \langle a_j | \hat{\rho}_A(t) | a_j \rangle , \quad (7.43)$$

where $\{|a_j\rangle\}$ is the set of eigenstates of \hat{O}_A .

$S_{pointer}$ is an entirely information-theoretic construction and is based on the probability distribution of $\hat{\rho}_A(t)$ in the basis of \hat{O}_A . It is insensitive to any ordering structure of eigenvalues and peaked states in this space. $S_{pointer}$ measures how far the spread of the probability distribution is from being completely certain, but does not capture its variance structure pertaining to a certain set of eigenvalues. Fortunately, as we will now see, for the class of peaked states $|\psi(0)\rangle_{CPO}$ we are considering, changes in $S_{pointer}$ correlate with a change in the variance $d \left(\Delta^2 \hat{O}_A \right) / dt$ of the state itself.

To better understand this connection, let us first compute $\ddot{S}_{pointer}(0)$ in the pointer basis selected in the Quantum Measurement Limit and look for features of the Hamiltonian that lead to small change in $S_{pointer}$ and its correlation with $d \left(\Delta^2 \hat{O}_A \right) / dt$. Our goal is to be able to compare pointer entropy with linear entanglement entropy computed in Appendix (7.8). As we saw, a quantifier for entanglement robustness of unentangled states is $\ddot{S}_{lin}(0)$, and on similar lines we would like to compute $\ddot{S}_{pointer}(0)$. Let us compute $\dot{S}_{pointer}$ explicitly to help us get to $\ddot{S}_{pointer}(0)$. Since we want an expression for $\ddot{S}_{pointer}(0)$, we will just retain $\mathcal{O}(t)$ in the following $\dot{S}_{pointer}$ calculation.

From the definition of $S_{pointer}$ of Eq. (7.42), we see,

$$\dot{S}_{pointer}(t) = -2 \sum_{j=1}^{d_A} p_j(t) \dot{p}_j(t) . \quad (7.44)$$

Following the construction in Appendix (7.8), we can write $\hat{\rho}_A(t)$ to $\mathcal{O}(t)$ as,

$$\begin{aligned} \hat{\rho}_A(t) &= \hat{\rho}_A(0) - it \left[\hat{H}_A, \hat{\rho}_A(0) \right] - it \sum_{\alpha} \lambda_{\alpha} \langle \hat{B}_{\alpha} \rangle_0 \left[\hat{A}_{\alpha}, \hat{\rho}_A(0) \right] \\ &\equiv \hat{\rho}_A(0) - it \left[\hat{H}_A^{\text{eff}}(0), \hat{\rho}_A(0) \right] + \mathcal{O}(t^2) , \end{aligned} \quad (7.45)$$

from which we get,

$$p_j(t) = \text{Tr} \left(\hat{\rho}_A(t) \hat{O}_j \right) = p_j(0) - it \langle \left[\hat{O}_j, \hat{H}_A^{\text{eff}}(0) \right] \rangle_0 + \mathcal{O}(t^2) . \quad (7.46)$$

To $\mathcal{O}(t)$ in the above equation, the effective self-Hamiltonian $\hat{H}_A^{\text{eff}}(0)$ contains a contribution from the interaction terms,

$$\hat{H}_A^{\text{eff}}(0) = \hat{H}_A + \sum_{\alpha} \lambda_{\alpha} \langle \hat{B}_{\alpha} \rangle_0 \hat{A}_{\alpha} . \quad (7.47)$$

In the QML limit, since $[\hat{O}_j, \hat{A}_\alpha] = 0 \forall \alpha, j$, this can be simplified further to depend only on \hat{H}_A ,

$$p_j(t) = p_j(0) - it \langle [\hat{O}_j, \hat{H}_A] \rangle_0 + \mathcal{O}(t^2) \quad (\text{QML}), \quad (7.48)$$

where $p_j(0) = \langle \hat{O}_j \rangle_0$.

To compute $\dot{S}_{pointer}(t)$, we use Eq. (7.110) for $d\hat{\rho}_A/dt$ to $\mathcal{O}(t)$ and notice that, as remarked in section 7.4, the diagonal entries of the decoherence term $\mathcal{D}(\hat{\rho}_A(t))$ in the pointer basis vanish identically, giving the diagonal entries of $d\hat{\rho}_A/dt$ in the pointer basis as shown in Eq. (7.20),

$$\left[\frac{d}{dt} \hat{\rho}_A(t) \right]_{jj} = \left(-i [\hat{H}_A(t), \hat{\rho}_A(t)]_{jj} \right) + \mathcal{O}(t^2), \quad (7.49)$$

which gives us,

$$\begin{aligned} \dot{p}_j(t) &= \text{Tr} \left(\hat{O}_j \frac{d}{dt} \hat{\rho}_A(t) \right) \\ &= -i \text{Tr} \left([\hat{H}_A, \hat{\rho}_A(t)] \hat{O}_j \right) + \mathcal{O}(t^2). \end{aligned} \quad (7.50)$$

Substituting for $\hat{\rho}_A(t)$ to $\mathcal{O}(t)$ from Eq. (7.45), we get,

$$\begin{aligned} \dot{p}_j(t) &= \dot{p}_j(0) - t \text{Tr} \left([\hat{H}_A, [\hat{H}_A, \hat{\rho}_A(0)]] \hat{O}_j \right) - \\ &t \sum_{\alpha} \lambda_{\alpha} \langle \hat{B}_{\alpha} \rangle_0 \text{Tr} \left([\hat{H}_A, [\hat{A}_{\alpha}, \hat{\rho}_A(0)]] \hat{O}_j \right) + \mathcal{O}(t^2), \end{aligned} \quad (7.51)$$

where $\dot{p}_j(0) = -i \text{Tr} \left([\hat{H}_A, \hat{\rho}_A(0)] \hat{O}_j \right) = -i \langle [\hat{O}_j, \hat{H}_A] \rangle_0$. We can now further simplify this in the Quantum Measurement Limit when a consistent pointer observable exists, and after a few lines of trace manipulations we obtain,

$$\begin{aligned} \dot{p}_j(t) &= \dot{p}_j(0) - t \langle \hat{O}_j \hat{H}_A^2 + \hat{H}_A^2 \hat{O}_j - 2\hat{H}_A \hat{O}_j \hat{H}_A \rangle_0 - \\ &t \sum_{\alpha} \lambda_{\alpha} \langle \hat{B}_{\alpha} \rangle_0 \langle [\hat{O}_j, [\hat{H}_A, \hat{A}_{\alpha}]] \rangle_0 + \mathcal{O}(t^2). \end{aligned} \quad (7.52)$$

We can now string everything together to give us an expression for $\ddot{S}_{pointer}(0)$, by taking a time derivative of $\dot{S}_{pointer}(t)$ constructed out of Eqs. (7.48) and (7.52),

$$\begin{aligned} \ddot{S}_{pointer}(0) &= 2 \sum_{j=1}^{d_A} \langle [\hat{O}_j, \hat{H}_A] \rangle_0^2 + 2 \sum_{j=1}^{d_A} \left(p_j(0) \langle \hat{O}_j \hat{H}_A^2 + \hat{H}_A^2 \hat{O}_j - 2\hat{H}_A \hat{O}_j \hat{H}_A \rangle_0 + \right. \\ &\left. 2 \sum_{j=1}^{d_A} \left(p_j(0) \sum_{\alpha} \lambda_{\alpha} \langle \hat{B}_{\alpha} \rangle_0 \langle [\hat{O}_j, [\hat{H}_A, \hat{A}_{\alpha}]] \rangle_0 \right) \right). \end{aligned} \quad (7.53)$$

We see when there exists a consistent pointer observable, its pointer entropy for a peaked initial state correlates with the rate of change of variance $d(\Delta^2 \hat{O}_A)/dt$ as shown in Figure 7.4 (details in caption). One can then interpret the results of Figs. 7.3 and 7.4 together to correlate the pointer entropy growth with the collimation of the self-Hamiltonian, which will play a crucial role in determining how fast the pointer entropy spreads out, thus quantifying the predictability of the pointer observable. Self-Hamiltonians with a higher collimation will induce smaller spread and hence a slower growth in pointer entropy (and rate of change of variance) for peaked pointer states.

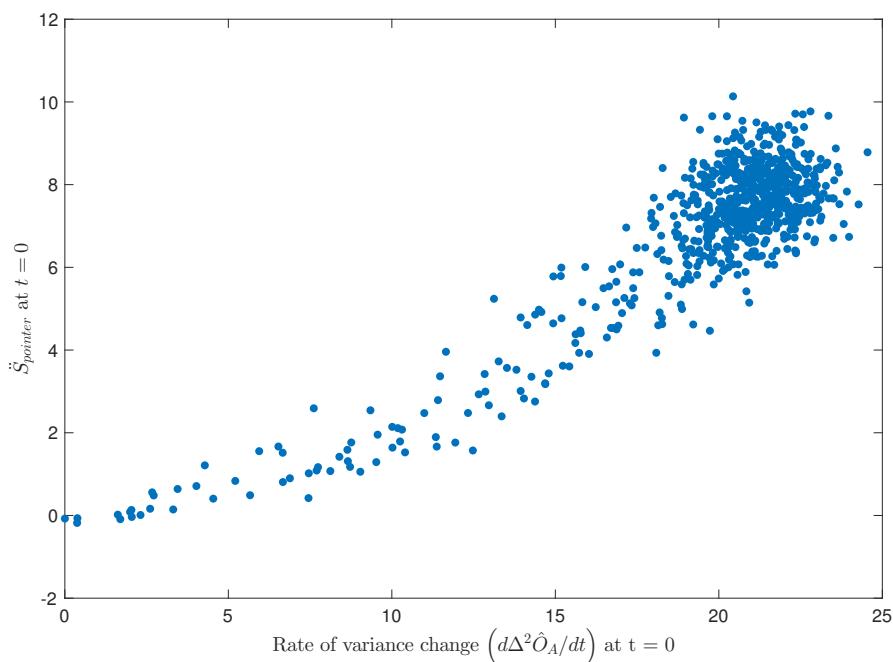


Figure 7.4: Plot showing correlation, in the Quantum Measurement Limit (QML), between pointer entropy $\check{S}_{pointer}(0)$ and the rate of change of variance of the pointer observable for a peaked state in pointer eigenspace. For peaked states in pointer eigenspace, low rate of change of variance implies a small spread in the pointer entropy and is characterized by self-Hamiltonians that are highly collimated in the conjugate direction picked out by the pointer observable. In this example, similar to fig. 7.3, we kept \hat{O}_A fixed at $\hat{O}_A \equiv \hat{\phi}_A$ and changed the self-Hamiltonian \hat{H}_A and computed the correlation for a peaked state in $\hat{\phi}_A$ eigenspace in a Hilbert space of $\dim \mathcal{A} = 27$.

With this connection between pointer entropy and rate of variance change established for cases that admit a consistent pointer observable in the QML, we can broaden our computation of $\check{S}_{pointer}(0)$ to a more general situation that will be useful in

quantifying a predictability measure for the Candidate Pointer Observable (CPO). Using the general expressions for $\hat{\rho}_A(t)$ and $d\hat{\rho}_A/dt$ from Eqs. (7.45) and (7.110), we find,

$$\ddot{S}_{pointer}(0) = -2 \sum_{j=1}^{d_A} \left(\dot{p}_j^2(0) + p_j(0)\ddot{p}_j(0) \right). \quad (7.54)$$

We refrain from writing the full expression here, but the important thing to remember is that for an arbitrary factorization, $\ddot{S}_{pointer}(0)$ for a peaked initial state for the Candidate Pointer Observable will serve as a quantifier for predictability of the candidate. As one goes closer to the QC factorization $\{\theta\}_\theta$, the CPO matches with a true pointer observable, and it becomes predictable for highly collimated self-Hamiltonians. In other factorizations, the value of $\ddot{S}_{pointer}(0)$ will typically be higher as a penalty for the factorization not admitting a good pointer observable.

The Algorithm

We can now summarize the Quantum Mereology Algorithm which sifts through various bipartite factorizations of Hilbert space and searches for the QC factorization. The algorithm will extremize an entropic quantity built from a combination of S_{lin} and $S_{pointer}$ to pick out the QC factorization which shows both features of robustness and predictability as outlined in Section 7.2.

For an arbitrary decomposition $\{\theta\}$,

1. Find the Candidate Pointer Observable $\hat{O}_{CPO} = \hat{O}_A \otimes \hat{O}_B$ from Eq. (7.40), which is the closest tensor product observable compatible with the interaction Hamiltonian.
2. Construct a set of states that represent peaked states of the CPO \hat{O}_A on \mathcal{A} , $|\psi_j(0)\rangle_{CPO} = |\tilde{\psi}_j(0)\rangle_A \otimes |\tilde{\psi}(0)\rangle_B$. They represent an initially predictable state for our subsystem under consideration \mathcal{A} having a definite value of the candidate pointer observable. To ensure quasi-classical conditions hold for all pointer states in the QC factorization, construct d_A number of such states, labeled by $j = 1, 2, \dots, d_A$. One possible prescription for these d_A states $\{|\tilde{\psi}_j(0)\rangle_A\}$ is to construct peaked states around each eigenstate of \hat{O}_A , and take the state on \mathcal{B} to be a uniform superposition of all eigenstates of \hat{O}_B in each case to represent a ready state for the candidate environment \mathcal{B} .
3. For each of these states, $|\psi(0)\rangle_{CPO}$, compute $\ddot{S}_{lin}(0)$ and $\ddot{S}_{pointer}(0)$ from Eqs. (7.10) and (7.54), respectively. These are measures of the quasi-classicality of

the factorization. Lower $\ddot{S}_{lin}(0)$ indicates a factorization whose pointer states (from the CPO) are robust to entanglement production, and lower $\ddot{S}_{pointer}(0)$ indicates a factorization which preserves predictability of classical states under evolution.

4. Define *Schwinger Entropy* (here, its second derivative) as follows,

$$\ddot{S}_{Schwinger} = \max\left(\ddot{S}_{lin}(0), \ddot{S}_{pointer}(0)\right). \quad (7.55)$$

Average over the d_A states from the eigenstates CPO to obtain the value of $\ddot{S}_{Schwinger}$ for the given factorization. We choose to label this quantity as Schwinger entropy to serve as a reminder that we are using Schwinger's unitary basis (from the GPOs) to define our construction in a finite-dimensional context.

5. Find the factorization that minimizes $\ddot{S}_{Schwinger}$. This will be the quasi-classical factorization.

Example

We now demonstrate the algorithm with a simple example where we recover the quasi-classical factorization by sifting through different factorizations of Hilbert space and selecting the one which minimizes Schwinger entropy for candidate classical states.. Let us take our complete quantum system to be described by two harmonic oscillators, coupled together (interacting) by their positions in the quasi-classical factorization. We take both these oscillators to have the same mass m and same frequency ω , and thus having their respective self-Hamiltonians,

$$\hat{H}_A = \frac{\hat{\pi}_A^2}{2m} + \frac{1}{2}m\omega^2\hat{\phi}_A^2, \quad (7.56)$$

$$\hat{H}_B = \frac{\hat{\pi}_B^2}{2m} + \frac{1}{2}m\omega^2\hat{\phi}_B^2. \quad (7.57)$$

The interaction term is modeled as oscillator A 's position $\hat{\phi}_A$ coupled to the position $\hat{\phi}_B$ of oscillator B with an interaction strength λ ,

$$\hat{H}_{int} = \lambda (\hat{\phi}_A \otimes \hat{\phi}_B). \quad (7.58)$$

This conventional way of writing the model makes physical sense to us, and implies a corresponding factorization of Hilbert space. As we now show, this choice matches our above criteria for a quasi-classical factorization as elaborated in Sections 7.3

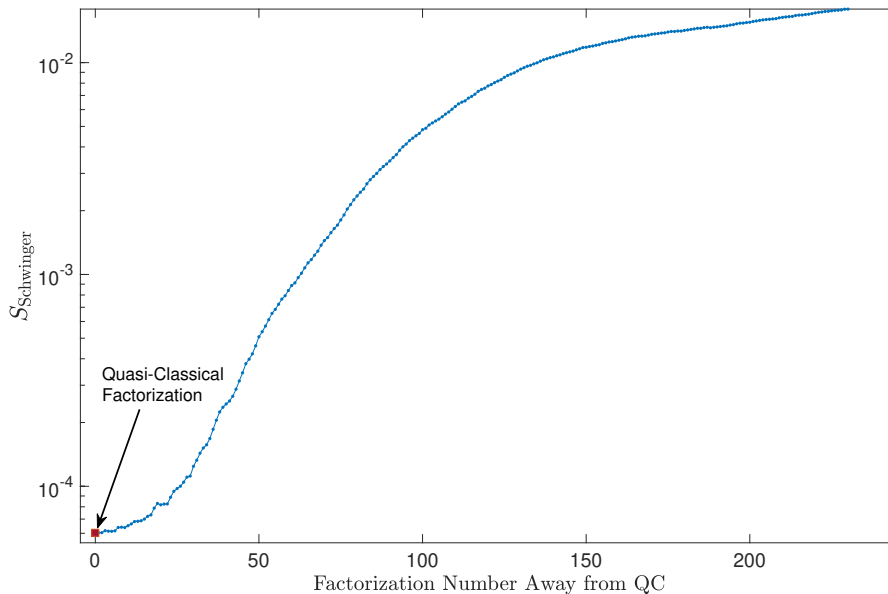


Figure 7.5: Quantum Mereology Algorithm: sifting through different factorizations of Hilbert space to recover the QC factorization by minimization of the Schwinger entropy. In the QC factorization, the quantum system is described by two harmonic oscillators coupled by their positions. The quasi-classical factorization (the first factorization we begin with) is marked by a red square. Details in the text.

and 7.4. The interaction Hamiltonian in the QC factorization takes the simple form $\hat{H}_{int} = \lambda(\hat{A} \otimes \hat{B})$ that is compatible with having low entropy pointer states robust to entanglement under evolution. The pointer observable of subsystem \mathcal{A} under consideration is the position $\hat{\phi}_A$ of that oscillator. The self-Hamiltonian is highly collimated with respect to $\hat{\phi}_A$, as can be seen by the quadratic power of $\hat{\pi}_A$ in \hat{H}_A . We choose values of the parameters m, ω, λ such that we are in the quantum measurement limit (QML) where the interaction term dominates.

We now demonstrate the Quantum Mereology algorithm by “forgetting” that we start in the QC factorization, and try to recover it by sifting through factorizations and select the QC one by minimization of the Schwinger entropy. We change factorizations by introducing incremental, random perturbations away from the identity operator (by making the parameters $\{\theta\}$ non-zero in Eq. 7.63) to construct the global unitary transformation $\tilde{U}(\theta)$. Since we are focusing on the quantum measurement limit, we make sure perturbations do not get large enough so as to break down the assumption of applicability of the QML regime (for example, a factorization change to make the two oscillators completely decoupled would no

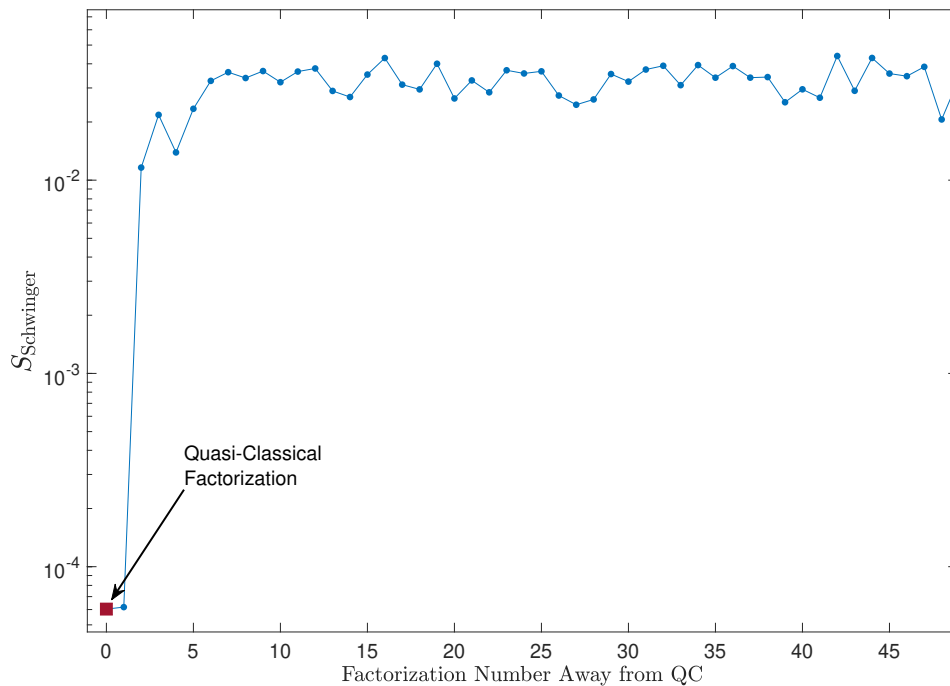


Figure 7.6: Quantum Mereology Algorithm: a run similar to figure 7.5 sifting through different factorizations of Hilbert space but this time with larger, successive perturbations away from the identity operator to generate the unitary transformation Λ . In the QC factorization, which minimizes the Schwinger entropy, the quantum system is described by two harmonic oscillators coupled by their positions. Factorizations away from QC quickly saturate to generic, large values of Schwinger entropy. The quasi-classical factorization (the first factorization we begin with) is marked by a red square. Details in the text.

longer be in the QML, and hence we do not focus on such factorizations in this paper). For each factorization, while the total Hamiltonian is left invariant, the form of the self and interaction terms are altered. We run the Quantum Mereology Algorithm as outlined in Section 7.5 with choosing eigenstates of the CPO \hat{O}_A as our peaked initial, low entropy states (one could construct peaked superpositions too which does not alter the results).

In figure 7.5, we plot the Schwinger entropy for many factorizations the algorithm sifts through, beginning with the QC factorization and then scrambling away. Since we are focusing on small times, we evolve quantum states to a characteristic time of $t_0 = 1/||\hat{H}||_2$ and use the Schwinger entropy $S_{\text{Schwinger}}$ at $t = t_0$ as the representative measure of classicality, instead of explicitly computing the second derivative at $t = 0$, $\ddot{S}_{\text{Schwinger}}(t = 0)$. This is done purely for convenience, and does not affect

the interpretation of picking out the QC factorization since for small times, both the linear entanglement entropy and pointer entropy grow as t^2 . It is seen that Schwinger entropy is minimized for the QC factorization, which exhibits features of both robustness and predictability. In figure 7.6, we plot the results of a similar run but this time with larger, successive perturbations away from the QC factorization (while still being in the quantum measurement limit). While in figure 7.5, we see a more gradual deviation from classicality, in 7.6, there is more rapid growth and saturation of the Schwinger entropy to larger values which are characteristic of generic, non-classical factorizations.

7.6 Discussion

In this paper we have developed a set of criteria, and an associated algorithm, for starting with an initially featureless Hilbert space \mathcal{H} and Hamiltonian \hat{H} , and factorizing \mathcal{H} into a system and environment, optimizing the extent to which the system exhibits quasi-classical behavior. The basic criteria we introduced were that system pointer states remain relatively robust against increasing entanglement with the environment, and that pointer observables evolve in relatively predictable ways. Both notions were quantified in terms of entropy: the linear entropy for entanglement robustness, and pointer entropy for predictability. Useful factorizations are those that minimize the growth of both of these entropies, which we suggested combining into a single ‘‘Schwinger entropy.’’

This work suggests a number of open questions and directions for future investigation. Let us briefly note some of them:

- While promising in principle, it is unclear how feasible our algorithm is in practice. Given nothing but the spectrum of a finite-dimensional Hamiltonian, it could take a long time to sift through the space of factorizations to find the one that minimizes the Schwinger entropy growth rate. It would be interesting to look for more computationally feasible algorithms, even if only approximate.
- We focused on how to factorize Hilbert space into system and environment, but ultimately we would want to continue to factorize the system into appropriate subsystems. We believe that the same basic strategy should apply, though locality and other considerations may come into play.
- We looked exclusively at the Quantum Measurement Limit, in which the system is continuously monitored by the environment. The other extreme case

of the Quantum Decoherence Limit is when the self-Hamiltonian dominates, and the pointer states are energy eigenstates of the self-Hamiltonian. We feel that the same essential concepts should apply, but it would be interesting to look at this case more explicitly.

- The stability of the quasi-classical factorization is another interesting question to study. Do quasi-classical features stay preserved under infinitesimal perturbations of the factorizations or is quasi-classicality finely tuned? We expect classicality to be a robust feature enhanced by the existence of multiple subsystems each redundantly recording information about the others. This ties back into the idea of Quantum Darwinism [153] and it would be interesting to investigate this question further.

As we mentioned at the start, in typical laboratory situations the choice of how to factorize Hilbert space is fairly evident, and the question of mereology doesn't arise. But as we consider more abstract theories, including those of emergent spacetime in quantum gravity [23, 24], our laboratory intuition may no longer be relevant, and an algorithm of the sort presented here can become important. The separation into system and environment that we considered here may be related to how states are redundantly specified in a quantum error-correcting code [24, 34]. It is certainly a central concern of the program of reconstructing the quasi-classical world from the spectrum of the Hamiltonian [22, 65]. Regardless, it is important to understand in principle why we impose the structures on Hilbert space that we do.

7.7 Appendix: Bases and Factorizations

To factorize a Hilbert space of finite dimension $\dim \mathcal{H} = D < \infty$ is to express it as a tensor product of N smaller factors,

$$\mathcal{H} \simeq \bigotimes_{\mu}^N \mathcal{H}_{\mu}. \quad (7.59)$$

The factors \mathcal{H}_{μ} have dimensions d_{μ} . These need not be equal for all μ , but their product must give the overall dimension, $\prod_{\mu}^N d_{\mu} = D$.

The most straightforward way to specify a factorization is in terms of a tensor-product basis that is adapted to it. For convenience we take all of our bases to be orthonormal. In each factor \mathcal{H}_{μ} we fix a basis,

$$\mathcal{H}_{\mu} \simeq \text{span}\{|e_i^{(\mu)}\rangle\}, \quad i = 1, 2, \dots, d_{\mu}. \quad (7.60)$$

We can then define basis vectors for \mathcal{H} as a whole by taking the tensor product of individual basis elements,

$$\mathcal{H} \simeq \bigotimes_{\mu=1}^N \text{span}\{|e_i^{(\mu)}\rangle\}. \quad (7.61)$$

Of course such bases are highly non-unique; unitary transformations within each separate factor will leave the associated factorization itself unchanged.

In practice, one can construct different factorizations of \mathcal{H} by starting with some reference factorization and associated tensor-product basis, then performing a unitary transformation that mixes factors. To implement the change in decomposition, we pick a special unitary matrix $\tilde{U} \in SU(D) \setminus \left(\bigotimes_{\mu=1}^N U(d_\mu) \right)$ that is characterized by $(D^2 - 1)$ real parameters $\{\theta_a \mid a = 1, 2, \dots, (D^2 - 1)\}$ and has $D^2 - 1$ traceless, Hermitian generators $\{\Lambda_a \mid a = 1, 2, \dots, (D^2 - 1)\}$, which can be identified with the Generalized Gell-Mann matrices (GGMM). These GGMMs come in three groups: symmetric, anti-symmetric and diagonal matrices. In the notation where E^{jk} is the $D \times D$ matrix with all zeros, except a 1 in the (j, k) location, the GGMMs have the following form, each identified with one of the Λ_a ,

$$\Lambda_{sym}^{jk} = E^{kj} + E^{jk} \ ; \ 1 \leq j < k \leq D, \quad (7.62a)$$

$$\Lambda_{antisym}^{jk} = -i \left(E^{jk} - E^{kj} \right) \ ; \ 1 \leq j < k \leq D, \quad (7.62b)$$

$$\Lambda_{diag}^l = \sqrt{\frac{2}{l(l+1)}} \left(-l E^{l+1, l+1} + \sum_{j=1}^l E^{jj} \right) \ ; \ 1 \leq l \leq D - 1. \quad (7.62c)$$

We work with special unitary instead of unitary since the global $U(1)$ phase is irrelevant to the physics of factorization changes and now we can express the factorization change unitary $\tilde{U}(\theta)$ as,

$$\tilde{U}(\theta) = \exp \left(\sum_{a=1}^{D^2-1} \theta_a \Lambda_a \right), \quad (7.63)$$

and factorization changes can be implemented on the reference decomposition.

In light of this parametrization, let us label decompositions by the set of parameters $\{\theta\}$, which are used to implement the factorization change relative to the reference decomposition $\{0\}$. This notation will help us succinctly show dependence of various quantities on the factorization of Hilbert space. Product states in the old tensor-product basis (such as basis states in this factorization) will now be entangled

in the new global basis identified with a new tensor product structure. Generally, operators that are local in their action to a certain sub-factor in a given decomposition such as $\hat{O}_\nu \equiv \hat{\mathbb{I}} \otimes \hat{\mathbb{I}} \otimes \cdots \otimes \hat{o}_\nu \otimes \cdots \otimes \hat{\mathbb{I}}$, which act non-trivially only on the ν -th subsystem, will generically act on more than one sub-factor in a different factorization. Locality of operators is a highly factorization-dependent statement and it has been shown [22] that most tensor factorizations of Hilbert space for a given Hamiltonian do not look local and the existence of dual local descriptions is rare and almost unique.

In a given decomposition, any operator $\hat{M} \in \mathcal{L}(\mathcal{H})$, the space of linear operators on \mathcal{H} can then be naturally decomposed as,

$$\hat{M} = \left(\frac{m_0}{D}\right) \hat{\mathbb{I}} + \sum_{\mu=1}^N \hat{M}_\mu^{\text{self}} + \hat{M}_{\text{int}}, \quad (7.64)$$

where $m_0 = \text{Tr}(\hat{M})$ is the trace of \hat{M} , the operator $\hat{M}_\mu^{\text{self}}$ is the (traceless) term that acts locally only on the \mathcal{H}_μ sub-factor and an interaction term, also traceless, connecting different sub-factors \hat{M}_{int} . The interaction term can be decomposed further as a sum of n -point interactions,

$$\hat{M}_{\text{int}} = \sum_{n=2}^N \left(\sum_{\mu_1 > \mu_2 > \cdots > \mu_n} \hat{M}_{\text{int}}(\mu_1, \mu_2, \cdots, \mu_n) \right), \quad (7.65)$$

where, $\hat{M}_{\text{int}}(\mu_1, \mu_2, \cdots, \mu_n)$ is a term connecting sub-factors labeled by $\mu_1, \mu_2, \cdots, \mu_n$. Any traceless, local term \hat{M}_μ that acts on a single sub-factor \mathcal{H}_μ can be expanded out in the basis of Generalize Gell-Mann operators $\hat{\Lambda}_a^\mu$ with $a = 1, 2, \cdots, (d_\mu^2 - 1)$, which are $(d_\mu^2 - 1)$ traceless, Hermitian generators of the $SU(d_\mu)$,

$$\hat{M}_\mu \equiv \hat{\mathbb{I}} \otimes \hat{\mathbb{I}} \otimes \cdots \otimes \hat{M}_\mu \otimes \cdots \otimes \hat{\mathbb{I}} = \hat{\mathbb{I}} \otimes \hat{\mathbb{I}} \otimes \cdots \otimes \sum_{a=1}^{d_\mu^2-1} m_a \hat{\Lambda}_a \otimes \cdots \otimes \hat{\mathbb{I}}. \quad (7.66)$$

In general, any operator \hat{M} can also be decomposed in the canonical operator basis formed from the defining tensor-product basis,

$$\hat{M} = \sum_{i,j=1}^D m_{ij} |e_i\rangle_{TPB} \langle e_j|. \quad (7.67)$$

Such expansions do not necessarily show the locality and interaction terms explicitly, but in the preferred, semi-classical decomposition, one would be able to arrange them in the form of familiar semi-classical terms in which features like robustness, quasi-separability and decoherence will be manifest.

7.8 Appendix: Evolution of the Linear Entropy

In this section we calculate the evolution of the linear entropy S_{lin} to $\mathcal{O}(t^2)$, leading to Eq. (7.10). Using the Zassenhaus expansion, which is a corollary of the Baker-Campbell-Hausdorff (BCH) lemma, one can separate the sum in the time evolution exponential $\hat{U}(t)$ as,

$$\hat{U}(t) = \exp(-i(\hat{H}_{\text{self}} + \hat{H}_{\text{int}})t), \quad (7.68)$$

$$\hat{U}(t) = \exp(-i\hat{H}_{\text{int}}t) \exp(-i\hat{H}_{\text{self}}t) \exp\left(-\frac{(-it)^2}{2} [\hat{H}_{\text{int}}, \hat{H}_{\text{self}}]\right) \exp(\mathcal{O}(t^3)). \quad (7.69)$$

We can move the $\exp\left(-\frac{(-it)^2}{2} [\hat{H}_{\text{int}}, \hat{H}_{\text{self}}]\right)$ past the $\exp(-i\hat{H}_{\text{self}}t)$ term to the left since the commutator we pick up is $\mathcal{O}(t^3)$ as can be explicitly checked by use of the Zassenhaus expansion again to get,

$$\hat{U}(t) = \exp(-i\hat{H}_{\text{int}}t) \exp\left(-\frac{(-it)^2}{2} [\hat{H}_{\text{int}}, \hat{H}_{\text{self}}]\right) \exp(-i\hat{H}_{\text{self}}t) \exp(\mathcal{O}(t^3)). \quad (7.70)$$

Further one can see that the first two pieces involving \hat{H}_{int} and $[\hat{H}_{\text{int}}, \hat{H}_{\text{self}}]$ in the above equation Eq. (7.70) can be combined into a sum of a single exponential since the non-commuting pieces will be $\mathcal{O}(t^3)$, and this gives us a succinct expression for $\hat{U}(t)$ to $\mathcal{O}(t^2)$,

$$U(t) = \exp(-i\hat{E}(t)t) \exp(-i\hat{H}_{\text{self}}t) + \mathcal{O}(t^3), \quad (7.71)$$

where,

$$\hat{E}(t) \equiv \hat{H}_{\text{int}} + \frac{it}{2} [\hat{H}_{\text{int}}, \hat{H}_{\text{self}}]. \quad (7.72)$$

Taking $\hat{U}(t)$ from Eq. (7.71), the time evolved state is $\hat{\rho}(t) = \hat{U}(t)\hat{\rho}(0)\hat{U}^\dagger(t)$ to $\mathcal{O}(t^2)$.

Let us define self-evolved states $\hat{\sigma}_A(t) = \exp(-i\hat{H}_A t)\hat{\rho}_A(0)\exp(i\hat{H}_A t)$ and $\hat{\sigma}_B(t) = \exp(-i\hat{H}_B t)\hat{\rho}_B(0)\exp(i\hat{H}_B t)$ and write the state $\hat{\rho}(t)$ as,

$$\hat{\rho}(t) = \exp(-i\hat{E}(t)t) (\hat{\sigma}_A \otimes \hat{\sigma}_B) \exp(i\hat{E}(t)t), \quad (7.73)$$

which can be expanded out to $\mathcal{O}(t^2)$ as,

$$\hat{\rho}(t) = (\hat{\sigma}_A \otimes \hat{\sigma}_B)_{\mathcal{O}(t^2)} - it [\hat{E}(t), (\hat{\sigma}_A \otimes \hat{\sigma}_B)] + \frac{(-it)^2}{2} [\hat{E}(t), [\hat{E}(t), \hat{\sigma}_A \otimes \hat{\sigma}_B]] + \mathcal{O}(t^3). \quad (7.74)$$

Let us now focus on one subsystem, say \mathcal{A} , and look at its reduced dynamics by computing its reduced density matrix $\hat{\rho}_A(t)$ by tracing out \mathcal{B} ,

$$\begin{aligned} \hat{\rho}_A(t) = \text{Tr}_B \hat{\rho}(t) = \hat{\sigma}_A(t) - it \text{Tr}_B \left[\hat{H}_{\text{int}} + \frac{it}{2} [\hat{H}_{\text{int}}, \hat{H}_{\text{self}}], (\hat{\sigma}_A \otimes \hat{\sigma}_B) \right] \\ - \frac{t^2}{2} \text{Tr}_B [\hat{H}_{\text{int}}, [\hat{H}_{\text{int}}, \hat{\rho}(0)]] + O(t^3). \end{aligned} \quad (7.75)$$

Written out (almost) explicitly using the diagonal form of \hat{H}_{int} of Eq. (7.5), $\hat{\rho}_A(t)$ takes the following form,

$$\begin{aligned} \hat{\rho}_A(t) = \hat{\sigma}_A(t) - it \sum_{\alpha} \lambda_{\alpha} \text{Tr}_B \left(\hat{A}_{\alpha} \hat{\sigma}_A \otimes \hat{B}_{\alpha} \hat{\sigma}_B - \hat{\sigma}_A \hat{A}_{\alpha} \otimes \hat{\sigma}_B \hat{B}_{\alpha} \right) \\ + \frac{t^2}{2} \sum_{\alpha} \lambda_{\alpha} \text{Tr}_B \left[[\hat{A}_{\alpha} \otimes \hat{B}_{\alpha}, \hat{H}_{\text{self}}], \hat{\sigma}_A(t) \otimes \hat{\sigma}_B(t) \right] \\ - \frac{t^2}{2} \sum_{\alpha, \beta} \lambda_{\alpha} \lambda_{\beta} \text{Tr}_B \left[\hat{A}_{\alpha} \otimes \hat{B}_{\beta}, [\hat{A}_{\alpha} \otimes \hat{B}_{\beta}, \hat{\rho}(0)] \right] + O(t^3). \end{aligned} \quad (7.76)$$

The partial trace over \mathcal{B} can be used to condense terms into expectation values of operators that act only on \mathcal{B} for a given state $\hat{\rho}_B$ since $\text{Tr}_B (\hat{O}_B \hat{\rho}_B) = \langle \hat{O}_B \rangle$. Let us compactly write, $\hat{\rho}_A(t) = \hat{\sigma}_A(t)_{O(t^2)} + T_1 + T_2 + T_3$, which can be simplified as,

$$\begin{aligned} T_1 = -it \sum_{\alpha} \lambda_{\alpha} \text{Tr}_B \left(\hat{A}_{\alpha} \hat{\sigma}_A \otimes \hat{B}_{\alpha} \hat{\sigma}_B - \hat{\sigma}_A \hat{A}_{\alpha} \otimes \hat{\sigma}_B \hat{B}_{\alpha} \right) + O(t^3) \\ = -it \sum_{\alpha} \lambda_{\alpha} \left([\hat{A}_{\alpha}, \hat{\sigma}_A(t)] \langle \hat{B}_{\alpha} \rangle^{\text{self}}(t) \right), \end{aligned} \quad (7.77)$$

where $\langle \hat{B}_{\alpha} \rangle_t^{\text{self}} = \text{Tr}_B (\hat{B}_{\alpha} \hat{\sigma}_B(t))$. We can write the other terms T_2 and T_3 to $O(t^2)$ as,

$$T_2 = \frac{t^2}{2} \sum_{\alpha} \lambda_{\alpha} \left([[\hat{A}_{\alpha}, \hat{H}_A], \hat{\rho}_A(0)] \langle \hat{B}_{\alpha} \rangle_0 + [\hat{A}_{\alpha}, \hat{\rho}_A(0)] \langle [\hat{B}_{\alpha}, \hat{H}_B] \rangle_0 \right), \quad (7.78)$$

and,

$$\begin{aligned} T_3 = \frac{-t^2}{2} \sum_{\alpha, \beta} \lambda_{\alpha} \lambda_{\beta} \left(\hat{A}_{\alpha} \hat{A}_{\beta} \hat{\rho}_A(0) \langle \hat{B}_{\alpha} \hat{B}_{\beta} \rangle_0 - \hat{A}_{\beta} \hat{\rho}_A(0) \hat{A}_{\alpha} \langle \hat{B}_{\alpha} \hat{B}_{\beta} \rangle_0 \right. \\ \left. - \hat{A}_{\alpha} \hat{\rho}_A(0) \hat{A}_{\beta} \langle \hat{B}_{\beta} \hat{B}_{\alpha} \rangle_0 + \hat{\rho}_A(0) \hat{A}_{\beta} \hat{A}_{\alpha} \langle \hat{B}_{\beta} \hat{B}_{\alpha} \rangle_0 \right). \end{aligned} \quad (7.79)$$

We next consider entanglement between the two subsystems \mathcal{A} and \mathcal{B} . A common measure is to use the von-Neumann entanglement entropy $S_{vN}(\hat{\rho}) = -\text{Tr}(\hat{\rho} \log \hat{\rho})$

for a given density matrix $\hat{\rho}$. However, the presence of the logarithm makes the entropy hard to analytically compute and give expressions for, hence we will focus on its leading order contribution, the linear entropy (which is the Tsallis second order entropy measure), $S_{lin}(\hat{\rho}) = (1 - \text{Tr} \hat{\rho}^2)$.

We can expand the self-evolved density matrix $\hat{\sigma}_A(t)$ to $\mathcal{O}(t^2)$ as,

$$\hat{\sigma}_A(t) = \hat{\rho}_A(0) - it [\hat{H}_A, \hat{\rho}_A(0)] + \frac{(-it)^2}{2} [\hat{H}_A, [\hat{H}_A, \hat{\rho}_A(0)]] + \mathcal{O}(t^3). \quad (7.80)$$

It can be explicitly checked that despite truncation upto $\mathcal{O}(t^2)$, in each order of the expansion, the self-evolved density operator $\hat{\sigma}_A(t)$ is pure and obeys $\hat{\sigma}_A^2(t) = \hat{\sigma}_A(t)$ and $\text{Tr} \hat{\sigma}_A(t) = 1$.

Let us now compute the linear entanglement entropy $S_{lin}(\hat{\rho}_A(t)) = (1 - \text{Tr} \hat{\rho}_A^2(t))$ for the reduced density matrix of \mathcal{A} given by Eq. (7.74), which corresponds to starting with an unentangled (and hence, zero entropy) state $\hat{\rho}(0)$. Using the cyclic property of trace, it can be shown that $\text{Tr}(\hat{\sigma}_A(t)T_1) = \text{Tr}(\hat{\sigma}_A(t)T_2) = 0$ to $\mathcal{O}(t^2)$, and hence we get,

$$S_{lin}(\hat{\rho}_A(t)) = 1 - \text{Tr}(\hat{\sigma}_A^2(t)) - \text{Tr}(T_1^2) - \text{Tr}(\hat{\sigma}_A(t)T_3) + \mathcal{O}(t^3), \quad (7.81)$$

which further using $\text{Tr} \hat{\sigma}_A(t) = \text{Tr} \hat{\sigma}_A^2(t) = 1$ reduces to,

$$S_{lin}(\hat{\rho}_A(t)) = -\text{Tr}(T_1^2) - \text{Tr}(\hat{\sigma}_A(t)T_3) + \mathcal{O}(t^3). \quad (7.82)$$

As we will do below – since we are working to $\mathcal{O}(t^2)$ – we will replace $\hat{\sigma}_A(t)$ with $\hat{\rho}_A(0)$ in any terms that have a factor of t^2 out-front. The remaining two terms in Eq. (7.82) can be computed to $\mathcal{O}(t^2)$ in a straightforward way,

$$\text{Tr}(T_1^2) = (-it)^2 \sum_{\alpha, \beta} \lambda_\alpha \lambda_\beta \langle \hat{B}_\alpha \rangle_0 \langle \hat{B}_\beta \rangle_0 \text{Tr}([\hat{A}_\alpha, \hat{\rho}_A(0)] [\hat{A}_\beta, \hat{\rho}_A(0)]), \quad (7.83)$$

which can be simplified by noting that for pure states $\hat{\rho}_A(0) = |\psi_A(0)\rangle \langle \psi_A(0)|$, certain trace terms simplify into product of expectation values, such as,

$$\text{Tr}(\hat{A}_\alpha \hat{\rho}_A(0) \hat{A}_\beta \hat{\rho}_A(0)) = \langle \hat{A}_\alpha \rangle_0 \langle \hat{A}_\beta \rangle_0. \quad (7.84)$$

Thus, further using such simplifications, we arrive at the following expressions for $\text{Tr}(T_1^2)$ and $\text{Tr}(\hat{\sigma}_A(t)T_3)$ to $\mathcal{O}(t^2)$,

$$\text{Tr}(T_1^2) = -t^2 \sum_{\alpha, \beta} \lambda_\alpha \lambda_\beta \langle \hat{B}_\alpha \rangle_0 \langle \hat{B}_\beta \rangle_0 \left(2 \langle \hat{A}_\alpha \rangle_0 \langle \hat{A}_\beta \rangle_0 - \langle \{\hat{A}_\alpha, \hat{A}_\beta\}_+ \rangle_0 \right), \quad (7.85)$$

$$\begin{aligned} \text{Tr}(\hat{\rho}_A(0)T_3) = \text{Tr}(\hat{\sigma}_A(t)T_3) = & -\frac{t^2}{2} \sum_{\alpha,\beta} \lambda_\alpha \lambda_\beta \left(\langle \hat{B}_\alpha \hat{B}_\beta \rangle_0 \langle \hat{A}_\alpha \hat{A}_\beta \rangle_0 - \langle \hat{B}_\alpha \hat{B}_\beta \rangle_0 \langle \hat{A}_\alpha \rangle_0 \langle \hat{A}_\beta \rangle_0 \right. \\ & \left. - \langle \hat{B}_\beta \hat{B}_\alpha \rangle_0 \langle \hat{A}_\alpha \rangle_0 \langle \hat{A}_\beta \rangle_0 + \langle \hat{B}_\beta \hat{B}_\alpha \rangle_0 \langle \hat{A}_\alpha \hat{A}_\beta \rangle_0 \right), \end{aligned} \quad (7.86)$$

where $\{\hat{O}_1, \hat{O}_2\}_+ = (\hat{O}_1 \hat{O}_2 + \hat{O}_2 \hat{O}_1)$ is the anticommutator of \hat{O}_1 and \hat{O}_2 . Putting these together in Eq. (7.82), we obtain the desired result of Eq. (7.10),

$$\begin{aligned} S_{lin}(\hat{\rho}_A(t)) = t^2 \sum_{\alpha,\beta} \lambda_\alpha \lambda_\beta & \left(\langle \hat{A}_\alpha \hat{A}_\beta \rangle_0 \langle \hat{B}_\alpha \hat{B}_\beta \rangle_0 + \langle \hat{A}_\beta \hat{A}_\alpha \rangle_0 \langle \hat{B}_\beta \hat{B}_\alpha \rangle_0 \right. \\ & \left. - \langle \hat{A}_\alpha \rangle_0 \langle \hat{A}_\beta \rangle_0 \left(\langle \{\hat{B}_\alpha, \hat{B}_\beta\}_+ \rangle_0 - \langle \hat{B}_\alpha \rangle_0 \langle \hat{B}_\beta \rangle_0 \right) \right) \quad (7.87) \\ & - \langle \hat{B}_\alpha \rangle_0 \langle \hat{B}_\beta \rangle_0 \left(\langle \{\hat{A}_\alpha, \hat{A}_\beta\}_+ \rangle_0 - \langle \hat{A}_\alpha \rangle_0 \langle \hat{A}_\beta \rangle_0 \right) \Big) + \mathcal{O}(t^3). \end{aligned}$$

7.9 Appendix: Generalized Pauli Operators

Here, we provide a brief review of generalized Pauli operators (GPOs) and their use to define finite-dimensional conjugate variables closely following the exposition of Ref. [10]. The interested reader is referred to Refs. [10, 76, 91] (and references therein) for more detail.

Consider a finite-dimensional Hilbert Space \mathcal{H} of dimension $\dim \mathcal{H} = d \in \mathbb{Z}^+$ with $d < \infty$. The GPO algebra on the space of linear operators $\mathcal{L}(\mathcal{H})$ acting on \mathcal{H} comes equipped with two unitary (but not necessarily Hermitian) operators as generators of the algebra, call them \hat{A} and \hat{B} , which satisfy the following commutation relation,

$$\hat{A}\hat{B} = \omega^{-1}\hat{B}\hat{A}, \quad (7.88)$$

where $\omega = \exp(2\pi i/d)$ is the d -th primitive root of unity. This commutation relation is also more commonly known as the Weyl braiding relation [77], and any further notions of commutations between conjugate, self-adjoint operators defined from \hat{A} and \hat{B} will be derived from this relation. In addition to being unitary, $\hat{A}\hat{A}^\dagger = \hat{A}^\dagger\hat{A} = \hat{\mathbb{1}} = \hat{B}\hat{B}^\dagger = \hat{B}^\dagger\hat{B}$, the algebra cyclically closes, giving it a cyclic structure in eigenspace,

$$\hat{A}^d = \hat{B}^d = \hat{\mathbb{1}}, \quad (7.89)$$

where $\hat{\mathbb{1}}$ is the identity operator on $\mathcal{L}(\mathcal{H})$.

The GPO algebra can be constructed for both even and odd values of d and both cases are important and useful in different contexts. Here, we focus on the case

of odd $d \equiv 2l + 1$, which will be useful in constructing conjugate variables whose eigenvalues can be thought of labeling lattice sites, centered around zero. While the subsequent construction can be done in a basis-independent way, we choose a hybrid route, switching between an explicit representation of the GPO and abstract vector space relations. Let us follow the convention that all indices used in this section (for the case of odd $d = 2l + 1$), for labeling states or matrix elements of an operator in some basis will run from $-l, (-l + 1), \dots, -1, 0, 1, \dots, l$. The operators are further specified by their eigenvalue spectrum, and it is identical for both the GPO generators \hat{A} and \hat{B} ,

$$\text{spec}(\hat{A}) = \text{spec}(\hat{B}) = \{\omega^{-l}, \omega^{-l+1}, \dots, \omega^{-1}, 1, \omega^1, \dots, \omega^{l-1}, \omega^l\}. \quad (7.90)$$

There exists a unique irreducible representation (up to unitary equivalences) (see [9] for details) of the generators of the GPO defined via Eqs. (7.21) and (7.89) in terms of $N \times N$ matrices

$$A = \begin{bmatrix} 0 & 0 & 0 & \dots & 1 \\ 1 & 0 & 0 & \dots & 0 \\ 0 & 1 & 0 & \dots & 0 \\ \cdot & \cdot & \dots & \cdot & \\ \cdot & \cdot & \dots & \cdot & \\ 0 & 0 & \dots & 1 & 0 \end{bmatrix}_{N \times N}. \quad (7.91)$$

$$B = \begin{bmatrix} \omega^{-l} & 0 & 0 & \dots & 0 \\ 0 & \omega^{-l+1} & 0 & \dots & 0 \\ \cdot & \cdot & \dots & \cdot & \\ \cdot & \cdot & \dots & \cdot & \\ 0 & 0 & 0 & \dots & \omega^l \end{bmatrix}_{N \times N}. \quad (7.92)$$

The $\hat{\cdot}$ has been removed to stress that these matrices are representations of the operators \hat{A} and \hat{B} in a particular basis, in this case, the eigenbasis \hat{B} (so that B is diagonal). More compactly, the matrix elements of operators \hat{A} and \hat{B} in the basis representation of eigenstates of \hat{B} ,

$$[A]_{jk} \equiv \langle b_j | \hat{A} | b_k \rangle = \delta_{j,k+1}, \quad (7.93)$$

$$[B]_{jk} \equiv \langle b_j | \hat{B} | b_k \rangle = \omega^j \delta_{j,k}, \quad (7.94)$$

where is the Kronecker Delta function. The operator \hat{A} acts as a “cyclic shift” operator for the eigenstates of \hat{B} , sending an eigenstate to the next,

$$\hat{A} |b_j\rangle = |b_{j+1}\rangle . \quad (7.95)$$

The unitary nature of these generators implies a cyclic structure which identifies $|b_{l+1}\rangle \equiv |b_{-l}\rangle$, so that $\hat{A} |b_l\rangle = |b_{-l}\rangle$. The operators \hat{A} and \hat{B} have the same relative action on the other’s eigenstates, since nothing in the algebra sets the two apart. It has already been seen in Eq. (7.95) that \hat{A} generates (unitary, cyclic) unit shifts in eigenstates of B and the opposite holds too: the operator \hat{B} generates unit shifts in eigenstates of \hat{A} (given by the relation $\hat{A} |a_k\rangle = \omega^k |a_k\rangle$, $k = -l, \dots, 0, \dots, l$) and has a similar action with a cyclic correspondence to ensure unitarity,

$$\hat{B} |a_k\rangle = |a_{k+1}\rangle , \quad (7.96)$$

with cyclic identification $|a_{l+1}\rangle \equiv |a_{-l}\rangle$. Hence we already have a set of operators that generate shifts in the eigenstates of the other, which is precisely what conjugate variables do and which is why we see that the GPOs provides a very natural structure to define conjugate variables on Hilbert Space. The GPO generators \hat{A} and \hat{B} have been extensively studied in various contexts in quantum mechanics, and offer a higher dimensional, non-Hermitian generalization of the Pauli matrices. In particular, for $d = 2$ it will be seen that $A = \sigma_1$ and $B = \sigma_3$, which recovers the Pauli matrices.

The defining notion for a pair of conjugate variables is the identification of two self-adjoint operators acting on Hilbert space, each of which generates translations in the eigenstates of the other. For instance, in (conventionally infinite-dimensional) textbook quantum mechanics, the momentum operator \hat{p} generates shifts/translations in the eigenstates of its conjugate variable, the position \hat{q} operator, and vice versa. Taking this as our defining criterion, we define a pair of Hermitian conjugate operators $\hat{\phi}$ and $\hat{\pi}$, acting on a finite-dimensional Hilbert space, each of which is the generator of translations in the eigenstates of its conjugate, with the following identification,

$$\hat{A} \equiv \exp(-i\alpha\hat{\pi}), \quad \hat{B} = \exp(i\beta\hat{\phi}), \quad (7.97)$$

where α and β are non-zero real parameters.

To further reinforce this conjugacy relation between operators \hat{A} and \hat{B} , we see that they are connected to each under a discrete Fourier transformation implemented by Sylvester’s Circulant Matrix S , which is a $N \times N$ unitary matrix ($SS^\dagger = S^\dagger S = \hat{\mathbb{I}}$),

connecting A and B ,

$$SAS^{-1} = B. \quad (7.98)$$

Sylvester's matrix has the following form, which we identify to be in the $\{ |b_j\rangle \}$ basis, with j and k running from $-l, \dots, 0, \dots, l$:

$$[S]_{jk} = \frac{\omega^{jk}}{\sqrt{N}}. \quad (7.99)$$

Since A and B are non-singular and diagonalizable, it follows that $\log A$ and $\log B$ exist, even though multivalued. In the case of odd dimension $d = 2l + 1$, their principle logarithms are well defined and we are able to find explicit matrix representations for operators $\hat{\phi}$ and $\hat{\pi}$. In particular, we can obtain matrix representation for $\hat{\pi}$ in the $|\phi_j\rangle$ basis,

$$\begin{aligned} \langle \phi_j | \hat{\pi} | \phi_{j'} \rangle &= \left(\frac{2\pi}{(2l+1)^2 \alpha} \right) \sum_{n=-l}^l n \exp \left(\frac{2\pi i (j-j') n}{2l+1} \right) \\ &= \begin{cases} 0, & \text{if } j = j' \\ \left(\frac{i\pi}{(2l+1)\alpha} \right) \operatorname{cosec} \left(\frac{2\pi l (j-j')}{2l+1} \right), & \text{if } j \neq j'. \end{cases} \end{aligned} \quad (7.100)$$

The matrix elements of $\hat{\pi}$ in the eigenbasis of $\hat{\phi}$ are non-local, in the sense that they have power-law-like decay in $(j - j')$, and hence connect arbitrary “far” eigenstates of $\hat{\phi}$. This is a feature of the finite-dimensional construction and in the infinite-dimensional limit $d \rightarrow \infty$, we recover the local form of $\hat{\phi}$ as $-id/d\phi$ as expected. Of course, $\hat{\phi}$ has common eigenstates with those of \hat{B} and $\hat{\pi}$ shares eigenstates with \hat{A} . The corresponding eigenvalue equations for $\hat{\phi}$ and $\hat{\pi}$ can be easily deduced using Eqs. (7.22) and (7.90),

$$\hat{\phi} |\phi_j\rangle = j \left(\frac{2\pi}{(2l+1)\beta} \right) |\phi_j\rangle, \quad j = -l, \dots, 0, \dots, l, \quad (7.101)$$

$$\hat{\pi} |\pi_j\rangle = j \left(\frac{2\pi}{(2l+1)\alpha} \right) |\pi_j\rangle, \quad j = -l, \dots, 0, \dots, l, \quad (7.102)$$

These conjugate variables defined on a finite-dimensional Hilbert space will not satisfy Heisenberg canonical commutation relation $[\hat{\phi}, \hat{\pi}] = i$ (in units where $\hbar = 1$), since by the Stone-von Neumann theorem there are no finite-dimensional representations of Heisenberg CCR. However, $\hat{\phi}$ and $\hat{\pi}$ still serve as a robust notion of

conjugate variables and their commutation can be derived from the more fundamental Weyl Braiding Relation of Eq. (7.21). In the large dimension limit $d \rightarrow \infty$, one recovers Heisenberg form of the CCR if the parameters α and β are constrained to obey $\alpha\beta = 2\pi/d$.

7.10 Appendix: Generic Evolution of Reduced Density Operators

We can further illustrate how decoherence is a non-generic feature as discussed in Section 7.3 by taking the general expression found for the reduced density operator $\hat{\rho}_A(t)$ to $\mathcal{O}(t^2)$ in the bipartite case discussed in Eq. (7.76) and studying it further to find conditions when off-diagonal elements in the pointer basis get suppressed relatively quickly leading to effective decoherence.

Let us compute the time derivative of the reduced density matrix, $\dot{\hat{\rho}}_A(t)$ to help us understand when decoherence is effective and leads to dynamic suppression of off-diagonal elements in the pointer basis. We will work explicitly to $\mathcal{O}(t)$ to keep a tractable number of terms, enough to help us see decoherence in action,

$$\dot{\hat{\rho}}_A(t) = \dot{\hat{\sigma}}_A(t) + \dot{T}_1 + \dot{T}_2 + \dot{T}_3 + \mathcal{O}(t^2), \quad (7.103)$$

where we can use the von-Neumann evolution equation for a density operator, $\dot{\hat{\sigma}}_A(t) = -i [\hat{H}_A, \hat{\sigma}_A(t)]$. The time derivatives of T_2 and T_3 are easy to take from Eqs. (7.78) and (7.79) since they both have a factor of t^2 out-front. The time derivative of T_1 can be computed to $\mathcal{O}(t)$ as follows,

$$\begin{aligned} \dot{T}_1 = & \left(-i \sum_{\alpha} \lambda_{\alpha} \langle \hat{B}_{\alpha} \rangle_t^{\text{self}} [\hat{A}_{\alpha}, \hat{\sigma}_A(t)] \right) - it \sum_{\alpha} \lambda_{\alpha} \langle \dot{\hat{B}}_{\alpha} \rangle_0 [\hat{A}_{\alpha}, \hat{\rho}_A(0)] \\ & - it \sum_{\alpha} \lambda_{\alpha} \langle \hat{B}_{\alpha} \rangle_0 [\hat{A}_{\alpha}, \dot{\hat{\sigma}}_A(t)] + \mathcal{O}(t^2), \end{aligned} \quad (7.104)$$

where to retain Eq. (7.104) to $\mathcal{O}(t)$, we can write $\dot{\hat{\sigma}}_A(t)_{\mathcal{O}(t)} = -i [\hat{H}_A, \hat{\rho}_A(0)]$ and from the expression for $\langle \hat{B}_{\alpha} \rangle_t^{\text{self}}$,

$$\begin{aligned} \langle \hat{B}_{\alpha} \rangle_t^{\text{self}} = & \text{Tr} (\hat{\sigma}_B(t) \hat{B}_{\alpha}) = \langle \hat{B}_{\alpha} \rangle_0 - it \text{Tr} ([\hat{H}_B, \hat{\rho}_B(0)] \hat{B}_{\alpha}) \\ & - \frac{t^2}{2} \text{Tr} ([\hat{H}_B, [\hat{H}_B, \hat{\rho}_B(0)]] \hat{B}_{\alpha}) + \mathcal{O}(t^3), \end{aligned} \quad (7.105)$$

we can extract the $\langle \dot{\hat{B}}_{\alpha} \rangle_0$ which will contribute to Eq. (7.104) to $\mathcal{O}(t)$,

$$\langle \dot{\hat{B}}_{\alpha} \rangle_0 = i \langle [\hat{H}_B, \hat{B}_{\alpha}] \rangle_0. \quad (7.106)$$

Plugging these in Eq. (7.103), we find the term with $\langle \hat{B}_\alpha \rangle_0$ cancels with one of the terms in \dot{T}_2 to yield,

$$\begin{aligned} \dot{\hat{\rho}}_A(t) = & -i [\hat{H}_A^{\text{eff}}(t), \hat{\sigma}_A(t)] - t \sum_{\alpha} \lambda_{\alpha} \langle \hat{B}_{\alpha} \rangle_0 \left([\hat{A}_{\alpha}, [\hat{H}_A, \hat{\rho}_A(0)]] - [[\hat{A}_{\alpha}, \hat{H}_A], \hat{\rho}_A(0)] \right) \\ & + \dot{T}_3 + \mathcal{O}(t^2), \end{aligned} \quad (7.107)$$

where we have defined an effective self-Hamiltonian for \mathcal{A} , which weighs in a relevant contribution from the interaction terms \hat{A}_{α} ,

$$\hat{H}_A^{\text{eff}}(t) = \hat{H}_A + \sum_{\alpha} \lambda_{\alpha} \langle \hat{B}_{\alpha} \rangle_t^{\text{self}} \hat{A}_{\alpha} + \mathcal{O}(t^2). \quad (7.108)$$

Let us write this in a more suggestive way such that the evolution equation of $\dot{\hat{\rho}}_A(t)$ can be explicitly split into a unitary piece and a piece that will induce decoherence under the right conditions. To $\mathcal{O}(t)$, let us write $\hat{\sigma}_A(t) = \hat{\rho}_A(t)_{\mathcal{O}(t)} - (T_1)_{\mathcal{O}(t)}$ and substitute in Eq. (7.107) while also noticing that the term

$\left([\hat{A}_{\alpha}, [\hat{H}_A, \hat{\rho}_A(0)]] - [[\hat{A}_{\alpha}, \hat{H}_A], \hat{\rho}_A(0)] \right)$ condenses to $[\hat{H}_A, [\hat{A}_{\alpha}, \hat{\rho}_A(0)]]$,

$$\begin{aligned} \dot{\hat{\rho}}_A(t) = & -i [\hat{H}_A^{\text{eff}}(t), \hat{\rho}_A(t)] + t \sum_{\alpha} \lambda_{\alpha} \langle \hat{B}_{\alpha} \rangle_0 [\hat{H}_A, [\hat{A}_{\alpha}, \hat{\rho}_A(0)]] \\ & + t \sum_{\alpha, \beta} \lambda_{\alpha} \lambda_{\beta} \langle \hat{B}_{\alpha} \rangle_0 \langle \hat{B}_{\beta} \rangle_0 [\hat{A}_{\alpha}, [\hat{A}_{\beta}, \hat{\rho}_A(0)]] \\ & - t \sum_{\alpha} \lambda_{\alpha} \langle \hat{B}_{\alpha} \rangle_0 [\hat{H}_A, [\hat{A}_{\alpha}, \hat{\rho}_A(0)]] + \dot{T}_3 + \mathcal{O}(t^2). \end{aligned} \quad (7.109)$$

The term containing $[\hat{H}_A, [\hat{A}_{\alpha}, \hat{\rho}_A(0)]]$ cancels away and after substituting for \dot{T}_3 from Eq. (7.79) and collecting terms, we see that the final expression for $\dot{\hat{\rho}}_A(t)$ to $\mathcal{O}(t)$ is,

$$\begin{aligned} \dot{\hat{\rho}}_A(t) = & -i [\hat{H}_A^{\text{eff}}(t), \hat{\rho}_A(t)] - t \sum_{\alpha, \beta} \lambda_{\alpha} \lambda_{\beta} \left((\hat{A}_{\alpha} \hat{A}_{\beta} \hat{\rho}_A(0) - \hat{A}_{\beta} \hat{\rho}_A(0) \hat{A}_{\alpha}) \left(\langle \hat{B}_{\alpha} \hat{B}_{\beta} \rangle_0 - \langle \hat{B}_{\alpha} \rangle_0 \langle \hat{B}_{\beta} \rangle_0 \right) \right. \\ & \left. + (\hat{\rho}_A(0) \hat{A}_{\beta} \hat{A}_{\alpha} - \hat{A}_{\alpha} \hat{\rho}_A(0) \hat{A}_{\beta}) \left(\langle \hat{B}_{\beta} \hat{B}_{\alpha} \rangle_0 - \langle \hat{B}_{\beta} \rangle_0 \langle \hat{B}_{\alpha} \rangle_0 \right) \right) + \mathcal{O}(t^2). \end{aligned} \quad (7.110)$$

Thus, we see that the equation for $\dot{\hat{\rho}}_A(t)$ to $\mathcal{O}(t)$ splits into a term $(-i [\hat{H}_A^{\text{eff}}(t), \hat{\rho}_A(t)])$, which corresponds to unitary evolution of $\hat{\rho}_A(t)$ under the effective self-Hamiltonian $\hat{H}_A^{\text{eff}}(t)$ and a term that will be responsible for decoherence under right conditions.

Let us focus on this “decoherence” term $\mathcal{D}(\hat{\rho}_A)$ and not concern ourselves with the unitary evolution for the moment (the \supset representing that we are focusing only on the decoherence term),

$$\begin{aligned} \hat{\rho}_A(t) \supset \mathcal{D}(\hat{\rho}_A) \equiv & -t \sum_{\alpha, \beta} \lambda_\alpha \lambda_\beta \left(\left(\hat{A}_\alpha \hat{A}_\beta \hat{\rho}_A(0) - \hat{A}_\beta \hat{\rho}_A(0) \hat{A}_\alpha \right) \left(\langle \hat{B}_\alpha \hat{B}_\beta \rangle_0 - \langle \hat{B}_\alpha \rangle_0 \langle \hat{B}_\beta \rangle_0 \right) \right. \\ & \left. + \left(\hat{\rho}_A(0) \hat{A}_\beta \hat{A}_\alpha - \hat{A}_\alpha \hat{\rho}_A(0) \hat{A}_\beta \right) \left(\langle \hat{B}_\beta \hat{B}_\alpha \rangle_0 - \langle \hat{B}_\beta \rangle_0 \langle \hat{B}_\alpha \rangle_0 \right) \right) + \mathcal{O}(t^2). \end{aligned} \quad (7.111)$$

In the Quantum Measurement Limit, when there exists a consistent pointer basis $\{|a_j\rangle \mid j = 1, 2, \dots, d_A\}$ which will be selected such that it forms simultaneous eigenstates of all $\hat{A}_\alpha \forall \alpha$,

$$\hat{A}_\alpha |a_j\rangle = a_j^\alpha |a_j\rangle \quad \forall \alpha \text{ and } j = 1, 2, \dots, d_A. \quad (7.112)$$

This is a highly non-generic situation, since an arbitrary Hamiltonian in an arbitrary factorization will have non-commuting terms in \hat{H}_{int} and hence not admit a complete basis satisfying Eq. (7.112) to serve as a pointer basis. For decoherence to be effective, there would be a small number of consistent terms in \hat{H}_{int} being monitored by the other subsystem as discussed in Section 7.3.

Let us see this explicitly by considering the off-diagonal matrix element,

$\langle a_j | \hat{\rho}_A(t) | a_k \rangle$, $j \neq k$ of $\hat{\rho}_A(t)$ in the purported pointer basis $\{|a_j\rangle\}$. The decoherence term $\mathcal{D}(\hat{\rho}_A(t))$ in Eq. (7.111) can be further split into $\alpha = \beta$ terms and $\alpha \neq \beta$ ones. The cross-terms with $\alpha \neq \beta$ are not seen to have a definitive sign that is needed for decoherence to take place. On the other hand, let us look at the $\alpha = \beta$ terms of the matrix element with $j \neq k$,

$$[\hat{\rho}_A(t)]_{jk} \supset -t \sum_{\alpha} \lambda_\alpha^2 \left(\langle \hat{B}_\alpha^2 \rangle_0 - \langle \hat{B}_\alpha \rangle_0^2 \right) \langle a_j | \left(\hat{A}_\alpha^2 \hat{\rho}_A(0) - 2\hat{A}_\alpha \hat{\rho}_A(0) \hat{A}_\alpha + \hat{\rho}_A(0) \hat{A}_\alpha^2 \right) | a_k \rangle, \quad (7.113)$$

which can be further simplified using Eq. (7.112),

$$\left[\frac{d}{dt} \hat{\rho}_A(t) \right]_{jk} \supset -t \sum_{\alpha} \lambda_\alpha^2 \left(\langle \hat{B}_\alpha^2 \rangle_0 - \langle \hat{B}_\alpha \rangle_0^2 \right) (a_j - a_k)^2 [\hat{\rho}_A(0)]_{jk} + \mathcal{O}(t^2). \quad (7.114)$$

Now since we are working to $\mathcal{O}(t)$ in Eq. (7.114), we can replace $[\hat{\rho}_A(0)]_{jk}$ with $[\hat{\rho}_A(t)]_{jk}$ since corrections will contribute to $\mathcal{O}(t^2)$ due to the presence of the factor of t in the expansion,

$$\left[\frac{d}{dt} \hat{\rho}_A(t) \right]_{jk} \supset -t \left(\sum_{\alpha} \lambda_\alpha^2 \Delta^2(\hat{B}_\alpha)_0 (a_j - a_k)^2 \right) [\hat{\rho}_A(t)]_{jk} + \mathcal{O}(t^2). \quad (7.115)$$

The term in the parenthesis $\left(\sum_{\alpha} \lambda_{\alpha}^2 \Delta^2 (\hat{B}_{\alpha})_0 (a_j - a_k)^2\right)$ is positive definite since the term, $\Delta^2 (\hat{B}_{\alpha})_0 \equiv \left(\langle \hat{B}_{\alpha}^2 \rangle_0 - \langle \hat{B}_{\alpha} \rangle_0^2\right)$ is the variance of \hat{B}_{α} in the state $\hat{\rho}_A(0)$, and hence positive by construction. This leads to decoherence since off-diagonal terms in Eq. (7.115) get suppressed dynamically in the pointer basis selected by \hat{H}_{int} .

Thus, we see that for decoherence to be effective, there should exist a small number of consistent terms in \hat{H}_{int} being monitored by the other subsystems (\mathcal{B} in this case), which will give us a notion of pointer basis in which off-diagonal elements of $\hat{\rho}_A(t)$ are dynamically suppressed due to interaction with the environment. Most of our classic models of decoherence [168] indeed consist of a single term (or a small number of compatible terms) representing environmental monitoring of the form $\hat{H}_{\text{int}} = \lambda (\hat{A} \otimes \hat{B})$ and hence there will be decoherence in the eigenbasis of \hat{A} , which serve as pointer states. From Eq. (7.115), we can give an estimate for the decoherence time-scale τ_d for the (j, k) matrix element, focusing on the $\hat{H}_{\text{int}} = \lambda (\hat{A} \otimes \hat{B})$ for clarity,

$$(\tau_d)_{jk} \sim \frac{\sqrt{2}}{|\lambda| |a_j - a_k| |\Delta (\hat{B}_{\alpha})_0|}. \quad (7.116)$$

Thus, as we can see from the above Eq. (7.116), for higher interaction strength, there is more stronger monitoring of \mathcal{A} by \mathcal{B} and hence faster decoherence. More variance of \hat{B} in the initial state allows for more support in state space for monitoring and quicker suppression of interference and also, we see that decoherence time-scales are inversely proportional to the spectral differences in \hat{A} . This can also be easily understood since more spacing between eigenvalues of \hat{A} would lead to inducing faster orthogonality in conditional states of \mathcal{B} , and hence more effective decoherence.

*Chapter 8***TOWARDS SPACE FROM HILBERT SPACE: FINDING
LATTICE STRUCTURES IN FINITE-DIMENSIONAL
QUANTUM SYSTEMS**

Field theories place one or more degrees of freedom at every point in space. Hilbert spaces describing quantum field theories, or their finite-dimensional discretizations on lattices, therefore have large amounts of structure: they are isomorphic to the tensor product of a smaller Hilbert space for each lattice site or point in space. Local field theories respecting this structure have interactions which preferentially couple nearby points. The emergence of classicality through decoherence relies on this framework of tensor-product decomposition and local interactions. We explore the emergence of such lattice structure from Hilbert-space considerations alone. We point out that the vast majority of finite-dimensional Hilbert spaces cannot be isomorphic to the tensor product of Hilbert-space subfactors that describes a lattice theory. A generic Hilbert space can only be split into a direct sum corresponding to a basis of state vectors spanning the Hilbert space; we consider setups in which the direct sum is naturally decomposed into two pieces. We define a notion of direct-sum locality which characterizes states and decompositions compatible with Hamiltonian time evolution. We illustrate these notions for a toy model that is the finite-dimensional discretization of the quantum-mechanical double-well potential. We discuss their relevance in cosmology and field theory, especially for theories which describe a landscape of vacua with different spacetime geometries.

This chapter is based on the following reference:

J. Pollack and A. Singh, “Towards space from Hilbert space: finding lattice structure in finite-dimensional quantum systems,” *Quant. Stud. Math. Found.* **6** no. 2, (2019) 181–200, [arXiv:1801.10168](https://arxiv.org/abs/1801.10168) [quant-ph]

8.1 Introduction

Mathematically, the basic objects of quantum mechanics are state vectors in an abstract Hilbert space. Yet the real world is well-described by one such state in one such space. It is natural to ask what additional features distinguish our state

and Hilbert space from generic ones. We know, for example, some details of the field content of our universe: it contains (at minimum) the fields in the Standard Model, a spin-two graviton, and potentially additional fields such as dark matter, an inflaton, etc. In particular, the quantum-mechanical theory which describes our universe has a description (in the semiclassical limit) as a theory of *fields*: that is, it has degrees of freedom which live at each point of some background spatial manifold (which in turn is a spatial slice of a four-dimensional spacetime geometry which solves Einstein's equations). Furthermore, to a very good approximation, the universe appears classical: we typically observe objects with definite values of classical variables (such as position and momentum) rather than in superpositions, and the time evolution of (expectation values of) these quantities obeys classical equations of motion. When considered as a point in a classical Hamiltonian phase space, it is also apparent that the current state of the universe is special: it is a low-entropy state far from equilibrium, with nontrivial evolution that exhibits an arrow of time.

Understanding the origin of all of these features is a vast research program. In this chapter we focus on one feature: the fact that the time evolution¹ of the state vector of the universe can be described as the time evolution of field-theoretic degrees of freedom living on a background space of definite dimension (and geometry). We are motivated to investigate this feature in particular because it seems to be a prerequisite for applying our most successful models of the emergence of classicality. The decoherence program [27, 154, 173, 174] explains how the unitary evolution of a single quantum-mechanical state is naturally viewed as a process involving the creation (via entropy production) of distinct classical branches which evolve independently without interference. The set of branches is selected by the Hamiltonian governing time evolution: when Hilbert space is decomposed into a preferred choice of subsystems [29, 114], the branches are the states which remain robust to the influence of the interactions between subsystems, i.e. in which the state of a given subsystem is preserved by interactions with the environment. This story relies crucially on the ability to decompose the Hilbert space into many interacting subsystems—or, equivalently, to identify local degrees of freedom [22]. Once these

¹In canonical quantum gravity, the Wheeler-DeWitt equation [4] implies that the action of the Hamiltonian is identically zero. Recovering a notion of nontrivial time evolution in quantum gravity can be regarded as one aspect of the problem of emergent time and is thus largely beyond the scope of our paper. We will assume for the purposes of our paper that we are given (the spectrum of) a Hamiltonian, either fundamental or emergent, and can use it to evolve state vectors in Hilbert space.

local degrees of freedom are identified, it seems plausible that space itself can be built up from considering the interactions between subsystems (c.f. [23, 40, 65, 153] and references therein), although this process is still incompletely understood. Or, more directly, the degrees of freedom can be organized into a spatial lattice or spin chain.

The goal of this chapter is to provide answers to two questions:

- When does a quantum-mechanical theory describe spatial degrees of freedom?
- When we know a theory *does* describe spatial degrees of freedom, to what extent can we identify them from purely quantum-mechanical data?

In investigating these questions we largely restrict ourselves to finite-dimensional Hilbert spaces. This is partly for convenience: understanding how such spaces can be decomposed is much more mathematically tractable (with no need, for example, to consider type III von Neumann algebras). Nevertheless, a number of arguments associated with complementarity and black hole entropy [18, 41, 175] suggest that the set of degrees of freedom accessible to any observer in a local region of space is actually finite [17]. These arguments are sharpest in an asymptotically de Sitter spacetime which is dominated by vacuum energy, where a horizon-sized patch of spacetime is a maximum-entropy thermal state with a finite entropy and a corresponding finite number of degrees of freedom [20, 21].

Given this restriction, we can answer the first question by checking when a finite-dimensional quantum-mechanical theory can describe a lattice theory. A simple number-theoretic argument, which we give in Section 8.2 below, gives a surprising answer to this question: almost never! That is, for almost all choices of finite positive integer N , independent of the Hamiltonian, there is *no* Hilbert space of dimension N which can describe a lattice theory with spatial dimension $\ll N$. We are therefore led to slightly generalize our setup, to include Hilbert spaces which can be decomposed into pieces which each describes a spatial lattice. As a toy model, we consider the finite-dimensional analog of the double-well potential. For a large enough barrier, low-lying states should decompose into a piece in the left well and a piece in the right well. We use the tools of generalized Clifford algebras (GCAs) (for a review, see [9] and references therein) to formalize this intuition. The lessons from this simple example should be applicable to more general examples of cosmological relevance, such as landscape potentials in which each minimum describes a different metastable vacuum solution.

The remainder of this chapter is organized as follows. In Section 8.2, we give a simple number-theoretic argument that almost all finite-dimensional Hilbert spaces are unable to describe lattice theories. In Section 8.3, we therefore move on to describe Hilbert spaces which are a direct sum of lattice theories. In Section 8.4, we build on this description to give a definition of *direct-sum locality*, which measures when a particular decomposition of a Hilbert space divides it into pieces which remain separate under the action of the Hamiltonian. In Section 8.5, we apply these definitions to a worked example: the double-well potential. We show how we can use the various measures of locality to identify a natural decomposition of the Hilbert space which successfully describes a spatial lattice theory. In Section 8.6, we argue that the strategy developed for the double-well potential should be of more general applicability to (finite-dimensional truncations of) field theory. Finally, we conclude this chapter in Section 8.7.

8.2 The Non-Genericity of Lattice Hilbert Spaces

Consider a finite-dimensional quantum-mechanical theory that lives on a spatial lattice, i.e. whose Hilbert space is isomorphic to a tensor product of smaller Hilbert spaces (we have used \simeq to denote Hilbert space isomorphism),

$$\mathcal{H}_{\text{lattice}} \simeq \mathcal{H}_{\text{site}}^{\otimes N_{\text{sites}}}. \quad (8.1)$$

If the lattice is embedded in a multidimensional space, we can further write

$$N_{\text{sites}} = \prod_{i=1}^{N_{\text{dim}}} N_{\text{sites}}^{(i)}. \quad (8.2)$$

Now consider the constraints that the factorization relation (8.1) places on the dimensionality of $\mathcal{H}_{\text{lattice}}$. We have seen that the dimension of the Hilbert spaces we are considering takes the form

$$|\mathcal{H}_{\text{lattice}}| = |\mathcal{H}_{\text{site}}|^{N_{\text{sites}}}. \quad (8.3)$$

So, just as the Hilbert space has N_{sites} subfactors, its dimension has $\sim N_{\text{sites}}$ prime factors (where the \sim covers the fact that $|\mathcal{H}_{\text{site}}|$ might itself have multiple prime factors). That is,

$$\# \text{ of prime factors of } |\mathcal{H}_{\text{lattice}}| \equiv \Omega(|\mathcal{H}_{\text{lattice}}|) \sim \ln |\mathcal{H}_{\text{lattice}}|. \quad (8.4)$$

The function $\Omega(n)$ counts the number of prime factors (including multiplicity) of the natural number n . It is closely related to $\omega(n)$, the number of distinct prime factors

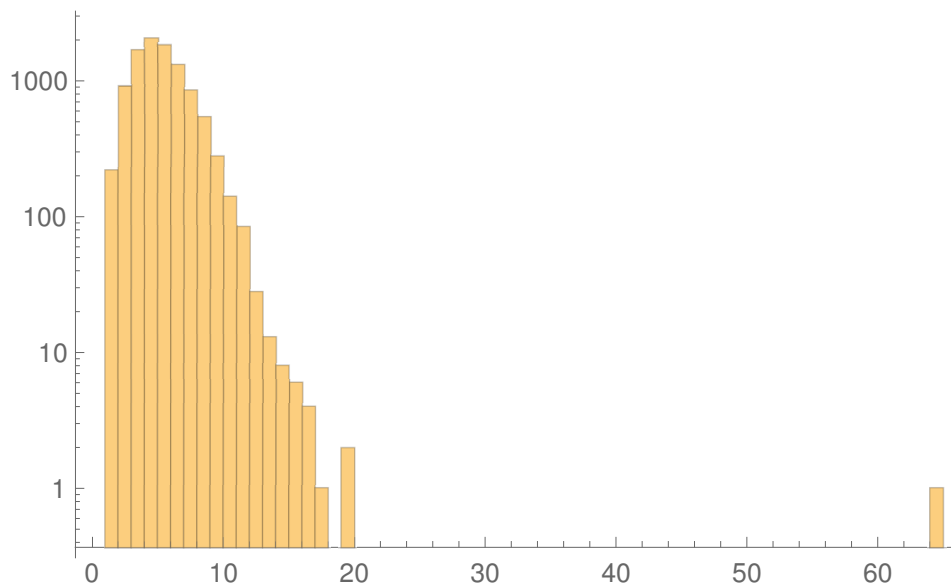


Figure 8.1: Histogram of $\Omega(n)$ for $2^{64} - 5000 < n < 2^{64} + 5000$. The mean is 4.85, the standard deviation is 2.21.

of n . Famously, the Hardy-Ramanujan theorem [176] says that asymptotically

$$\omega(n) \sim \ln \ln n, \text{ var}(\omega(n)) \sim \ln \ln n. \quad (8.5)$$

The total number of prime factors $\Omega(n)$ can be shown to have a similar asymptotic expansion (e.g. [177]):

$$\Omega(n) \sim \ln \ln n, \text{ var}(\Omega(n)) \sim \ln \ln n. \quad (8.6)$$

So, as the size of a Hilbert space gets larger, it becomes vanishingly rare for the Hilbert space to have a dimension of the right size for it to describe a lattice theory.

To gain some intuition for this phenomenon, consider Hilbert spaces around the same size as that of a $4 \times 4 \times 4$ lattice of qubits,

$$|\mathcal{H}_{\text{lattice}}| \approx 2^{64} \approx 1.8 \times 10^{19}. \quad (8.7)$$

We have

$$\ln |\mathcal{H}_{\text{lattice}}| \approx 64 \ln 2 \approx 44, \ln \ln |\mathcal{H}_{\text{lattice}}| \approx 3.8. \quad (8.8)$$

As Figures 8.1, 8.2, and 8.3 show, when we histogram the integers around 2^{64} , we indeed find that typical integers n in this range have $\Omega(n) \sim \ln \ln n$. In particular, the mean number of factors is 4.8 and the standard deviation around the mean is 2.1 – 2.2. 2^{64} itself is then an extreme—30 sigma!—outlier.

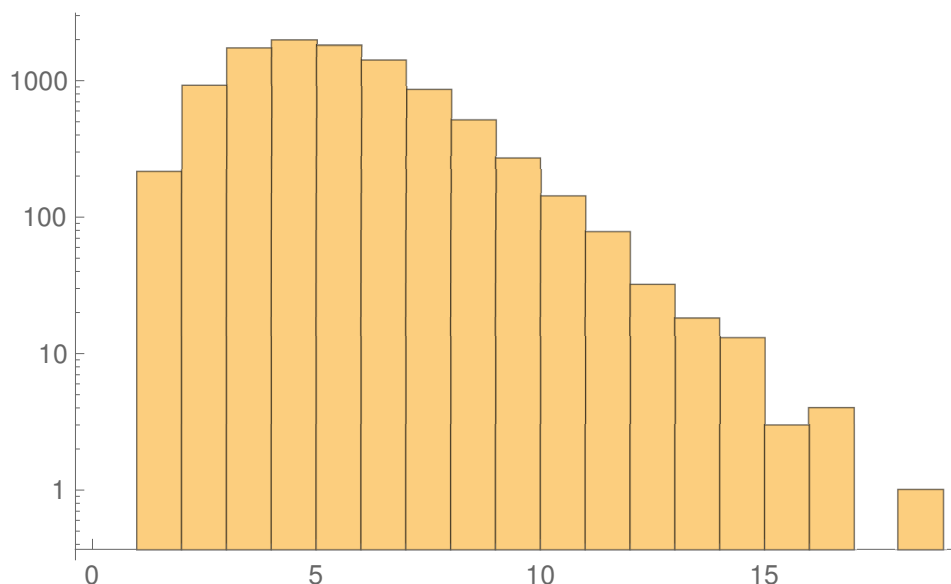


Figure 8.2: Histogram of $\Omega(n)$ for $2^{64} - 15000 < n < 2^{64} - 5000$. The mean is 4.84, the standard deviation is 2.13.

8.3 Direct-Sum Hilbert Spaces

In the previous section we argued that large Hilbert spaces—like the one which describes our own universe, which must be at least as large as $\exp(S_{dS}) \sim \exp(10^{122})$ to describe our Hubble volume—are vanishingly unlikely to decompose in the manner necessary to describe a lattice quantum field theory. On the other hand, we can always identify subspaces of a large Hilbert space—for example, those with dimension equal to the largest power of 2 smaller than the dimensionality of the Hilbert space—which might themselves be decomposed into a product over lattice sites:

$$\mathcal{H} = \mathcal{H}_{\text{lattice}} \oplus \mathcal{H}_{\text{remainder}}, |\mathcal{H}_{\text{lattice}}| = 2^{\lfloor \log_2 n \rfloor} \equiv n_{\text{lattice}} \implies \Omega(n_{\text{lattice}}) \sim \ln n_{\text{lattice}} \sim \ln |\mathcal{H}|. \quad (8.9)$$

Could the Hilbert space of our universe be of this form? In such a situation, a generic state in \mathcal{H} would be a superposition of a state in the lattice subspace and a state in the (typically non-geometric) remainder space. Put another way, an initial “geometric” state in the lattice Hilbert space is not constrained to remain within it under the action of the Hamiltonian: part of it can “leak out” into the remainder of the Hilbert space. This is not a familiar situation in standard quantum field theory, where the use of a unitary S-matrix is predicated on both initial and final asymptotic states being the vacuum of a field theory on a fixed background. However, we have

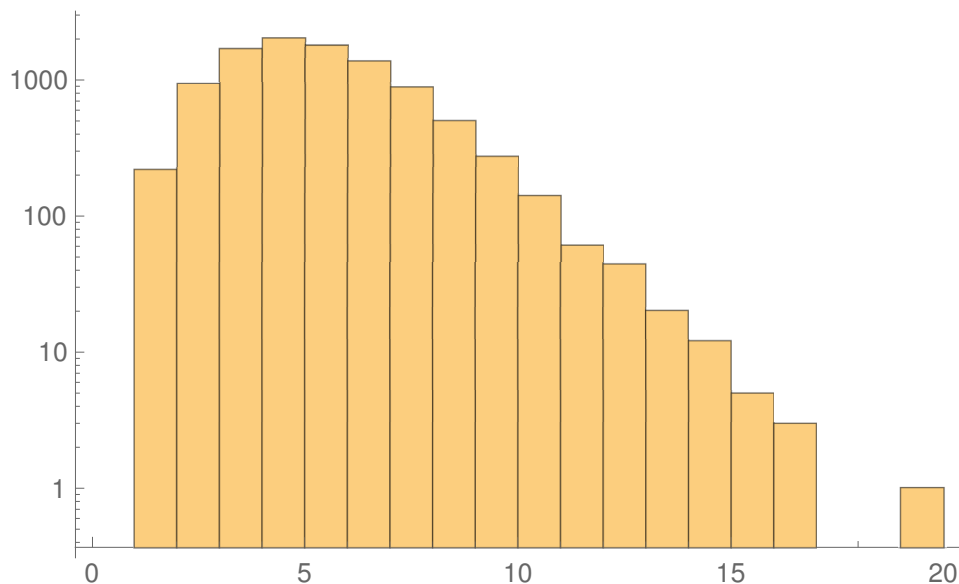


Figure 8.3: Histogram of $\Omega(n)$ for $2^{64} + 5000 < n < 2^{64} + 15000$. The mean is 4.84, the standard deviation is 2.13.

used language meant to suggest situations where this does occur: barrier decay in quantum mechanics or, in quantum field theory in curved space, the decay of metastable vacua by bubble nucleation.

In the latter case, one typically considers states localized around particular (meta)stable vacua, which are each given geometric interpretations, but a generic state describes a superposition of field configurations of different background geometries. That is, states in such a theory with multiple vacua are necessarily not states in a single field theory, but superpositions of states in different field theories, and thus a finite-dimensional version of such a theory does not have a Hilbert space with the tensor-product structure of a single lattice theory, but is instead a sum of such tensor-product spaces. We discuss the field-theoretic interpretations of our results further in Section 8.6 below. In the remainder of this section, we develop a formalism for the simplest such system: Hilbert spaces which divide into two pieces, each of which describes a lattice.

Suppose we have a Hilbert space \mathcal{H} with a finite dimension $\dim \mathcal{H} = N < \infty$. Given an operator $\hat{O} \in \mathcal{L}(\mathcal{H})$, we can write the eigenstates of the operator

$$\hat{O} |o_i\rangle = O_i |o_i\rangle \quad (8.10)$$

(dealing with degeneracies as necessary so that the $\{|o_i\rangle, i = 1, 2, \dots, N\}$ are an

orthonormal basis for \mathcal{H}) and decompose a generic state $|\Psi\rangle \in \mathcal{H}$ as

$$|\Psi\rangle = \sum_i c_i^{(\hat{O})} |o_i\rangle. \quad (8.11)$$

We can thus also decompose the Hilbert space as a direct sum of one-dimensional subspaces,

$$\mathcal{H} = \bigoplus_i \mathcal{H}_i^{(\hat{O})}, \quad (8.12)$$

with $\mathcal{H}_i^{(\hat{O})} \simeq \mathbb{C}$ the one-dimensional Hilbert space consisting of scalar multiples of $|o_i\rangle$. Let us define a choice of *scrambling* of this direct-sum decomposition by choosing a permutation σ of our set of ordered eigenstates $(1, 2, 3, \dots, N)$ followed by a division into two mutually exclusive and exhaustive sets A_σ and B_σ , of cardinality $|A_\sigma| = m$ and $|B_\sigma| = N - m$,

$$\sigma(1, \dots, N) = (\sigma_1, \dots, \sigma_N) = (\sigma_1, \dots, \sigma_m) \cup (\sigma_{m+1}, \dots, \sigma_N) \equiv A_\sigma \cup B_\sigma, \quad (8.13)$$

where, of course, viewed as unordered sets, we have $A_\sigma \cup B_\sigma = \{1, 2, 3, \dots, N\}$ and $A_\sigma \cap B_\sigma = \emptyset$. We will denote the canonical, ordered set $(1, 2, 3, \dots, N)$ as the one corresponding to $\sigma = \text{id}$ (i.e. the identity permutation). This allows us to write our Hilbert space \mathcal{H} as a direct sum of two Hilbert spaces of dimension m and $N - m$, respectively:

$$\mathcal{H} \simeq \mathcal{H}_{A_\sigma}^{(\hat{O})} \oplus \mathcal{H}_{B_\sigma}^{(\hat{O})}, \quad (8.14)$$

where

$$\mathcal{H}_{A_\sigma}^{(\hat{O})} \equiv \bigoplus_{j \in A_\sigma} \mathcal{H}_j^{(\hat{O})} \quad \text{and} \quad \mathcal{H}_{B_\sigma}^{(\hat{O})} \equiv \bigoplus_{j' \in B_\sigma} \mathcal{H}_{j'}^{(\hat{O})}. \quad (8.15)$$

Let us denote this choice of direct-sum decomposition as $D_\oplus \equiv \{\hat{O}, \sigma, m\}$ which consists of a choice of the operator \hat{O} , the permutation σ , and subspace size m as defined above.

Our formalism thus far has been totally generic: it describes all possible partitions of a Hilbert space of dimension N into two parts. We would like, however, to find the particular partitions (if there are any) which reflect genuine features of the theory. In particular, as we discussed above, useful partitions should be approximately preserved under time evolution, so that geometric states localized in one of the Hilbert spaces only gradually leak into the other one. We say that partitions where this is the case exhibit *direct-sum locality*. To diagnose it, we will need measures which depend not only on N and \hat{O} , but also on the Hamiltonian \hat{H} .

First consider the special case $\hat{O} = \hat{H}$. We can decompose any state $|\Psi\rangle$ in terms of energy eigenstates $|e_i\rangle$, where each $\mathcal{H}_i^{(\hat{H})}$ is (isomorphic to) the set of vectors in \mathbb{C}^N proportional to $|e_i\rangle$. A natural division of the energy eigenstates is the states below/above the energy E_m of the m -th energy eigenstate (with the energy eigenstates arranged in an ascending order with $|e_1\rangle$ being the ground state):

$$A_0 = \{1, 2, \dots, m\} \quad (8.16)$$

$$\mathcal{H}^{(\hat{H}_{A_0})} = \bigoplus_{j \in A_0} \mathcal{H}_j^{(\hat{H})}. \quad (8.17)$$

This decomposition is (unsurprisingly) trivial with respect to the Hamiltonian: time evolution only evolves states within the subspaces, and there is no interaction between $\mathcal{H}^{(\hat{H}_{A_0})}$ and $\mathcal{H}^{(\hat{H}_{B_0})}$. Every state in this trivial decomposition with support on a single piece is equally local in the direct-sum sense; time evolution does not spread any such state across the entire Hilbert space. Such a decomposition thus does not provide a means of applying the lessons of the decoherence program to identify classical states, as discussed in the Introduction; since there is no interaction between subsystems, there is no notion of robustness.

Instead, we should consider the action of \hat{H} on a Hilbert space divided generically as $\mathcal{H} = \mathcal{H}_{A_\sigma}^{(\hat{O})} \oplus \mathcal{H}_{B_\sigma}^{(\hat{O})}$. To belabor the point, we can write

$$|o_i\rangle = \sum_j \langle e_j | o_i \rangle |e_j\rangle \quad (8.18)$$

and

$$|e_j\rangle = \sum_k \langle o_k | e_j \rangle |o_k\rangle. \quad (8.19)$$

so

$$\begin{aligned} e^{-i\hat{H}t} |o_i\rangle &= \sum_j e^{-iE_j t} \langle e_j | o_i \rangle |e_j\rangle \\ &= \sum_{j,k} e^{-iE_j t} \langle e_j | o_i \rangle \langle o_k | e_j \rangle |o_k\rangle = \sum_k \left(\sum_j e^{-iE_j t} \langle e_j | o_i \rangle \langle o_k | e_j \rangle \right) |o_k\rangle, \end{aligned} \quad (8.20)$$

i.e. time evolution evolves an eigenstate of \hat{O} into a superposition of eigenstates. In particular, for generic \hat{O} , the time evolution of $|o_i\rangle$ will have support on both $\mathcal{H}_{A_\sigma}^{(\hat{O})}$ and $\mathcal{H}_{B_\sigma}^{(\hat{O})}$.

Thus, the Hamiltonian \hat{H} for the system under this direct-sum decomposition $D_\oplus(\hat{O}, \sigma, m)$ of Eq. (8.14) can be decomposed into a term \hat{H}_{A_σ} which acts non-trivially only on the part of the state supported on $\mathcal{H}_{A_\sigma}^{(\hat{O})}$, a term \hat{H}_{B_σ} acting only

on part of states supported on $\mathcal{H}_{B_\sigma}^{(\hat{O})}$, and finally a *tunneling* term $\hat{H}_{\text{tunnel}(\sigma)}$ which swaps support between $\mathcal{H}_{A_\sigma}^{(\hat{O})}$ and $\mathcal{H}_{B_\sigma}^{(\hat{O})}$ (we have suppressed the superscript (\hat{O}) on the terms in the Hamiltonian to avoid clutter in our notation),

$$\hat{H} = \hat{H}_{A_\sigma} + \hat{H}_{B_\sigma} + \hat{H}_{\text{tunnel}(\sigma)}. \quad (8.21)$$

One could work in the eigenbasis of \hat{O} to express the Hamiltonian \hat{H} as a matrix and under the scrambling permutation $\{A_\sigma, B_\sigma\}$, in which case the terms \hat{H}_{A_σ} and \hat{H}_{B_σ} would represent diagonal blocks while $\hat{H}_{\text{tunnel}(\sigma)}$ would be the off-diagonal piece. In the next section, we seek measures of direct-sum locality which depend on this decomposition of the Hamiltonian.

8.4 Direct-Sum Locality and Robustness

In the previous sections, we established the rarity of lattice structures in a generic Hilbert space and motivated the use of direct-sum constructions as tools for finding lattice-like factorizations where locality can be made manifest. As discussed in Section 8.3, a finite-dimensional Hilbert space \mathcal{H} can be decomposed into a direct sum of two subspaces labeled by $D_\oplus(\hat{O}, \sigma, m)$, which is specified by a choice of the operator \hat{O} whose eigenstates are used to define the direct-sum decomposition and a partition of these eigenstates into two sets.

In this section, we tackle the problem of finding a suitable measure to quantify the *direct-sum locality* of states in the context of a direct-sum decomposition. Locality in such a context means that states which begin localized in one subspace in the decomposition will remain localized under time evolution by the Hamiltonian and not spread substantially into the other direct-sum subspace(s). Hence, such states evolve mostly unitarily within that subspace with little or no tunneling into other direct-sum subspaces. We emphasize that direct-sum locality is a highly non-generic property, exhibited only by a subset of states in Hilbert space in a particular choice of direct-sum decomposition.

To make the notion of direct-sum locality concrete, we need to specify what we mean by “localized in a subspace.” Consider an arbitrary state $|\phi\rangle \in \mathcal{H}$, which in general, has non-trivial support on the full Hilbert space. We would like to define a super-operator $\text{Pr}_{A_\sigma}^{(\hat{O})}$ which takes $|\phi\rangle$ and returns a state $|\phi\rangle_{A_\sigma}$ living in $\mathcal{H}_{A_\sigma}^{(\hat{O})}$ which corresponds to the support of $|\phi\rangle$ on $\mathcal{H}_{A_\sigma}^{(\hat{O})}$ (and a similar super-operator $\text{Pr}_{B_\sigma}^{(\hat{O})}$). The

natural tool to use is the projection operator \hat{P}_{A_σ} onto $\mathcal{H}_{A_\sigma}^{(\hat{O})} \subset \mathcal{H}$:

$$\hat{P}_{A_\sigma}^{(\hat{O})} \equiv \sum_{j \in A_\sigma} |o_j\rangle \langle o_j|, \quad (8.22)$$

where, as usual for a projector, $(\hat{P}_{A_\sigma}^{(\hat{O})})^2 = \hat{P}_{A_\sigma}^{(\hat{O})}$. Now $\hat{P}_{A_\sigma}^{(\hat{O})} |\phi\rangle$ is not a state vector, because it need not have unit norm:

$$0 \leq \langle \phi | \hat{P}_{A_\sigma}^{(\hat{O})} | \phi \rangle \leq 1. \quad (8.23)$$

When the norm is nonzero, we can recover a normalized state by dividing by the norm. When the norm is zero, however, there is no unambiguous way to do this. This is, in fact, desirable: the norm is zero only when a state $|\phi\rangle$ in fact has no support on $\mathcal{H}_{A_\sigma}^{(\hat{O})}$. What this means is that our super-operator $\text{Pr}_{A_\sigma}^{(\hat{O})}$ does not map strictly from states in \mathcal{H} onto states in $\mathcal{H}_{A_\sigma}^{(\hat{O})}$, but onto either states or the null element² $\mathbf{0}_{\mathcal{H}_{A_\sigma}^{(\hat{O})}} \in \mathcal{H}_{A_\sigma}$. Hence the action of $\text{Pr}_{A_\sigma}^{(\hat{O})}$ is defined³ as follows:

$$\text{Pr}_{A_\sigma}^{(\hat{O})} : \mathcal{H} \rightarrow \mathcal{H}_{A_\sigma}^{(\hat{O})} \subset \mathcal{H}, \quad |\phi\rangle \mapsto |\phi\rangle_{A_\sigma}, \quad (8.24)$$

with

$$|\phi\rangle_{A_\sigma} = \begin{cases} \frac{\hat{P}_{A_\sigma}^{(\hat{O})} |\phi\rangle}{\langle \phi | \hat{P}_{A_\sigma}^{(\hat{O})} | \phi \rangle}, & \langle \phi | \hat{P}_{A_\sigma}^{(\hat{O})} | \phi \rangle > 0 \\ \mathbf{0}_{\mathcal{H}_{A_\sigma}^{(\hat{O})}}, & \langle \phi | \hat{P}_{A_\sigma}^{(\hat{O})} | \phi \rangle = 0. \end{cases} \quad (8.25)$$

We can now proceed to quantify the spread of an arbitrary state $|\psi\rangle$ in a given direct-sum decomposition $D_\oplus(\hat{O}, \sigma, m)$ by projecting it onto $\mathcal{H}_{A_\sigma}^{(\hat{O})}$ using $\text{Pr}_{A_\sigma}^{(\hat{O})}$ and checking to what extent time evolution, given by the action of the Hamiltonian \hat{H} (8.21), evolves the projected state to have non-trivial support on $\mathcal{H}_{B_\sigma}^{(\hat{O})}$. For any state $|\psi\rangle$, let us take our initial state $|\psi(0)\rangle$ to be the projection of $|\psi\rangle$ on $\mathcal{H}_{A_\sigma}^{(\hat{O})}$, $|\psi(0)\rangle \equiv |\psi\rangle_{A_\sigma}$, using Eq. (8.25).

For concreteness, we will look at small time evolution of this state. This is physically justified since we expect that in arbitrary choices of direct-sum decompositions,

²Recall that because Hilbert spaces are vector spaces, they have a null element $\mathbf{0}_{\mathcal{H}} \in \mathcal{H}$ with $\|\mathbf{0}_{\mathcal{H}}\| = 0$. Because state vectors are (equivalence classes of) vectors in the Hilbert space with unit norm, $\mathbf{0}_{\mathcal{H}}$ is not itself a physical state, but it is nonetheless an element of the Hilbert space.

³To avoid clutter, we have neglected a superscript (\hat{O}) on our projected states, e.g. writing $|\phi\rangle_{A_\sigma}$ rather than $|\phi\rangle_{A_\sigma}^{(\hat{O})}$, but it should be understood that any projected state (in any direct-sum subspace) is dependent on the choice of \hat{O} .

generic states $|\psi\rangle$ projected down to $\mathcal{H}_{A\sigma}^{(\hat{O})}$ will spread over the entire Hilbert space on very short time scales, representing their non-locality and lack of robustness in a direct-sum sense, whereas robust states (whose properties we will discuss below) would stay localized in the subspace they begin with. The time-evolved state, explicitly written to $\mathcal{O}(t^2)$, is

$$|\psi(t)\rangle = \exp(-i\hat{H}t) |\psi(0)\rangle = \left(\hat{\mathbb{1}} - it\hat{H} - \frac{t^2}{2}\hat{H}^2 + \mathcal{O}(t^3) \right) \frac{\hat{P}_{A\sigma}^{(\hat{O})} |\psi\rangle}{\langle\psi|\hat{P}_{A\sigma}^{(\hat{O})}|\psi\rangle}. \quad (8.26)$$

Substituting the form (8.21) of the Hamiltonian yields

$$\begin{aligned} |\psi(t)\rangle &= \frac{\hat{P}_{A\sigma}^{(\hat{O})} |\psi\rangle}{\langle\psi|\hat{P}_{A\sigma}^{(\hat{O})}|\psi\rangle} - \frac{it}{\langle\psi|\hat{P}_{A\sigma}^{(\hat{O})}|\psi\rangle} (\hat{H}_{A\sigma} + \hat{H}_{\text{tunnel}(\sigma)}) \hat{P}_{A\sigma}^{(\hat{O})} |\psi\rangle \\ &- \frac{t^2}{2\langle\psi|\hat{P}_{A\sigma}^{(\hat{O})}|\psi\rangle} \left(\hat{H}_{A\sigma}^2 + \hat{H}_{\text{tunnel}(\sigma)}^2 + \hat{H}_{B\sigma}\hat{H}_{\text{tunnel}(\sigma)} + \hat{H}_{\text{tunnel}(\sigma)}\hat{H}_{A\sigma} \right) \hat{P}_{A\sigma}^{(\hat{O})} |\psi\rangle + \mathcal{O}(t^3), \end{aligned} \quad (8.27)$$

where we have simplified the expression using the orthogonality properties of the projected state,

$$\hat{H}_{B\sigma}\hat{P}_{A\sigma}^{(\hat{O})} = \hat{H}_{B\sigma}\hat{H}_{A\sigma}\hat{P}_{A\sigma}^{(\hat{O})} = \hat{H}_{A\sigma}\hat{H}_{\text{tunnel}(\sigma)}\hat{P}_{A\sigma}^{(\hat{O})} = 0. \quad (8.28)$$

Recall that the tunneling term $\hat{H}_{\text{tunnel}(\sigma)}$ swaps support of states localized in either subspace, such that its action on states completely localized in $\mathcal{H}_{A\sigma}^{(\hat{O})}$ will transform them to states with support only in $\mathcal{H}_{B\sigma}^{(\hat{O})}$ and *vice versa*.

Eq. (8.27) makes clear that the time-evolved state $|\psi(t)\rangle$ has support over the full Hilbert space \mathcal{H} , as expected due to the presence of the tunneling term $\hat{H}_{\text{tunnel}(\sigma)}$, even though the initial state $|\psi(0)\rangle$ was constructed to be localized only in $\mathcal{H}_{A\sigma}^{(\hat{O})}$. We would like to quantify how much support $|\psi(t)\rangle$ has in $\mathcal{H}_{B\sigma}^{(\hat{O})}$. This can be achieved by projecting $|\psi(t)\rangle$ to $\mathcal{H}_{B\sigma}^{(\hat{O})}$ using a projection operator $\hat{P}_{B\sigma}^{(\hat{O})}$ (defined in the same manner as Eq. (8.25) to truncate support of states to $\mathcal{H}_{B\sigma}^{(\hat{O})}$ only), but this time, *without* normalizing the result of the projection, so that we can explicitly measure the support in $\mathcal{H}_{B\sigma}^{(\hat{O})}$. We see that

$$\begin{aligned} \hat{P}_{B\sigma}^{(\hat{O})} |\psi(t)\rangle &= -\frac{it}{\langle\psi|\hat{P}_{A\sigma}^{(\hat{O})}|\psi\rangle} \hat{H}_{\text{tunnel}(\sigma)} \hat{P}_{A\sigma}^{(\hat{O})} |\psi\rangle \\ &- \frac{t^2}{2\langle\psi|\hat{P}_{A\sigma}^{(\hat{O})}|\psi\rangle} (\hat{H}_{B\sigma}\hat{H}_{\text{tunnel}(\sigma)} + \hat{H}_{\text{tunnel}(\sigma)}\hat{H}_{A\sigma}) \hat{P}_{A\sigma}^{(\hat{O})} |\psi\rangle \in \mathcal{H}_{B\sigma}^{(\hat{O})} \subset \mathcal{H}. \end{aligned} \quad (8.29)$$

The support of $|\psi(t)\rangle$ in $\mathcal{H}_{B_\sigma}^{(\hat{O})}$ is given by the overlap of Eq. (8.29) with the time-evolved state $|\psi(t)\rangle$ itself, which is, to $\mathcal{O}(t^2)$,

$$\langle\psi(t)|\hat{P}_{B_\sigma}^{(\hat{O})}|\psi(t)\rangle = \frac{\langle\psi|\hat{P}_{A_\sigma}^{(\hat{O})}\hat{H}_{\text{tunnel}(\sigma)}^2\hat{P}_{A_\sigma}^{(\hat{O})}|\psi\rangle}{\langle\psi|\hat{P}_{A_\sigma}^{(\hat{O})}|\psi\rangle^2}t^2. \quad (8.30)$$

The coefficient of t^2 defines the *Tunneling Spread* $\mathbb{T}(|\psi\rangle, A_\sigma, D_\oplus)$ of the state $|\psi\rangle$ in the subspace $\mathcal{H}_{A_\sigma}^{(\hat{O})}$ in the decomposition $D_\oplus(\hat{O}, \sigma, m)$:

$$\begin{aligned} \mathbb{T}(|\psi\rangle, A_\sigma, D_\oplus) &\equiv \frac{1}{2} \frac{d^2}{dt^2} (\langle\psi(t)|\hat{P}_{B_\sigma}^{(\hat{O})}|\psi(t)\rangle) = \frac{\langle\psi|\hat{P}_{A_\sigma}^{(\hat{O})}\hat{H}_{\text{tunnel}(\sigma)}^2\hat{P}_{A_\sigma}^{(\hat{O})}|\psi\rangle}{\langle\psi|\hat{P}_{A_\sigma}^{(\hat{O})}|\psi\rangle^2} \\ &= \langle\psi_{A_\sigma}|\hat{H}_{\text{tunnel}(\sigma)}^2|\psi_{A_\sigma}\rangle. \end{aligned} \quad (8.31)$$

The tunneling spread is a time-independent quantity, but characterizes the robustness of initially localized states under time evolution in a given direct-sum decomposition. It is evident that the tunneling Hamiltonian plays a crucial role in determining the spread of localized states in the direct-sum. Note also the strong dependence on the choice of state $|\psi\rangle$ and decomposition D_\oplus (and hence, $\hat{P}_{A_\sigma}^{(\hat{O})}$), as expected.

Before closing this section, we define two other important quantities which will be used in our toy model of Section 8.5 below. As noted in Section 8.3, we label the energy eigenstates of \hat{H} as $\{|e_i\rangle\}$, $i = 1, 2, \dots, N$ with corresponding energies E_i , respectively. We will be interested in studying the evolution of energy eigenstates projected down to $\mathcal{H}_{A_\sigma}^{(\hat{O})}$ using a projection operator $\hat{P}_{A_\sigma}^{(\hat{O})}$ (as defined in Eq. 8.25). Define the normalized, projected energy eigenstates by

$$|E_n\rangle_{A_\sigma} \equiv \frac{\hat{P}_{A_\sigma}^{(\hat{O})}|E_n\rangle}{\langle E_n|\hat{P}_{A_\sigma}^{(\hat{O})}|E_n\rangle} \in \mathcal{H}_{A_\sigma}^{(A_\sigma)} \subset \mathcal{H}. \quad (8.32)$$

These states have energy expectation values

$$(E_n)_{A_\sigma} \equiv \frac{\langle E_n|\hat{P}_{A_\sigma}^{(\hat{O})}\hat{H}\hat{P}_{A_\sigma}^{(\hat{O})}|E_n\rangle}{\langle E_n|\hat{P}_{A_\sigma}^{(\hat{O})}|E_n\rangle}. \quad (8.33)$$

We would also like to quantify the degree of scrambling of a direct-sum decomposition as a whole. The tunneling spread captures the robustness of an individual state by taking the expectation value of $\hat{H}_{\text{tunnel}(\sigma)}^2$ with respect to the projected state. As a

quantifier of how scrambled our decomposition is, we take the trace $\text{Tr} \left(\hat{H}_{\text{tunnel}(\sigma)}^2 \right)$ in the basis $\{|o_j\rangle\}$ of \hat{O} eigenstates :

$$\text{Tr} \left(\hat{H}_{\text{tunnel}(\sigma)}^2 \right) = \sum_{j=1}^N \langle o_j | \hat{H}_{\text{tunnel}(\sigma)}^2 | o_j \rangle = \sum_{j=1}^N \left(\mathbb{T}(|o_j\rangle, A_\sigma, D_\oplus) + \mathbb{T}(|o_j\rangle, B_\sigma, D_\oplus) \right). \quad (8.34)$$

The last equality follows because the projectors act trivially on the $\{|o_j\rangle\}$.

8.5 A Worked Example: The Double-Well Potential

In this section, we apply this construction of direct sums and direct-sum locality to a simple, concrete example: the quantum-mechanical double-well potential. While the usual construction of the double-well potential in standard, non-relativistic quantum mechanics textbooks is based on an infinite-dimensional Hilbert space $\mathbb{L}^2(\mathbb{R})$ with position and momentum operators, we will construct an analogous finite-dimensional version of the same, in line with our motivation for considering locally finite-dimensional Hilbert spaces of the type relevant for quantum gravity. As we will see, the double-well potential plays very naturally with the direct-sum decomposition and can be used to illustrate features of direct-sum locality very cleanly.

Let us define the Hamiltonian for our double-well system in the standard way,

$$\hat{H} = \frac{\hat{\pi}^2}{2} + \hat{V}(\hat{\phi}), \quad (8.35)$$

where $\hat{\pi}$ and $\hat{\phi}$ are finite-dimensional analogues of the momentum and position operators which we will define below. The ‘‘potential’’ $\hat{V}(\hat{\phi})$ is taken to be,

$$\hat{V}(\hat{\phi}) = \begin{cases} V_0 & \phi_j = 0 \\ V_{\text{edge}} & \phi_j = \pm l \Delta \phi \\ 0 & \text{elsewhere,} \end{cases} \quad (8.36)$$

where V_0 is a positive, real number representing the central barrier potential and V_{edge} is the positive potential at the edges of our ϕ -lattice. The separation between eigenvalues of $\hat{\phi}$ is denoted by $\Delta \phi$ which is defined in Eqs. (8.37) and (8.38) below. We have numerically implemented this system in MATLAB for a Hilbert space of dimension $N = 301$, with $V_{\text{edge}} = 3V_0 = 10 \|\hat{\pi}^2/2\|_2$ to ensure that the central barrier is lower than the edge barriers. In Figure 8.4, we plot this double-well potential and show the lowest two and one of the higher energy eigenstates represented in ϕ -space. As expected and well-known from quantum mechanics, the low-lying states

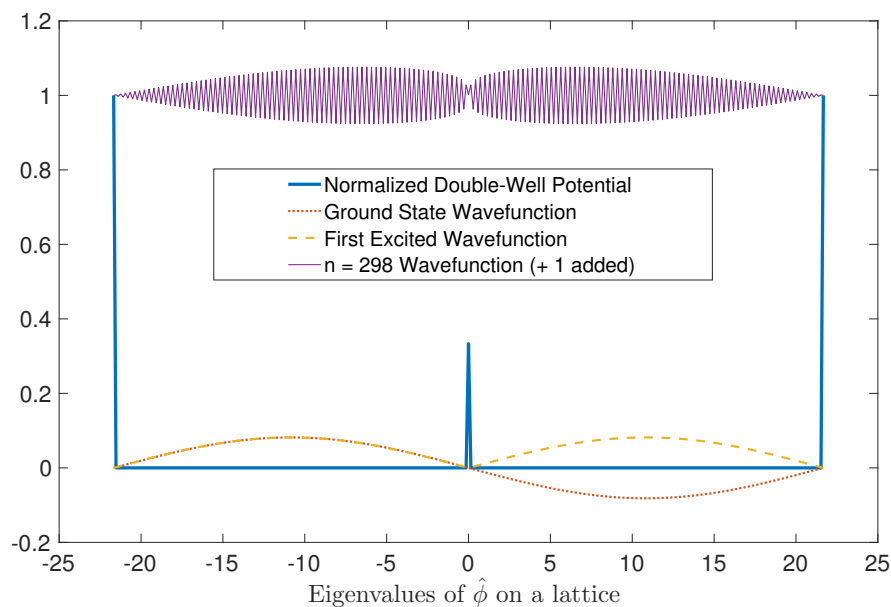


Figure 8.4: The $\hat{\phi}$ -representation of the double-well potential $\hat{V}(\hat{\phi})$ for a Hilbert space of dimension $N = 301$ is plotted. Along with it, we show the lowest two energy eigenstates and one of the highest ones ($n = 298$) for a Hilbert space corresponding to $N = 301$. We have added $+1$ by hand to the wave function of the $n = 298$ state to cleanly separate it from the low-lying one and demonstrate how higher energy states are delocalized across the two wells. Eigenstates $n = 299, 300, 301$ are very high energy states localized near the barriers of the potential as a result of the the finite-dimensional, cyclic structure of $\hat{\phi}$, as can be seen in Fig. 8.5. The state $n = 299$ is peaked around the central barrier, and $n = 300, 301$ are peaked at the edges.

represent superpositions of localized states within each well, whereas higher energy states are delocalized over the full double well.

In addition, we plot the energy eigenvalues (spectrum) of the Hamiltonian in Figure 8.5, where the expected double degeneracy of the lower eigenvalues is demonstrated. A few of the higher most eigenvalues are exceptionally large; this is a consequence of working with a Hilbert space of a relatively small size ($N = 301$ in our case) with a cyclic structure. Such states of extremely high energy will not be explicitly studied here, but they will induce stray effects in the results and plots to follow which do not bear any physical significance on our main results.

There is an obstacle to defining $\hat{\pi}$ and $\hat{\phi}$ in the same way as in standard one-dimensional quantum mechanics. It is well known that Heisenberg's canonical

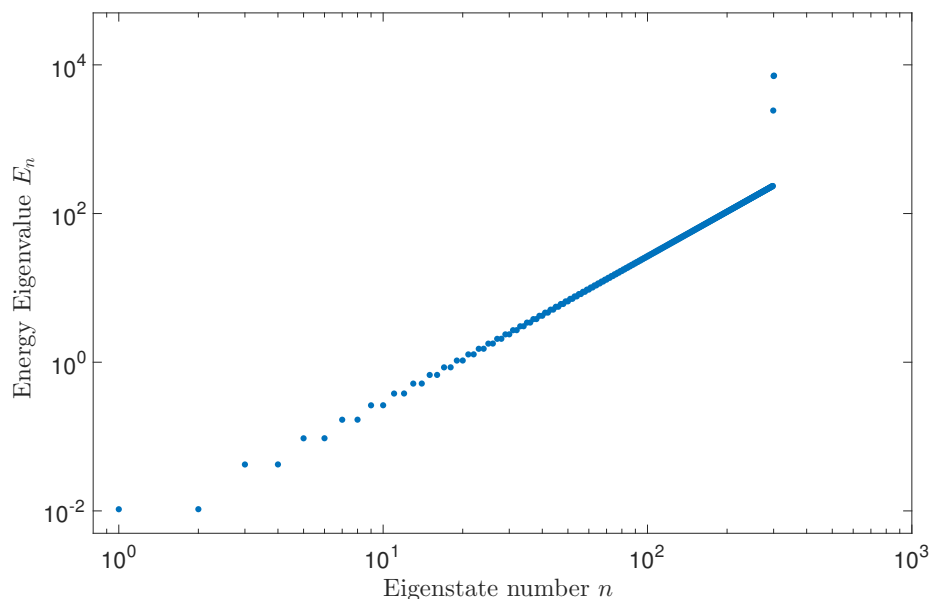


Figure 8.5: Energy spectrum of the double-well Hamiltonian of Eq. (8.35). One can easily notice the (approximate) double degeneracy in the low-lying eigenvalues (corresponding to the two symmetric wells). The last three (the highest two are indistinguishable on the plot) highly-energetic eigenstates are an artifact of working in a finite-dimensional space with a relatively small N with the algebra of conjugate variables having a cyclic structure. They cause spurious features in other plots, but have no bearing on our physical results.

commutation relation (CCR) between pairs of conjugate variables has no finite-dimensional irreducible representations. However, its exponential form, given by Weyl [77], does admit finite-dimensional representations, based on the Generalized Clifford Algebra (GCA) ([9] for a review), and can be used to construct finite-dimensional conjugate variables which reduce to the usual ones obeying Heisenberg’s CCR in the infinite-dimensional limit (see, for example, [76, 91, 94]). We give a short introduction to the GCA as an appropriate construction of finite-dimensional conjugate variables in the Appendix. It should be noted that, as explained in the Appendix, the form of the momentum operator in finite dimensions is non-local in the sense that matrix elements of $\hat{\pi}$ in the eigenbasis of $\hat{\phi}$ demonstrate power law-like decay, connecting arbitrary “far” $\hat{\phi}$ eigenstates. While this may seem counter-intuitive, we note that in the usual infinite-dimensional limit, we recover the usual local representation of $\hat{\pi}$ as $-id/d\phi$ in the $\hat{\phi}$ basis. Our goal in this chapter, and particularly through this example is to demonstrate that there exists a preferred

decomposition of Hilbert space in which dynamics is *most local* as compared to others, and this decomposition can serve as a starting point for the emergence of classical behavior, and in particular having a momentum operator with non-local matrix elements in finite-dimensions is not an obstacle towards this goal.

The appropriate way to define $\hat{\pi}$ and $\hat{\phi}$ is therefore by using the GCA. We denote the Hilbert space of our Double-Well (DW) system as \mathcal{H}_{DW} , with an odd, finite dimension $N = 2l + 1$. (The odd dimension is chosen so that our field variable ϕ can lie on a one-dimensional lattice centered around 0.) On $\mathcal{L}(\mathcal{H}_{DW})$, we associate a pair of conjugate variables $\hat{\phi}$ and $\hat{\pi}$ which form a GCA. From the point of view of the GCA, $\hat{\phi}$ and $\hat{\pi}$ are on the same footing, so we need to make a choice of which operator to assign to position and which to momentum. As already noted, the operator corresponding to a ‘‘lattice’’ variable is chosen to be $\hat{\phi}$, which has eigenvalues

$$\{\phi_j = j\Delta\phi, j = -l, (-l+1), \dots, 0, \dots, (l-1), l\}, \quad (8.37)$$

where $\Delta\phi$ is a positive real number constrained by the algebra to obey

$$(2l+1)\Delta\phi\Delta\pi = 2\pi \quad (8.38)$$

and $\Delta\pi$ is the uniform difference between eigenvalues of $\hat{\pi}$. This constraint ensures that Heisenberg’s canonical commutation relation is recovered in the infinite-dimensional $N \rightarrow \infty$ limit. In our numerical implementation, we have taken $\Delta\phi = \Delta\pi = \sqrt{2\pi/(2l+1)}$ and $l = 150$.

Thus eigenstates of $\hat{\phi}$ can be thought of labeling sites on a 1-D lattice with cyclic boundary conditions as specified by the GCA. The conjugate variable to $\hat{\phi}$ is $\hat{\pi}$ which generates translations in the eigenspace of $\hat{\phi}$ (and vice versa). For our purposes, we will use $\hat{\phi}$ and $\hat{\pi}$ in analogy to position and momentum operators in standard textbook quantum mechanics in one spatial dimension on $\mathbb{L}^2(\mathbb{R})$, but here representing bounded operators on a finite-dimensional Hilbert space.

Having defined the system, we can proceed to study different choices of scramblings σ . Because the system defines a symmetric double-well potential, we expect that the only good choices are those which keep the size m of A_σ fixed at $m = l$. In particular, we start from the ordered, canonical ϕ -lattice $(-l, -l+1, \dots, 0, \dots, l-1, l)$ and sequentially build up different scramblings by swapping a pair of randomly chosen sites from A_σ and B_σ separated by the barrier fixed at $\phi = 0$. In the canonical, ordered decomposition, the Hamiltonian is the sum of a local kinetic term and

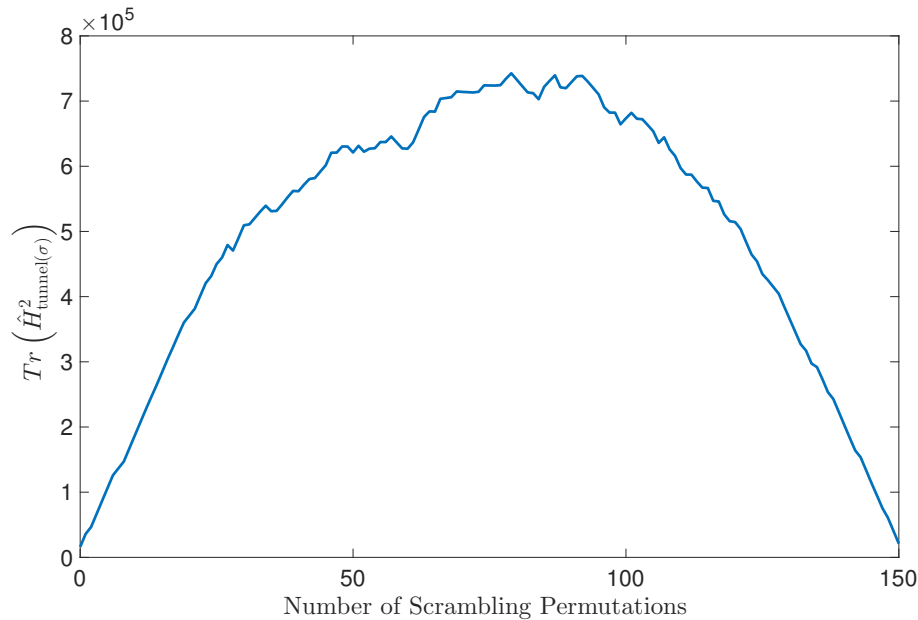


Figure 8.6: The trace of the square of the tunneling term in the Hamiltonian $\text{Tr}\left(\hat{H}_{\text{tunnel}(\sigma)}^2\right)$ for different decompositions building up from the canonical, ordered $(-l, -l+1, \dots, -1) \cup (0, 1, 2, \dots, l)$ decomposition. This quantity acts as a measure of the strength of the tunneling term for the choice $\hat{O} \equiv \hat{\phi}$ and quantifies the scrambling of the decomposition as discussed in the text.

a potential (a highly non-generic feature), and as one scrambles away from it and becomes more non-local, the tunneling term becomes more important. This behavior is seen in Figure 8.6, where $\text{Tr}\left(\hat{H}_{\text{tunnel}(\sigma)}^2\right)$ (which we defined in Eq. 8.34 in Section 8.4 as a measure of how scrambled the decomposition is) correlates with the number of scrambling swaps applied to the canonical, ordered lattice.

As expected, since we are working with a Hilbert space corresponding to $l = 150$ and swapping pairs of sites sequentially across the central barrier, the decomposition becomes more non-local (and hence has higher $\text{Tr}\left(\hat{H}_{\text{tunnel}(\sigma)}^2\right)$) until reaching $\approx l/2$ swaps, after which we start approaching the case where the two wells are swapped entirely (up to internal scramblings within each well which are inconsequential for our purposes, since the potential energy defined on such well configurations is zero and the Hamiltonian reduces to just a local kinetic term within each well).

We next study the properties of individual energy eigenstates $|E_n\rangle$ of the double-well Hamiltonian of Eq. (8.35) and their projected counterparts $|E_n\rangle_{A_\sigma}$ on $\mathcal{H}_{A_\sigma}^{(\hat{O})}$. We compute the tunneling spread for each projected eigenstates in different choices of

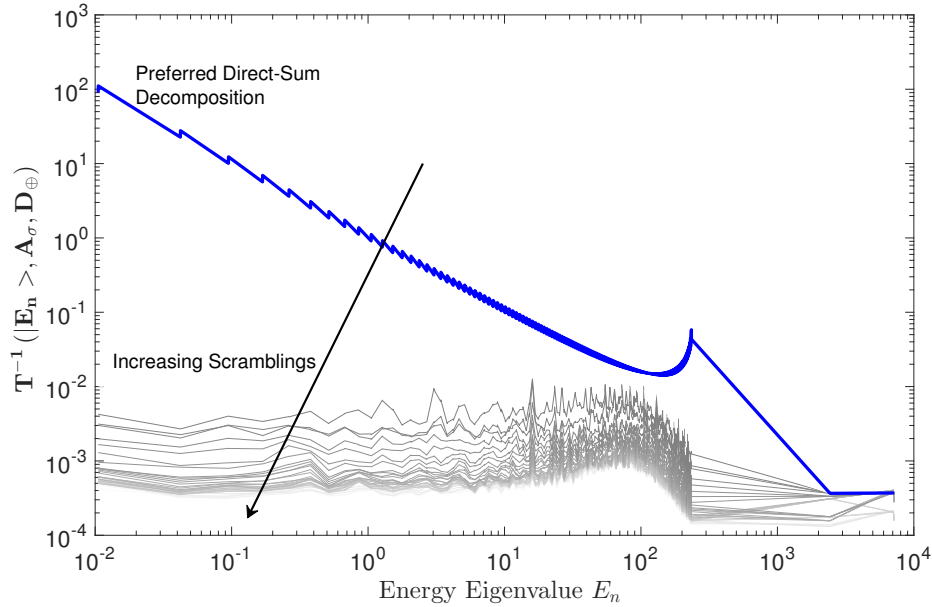


Figure 8.7: Plot showing the dependence of Tunneling Spread $\mathbb{T}(|\psi\rangle, A_\sigma, D_\oplus)$ on energy eigenstates (represented by their eigenvalues E_n) of the double-well Hamiltonian expressed in different direct-sum decompositions $D_\oplus(\hat{\phi}, \sigma, m = l)$ of \mathcal{H}_{DW} . There exists a preferred decomposition into direct sum subspaces (the canonical, ordered $(-l, -l + 1, \dots, -1) \cup (0, 1, 2, \dots, l)$ one) in which low-lying energy states have very small tunneling spreads and hence represent robust, localized states in the direct-sum subspace. Other decompositions are near-generic where there is no manifestation of direct-sum locality. Notice the log scale on the y-axis representing the tunneling spread. The very-high energy behavior is a consequence of the three largest energy eigenstates, which are artifacts of finite-dimensional, cyclic constructions and do not bear any physical significance for our results.

direct-sum scramblings, based on the operator $\hat{\phi}$, but varying σ by swapping sites in the same way as described above. The results are plotted in Figure 8.7.

We see that there exists a preferred decomposition of \mathcal{H}_{DW} into two subspaces based on $\hat{\phi}$, in which the low-lying energy states offer a very natural set of robust, localized states within the $\mathcal{H}_{A_\sigma}^{(\hat{\phi})}$ direct-sum subspace, acting as semiclassical states which maintain their support under evolution by the Hamiltonian. Changing the scrambling even slightly destroys the strong correlation we see for the preferred decomposition. As one goes on further scrambling the canonical decomposition, by continually swapping lattice sites across the central barrier, the tunneling spread systematically increases, but occupies a “degenerate band” indicating how generically non-local arbitrary decompositions are. In addition, as expected, even with the correct choice

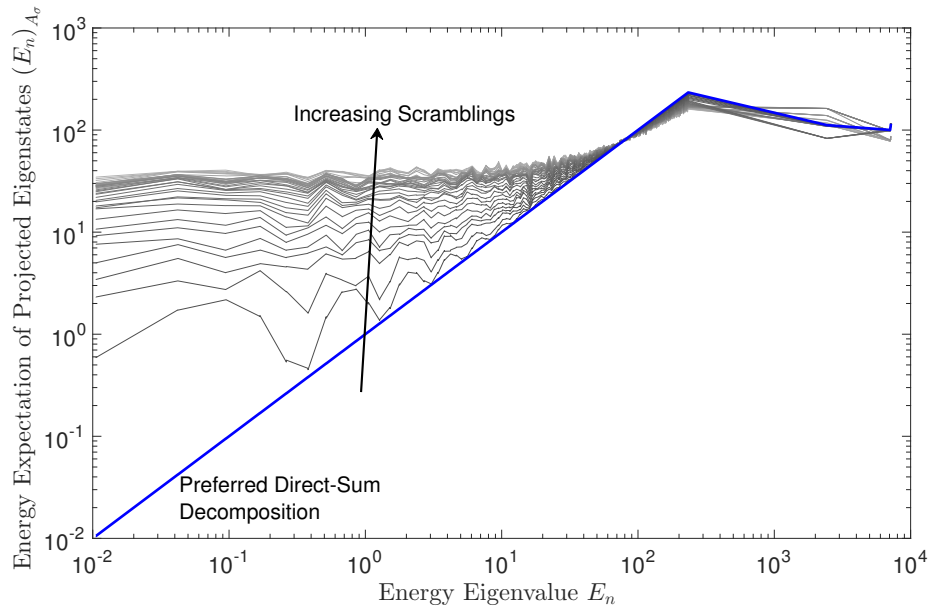


Figure 8.8: Plot showing correlation between E_n and $(E_n)_{A_\sigma}$ for different choices of scramblings $D_\oplus = \{\phi, \sigma, m\}$ in the double-well toy model. Only in the canonical, preferred decomposition do the low-lying eigenstates of \hat{H} serve as low energy states which can be localized within a given direct-sum subspace. The very-high energy behavior is a consequence of the three largest energy eigenstates, which are artifacts of finite-dimensional, cyclic constructions and do not bear any physical significance for our results.

of decomposition, it is only the low-lying states which exhibit robustness and locality. Higher-energy states are already delocalized to begin with (as seen in Figure 8.4) and approach the generic band of states for any choice of scramblings.

Such ideas can be further understood by studying the correlation between E_n , the energy eigenvalues of the Hamiltonian, and the expectation value of the energy of the *projected* states, $|E_n\rangle_{A_\sigma}$, defined as $(E_n)_{A_\sigma}$ in Eq. (8.33) above. As shown in Figure 8.8, in the canonical, preferred decomposition discussed above, low-lying eigenstates of the Hamiltonian inherit their low energy features when projected down to the $\mathcal{H}_{A_\sigma}^{(\phi)}$ subspace and can describe localized states which are robust under time evolution (as described by Figure 8.7). For decompositions successively more scrambled from the canonical, the low-lying eigenstates lose their role as localized states because they are mapped to energetically unfavoured states once projected onto the direct-sum subspace. This further demonstrates how arbitrary decompositions place all states on equal footing once projected; only in the preferred

decomposition, which respects the system's dynamics, are localization features in the low-lying states made manifest.

Now that we have discussed ideas of direct-sum locality in a concrete example of the double-well potential and seen the interesting, non-generic features of the preferred direct-sum decomposition, let us interpret these ideas in the context of cosmology and field theory.

8.6 Towards Field Theory

The toy model considered in the previous section demonstrated features that we expect are generic in situations where a lattice theory on a semiclassical spatial background can be described on direct-sum sectors of the Hilbert space. In particular, they illustrate how to select a preferred direct-sum decomposition under which the low-lying states of the Hamiltonian can represent robust, semiclassical states which remain localized under time evolution.

It is important to point out, however, that in our construction above there was no notion of tensor factorization of Hilbert space. Explicitly, the analog of position in our finite-dimensional toy model was labeled by the eigenvalues of the operator $\hat{\phi}$. As we take the dimension of the Hilbert space to infinity to recover one-dimensional quantum mechanics, $\hat{\phi}$ reduces to the position operator \hat{x} . There is thus no real sense in which degrees of freedom in the Hilbert space of the model are actually localized at a given position. Contrast this with field-theory, in which the analogous operators measure the field value at a particular point, $\hat{\phi}_x$.

In other words, our toy model was a first quantized, not a second quantized theory, and we should not expect either the left or right Hilbert subspaces to factorize in the manner required of a lattice field theory. Its goal was to demonstrate, as a proof of principle, how there can exist a preferred direct-sum decomposition for a given Hamiltonian for which we can recover robust, semi-classical structure in different direct-sum subspaces. To extend these ideas to Hilbert spaces where lattice structure exists, we first require an appropriate number-theoretic division into direct sums in which each sum allows a tensor factorization, as discussed in Section 8.2 above. However, even once we have checked that such a tensor factorization can exist, the success of the decoherence program within each such direct-sum factor requires a specific, non-generic direct-sum decomposition which is chosen based on locality characteristics governed by the Hamiltonian. It is this choice of decomposition which our results on the toy model in the previous section can inform.

In Section 8.3 above, we suggested that theories in which each term in the direct sum describes a geometric field theory occur frequently in quantum field theory in curved space. Whenever we have a theory that describes multiple (meta)stable vacua, such as those invoked in landscape eternal inflation [178], string-theoretic mechanisms for producing de Sitter solutions [179], or for anthropic purposes [180], we should decompose the Hilbert space of the theory into a sum of subspaces which describe field theory around the geometry corresponding to each individual vacuum in the theory (see [181, 182] for related ideas). Interactions between the subspaces, which we have referred to as tunneling terms, play the dual role of describing transitions between the vacua and determining which states of the field theories remain robust under time evolution. They also determine what the ultimate ground state of the theory is, as states initially localized within a particular vacuum eventually relax to a particular superposition of states across all of the vacua [183].

Let us finally return to the questions we asked in the Introduction if this chaptee. Given only the Hilbert space data of a theory—that is, its dimension and the spectrum of its Hamiltonian—how could we deduce that such a theory describes a landscape of field theories of this sort? And how could we identify the local degrees of freedom within each field theory? The answer we have presented in the last several sections is to vary across the operators \hat{O} and choice of decompositions (σ, m) which define a direct-sum decomposition $D_{\oplus}(\hat{O}, \sigma, m)$. (If we are considering more arbitrary decompositions into more than two pieces, we should replace the size m with the dimensionalities $\{m_i\}$ of each subspace.) Then we should compare the measures of direct-sum locality we defined in Section 8.4 above—in particular, the tunneling spread $\mathbb{T}(|\psi\rangle, A_{\sigma}, D_{\oplus})$ (8.31) and the size of the tunneling term $\text{Tr}(\hat{H}_{\text{tunnel}(\sigma)}^2)$ (8.34)—across different decompositions. Once we have identified a particular decomposition in which low-lying states in a particular subspace remain robust under the action of the Hamiltonian, such as the canonical decomposition into left and right in our toy model above, we can use the familiar methods of decoherence within the subspaces to identify the local degrees of freedom. That is, we can write each subspace as a tensor product of smaller factors and identify the choice of basis in which interactions between the factor act like a monitoring environment.

8.7 Conclusion

In this chapter we have tried to take some preliminary steps towards understanding the conditions under which lattice or geometrical structures emerge from Hilbert-

space dynamics. We have introduced the notion of *direct-sum decompositions* of a Hilbert space which partition the Hilbert space into multiple pieces spanned by subsets of the eigenstates of an operator. We argued that preferred decompositions which allow the possibility of local degrees of freedom can be identified by the existence in such decompositions of states with low *tunneling spread*, which remain robust under time evolution. We studied the selection of a canonical decomposition in a simple toy model, the finite-dimensional discretization of the double-well potential.

Much work remains to be done in order to fill out the entire research program we mentioned in the Introduction: understanding how the classical, geometric world we observe emerges from a fundamental Hilbert space. With respect to our particular problem, it would be interesting to more explicitly understand under what conditions landscapes of vacua, which seem to be ubiquitous in our models of quantum gravity, can emerge. In particular nothing in the direct-sum understanding we have sketched in this paper seems to preclude the different metastable vacua from differing dramatically, for example in having different numbers of fundamental fields or even differing numbers of dimensions. In addition, there is some tension between a description of spacetime with a lattice structure and the existence of gauge symmetries or diffeomorphism invariance [46, 47, 184–186], which might be solved by introducing additional “edge modes” in addition to degrees of freedom located at lattice sites. Describing the Hilbert spaces of such theories as direct-sum decompositions would require additional generalization.

8.8 Appendix: A Primer on Generalized Clifford Algebra

Consider a finite-dimensional Hilbert Space \mathcal{H} of dimension $\dim \mathcal{H} = N \in \mathbb{Z}^+$ with $N < \infty$. A Generalized Clifford Algebra(GCA) on the space of linear operators $\mathcal{L}(\mathcal{H})$ acting on \mathcal{H} comes equipped with two unitary (but not necessarily hermitian) operators as generators of the algebra, \hat{A} and \hat{B} , which satisfy the following commutation relation,

$$\hat{A}\hat{B} = \omega^{-1}\hat{B}\hat{A}, \quad (8.39)$$

where $\omega = \exp(2\pi i/N)$ is the N -th primitive root of unity. This commutation relation is also more commonly known as the Weyl braiding relation and any further notions of commutations between conjugate, self-adjoint operators (which will be defined from \hat{A} and \hat{B}) will be derived from this fundamental braiding relation. In addition to being unitary, $\hat{A}\hat{A}^\dagger = \hat{A}^\dagger\hat{A} = \hat{\mathbb{1}} = \hat{B}\hat{B}^\dagger = \hat{B}^\dagger\hat{B}$, the algebra cyclically

closes, giving it a cyclic structure in eigenspace,

$$\hat{A}^N = \hat{B}^N = \hat{\mathbb{I}}, \quad (8.40)$$

where $\hat{\mathbb{I}}$ is the identity operator on $\mathcal{L}(\mathcal{H})$. The GCA can be constructed for both even and odd values of N and both cases are important and useful in different contexts. Here, we focus on the case of odd $N \equiv 2l + 1$ which will be useful in constructing conjugate variables whose eigenvalues can be thought of labelling lattice sites, centered around 0. While all of the subsequent construction can be done in a basis-independent way, we choose a hybrid route, routinely switching between an explicit representation of the GCA and abstract vector space relations. Let us follow the convention that all indices used in this section (for the case of odd $N = 2l + 1$), for labelling states or matrix elements of an operator in some basis etc. will run from $-l, (-l + 1), \dots, -1, 0, 1, \dots, l$. The operators are further specified by their eigenvalue spectrum, and it is identical for both the GCA generators \hat{A} and \hat{B} ,

$$\text{spec}(\hat{A}) = \text{spec}(\hat{B}) = \{\omega^{-l}, \omega^{-l+1}, \dots, \omega^{-1}, 1, \omega^1, \dots, \omega^{l-1}, \omega^l\}. \quad (8.41)$$

There exists a unique irreducible representation (up to unitary equivalences) (see review [9] for details) of the generators of the GCA defined via Eqs. (8.39) and (8.40) in terms of $N \times N$ matrices

$$A = \begin{bmatrix} 0 & 0 & 0 & \dots & 1 \\ 1 & 0 & 0 & \dots & 0 \\ 0 & 1 & 0 & \dots & 0 \\ \cdot & \cdot & \dots & \cdot & \\ \cdot & \cdot & \dots & \cdot & \\ 0 & 0 & \dots & 1 & 0 \end{bmatrix}_{N \times N}, \quad (8.42)$$

$$B = \begin{bmatrix} \omega^{-l} & 0 & 0 & \dots & 0 \\ 0 & \omega^{-l+1} & 0 & \dots & 0 \\ \cdot & \cdot & \dots & \cdot & \\ \cdot & \cdot & \dots & \cdot & \\ 0 & 0 & 0 & \dots & \omega^l \end{bmatrix}_{N \times N}. \quad (8.43)$$

The $\hat{\cdot}$ has been removed to stress that these matrices are representations of the operators \hat{A} and \hat{B} in a particular basis, in this case, the eigenbasis \hat{B} (so that B is

diagonal). More compactly, the matrix elements of operators \hat{A} and \hat{B} in the basis representation of eigenstates of \hat{B} ,

$$[A]_{jk} \equiv \langle b_j | \hat{A} | b_k \rangle = \delta_{j,k+1}, \quad (8.44)$$

$$[B]_{jk} \equiv \langle b_j | \hat{B} | b_k \rangle = \omega^j \delta_{j,k}, \quad (8.45)$$

with the indices j and k running from $-l, \dots, 0, \dots, l$ and δ_{jk} is the Kronecker Delta function. Consider the set $\{|b_j\rangle\}$, $j = -l, \dots, l$ of states to be the set of eigenstates of \hat{B} ,

$$\hat{B} |b_j\rangle = \omega^j |b_j\rangle, \quad j = -l, \dots, 0, \dots, l \quad (8.46)$$

As can be evidently seen in the matrix representation of \hat{A} in Eq. (8.42), the operator \hat{A} acts as a ‘‘cyclic shift’’ operator for the eigenstates of \hat{B} , sending an eigenstate to the next,

$$\hat{A} |b_j\rangle = |b_{j+1}\rangle. \quad (8.47)$$

The unitary nature of these generators implies a cyclic structure which identifies $|b_{l+1}\rangle \equiv |b_{-l}\rangle$, so that $\hat{A} |b_l\rangle = |b_{-l}\rangle$. The operators \hat{A} and \hat{B} have the same relative action on one another’s eigenstates, since nothing in the algebra sets the two apart. It has already been seen in Eq. (8.47) that \hat{A} generates (unitary, cyclic) unit shifts in eigenstates of B , and the opposite holds too: the operator \hat{B} generates unit shifts in eigenstates of \hat{A} (given by the relation $\hat{A} |a_k\rangle = \omega^k |a_k\rangle$, $k = -l, \dots, 0, \dots, l$) and has a similar action with a cyclic correspondence to ensure unitarity,

$$\hat{B} |a_k\rangle = |a_{k+1}\rangle, \quad (8.48)$$

with cyclic identification $|a_{l+1}\rangle \equiv |a_{-l}\rangle$. Hence, we already have a set of operators which generate shifts in the eigenstates of the other, which is precisely what conjugate variables do and which is why we see that the GCA provides a very natural structure to define conjugate variables on Hilbert Space. The GCA generators \hat{A} and \hat{B} have been extensively studied in various contexts in quantum mechanics, and are often referred to as ‘‘Clock and Shift’’ matrices in the literature and offer a higher dimensional, non-Hermitian generalisation of the Pauli matrices. In particular, for sake of completeness, we mention that for $N = 2$, it will be seen that $A = \sigma_1$ and $B = \sigma_3$, which recovers the famous Pauli matrices.

The defining notion for a pair of conjugate variables is the identification of two self-adjoint operators acting on Hilbert space, each of which generates translations in the eigenstates of the other. For instance, in (conventionally infinite-dimensional)

textbook quantum mechanics, the momentum operator \hat{p} generates shifts/translations in the eigenstates of its conjugate variable, the position \hat{q} operator and vice versa. Taking this as our defining criterion, we would like to define a pair of conjugate operators $\hat{\phi}$ and $\hat{\pi}$, acting on a finite-dimensional Hilbert space, each of which is the generator of translations in the eigenstates of its conjugate, with the following identification,

$$\hat{A} \equiv \exp(-i\alpha\hat{\pi}), \quad \hat{B} = \exp(i\beta\hat{\phi}), \quad (8.49)$$

where α and β are non-zero real parameters which set the scale of the eigen-spectrum of the operators $\hat{\phi}$ and $\hat{\pi}$. They are bounded operators on \mathcal{H} and, due to the virtue of the GCA generators \hat{A} and \hat{B} being unitary, the conjugate operators $\hat{\phi}$ and $\hat{\pi}$ are self-adjoint satisfying $\hat{\phi}^\dagger = \hat{\phi}$ and $\hat{\pi}^\dagger = \hat{\pi}$. The operator $\hat{\pi}$ is the generator of translations of $\hat{\phi}$ and vice versa.

To further reinforce this conjugacy relation between operators \hat{A} and \hat{B} , we see that they are connected to each other under a discrete Fourier transformation implemented by Sylvester's Circulant Matrix S , which is a $N \times N$ unitary matrix ($SS^\dagger = S^\dagger S = \hat{\mathbb{I}}$), connecting A and B ,

$$SAS^{-1} = B. \quad (8.50)$$

The Sylvester's matrix has the following form, which we identify to be in the $\{|\phi_j\rangle\}$ basis,

$$[S]_{jk} = \frac{\omega^{jk}}{\sqrt{N}}, \quad (8.51)$$

with the indices j and k running from $-l, \dots, 0, \dots, l$. Let us now solve for the conjugate operators $\hat{\phi}$ and $\hat{\pi}$ explicitly by finding their matrix representations in the $|\phi_j\rangle$ basis. By virtue of being diagonal, the logarithm of B is taken rather easily,

$$\log B = (\log \omega) \text{diag}(-l, -l+1, \dots, 0, \dots, l-1, l), \quad (8.52)$$

and hence, we have the matrix representation of $\hat{\phi}$,

$$\langle \phi_j | \hat{\phi} | \phi_{j'} \rangle = j \left(\frac{2\pi}{(2l+1)\beta} \right) \delta_{jj'}, \quad (8.53)$$

which is diagonal in the $|\phi_j\rangle$ basis as expected. To find a representation of $\hat{\pi}$ in the $|\phi_j\rangle$ basis requires a little extra work to compute $\log A$ which is again done with the help of Sylvester's matrix,

$$\log A = S^{-1} (\log B) S. \quad (8.54)$$

Since A and B are non-singular and diagonalizable, it follows, as shown, that $\log A$ and $\log B$ exist, even though multivalued. In the case of odd dimension $N = 2l + 1$, their principle logarithms are well defined and we are able to find explicit matrix representations for operators $\hat{\phi}$ and $\hat{\pi}$ as above. We have already mentioned the conjugate properties of operators $\hat{\phi}$ and $\hat{\pi}$ which are connected through the Sylvester's operator. Using this expression for $\log A$ from Eq. (8.54), we can obtain matrix representation for $\hat{\pi}$ in the $|\phi_j\rangle$ basis rather easily,

$$\langle \phi_j | \hat{\pi} | \phi_{j'} \rangle = \left(\frac{2\pi}{(2l+1)^2 \alpha} \right) \sum_{n=-l}^l n \exp \left(\frac{2\pi i (j-j') n}{2l+1} \right), \quad (8.55)$$

which can be further simplified to give,

$$\langle \phi_j | \hat{\pi} | \phi_{j'} \rangle = \begin{cases} 0, & \text{if } j = j' \\ \left(\frac{i\pi}{(2l+1)\alpha} \right) \operatorname{cosec} \left(\frac{2\pi l(j-j')}{2l+1} \right), & \text{if } j \neq j'. \end{cases} \quad (8.56)$$

It should be noted at this point that the matrix elements of $\hat{\pi}$ in the eigenbasis of $\hat{\phi}$ are non-local in the sense that they have power law-like decay in $(j-j')$ and hence connect arbitrary "far" eigenstates of $\hat{\phi}$. This is a feature of the finite-dimensional construction and in the infinite-dimensional limit $N \rightarrow \infty$, we recover the local form of $\hat{\phi}$ as $-id/d\phi$ as expected. Of course, $\hat{\phi}$ has common eigenstates with those of \hat{B} and $\hat{\pi}$ shares eigenstates with \hat{A} . Let us, for the sake of clarity and convenience, label the eigenstates of $\hat{\phi}$ as $|\phi_j\rangle$ and those of $\hat{\pi}$ as $|\pi_j\rangle$ with the index j running from $-l, \dots, 0, \dots, l$. The corresponding eigenvalue equations for $\hat{\phi}$ and $\hat{\pi}$ can be easily deduced using Eqs. (8.49) and (8.41),

$$\hat{\phi} |\phi_j\rangle = j \left(\frac{2\pi}{(2l+1)\beta} \right) |\phi_j\rangle, \quad j = -l, \dots, 0, \dots, l, \quad (8.57)$$

$$\hat{\pi} |\pi_j\rangle = j \left(\frac{2\pi}{(2l+1)\alpha} \right) |\pi_j\rangle, \quad j = -l, \dots, 0, \dots, l. \quad (8.58)$$

These conjugate variables defined on a finite-dimensional Hilbert space will *not* satisfy Heisenberg's Canonical Commutation relation (CCR) $[\hat{\phi}, \hat{\pi}] = i$ (in units where $\hbar = 1$) since it is well known by the Stone-von Neumann theorem, there are no finite-dimensional representations of Heisenberg's CCR. However, $\hat{\phi}$ and $\hat{\pi}$ still serve as a robust notion of conjugate variables and their commutation can be derived from the more fundamental Weyl Braiding Relation of Eq. (8.39). In the large dimension limit $N \rightarrow \infty$, one recovers Heisenberg's form of the CCR if

the parameters α and β are constrained to obey $\alpha\beta = 2\pi/N$. This completes our lightning review of GCA and conjugate variables on a finite-dimensional Hilbert space.

Part IV

Quantum State-Reduction

QUANTUM DECIMATION IN HILBERT SPACE: COARSE-GRAINING WITHOUT STRUCTURE

We present a technique to coarse-grain quantum states in a finite-dimensional Hilbert space. Our method is distinguished from other approaches by not relying on structures such as a preferred factorization of Hilbert space or a preferred set of operators (local or otherwise) in an associated algebra. Rather, we use the data corresponding to a given set of states, either specified independently or constructed from a single state evolving in time. Our technique is based on principle component analysis (PCA), and the resulting coarse-grained quantum states live in a lower dimensional Hilbert space whose basis is defined using the underlying (isometric embedding) transformation of the set of fine-grained states we wish to coarse-grain. Physically, the transformation can be interpreted to be an “entanglement coarse-graining” scheme that retains most of the global, useful entanglement structure of each state, while needing fewer degrees of freedom for its reconstruction. This scheme could be useful for efficiently describing collections of states whose number is much smaller than the dimension of Hilbert space, or a single state evolving over time.

This chapter is based on the following reference:

A. Singh and S. M. Carroll, “Quantum decimation in Hilbert space: Coarse-graining without structure,” *Phys. Rev.* **A97** no. 3, (2018) 032111, [arXiv:1709.01066 \[quant-ph\]](#)

9.1 Introduction

One of the challenges of doing practical calculations in quantum mechanics is that Hilbert space is very big: the number of dimensions is exponential in the number of degrees of freedom. Furthermore, not all degrees of freedom are created equal; some might be microscopic or high-energy and hard to access, while others may be irrelevant to certain dynamical questions. It is therefore very often useful to coarse-grain, modeling quantum systems defined by states on some Hilbert space \mathcal{H} by states in some lower-dimensional Hilbert space $\tilde{\mathcal{H}}$, under conditions where the coarse-grained dynamics suffices to capture important properties of the system.

In practice, coarse-graining procedures typically rely on the existence of structure in Hilbert space that exists as part of the quantum system under consideration, and use that structure to define a renormalization group (RG) flow [188–193]. For example, there might be a notion of emergent space [22, 23] and associated locality. We imagine some decomposition of Hilbert space into local factors,

$$\mathcal{H} = \bigotimes_i \mathcal{H}_i, \quad (9.1)$$

where the factors \mathcal{H}_i come equipped with some nearest-neighbor structure (specifying when \mathcal{H}_i and \mathcal{H}_j are nearby), typically characterized by the form of interactions between factors in the Hamiltonian. Then it makes sense to coarse-grain spatially, grouping together nearby factors, as in the classic block-spin approach to the Ising model [188, 194]. Alternatively, one might appeal to the energy spectrum of the Hamiltonian, constructing an effective theory of low-energy states by integrating out high-energy ones.

In quantum information theory, data compression has received a lot of attention over the last few decades and a considerable amount of work has been done. A lot of motivation for such techniques comes from quantum computation, and many different approaches have been suggested, including but not limited to Schumacher’s data compression [195], one-shot compression techniques [196], the Johnson-Lindenstrauss lemma [197, 198] and its limitations in quantum dimensional reduction [199], by application of elementary quantum gates [200], and even considering overlapping qubits [201], amongst others [202, 203] (and references therein).

In this chapter, we pursue a different road to coarse-graining. We imagine that we are given some particular set of states (or one state as a function of time) in Hilbert space, but no preferred notion of locality or energy, or a preferred factorization into individual degrees of freedom. Our specific motivation comes from quantum gravity and quantum cosmology, where notions of locality and energy are more subtle than in traditional laboratory settings, but the technique might be of wider applicability. Our method represents another technique in the literature on compression quantum information and coarse-graining, but with an emphasis on the fact that the construction is based solely on structure of a set of given quantum states, without relying on any additional, preferred structure in Hilbert space. In particular, we use principle component analysis (PCA) [204] to use a set of states $\{|\psi^{(\mu)}\rangle\} \in \mathcal{H}$ to define a vector subspace $\tilde{\mathcal{H}} \subset \mathcal{H}$, such that a coarse-graining map onto $\tilde{\mathcal{H}}$ captures the most important information about the original states (in a sense

we make precise below). We refer to this procedure as “quantum decimation in Hilbert space”: a scheme where we coarse-grain quantum states by decimating or discarding irrelevant features determined by the structure of the states themselves, without presuming additional structure on Hilbert space. (Our method is distinct from past usage of the term “quantum decimation” in the literature [205–207], which refers to application of RG ideas to spin chains, Hubbard models and the like.) The idea of the PCA is to express the information contained in the original states in the most efficient way possible, by identifying the basis vectors along which most of the variation occurs, and attaching a systematic notion of the relative importance of different basis vectors. This helps us identify global, important features of the state (determined by the states themselves) and physically one can relate this to preserving most of the relevant entanglement structure of the states (in any arbitrarily associated tensor factorization to Hilbert space).

The chapter is organized as follows. In Section (9.2), we construct the principle component basis for the set of fine-grained states we wish to coarse-grain, and define a PCA compression map which removes redundancy in the basis used to describe our states. In Section (9.3), we develop the details of the coarse-graining isometry based on decimation of the PCA expansion and discuss the physical question of “what are we coarse-graining?” and a possible application of the procedure in coarse-graining time evolution of a system. In section (9.4), we compare it with other conventional coarse-graining schemes and data compression techniques in quantum information, and conclude.

9.2 Constructing the Principle Component Basis

Setting the Stage

Consider a finite-dimensional Hilbert space \mathcal{H} of dimension $D = \dim \mathcal{H}$, equipped with a global basis $\{|i\rangle\}$ with $i = 1, 2, \dots, D$. “Global” indicates that the basis spans all of \mathcal{H} , and this choice of this basis is left arbitrary at this stage. Typically, this global basis can be identified with a tensor product structure which identifies degrees of freedom corresponding to subsystems. While in any practical setup such as many-body theory or quantum computation, one typically assumes a highly non-generic and preferred tensor factorization of \mathcal{H} based on the Hamiltonian [28, 29] where features like locality and classical emergence might be manifest, we do not assume any such preferred structure. Our technique, at the “data-compression” stage, works even without associating a tensor product structure to Hilbert space, but its interpretation (which we offer in section 9.3) relies on the existence of an arbitrary

factorization $\mathcal{H} = \bigotimes_j \mathcal{H}_j$, not necessarily corresponding to a quasi-classical one. A normalized state $|\psi\rangle \in \mathcal{H}$ can be expanded in this global basis,

$$|\psi\rangle = \sum_{i=1}^D c_i |i\rangle, \quad (9.2)$$

with $c_i = \langle i|\psi\rangle$ and $\sum_{i=1}^D |c_i|^2 = 1$.

Now imagine that we are given M states in \mathcal{H} , labeled by $\{|\psi^{(\mu)}\rangle\}$, $\mu = 1, 2, \dots, M$, which we will call the *specifying states*. Our goal is to harness the structure of these specifying states in \mathcal{H} to construct a coarse-graining procedure that will allow us to project them down to a subspace $\tilde{\mathcal{H}}$ that preserves as much relevant information as possible. Each $|\psi^{(\mu)}\rangle$ be expanded in the chosen global basis,

$$|\psi^{(\mu)}\rangle = \sum_{i=1}^D c_i^{(\mu)} |i\rangle, \quad (9.3)$$

with $\sum_{i=1}^D |c_i^{(\mu)}|^2 = 1$. It will be convenient to package these components as a $(D \times 1)$ column vector, which we call $[C^{(\mu)}]$,

$$[C^{(\mu)}]_{D \times 1} = \begin{bmatrix} c_1^{(\mu)} \\ c_2^{(\mu)} \\ \cdot \\ \cdot \\ c_D^{(\mu)} \end{bmatrix}. \quad (9.4)$$

We now bundle together the coefficients of all of the specifying states into a matrix $[C]$, of order $(D \times M)$, which we call our *augmented matrix*:

$$[C]_{D \times M} = [C^{(1)}; C^{(2)}; \dots; C^{(M)}] \equiv \begin{bmatrix} c_1^{(1)} & c_1^{(2)} & \dots & c_1^{(M)} \\ c_2^{(1)} & c_2^{(2)} & \dots & c_2^{(M)} \\ \cdot & \cdot & \dots & \cdot \\ \cdot & \cdot & \dots & \cdot \\ c_D^{(1)} & c_D^{(2)} & \dots & c_D^{(M)} \end{bmatrix}. \quad (9.5)$$

The basic idea of coarse-graining is to reduce the effective dimensionality of Hilbert space, thus giving an effective description of the state, while retaining the global or

Table 9.1: List of Important Notation Used

\mathcal{H}	Hilbert space of (fine-grained) dimension $D = \dim \mathcal{H}$.
$\{ i\rangle\}$	Global basis of \mathcal{H} , $i = 1, 2, \dots, D$.
$\{ \psi^{(\mu)}\rangle\}$	Set of M specifying states in \mathcal{H} , $\mu = 1, 2, \dots, M$.
$\tilde{\mathcal{H}}_{(d)}$	Hilbert space of (coarse-grained) dimension $d = \dim \tilde{\mathcal{H}}_{(d)}$ with $\tilde{\mathcal{H}}_{(d)} \subset \mathcal{H}$ and $d \leq (M + 1) < D$.
$[C^{(\mu)}]$	Column-vector containing coefficients $c_i^{(\mu)}$ of $ \psi^{(\mu)}\rangle$ in the global $ i\rangle$ basis.
$[C]$	Augmented Matrix containing all M specifying states as column vectors.
$\bar{c}^{(\mu)}$	Mean value of the coefficients of $ \psi^{(\mu)}\rangle$ in the global basis.
$[O_D]$	Un-normalized, uniform superposition state in \mathcal{H} .
$[\Delta C]$	Augmented Matrix of deviation of each state from its mean value.
$\{e_k\}$	Set of non-zero singular values of $[\Delta C]^\dagger [\Delta C]$ and $[\Delta C] [\Delta C]^\dagger$, $k = 1, 2, \dots, M$.
$[\hat{\Phi}]$	Un-normalized PCA basis vectors organized as a matrix.
$[\hat{\mathcal{W}}]$	Un-normalized PCA weights organized as a matrix.
$[\Phi]$	Normalized PCA basis vectors organized as a matrix.
$[\mathcal{W}]$	Normalized PCA weights organized as a matrix.
$\{ \phi_j\rangle\}$	PCA basis vectors in $\tilde{\mathcal{H}}_{(d)}$ with $j = 0, 1, \dots, (d - 1)$.
$\hat{\Pi}_{(d)}$	Projection Map from fine-grained states in \mathcal{H} to coarse-grained states in $\tilde{\mathcal{H}}_{(d)}$.
$[\mathcal{T}_d]$	Truncation matrix of order $d \times (M + 1)$ with $[\mathcal{T}_d]_{ab} = \delta_{ab}$
$[G_d]$	Net coarse-graining transformation defined as $[G_d] = [\mathcal{T}_d] [\Phi]^\dagger$.

large-scale physics of the state. Our current structure does not assume any notion of space or any associated notion of locality, or indeed any specific Hamiltonian. All we are working in is Hilbert space and an associated global basis. An idea of coarse-graining in such a setup would need to be equipped with the understanding of ‘‘What are we coarse-graining?’’ and ‘‘What are we losing under such a transformation?’’ since our regular ideas of spatial scales, lattices, and locality are not present in the current scheme. This allows us to construct a more general prescription using Hilbert space ideas, which does not assume any preferred decomposition into subsystems or preferred observables, local or otherwise. These ideas are further discussed in Sections (9.3) and (9.4).

We propose to perform principle component analysis (PCA) on the specifying states

as a technique to reduce the dimensionality of our Hilbert space, thus resulting in a coarse-grained description for the specifying states. The resulting PCA coarse-graining prescription will be useful to coarse-grain the same set of specifying states only (unless there is some relationship between a separate state and the specifying states). The PCA transforms the input into a set of linearly uncorrelated principle components, thus reducing any redundancy in describing the specifying states. As is common in any PCA application, the first step is to remove the column-wise mean of the matrix $[C]$, which helps to isolate the sources of variance in the set of specifying states. A mean-subtracted input allows the PCA components to have variance in reconstruction over and above the mean in a systematic way, where the k th component is more important in adding back variance as compared to the $(k + 1)$ st component. It is worth pointing out at this stage and as we will see, in our use of the PCA, that the mean subtraction will be an important step in our physical interpretation of the coarse-graining transformation.

Let us begin by subtracting the column-wise mean from the structure of our specifying states $\{|\psi^{(\mu)}\rangle\}$ described by the augmented matrix $[C]$. Let $\bar{C}^{(\mu)}$ be the mean of the $(D \times 1)$ column vector $[C^{(\mu)}]$, which is also the μ th column of $[C]$,

$$\bar{C}^{(\mu)} = \frac{1}{D} \sum_{j=1}^D c_j^{(\mu)}. \quad (9.6)$$

We also define an un-normalized, uniform superposition state whose representation in the global $\{|i\rangle\}$ basis is the $(D \times 1)$ column vector $[O_D]$ with all entries equal to unity,

$$[O_D]_{D \times 1} \equiv \begin{bmatrix} 1 \\ 1 \\ \cdot \\ \cdot \\ \cdot \\ 1 \end{bmatrix}. \quad (9.7)$$

While this uniform state $[O_D]$ is basis-dependent, we will argue in Section (9.3) that the relative inner product structure between the specifying states will be invariant under the coarse-graining for *any* choice of global basis. Each choice of basis lends its own features which will be taken into account by the coarse-graining prescription, while at the same time, keeping the relative structure of the states invariant and

offering a uniform interpretation in terms of entanglement coarse-graining for any associated tensor product structure to the chosen basis.

Based on this, one can define the mean augmented matrix $[\bar{C}]$ as the following $(D \times M)$ matrix,

$$[\bar{C}] = \left[\bar{C}^{(1)} O_D; \bar{C}^{(2)} O_D; \dots; \bar{C}^{(M)} O_D \right], \quad (9.8)$$

and thus, the μ th column of $[\bar{C}]$ is simply,

$$\bar{C}^{(\mu)} O_D = \frac{1}{D} \sum_{j=1}^D c_j^{(\mu)} \begin{bmatrix} 1 \\ 1 \\ \cdot \\ \cdot \\ \cdot \\ 1 \end{bmatrix}. \quad (9.9)$$

One can now define the deviation of each of the specifying states from their respective means as,

$$[\Delta C]_{D \times M} = [C]_{D \times M} - [\bar{C}]_{D \times M}, \quad (9.10)$$

which will serve as a description of our states $\{|\psi^{(\mu)}\rangle\}$ based on the deviations of the coefficients from the mean $\bar{C}^{(\mu)}$ of each of the specifying states.

Implementing the Principle Component Analysis

Starting with M specifying states $\{|\psi^{(\mu)}\rangle\}$ in the D -dimensional Hilbert space \mathcal{H} , we have decomposed them into a set of mean values organized into a matrix $[\bar{C}]_{D \times M}$ and a set of deviations $[\Delta C]_{D \times M}$. In what follows, we focus on the case with $D > M + 1$ (the “+1” to become clear later), *i.e.* with fewer states than the dimension of the space they live in. This is usually the relevant case, since state vectors describing physical systems commonly live in very large Hilbert spaces and the number of states one might wish to understand is much smaller. In the other limit with more states than dimensions, one would generically need the full support of the Hilbert space to describe them and a PCA based coarse-graining technique may not be very useful. The matrix $[\Delta C]$ captures all the information there is in our set of specifying states in the choice of basis, modulo the mean of each state which just adds a uniform contribution along each of the basis directions. We can think of $[\Delta C]$ as characterizing the deviation of the state from being a uniform superposition (in the average sense), which as we will see, will be important in interpreting the

technique as an entanglement coarse-graining under any associated tensor product structure $\mathcal{H} = \bigotimes_j \mathcal{H}_j$.

We now perform a principle component analysis on the matrix $[\Delta C]$, which is implemented via a singular value decomposition (SVD). While one can directly perform a PCA on the coefficient matrix $[C]$ and work out the technique on similar lines as described below, we feel that delineating these different contributions makes the process rather clear and better physically motivated. We decompose $[\Delta C]$ as,

$$[\Delta C]_{D \times M} = [\mathcal{A}]_{D \times D} [\mathcal{D}]_{D \times M} [\hat{\mathcal{W}}]_{M \times M}, \quad (9.11)$$

where $[\mathcal{A}]$ and $[\hat{\mathcal{W}}]$ are unitary matrices and $[\mathcal{D}]$ is a diagonal matrix with M non-zero singular values $\{e_k, k = 1, 2, \dots, M\}$ of $[\Delta C]$ on the diagonal,

$$[\mathcal{D}]_{D \times M} = \begin{bmatrix} e_1 & 0 & \cdots & 0 \\ 0 & e_2 & \cdots & 0 \\ \cdot & \cdot & \cdots & \cdot \\ \cdot & \cdot & \cdots & \cdot \\ 0 & 0 & \cdots & e_M \\ 0 & 0 & \cdots & 0 \\ \cdot & \cdot & \cdots & \cdot \\ 0 & 0 & \cdots & 0 \end{bmatrix}. \quad (9.12)$$

These non-zero singular values are the square roots of the non-zero eigenvalues of $[\Delta C]^\dagger [\Delta C]$ and $[\Delta C] [\Delta C]^\dagger$. Following standard PCA procedure, we arrange the singular values on the diagonal in $[\mathcal{D}]$ in descending order, which helps capture the systematic addition of variance by the PCA,

$$e_1 \geq e_2 \geq \cdots \geq e_M. \quad (9.13)$$

It is most convenient to write the deviations from the mean as

$$[\Delta C]_{D \times M} = [\hat{\Phi}]_{D \times M} [\hat{\mathcal{W}}]_{M \times M}, \quad (9.14)$$

where the $D \times M$ matrix

$$[\hat{\Phi}]_{D \times M} \equiv [\mathcal{A}]_{D \times D} [\mathcal{D}]_{D \times M} \quad (9.15)$$

defines the PCA basis, and the $M \times M$ matrix $[\hat{\mathcal{W}}]$ defines the (un-normalized) PCA weights. The hat symbol ($\hat{\cdot}$) here is used to stress that the variable is not

normalized. The use of hat ($\hat{\cdot}$) to denote operators, whenever used, will be clear from context. Written explicitly,

$$[\Delta C] = \left[\hat{\phi}_1; \hat{\phi}_1; \cdots; \hat{\phi}_M \right]_{D \times M} \begin{bmatrix} \hat{w}_1^{(1)} & \hat{w}_1^{(2)} & \cdots & \hat{w}_1^{(M)} \\ \hat{w}_2^{(1)} & \hat{w}_2^{(2)} & \cdots & \hat{w}_2^{(M)} \\ \cdot & \cdot & \cdots & \cdot \\ \cdot & \cdot & \cdots & \cdot \\ \hat{w}_D^{(1)} & \hat{w}_D^{(2)} & \cdots & \hat{w}_D^{(M)} \end{bmatrix}_{M \times M} . \quad (9.16)$$

The columns $[\hat{\phi}_j]_{D \times 1} \equiv e_j [\mathcal{A}_j]_{D \times 1}$ $j = 1, 2, \dots, M$, are the components of the M new PCA basis vectors in the original global $\{|i\rangle\}$ basis, and $\hat{w}_j^{(\mu)}$ is the j -th un-normalized PCA weight for the specifying state $|\psi^{(\mu)}\rangle$.

Thus, the deviation from the mean of $|\psi^{(\mu)}\rangle$ can be reconstructed as,

$$\left[\Delta C^{(\mu)} \right]_{D \times 1} = \sum_{j=1}^M \hat{w}_j^{(\mu)} [\hat{\phi}_j]_{D \times 1} . \quad (9.17)$$

The columns of $[\mathcal{A}]_{D \times D}$, which we denote as $[\mathcal{A}_i]_{D \times 1}$, $i = 1, 2, \dots, D$ form an orthonormal basis for the global Hilbert space \mathcal{H} , since $[\mathcal{A}]$ is unitary, while just the first M states in $[\mathcal{A}]_{D \times D}$ selected by the M non-zero singular values $\{e_k, k = 1, 2, \dots, M\}$ are needed to form a complete basis for our specifying states $|\psi^{(\mu)}\rangle$ we wish to coarse-grain. This step forms the information compression step: we have chosen a smaller set of linearly independent vectors who span a vector subspace that includes all of our specifying states $|\psi^{(\mu)}\rangle$. However, the scaling of each of these columns with the singular values e_j to get $[\hat{\phi}_j]$ renders the basis vectors un-normalized. Once this compression step is done, we can normalize our PCA basis states by associating the singular values with the PCA weights, by defining

$$w_j^{(\mu)} = e_j \hat{w}_j^{(\mu)}, \quad j = 1, 2, \dots, M \quad \text{and} \quad \forall \mu . \quad (9.18)$$

This lets us define the normalized PCA basis vectors as simply the first M columns of the unitary $[\mathcal{A}]$,

$$[\phi_j]_{D \times 1} = [\mathcal{A}_j]_{D \times 1}, \quad j = 1, 2, \dots, M \quad \text{and} \quad \forall \mu . \quad (9.19)$$

Thus, we have mapped the D coefficients of each state $[C^{(\mu)}]$ to M coefficients of the PCA expansion in the PCA basis $[\Phi]$ as obtained above, in addition to the mean

coefficient of each state. To reconstruct the full state $|\psi^{(\mu)}\rangle$, we add the mean $\bar{C}^{(\mu)}$ multiplied by $[O_D]$ to obtain back $[C^{(\mu)}]$,

$$|\psi^{(\mu)}\rangle \equiv [C^{(\mu)}] = \bar{C}^{(\mu)} [O_D]_{D \times 1} + \sum_{i=1}^M w_i^{(\mu)} [\phi_i]_{D \times 1}. \quad (9.20)$$

In what follows, to avoid clutter in our equations, we drop the explicit use of the square brackets $[.]$, which we have been using to denote matrices so far.

The μ th state $|\psi^{(\mu)}\rangle$ is normalized, hence we obtain the matrix representation of the normalization condition $\langle \psi^{(\mu)} | \psi^{(\mu)} \rangle = 1$ to be the following,

$$|\bar{C}^{(\mu)}|^2 O_D^\dagger O_D + \sum_{i=1}^M \sum_{k=1}^M w_i^{(\mu)} (w_k^{(\mu)})^* \phi_k^\dagger \phi_i + \sum_{k=1}^M w_k^{(\mu)} O_D^\dagger \phi_k + \sum_{k=1}^M (w_k^{(\mu)})^* \phi_k^\dagger O_D = 1. \quad (9.21)$$

Before we further simplify the normalization condition, consider contracting the state $|\psi^{(\mu)}\rangle$ in Eq. (9.20) with $[O_D]$,

$$O_D^\dagger C^{(\mu)} = \sum_{j=1}^D c_j^{(\mu)} = \bar{C}^{(\mu)} O_D^\dagger O_D + \sum_{k=1}^M w_k^{(\mu)} O_D^\dagger \phi_k. \quad (9.22)$$

One can now use the fact that $O_D^\dagger O_D = D$ and $\sum_{j=1}^D c_j^{(\mu)} = D \bar{C}^{(\mu)}$ to get,

$$\sum_{k=1}^M w_k^{(\mu)} O_D^\dagger \phi_k = 0 = \sum_{k=1}^M (w_k^{(\mu)})^* \phi_k^\dagger O_D. \quad (9.23)$$

In addition to this, due to the mean subtraction in each column in Eq. (9.10), each of the PCA basis vectors $[\phi_j]$, $j = 1, 2, \dots, M$ has a zero mean $O_D^\dagger \phi_j = \phi_j^\dagger O_D = 0$. Hence, not only is the summand of Eq. (9.23) zero, but each term vanishes separately. The PCA basis vectors $[\phi_j]_{D \times 1}$ are the columns of a unitary matrix, and are therefore orthonormal, $\phi_k^\dagger \phi_i = \delta_{ik}$. We can therefore use Eq. (9.23) to get the normalization condition for the μ th state $|\psi^{(\mu)}\rangle$ as,

$$|\sqrt{D} \bar{C}^{(\mu)}|^2 + \sum_{k=1}^M |w_k^{(\mu)}|^2 = 1 \quad \forall \mu = 1, 2, \dots, M. \quad (9.24)$$

Thus, we have mapped the D coefficients of each state $|\psi^{(\mu)}\rangle$ in the global basis to a mean value $\bar{C}^{(\mu)}$ and M coefficients in the PCA basis $[\Phi]$, thus needing $M + 1$ coefficients in this new basis to characterize the state.

At this stage, we have captured the full information of each specifying state $|\psi^{(\mu)}\rangle$ in the $M + 1$ coefficients and the constructed PCA basis. The dimensional reduction is

not a result of integrating out small scale physics, rather it is simply a smart choice of basis, which minimizes redundancy in the description of our specifying states $\{|\psi^{(\mu)}\rangle\}$. We also know that $O_D^\dagger \phi_j = 0$, making it orthogonal to all of the other PCA basis vectors, and is hence a linearly independent vector whose contribution is needed to reconstruct $\{|\psi^{(\mu)}\rangle\}$ from the $M + 1$ coefficients. This motivates us to identify the “zeroth” component of the PCA basis ϕ_0 and the corresponding PCA weight to be the mean contribution,

$$\phi_0 \equiv \frac{1}{\sqrt{D}} O_D, \quad w_0^{(\mu)} \equiv \sqrt{D} \bar{C}^{(\mu)}. \quad (9.25)$$

The PCA basis now has $M + 1$ basis and each contribution (mean and otherwise) is treated homogeneously, and one can express the basis set as $[\Phi] = [\phi_0; \phi_1; \dots; \phi_M]$. Thus we have (notice the sum runs from zero now),

$$|\psi^{(\mu)}\rangle \equiv [C^{(\mu)}] = \sum_{j=0}^M w_j^{(\mu)} [\phi_j]_{D \times 1}. \quad (9.26)$$

Notice, we have added a factor of \sqrt{D} to keep ϕ_0 normalized like the other PCA basis vectors. Normalization of the state $|\psi^{(\mu)}\rangle$ is now simply written as, following Eq. (9.24),

$$\sum_{k=0}^M |w_k^{(\mu)}|^2 = 1 \quad \forall \mu = 1, 2, \dots, M. \quad (9.27)$$

Mapping onto the PCA Subspace

The PCA procedure discussed above provides us with $M + 1$ vectors (the PCA basis) $[\Phi]$, which span and act as a basis in a vector subspace containing our M specifying states. Let us denote this subspace as $\tilde{\mathcal{H}}_{(M+1)}$ with $\tilde{\mathcal{H}}_{(M+1)} \subset \mathcal{H}$. For each of the PCA basis vector $[\phi_j]$, $j = 0, 1, \dots, M$, we can identify the corresponding state vector $|\phi_j\rangle \in \tilde{\mathcal{H}}_{(M+1)}$. This set of PCA vectors $\{|\phi_j\rangle\}$ forms a complete, orthonormal basis set for $\tilde{\mathcal{H}}_{(M+1)}$ and our specifying states can be expanded in this basis for $\tilde{\mathcal{H}}_{(M+1)}$ following Eq. (9.26),

$$|\psi^{(\mu)}\rangle = \sum_{j=0}^M w_j^{(\mu)} |\phi_j\rangle. \quad (9.28)$$

The j -th basis state $|\phi_j\rangle \in \tilde{\mathcal{H}}_{M+1}$ is embedded in the larger D -dimensional space \mathcal{H} and is connected to its representation in the global $\{|i\rangle\} \in \mathcal{H}$ basis via its matrix representation $[\phi_j]$ of Eq. (9.19).

Once this subspace $\tilde{\mathcal{H}}_{(M+1)}$ has been defined and its basis identified, one can work with the specifying states exclusively in this subspace by mapping the state $|\psi^{(\mu)}\rangle$ from the larger space \mathcal{H} to $\tilde{\mathcal{H}}_{(M+1)}$ by using an operator $\hat{\Pi}_{(M+1)}$. To understand the action of $\hat{\Pi}_{(M+1)}$ on the specifying states, we first connect the PCA weights $w_j^{(\mu)}$ with the global expansion coefficients $c_i^{(\mu)}$. For $|\psi^{(\mu)}\rangle$, by contracting both sides of $\sum_{i=1}^D c_i^{(\mu)} |i\rangle = \sum_{j=0}^M w_j^{(\mu)} |\phi_j\rangle$ by $\langle\phi_k|$ and using the orthonormality of the PCA basis $\langle\phi_k|\phi_j\rangle = \delta_{kj}$, we find

$$w_j^{(\mu)} = \sum_{i=1}^D c_i^{(\mu)} \langle\phi_j|i\rangle . \quad (9.29)$$

Thus, mapping to the $\tilde{\mathcal{H}}_{(M+1)}$ space is achieved by,

$$\hat{\Pi}_{(M+1)} = \sum_{j=0}^M |\phi_j\rangle \langle\phi_j| . \quad (9.30)$$

This, of course, keeps the specifying states unaltered, while mapping them onto the $\tilde{\mathcal{H}}_{(M+1)}$ subspace with their expansion in the PCA basis, thus compressing the support needed to describe them. Also, any other vector $|\alpha\rangle \in \tilde{\mathcal{H}}_{(M+1)} \subset \mathcal{H}$ can be similarly mapped down from a D -dimensional to an $M+1$ dimensional space. While arbitrary states in \mathcal{H} not completely supported on $\tilde{\mathcal{H}}_{(M+1)}$ can be mapped to $\tilde{\mathcal{H}}_{(M+1)}$ using $\hat{\Pi}_{(M+1)}$, such a map will non-systematically, and perhaps non-desirably, alter the structure of the state.

Our focus in this chapter is to coarse-grain the specifying states: the PCA map $\hat{\Pi}_{(M+1)}$ acts as the dimension compression step which can now be coarse-grained as described in Section (9.3).

9.3 Coarse-Graining via Decimation

Truncation of the PCA Expansion and Coarse-Graining

With this technology in hand, we can now explore how to systematically coarse-grain our states $\{|\psi^{(\mu)}\rangle\}$ to further lower-dimensional Hilbert spaces. With the PCA basis alone, we have already reduced the effective dimensionality of the underlying vector space from D to $M+1$ using the PCA map $\hat{\Pi}_{(M+1)}$ without any loss in the description of the state, since the PCA simply chooses a smart basis which removes redundancy in their description. We now discuss the decimation prescription, in which we truncate the PCA expansion of Eq. (9.28) as a method of coarse-graining, explicitly reducing the dimensionality of Hilbert space at the expense of throwing away certain features of the state.

Currently, a state $|\psi^{(\mu)}\rangle$ is expanded in the PCA basis $[\Phi]$, as done in Eq. (9.26) in the matrix representation describing its reconstruction in the global D -dimensional space \mathcal{H} . The M non-zero singular values e_k , $k = 1, 2, \dots, M$ are arranged in descending order in the diagonal matrix $[\mathcal{D}]$ in Eq. (9.11). The PCA endows us with a systematic control of the contribution of different PCA components in reconstruction of the state. Thus, the $j = 1$ component of the PCA, $w_1^{(\mu)}\phi_1$, carries *maximum variance* in reconstructing the state $[C^{(\mu)}]$ over and above the zeroth component ($j = 0$) *i.e.* the state mean $\bar{C}^{(\mu)}$. The next $j = 2$ orthonormal component $w_2^{(\mu)}\phi_2$ has lesser variance than the $j = 1$ component, and so on. The k -th component is more important than the $(k + 1)$ -st component in adding back variance over and above the mean to reconstruct the state.

Since the tailing PCA components contribute little to the reconstruction of the state as compared to the preceding components, one could, depending on the required accuracy of reconstruction, neglect some of these tailing terms in the series to obtain an effective, coarse-grained description of the state. To better understand relative importance of different PCA components in reconstructing the specifying states, one can look at the fractional contribution/importance (Imp) of the k -th PCA component,

$$\text{Imp}(\phi_k) = \frac{e_k}{\sum_{j=1}^M e_j}, \quad k = 1, 2, \dots, M. \quad (9.31)$$

Thus, in addition to the mean term $w_0^{(\mu)}\phi_0 \equiv \bar{C}^{(\mu)}O_D$, one could choose the next $(d - 1)$ PCA terms with $1 \leq (d - 1) \leq M$ in the expansion as a coarse-grained description of the state,

$$|\psi^{(\mu)}\rangle_{CG(d)} \equiv [C^{(\mu)}]_{CG(d)} = \sum_{k=0}^{d-1} w_k^{(\mu)} [\phi_k], \quad (9.32)$$

where the contributions of the $k = d$ to M components have been truncated and neglected. In the above equation and in what follows, “CG(d)” indicates that the state has been coarse-grained (CG) to a d -dimensional reconstruction. The choice of d can be made depending on the various fractional contributions (Eq. 9.31) of the PCA basis and the required accuracy of the coarse-grained description. We have thus effectively mapped the D coefficients of the state $|\psi^{(\mu)}\rangle$ in the original (global) basis to $d \leq (M + 1) < D$ components in the truncated/coarse-grained PCA basis.

Following the discussion in subsection (9.2), we now construct a d -dimensional vector subspace $\tilde{\mathcal{H}}_{(d)}$ with $\tilde{\mathcal{H}}_{(d)} \subset \tilde{\mathcal{H}}_{(M+1)} \subset \mathcal{H}$, which covers the support of the CG(d) coarse-grained specifying states. The first d PCA vectors $[\phi_j]$, $j =$

$0, 1, 2, \dots, d-1$ form an orthonormal basis for $\tilde{\mathcal{H}}_{(d)}$ and can be identified with their corresponding set of basis state vectors $|\phi_j\rangle$, $j = 0, 1, 2, \dots, d-1$. Before we construct the coarse-graining map, it is important to notice that truncating the PCA series renders the states un-normalized. Since we would like our coarse-grained vectors to be good quantum states satisfying probability summing to unity, we normalize the states by hand. A coarse-graining map $\hat{\Pi}_{(d)}$ can be constructed which projects and coarse-grains the state to $\tilde{\mathcal{H}}_{(d)}$ and normalizes it as well,

$$\hat{\Pi}_{(d)} : \mathcal{H} \rightarrow \tilde{\mathcal{H}}_{(d)} \quad (9.33)$$

$$|\psi^{(\mu)}\rangle \mapsto |\psi^{(\mu)}\rangle_{CG(d)} = \frac{\sum_{j=0}^{d-1} w_j^{(\mu)} |\phi_j\rangle}{\|\sum_{k=0}^{d-1} w_k^{(\mu)} |\phi_k\rangle\|}. \quad (9.34)$$

As before, the basis states $|\phi_j\rangle$ are embedded in the original space \mathcal{H} via their matrix representations (Eq. (9.19)). We see $2 \leq d \leq (M+1)$, and $d=2$ is the most coarse-grained description of the specifying states as effective qubits, whereas the other limit $d=(M+1)$ takes it back to the full non-coarse-grained, albeit PCA-compressed description, as discussed in subsection 9.2. One can also define a series of nested subspaces

$$\tilde{\mathcal{H}}_{(2)} \subset \tilde{\mathcal{H}}_{(3)} \subset \dots \subset \tilde{\mathcal{H}}_{(M+1)} \subset \mathcal{H}, \quad (9.35)$$

and a corresponding sequence of maps $\hat{\Pi}_{(d)}$, $d = 2, 3, \dots, M+1$, which progressively coarse-grain from just the PCA compression ($d = M+1$) to a maximally coarse-grained description as an effective qubit ($d = 2$).

One can also consider a coarse-graining application where we admit non-normalized coarse-grained states, possibly due to inaccuracies in experimental setups or numerical precision. In that case, we can choose the coarse-grained dimension d such that,

$$\sum_{k=0}^{d-1} |w_k^{(\mu)}|^2 = 1 - \epsilon, \quad (9.36)$$

for some ϵ small enough to not be detected experimentally or within numerical errors.

The Coarse-Graining Isometry and Expectation Values

Let us recap what we have accomplished so far. We have coarse-grained each of our specifying states from a D -dimensional description in \mathcal{H} to a state living in the d -dimensional Hilbert space $\tilde{\mathcal{H}}_{(d)}$ with $d \leq M+1 < D$, and identified the d expansion coefficients in the (truncated) PCA $\{|\phi_i\rangle\}$, $i = 0, 2, \dots, (d-1)$ basis

in $\tilde{\mathcal{H}}_{(d)}$. Each of these basis states is connected to the fine-grained D -dimensional embedding in \mathcal{H} via its matrix representation, as found in Section (9.2). In this section, we aim to package our results and formally define a transformation that directly relates the d coarse-grained coefficients to the D fine-grained coefficients.

The PCA compression of $|\psi^{(\mu)}\rangle$ lives in $\tilde{\mathcal{H}}_{(M+1)}$ and is described by $M+1$ coefficients $\{w_j^{(\mu)}, j = 0, 1, \dots, M\}$. Let us denote this column by $[W^{(\mu)}]$, which is connected to the fine-grained description of the state $|\psi^{(\mu)}\rangle$ via the PCA basis $[\Phi]_{D \times (M+1)}$ following inversion of Eq. (9.26) as,

$$\left[W^{(\mu)} \right]_{(M+1) \times 1} = [\Phi]_{(M+1) \times D}^\dagger \left[C^{(\mu)} \right]. \quad (9.37)$$

The PCA basis matrix, whose columns form an orthonormal basis in $\tilde{\mathcal{H}}_{(M+1)}$, defines an isometric embedding, $[\Phi]^\dagger [\Phi] = \mathbb{I}_{(M+1)}$, but in general $[\Phi] [\Phi]^\dagger \neq \mathbb{I}_D$ as expected, where \mathbb{I}_p is the p -dimensional identity. However, $[\Phi] [\Phi]^\dagger$ acts as the identity in the subspace where our specifying states reside. This is tantamount to saying that the PCA projection $\hat{\Pi}_{(M+1)}$ leaves the specifying states invariant,

$$[\Phi] [\Phi]^\dagger \left[C^{(\mu)} \right] = \left[C^{(\mu)} \right], \forall \mu = 1, 2, \dots, M. \quad (9.38)$$

Before describing truncation of the PCA series as an effective coarse-grained description of the state, it is instructive to understand how inner products of states are related in the two descriptions. Combining Eqs. (9.37) and (9.38), it is easily seen that the inner product $\langle \psi^{(\nu)} | \psi^{(\mu)} \rangle$ is preserved while transforming from the global D -dimensional to the PCA $(M+1)$ -dimensional description,

$$\langle \psi^{(\nu)} | \psi^{(\mu)} \rangle = \left[C^{(\nu)} \right]^\dagger \left[C^{(\mu)} \right] = \left[W^{(\nu)} \right]^\dagger \left[W^{(\mu)} \right]. \quad (9.39)$$

At this stage, one might worry about the basis-dependence of the PCA prescription outlined in Section (9.2), since the uniform, un-normalized state $[O_D]$ is a basis-dependent construction. Under different choices of global basis $\{|i\rangle\}$ that lead to different augmented matrices $[C]$, one would end up with a different set of PCA basis vectors and weights, with the zeroth vector always identified as the uniform superposition state. However, this is not an issue since the relative inner product structure of the specifying states is invariant under change of global basis by a unitary transformation. This can be easily verified by using Eqs. (9.37) and (9.38) for two different choices of global basis where the coefficients of the specifying states are connected by some unitary transformation $[\Lambda]$. The PCA compression,

while preserving overlaps between our set of specifying states in any arbitrary choice of basis, then also preserves the pairwise distances between states,

$$\| |\psi^\mu - \psi^\nu\rangle \|^2 = \langle \psi^\mu - \psi^\nu | \psi^\mu - \psi^\nu \rangle = 2 - 2 \operatorname{Re} (\langle \psi^\mu | \psi^\nu \rangle) , \quad (9.40)$$

and under truncation of the PCA expansion of Eq. (9.32), we preserve these overlaps and pairwise distances upto some error scale determined by the choice d of the coarse-grained subspace.

The next step of coarse-graining via truncating the PCA expansion to the first d coefficients of $[W^{(\mu)}]$ as a coarse-grained description of the state $|\psi^{(\mu)}\rangle$ can be achieved by a truncation matrix $[\mathcal{T}_d]$ that is of order $d \times (M + 1)$ and is a diagonal matrix with ones on the diagonal, $[\mathcal{T}_d]_{ab} = \delta_{ab}$. Using this truncation matrix, the d coefficients of the *un-normalized* coarse-grained state $|\psi^{(\mu)}\rangle_{CG(d)}$, which we call $[W_{CG(d)}^{(\mu)}]$, can be obtained as,

$$\left[W_{CG(d)}^{(\mu)} \right]_{d \times 1} = [\mathcal{T}_d] [W^{(\mu)}] = [\mathcal{T}_d] [\Phi]^\dagger [C^{(\mu)}] \equiv [G_d] [C^{(\mu)}] , \quad (9.41)$$

where we have defined the net coarse-graining transformation as $[G_d] = [\mathcal{T}_d] [\Phi]^\dagger$, which satisfies $[G_d] [G_d]^\dagger = \mathcal{I}_d$. This transformation captures both the PCA basis change and the truncation to retain the first d components. Normalization of the coarse-grained state can be done by hand, as described in subsection (9.3).

Another aspect is the behavior of expectation values of Hermitian operators under our coarse-graining transformation. Consider a Hermitian operator $\hat{O} \in \mathcal{L}(\mathcal{H})$, which in the global basis for \mathcal{H} has a matrix representation $[O]_{D \times D}$, whose expectation in the μ th state is

$$\langle \hat{O} \rangle_{FG}^{(\mu)} = \langle \psi^{(\mu)} | \hat{O} | \psi^{(\mu)} \rangle \equiv [C^{(\mu)}]^\dagger [O] [C^{(\mu)}] , \quad (9.42)$$

where the subscript FG is to emphasize that we compute this expectation in the fine-grained, global description in \mathcal{H} . One can construct the coarse-grained matrix representation of \hat{O} using our coarse-graining transformation $[G]$ as follows,

$$[O_{CG(d)}]_{d \times d} = [G_d] [O] [G_d]^\dagger , \quad (9.43)$$

whose expectation value is computed with respect to the coarse-grained state $[W_{CG(d)}^{(\mu)}]$,

$$\langle \hat{O} \rangle_{CG(d)}^{(\mu)} = [W_{CG(d)}^{(\mu)}]^\dagger [O_{CG(d)}] [W_{CG(d)}^{(\mu)}] , \quad (9.44)$$

$$\langle \hat{O} \rangle_{CG(d)}^{(\mu)} = \left[C^{(\mu)} \right]^\dagger \left([G_d]^\dagger [G_d] [O] [G_d]^\dagger [G_d] \right) \left[C^{(\mu)} \right]. \quad (9.45)$$

Depending on how well/poorly we decide to coarse-grain by choosing d , and the details and correlations in the specifying states, the coarse-grain expectations will differ from the fine-grained value, though the coarse-grained expectation $\langle \hat{O} \rangle_{CG(d)}^{(\mu)}$ approaches the fine-grained value as $d \rightarrow M+1$, and they are equal when $d = M+1$.

Decimation and Entanglement

Having developed a coarse-graining prescription based on a PCA transformation and further truncation of the expansion, our next task is to better understand what microscopic information is lost in the course of this transformation. Ours is an unconventional coarse-graining prescription, since it is solely founded on the details of the quantum state given in some global basis. Most coarse-graining schemes assume more structure than this, be it a preferred split of the Hilbert space into tensor factors, a notion of locality in space, or energy modes beyond a certain cutoff that are to be integrated out. All we have is Hilbert space, a notion of a basis and a set of quantum states. A brief comparison of our PCA prescription with other conventional schemes will be done in Section (9.4).

The basic question we wish to answer in this section is, what are we really losing when we perform the PCA and truncate the state description to retain the first d components? What information are we discarding with the remaining $(M+1-d)$ components?

To understand this, let us refer to the tensor product structure associated with the global fine-grained Hilbert space $\mathcal{H} = \bigotimes_j \mathcal{H}_j$. In most physical applications, one has a notion of subsystems, and correspondingly the global Hilbert space \mathcal{H} can be factorized preferentially as a tensor product of Hilbert spaces of each such subsystem. In what follows, we minimally assume some arbitrary tensor factorization of \mathcal{H} , not necessarily equipped with some preferred decomposition governed by the Hamiltonian [28, 29, 114] that might have notions of emergent space, locality, classical equations of motion, and the like. Our interpretation of the technique as an entanglement coarse-graining just uses the existence of such a tensor product structure, and not in being special in any particular way, though since we are working on more general grounds, our method can be adapted to more physically familiar cases.

For concreteness, let us associate a tensor product structure with \mathcal{H} of $D = 2^n$ such that it can be thought of as the Hilbert space of n qubits $\mathcal{H} = (\mathcal{H}_2)^{\otimes n}$, where \mathcal{H}_2 is

the Hilbert space of a qubit. The argument which follows does not hinge on such a qubit factorization, but will work for any arbitrary factorization chosen. Let us write down the reconstruction of the μ -th specifying state by explicitly writing out the mean term, the next $(d - 1)$ terms being retained, and the $M + 1 - d$ truncated terms,

$$\left[C^{(\mu)} \right] = \bar{C}^{(\mu)} [O_D] + \sum_{k=1}^{d-1} w_k^{(\mu)} [\phi_k] + \sum_{l=d}^{M+1} w_l^{(\mu)} [\phi_l] . \quad (9.46)$$

The mean term $\bar{C}^{(\mu)} [O_D]$ has by construction all the same entries. A state of n qubits $\sim [O_D]$ represents a completely separable (product) state of the qubits, and thus has no entanglement between the constituent sub-factors. Thus, the mean state or the ϕ_0 contribution sets a baseline state with the property of having no entanglement amongst its components. One can think of a different tensor structure to \mathcal{H} in terms of qudits, but the mean $\bar{C}^{(\mu)} [O_D]$ term still represents an unentangled state of the constituent sub-factors.

The next $(d - 1)$ terms in the PCA expansion of Eq. (9.46), $w_k^{(\mu)} [\phi_k]$, $k = 1, 2, \dots, (d - 1)$ add most of the variance over and above the mean in reconstructing the (resultant, un-normalized) state. Thus, this sum of $(d - 1)$ terms adds most of the relevant entanglement structure of the state in the chosen tensor factorization of \mathcal{H} . Of course, one may choose a factorization of \mathcal{H} under which the μ -th specifying state may be unentangled to begin with and this argument of adding back relevant entanglement would not be particularly useful. But for a generic decomposition, this understanding of entanglement coarse-graining would be a good notion for what our prescription is coarse-graining. The higher-order terms for $w_l^{(\mu)} [\phi_l]$, $l = d, d + 1, \dots, (M + 1)$ have a negligible (up to the coarse-graining scale set by choice of d) contribution in adding back variance to reconstruct the state, and hence also add minimal entanglement to the structure of the state in the chosen Hilbert space factorization.

As an example, we numerically constructed $M = 250$ specifying states of dimension $D = 2^{10}$. Each coefficient of these states was chosen from a pseudo-random distribution and then normalized. Following this, we performed our PCA-decimation procedure and reduced the dimensionality of each state to d under the map $\hat{\Pi}_{(d)}$ (hence our coarse-grained states are normalized). The coarse-graining dimension d was varied from $d = 1$, corresponding to retaining only the separable $[O_D]$ term, to $d = M + 1$, corresponding to no truncation, only PCA compression. Now one can think of each state to be composed out of $n = 10$ qubits, and we can quantify the

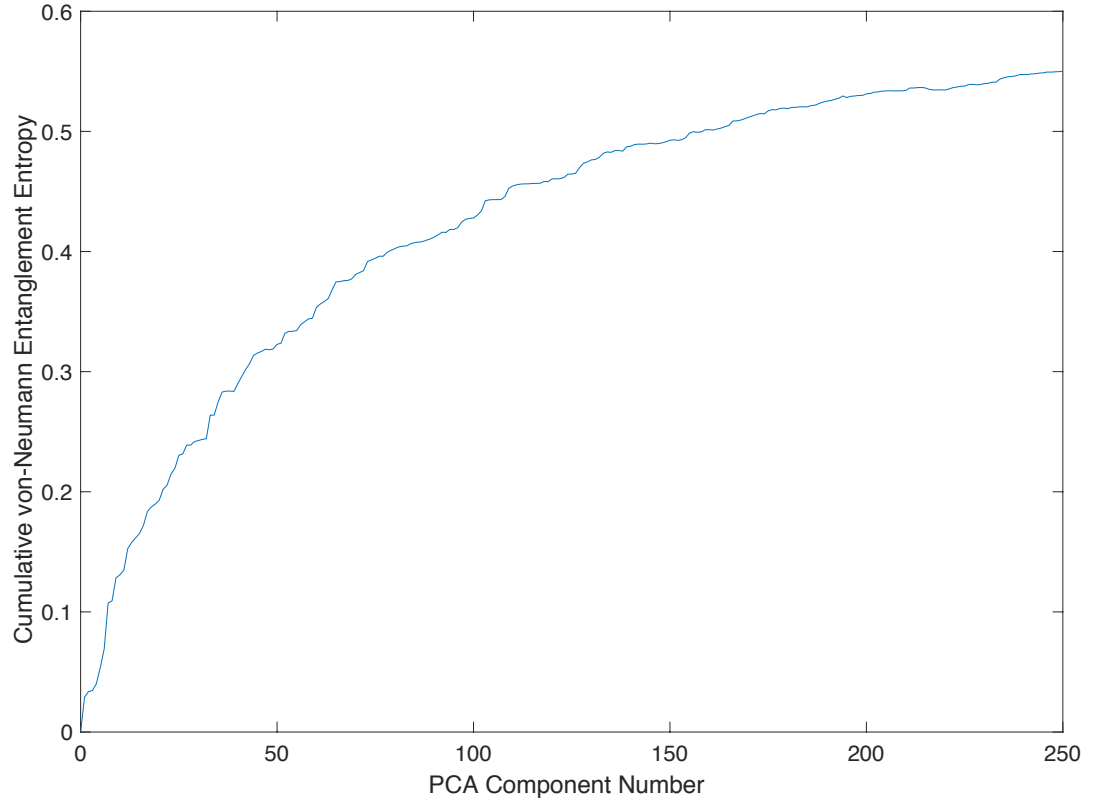


Figure 9.1: Plot of von Neumann entanglement entropy of a constituent qubit of a state as a function of the number of PCA components retained in reconstructing the state.

entanglement structure by looking at the von Neumann entanglement entropy for these qubits in each of the specifying states. For instance, in the μ -th specifying state $|\psi^{(\mu)}\rangle$, one can compute the entanglement entropy of the q -th qubit, $q = 1, 2, \dots, n$ (number of qubits) as

$$S_q^{(\mu)} = -\text{Tr}_q \left(\hat{\rho}_q^{(\mu)} \log \hat{\rho}_q^{(\mu)} \right), \quad (9.47)$$

where

$$\hat{\rho}_q^{(\mu)} = \text{Tr}_{\bar{q}} \left(|\psi^{(\mu)}\rangle \langle \psi^{(\mu)}| \right). \quad (9.48)$$

Figure (1) plots the cumulative von Neumann entanglement entropy of a chosen, constituent qubit in one of the constructed $M = 250$ states (again, chosen as a representative) as a function of the number of PCA components d retained in recon-

structuring the state. The idea of the plot is the saturation of the added entanglement entropy as one goes to more number of PCA components used to reconstruct the state. It is seen that only a few components are required to capture most of the entanglement structure while the higher orders have smaller contribution. By retaining the first d components in the expansion, we recover the state $|\psi^{(\mu)}\rangle$ within error bounds (determined by the choice of d) in a way that we preserve the global or most relevant entanglement structure of the constituent sub-factors and lose irrelevant entanglement by truncating the higher $> d$ components.

The amount of correlations between the specifying states will be an important factor in determining how quickly the entanglement curve (as in Fig. 1) saturates. In general, for higher correlations amongst the specifying states, fewer PCA components would be required for most of the reconstruction, and one will expect a quick saturation in the entanglement build-up. In this sense, our PCA decimation coarse-graining prescription is related to entanglement coarse-graining, and is in the spirit of ignoring microscopic degrees of freedom and retaining large scale/global features; in this case, throwing away small, irrelevant entanglement while holding on the basic large scale structure of the state.

Coarse-Grained Time Evolution of a Quantum System

We have based our coarse-graining prescription on very little structure in Hilbert space: equipped only with a global basis and a set of specifying states, our PCA decimation procedure maps states from a D -dimensional Hilbert space \mathcal{H} to $d < D$ dimensional space $\tilde{\mathcal{H}}_{(d)}$ while retaining most of the global, relevant entanglement structure in the state (in some associated factorization). It is natural to ask in what setups can one adapt and put this coarse-graining prescription to use.

One possible application involves coarse-graining the discretized time evolution of a given initial state $|\psi(t=0)\rangle \equiv |\psi(0)\rangle \in \mathcal{H}$ of dimension $D = \dim \mathcal{H}$ with a global basis $|i\rangle$, $i = 1, 2, \dots, D$. The dynamics of states in \mathcal{H} are governed by some known and specified Hamiltonian \hat{H} . Consider unitarily evolving the initial state at $(M-1)$ time steps governed by some specified/chosen time step Δt , such that the state at the j -th time step $t_j = j\Delta t$, $j = 0, 1, \dots, (M-1)$, is given by (we take units in which $\hbar = 1$),

$$|\psi(t_j)\rangle \equiv \hat{U}(t_j) |\psi(0)\rangle = \exp(-i\hat{H}t_j) |\psi(0)\rangle, \quad j = 0, 1, 2, \dots, (M-1). \quad (9.49)$$

We thus have a collection of M states living in a D -dimensional Hilbert space \mathcal{H} . In the case when the number of time evolved states satisfy $D > (M+1)$, these M states

can act as our set of specifying states to undergo the PCA decimation prescription to be coarse-grained to a lower d ($\leq (M + 1) < D$) dimensional Hilbert space,

$$|\psi(t_j)\rangle_{CG(d)} = \hat{\Pi}_{(d)} |\psi(t_j)\rangle, \quad j = 0, 1, 2, \dots, (M - 1). \quad (9.50)$$

If the Hamiltonian has desirable physical features such as locality, and if the time step is not too large, one would expect a high amount of correlation amongst the time evolved states. In this case, only a very few number of PCA basis components would be required to reconstruct the state. One can also find a coarse-grained representation of the Hamiltonian in the lower-dimensional $\tilde{\mathcal{H}}_{(d)}$ space,

$$[H_{CG(d)}]_{d \times d} = [G_d] [H] [G_d]^\dagger, \quad (9.51)$$

where $[H]$ is the matrix representation of \hat{H} in the global basis in \mathcal{H} . Thus, using our PCA decimation prescription, one can compute a coarse-grained version of the time evolution of the state and use it as a proxy to study time-dependent features of the quantum system under consideration.

9.4 Epilogue and Conclusion

Coarse-graining is a very important theme in understanding the behavior of realistic quantum systems which live in large Hilbert spaces of very large dimension. Many quantum coarse-graining schemes [208–215] integrate out or eliminate irrelevant degrees of freedom to produce a coarse-grained description of the system. Renormalization Group techniques [188–193] have been the cornerstone of coarse-graining ideas, and have proven to be extremely powerful and useful tools in physics. In particular, popular quantum coarse-graining schemes include Density Matrix Renormalization Group (DMRG) [208, 216] and Entanglement Renormalization [209] and their numerical implementations [217–225]. These, and many other coarse-graining schemes, assume substantial structure on Hilbert space. For instance, techniques like DMRG define an RG flow on the space of density matrices and serve as an effective truncation of Hilbert space of strongly correlated quantum many-body systems. Focusing on the low-energy properties of a system with a known Hamiltonian, one assumes a notion of spatial locality and factorizability into state spaces on the lattice, and numerical implementations further assume a preferred split into a system and an environment over which the trace is carried out to compute the properties at the level of the system. Similarly, in Entanglement Renormalization and its numerical implementations like MERA [209], one has a local lattice structure and aims to compute ground state properties for the system

by defining a real space RG to dispose off small-distance degrees of freedom and entanglement (by the use of disentangling isometries, followed by block-decimation prescriptions). All coarse-graining schemes come equipped with an understanding of what global properties of the system one aims to retain, such as optimizing observable expectation values or correlation functions or entanglement between sub-systems; and which features are discarded which usually correspond to small scale entanglement, or high-energy modes, etc.

Techniques in quantum information theory to compress data and allow for dimensional reduction also form an interesting set of ideas to coarse-grain quantum information. Such schemes depend on the context at hand: for example, focusing on a typical subspace and ignoring its orthogonal complement, without much loss of fidelity, such as in Schumacher's noiseless quantum coding theorem, or compressing quantum information in a collection of qubits using elementary quantum circuit operations. Each technique has a specific aim and contextual validity, like the Johnson-Lindenstrauss lemma allows us to preserve pairwise distances up to a certain specified error tolerance and the dimension of the reduced subspace is then determined by this specified error and the number of points in the data set, and not on the dimensionality of the original space. Constructive implementations of the Johnson-Lindenstrauss lemma can be done via random projection and heavily relies on the Euclidean norm to measure pairwise distances, while on the other hand, dimensional reduction using PCA relies on specification of the dimension of the reduced subspace and projects onto a linear subspace. Thus, each technique has its range of validity and can be used depending on the physical system at hand.

While such methods are very useful, it is interesting to ask how one might coarse-grain a set of given quantum states in a Hilbert space which may or may not be associated with a Hamiltonian or the usual assumed structure on the space. In an effort in this direction, motivated by questions in quantum spacetime and emergent classicality, we have developed a coarse-graining prescription which uses Principle Component Analysis to first compress the dimensionality of Hilbert space by identifying a non-redundant basis (the PCA basis), followed by truncation of the last few PCA terms which contribute very little in reconstruction of the state. Physically, one can interpret this scheme as an entanglement coarse-graining (in some arbitrarily associated factorization to Hilbert space) where, upon discarding the low importance terms, one only loses little and irrelevant entanglement structure of the state, while retaining major features in the reconstruction. One expects similarities between our

PCA decimation scheme and other conventional coarse-graining prescriptions in the addition of appropriate structure. We feel this prescription is of a general nature, developed on a Hilbert space with very little structure, and can serve as a reliable means of first-principles quantum coarse-graining.

QUANTUM STATE REDUCTION: GENERALIZED BIPARTITIONS FROM ALGEBRAS OF OBSERVABLES

Reduced density matrices are a powerful tool in the analysis of entanglement structure, approximate or coarse-grained dynamics, decoherence, and the emergence of classicality. It is straightforward to produce a reduced density matrix with the partial-trace map by “tracing out” part of the quantum state, but in many natural situations this reduction may not be achievable. We investigate the general problem of identifying how the quantum state reduces given a restriction on the observables. For example, in an experimental setting, the set of observables that can actually be measured is usually modest (compared to the set of all possible observables) and their resolution is limited. In such situations, the appropriate state-reduction map can be defined via a *generalized bipartition*, which is associated with the structure of irreducible representations of the algebra generated by the restricted set of observables. One of our main technical results is a general, not inherently numeric, algorithm for finding irreducible representations of matrix algebras. We demonstrate the viability of this approach with two examples of limited-resolution observables. The definition of quantum state reductions can also be extended beyond algebras of observables. To accomplish this task we introduce a more flexible notion of bipartition, the *partial bipartition*, which describes coarse-grainings preserving information about a limited set (not necessarily algebra) of observables. We describe a variational method to choose the coarse-grainings most compatible with a specified Hamiltonian, which exhibit emergent classicality in the reduced state space. We apply this construction to the concrete example of the 1-D Ising model. Our results have relevance for quantum information, bulk reconstruction in holography, and quantum gravity.

This chapter is based on the following reference:

O. Kabernik, J. Pollack, and A. Singh, “Quantum state reduction: Generalized bipartitions from algebras of observables,” *Phys. Rev. A* **101** no. 3, (2020) 032303, [arXiv:1909.12851](https://arxiv.org/abs/1909.12851) [quant-ph]

10.1 Introduction and Motivation

How do we describe the state of a system about which we have only limited information? In the most general form, this is a question for probabilists: the best that can be done in the Bayesian approach, for example, is to make our best guess in the form of a distribution over the possible states of the system compatible with what is already known and update this guess as we learn new information. In physical applications, however, we typically encounter situations in which we can only make certain types of measurements on a system. For example, we might only be able to measure extensive, macroscopic quantities of a gas; or we might be able to probe only classical observables of a quantum system.

In classical statistical mechanics, one usually proceeds by enumerating the possible “microstates” of the underlying microphysical system (for example, a gas of N point particles in a finite volume with positions, momenta, and possible interactions). Then we partition the microstates into “macrostates” by collecting together the states with approximately the same values of some coarse-grained extensive property which probes the average behavior of the particles (for example, temperature, or some hydrodynamic quantity like viscosity). In other words, we choose a particular statistical ensemble, write the appropriate partition function, and use it as the generating functional for macroscopic observables. When certain assumptions are valid, it is then valid to track the values of the macroscopic quantities without reference to the underlying microscopic physics. These assumptions have to do with compatibility between the macroscopic observables and the microscopic dynamics of the theory. We want the values of the macroscopic variables to evolve continuously in time, which requires that the time evolution of a macrostate to itself be a macrostate to some approximation; that is, if two microstates are in the same macrostate at one time, there should exist another set of macrostates for the system at a later time such that the time-evolved microstates will usually be in the same new macrostate. Of course, this picture can be generalized in various ways by relaxing some of the assumptions, or by working with probability distributions over microstates instead of partitions [226–228].

In quantum mechanics, the story is usually told differently. Given a Hilbert space \mathcal{H} , we can work with pure states $|\psi\rangle \in \mathcal{H}$ or mixed states $\rho \in \mathcal{L}(\mathcal{H})$, which can be thought of as classical statistical mixtures of the states $\{|\psi\rangle_i\}$ in the basis $\{|\psi\rangle_i \langle\psi|_i\}$ in which ρ is diagonal. When the Hilbert space has a tensor-product structure, $\mathcal{H} \cong \mathcal{H}_A \otimes \mathcal{H}_{\bar{A}}$, there is a natural state-reduction map, the partial-trace map $\text{Tr}_{\bar{A}}$,

which maps mixed states in $\mathcal{L}(\mathcal{H})$ to mixed states in $\mathcal{L}(\mathcal{H}_A)$ via $\rho \mapsto \rho_A \equiv \text{Tr}_{\bar{A}} \rho$. Then the reduced state ρ_A preserves information about operators acting only on \mathcal{H}_A , in the sense that the expectation value of $O_A \otimes I_{\bar{A}}$, with $I_{\bar{A}}$ the identity operator on $\mathcal{H}_{\bar{A}}$, acting on ρ is the same as the expectation value of O_A acting on ρ_A , for all states ρ and linear operators O_A .

So far this picture seems quite different from the classical one summarized above. Certainly, if we have a $3N$ - or $6N$ -dimensional configuration space or phase space, we can consider the reduced spaces generated by projection onto some lower-dimensional subspace. We can then ask the question of what the reduced dynamics in this subspace look like. In particular, we might find that the new dynamics is dissipative, if the particles traced out act as a heat bath for the ones kept in the description, or, in the opposite extreme, that the kept particles only act amongst themselves and can be described without reference to the remainder. If we did not actually know which coordinates in the phase space corresponded to the positions or momenta of individual particles, we might hope to identify them by looking for subspace projections with particularly simple reduced dynamics.

The quantum analog of this process is known as the *decoherence program* [27, 154, 173, 174, 229]. In this program, one is given, or looks for, decompositions of \mathcal{H} into a system and environment, $\mathcal{H} \cong \mathcal{H}_S \otimes \mathcal{H}_E$. This induces a decomposition of the Hamiltonian $H = H_S \otimes I_E + H_{int} + I_S \otimes H_E$. For certain choices of the Hamiltonian and sets of initial states—for example, interaction-dominated Hamiltonians and initial product states—the action of the environment, to a good approximation, is to take an initial state of the system to a superposition of system states, in some basis, which evolve without interfering. When this happens, we say that the initial state has *branched*, and the set of system states whose evolution is preserved by the environment are the *classical states* of the system. (We will review the decoherence program in more detail below.)

However, it is easy to see that most coarse-grainings cannot be described in the decoherence picture. Most observables do not take the simple form of acting on a single tensor factor, even when such a factorization of the Hilbert space exists. In particular, the sorts of *collective* observables which correspond to the averaged, macroscopic properties featured in statistical mechanics do not take this form¹. That is, we do *not* expect, even approximately, a factorization of the form

¹There are more general contexts, such as virtual subsystems [156, 157], in which collective observables can nevertheless be thought of as acting on a collective Hilbert space. We discuss the

$\mathcal{H} \cong \mathcal{H}_{\text{collective}} \otimes \mathcal{H}_{\text{other}}$ for the sorts of collective observables we might measure in a laboratory.

A similar situation arises in field theories, in which we often wish to construct some notion of a state restricted to a finite spatial region. It is well known [12, 13] that even in the simplest field theories, we cannot simply apply the naive partial-trace map to construct the reduced state as discussed above. There is, nevertheless, a good notion of algebras of observables restricted to a spatial region, which is provided by modular theory (e.g. [230–232]), and in many cases, we can pass to a (finite-dimensional) latticization, for example a tensor network, in which these issues do not arise. When the theory has a gauge symmetry, however, the physical Hilbert space is restricted to states which obey global constraints like a Gauss law, and we cannot consistently restrict to subregions in a gauge-invariant way. The approach of the edge modes program [233–235] is to embed the physical Hilbert space into a larger, “ungauged” Hilbert space in which the constraints have been removed and subregions are well-defined.

Given that many natural coarse-grainings of quantum systems cannot be captured by the partial-trace map, it is natural to consider more general state-reduction maps. It is only when such a map can be constructed from a physically-motivated coarse-graining that we are furnished with a true reduced density matrix to which we can apply the well-developed machinery of decoherence, von Neumann entropy, etc. The main goal of this paper is to provide such an interpretation for a large class of general quantum coarse-grainings.

We will provide an algorithm which takes a (finite) set of observables on a (finite-dimensional) Hilbert space and outputs a decomposition of the Hilbert space into irreducible representations of the algebra generated by the observables. Such a decomposition will be called a *generalized bipartition*. The state-reduction map is then defined by tracing out tensor factors of subspaces that appear in this decomposition which is not equivalent to a partial-trace of any single tensor factor of the original Hilbert space. However, like the usual partial-trace map, such state reductions preserve the expectation values of all observables in this algebra. Furthermore, unitary dynamics on \mathcal{H} will induce some (typically) non-unitary dynamics on the reduced state so, as with the usual partial-trace reductions, we can perform a decoherence analysis to determine what observables behave classically.

relation of our work to the previous literature in Subsection 10.1 below.

There are many cases in which a coarse-graining is operationally well-described as having access to all elements in a subalgebra of observables. In some cases, however, it is more appropriate to consider only a restricted *set* of observables which need not comprise an algebra. Classical experimenters, for example, though they might be able to devise setups to measure the (coarse-grained) position and momentum of some system in a lab, would have trouble implementing arbitrary superpositions of these operators. We are thus motivated to define *partial bipartitions*, which implement more general state-reduction maps. Partial bipartitions are best-suited to a *variational* approach, in which one scans over possible coarse-grainings with the goal of determining which restricted set of observables is “most classical” [29, 172].

Summary of Results

Because of the very general nature of our subject, we have chosen to make this chapter as self-contained as possible, often at the expense of brevity. In this subsection, we summarize the explicit results of the paper for the benefit of the busy reader.

- A *generalized bipartition* (10.17) is a direct-sum decomposition of a Hilbert space \mathcal{H} into a sum of bipartite blocks $\mathcal{H}_q \cong \mathcal{H}_{A_q} \otimes \mathcal{H}_{B_q}$:

$$\mathcal{H} \cong \bigoplus_q \mathcal{H}_q \cong \bigoplus_q \mathcal{H}_{A_q} \otimes \mathcal{H}_{B_q}, \quad (10.1)$$

where each sector \mathcal{H}_q is spanned by a set of basis elements $\{|e_{ik}^q\rangle\}$ and the isometry between \mathcal{H}_q and $\mathcal{H}_{A_q} \otimes \mathcal{H}_{B_q}$ maps the basis element $|e_{ik}^q\rangle$ to the product state $|a_i^q\rangle |b_k^q\rangle$, with $\{a_i^q\}$ and $\{b_k^q\}$ being the bases for \mathcal{H}_{A_q} and \mathcal{H}_{B_q} , respectively. The index structure of the $|e_{ik}^q\rangle$ can be conveniently represented as a block-diagonal table, which we refer to as a *bipartition table* (10.16):

$$\begin{array}{|c|c|c|}
 \hline
 e_{11}^1 & e_{12}^1 & \cdots \\
 \hline
 e_{21}^1 & e_{22}^1 & \cdots \\
 \hline
 \vdots & \vdots & \ddots \\
 \hline
 \end{array}
 \begin{array}{|c|c|}
 \hline
 e_{11}^2 & \cdots \\
 \hline
 \vdots & \ddots \\
 \hline
 \end{array}
 \cdots \quad (10.2)$$

The upper index of $|e_{ik}^q\rangle$ labels the block, and the lower indices label the position within the block.

- Generalized bipartitions are interesting for (at least) two reasons. First, they provide a natural way of talking about “the degrees of freedom in B” and “the set of measurements which can be performed on B.” In particular, consider the *bipartition operators* (10.24):

$$S_{kl}^q := I_{A_q} \otimes |b_k^q\rangle \langle b_l^q| = \sum_i |e_{ik}^q\rangle \langle e_{il}^q|. \quad (10.3)$$

The linear combinations of the S_{kl}^q comprise the space of linear operators that act on a Hilbert space (isomorphic to) $\mathcal{H}_B := \bigoplus_q \mathcal{H}_{B_q}$. The bipartition operators can therefore be used to define a state-reduction map $tr_{(A)}$, distinct from the standard partial-trace map tr_A , from \mathcal{H} to \mathcal{H}_B (10.159):

$$\rho_B = tr_{(A)}(\rho) := \sum_q \sum_{k,l} tr(S_{kl}^q \rho) |b_l^q\rangle \langle b_k^q| = \sum_q tr_{A_q}(\rho_q) \in \mathcal{L}(\mathcal{H}_B), \quad (10.4)$$

where ρ_q is the projection of the state ρ onto the sector \mathcal{H}_q . (There is an analogous state-reduction map onto \mathcal{H}_A produced from the dual generalized bipartition, which represents the isometry $\mathcal{H} \cong \bigoplus_q \mathcal{H}_{B_q} \otimes \mathcal{H}_{A_q}$; its bipartition table is constructed by taking the transpose of each block in the original table.)

- Second, generalized bipartitions are interesting because they appear in the foundational result of the representation theory of operator algebras, the Wedderburn decomposition theorem (Theorem 10.2.2). In our language, subject to technical details which we discuss in the main presentation of the theorem below, the decomposition theorem says that any subalgebra \mathcal{A} of $\mathcal{L}(\mathcal{H})$ induces a generalized bipartition of \mathcal{H} , such that the subalgebra is identical to the set of operators which are linear combinations of the bipartition operators S_{kl}^q which act on \mathcal{H}_B alone. The generalized bipartition thus provides a decomposition of \mathcal{H} into irreducible representations of \mathcal{A} . That is, any subalgebra furnishes a generalized bipartition, and any identification of degrees of freedom given by a bipartition table defines a subalgebra. We emphasize that the decomposition theorem is not constructive: it says only that given a subalgebra, such a decomposition must exist.
- The main technical accomplishment of the paper is to provide an explicit construction of the generalized bipartition (that is, the irrep decomposition) of the (finitely generated) algebra \mathcal{A} . This is accomplished by Algorithm 1, whose correctness is established in Theorem 10.4.10 via a number of

intermediate lemmas. We refer the reader to Section 10.4 for details. The main idea of the algorithm is based on the fact that projections whose rank cannot be reduced within the algebra are the fundamental building blocks of the algebra. Such minimal projections can be distilled from the initial spectral projections of the generators by breaking them into projections of smaller rank with an operation we call *scattering*:

$$\begin{array}{ccc}
 \Pi_1 & \searrow & \Pi_1^{(\lambda_1)} + \Pi_1^{(\lambda_2)} + \dots + \Pi_1^{(0)} \\
 & \text{---} & \\
 \Pi_2 & \nearrow & \Pi_2^{(\lambda_1)} + \Pi_2^{(\lambda_2)} + \dots + \Pi_2^{(0)}.
 \end{array} \tag{10.5}$$

The result on the right-hand side of this operation is given by the spectral decomposition of the operator $\Pi_1\Pi_2\Pi_1$. Once all projections have been scattered into minimal projections, we consider a graph, which we call a *reflection network*, that consists of the minimal projections as vertices with edges defined by their orthogonality relations. Under certain conditions, such a reflection network naturally corresponds to a bipartition table. We leverage this correspondence to identify the irrep decomposition with this bipartition table.

- The main application of the algorithm that we will focus on is the idea that operational constraints lead to state reductions. The prototypical example of that is the system-environment split in the context of the decoherence program. There, the operational constraints are defined by the observer's inability to control or measure the environment which leads to the state-reduction map implemented by tracing out the environment. In Section 10.3, we formalize the idea that any operational constraints given by some restricted set of observables, lead to a state-reduction map; this is what we call *operational approach to decoherence*. The correspondence between operational constraints and state reductions is obtained by constructing the generalized bipartition associated with the algebra of restricted observables.
- In the context of the operational approach, we will study two, relatively straightforward, examples of state reductions. One of the examples is concerned with the operational constraints of an observer unable to distinguish spin and orbital angular momentum components; this leads to superselection of the total angular momentum sectors. This example is interesting not because of the conclusion – it can be deduced from the standard formalism

of angular momentum addition – but because we can reach this conclusion independently by analytically applying our algorithm. Remarkably, even the correct Clebsch-Gordan coefficients come out as byproducts of this construction. The second example finds the state reduction map corresponding to an observer’s inability to resolve a bound pair of particles on a lattice. This example also results in superselection, but in this case, the two sectors are the symmetric and the anti-symmetric configurations of the pair.

- The machinery of bipartition tables can be applied more generally than matrix algebras or generalized bipartitions. In particular, the state-reduction map $tr_{(A)}$ still produces a valid reduced state in \mathcal{H}_B if some of the entries in the bipartition table are removed. The resulting bipartition table, which defines a *partial bipartition* (10.164), is still block-diagonal, but not all of the blocks are rectangular:

$$\begin{array}{|c|c|c|}
 \hline
 e_{1;1,1} & e_{1;1,2} & \dots \\
 \hline
 e_{1;2,1} & \ddots & \\
 \hline
 \vdots & & \\
 \hline
 \end{array}
 \qquad
 \begin{array}{|c|c|c|}
 \hline
 e_{2;1,1} & e_{2;1,2} & \dots \\
 \hline
 e_{2;2,1} & \ddots & \\
 \hline
 \vdots & & \\
 \hline
 \end{array}
 \qquad
 \dots$$

(10.6)

The bipartition operators still correspond to the spanning set of all linear operators in this reduced space, but, in general, they no longer span an algebra. In particular, the last equality in (10.4) does not hold for a non-rectangular block. Hence the state-reduction map is not related to the usual partial-trace, since \mathcal{H}_{B_q} need not be a tensor factor of \mathcal{H}_q ; we instead say that \mathcal{H}_{B_q} is a *partial subsystem* of \mathcal{H}_q and write

$$\mathcal{H}_q \cong \mathcal{H}_{A_q} \otimes \mathcal{H}_{B_q}. \quad (10.7)$$

The same relation holds² between the collection of all the degrees of freedom in B and the full Hilbert space: $\mathcal{H} \cong \mathcal{H}_A \otimes \mathcal{H}_B$.

- Using the machinery of partial bipartitions, we can capture very general coarse-grainings of Hilbert space, since in most cases, the coarse-grained space which will preserve some relevant information will not correspond to a factor of Hilbert space. For example, it may be specified by a restricted set of observables which do not necessarily form an algebra. A particular interesting case which we consider in detail in this chapter is to look for coarse-graining of a collection of N underlying degrees of freedom (such as N particles) based on a *collective* or average feature of these degrees of freedom while tracing out the internal features. We focus on obtaining such a partial bipartition, $\mathcal{H} \cong \mathcal{S}_{\text{collective}} \otimes \mathcal{S}_{\text{internal}}$, where $\mathcal{S}_{\text{collective}}$ is the partial subsystem representing the coarse-graining which exhibits classical behavior under evolution by the Hamiltonian. This is a variational approach where we iterate over all possible bipartitions which define the split—that is, rearrangements of the elements inside the blocks of the bipartition table—and preferentially choose the one(s) which is (are) most compatible with the Hamiltonian and demonstrates quasi-classical features. Classicality is marked by the existence of macroscopic pointer states compatible with the Hamiltonian, superposition of which exhibit fast dynamical decoherence.
- To define the coarse-graining $\mathcal{S}_{\text{collective}}$, we search for the collective observable M_c , of the form

$$M_c = \sum_{\mu=1}^N M_{\mu}, \quad (10.9)$$

where each M_{μ} acts only on the μ -th particle, most compatible or stationary with respect to the Hamiltonian, by minimizing the norm of $[H, M_c]$ as in Eq. (10.178). Similar to the notion of predictability sieve[170] in the decoherence

²Formally, we can embed \mathcal{H} into the larger Hilbert space

$$\mathcal{H}_A \otimes \mathcal{H}_B := \left(\bigoplus_q \mathcal{H}_{A_q} \right) \otimes \left(\bigoplus_q \mathcal{H}_{B_q} \right) = \bigoplus_{q,q'} \mathcal{H}_{A_q} \otimes \mathcal{H}_{B_{q'}}, \quad (10.8)$$

so that \mathcal{H} comprises the diagonal entries $q = q'$, and then the partial-trace map tr_A on this bipartite Hilbert space does indeed map those states in $\mathcal{H}_A \otimes \mathcal{H}_B$ supported on \mathcal{H} to states on \mathcal{H}_B . Hence, we can obtain the reduced density matrix ρ_B by tracing out degrees of freedom, at the cost of working with a larger, auxiliary Hilbert space. As we will discuss below, this procedure is closely related to passing from the physical to the “ungauged” Hilbert space when computing the entropy of subregions of states in theories with gauge symmetries.

literature, eigenstates of M_c will define robust, pointer states of the system since they are most compatible with the Hamiltonian. Given the underlying N degrees of freedom, the eigenstates of M_c furnish a factorizable basis for Hilbert space, and eigenstates with distinct eigenvalues will label macroscopically distinct pointer states. These can be used to label and construct different columns of the bipartition table which specify the coarse-graining. Pointer states identified in this manner are special low-entropy states which stay robust to entanglement production under evolution. This is a telltale sign of a classical variable which does not arbitrarily entangle with all other degrees of freedom on short timescales. In this sense, eigenstates of the collective observable chosen by the compatibility condition of Eq. (10.178) are classical, macroscopic pointer states which capture an average, collective property of the underlying degrees of freedom which is as robust under evolution as possible.

- Based on the transition structure of the Hamiltonian written in the factorized M_c basis, we can split our Hilbert space into superselection sectors which never interact and hence form disjoint blocks of our bipartition table. To fix the remaining freedom within each block of the bipartition table, we need to fix the alignment of the rows for which we return to the question of quasiclassicality. A defining feature of our coarse-graining should be that dynamics in the reduced space constructed from the state-reduction map defined by the bipartition table will reflect features of classicality. After identifying the column structure of the bipartition table based on compatibility of a collective observable M_c with the Hamiltonian, we focus on effective dynamical decoherence by the Hamiltonian. Hence, we expect the row alignment of the bipartition table to be such that Hamiltonian evolution decoheres superpositions of macroscopic pointer states by “interaction” with $\mathcal{S}_{\text{internal}}$. We quantify the entanglement production of a pure state $\rho(t) = |\psi(t)\rangle\langle\psi(t)| \in \mathcal{L}(\mathcal{H})$ evolving under evolution by the Hamiltonian using linear entanglement entropy,

$$S_{\text{lin}}(t) = 1 - \text{Tr}(\rho_c^2(t)) , \quad (10.10)$$

where

$$\rho_c(t) \equiv \text{Tr}_{(\mathcal{S}_{\text{internal}})} \rho(t) , \quad (10.11)$$

is the reduced state which $\rho(t)$ gets mapped to by the state-reduction map $\text{Tr}_{(\mathcal{S}_{\text{internal}})}$. We iterate over all finite, discrete permutations of row alignments

to select (the class of) bipartition table(s) which maximize entanglement production. This is done for a set of candidate classical states which are taken to be natural extensions of the unentangled, initial ready states in the decoherence literature.

- Using this algorithm to obtain the classical coarse-graining of an underlying N degrees of freedom based on a collective feature compatible with the Hamiltonian, we analyze the Ising model in 1-D. We see the emergence of different coarse-grainings depending on whether the nearest neighbor spin interaction or the external magnetic field dominates the Hamiltonian, a phenomenon akin to a phase transition. Depending on the preferentially selected collective compatible observable, either the total spin-z or total spin-x of the Ising chain, the coarse-graining may or may not exhibit superselection sectors. In both cases, the dimension of the coarse-grained space is $\sim O(N)$ compared to the original Hilbert space, which has dimension $\sim O(2^N)$. The classical coarse-grainings picked out exhibit fast dynamical decoherence between eigenstates of the compatible macroscopic variable and lead to emergent quasi-classicality. We exhibit numerical results for the case of $N = 3$ and $N = 4$ spins, where the results are simple. Often a class of such quasi-classical bipartition tables (and hence, coarse-grainings) will get selected which reflects a symmetry between different underlying degrees of freedom from the point of view of the Hamiltonian. This setup can be generalized to other physical systems to study classical coarse-grainings determined by the Hamiltonian itself.

Previous Work

Because of the general nature of our subject, there is a vast body of interesting related work. Here we will only briefly mention some of the previous work directly related to the core problem of state reduction based on observables.

The idea that tensor product structures and virtual subsystems can be identified with algebras of observables was originally introduced by Zanardi *et al*, in [156, 157]. Subsequently, this operator algebraic description has found applications in diverse settings such as quantum error correction [236, 237], the study of entanglement in systems of identical particles [238, 239], and Hamiltonian induced factorization of Hilbert spaces [22, 29]). The picture of bipartition tables that we introduce here is a complementary perspective on virtual subsystems, tensor products and operator algebras that clarifies their common structure and its transformations.

A generalization of the notion of *subsystem* has been explored in [240, 241] where entanglement has been identified with respect to a set of preferred observables rather than a tensor product structure. Our idea of partial bipartition is also a generalization of the notion of *subsystem* that arises naturally from the picture of bipartition tables and it also induces a preferred set of observables. However, it is not currently clear whether there is a direct correspondence that goes both ways between sets of observables and partial bipartitions.

As discussed above, one of our major results is an algorithm for directly computing the irrep decomposition of a Hilbert space with respect to a subalgebra \mathcal{A} . Our goal is to propose a procedure that is not inherently numeric that could be used, at least in principle, in abstract symbolic derivations of tensor product structures induced by algebras of observables. We mention two approaches to the same problem that are known in the literature, but they do not fully satisfy our original goal.

First, a numerical algorithm for the matrix-algebra problem was previously given by Murota *et al.*, [242] in the context of semidefinite programming (see [243] for its adaptation in the physics literature). A key step in their algorithm involves sampling for a random matrix in the algebra, which is inherently numeric and requires the ability to span the operator space of the algebra. Our approach does not require sampling from the algebra and it has no prerequisite of being able to span the algebra. Second, in a more physical context, Holbrook *et al.*, [244] have proposed an algorithm for computing the noise commutant of an error algebra associated with a noisy channel. Similarly to our approach, they also propose an inherently non-numeric algorithm that relies on minimal projections as the fundamental building blocks of the algebra. However, their algorithm also requires the ability to span the operator space of the algebra, a prerequisite that is not easy to satisfy without numerics.

Beyond the specific algorithm, we are concerned with the general phenomenon wherein we can assign definite classical dynamics to a set of observables, along the lines of the decoherence program but without a bipartite Hilbert space. In a series of papers (e.g. [159–162]; see also [163]), Castagnino, Lombardi, and collaborators have developed the self-induced decoherence (SID) program, which conceptualizes decoherence as a dynamical process which identifies the classical variables by inspection of the Hamiltonian, without the need to explicitly identify a set of environment degrees of freedom. The variational approach we sketch in Section 10.7 is similarly concerned with the dynamical selection of a preferred set

of observables.

Finally, similar physical motivations but different mathematical methods have led Kofler and Brukner [164] to study the emergence of classicality under restriction to coarse-grained measurements, and Duarte *et al.*, [245] to study state-reduction for blurred and saturated detectors. We believe that, in principle, the consequence of such reduced resolution measurements can be studied in a unified way as algebras of coarse-grained observables.

Organization of the Chapter

Because this chapter is aimed at a broad audience, and mostly uses the tools of fundamental quantum mechanics along with linear algebra and representation theory, we have attempted to keep it self-contained and pedagogical to the extent possible. In Section 10.2, we accordingly review the technical and conceptual tools we will use in the remainder of the paper. In particular, we review the concept of generalized bipartitions and bipartition tables introduced by one of us in [246], as well as results from the mathematical literature on representations of matrix algebras.

The remainder of the chapter is concerned with the application of these tools to physical situations. We will mostly be concerned with an operational approach, in which we assume a lab-like setup in which a set of accessible observables has been specified, and investigate the decoherences of the resulting states. In Section 10.3, we set up this general operational problem and its relation to the decoherence program, which we review. In Section 10.4, we then present the general algorithm for passing from an operator algebra to a bipartition. Given this mechanism for producing a reduced state containing the desired coarse-grained information, we can use the tools of the decoherence program to investigate the dynamics and classicality of the reduced states. Having specified the general algorithm, we specialize in Section 10.5 to physically relevant examples. In particular, we focus on the common case where the experimentalist only has access to coarse-grained, collective observables, where the generalized bipartition table takes a particularly simple form and superselection sectors are induced by the operator algebra.

In Section 10.6, we return to the general problem of coarse-graining from observables and discuss the state-reduction maps which arise when the set of observables need not form an algebra. In Section 10.7 we use the tools of the previous section and ideas from the decoherence program to initiate a more abstract, variational approach in which the goal is to determine the “most classical” set of observables

given only a Hilbert space with a specified Hamiltonian. To build intuition for the general case, we focus in Section 10.8 on the Ising Model, where numerical calculations are tractable. In Section 10.9, we conclude by sketching some of the potential applications of our work for quantum information, holography, and quantum gravity.

10.2 Preliminaries

Setup and Notation

Unless stated otherwise, all Hilbert spaces will be complex and finite-dimensional and the notions of *linear operator* and *matrix* will be used interchangeably. We will denote with $\mathcal{L}(\mathcal{H})$ the space of linear operators on the Hilbert space \mathcal{H} . Isometric Hilbert spaces will be identified by the relation $\mathcal{H}_1 \cong \mathcal{H}_2$ associated with some isometry V between the spaces (most of the time, isometric Hilbert spaces will arise when we relabel or reinterpret the basis elements).

An *orthogonal projection* $\Pi \in \mathcal{L}(\mathcal{H})$ is defined by the property $\Pi = \Pi^\dagger = \Pi^2$. In the following, we will refer to such an operator simply as a *projection*, implying an *orthogonal projection* as defined here. This should not be confused with the notion of *pairwise* orthogonal projections which refers to a set of projections $\{\Pi_k\}$ such that $\Pi_k \Pi_{k'} = \delta_{kk'} \Pi_k$ (we will sometimes omit *pairwise* when referring to such sets). The *eigenspace* of a projection Π is the subspace of \mathcal{H} on which Π acts as the identity. Similarly, an *eigenbasis* of Π refers to a set of orthonormal vectors that span the eigenspace of Π . The *rank* of a projection is also the dimension of its eigenspace; we will often use this relation implicitly.

A *partial isometry* $S \in \mathcal{L}(\mathcal{H})$ is defined by the properties $SS^\dagger = \Pi_{\text{fin}}$ and $S^\dagger S = \Pi_{\text{in}}$ where Π_{in} and Π_{fin} are projections. A partial isometry S acts as an isometry on the eigenspace of Π_{in} , mapping it to the eigenspace of Π_{fin} (both projections have the same rank), and it annihilates vectors that are orthogonal to the eigenspace of Π_{in} (the kernel of S is the kernel of Π_{in}). Every projection Π is also a partial isometry ($\Pi_{\text{in}} = \Pi_{\text{fin}} = \Pi$), so we will say that S is a *proper* partial isometry if it is a partial isometry, but it is not a projection.

A *graph* $G := \{V, E\}$ is defined by a set of vertices $V := \{v_i\}$ and a set of edges $E := \{(v_i, v_j)\}$. A *path* p on the graph is an ordered set of vertices $p = (v_{i_1}, v_{i_2}, \dots)$ such that every consecutive pair is connected by an edge $(v_{i_k}, v_{i_{k+1}}) \in E$. The path p is called *simple* if every vertex appears at most once in p . We will say that a pair of vertices $v_1, v_2 \in V$ is *connected by a path* if there is a path p such that v_1 is its first vertex and v_2 is its last. A *connected component* is a subset of vertices $C \subseteq V$ such

that every pair $v_1, v_2 \in C$ is connected by a path, and every pair $v_1 \in C, v_2 \in V \setminus C$ is not connected by a path.

Generalized Bipartitions and Bipartition Tables

A *bipartite system* is a system that consists of two distinct subsystems A and B . A bipartition of a system is an explicit specification of these subsystems. When the system is bipartite by construction—the system of two qubits, for example—it comes with a natural bipartite structure $\mathcal{H} \cong \mathcal{H}_A \otimes \mathcal{H}_B$. The Hilbert space of the whole system is constructed from the tensor product of two Hilbert spaces and the bases are naturally constructed from products of local bases. Such a construction, however, is not necessary and we can always impose a bipartition after the fact by selecting a bipartite tensor product structure in any (non-prime dimensional) Hilbert space. Different bipartitions of the Hilbert space identify different subsystems that are not necessarily physical in the usual sense, but are associated with distinct degrees of freedom that define a virtual subsystem [156].

Formally, given a d -dimensional Hilbert space \mathcal{H} such that $d = d_A d_B$, we can introduce an auxiliary bipartite Hilbert space $\mathcal{H}_A \otimes \mathcal{H}_B$ with dimensions $\dim \mathcal{H}_A = d_A$ and $\dim \mathcal{H}_B = d_B$. By isometrically mapping the original Hilbert space \mathcal{H} into $\mathcal{H}_A \otimes \mathcal{H}_B$, we impose a tensor product structure that might not have been explicitly present beforehand. Different choices of the isometry $V : \mathcal{H} \rightarrow \mathcal{H}_A \otimes \mathcal{H}_B$ specify different choices of bipartition, and the isometry V itself is fully described by some orthonormal basis $|e_{ik}\rangle$ in \mathcal{H} where $i = 1 \dots d_A$ and $k = 1 \dots d_B$ such that $V |e_{ik}\rangle = |a_i\rangle |b_k\rangle$, where the elements $|e_{ik}\rangle$ and $|a_i\rangle |b_k\rangle$ are pairs of right and left singular vectors of V . The choice of bipartition is therefore conveniently summarized by choosing the elements $|e_{ik}\rangle$ and arranging them into a rectangular table such that the i, k indices correspond to the row and column of the element, respectively:

$$\begin{array}{c}
 \begin{array}{cccc}
 & b_1 & b_2 & \cdots & b_{d_B} \\
 a_1 & e_{11} & e_{12} & \cdots & e_{1d_B} \\
 a_2 & e_{21} & e_{22} & \cdots & e_{2d_B} \\
 \vdots & \vdots & \vdots & \ddots & \vdots \\
 a_{d_a} & e_{d_a 1} & e_{d_a 2} & \cdots & e_{d_a d_B}
 \end{array} \\
 \end{array} \tag{10.12}$$

The rows of this table are associated with the degree of freedom of subsystem A

and the columns are associated with the degree of freedom of subsystem B . We will refer to such tables, which one of us first introduced in [246], as *bipartition tables* (BPTs). It should be clear that for each bipartition table there is another, trivially related one derived by swapping the row and column indices, which simply swaps the first and second systems in the bipartition.

As a simple example, consider a system of two qubits and the product basis $\{|00\rangle, |01\rangle, |10\rangle, |11\rangle\}$. The BPT

$$\begin{array}{cc}
 & \begin{array}{cc} 0_B & 1_B \end{array} \\
 \begin{array}{c} 0_A \\ 1_A \end{array} & \begin{array}{|cc|} \hline 00 & 01 \\ \hline 10 & 11 \\ \hline \end{array}
 \end{array} \tag{10.13}$$

represents the natural tensor product structure given by construction, with each of the elements placed at the row and column that corresponds to the values of the qubits. The subsystems A and B in this case are the qubits themselves.

A minor rearrangement of the two qubit BPT

$$\begin{array}{cc}
 & \begin{array}{cc} \text{even}_B & \text{odd}_B \end{array} \\
 \begin{array}{c} 0_A \\ 1_A \end{array} & \begin{array}{|cc|} \hline 00 & 01 \\ \hline 11 & 10 \\ \hline \end{array}
 \end{array} \tag{10.14}$$

results in a new tensor product structure where we relabeled the columns to better match their new meaning. Here, the value of the left qubit still varies with rows, but what now varies with columns is the overall parity of the two qubits, so subsystem A is still interpreted as the left qubit, but subsystem B is now associated with the parity degree of freedom. The isometry defined by this BPT is

$$V = |0_A\rangle |\text{even}_B\rangle \langle 00| + |0_A\rangle |\text{odd}_B\rangle \langle 01| + |1_A\rangle |\text{odd}_B\rangle \langle 10| + |1_A\rangle |\text{even}_B\rangle \langle 11|, \tag{10.15}$$

so with respect to this bipartition, the entangled Bell state $|00\rangle + |11\rangle$ maps to $|0_A\rangle |\text{even}_B\rangle + |1_A\rangle |\text{even}_B\rangle$, which is not entangled. From now on, we will not explicitly label the rows and columns on BPTs, but we will implicitly use the fact

that the rows and columns represent the individual degrees of freedom of the two subsystems in the bipartition.

The visual representation of BPTs can also be extended to capture direct-sum decompositions of Hilbert spaces. By arranging basis elements into a block-diagonal table,

$$\begin{array}{|c|c|c|} \hline e_{11}^1 & e_{12}^1 & \cdots \\ \hline e_{21}^1 & e_{22}^1 & \cdots \\ \hline \vdots & \vdots & \ddots \\ \hline \end{array} \quad \begin{array}{|c|c|} \hline e_{11}^2 & \cdots \\ \hline \vdots & \ddots \\ \hline \end{array} \quad \cdots \quad (10.16)$$

we can specify Hilbert-space decompositions of the form

$$\mathcal{H} \cong \bigoplus_q \mathcal{H}_{A_q} \otimes \mathcal{H}_{B_q}, \quad (10.17)$$

where the sector q is spanned by the basis elements $|e_{ik}^q\rangle$ of the block q and each sector is further decomposed into a tensor product of two subsystems according to the arrangement of elements inside the block. We will refer to decompositions of the form (10.17) as *generalized bipartitions*, and by BPT we will imply the generalized form (10.16). In Sections 10.6-10.8, we will further generalize this idea to non-rectangular BPTs that capture the notion of *partial bipartitions*, associated with decompositions that cannot be expressed as in Eq. (10.17).

As an example, consider the 3 spin- $\frac{1}{2}$ system decomposed into total spin sectors:

$$\mathcal{H} = \frac{1}{2} \otimes \frac{1}{2} \otimes \frac{1}{2} \cong \frac{3}{2} \oplus \frac{1}{2} \oplus \frac{1}{2}. \quad (10.18)$$

The bases that correspond to each total spin sector are $|\frac{3}{2}, m\rangle$, $|\frac{1}{2}, m, 1\rangle$, $|\frac{1}{2}, m, 2\rangle$, where m varies from $\frac{3}{2}$ to $-\frac{3}{2}$ in integer steps and 1, 2 label the two distinct sectors of total spin $\frac{1}{2}$. The BPT

$\frac{3}{2}, \frac{3}{2}$	$\frac{3}{2}, \frac{1}{2}$	$\frac{3}{2}, -\frac{1}{2}$	$\frac{3}{2}, -\frac{3}{2}$		
				$\frac{1}{2}, \frac{1}{2}, 1$	$\frac{1}{2}, -\frac{1}{2}, 1$
				$\frac{1}{2}, \frac{1}{2}, 2$	$\frac{1}{2}, -\frac{1}{2}, 2$

(10.19)

represents the direct-sum decomposition of the Hilbert space into total spin sectors. By stacking the two rows of total spin $\frac{1}{2}$ into a single block,

$\frac{3}{2}, \frac{3}{2}$	$\frac{3}{2}, \frac{1}{2}$	$\frac{3}{2}, -\frac{1}{2}$	$\frac{3}{2}, -\frac{3}{2}$		
				$\frac{1}{2}, \frac{1}{2}, 1$	$\frac{1}{2}, -\frac{1}{2}, 1$
				$\frac{1}{2}, \frac{1}{2}, 2$	$\frac{1}{2}, -\frac{1}{2}, 2$

(10.20)

we specify a different, more subtle decomposition of the Hilbert space. We now have two sectors, one associated with total spin $\frac{3}{2}$ and the other with total spin $\frac{1}{2}$ where the $\frac{1}{2}$ sector is further decomposed into a tensor product

$$\mathcal{H} \cong \frac{3}{2} \oplus \left(\mathcal{N}_{\frac{1}{2}} \otimes \frac{1}{2} \right). \quad (10.21)$$

The virtual subsystem $\mathcal{N}_{\frac{1}{2}}$ is usually referred to as the *multiplicity* subsystem while $\frac{1}{2}$ still represents the total spin- $\frac{1}{2}$ magnetization degree of freedom. The multiplicity subsystem $\mathcal{N}_{\frac{1}{2}}$ is also well known as the prototypical example of a *noiseless subsystem* [247], which encodes information in the relational degrees of freedom that are invariant under collective rotations. In general, such bipartitions naturally arise from the structure of irreducible representations of symmetry groups, as we will see below.

Matrix Algebras and Their Representation

We will now summarize the relevant results of the representation theory of finite-dimensional operator algebras and relate them to the BPT picture of the previous subsection. Our exposition will emphasize the structural details of the representation

theory at the expense of mathematical rigor. The mathematically inclined reader is referred to [248] or [249].

Let us first define what we mean by a matrix algebra.³

Definition 10.2.1. A matrix algebra is a subset $\mathcal{A} \subseteq \mathcal{L}(\mathcal{H})$ such that for any $M_1, M_2 \in \mathcal{A}$ and $c \in \mathbb{C}$:

$$(1) M_1 + M_2 \in \mathcal{A}$$

$$(2) M_1 M_2 \in \mathcal{A}$$

$$(3) cM_1 \in \mathcal{A}$$

$$(4) M_1^\dagger \in \mathcal{A}$$

For example, the set $\mathcal{L}(\mathcal{H})$ is a *full* matrix algebra on \mathcal{H} . From here on, we will use the term *algebra* to mean *matrix algebra* as defined above.

Any finite (or infinite) set of matrices $\mathcal{M} := \{M_1, M_2, \dots, M_n\}$ can generate the algebra $\mathcal{A} := \langle M_1, M_2, \dots, M_n \rangle$ (which the angled brackets denote) by taking the closure of \mathcal{M} with respect to operations in the above definition. It should be clear then that the algebra $\langle M_1, M_2, \dots, M_n \rangle$ is spanned by linear combinations of products of elements $\{M_1, M_2, \dots, M_n\} \cup \{M_1^\dagger, M_2^\dagger, \dots, M_n^\dagger\}$.

The central result of representation theory of matrix algebras is known as Wedderburn decomposition [250], and it can be stated in the following way:

Theorem 10.2.2. (*Wedderburn Decomposition*) For every algebra $\mathcal{A} \subseteq \mathcal{L}(\mathcal{H})$, the Hilbert space \mathcal{H} decomposes into

$$\mathcal{H} \cong \left[\bigoplus_q \mathcal{H}_{A_q} \otimes \mathcal{H}_{B_q} \right] \oplus \mathcal{H}_0 \quad (10.22)$$

such that every element $M \in \mathcal{A}$ is of the form

$$M = \left[\bigoplus_q I_{A_q} \otimes M_{B_q} \right] \oplus 0, \quad (10.23)$$

where I_{A_q} is the identity on \mathcal{H}_{A_q} and M_{B_q} is any matrix on \mathcal{H}_{B_q} , and all matrices of this form are elements of \mathcal{A} .

³In the literature, matrix algebras are often referred to as von Neumann algebras or C^* -algebras, even when only finite-dimensional spaces are involved. We prefer the term “matrix algebra” to emphasize the fact that we are dealing with a simpler, finite-dimensional case where we need not be concerned with the subtleties of infinite-dimensional spaces.

(For a contemporary exposition of the proof see Section 2.7 in [248] or Appendix A of [34].)

In the language of representation theory, Eq. (10.22) is the decomposition of \mathcal{H} into irreducible representations (irreps) of the algebra \mathcal{A} . The tensor factors \mathcal{H}_{B_q} in the bipartition are associated with distinct irreps of \mathcal{A} while the tensor factors \mathcal{H}_{A_q} are associated with the multiplicity of distinct irreps. It is important to note the significance of the fact that not only all $M \in \mathcal{A}$ are of the form (10.23), but that *any* matrix of this form is necessarily an element of \mathcal{A} . Therefore, the decomposition (10.22) is the defining structure of an algebra that selects the elements of the algebra to be *all* the matrices that act nontrivially only on the tensor factors \mathcal{H}_{B_q} in the decomposition. The null space \mathcal{H}_0 is the space where the algebra is not supported and its elements act on \mathcal{H}_0 as the null matrix. From now on, we will ignore the null space in the decomposition and assume the Hilbert space \mathcal{H} to exclude \mathcal{H}_0 .⁴

As was discussed in Sec. 10.2, decompositions such as (10.22) are generalized bipartitions that correspond to a BPT of the form (10.16). This correspondence and the result of Theorem 10.2.2 suggest that the defining structure of an algebra is explicitly captured by a BPT. We can therefore explicitly specify algebras with BPTs and vice versa via this correspondence.

In order to see what the BPT tells us about the structure of an algebra, we consider the basis $\{|e_{ik}^q\rangle\}$ that corresponds to the decomposition (10.22) in the sense that, for every sector q , there are product bases $\{|a_i^q\rangle |b_k^q\rangle\}$ of $\mathcal{H}_{A_q} \otimes \mathcal{H}_{B_q}$ such that $|e_{ik}^q\rangle = |a_i^q\rangle |b_k^q\rangle$ (note that this definition is not unique and any choice of local basis $|a_i^q\rangle$ and $|b_k^q\rangle$ can work). According to Eq. (10.23), all matrices in the algebra can be constructed from linear combinations of the operators

$$S_{kl}^q := I_{A_q} \otimes |b_k^q\rangle \langle b_l^q| = \sum_i |e_{ik}^q\rangle \langle e_{il}^q|. \quad (10.24)$$

These operators, which we will call *bipartition operators* (BPOs), are partial isometries, and they form an (unnormalized) operator basis for the algebra.

Now consider the BPT constructed with the basis $|e_{ik}^q\rangle$:

⁴In the cases that we will consider, \mathcal{H}_0 does not appear in the decomposition. Even when \mathcal{H}_0 does appear, it simply means that that part of the Hilbert space is irrelevant for operators of the algebra.

$$\begin{array}{ccc|cc}
e_{11}^1 & e_{12}^1 & \cdots & & \\
e_{21}^1 & e_{22}^1 & \cdots & & \\
\vdots & \vdots & \ddots & & \\
\hline
& & & e_{11}^2 & \cdots \\
& & & \vdots & \ddots \\
& & & & \ddots \\
& & & & \ddots
\end{array} \quad (10.25)$$

and the subspaces selected by the basis elements of the distinct rows and columns. The BPO S_{kl}^q acts by mapping the basis element in column l of block q to the parallel element in column k of the same block; this is a partial isometry between subspaces of the columns. Since the basis elements inside each row are mapped to themselves by the BPOs, and since the BPOs span the algebra, distinct rows of the BPT define invariant subspaces of the algebra. The row subspaces are *minimal* invariant subspaces (they do not contain smaller invariant subspaces) because BPOs act on these subspaces as the full matrix algebra which is irreducible [249].

Column subspaces are also a meaningful part of the matrix algebra structure. The projection operator on the subspace of column k in block q is just a special case of a BPO (projections are the trivial partial isometries from subspaces to themselves):

$$S_{kk}^q = \sum_i |e_{ik}^q\rangle \langle e_{ik}^q|. \quad (10.26)$$

The adjoint action of the projection S_{kk}^q on any other BPO results in

$$S_{kk}^q S_{k'l'}^{q'} S_{kk}^q = \delta_{qq'} \delta_{kk'} \delta_{kl'} S_{kk}^q. \quad (10.27)$$

Since every element of the algebra is a linear combination of BPOs, the adjoint action of S_{kk}^q on any $M \in \mathcal{A}$ must result in

$$S_{kk}^q M S_{kk}^q \propto S_{kk}^q. \quad (10.28)$$

Projections in the algebra for which Eq. (10.28) holds for all elements $M \in \mathcal{A}$ are the key building blocks of the algebra:

Definition 10.2.3. A projection $\Pi \in \mathcal{A}$ is called a minimal projection if for every $M \in \mathcal{A}$, we have $\Pi M \Pi \propto \Pi$.⁵

⁵This property is equivalent to a different, more common defining property: Π_{\min} is minimal if for all projections $\Pi \in \mathcal{A}$ such that $\Pi \Pi_{\min} = \Pi$ it implies that either $\Pi = 0$ or $\Pi = \Pi_{\min}$. We prefer to define it the other way because this is the only property of minimal projections that we will use.

Not only are all S_{kk}^q 's minimal projections, they are also the maximal set of such projections.

Definition 10.2.4. A set of projections $\{\Pi_k\} \subseteq \mathcal{A}$ is called a maximal set of minimal projections (MSMP) if every Π_k is minimal and all Π_k are pairwise orthogonal and sum to the identity element $I_{\mathcal{A}} := \sum_k \Pi_k$ of the algebra.

The columns of a BPT are therefore a concise summary of a particular choice of MSMP given by the BPOs $\{S_{kk}^q\}$ (the non-uniqueness of this choice traces back to the freedom to choose the local basis $|b_k^q\rangle$).

The commutant \mathcal{A}' of an algebra \mathcal{A} is the set of all matrices that commute with every element of \mathcal{A}

$$\mathcal{A}' := \{M' \in \mathcal{L}(\mathcal{H}) \mid [M', M] = 0, \forall M \in \mathcal{A}\}, \quad (10.29)$$

and is itself also an algebra. The irrep decomposition for \mathcal{A}' is essentially the same as for \mathcal{A} with the roles of the tensor factors \mathcal{H}_{A_q} and \mathcal{H}_{B_q} reversed. That is, if

$$\mathcal{H} \cong \bigoplus_q \mathcal{H}_{A_q} \otimes \mathcal{H}_{B_q} \quad (10.30)$$

is the irrep decomposition for \mathcal{A} , then all $M' \in \mathcal{A}'$ are of the form

$$M' = \bigoplus_q M'_{A_q} \otimes I_{B_q}. \quad (10.31)$$

For the BPTs, this implies a reversal of roles between rows and columns. Given the BPT of \mathcal{A} , we can get the BPT of \mathcal{A}' by rotating rows into columns; we will call this transformation a *transpose*. Consequently, BPOs constructed from a transposed BPT span the commutant of the algebra.

A simple example of an algebra is the full matrix algebra $\mathcal{L}(\mathcal{H})$. The BPT of this algebra is just a single row of all basis elements $|e_k\rangle$ (the choice of basis is arbitrary).

e_1	e_2	\cdots	e_d
-------	-------	----------	-------

(10.32)

The BPOs defined by this table are just the matrix units

$$S_{kl} = |e_k\rangle \langle e_l| \quad (10.33)$$

that span all the matrices in the algebra. The transpose of this BPT results in a single column that corresponds to a single BPO that is the identity matrix I . This means that the commutant of the full matrix algebra $\mathcal{L}(\mathcal{H})$ consists of the span of I , as expected.

Another important example of an algebra is the algebra $\langle M \rangle$ generated by a single self-adjoint matrix M . By definition, $\langle M \rangle$ is the set of all matrices spanned by M^n for all natural n . The key fact about this algebra is that it contains, and therefore can be spanned by, the spectral projections of M :

Proposition 10.2.5. *Let M be a self-adjoint matrix with the spectral decomposition*

$$M = \sum_k \lambda_k \Pi_k \quad (10.34)$$

where λ_k are distinct (non-zero) eigenvalues and Π_k are projections on eigenspaces. Then

$$\langle M \rangle = \text{span} \{ \Pi_k \}. \quad (10.35)$$

This fact can be shown by first identifying the identity element $I_{\langle M \rangle}$ in this algebra (it does not have to be the full identity matrix). The identity element is constructed using the minimal polynomial $p(x)$ of M (that is, the smallest degree polynomial for which $p(M) = 0$) and the fact that for self-adjoint matrices the minimal polynomial is of the form $p(x) = f(x)$ or $p(x) = xf(x)$ where f is such that $f(0) \neq 0$. Then

$$I_{\langle M \rangle} := \frac{f(M) - If(0)}{-f(0)} \in \langle M \rangle \quad (10.36)$$

acts as the identity on M , and uniqueness of the identity implies that

$$I_{\langle M \rangle} = \sum_k \Pi_k. \quad (10.37)$$

With the identity, we can re-express the spectral projections as

$$\Pi_k = \prod_{l \neq k} \frac{M - \lambda_l I_{\langle M \rangle}}{\lambda_k - \lambda_l} \in \langle M \rangle. \quad (10.38)$$

Since every natural power of M is in the span of spectral projections, Π_k 's span the whole algebra $\langle M \rangle$.

The projections Π_k are in fact the MSMP of $\langle M \rangle$, since for all powers n , we have

$$\Pi_k M^n \Pi_k = (\lambda_k)^n \Pi_k \quad (10.39)$$

and clearly they are pairwise orthogonal and sum to the identity. Since the MSMP $\{\Pi_k\}$ spans $\langle M \rangle$, these are the only BPOs in this algebra. From a complete set of BPOs, it is easy to build a BPT. In general, we have seen that each minimal projection defines a column and columns in the same block are related to each other by a proper partial isometry. In this case, there are no proper partial isometries so each column is its own block.

$$(10.40)$$

The height of each column is the rank of the projection and the arrangement of basis elements inside the columns is not important in this case. The irrep decomposition implied by this BPT decomposes the Hilbert space into sectors of distinct eigenspaces of M

$$\mathcal{H} \cong \bigoplus_k \mathcal{H}_{A_k} \otimes h_{B_k} \quad (10.41)$$

where the tensor factors B (associated with the columns in each block) are one dimensional and the tensor factors A (associated with the rows in each block) are of dimension equal to the rank of Π_k . Eq. (10.23) is then the statement that all elements of $\langle M \rangle$ are given by the span of Π_k . Under transpose, each block of the BPT becomes a row specifying the full matrix algebra on that eigenspace of M . The commutant is then the direct sum of full matrix algebras on the eigenspaces of M , which is also what Eq. (10.31) implies.

As we have seen, the structure of the algebra generated by a single self-adjoint matrix M is fully characterized by the spectral decomposition of M . Our derivation of the irrep decomposition by constructing a BPT from BPOs ended up being a roundabout way of decomposing the Hilbert space into eigenspaces of M . We will see in Section 10.4 that this approach generalizes to algebras generated by multiple elements $\langle M_1, M_2 \dots \rangle$. In that case, spectral projections of generators are not sufficient to characterize the structure of the algebra, but they can be used to produce a complete set of BPOs that will specify a BPT and so the irrep decomposition.

The last special case of an algebra that is very useful is the *group algebra*. A group algebra is an algebra generated by matrices that form a group. The same matrices that generate the group generate the group algebra, however, the term “generate” in the context of matrix algebras means that we also include linear combinations of the group elements. That is, if \mathcal{G} is a (finite or Lie) group generated by L_1, L_2, \dots , then the group algebra $\mathbb{C}\mathcal{G}$ is the span of elements of \mathcal{G}

$$\mathbb{C}\mathcal{G} := \langle L_1, L_2, \dots \rangle = \text{span} \{ \mathcal{G} \}. \quad (10.42)$$

An important fact about group algebras is that their irrep decomposition is the same as the irrep decomposition for the group.

Proposition 10.2.6. *Let \mathcal{G} be a finite or Lie unitary group generated by L_1, L_2, \dots acting on the Hilbert space \mathcal{H} . If*

$$\mathcal{H} \cong \bigoplus_q \mathcal{H}_{A_q} \otimes \mathcal{H}_{B_q} \quad (10.43)$$

is the irrep decomposition of \mathcal{H} such that all elements $U(g) \in \mathcal{G}$ are of the form

$$U(g) = \bigoplus_q I_{A_q} \otimes U_q(g) \quad (10.44)$$

where $U_q(g)$ are irreducible, then (10.43) is the irrep decomposition for the group algebra

$$\mathbb{C}\mathcal{G} = \langle L_1, L_2, \dots \rangle. \quad (10.45)$$

This fact follows from the observation that if a subspace is invariant under the action of the group, then it is invariant under the action of the group algebra, since linear combinations of group elements preserve the same subspaces as the elements themselves. The same reasoning establishes that invariant subspaces that are equivalent representations for group elements are also equivalent for linear combinations of group elements. This leads to the conclusion that groups and their algebras have the same minimal invariant subspaces with the same equivalences, which means that they have the same irrep structure, hence the same irrep decomposition.

Proposition 10.2.6 will allow us to construct the irrep decomposition for group algebras using the known irreps of groups. For example, going back to the 3 spin- $\frac{1}{2}$ case, Eq. (10.21) is the irrep decomposition associated with the $SU(2)$ group of collective rotations on the spins. It is constructed by recognizing the total spin basis (via the Clebsch-Gordan coefficients) that identify the minimal invariant subspaces

of total spin $\frac{3}{2}$ and $\frac{1}{2}$ that decompose the Hilbert space into irreps of $SU(2)$. Since the group of total rotations is generated by the total spin operators J_x, J_y, J_z , we can conclude that the irrep decomposition of the algebra generated by J_x, J_y, J_z is given by the irrep decomposition (10.21).

10.3 Operational Approach to Decoherence

The Decoherence Program

In this subsection, we review some basic aspects of the decoherence program, which we will apply below to the reduced states produced by our generalized state-reduction maps. The decoherence program is a well-established field with an extensive literature and our treatment here will be terse. The reader already familiar with its details is invited to proceed to the next subsection. Conversely, more details can be found, for example, in the review [229] or the textbook [168]. Several formulations of the decoherence program exist; here we discuss only the ‘‘Zurekian’’ framework.

The (Zurekian) decoherence program is a formalism for describing the circumstances under which a system can be classically measured. Recall that the Born rule states that the possible results of measuring an observable \mathcal{O} in a state $|\psi\rangle$ of a system represented by the Hilbert space \mathcal{H}_S are the eigenstates $|o_i\rangle$ of the observables, with a probability $|\langle o_i|\psi\rangle|^2$ of obtaining each individual outcome. From the point of view of the system alone, the (projective) measurement process is non-unitary; for example, if the $|o_i\rangle$ are not eigenstates of the system’s Hamiltonian so that $\langle o_i(t)|o_j(t)\rangle \neq \delta_{ij}$, time evolution will act differently on the initial state and the post-measurement state. In particular, interference terms will be suppressed in the post-measurement state, which no longer evolves coherently.

The Zurekian decoherence program implements this ‘‘de-coherence’’ process, which is effectively non-unitary for the system alone, as a unitary process on a larger Hilbert space consisting of the tensor product⁶ $\mathcal{H} \simeq \mathcal{H}_S \otimes \mathcal{H}_E$ of the original system and an environment \mathcal{H}_E . If the Hamiltonian contains interaction terms between the system and environment degrees of freedom, then an initial product state can evolve into an entangled state of the system and environment:

$$|\Psi(t=0)\rangle = |\psi\rangle_S |e_0\rangle_E \rightarrow |\Psi(t)\rangle = \sum_i c_i(t) |s_i(t)\rangle_S |e_i(t)\rangle_E. \quad (10.46)$$

⁶Although some careful treatments require a tripartite system-apparatus-environment split (e.g. [183, 229, 251]), here we will only split out the system from the environment; when such distinctions are important, we have in mind that the system is small and quantum so that a (large, classical) apparatus is a subsystem of the environment.

In fact for any choice of initial state and time evolution, this decomposition can be performed exactly at any moment in time for a particular choice of orthonormal bases for the system and environment (the Schmidt decomposition). However, as the time dependence indicates, decompositions at different times are generically unrelated; in particular, the state $|s_i(\tau)\rangle_S |e_i(\tau)\rangle_E$ is not the Hamiltonian evolution of $|s_i(t)\rangle_S |e_i(t)\rangle_E$.

For the particular states and interactions that admit decoherence, however, there exists, at least approximately, a decomposition of the entangled state into “branches” which evolve independently of each other; that is, a choice of bases in which $U_{\tau-t} |s_i(t)\rangle_S |e_i(t)\rangle_E \approx |s_i(\tau)\rangle_S |e_i(\tau)\rangle_E \forall i$, so that the c_i are constant⁷:

$$|\Psi(t)\rangle \approx \sum_i c_i |s_i(t)\rangle_S |e_i(t)\rangle_E. \quad (10.47)$$

Hence there is a one-to-one association of system states $|s_i\rangle_S$ and environment states $|e_i\rangle_E$ in the “pointer basis” given by the decomposition. It immediately follows⁸ from Eq. (10.47) that the reduced density matrix describing the state of the system is

$$\rho_S = \text{Tr}_E |\Psi\rangle\langle\Psi| \approx \sum_i |c_i|^2 |s_i\rangle\langle s_i|, \quad (10.48)$$

so the system can be described to good approximation as a statistical mixture of the states $|s_i\rangle_S$, in agreement with the action of the Born rule on the system alone. If we only have access to the information in the system, we can check for the presence of decoherence by looking for a choice of basis in which the reduced density matrix becomes, and remains, approximately diagonal.

We comment briefly on the physical significance of the conditions (10.47) and (10.48). The branch label i picks out a distinct state of the system and, crucially,

⁷If the Hamiltonian is time-dependent, as it is, for example, if the interaction only occurs in a specific period of time, then we should interpret this condition as holding in some finite time interval. Intuitively this condition says that, after the measurement-causing interaction occurs, the environment should, at least temporarily, record the state of the system[153, 252].

⁸Actually Eq. (10.47) is more general: it describes a situation in which the system-environment product kets are orthonormal, but in which the system or environment kets need not individually be orthonormal. In particular it is easy to imagine situations (for example, a measurement apparatus that can record the state of a spin in multiple different bases) in which the system states $|s_i\rangle_S$ need not be orthonormal, or even where the sum is over a larger number of terms than the dimensionality of the system. In this case, we should not expect the reduced density matrix to be a good record of the actual branches. See Sec. 2 of [183] for further discussion of this point. In practice, we expect that we can deal with such cases by moving degrees of freedom from the environment into the system (in the above example, the choice of which basis to measure in) until the system states are themselves orthogonal.

a state of the environment $|e_i\rangle_E$ which is one-one correlated with the state of the system. Because each of the environment states $|e_i\rangle_E$ has zero (or very small) overlap with the environment state associated with other system states, we say that the environment is *monitoring* the state of the system, or keeping a record of it. Again, this is a dynamical process: the environment starts in a particular initial ready state which is not entangled with the initial state of the system, but interactions between the system and environment cause the environment to *record* the state of the system. It is often convenient to decompose the Hamiltonian generating time evolution on the total Hilbert space into pieces denoting evolution in the system and environment alone, as well as an interaction Hamiltonian connecting the two factors:

$$H = H_S + H_E + H_{\text{int}}. \quad (10.49)$$

In general, a decoherence analysis requires conditions on all of these components, but when decoherence occurs in the limit that the interaction strength is much larger than the other two terms (for a suitable choice of norm), the branches are simply given by the eigenstates of the interaction Hamiltonian.

Because the overall state starts as a product state but ends as an entangled superposition of branches, we see that decoherence is associated with entropy production, visible as the Shannon entropy of the classical probability distribution $|c_i|^2$ over system states. In fact the connection between decoherence, entropy growth, and the production of records in the environment can be made more precise [153]. In laboratory settings, for example when the environment includes photons and air molecules bouncing off an experimental apparatus, we expect that the environment in fact contains very many highly redundant records of the system state [252].

We emphasize that in most setups the situations which lead to decoherence are non-generic. The decoherence program requires, in particular, an initial (low-entropy) product state between the system and the environment, a special initial “ready” state of the environment which will subsequently be able to record the state of the system, and dynamics which allow the system to interact with the environment while still admitting effective non-dissipative evolution in the system alone after branching has occurred. If, instead of analyzing a particular measurement apparatus, we want to use the decoherence formalism to determine which states are classical, we need to vary over some of these initial specifications. In particular, if we do not start a preferred identification of the system, but instead, like in cosmology, wish to pick out the natural classical degrees of freedom, we need to vary over possible

system-environment decompositions [29].

State Reduction from Operational Constraints

In the study of decoherence, we usually start by postulating the system-environment split $\mathcal{H} = \mathcal{H}_E \otimes \mathcal{H}_S$. The state-reduction map $tr_E : \mathcal{H} \rightarrow \mathcal{H}_S$ is then characterized by demanding

$$tr (I_E \otimes O_S \rho) = tr (O_S tr_E (\rho)) \quad (10.50)$$

for all ρ and O_S , which leads to the definition of the partial-trace map. The reduced state $tr_E (\rho)$ is understood as the state of the subsystem \mathcal{H}_S and unitary evolution of ρ (usually) results in a loss of coherence for $tr_E (\rho)$.

The operational justification for the system-environment split $\mathcal{H}_E \otimes \mathcal{H}_S$ comes from an assertion that only measurements of the form $I_E \otimes O_S$ are allowed. In the language of matrix algebras (see Section 10.2) we can say that the allowed measurements $I_E \otimes O_S$ form an algebra and the system-environment split $\mathcal{H}_E \otimes \mathcal{H}_S$ comes from the irrep decomposition of this algebra. By taking this perspective, we do not have to postulate the system-environment split; instead we derive it as the irrep decomposition of the algebra of allowed observables. This suggests a strictly operational approach to decoherence where the algebra of allowed observables is the primary object from which the Hilbert-space bipartition and the state-reduction map are derived.

In this operational approach, we start with a Hilbert space \mathcal{H} and an algebra $\mathcal{A} \subseteq \mathcal{L}(\mathcal{H})$ that reflects our operational constraints. The assumption is that in principle, all observables $O \in \mathcal{A}$ can be measured, but nothing else. This is the generalization of the earlier assumption that only observables of the form $I_E \otimes O_S$ are allowed. This of course may be an overstatement of the practical reality, in which not all $O \in \mathcal{A}$ are in fact measurable, but it is still a useful assumption that outlines what definitely cannot be measured. (Similarly, when we make the usual system-environment split, we do not actually consider all $I_E \otimes O_S$ to be measurable, but it is still a useful assumption that outlines the boundary of the inaccessible environment). In Sections 10.6-10.8 below, we will introduce a more flexible notion of bipartition that captures restrictions to observables that do not have to form an algebra.

With the algebra $\mathcal{A} \subseteq \mathcal{L}(\mathcal{H})$, the Hilbert space decomposes into the generalized bipartition (see Theorem 10.2.2)

$$\mathcal{H} \cong \bigoplus_q \mathcal{H}_{E_q} \otimes \mathcal{H}_{S_q} \quad (10.51)$$

where only subsystems \mathcal{H}_{S_q} are accessible with observables restricted to $O \in \mathcal{A}$. This decomposition generalizes the usual system-environment split in that it can identify multiple superselection sectors, each of which is split into system and environment. The superselection sectors are manifestations of the fact that superpositions between state vectors in different sectors are unobservable and unpreparable with the given operational constraints. The reduced Hilbert space is therefore given by

$$\mathcal{H}_{\{S_q\}} := \bigoplus_q \mathcal{H}_{S_q} \quad (10.52)$$

where the observables $\bigoplus_q I_{E_q} \otimes O_{S_q} \in \mathcal{A}$ reduce to $\bigoplus_q O_{S_q}$. Now the state-reduction map $tr_{\{E_q\}}$ can be defined in two steps: first, impose the superselection rules; second, discard the environments:

$$tr_{\{E_q\}} : \rho \mapsto \bigoplus_q \Pi_q \rho \Pi_q \mapsto \bigoplus_q tr_{E_q} (\Pi_q \rho \Pi_q) \quad (10.53)$$

where Π_q are projections on the superselection sectors. Finally, the analog of Eq. (10.50)

$$tr \left(\left(\bigoplus_q I_{E_q} \otimes O_{S_q} \right) \rho \right) = tr \left(\left(\bigoplus_q O_{S_q} \right) tr_{\{E_q\}} (\rho) \right) \quad (10.54)$$

can be shown to hold by considering the trace on each sector q separately and applying Eq. (10.50).

We can now see that restriction of observables to an algebra manifests itself in two ways: superselection and system-environment split. Superselection is responsible for eliminating some of the reduced state's coherence terms by fiat, since no observable that could detect such coherences is measurable in principle. The system-environment split, on the other hand, is responsible for eliminating the coherence terms dynamically. That is, even if some superpositions could be detected in principle, they become entangled with the environment so rapidly that we cannot actually see them; this is the idea of environment-induced superselection or *einselection* [253]. In general, both superselection and einselection can play a role in the appearance of classical reality.

A very simple case of classicality from superselection comes up when we restrict the measurements to a single observable O . The algebra generated by O is spanned by the spectral projections Π_k (see Proposition 10.2.5) associated with the distinct measurement outcomes. The irrep decomposition is then the decomposition of \mathcal{H}

into the eigenspaces of O

$$\mathcal{H} \cong \bigoplus_k \mathcal{H}_{E_k} \otimes h_{S_k} \cong \bigoplus_k \mathcal{H}_{E_k} \quad (10.55)$$

where the system parts h_{S_k} are one-dimensional and can be absorbed into \mathcal{H}_{E_k} . The state-reduction map (10.53) then becomes

$$\rho \mapsto \bigoplus_k \text{tr}(\Pi_k \rho) \quad (10.56)$$

which is the reduction of ρ into a classical probability distribution over the outcomes k . Therefore, when only one observable can be measured, all quantum states are operationally equivalent to classical probability distributions and no coherence effects can be observed.

The more interesting cases involve more than one observable. For example, in a laboratory settings, it is common to have a single readout (measurement) operation O supplemented by a set of control operations $\{U_\alpha\}$. Then the allowed measurements consist of the set $\{O_\alpha := U_\alpha^\dagger O U_\alpha\}$ for all α . Such sets can be as simple as position and momentum $\{X, P\}$ or the angular momentum operators $\{J_x, J_y, J_z\}$. When the underlying system consists of many particles for which we can only measure the collective version of these observables, or when there is a single particle but the observables have limited resolution, we can expect non-trivial manifestations of superselection and einselection effects.

This leads us to the main technical difficulty of the operational approach: finding the irrep decomposition of algebras generated by $\{O_\alpha\}$. In the cases where $\{O_\alpha\}$ forms a group with a known representation structure, the irrep decomposition is given by the group's irreps (see Proposition 10.2.6). In other cases, however, we need a systematic way of constructing the irrep decomposition from the generating set of observables $\{O_\alpha\}$. The solution of this problem is the subject of the next section, and one of the main technical results of this paper.

10.4 Irrep Decomposition of Matrix Algebras by Scattering of Projections

The problem that we will address here is the following:

Given a finite set of self-adjoint matrices $\{M_1, M_2, \dots, M_n\}$ that generate the algebra \mathcal{A} , find the irrep decomposition of \mathcal{A} as in Theorem 10.2.2.

As was discussed in Section 10.2, the explicit specification of an irrep structure can be given by a choice of basis arranged into a bipartition table (BPT), with

the columns specifying a maximal set of minimal projections (MSMP) and the alignment of rows specifying the partial isometries that map between the columns. Conversely, given an MSMP and partial isometries that map between them, we can construct a BPT by following our definitions of the rows and columns. This suggests that in order to find the irrep structure of an algebra, we need to find an MSMP and the partial isometries that map between them.

According to its definition (Definition 10.2.4), an MSMP is called maximal because it resolves the identity element of the algebra, but this does not mean that it alone can generate the whole algebra. In the BPT picture, the elements of the MSMP determine the columns, but are oblivious to how the columns are aligned with each other. In order to construct the BPT, we will only need to supplement the MSMP with additional minimal projections that will allow it to generate the algebra. These additional projections define the partial isometries that map between the elements of the MSMP, which determines the alignment of columns in the BPT. The main task of the irrep decomposition algorithm is then to find a set of minimal projections that generates the algebra and contains an MSMP.

Before we go into specifics, let us outline the 4 main steps of the algorithm that we develop in this section:

1. Construct the initial set of projections from the spectral projections of the generators $\{M_1, M_2, \dots, M_n\}$.
2. Keep applying the rank-reducing operation called *scattering* on the set of projections until no further reduction is possible; this produces the final set of projections.
3. Verify that the final set of projections (which generates the algebra by construction) consists of minimal projections and contains an MSMP.
4. Use the final set of projections to construct the BPT.

Step 1 is a conversion of the input from self-adjoint operators to their spectral projections. Step 2, the heart of the algorithm, uses the scattering operation that we will define in Section 10.4. Step 3 is necessary because Step 2 is not guaranteed to produce minimal projections (although this is what happens in practice); we will explain how to deal with this in Section 10.4. Step 4 is the construction of the basis elements that populate the rows and columns of the BPT, which we will define in

Section 10.4. The formal definition of the algorithm and the proof of its correctness are deferred to Section 10.4.

In the following, it will be beneficial to have a concrete example to consider as we go over the details of the algorithm. For this purpose, we will now introduce a toy example that will be used throughout this section to illustrate the steps of the algorithm.

Toy Example

The example that we will consider here is a quantum system described by an eight-dimensional Hilbert space. The system itself and the measurements that we will consider are not motivated by physical considerations, but by their simplicity and ability to illustrate the key aspects of the algorithm. More physically-motivated examples will be considered in Section 10.5 below.

The toy example consists of the Hilbert space \mathcal{H} , spanned by the eight basis elements $\{|i\rangle\}_{i=1,\dots,8}$, and two incompatible projective measurements given by the self-adjoint operators Z and X . (This choice of names is only meant to be suggestive of their non-commutativity; we will remain agnostic to the physical nature of this system.) The problem is to find the irreps of the algebra $\langle Z, X \rangle$ which will allow us to simultaneously block-diagonalize the two non-commuting observables. Once we have this structure, it will be apparent what information encoded in the quantum states is accessible with the measurements Z, X , and what is not.

The observables Z and X have two outcomes associated with the spectral projections $\{\Pi_{Z;1}, \Pi_{Z;2}\}$ and $\{\Pi_{X;1}, \Pi_{X;2}\}$ ⁹ that sum to the identity. The spectral projections are defined as follows:

$$\Pi_{Z;1} := |1\rangle\langle 1| + |2\rangle\langle 2| + |3\rangle\langle 3| + |4\rangle\langle 4| \quad (10.57)$$

$$\Pi_{X;1} := |_{-}^{+37}\rangle\langle_{-}^{+37}| + |_{-}^{+1256}\rangle\langle_{-}^{+1256}|, \quad (10.58)$$

where we have used the shorthand notation

$$|_{-j_1, j_2, \dots}^{+i_1, i_2, \dots}\rangle := \frac{1}{\sqrt{N}} (|i_1\rangle + |i_2\rangle + \dots - |j_1\rangle - |j_2\rangle - \dots) \quad (10.59)$$

⁹We do not need to know their eigenvalues, but we will assume that they are nonzero. We can always shift all eigenvalues of the observable, without changing any physical predictions, so none of them are zero.

(\sqrt{N} is the normalization) so

$$|_{-}^{+37}\rangle := \frac{1}{\sqrt{2}} (|3\rangle + |7\rangle) \quad (10.60)$$

$$|_{-}^{+1256}\rangle := \frac{1}{2} (|1\rangle + |2\rangle + |5\rangle + |6\rangle). \quad (10.61)$$

Their complementary projections are given by $\Pi_{Z;2} := I - \Pi_{Z;1}$, $\Pi_{X;2} := I - \Pi_{X;1}$.

As was discussed in Proposition 10.2.5, the spectral projections of each self-adjoint operator are part of the algebra that it generates, and the algebra $\langle Z, X \rangle$ is also generated by $\langle \Pi_{Z;1}, \Pi_{Z;2}, \Pi_{X;1}, \Pi_{X;2} \rangle$. This replacement of generators from self-adjoint matrices to their spectral projections is Step 1 of the algorithm. We will continue this example after we define and prove some facts about the scattering algorithm.

Scattering of Projections

Scattering is the basic operation that we will use to break down the spectral projections of the generators into smaller rank projections.

Definition 10.4.1. *Scattering is an operation on a pair of projections Π_1, Π_2 that produces a pair of sets of projections $\{\Pi_1^{(\lambda)}\}, \{\Pi_2^{(\lambda)}\}$. The elements in each set come from the spectral decompositions*

$$\Pi_1 \Pi_2 \Pi_1 = \sum_{\lambda \neq 0} \lambda \Pi_1^{(\lambda)} \quad (10.62)$$

$$\Pi_2 \Pi_1 \Pi_2 = \sum_{\lambda \neq 0} \lambda \Pi_2^{(\lambda)} \quad (10.63)$$

(the sums are over unique non-zero eigenvalues λ) with the addition of null projections defined by¹⁰

$$\Pi_{i=1,2}^{(0)} := \Pi_i - \sum_{\lambda \neq 0} \Pi_i^{(\lambda)}. \quad (10.64)$$

It will be very convenient to consider the null projections $\Pi_i^{(0)}$ as just the $\lambda = 0$ elements of the set of spectral projections $\{\Pi_i^{(\lambda)}\}$, even when $\Pi_i^{(0)} = 0$ in Eq. (10.64). Also note that, although the definition does not say so explicitly, the spectrum λ in both Eq. (10.62) and (10.63) is the same (we will prove this in Lemma 10.4.4 below).

¹⁰Null projections should not be confused with projections on the kernel of $\Pi_i \Pi_j \Pi_i$. The kernel projections are given by $I - \sum_{\lambda} \Pi_i^{(\lambda)}$ which is not the same as Eq. (10.64).

From this definition, we see that all the projections in the set $\{\Pi_i^{(\lambda)}\}$ are pairwise orthogonal and sum to their predecessor

$$\Pi_i = \Pi_i^{(\lambda_1)} + \Pi_i^{(\lambda_2)} + \dots + \Pi_i^{(0)}, \quad (10.65)$$

so they are of lower rank than their predecessor Π_i . Thus, in analogy with the scattering of particles, the scattering of projections “breaks” them into smaller constituents (the “interaction” in this analogy is the adjoint action of Eq. (10.62),(10.63))

$$\begin{array}{ccc} \Pi_1 & \searrow & \Pi_1^{(\lambda_1)} + \Pi_1^{(\lambda_2)} + \dots + \Pi_1^{(0)} \\ & \swarrow \quad \searrow & \\ \Pi_2 & \nearrow & \Pi_2^{(\lambda_1)} + \Pi_2^{(\lambda_2)} + \dots + \Pi_2^{(0)} \end{array} \quad (10.66)$$

This defines scattering in the general case. There is also a special case that is important enough to have its own definition:

Definition 10.4.2. *A pair of projections Π_1, Π_2 is called reflecting if both projections remain unbroken by scattering, that is*

$$\Pi_1 \Pi_2 \Pi_1 = \lambda \Pi_1 \quad (10.67)$$

$$\Pi_2 \Pi_1 \Pi_2 = \lambda \Pi_2 \quad (10.68)$$

where the coefficient λ is called the reflection coefficient. We will say that Π_1, Π_2 are properly reflecting if the reflection coefficient is not 0 (i.e. they are not orthogonal, $\Pi_1 \Pi_2 \neq 0$).

It should be clear that rank 1 projections are always reflecting (however, reflecting projections can be of any rank). Another couple of useful facts about reflecting projections are given by the following proposition:

Proposition 10.4.3. *Let Π_1, Π_2 be a pair of properly reflecting projections with the reflection coefficient $\lambda \neq 0$, then:*

(1) Π_1 and Π_2 have the same rank.

(2) $\Pi_1 = \Pi_2$ if $\lambda = 1$.

Proof. We take the trace on both sides of Eq. (10.67), (10.68) and use the cyclic property of the trace to get

$$\text{tr}(\Pi_1 \Pi_2) = \lambda \text{tr}(\Pi_1) \quad (10.69)$$

$$\text{tr}(\Pi_1 \Pi_2) = \lambda \text{tr}(\Pi_2) \quad (10.70)$$

Since the λ 's are the same (this will be proven in general in Lemma 10.4.4), then $tr(\Pi_1) = \frac{tr(\Pi_1\Pi_2)}{\lambda} = tr(\Pi_2)$ so they must have the same rank.

If, in addition, $\lambda = 1$ then

$$0 = \Pi_1 - \Pi_1\Pi_2\Pi_1 = (\Pi_1 - \Pi_1\Pi_2)(\Pi_1 - \Pi_1\Pi_2)^\dagger \quad (10.71)$$

$$0 = \Pi_2 - \Pi_2\Pi_1\Pi_2 = (\Pi_2 - \Pi_2\Pi_1)(\Pi_2 - \Pi_2\Pi_1)^\dagger \quad (10.72)$$

so

$$0 = \Pi_1 - \Pi_1\Pi_2 \quad (10.73)$$

$$0 = (\Pi_2 - \Pi_2\Pi_1)^\dagger. \quad (10.74)$$

Thus, $\Pi_1 = \Pi_1\Pi_2 = \Pi_2$. □

The importance of reflecting projections is that they do not break under scattering (this choice of terminology is a continuation of our commitment to the analogy with particles). In Step 2 of the algorithm, we will apply the scattering operation on pairs of projections until no further reduction is possible. The impossibility of reduction is then the case of all projections being pairwise reflecting. We are guaranteed to reach entirely reflecting projections because scattering produces projections of smaller rank (unless it reflects) and projections of rank 1 are always reflecting.

The most important fact about scattering is that regardless of what the initial projections Π_1, Π_2 are, the resulting projections are a series of reflecting pairs $\{\Pi_1^{(\lambda)}, \Pi_2^{(\lambda)}\}$ with reflection coefficients λ , and every pair $\{\Pi_1^{(\lambda)}, \Pi_2^{(\lambda)}\}$ is orthogonal to any other pair $\{\Pi_1^{(\lambda')}, \Pi_2^{(\lambda')}\}$.

Lemma 10.4.4. *Let Π_1, Π_2 be the initial projections and $\{\Pi_1^{(\lambda)}\}, \{\Pi_2^{(\lambda)}\}$ be the sets of post scattering projections given by Definition 10.4.1, then:*

- (1) *The spectrum of eigenvalues λ is the same in both sets.*
- (2) *For all $\lambda \neq \lambda'$, the pairs of projections $\Pi_1^{(\lambda)}, \Pi_2^{(\lambda')}$ are orthogonal.*
- (3) *For all λ , the pairs of projections $\Pi_1^{(\lambda)}, \Pi_2^{(\lambda)}$ are reflecting with reflection coefficient λ .*

Proof. We begin by taking λ and $\Pi_1^{(\lambda)}$ to be the eigenvalues and the spectral projections in the decomposition of $\Pi_1\Pi_2\Pi_1$ and assume nothing about the spectral decomposition of $\Pi_2\Pi_1\Pi_2$.

First, note that $\Pi_1^{(\lambda)}\Pi_1 = \Pi_1\Pi_1^{(\lambda)} = \Pi_1^{(\lambda)}$ for all λ as can be seen from Eq. (10.65) and the fact that all spectral projections (including $\Pi_1^{(0)}$) are pairwise orthogonal. Then, if we act on both sides of Eq. (10.62) by the adjoint with $\Pi_1^{(\lambda)}$ and $\Pi_1^{(\lambda')}$, we get

$$\Pi_1^{(\lambda)}\Pi_2\Pi_1^{(\lambda')} = \delta_{\lambda\lambda'}\lambda\Pi_1^{(\lambda)}. \quad (10.75)$$

This equation holds for all λ including $\lambda = 0$, and it does not matter whether $\Pi_1^{(0)}$ vanishes ($\Pi_1^{(0)} = 0$) or not. In particular $\Pi_1^{(0)}\Pi_2\Pi_1^{(0)} = 0$, so $\Pi_1^{(0)}\Pi_2 = 0$ because otherwise we would reach a contradiction,

$$0 \neq \left(\Pi_1^{(0)}\Pi_2\right) \left(\Pi_1^{(0)}\Pi_2\right)^\dagger = \left(\Pi_1^{(0)}\Pi_2\right) \left(\Pi_2\Pi_1^{(0)}\right) = \Pi_1^{(0)}\Pi_2\Pi_1^{(0)} = 0. \quad (10.76)$$

Therefore, $\Pi_1^{(0)}\Pi_2 = \Pi_2\Pi_1^{(0)} = 0$. This allows us to write

$$\Pi_2\Pi_1\Pi_2 = \Pi_2\left(\Pi_1 - \Pi_1^{(0)}\right)\Pi_2 = \Pi_2\left(\sum_{\lambda \neq 0} \Pi_1^{(\lambda)}\right)\Pi_2 = \sum_{\lambda \neq 0} \lambda \left(\frac{1}{\lambda}\Pi_2\Pi_1^{(\lambda)}\Pi_2\right). \quad (10.77)$$

The last step suggests the definition

$$\tilde{\Pi}_2^{(\lambda)} := \frac{1}{\lambda}\Pi_2\Pi_1^{(\lambda)}\Pi_2. \quad (10.78)$$

These operators are clearly self-adjoint and, using Eq. (10.75), we can see that

$$\tilde{\Pi}_2^{(\lambda)}\tilde{\Pi}_2^{(\lambda')} = \frac{1}{\lambda\lambda'}\Pi_2\Pi_1^{(\lambda)}\Pi_2\Pi_1^{(\lambda')}\Pi_2 = \delta_{\lambda\lambda'}\frac{1}{\lambda}\Pi_2\Pi_1^{(\lambda)}\Pi_2 = \delta_{\lambda\lambda'}\tilde{\Pi}_2^{(\lambda)}, \quad (10.79)$$

so they are pairwise orthogonal projections. Since the λ 's are distinct and $\tilde{\Pi}_2^{(\lambda)}$ are pairwise orthogonal projections, Eq. (10.77) must be the spectral decomposition of $\Pi_2\Pi_1\Pi_2$. Thus, $\tilde{\Pi}_2^{(\lambda)} = \Pi_2^{(\lambda)}$, and the spectrum is the same for both $\Pi_1\Pi_2\Pi_1$ and $\Pi_2\Pi_1\Pi_2$. This proves claim 1.

Now, if we use Eq. (10.78) as the definition of $\Pi_2^{(\lambda')}$ and simplify with Eq. (10.75), we get the identity

$$\Pi_1^{(\lambda)}\Pi_2^{(\lambda')} = \Pi_1^{(\lambda)}\Pi_2\Pi_1^{(\lambda')}\Pi_2\frac{1}{\lambda'} = \delta_{\lambda\lambda'}\Pi_1^{(\lambda)}\Pi_2. \quad (10.80)$$

This proves claim 2. In particular, for $\lambda = \lambda'$, if we multiply this identity with its own adjoint on both sides and again use Eq. (10.75) and (10.78), we get

$$\Pi_1^{(\lambda)}\Pi_2^{(\lambda)}\Pi_1^{(\lambda)} = \Pi_1^{(\lambda)}\Pi_2\Pi_1^{(\lambda)} = \lambda\Pi_1^{(\lambda)} \quad (10.81)$$

$$\Pi_2^{(\lambda)}\Pi_1^{(\lambda)}\Pi_2^{(\lambda)} = \Pi_2\Pi_1^{(\lambda)}\Pi_2 = \lambda\Pi_2^{(\lambda)} \quad (10.82)$$

which proves claim 3. \square

Lemma 10.4.4 tells us that almost all projections that come out of scattering are pairwise orthogonal. In particular, each of the null projections $\Pi_1^{(0)}, \Pi_2^{(0)}$ is orthogonal to all other projections and only the pairs $\Pi_1^{(\lambda)}, \Pi_2^{(\lambda)}$ for $\lambda \neq 0$ are not orthogonal but properly reflecting. It is also interesting to note that if there is $\lambda = 1$ in the spectrum, then $\Pi_1^{(1)} = \Pi_2^{(1)}$ (see Proposition 10.4.3), which occurs if the initial projections project onto intersecting subspaces so $\Pi_i^{(1)}$ is the projection on their intersection. We can avoid scattering these projections twice in future iterations of the algorithm by eliminating such duplicates. Lastly, note that Eq. (10.78) tells us how to get the post-scattering projections $\Pi_2^{(\lambda \neq 0)}$ from the post-scattering projections $\Pi_1^{(\lambda \neq 0)}$ (for $\Pi_i^{(\lambda=0)}$ we use Eq. (10.64)) so we only need to calculate the spectral decomposition once for $\Pi_1 \Pi_2 \Pi_1$.

We now define a graph structure for a set of projections:

Definition 10.4.5. A (proper) reflection network associated with the set of reflecting projections $\{\Pi_v\}$ is the graph $G = \{V, E\}$ where the vertices are the projections $V := \{\Pi_v\}$ and every properly reflecting pair is connected by an edge $E := \{(\Pi_v, \Pi_u) \mid \Pi_v \Pi_u \neq 0\}$ (only orthogonal reflecting projections do not share an edge). An improper reflection network is the generalization of the above where not all projections are known to be reflecting. In that case, there are two kinds of edges: one kind for properly reflecting pairs (black solid edge) and one for unknowns (red dashed edge).

In general, reflection networks may have multiple connected components formed by subsets of projections that are orthogonal to every projection outside the subset. It does not mean, however, that projections in the same connected component cannot be orthogonal; as long as there is a sequence of proper reflection (or unknown) relations connecting the projections, they will be in the same component. Also note that, according to Proposition 10.4.3, all projections in the same connected component of a proper reflection network must be of the same rank.

We will now consider how the scattering operation affects the reflection network by focusing on a pair of projections in the network. According to Lemma 10.4.4, in general a pair of projections $\{\Pi_1, \Pi_2\}$ with unknown relations (red edge) scatters into a series of pairs of reflecting projections $\{\Pi_1^{(\lambda)}, \Pi_2^{(\lambda)}\}$ (black edges unless $\lambda = 0$ then no edge), and each pair in the series is orthogonal to all other pairs (no edges); see Fig 10.1(a). Fig 10.1(b) illustrates the special case where Π_1 did not break under scattering so $\Pi_1 \equiv \Pi_1^{(\lambda_1)}$. The case where both $\{\Pi_1, \Pi_2\}$ do not break (not shown)

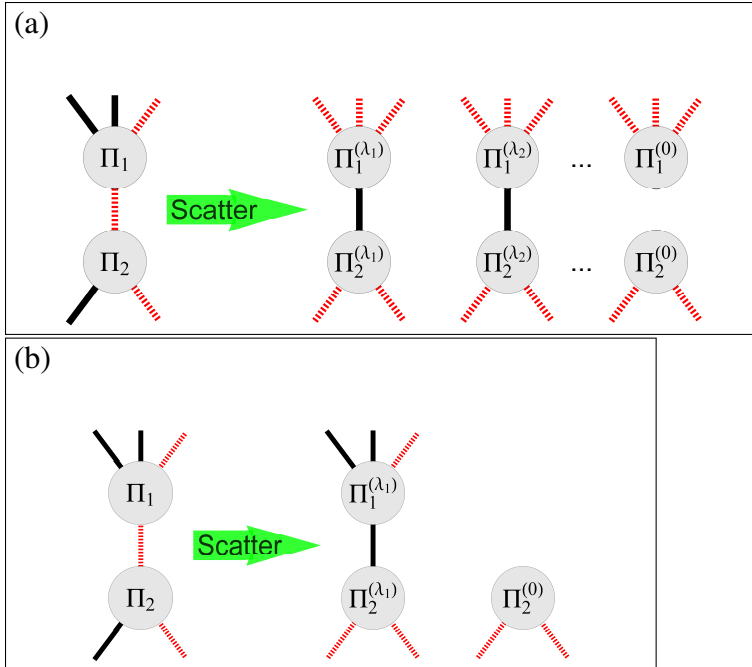


Figure 10.1: Update rules for reflection relations after scattering. The red (dashed) edges represent unknown reflection relations, black (solid) edges represent properly-reflecting pairs, absent edges represent orthogonal pairs. One-sided edges stand for the reflection relations with other projections in the rest of the network. (a) In the generic case where each $\Pi_{i=1,2}$ breaks down into $\{\Pi_i^{(\lambda_k)}\}$, the result is a series of properly reflecting pairs (for $\lambda = 0$ the pair is orthogonal) as described in Lemma 10.4.4. All the external edges are inherited by $\{\Pi_i^{(\lambda_k)}\}$ from Π_i with the black (solid) edges being reset to red (dashed). (b) In the special case where Π_1 did not break down under scattering, we know $\Pi_1 \equiv \Pi_1^{(\lambda_1)}$. In this case, Π_2 may break down to at most two projections (if it also did not break down, then Π_1, Π_2 should just be relabeled as reflecting) such that $\Pi_1^{(\lambda_1)}, \Pi_2^{(\lambda_1)}$ are properly reflecting and $\Pi_2^{(0)}$ is orthogonal to both. In (b) the update rule of external edges differs from the generic case (a) in that for unbroken projection $\Pi_1^{(\lambda_1)}$, the black (solid) edges are not reset to red (dashed).

implies that they are reflecting and the red edge between them is set to black or omitted, depending on whether $\lambda = 0$.

Since both projections $\{\Pi_1, \Pi_2\}$ are part of a larger network, we also have to specify how the resulting projections $\{\Pi_i^{(\lambda_k)}\}$ inherit the relations with the rest of the elements in the network. First, we note that orthogonality with other projections is preserved under scattering so we do not need to add new edges that we did not already have. Red edges also do not need to be updated since every unknown relation

that Π_i had is still unknown for $\Pi_i^{(\lambda_k)}$. Proper reflection relations, however, do not survive when one of the projections is broken down into smaller rank projections, because properly reflecting projections must have the same rank (see Proposition 10.4.3). Therefore, black edges that Π_i had before scattering should be reset to red when inherited by $\Pi_i^{(\lambda_k)}$, unless the projection did not break, like in Fig 10.1(b), in which case the black edges remain intact.

Procedure

As we mentioned before, Step 1 of the algorithm produces the spectral projections of the generators. Formally, we will refer to this step of the algorithm as the procedure `GETALLSPECTRALPROJECTIONS`, but we will not explicitly define it as it is self-evident.

We now have the definitions and the facts to define the procedure of Step 2 of the algorithm:

```

1: procedure SCATTERALLPROJECTIONS(SpecProjs)
2:   Projs  $\leftarrow$  SpecProjs
3:   Relations  $\leftarrow$  INITIALIZEREFLERATIONRELATIONS(Projs)
4:   ReflectNet  $\leftarrow$  {Projs, Relations}
5:   while ISEVERYTHINGREFLECTING(ReflectNet) is false do
6:     Pair  $\leftarrow$  PICKNONREFLECTPAIR(ReflectNet)
7:     PostScatPair  $\leftarrow$  SCATTERPROJECTIONSPAIR(Pair)
8:     ReflectNet  $\leftarrow$  UPDATEREFLECTIONNETWORK(ReflectNet, Pair, PostScatPair)
9:   end while
10:  return ReflectNet
11: end procedure

```

The procedure starts by constructing the improper reflection network from the initial spectral projections and initializing all edges to red except the ones that are known to be reflecting (like rank 1 or orthogonal projections). It then proceeds to iterations where it picks a pair of projections connected by a red edge,¹¹ scatters it,¹² and updates the relations in the network according to the rules given in Fig. 10.1. The

¹¹For better efficiency, we should prioritize projections of lowest rank. Such projections are less likely to break down under scattering, which will reduce the number of resets of proper reflection relations that happen when we update the network after scattering.

¹²As was discussed after Lemma 10.4.4, the projections in *Pair* may intersect on a subspace and the projection on this subspace will appear twice in *PostScatPair*. Eliminating such duplicate projections is not necessary for the success of the algorithm, but it will improve efficiency.

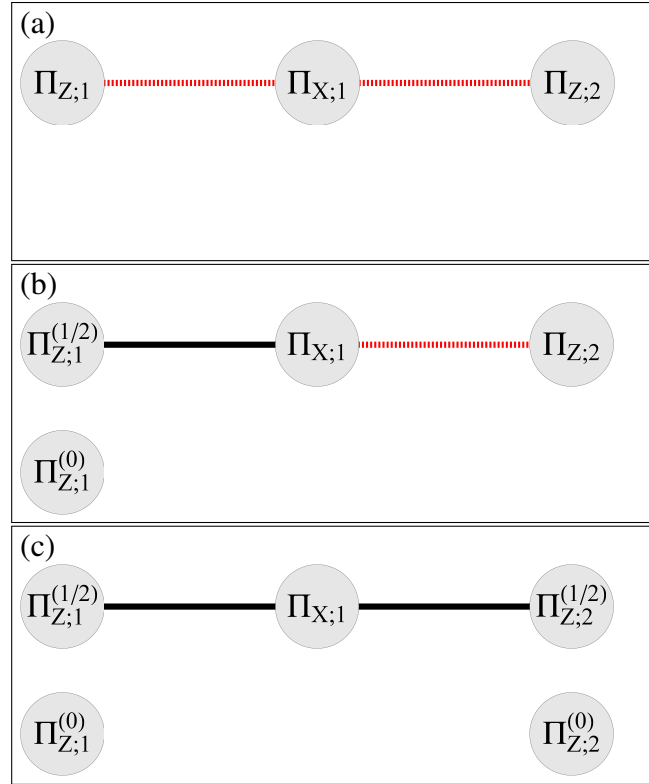


Figure 10.2: Evolution of the reflection network of the toy model during two scattering iterations. The red (dashed) edges represent unknown reflection relations, black (solid) edges represent properly reflecting pairs, absent edges represent orthogonal pairs. (a) is the initial improper reflection network. (b) is the intermediate network after one scattering iteration. (c) is the final proper reflection network after two scatterings.

procedure `SCATTERALLPROJECTIONS` finishes when the reflection network is proper: that is, when all projections are reflecting (all edges are black). This procedure is guaranteed to terminate because every scattering iteration either identifies a previously unknown reflecting pair or scatters a pair into a series of reflecting pairs of lower rank. Eventually, all projections will either be reflecting, or they will be reduced to rank 1 and thus again must be reflecting.

Toy Example (continued)

Before we consider the initial reflection network, we note that one of the four initial spectral projections $\{\Pi_{Z;1}, \Pi_{Z;2}, \Pi_{X;1}, \Pi_{X;2}\}$ is redundant in generating the algebra. That is because $\Pi_{X;2} = I - \Pi_{X;1} = \Pi_{Z;1} + \Pi_{Z;2} - \Pi_{X;1}$ so the algebra generated just by $\{\Pi_{Z;1}, \Pi_{Z;2}, \Pi_{X;1}\}$ is the same as before.

The initial improper reflection network is shown in Fig 10.2(a). We begin by scattering the pair $\{\Pi_{Z;1}, \Pi_{X;1}\}$

$$\Pi_{Z;1}\Pi_{X;1}\Pi_{Z;1} = \Pi_{Z;1} |_{-}^{+37}\rangle \langle_{-}^{+37}| \Pi_{Z;1} + \Pi_{Z;1} |_{-}^{+1256}\rangle \langle_{-}^{+1256}| \Pi_{Z;1} \quad (10.83)$$

$$= \frac{1}{2} |3\rangle \langle 3| + \frac{1}{2} |_{-}^{+12}\rangle \langle_{-}^{+12}|. \quad (10.84)$$

There is only one eigenvalue $\lambda = \frac{1}{2}$ here which identifies a single spectral projection

$$\Pi_{Z;1}^{(1/2)} = |3\rangle \langle 3| + |_{-}^{+12}\rangle \langle_{-}^{+12}|. \quad (10.85)$$

Thus, the rank 4 projection $\Pi_{Z;1}$ breaks into two rank 2 projections $\Pi_{Z;1} = \Pi_{Z;1}^{(1/2)} + \Pi_{Z;1}^{(0)}$ (see Definition 10.4.1), where

$$\Pi_{Z;1}^{(0)} = |4\rangle \langle 4| + |_{-2}^{+1}\rangle \langle_{-2}^{+1}|. \quad (10.86)$$

In principle, the breaking of the second projection $\Pi_{X;1}$ in the scattering is calculated using Eq. (10.78) resulting in

$$\Pi_{X;1}^{(1/2)} = \frac{1}{1/2} \Pi_{X;1} \Pi_{Z;1}^{(1/2)} \Pi_{X;1} = |_{-}^{+37}\rangle \langle_{-}^{+37}| + |_{-}^{+1256}\rangle \langle_{-}^{+1256}| = \Pi_{X;1}, \quad (10.87)$$

which tells us that $\Pi_{X;1}$ did not break (when the scattering has only one non-zero eigenvalue, as in this case, we already know at least one of the projections does not break). The reflection network after the first scattering is shown in Fig 10.2(b).

Repeating the same for the scattering of $\Pi_{Z;2}$ with $\Pi_{X;1}$, we get

$$\Pi_{Z;2}\Pi_{X;1}\Pi_{Z;2} = \frac{1}{2} |7\rangle \langle 7| + \frac{1}{2} |_{-}^{+56}\rangle \langle_{-}^{+56}| \quad (10.88)$$

so $\Pi_{Z;2} = \Pi_{Z;2}^{(1/2)} + \Pi_{Z;2}^{(0)}$ and

$$\Pi_{Z;2}^{(1/2)} = |7\rangle \langle 7| + |_{-}^{+56}\rangle \langle_{-}^{+56}| \quad (10.89)$$

$$\Pi_{Z;2}^{(0)} = |8\rangle \langle 8| + |_{-6}^{+5}\rangle \langle_{-6}^{+5}|. \quad (10.90)$$

As before, $\Pi_{X;1}$ does not break in the scattering.

The final proper reflection network is shown in Fig 10.2(c).

Minimality and Completeness of Reflecting Projections

Now, we will examine the properties of the set of projections that comes out of Step 2 of the algorithm. As we discussed above, this step finishes when all projections are pairwise reflecting. In order to construct the BPT, we will need at least one MSMP and any additional minimal projections required to generate the whole algebra. Thus, we will have to establish whether the final set of reflecting projections meets the following criteria:

1. *Minimality*: All projections in the final set are minimal (Definition 10.2.3).
2. *Completeness*: The final set contains at least one MSMP (Definition 10.2.4).

We will now introduce correction procedures for when these criteria are not met.

Minimality

Minimality of the reflecting projections can be established by considering the paths in the reflection network. Each path is given by a sequence of vertices $\mathbf{v} = (v_1, v_2, \dots, v_n)$ that specify the projections along the path. By taking the product of all projections along the path and normalizing with reflection coefficients¹³, we define the operator

$$S_{\mathbf{v}} := \frac{\Pi_{v_1} \Pi_{v_2} \dots \Pi_{v_n}}{\sqrt{\lambda_{v_1 v_2} \lambda_{v_2 v_3} \dots \lambda_{v_{n-1} v_n}}}. \quad (10.91)$$

Such an operator will be referred to as a *path isometry* since it is a partial isometry from the eigenspace of Π_{v_n} to the eigenspace of Π_{v_1} along the path \mathbf{v} (the operator $S_{\mathbf{v}}^\dagger$ is a path isometry in the opposite direction). In order to see that this is the case, consider the path between two neighboring projections Π_v, Π_u such that $S_{(v,u)} = \frac{1}{\sqrt{\lambda_{vu}}} \Pi_v \Pi_u$. This is a partial isometry because

$$S_{(v,u)} S_{(v,u)}^\dagger = \frac{1}{\lambda_{vu}} \Pi_v \Pi_u \Pi_v = \Pi_v \quad (10.92)$$

$$S_{(v,u)}^\dagger S_{(v,u)} = \frac{1}{\lambda_{vu}} \Pi_u \Pi_v \Pi_u = \Pi_u. \quad (10.93)$$

The general case follows in the same way by considering $S_{\mathbf{v}} S_{\mathbf{v}}^\dagger$, $S_{\mathbf{v}}^\dagger S_{\mathbf{v}}$ and reducing the products of projections by applying the reflection relations.

The minimality of reflecting projections can then be established with the help of the following lemma:

Lemma 10.4.6. *Let $\{\Pi_v\}$ be a set of projections forming a proper reflection network and let $\{S_{\mathbf{v}}\}$ be the set of all path isometries in the network as defined by Eq. (10.91). Then, the following statements are equivalent:*

- (1) Every Π_v is a minimal projection in the algebra $\mathcal{A} := \langle \{\Pi_v\} \rangle$.
- (2) $S_{\mathbf{v}} \propto S_{\mathbf{u}}$ for all paths \mathbf{v}, \mathbf{u} that share the same initial and final vertices.

¹³In practice, we do not need to remember the reflection coefficients in order to construct these operators, since at each step the normalization is given by the non-zero singular value (which is unique, since all projections are reflecting) of $\Pi_{v_1} \Pi_{v_2} \dots \Pi_{v_n}$.

Proof. Every element $M \in \mathcal{A}$ is a linear combination of products of $\{\Pi_v\}$ so $\mathcal{A} = \text{span}\{S_v\}$. Then, by Definition 10.2.3 and linearity, the projections $\{\Pi_v\}$ are minimal if and only if $\Pi_v S_v \Pi_v \propto \Pi_v$ for all v and v . When $\Pi_v S_v = 0$ or $S_v \Pi_v = 0$, the relation $\Pi_v S_v \Pi_v = 0 \propto \Pi_v$ holds trivially. Let us then consider $\Pi_v S_v \Pi_v \neq 0$ for some $v := (v_1, v_2, \dots, v_n)$, which implies that $v' := (v, v_1, v_2, \dots, v_n, v)$ is a circular path from Π_v to itself. Recalling the definition in Eq. (10.91), we can use both $\Pi_v S_v \Pi_v \propto S_{v'}$ and $S_{v'} \propto \Pi_v S_v \Pi_v$, since the proportionality factor is not 0. Thus, if statement 2 holds, then $S_{v'} \propto S_{(v,v)}$ and

$$\Pi_v S_v \Pi_v \propto S_{v'} \propto S_{(v,v)} = \Pi_v. \quad (10.94)$$

This proves $2 \Rightarrow 1$.

If statement 1 holds, then $\Pi_v S_v \Pi_v \propto \Pi_v$ and

$$S_{v'} \propto \Pi_v S_v \Pi_v \propto \Pi_v. \quad (10.95)$$

This proves statement 2 for all circular paths v' since all $S_{v'}$ are (properly) proportional to the same initial projection Π_v and thus to each other. For non circular paths $v = (v_1, \dots, v_n)$, $u = (u_1, \dots, u_m)$ with $v_1 = u_1$ and $v_n = u_m$, let us assume that $S_v \not\propto S_u$ so $S_v S_u^\dagger \not\propto S_u S_u^\dagger$. Then the path isometry $S_{v'} = S_v S_u^\dagger$ defined by the circular path $v' := (v_1, \dots, v_n = u_m, \dots, u_1)$ is proportional to its initial projection $S_v S_u^\dagger \propto \Pi_{v_1} = \Pi_{u_1} = S_u S_u^\dagger$, in contradiction to $S_v S_u^\dagger \not\propto S_u S_u^\dagger$. Therefore, $S_v \propto S_u$ proving $1 \Rightarrow 2$. \square

Thus, by checking whether the path isometries in a reflection network depend only on the initial and final vertices and are independent of the paths taken, we can verify that the projections are minimal. In practice, it is not necessary to check all paths as there is usually a lot of order in the reflection network and path independence can be established based on this order. Things are even simpler when the projections are of rank 1 (recall all projections in the same connected component of a reflection network must have the same rank), then there is nothing to check since rank 1 projections are always minimal.

In addition to providing a testable criterion for minimality, Lemma 10.4.6 also implies a correction for the case where the reflecting projections are not minimal.

Proposition 10.4.7. *In the setting of Lemma 10.4.6, let v, u be two paths that share the same initial $v_1 = u_1$ and final $v_n = u_m$ vertices but $S_v \not\propto S_u$. Then, the spectral projections $\{\Pi^{(\omega)}\}$ of $U := S_v S_u^\dagger$ have the following properties:*

- (1) Each $\Pi^{(\omega)}$ is in the algebra $\mathcal{A} := \langle \{\Pi_v\} \rangle$.
- (2) Each $\Pi^{(\omega)}$ is not reflecting with Π_{v_1} .

Proof. First note that the operator U is a unitary on the eigenspace of Π_{v_1} since $UU^\dagger = U^\dagger U = \Pi_{v_1}$. Since U is in \mathcal{A} , and it is a normal operator, all its spectral projections are also in \mathcal{A} [249]. This proves statement 1.

From $S_v \not\propto S_u$, we have $U = S_v S_u^\dagger \not\propto S_u S_u^\dagger = \Pi_{v_1}$. Since $U = \sum_\omega \omega \Pi^{(\omega)}$ and $\Pi_{v_1} = \sum_\omega \Pi^{(\omega)}$ but $U \not\propto \Pi_{v_1}$ then there must be more than one spectral projection $\Pi^{(\omega)}$. Therefore, $\Pi_{v_1} \Pi^{(\omega)} \Pi_{v_1} = \Pi^{(\omega)} \not\propto \Pi_{v_1}$, proving statement 2. \square

So, if the minimality condition of statement 2 in Lemma 10.4.6 does not hold, we can take $U := S_v S_u^\dagger$ for the two paths that violate it and use its spectral projections $\{\Pi^{(\omega)}\}$ to scatter Π_{v_1} . By scattering the projections in the connected component of Π_{v_1} with the spectral projections $\{\Pi^{(\omega)}\}$ until everything is reflecting again, we will break down the connected component into a reflection network of smaller rank projections. Then we can check the condition of minimality again and repeat until it is satisfied.

Procedure

As was shown in Lemma 10.4.6, in principle minimality of a reflection network can be established by checking all path isometries connecting every pair of projections and verifying that they are proportional to one another. We will formally refer to this procedure as `ESTABLISHMINIMALITY`. This, of course, is not a computationally tractable solution because of the exponentially large number of paths in all but the most degenerate networks. Nonetheless, when dealing with concrete examples, path invariance of path isometries can be shown based on the specifics of the problem; this is what we mean in practice when referring to the `ESTABLISHMINIMALITY` procedure.

Even though we have not encountered non-minimal reflection networks following the scattering procedure, we do know that such networks exist.¹⁴ Therefore, for the sake of completeness, we have mentioned that even in such cases there is a way to proceed, given by Proposition 10.4.7.

¹⁴Non-minimal reflection networks can be constructed directly by carefully choosing the reflecting projections. It is an open question whether there are conditions that guarantee that the reflecting projections that come out from the scattering procedure are always minimal. If that is not the case, a tractable procedure that establishes minimality of the reflection network without relying on the specifics of the problem would be desirable.

Toy Example (continued)

In the network shown in Fig 10.2(c), we have three connected components, but only the component $\{\Pi_{Z;1}^{(1/2)}, \Pi_{X;1}, \Pi_{Z;2}^{(1/2)}\}$ has any paths. For every pair of projections in this component, there is only one simple path (that is a path that has no repeating vertices) between them, so paths invariance trivially holds for simple paths.

Every non-simple path is of the form $((\cdot), \Pi_{X;1}, (\cdot), \Pi_{X;1}, \dots, (\cdot), \Pi_{X;1}, (\cdot), \Pi_{X;1}, (\cdot))$ where (\cdot) is a placeholder for any of the other two projections in the component, and it may be empty at the boundaries. Any path isometry of such path is proportional to the path isometry of the simple path $((\cdot), \Pi_{X;1}, (\cdot))$, because of the reflection relation $\Pi_{X;1} (\cdot) \Pi_{X;1} \propto \Pi_{X;1}$. Therefore, in this network all path isometries between every pair are proportional to one another.

Completeness

Completeness requires the reflection network to contain at least one MSMP as defined in Definition 10.2.4. That is, assuming that the minimality of projections has been established, we must identify a set of pairwise orthogonal projections that sum to the identity of the algebra. Since the initial projections in step 1 of the algorithm are the spectral projections of observables, they must resolve the identity (otherwise the probabilities of outcomes will not sum to 1). The scattering at step 2 breaks them down into smaller ranks, but they continue to resolve the identity. This means that completeness is a given if the initial projections resolve the identity to begin with. However, in more general applications of the algorithm where we do not assume the inputs to consist of identity-resolving projections, it turns out that we can still reconstruct an MSMP.

Given the reflection network of projections $\{\Pi_v\}$ and the algebra $\mathcal{A} := \langle\{\Pi_v\}\rangle$, we will assume that all Π_v are minimal in \mathcal{A} (that is, minimality has to be established before checking completeness). Consider the largest subset of pairwise orthogonal projections $\{\Pi_{v_k}\} \subseteq \{\Pi_v\}$, with $\Pi_{v_k} \Pi_{v_l} = \delta_{kl} \Pi_{v_k}$, which is a maximal independent set of vertices in the network (this set does not have to be unique). The subset $\{\Pi_{v_k}\}$ is an MSMP if the operator

$$I_{\mathcal{A}} := \sum_k \Pi_{v_k} \quad (10.96)$$

is such that $I_{\mathcal{A}} \Pi_v = \Pi_v$ for all v . If it is not, we can use the result of the following lemma to complete the subset into an MSMP.

Lemma 10.4.8. *Let $\{\Pi_{v_k}\}$ be the largest subset of pairwise orthogonal projections in the reflection network of $\{\Pi_v\}$, where all Π_v are minimal in the algebra $\mathcal{A} := \langle \{\Pi_v\} \rangle$. If there is a v such that $I_{\mathcal{A}}\Pi_v \neq \Pi_v$, then, with the appropriate normalization factor c , the operator (here I is the full identity matrix and $I_{\mathcal{A}}$ is given by Eq. (10.96))*

$$\tilde{\Pi}_v := \frac{1}{c} (I - I_{\mathcal{A}}) \Pi_v (I - I_{\mathcal{A}}), \quad (10.97)$$

has all of the following properties:

- (1) $\tilde{\Pi}_v$ is a minimal projection in \mathcal{A} .
- (2) $\tilde{\Pi}_v$ is orthogonal to all $\{\Pi_{v_k}\}$.
- (3) The operator $\tilde{I}_{\mathcal{A}} := I_{\mathcal{A}} + \tilde{\Pi}_v$ is such that $\tilde{I}_{\mathcal{A}}\Pi_v = \Pi_v$.

Proof. If we distribute the terms in Eq. (10.97), we will get $c\tilde{\Pi}_v = \Pi_v - I_{\mathcal{A}}\Pi_v - \Pi_v I_{\mathcal{A}} + I_{\mathcal{A}}\Pi_v I_{\mathcal{A}}$ so $\tilde{\Pi}_v$ is an operator in \mathcal{A} . It is clearly self-adjoint and it squares to

$$\tilde{\Pi}_v \tilde{\Pi}_v = \frac{1}{c^2} (I - I_{\mathcal{A}}) \Pi_v (I - I_{\mathcal{A}}) \Pi_v (I - I_{\mathcal{A}}). \quad (10.98)$$

Since all Π_v are minimal, $\Pi_v (I - I_{\mathcal{A}}) \Pi_v = \Pi_v - \Pi_v I_{\mathcal{A}} \Pi_v = (1 - \alpha) \Pi_v$, where α is the proportionality factor in the minimality relation $\Pi_v I_{\mathcal{A}} \Pi_v \propto \Pi_v$, and α is not 1 because that would contradict $I_{\mathcal{A}}\Pi_v \neq \Pi_v$. Thus, for $c = 1 - \alpha$, Eq. (10.98) is equal to $\tilde{\Pi}_v$, so $\tilde{\Pi}_v$ is a projection. It is minimal because for any matrix $M \in \mathcal{A}$,

$$\tilde{\Pi}_v M \tilde{\Pi}_v = \frac{1}{c^2} (I - I_{\mathcal{A}}) \Pi_v \tilde{M} \Pi_v (I - I_{\mathcal{A}}) \quad (10.99)$$

where $\tilde{M} := (I - I_{\mathcal{A}}) M (I - I_{\mathcal{A}})$ is also in \mathcal{A} , so $\Pi_v \tilde{M} \Pi_v \propto \Pi_v$ and $\tilde{\Pi}_v M \tilde{\Pi}_v \propto \tilde{\Pi}_v$. This proves statement 1. Statement 2 follows from $(I - I_{\mathcal{A}}) \Pi_{v_k} = \Pi_{v_k} - \Pi_{v_k} = 0$ so $\tilde{\Pi}_v \Pi_{v_k} = 0$. Lastly, using the minimality of Π_v and $c = 1 - \alpha$ once again, we get

$$\tilde{\Pi}_v \Pi_v = \frac{1}{c} (I - I_{\mathcal{A}}) \Pi_v (I - I_{\mathcal{A}}) \Pi_v = (I - I_{\mathcal{A}}) \Pi_v \quad (10.100)$$

so $\tilde{I}_{\mathcal{A}}\Pi_v = I_{\mathcal{A}}\Pi_v + (I - I_{\mathcal{A}}) \Pi_v = \Pi_v$. This proves statement 3. \square

Procedure

The procedure to establish completeness is only necessary if the initial projections are not known to resolve the identity.

- 1: **procedure** ESTABLISHCOMPLETENESS(*ReflectNet*)
- 2: $MSMP \leftarrow \text{PICKMAXINDEPENDENTSET}(\textit{ReflectNet})$

```

3:   for all  $\Pi \in (\text{ReflectNet} \text{ excluding MSMP})$  do
4:     if  $\text{SUMALL}(\text{MSMP})\Pi \neq \Pi$  then
5:        $\tilde{\Pi} \leftarrow \text{CONSTRUCTCOMPLEMENTARYPROJ}(\text{MSMP}, \Pi)$ 
6:        $\text{MSMP} \leftarrow \text{ADDPROJ}(\text{MSMP}, \tilde{\Pi})$ 
7:        $\text{ReflectNet} \leftarrow \text{ADDPROJ}(\text{ReflectNet}, \tilde{\Pi})$ 
8:     end if
9:   end for
10:  return  $\text{ReflectNet}$ 
11: end procedure

```

Completeness is achieved by choosing a maximal independent set of orthogonal projections in the network $\{\Pi_{v_k}\}$,¹⁵ and testing whether $I_{\mathcal{A}} = \sum_k \Pi_{v_k}$ acts as the identity on all projections in the network. If it does, then $\{\Pi_{v_k}\}$ is the MSMP. If it does not, then for each projection such that $I_{\mathcal{A}}\Pi_v \neq \Pi_v$, we construct the complementary projection $\tilde{\Pi}_v$ as defined in Eq. (10.97) and add it to the network¹⁶ and the independent set of orthogonal projections $\{\Pi_{v_k}\}$. Lemma 10.4.8 ensures that the final set $\{\Pi_{v_k}\}$ always consists of pairwise orthogonal minimal projections in the algebra that sum to the identity, i.e. an MSMP.

Toy Example (continued)

In our example, the initial projections resolve the identity $\Pi_{Z;1} + \Pi_{Z;2} = I$, so, as expected, the maximal independent set in the reflection network of Fig. 10.2(c) is the MSMP since $\Pi_{Z;1}^{(1/2)} + \Pi_{Z;1}^{(0)} + \Pi_{Z;2}^{(1/2)} + \Pi_{Z;2}^{(0)} = I$.

In order to demonstrate how the MSMP can be constructed even if it initially is missing, we will drop $\Pi_{Z;2}$ and consider the algebra generated by $\langle \Pi_{Z;1}, \Pi_{X;1} \rangle$. As we calculated before, after scattering, we have a proper reflection network consisting of the reflecting pair $\{\Pi_{Z;1}^{(1/2)}, \Pi_{X;1}\}$ and the projection $\Pi_{Z;1}^{(0)}$ orthogonal to both; see Fig 10.3(a). The maximal independent set consists of $\{\Pi_{Z;1}^{(1/2)}, \Pi_{Z;1}^{(0)}\}$, but $I_{\mathcal{A}} := \Pi_{Z;1}^{(1/2)} + \Pi_{Z;1}^{(0)} = \Pi_{Z;1}$ does not act as the identity on $\Pi_{X;1}$. Using Eq. (10.97),

¹⁵Actually, any subset of pairwise orthogonal projections will do, but a maximal independent set is what we end up constructing anyway.

¹⁶When adding a new minimal projection to the network, we need to establish its reflection relations with all existing elements. The minimality of projections ensures that it will not trigger new scattering and breakdowns, but we do need to know which existing projections are orthogonal to the new element and which are not.

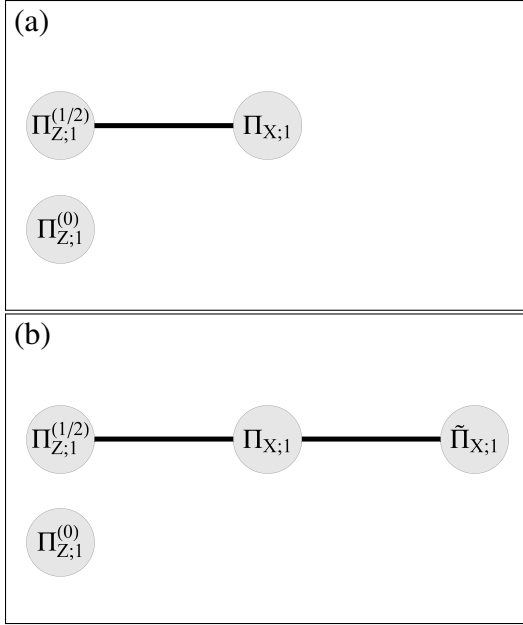


Figure 10.3: Completion of a reflection network lacking an MSMP (a), to the one that has an MSMP (b).

we construct the complementary projection in this algebra

$$\tilde{\Pi}_{X;1} := \frac{1}{c} (I - \Pi_{Z;1}) \Pi_{X;1} (I - \Pi_{Z;1}) = \frac{1}{c} \Pi_{Z;2} \Pi_{X;1} \Pi_{Z;2} = \frac{1}{c} \left(\frac{1}{2} |7\rangle \langle 7| + \frac{1}{2} |_{-}^{+56}\rangle \langle_{-}^{+56}| \right), \quad (10.101)$$

choosing $c = \frac{1}{2}$ for proper normalization, and add it to the network. The new projection $\tilde{\Pi}_{X;1}$ is orthogonal to both $\{\Pi_{Z;1}^{(1/2)}, \Pi_{Z;1}^{(0)}\}$, and is reflecting with $\Pi_{X;1}$, which results in the reflection network shown in Fig 10.3(b). Now the maximal independent set sums to $I_{\mathcal{A}} := \Pi_{Z;1}^{(1/2)} + \Pi_{Z;1}^{(0)} + \tilde{\Pi}_{X;1}$ and we can check that it acts as the identity on $\Pi_{X;1}$, so $\{\Pi_{Z;1}^{(1/2)}, \Pi_{Z;1}^{(0)}, \tilde{\Pi}_{X;1}\}$ is our MSMP.

Construction of Bipartition Tables from Minimal Projections

As discussed at the start of the section, the structure captured by a reflection network that meets the criteria of minimality and completeness can be translated into a bipartition table in the following way: the elements of an MSMP correspond to columns of the BPT. The isometries between the columns are given by the path isometries between the elements of the MSMP (minimality ensures that the particular choice of path is inconsequential). Elements of the MSMP that are not connected by any path in the network are not related by an isometry, so cannot be in the same block of the BPT. That is, distinct connected components of the reflection network correspond to distinct blocks of the BPT.

The formal construction of the BPT relies on the proof of the following lemma:

Lemma 10.4.9. *Let $\{\Pi_v\}$ be projections of a reflection network for which minimality and completeness holds, and let $\{\Pi_{v_k}\} \subseteq \{\Pi_v\}$ be an MSMP. Then, there is a BPT with the BPOs $\{S_{kl}^q\}$ such that every S_{kl}^q is a path isometry in the network and the set $\{S_{kl}^q\}$ spans the algebra $\mathcal{A} := \langle \{\Pi_v\} \rangle$.*

Proof. In order to construct the aforementioned BPT, we will first select a subset of path isometries in the network to be the BPOs.¹⁷ Let $\{\Pi_{v_k^q}\}$ be all the elements of the MSMP that belong to the connected component q and let $\Pi_{v_1^q}$ be a single, arbitrarily chosen element. We first select the path isometries $\{S_{k1}^q\}$ by arbitrarily choosing a path from $\Pi_{v_1^q}$ to each $\Pi_{v_k^q}$ for $k > 1$ and $S_{11}^q := \Pi_{v_1^q}$. We then define the BPOs for all $k, l \geq 1$ to be $S_{kl}^q := S_{k1}^q S_{l1}^{q\dagger}$ which are just path isometries from $\Pi_{v_l^q}$ to $\Pi_{v_k^q}$ that go through $\Pi_{v_1^q}$.

For each connected component q , we now construct the corresponding block of the BPT. First, we choose an orthonormal basis $\{|e_{i1}^q\rangle\}_{i=1..r_q}$ for the eigenspace of $\Pi_{v_1^q}$, where r_q is the rank of projections in the q th component. Then, we populate the first column of the block with $|e_{i1}^q\rangle$, such that i is the row index, and each subsequent column $k > 1$ is populated by the basis $|e_{ik}^q\rangle := S_{k1}^q |e_{i1}^q\rangle$. As a result,

$$S_{kl}^q = S_{k1}^q S_{l1}^{q\dagger} = S_{k1}^q \Pi_{v_1^q} S_{l1}^{q\dagger} = \sum_{i=1..r_q} S_{k1}^q |e_{i1}^q\rangle \langle e_{i1}^q| S_{l1}^{q\dagger} = \sum_{i=1..r_q} |e_{ik}^q\rangle \langle e_{il}^q|, \quad (10.102)$$

so $\{S_{kl}^q\}$ are indeed the BPOs of this block of the BPT.

Since \mathcal{A} is spanned by products of $\{\Pi_v\}$ which are proportional to path isometries $\{S_v\}$, it suffices to show that every S_v is spanned by $\{S_{kl}^q\}$ in order to show that $\{S_{kl}^q\}$ spans \mathcal{A} . If $\{\Pi_{v_k^q}\}$ is a MSMP, then by definition $I_{\mathcal{A}} = \sum_{q,k} \Pi_{v_k^q}$ is the identity of the algebra and

$$S_v = I_{\mathcal{A}} S_v I_{\mathcal{A}} = \sum_{kl} \Pi_{v_k^q} S_v \Pi_{v_l^q}, \quad (10.103)$$

where q is the connected component that contains the path v . Every non-vanishing term $\Pi_{v_k^q} S_v \Pi_{v_l^q}$ is proportional to the path isometry $S_{(v_k^q, v, v_l^q)}$ from $\Pi_{v_l^q}$ to $\Pi_{v_k^q}$ along the path v . Furthermore, if minimality holds, then according to Lemma 10.4.6 path isometries are path-independent, so $S_{(v_k^q, v, v_l^q)} \propto S_{kl}^q$. Therefore, either

¹⁷It should be noted that the selection of BPOs is not unique and depends on the arbitrary selection of paths between the elements of the MSMP. This freedom, however, only changes the individual BPOs by a constant factor, which does not affect the generalized bipartition structure captured by the BPT.

$\Pi_{v_k^q} S_v \Pi_{v_l^q} = 0$ or $\Pi_{v_k^q} S_v \Pi_{v_l^q} \propto S_{kl}^q$, so Eq. (10.103) implies that S_v is in the span of $\{S_{kl}^q\}$. \square

The practical takeaway from this lemma is that in order to construct the BPT of an algebra generated by a reflection network, we need to (arbitrarily) pick a basis $\{|e_{i1}^q\rangle\}_{i=1..r_q}$ for the eigenspace of a single MSMP element $\Pi_{v_1^q}$ in each connected component q , and map those basis elements to the eigenspaces of the rest of MSMP $\{\Pi_{v_k^q}\}$ in q using (arbitrarily chosen) path isometries $\{S_{k1}^q\}$. The resulting set $\{|e_{ik}^q\rangle\}$ are the basis elements that reside in block q , row i , column k of the BPT.

Procedure

The procedure for constructing the BPT is essentially what we did in the proof of Lemma 10.4.9

```

1: procedure CONSTRUCTIRREPBASIS(ReflectNet)
2:   BPT  $\leftarrow$  {}
3:   for all ConnComp  $\subseteq$  ReflectNet do
4:     Block  $\leftarrow$  {}
5:     MaxIndepSet  $\leftarrow$  PICKMAXINDEPENDENTSET(ConnComp)
6:      $\Pi_1$   $\leftarrow$  PICKANYELEMENT(MaxIndepSet)
7:     FirstColumnBasis  $\leftarrow$  CONSTRUCTEIGENBASIS( $\Pi_1$ )
8:     Block  $\leftarrow$  ADDCOLUMN(Block, FirstColumnBasis)
9:     for all  $\Pi_{k \neq 1} \in$  MaxIndepSet do
10:       $S_{k1}$   $\leftarrow$  CONSTRUCTPATHISOMETRY(ConnComp,  $\Pi_1$ ,  $\Pi_k$ )
11:      NewColumnBasis  $\leftarrow$  MAPBASIS( $S_{k1}$ , FirstColumnBasis)
12:      Block  $\leftarrow$  ADDCOLUMN(Block, NewColumnBasis)
13:     end for
14:     BPT  $\leftarrow$  ADDBLOCK(BPT, Block)
15:   end for
16:   return BPT
17: end procedure

```

For each connected component, the procedure chooses a maximal independent set of orthogonal projections, which is the subset of the MSMP in the component, and uses it to construct the columns of a single block of the BPT. In order to construct the block, it arbitrarily picks a single projection Π_1 in the MSMP and arbitrarily constructs the basis that span its eigenspace; these basis become the first column

of the block. The rest of the columns are constructed by picking each of $\Pi_{k \neq 1}$ in the MSMP and constructing a path isometry S_{k1} from the eigenspace of Π_1 to Π_k . The path isometry S_{k1} is then used to map the elements of the first column to the elements of the k th column. Once each block is constructed, it is added to the BPT.

Toy Example (continued)

In the reflection network of Fig. 10.2(c), there are three connected components, but two of them, $\{\Pi_{Z;1}^{(0)}\}$ and $\{\Pi_{Z;2}^{(0)}\}$, consist of a single projection which correspond to blocks with a single column. Arbitrarily choosing to use the same basis as we have

used before, these single column blocks are $\begin{bmatrix} 4 \\ +1 \\ -2 \end{bmatrix}$ and $\begin{bmatrix} 8 \\ +5 \\ -6 \end{bmatrix}$.

For the remaining block, we identify $\{\Pi_{Z;1}^{(1/2)}, \Pi_{Z;2}^{(1/2)}\}$ to be the block's maximal independent set. We pick $\Pi_{Z;1}^{(1/2)}$ to be the projection associated with the first

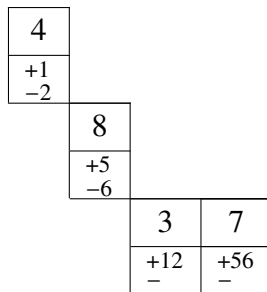
column and we pick its basis to be $\begin{bmatrix} 3 \\ +12 \\ - \end{bmatrix}$. The path isometry that maps the first

column to the second column associated with $\Pi_{Z;2}^{(1/2)}$ is constructed by taking the only simple path between them (we have fixed the normalization after the fact)

$$S_{21} \propto \Pi_{Z;2}^{(1/2)} \Pi_{X;1} \Pi_{Z;1}^{(1/2)} = \frac{1}{2} |7\rangle \langle 3| + \frac{1}{2} |_{-}^{+56}\rangle \langle_{-}^{+12}|. \tag{10.104}$$

Then, by mapping the first column using this isometry, we get the second column

$\begin{bmatrix} 7 \\ +56 \\ - \end{bmatrix}$.¹⁸ Combining all the columns into blocks completes the construction of the BPT,



¹⁸Although we already identified this basis when we first wrote the projection $\Pi_{Z;2}^{(1/2)}$, we could not know *a priori* how the path isometry would map the eigenbasis between projections. It is only due to the simplicity of this toy example that the basis we used to express the projections after scattering ended up as the basis in the BPT.

The above BPT tells us that the Hilbert space decomposes into irreps as

$$\mathcal{H} = \mathcal{H}_{A_1} \oplus \mathcal{H}_{A_2} \oplus \mathcal{H}_{A_3} \otimes \mathcal{H}_{B_3}, \quad (10.105)$$

where A_q are the subsystems associated with the multiplicity of irreps and B_q are the subsystems on which the algebra acts irreducibly. In this case, blocks 1 and 2 (the single column blocks) specify one-dimensional irreps, so the one-dimensional subsystems $B_{q=1,2}$ are absorbed into the two-dimensional multiplicities $A_{q=1,2}$. The last block specifies a two dimensional irrep B_3 , with a two-dimensional multiplicity A_3 .

According to Theorem 10.2.2, with respect to this irrep decomposition, all operators in the algebra are of the form

$$M = c_1 I_{A_1} + c_2 I_{A_2} + I_{A_3} \otimes M_{B_3} \quad (10.106)$$

for any scalars c_1, c_2 , and 2×2 matrices M_{B_3} . In particular, the generators $\{Z, X\}$ can also be presented in this form. To see this explicitly, we change the original basis into the irrep basis given by the BPT (reading the BPT from left to right, top to bottom)

$$\{|1\rangle, |2\rangle, |3\rangle, |4\rangle, |5\rangle, |6\rangle, |7\rangle, |8\rangle\} \mapsto \{|4\rangle, |_{-2}^{+1}\rangle, |8\rangle, |_{-6}^{+5}\rangle, |3\rangle, |7\rangle, |_{-}^{+12}\rangle, |_{-}^{+56}\rangle\}. \quad (10.107)$$

Assuming $Z = a\Pi_{Z;1} + b\Pi_{Z;2}$ and $X = c\Pi_{X;1} + d\Pi_{X;2}$, for some eigenvalues a, b, c, d , we re-express their matrices using the irrep basis, thus simultaneously

is then given by reinterpreting the basis $|e_{ik}^q\rangle$ as the product basis $|a_i^q\rangle|b_k^q\rangle$ of $\mathcal{H}_{A_q} \otimes \mathcal{H}_{B_q}$ (formally, we will define the isometry $V := \sum_{q,i,k} |a_i^q\rangle|b_k^q\rangle\langle e_{ik}^q|$ that maps \mathcal{H} into $\bigoplus_q \mathcal{H}_{A_q} \otimes \mathcal{H}_{B_q}$ and thus specifies the decomposition).

With the procedures defined in the previous subsections, the top-level procedure of the algorithm is as follows:

Algorithm 1 Irrep decomposition of matrix algebra

```

1: procedure IRREPDECOMPOSITION( $\mathcal{M}$ )
2:    $SpecProjs \leftarrow$  GETALLSPECTRALPROJECTIONS( $\mathcal{M}$ )
3:    $ReflectNet \leftarrow$  SCATTERALLPROJECTIONS( $SpecProjs$ )
4:    $ReflectNet \leftarrow$  ESTABLISHMINIMALITY( $ReflectNet$ )
5:    $ReflectNet \leftarrow$  ESTABLISHCOMPLETENESS( $ReflectNet$ )
6:    $BPT \leftarrow$  CONSTRUCTIRREPBASIS( $ReflectNet$ )
7:   return  $BPT$ 
8: end procedure

```

The algorithm returns a BPT since this is the natural data structure to organize the irrep basis.

The correctness of this algorithm follows from the proof of the following theorem:

Theorem 10.4.10. *Let \mathcal{H} be a finite-dimensional Hilbert space, $\mathcal{M} \subseteq \mathcal{L}(\mathcal{H})$ a finite set of self-adjoint matrices, and $\mathcal{A} := \langle \mathcal{M} \rangle$ the matrix algebra generated by \mathcal{M} . Then, Algorithm 1 produces the basis $\{|e_{ik}^q\rangle\}$ of \mathcal{H} such that the isometry $V := \sum_{q,i,k} |a_i^q\rangle|b_k^q\rangle\langle e_{ik}^q|$ explicitly specifies the irrep decomposition*

$$\mathcal{H} \cong \bigoplus_q \mathcal{H}_{A_q} \otimes \mathcal{H}_{B_q} \quad (10.111)$$

defined in Theorem 10.2.2 for the algebra \mathcal{A} .

Proof. From Proposition 10.2.5, we know that for each $M \in \mathcal{M}$, the spectral projections of M generate the algebra $\langle M \rangle$ so the set of projections produced by GETALLSPECTRALPROJECTIONS generates \mathcal{A} .

During the procedure SCATTERALLPROJECTIONS, we break down pairs of projections $\{\Pi_1, \Pi_2\}$ by the scattering operation as defined in Definition 10.4.1. The resulting projections $\{\Pi_1^{(\lambda)}, \Pi_2^{(\lambda)}\}$ are in the algebra generated by $\{\Pi_1, \Pi_2\}$ because – again using Proposition 10.2.5 – they are the spectral projections of the operators $\Pi_i \Pi_j \Pi_i$ that are in the algebra generated by $\{\Pi_1, \Pi_2\}$ (for null elements $\Pi_i^{(0)}$ it is true by the

definition of Eq. (10.64)). Conversely, the predecessor projections $\{\Pi_1, \Pi_2\}$ are in the algebra generated by $\{\Pi_1^{(\lambda)}, \Pi_2^{(\lambda)}\}$ because each $\{\Pi_i^{(\lambda)}\}$ sums to Π_i . Therefore, the elements $\{\Pi_1, \Pi_2\}$ before, and the elements $\{\Pi_1^{(\lambda)}, \Pi_2^{(\lambda)}\}$ after scattering, generate the same algebra. So, after every iteration of scattering, the resulting reflection network generates the same algebra \mathcal{A} as before.

The procedure SCATTERALLPROJECTIONS keeps track of the known and unknown reflection relations as the network evolves, so when it stops, all pairs of projections must be reflecting. This procedure is guaranteed to stop because, according to Lemma 10.4.4, every scattering iteration either identifies a previously unknown reflecting pair, or the pair scatters into a series of reflecting pairs of lower rank. Eventually, all projections will either be reflecting or they will be reduced to rank 1 and then they must again be reflecting. Therefore, the procedure SCATTERALLPROJECTIONS produces, in a finite number of iterations, a proper reflection network that consists of projections that generate \mathcal{A} .

The procedure ESTABLISHMINIMALITY establishes that all elements of a proper reflection network are minimal projections of the algebra \mathcal{A} by checking the condition of minimality given by Lemma 10.4.6.

The procedure ESTABLISHCOMPLETENESS completes the maximal orthogonal set of projections in the reflection network to an MSMP as prescribed by Lemma 10.4.8.

At this point, we have a reflection network that generates \mathcal{A} and is known to be minimal and complete, so the conditions of Lemma 10.4.9 hold. The procedure CONSTRUCTIRREPBASIS constructs the basis $\{|e_{ik}^q\rangle\}$ according to the procedure described in the proof of Lemma 10.4.9, so the partial isometries

$$S_{kl}^q := \sum_i |e_{ik}^q\rangle \langle e_{il}^q| \quad (10.112)$$

are the path isometries given by that Lemma that span the algebra \mathcal{A} .

With respect to the decomposition (10.111) specified by the isometry $V := \sum_{q,i,k} |a_i^q\rangle |b_k^q\rangle \langle e_{ik}^q|$, the operators S_{kl}^q take the form

$$VS_{kl}^q V^\dagger = \sum_i |a_i^q\rangle |b_k^q\rangle \langle a_i^q| \langle b_l^q| = I_{A_q} \otimes |b_k^q\rangle \langle b_l^q|, \quad (10.113)$$

so they span all matrices of the form

$$M = \bigoplus_q I_{A_q} \otimes M_{B_q}. \quad (10.114)$$

Therefore, with respect to the decomposition (10.111), the algebra

$$\mathcal{A} = \text{span} \{S_{kl}^q \cong I_{A_q} \otimes |b_k^q\rangle \langle b_l^q|\} \quad (10.115)$$

consists of all, and only, the matrices of the form (10.114), as promised by Theorem 10.2.2. \square

10.5 Examples of State Reduction via Irrep Decomposition of Operational Constraints

Particle with Orbital and Spin Angular Momentum

Here, we consider a single particle with orbital angular momentum l and spin $1/2$. In light of our discussion in Section 10.3, we would like to know how the quantum state of the particle reduces if operationally we cannot distinguish between spin and orbital angular momentum and are constrained to measurements of total angular momentum. This question, of course, can be addressed with the standard formalism of group representation theory (or “addition of angular momentum” as it is called in physics textbooks). From this formalism, we know that the total angular momentum operators are reducible and split the Hilbert space of a spin-orbit particle into $l + 1/2$ and $l - 1/2$ sectors of total angular momentum, which are captured by Clebsch-Gordan coefficients. We will now show that the same conclusion can be reached, including the particular Clebsch-Gordan coefficients, without relying on the formalism of angular momentum addition, but by instead using the scattering of projections as described in Section 10.4.

The Hilbert space of a spin $1/2$ particle with orbital angular momentum l is the tensor product $\mathcal{H}_L \otimes \mathcal{H}_S$ of orbital and spin degrees of freedom of dimensions $2l + 1$ and 2 respectively. The total angular momentum component along the r axis (where r can stand for any direction) is given by the operator

$$J_r := L_r \otimes I + I \otimes S_r, \quad (10.116)$$

where L_r and S_r are the operators of orbital angular momentum and spin along r . Given our operational constraints, we should look for the irrep structure of the algebra $\langle\{J_r\}\rangle$ where r assumes all directions.

We will denote with $|r; m_L, m_S\rangle$ the simultaneous eigenstates of $L_r \otimes I$ and $I \otimes S_r$ with the eigenvalues $m_L = -l, \dots, l$ and $m_S = \pm \frac{1}{2}$ respectively; we will call these states the spin-orbit basis. Then, since $J_r |r; m_L, m_S\rangle = m_J |r; m_L, m_S\rangle$ where $m_J = m_L + m_S$,

the spectral decomposition of J_r is given by

$$J_r = \sum_{m_J = -l - \frac{1}{2}}^{l + \frac{1}{2}} m_J \Pi_{r; m_J} \quad (10.117)$$

and the spectral projections are

$$\Pi_{r; m_J} := \begin{cases} |r; \pm l, \pm \frac{1}{2}\rangle \langle r; \pm l, \pm \frac{1}{2}| & |m_J| = l + \frac{1}{2} \\ \sum_{m_S = \pm 1/2} |r; m_J - m_S, m_S\rangle \langle r; m_J - m_S, m_S| & |m_J| < l + \frac{1}{2}. \end{cases} \quad (10.118)$$

Note that two of the spectral projections (with $|m_J| = l + \frac{1}{2}$) are rank 1 and the rest are rank 2.

The algebra generated by $\{J_r\}$, for all r , is also generated by just the two operators $\{J_z, J_x\}$. This is because the rotations $e^{-i\theta J_x}$ and $e^{-i\varphi J_z}$ are elements of the algebra $\langle J_z, J_x \rangle$ and every J_r can be produced by rotating $e^{-i\varphi J_z} e^{-i\theta J_x} J_z e^{i\theta J_x} e^{i\varphi J_z}$ with the appropriate angles θ, φ . Therefore, in order to find the irrep structure of the algebra $\langle \{J_r\} \rangle$, it is sufficient to consider the algebra generated by the spectral projections $\{\Pi_{z; m_J}, \Pi_{x; m_J}\}$ of $\{J_z, J_x\}$. In the following, we denote with r the variable that takes the values of the two axis z, x and similarly for the capitalized version $R = Z, X$, which we will later use to label states.

The initial improper reflection network consists of all projections $\{\Pi_{z; m_J}, \Pi_{x; m_J}\}$ for $m_J = -l - \frac{1}{2}, \dots, l + \frac{1}{2}$. Our scattering strategy will be to take the rank 1 projection $\Pi_{x; l + \frac{1}{2}}$ and use it to break all the rank 2 projections $\Pi_{z; m_J}$, and similarly, take the rank 1 projection $\Pi_{z; -l - \frac{1}{2}}$ and use it to break all the rank 2 projections $\Pi_{x; m_J}$.²⁰ These scatterings will result in all projections reducing to rank 1, so the reflection network becomes proper and minimal. After that, we will only have to identify the connected components of this network.

The scattering of the pairs $\Pi_{z; m_J}, \Pi_{x; l + \frac{1}{2}}$ and $\Pi_{x; m_J}, \Pi_{z; -l - \frac{1}{2}}$ comes down to the spectral decomposition of

$$\Pi_{z; m_J} \Pi_{x; l + \frac{1}{2}} \Pi_{z; m_J} = \Pi_{z; m_J} |x; l, \frac{1}{2}\rangle \langle x; l, \frac{1}{2}| \Pi_{z; m_J} \quad (10.119)$$

$$\Pi_{x; m_J} \Pi_{z; -l - \frac{1}{2}} \Pi_{x; m_J} = \Pi_{x; m_J} |z; -l, -\frac{1}{2}\rangle \langle z; -l, -\frac{1}{2}| \Pi_{x; m_J}. \quad (10.120)$$

²⁰The strategy of choosing the scattering pairs is not important from the perspective of the raw algorithm we presented in the previous section, but it does make a difference in how hard it is to carry it out analytically, as we are doing here.

Since $\Pi_{r;\pm l \pm \frac{1}{2}}$ ($r = x, z$) are rank 1, they do not break, so we only need to figure out how the remaining $\Pi_{r;m_J}$ break in these scatterings. For that purpose, we define the following states and the associated projections

$$|Z; l + \frac{1}{2}, m_J\rangle := \frac{1}{\sqrt{N_{m_J}}} \Pi_{z;m_J} |x; l, \frac{1}{2}\rangle \quad \Pi_{z;m_J}^{(l+\frac{1}{2})} := |Z; l + \frac{1}{2}, m_J\rangle \langle Z; l + \frac{1}{2}, m_J| \quad (10.121)$$

$$|X; l + \frac{1}{2}, m_J\rangle := \frac{1}{\sqrt{N_{m_J}}} \Pi_{x;m_J} |z; -l, -\frac{1}{2}\rangle \quad \Pi_{x;m_J}^{(l+\frac{1}{2})} := |X; l + \frac{1}{2}, m_J\rangle \langle X; l + \frac{1}{2}, m_J| \quad (10.122)$$

with the (unimportant) normalization factor $\sqrt{N_{m_J}}$. The capitalized labels Z, X of the axis symbolize the fact that these are the eigenstates of total angular momentum with eigenvalue $l + \frac{1}{2}$, as we will see shortly. The scatterings can then be expressed as

$$\Pi_{z;m_J} \Pi_{x;l+\frac{1}{2}} \Pi_{z;m_J} = N_{m_J} \Pi_{z;m_J}^{(l+\frac{1}{2})} \quad (10.123)$$

$$\Pi_{x;m_J} \Pi_{z;-l-\frac{1}{2}} \Pi_{x;m_J} = N_{m_J} \Pi_{x;m_J}^{(l+\frac{1}{2})}, \quad (10.124)$$

so the rank 1 projections $\Pi_{r;m_J}^{(l+\frac{1}{2})}$ are one of the spectral projections that come out of scattering, corresponding to the eigenvalue N_{m_J} . For $|m_J| = l + \frac{1}{2}$, there is no additional spectral projection since the projections $\Pi_{r;\pm l \pm \frac{1}{2}}$ are rank 1 and they do not break, so $\Pi_{r;\pm l \pm \frac{1}{2}} = \Pi_{r;\pm l \pm \frac{1}{2}}^{(l+\frac{1}{2})}$, or equivalently, $|R; l + \frac{1}{2}, \pm(l + \frac{1}{2})\rangle = |r; \pm l, \pm \frac{1}{2}\rangle$. For $|m_J| < l + \frac{1}{2}$, the second spectral projection is given by $\Pi_{r;m_J} - \Pi_{r;m_J}^{(l+\frac{1}{2})}$ and it corresponds to the eigenvalue 0. Since this is just the projection on the orthogonal complement of $|R; l + \frac{1}{2}, m_J\rangle$ in the eigenspace of $\Pi_{r;m_J}$, we will have to identify the orthogonal complements of the states $|R; l + \frac{1}{2}, m_J\rangle$.

Using their definition above, the states $|Z; l + \frac{1}{2}, m_J\rangle$, for $|m_J| < l + \frac{1}{2}$, can be expressed (without worrying about the normalization) as

$$|Z; l + \frac{1}{2}, m_J\rangle \propto \Pi_{z;m_J} |x; l, \frac{1}{2}\rangle \quad (10.125)$$

$$= \sum_{m_S=\pm 1/2} |z; m_J - m_S, m_S\rangle \langle z; m_J - m_S, m_S|x; l, \frac{1}{2} \quad (10.126)$$

$$\propto |z; m_J - \frac{1}{2}, \frac{1}{2}\rangle d_{m_J-\frac{1}{2}, l}^l \left(\frac{\pi}{2}\right) + |z; m_J + \frac{1}{2}, -\frac{1}{2}\rangle d_{m_J+\frac{1}{2}, l}^l \left(\frac{\pi}{2}\right). \quad (10.127)$$

Here, we have used the Wigner's "small" d-matrix element [254] $d_{m_J - m_S, l}^l\left(\frac{\pi}{2}\right)$ that is obtained from the orbital part of the inner product (the spin part gives $1/\sqrt{2}$ which we disregard as a normalization factor). In particular, the specific d-matrix elements we need are given by

$$d_{m_J \mp \frac{1}{2}, l}^l\left(\frac{\pi}{2}\right) = \left(\frac{1}{\sqrt{2}}\right)^{2l} \sqrt{\binom{2l}{l - m_J \pm \frac{1}{2}}} \quad (10.128)$$

so, using this expression and normalizing, we obtain the state

$$\begin{aligned} |Z; l + \frac{1}{2}, m_J\rangle &= |z; m_J - \frac{1}{2}, \frac{1}{2}\rangle \sqrt{\frac{l - m_J - \frac{1}{2}}{2l + 1}} + |z; m_J + \frac{1}{2}, -\frac{1}{2}\rangle \sqrt{\frac{l - m_J + \frac{1}{2}}{2l + 1}} \\ &= |z; m_J - \frac{1}{2}, \frac{1}{2}\rangle c_-^{l+1, m_J} + |z; m_J + \frac{1}{2}, -\frac{1}{2}\rangle c_+^{l+1, m_J}. \end{aligned}$$

The coefficients $c_{\pm}^{l+1, m_J} := \sqrt{\frac{l - m_J \pm \frac{1}{2}}{2l + 1}}$ are the well-known Clebsch-Gordan coefficients that arise in spin-orbit coupling, so we know the states $|Z; l + \frac{1}{2}, m_J\rangle$ are the states of total angular momentum $l + 1/2$ with m_J component along the z axis. Its orthogonal complement in the two-dimensional subspace spanned by $\{|z; m_J - \frac{1}{2}, \frac{1}{2}\rangle, |z; m_J + \frac{1}{2}, -\frac{1}{2}\rangle\}$ is just the antipodal point of $|Z; l + \frac{1}{2}, m_J\rangle$ on the Bloch sphere:

$$|Z; l - \frac{1}{2}, m_J\rangle := |z; m_J - \frac{1}{2}, \frac{1}{2}\rangle c_+^{l+1, m_J} - |z; m_J + \frac{1}{2}, -\frac{1}{2}\rangle c_-^{l+1, m_J}. \quad (10.129)$$

With this arrangement of Clebsch-Gordan coefficients, these states are the states of total angular momentum $l - 1/2$ with m_J component along the z axis.

The same characterization for the $|X; l + \frac{1}{2}, m_J\rangle$ states can be derived from the observation

$$|X; l + \frac{1}{2}, m_J\rangle = \frac{1}{\sqrt{N_{m_J}}} \Pi_{x; m_J} |z; -l, -\frac{1}{2}\rangle \quad (10.130)$$

$$= \frac{1}{\sqrt{N_{m_J}}} e^{-i\frac{\pi}{2}J_y} \Pi_{z; m_J} e^{i\frac{\pi}{2}J_y} e^{-i\frac{\pi}{2}J_y} |x; l, \frac{1}{2}\rangle \quad (10.131)$$

$$= e^{-i\frac{\pi}{2}J_y} |Z; l + \frac{1}{2}, m_J\rangle \quad (10.132)$$

so their orthogonal complements are

$$|X; l - \frac{1}{2}, m_J\rangle := e^{-i\frac{\pi}{2}J_y} |Z; l - \frac{1}{2}, m_J\rangle. \quad (10.133)$$

With the rank 1 projections $\Pi_{r;m_J}^{(l-\frac{1}{2})}$ on the states $|R; l - \frac{1}{2}, m_J\rangle$, we can finally conclude that for $|m_J| < l + \frac{1}{2}$, the projections $\Pi_{z;m_J}$ break into $\Pi_{z;m_J}^{(l+\frac{1}{2})} + \Pi_{z;m_J}^{(l-\frac{1}{2})}$ and $\Pi_{x;m_J}$ break into $\Pi_{x;m_J}^{(l+\frac{1}{2})} + \Pi_{x;m_J}^{(l-\frac{1}{2})}$. The resulting reflection network consists of the projections $\left\{ \Pi_{z;m_J}^{(l+\frac{1}{2})}, \Pi_{x;m_J}^{(l+\frac{1}{2})}, \Pi_{z;m_J}^{(l-\frac{1}{2})}, \Pi_{x;m_J}^{(l-\frac{1}{2})} \right\}$ for $m_J = -l - \frac{1}{2}, \dots, l + \frac{1}{2}$ where the four projections $\Pi_{z;\pm l \pm \frac{1}{2}}^{(l+\frac{1}{2})}, \Pi_{x;\pm l \pm \frac{1}{2}}^{(l+\frac{1}{2})}$ (for $|m_J| = l + \frac{1}{2}$) are just relabeled $\Pi_{z;\pm l \pm \frac{1}{2}}, \Pi_{x;\pm l \pm \frac{1}{2}}$ and the rest are the result of scatterings. Since all projections are rank 1, this is a proper minimal reflection network.

From the fact that $|X; l \pm \frac{1}{2}, m_J\rangle = e^{-i\frac{\pi}{2}J_y} |Z; l \pm \frac{1}{2}, m_J\rangle$ and that states of different total angular momentum are orthogonal to each other, it should be clear that all $\left\{ \Pi_{z;m_J}^{(l+\frac{1}{2})}, \Pi_{x;m_J}^{(l+\frac{1}{2})} \right\}$ are orthogonal to all $\left\{ \Pi_{z;m_J}^{(l-\frac{1}{2})}, \Pi_{x;m_J}^{(l-\frac{1}{2})} \right\}$. At the same time, all $\left\{ \Pi_{z;m_J}^{(l+\frac{1}{2})} \right\}$ are properly reflecting with all $\left\{ \Pi_{x;m_J}^{(l+\frac{1}{2})} \right\}$ and similarly for $l - \frac{1}{2}$. Therefore, the reflection network has two connected components for $l + \frac{1}{2}$ and $l - \frac{1}{2}$. We choose the maximal independent sets in the connected components to be $\left\{ \Pi_{z;m_J}^{(l+\frac{1}{2})} \right\}$ and $\left\{ \Pi_{z;m_J}^{(l-\frac{1}{2})} \right\}$. Since all projections are rank 1, there is no freedom in the alignment of columns in the BPT; it is just two blocks with a single row of eigenbasis of $\left\{ \Pi_{z;m_J}^{(l+\frac{1}{2})} \right\}$ and $\left\{ \Pi_{z;m_J}^{(l-\frac{1}{2})} \right\}$:

$l + \frac{1}{2}, l + \frac{1}{2}$	\cdots	$l + \frac{1}{2}, -l - \frac{1}{2}$			
			$l - \frac{1}{2}, l - \frac{1}{2}$	\cdots	$l - \frac{1}{2}, -l + \frac{1}{2}$

Each cell corresponds to the state $|Z; l \pm \frac{1}{2}, m_J\rangle$, where we have suppressed the Z axis label.

The resulting Hilbert space decomposition

$$\mathcal{H}_L \otimes \mathcal{H}_S \cong \mathcal{H}^{(l+\frac{1}{2})} \oplus \mathcal{H}^{(l-\frac{1}{2})} \quad (10.134)$$

indicates that the restriction to total angular momentum measurements will result in a superselection between the two total angular momentum sectors. The accessible state is therefore obtained, according to Eq. (10.53) of Section 10.3, from the state-

reduction map

$$\rho \longmapsto \Pi^{(l+\frac{1}{2})} \rho \Pi^{(l+\frac{1}{2})} + \Pi^{(l-\frac{1}{2})} \rho \Pi^{(l-\frac{1}{2})}, \quad (10.135)$$

where $\Pi^{(l\pm\frac{1}{2})}$ are projections on the sectors $\mathcal{H}^{(l\pm\frac{1}{2})}$. So the coherence terms between total angular momentum sectors are unobservable if only total angular momentum measurements are allowed.

This conclusion is of course not surprising if we know the theory of angular momentum addition. But, the fact that the same result, including the explicit derivation of the total angular momentum states $|Z; l \pm \frac{1}{2}, m_J\rangle$ in the spin-orbit basis, can be obtained by scattering of projections, is a strong confirmation of the viability of this approach to derivation of irreps. In the next example, we will consider a case where the group representation theory is not as well developed, yet the projection-scattering method yields the irrep decomposition in a straight forward way.

A Bound Pair of Particles on a Lattice

In this example, we consider a periodic one-dimensional lattice of length D with two identical particles on it. The two particles are assumed to be bound in the sense that their relative position and relative momentum cannot exceed 1 lattice site. This is a simple toy model for a bound pair of particles on a lattice that oscillate around a common center of mass with limited energy. The operational constraint that we will consider is the inability to resolve the composite pair as two separate particles, which is manifested by a restriction to the center of mass measurements $\{X_{cm}, P_{cm}\}$ of both position and momentum. Once again, as was discussed in Section 10.3, the main challenge is to find the irrep structure of the algebra $\langle X_{cm}, P_{cm} \rangle$.

The D^2 dimensional Hilbert space $\mathcal{H}_1 \otimes \mathcal{H}_2$ is spanned by the position basis $|x; n_1, n_2\rangle$ for $n_i = 0, \dots, D-1$. The momentum basis states $|p; m_1, m_2\rangle$ are related to the position basis via the lattice Fourier transform

$$|p; m_1, m_2\rangle := F |x; m_1, m_2\rangle = \frac{1}{D} \sum_{n_1, n_2=0}^{D-1} e^{i2\pi(m_1 n_1 + m_2 n_2)/D} |x; n_1, n_2\rangle. \quad (10.136)$$

The center of mass operators are given by

$$X_{cm} := \frac{1}{2} (X_1 \otimes I_2 + I_1 \otimes X_2) \quad (10.137)$$

$$P_{cm} := \frac{1}{2} (P_1 \otimes I_2 + I_1 \otimes P_2), \quad (10.138)$$

where X_i, P_i are the position and momentum operators on each particle. In general, $X_{cm} |x; n_1, n_2\rangle = n_{cm} |x; n_1, n_2\rangle$ where $n_{cm} = (n_1 + n_2) / 2$, but, assuming that the particles cannot occupy the same lattice site simultaneously,²¹ in the bound state we have $n_2 = n_1 \pm 1$ so $n_{cm} = n_1 \pm 1/2$. For a shorter notation, we will use the integer n instead of the half-integer n_{cm} related by $n_{cm} = n + 1/2$. Then, for each possible eigenvalue n_{cm} for bound particles, there are two possible eigenstates $|x; n, n + 1\rangle$ and $|x; n + 1, n\rangle$. The same notation applies to P_{cm} .

Therefore, the spectral projections of X_{cm} and P_{cm} , when considering bound particles that cannot occupy the same site, are given by

$$\Pi_{x;n} := |x; n, n + 1\rangle \langle x; n, n + 1| + |x; n + 1, n\rangle \langle x; n + 1, n| \quad (10.139)$$

$$\Pi_{p;m} := |p; m, m + 1\rangle \langle p; m, m + 1| + |p; m + 1, m\rangle \langle p; m + 1, m| \quad (10.140)$$

for $n, m = 0, \dots, D - 1$ and the summation is modulo D . The algebra $\langle X_{cm}, P_{cm} \rangle$ is then generated by the improper reflection network of $\{\Pi_{x;n}, \Pi_{p;m}\}$, which we will now reduce to a proper network by scattering of projections.

The result of scattering of any pair of projections $\{\Pi_{x;n}, \Pi_{p;m}\}$ depends on the spectral decomposition of $\Pi^{n;x} \Pi^{m;p} \Pi^{n;x}$. For this calculation, we first define the states

$$|\chi_n(\varphi)\rangle := \frac{1}{\sqrt{2}} (|x; n, n + 1\rangle + e^{i\varphi} |x; n + 1, n\rangle) \quad (10.141)$$

$$|\psi_m(\varphi)\rangle := \frac{1}{\sqrt{2}} (|p; m, m + 1\rangle + e^{i\varphi} |p; m + 1, m\rangle). \quad (10.142)$$

Then, using the Fourier transform of Eq. (10.136), we derive

$$\Pi_{x;n} \Pi_{p;m} \Pi_{x;n} = \Pi_{x;n} |p; m, m + 1\rangle \langle p; m, m + 1| \Pi_{x;n} + \Pi_{x;n} |p; m + 1, m\rangle \langle p; m + 1, m| \Pi_{x;n} \quad (10.143)$$

$$= \frac{2}{D^2} |\chi_n\left(-\frac{2\pi}{D}\right)\rangle \langle \chi_n\left(-\frac{2\pi}{D}\right)| + \frac{2}{D^2} |\chi_n\left(\frac{2\pi}{D}\right)\rangle \langle \chi_n\left(\frac{2\pi}{D}\right)|. \quad (10.144)$$

The two states $|\chi_n\left(\pm\frac{2\pi}{D}\right)\rangle$ are not orthogonal to each other, so this is not yet the spectral decomposition. One can check that the eigenstates of $\Pi_{x;n} \Pi_{p;m} \Pi_{x;n}$ are

²¹We refrain from calling the particles fermions because we have no reason to assume that their states must be anti-symmetric under particle exchange.

$|\chi_n(0)\rangle$ and $|\chi_n(\pi)\rangle$ with the distinct eigenvalues $\frac{2}{D^2} \left(1 \pm \cos\left(\frac{2\pi}{D}\right)\right)$. (One can also visualize this fact using the representation of $|\chi_n(\pm\frac{2\pi}{D})\rangle$ as two vectors in the $x-y$ plane of the Bloch sphere of the qubit spanned by $|x;n,n+1\rangle$ and $|x;n+1,n\rangle$.) Thus, the projection $\Pi_{x;n}$ breaks into $\Pi_{x;n}^{(0)} + \Pi_{x;n}^{(\pi)}$, where $\Pi_{x;n}^{(\varphi)} := |\chi_n(\varphi)\rangle \langle \chi_n(\varphi)|$, and this result does not depend on the m argument of $\Pi_{p;m}$. A similar calculation for the scattering of $\Pi_{p;m}$ via the spectral decomposition of $\Pi_{p;m}\Pi_{x;n}\Pi_{p;m}$, results in it breaking into $\Pi_{p;m}^{(0)} + \Pi_{p;m}^{(\pi)}$ where $\Pi_{p;m}^{(\varphi)} := |\psi_m(\varphi)\rangle \langle \psi_m(\varphi)|$.

Therefore, by scattering all (arbitrarily chosen) pairs $\Pi_{x;n}, \Pi_{p;m}$, the initial reflection network reduces to $\left\{\Pi_{x;n}^{(0)}, \Pi_{x;n}^{(\pi)}, \Pi_{p;m}^{(0)}, \Pi_{p;m}^{(\pi)}\right\}$ for $n, m = 0, \dots, D-1$. Since now all projections are rank 1, the network is again proper and minimal. In order to see how it decomposes into connected components, we note that for $a, b = 0, 1$ we have (using $e^{-ia\pi} = e^{ia\pi}$)

$$\langle \chi_n(a\pi) | \psi_m(b\pi) \rangle = \sqrt{2} \cos\left(\frac{(b+a)\pi}{2}\right) \left(e^{i2\pi/D} + e^{-i2\pi/D}\right) e^{i(b+a)\pi/2} e^{i2\pi(2nm+m+n)/D}. \quad (10.145)$$

The cosine term tells us that these states are orthogonal for $a \neq b$ and are not orthogonal for $a = b$. Then the subsets $\left\{\Pi_{x;n}^{(0)}, \Pi_{p;m}^{(0)}\right\}$ and $\left\{\Pi_{x;n}^{(\pi)}, \Pi_{p;m}^{(\pi)}\right\}$ form two separate connected components in the network.

We choose the maximal independent sets in the connected components to be $\left\{\Pi_{x;n}^{(0)}\right\}$ and $\left\{\Pi_{x;n}^{(\pi)}\right\}$. (This choice is arbitrary; we could just as well have chosen the momentum basis.) Then, similarly to the example of a particle with orbital and spin angular momentum, the BPT is just two blocks with single rows of eigenbasis of $\left\{\Pi_{x;n}^{(0)}\right\}$ and $\left\{\Pi_{x;n}^{(\pi)}\right\}$:

$\chi_0(0)$	$\chi_1(0)$	\cdots	$\chi_{D-1}(0)$		$\chi_0(\pi)$	$\chi_1(\pi)$	\cdots	$\chi_{D-1}(\pi)$
-------------	-------------	----------	-----------------	--	---------------	---------------	----------	-------------------

This BPT indicates the irrep decomposition into two sectors:

$$\mathcal{H}_1 \otimes \mathcal{H}_2 \cong \mathcal{H}^{(0)} \oplus \mathcal{H}^{(\pi)}. \quad (10.146)$$

Thus we learn that, under restriction to the center of mass measurements, the Hilbert space splits into two superselection sectors with symmetric $|\chi_n(0)\rangle$ and anti-symmetric $|\chi_n(\pi)\rangle$ configurations of the bound pair of particles. We can now

see that this BPT specifies the commutant algebra of particle exchange symmetry, and indeed, X_{cm} and P_{cm} commute with exchange of particles so they belong to the commutant of this symmetry. This, however, does not mean that a priori it was obvious that $\{X_{cm}, P_{cm}\}$ generate the whole commutant algebra of this symmetry; it is possible that they only generate a subalgebra of the commutant. Only by explicitly finding the irreps with the projection scattering method we can be certain that $\langle X_{cm}, P_{cm} \rangle$ is the commutant algebra of particle exchange.

As discussed in Section 10.3, the bound pair's state reduces by enforcing the superselection with projections on the superselection sectors $\mathcal{H}^{(0)}$, $\mathcal{H}^{(\pi)}$:

$$\rho \longmapsto \Pi^{(0)}\rho\Pi^{(0)} + \Pi^{(\pi)}\rho\Pi^{(\pi)}. \quad (10.147)$$

This state reduction accounts for the operational constraints of an observer that cannot resolve the individual particles. From such an observer's perspective, each sector $q\pi$ for $q = 0, 1$ is effectively a single composite particle with position states $|\chi_n(q\pi)\rangle$ and momentum states $|\psi_n(q\pi)\rangle = F|\chi_n(q\pi)\rangle$. The distinction between the two sectors is then associated with some "charge" $q = 0, 1$ of the composite particle. Whether this charge is constant in time depends on the full dynamics of the system. If the charge is not conserved, meaning the dynamics have tunneling terms between the symmetric and anti-symmetric states of the pair, the constrained observer can describe the charge variation as the result of interactions with an "environment." The "environment" in this case is the composite particle's intrinsic degrees of freedom, which are inaccessible with $\{X_{cm}, P_{cm}\}$.

10.6 Beyond Matrix Algebras: Partial Bipartitions

Thus far we have discussed the case of matrix algebras, where Hilbert space is decomposed into a collection of direct-sum sectors of tensor products. These generalized bipartitions, as described by Eq. (10.17), are represented using their bipartition table (BPT) structure as block-diagonal arrangements of rectangular tables. We will now extend this construction of generalized bipartitions to include the case where some or all of the direct-sum sectors are represented by *non-rectangular* tables. We will refer to these non-rectangular cases as *partial bipartitions*. The power of partial bipartitions will be relevant when, for example, the set of measurements that can be implemented by an observer in the laboratory does not form an algebra.

As a motivating example, consider two spin- $\frac{1}{2}$ particles, spanned by the total spin basis labeled by $\{|S_z, \mu\rangle\}$, where S_z is the total spin-z of the two spins and μ labels

the information about the multiplet nature of the state, with $\mu = s$ for singlet and $\mu = t$ for triplet. A relevant situation is when an experimenter in the lab only has access to measurements of the total spin of the two particles, and not the multiplet information of the quantum state. Written in terms of the computational tensor product basis $\{|0\rangle, |1\rangle\}^{\otimes 2}$, we have

$$|1, t\rangle = |1, 1\rangle \quad (10.148)$$

$$|0, s\rangle = \frac{|01\rangle - |10\rangle}{\sqrt{2}} \quad (10.149)$$

$$|0, t\rangle = \frac{|01\rangle + |10\rangle}{\sqrt{2}} \quad (10.150)$$

$$|-1, t\rangle = |00\rangle . \quad (10.151)$$

This four-dimensional Hilbert space is *not* factorizable into a tensor product structure where one factor describes the total spin-z degree of freedom and the other factor corresponding to the multiplet information. Partial bipartitions offer a natural construction to capture such splits of Hilbert space. Partial bipartitions were first introduced in [246] in the context of quantum coarse-graining and some examples were discussed. In this paper, we will use the concept of partial bipartitions in Sections 10.7 and 10.8 below, where we will discuss decoherence and coarse-graining of Hilbert space using a variational approach based on an underlying Hamiltonian which governs evolution. Our exposition here of the concept and construction of partial bipartitions, in particular some of the notation, will be with an eye towards the variational approach.

Let us first consider the case of a single direct-sum factor, so that the BPT is a single non-rectangular table describing a partial bipartition. By virtue of being non-rectangular, the split of the Hilbert space is no longer that of a tensor product structure between the row and column degrees of freedom of the BPT, as was the case for a rectangular BPT, but rather captures a more general partition of the space into two. Consider a finite-dimensional Hilbert space \mathcal{H} of dimension $\dim \mathcal{H} = d < \infty$ spanned by a choice of orthonormal basis,

$$\mathcal{H} \cong \text{span}\{ |e_{ik}\rangle \} . \quad (10.152)$$

A partial bipartition of \mathcal{H} is specified by an arrangement of the d basis elements into a non-rectangular bipartition table, with N_C columns and N_R rows such that $d < N_C N_R$. As suggested by the notation, the basis element $|e_{ik}\rangle$ is located in the BPT in the i -th row with $i = 1, 2, \dots, N_R$ and k -th column with $k = 1, 2, \dots, N_C$.

The BPT is then specified by the heights $\{h_k\}$ for each of the N_C columns which is the number of basis elements which go in the k -th column. In what follows, we will focus on *compact* non-rectangular BPTs which correspond to the following conditions on the BPT:

1. The number of rows of the BPT is equal to the height of the largest column i.e. $\max\{h_k\} = N_R$.
2. The h_k basis elements which populate the k -th column are stacked together, starting from the first row without having any breaks in them.

A compact BPT minimizes loss of coherence under the action of the state-reduction map defined by the BPT. Such loss of coherence under state reduction is akin to superselection which is different than the dynamical decoherence induced by the Hamiltonian we will be interested in in the following sections. In Eq. (10.153) below, we depict a generic compact non-rectangular BPT specifying a partial bipartition of $\mathcal{H} \cong \mathcal{H}_A \otimes \mathcal{H}_B$. Arrows point toward the associated states of partial subsystems.

$$\begin{array}{ccccccc}
 e_{1,1} & \dots & e_{1,k} & \dots & e_{1,w_i} & \dots & e_{1,N_C} & \rightarrow & \alpha_1 \\
 \vdots & & \vdots \\
 e_{i,1} & \dots & e_{i,k} & \dots & e_{i,w_i} & & & \rightarrow & \alpha_i \\
 \vdots & \vdots & \vdots & \vdots & \vdots & & & & \vdots \\
 e_{h_k,1} & \dots & e_{h_k,k} & & & & & \rightarrow & \alpha_{h_k} \\
 \vdots & \vdots & & & & & & & \vdots \\
 e_{N_R,1} & \dots & & & & & & \rightarrow & \alpha_{N_R} \\
 \downarrow & & \downarrow & & \downarrow & & \downarrow & & \\
 \beta_1 & \dots & \beta_k & \dots & \beta_{w_i} & \dots & \beta_{N_C} & &
 \end{array}$$

(10.153)

It should be noted that as long as the compact form condition is met, there is still some freedom, albeit inconsequential, in the locational arrangement of basis elements in the BPT which will have no consequence in the state-reduction map defined by the BPT. For example, in Eq. (10.153), one can swap any two columns,

which is equivalent to swapping the order of basis in the reduced state space, and that will still leave the partial bipartition encoded in the BPT.

As we discussed in Section 10.2, since generalized bipartitions describe tensor-product splits of Hilbert space, and direct-sum sectors thereof, we can immediately infer that a partial bipartition describes splits of Hilbert space more general than tensor factorization. The span of the row (column) kets $\{|\alpha_i\rangle\}_{i=1}^{N_R}$ ($\{|\beta_k\rangle\}_{k=1}^{N_C}$) is defined to be the row (column) Hilbert space \mathcal{H}_A (\mathcal{H}_B) as illustrated in Eq. (10.153). These can be identified as *partial subsystems* of the full underlying Hilbert space \mathcal{H} and we represent this partial factorization as,

$$\mathcal{H} \cong \mathcal{H}_A \otimes \mathcal{H}_B. \quad (10.154)$$

One can always isometrically embed a partial bipartition of a Hilbert space into a larger tensor product Hilbert space defined by $\mathcal{H}_{AB} \cong \mathcal{H}_A \otimes \mathcal{H}_B$, such that for every $|e_{ik}\rangle \in \mathcal{H}$, there is a matching $|\alpha_i\rangle |\beta_k\rangle \in \mathcal{H}_{AB}$ but not vice-versa. The extra pairs in \mathcal{H}_{AB} which do not have a match in \mathcal{H} correspond to the missing elements of the BPT that would complete it to a rectangular, and hence, tensor product form.

Tensor product structures which correspond to generalized bipartitions are thus a special case of partial bipartitions which have rectangular BPTs, satisfying the condition $d = N_C N_R$.

Once the partial subsystem \mathcal{H}_A is identified, we can define a state-reduction map which will “trace” out \mathcal{H}_A , akin to a partial-trace map in the case of tensor products, but defined appropriately for partial subsystems. We denote this state-reduction map for the case of partial subsystems as $tr_{(A)}$ which maps the density matrices between the operator spaces as

$$tr_{(A)} : \mathcal{L}(\mathcal{H}) \longrightarrow \mathcal{L}(\mathcal{H}_B), \quad (10.155)$$

so the reduced state-space is indeed described by the partial subsystem \mathcal{H}_B as expected. We use a bracketed subscript (A) in $tr_{(A)}$ to denote the state-reduction map of a partial system, as opposed to the unbracketed one tr_A , which refers to the usual partial-trace map for tensor factors.

The action of $tr_{(A)}$ on the matrix elements in the bipartition basis $|e_{i,k}\rangle$,

$$tr_{(A)} : |e_{i,k}\rangle \langle e_{j,l}| \longmapsto \delta_{ij} |\beta_k\rangle \langle \beta_l|, \quad (10.156)$$

thus traces over the row indices i, j as if they label basis elements of a proper tensor factor of Hilbert space.

Based on the BPT structure, the original Hilbert space \mathcal{H} can be decomposed into direct-sum sectors, each corresponding to the subspace spanned by basis elements of a single column,

$$\mathcal{H} \cong \bigoplus_{k=1}^{N_C} \mathcal{H}_k . \quad (10.157)$$

Similar to the case of generalized bipartitions, we can define bipartition operators (BPOs) for partial subsystems,

$$S_{kl} = \sum_{i=1}^{\min(h_k, h_l)} |e_{i,k}\rangle \langle e_{i,l}| , \quad k, l = 1, 2, 3, \dots, N_C , \quad (10.158)$$

that map between columns of the bipartition table by preserving the row index i of each element (where it should be understood that the element is skipped in the sum if the row is not present in the destination column). BPOs of the form S_{kk} correspond to projectors on the column \mathcal{H}_k subspace and the ones of the form S_{kl} with $k \neq l$ implement partial isometries from (a subspace of) \mathcal{H}_l to (a subspace of) \mathcal{H}_k (depending on which dimension is lower). Written in terms of bipartition operators, the state-reduction map maps a density matrix $\rho \in \mathcal{L}(\mathcal{H})$ to a reduced, traced out state $\rho_B \in \mathcal{L}(\mathcal{H}_B)$,

$$\rho_B = \text{tr}_{(A)}(\rho) = \sum_{k,l=1}^{N_C} \text{tr}(S_{kl}\rho) |\beta_l\rangle \langle \beta_k| . \quad (10.159)$$

As an illustrative example, consider the 6 dimensional Hilbert space \mathcal{H} spanned by the orthonormal basis $\{|s\rangle\}$ for $s = 1, \dots, 6$. A partial bipartition of \mathcal{H} is chosen such that in the basis $\{|s\rangle\}$, it is specified by the bipartition table,

1	2	3
4	5	
	6	

$$(10.160)$$

While one can identify a notational correspondence between states $\{|s\rangle\}$ and $\{|e_{i,k}\rangle\}$ using their row/column location in the BPT, we will stick with the $|s\rangle$ notation since it will allow ease of representation of matrix elements of operators in this basis, such as the density matrix. It should be noted that the above BPT is compact. Now, for a given density matrix ρ written in the bipartition basis $\{|s\rangle\}$ ordered by appearance

in the bipartition table (read from left to right and top to bottom), the action of the state-reduction map $tr_{(A)}$ to trace out the partial subsystem \mathcal{H}_A , is

$$\begin{pmatrix} \rho_{11} & \rho_{12} & \rho_{13} & \rho_{14} & \rho_{15} & \rho_{16} \\ \rho_{21} & \rho_{22} & \rho_{23} & \rho_{24} & \rho_{25} & \rho_{26} \\ \rho_{31} & \rho_{32} & \rho_{33} & \rho_{34} & \rho_{35} & \rho_{36} \\ \rho_{41} & \rho_{42} & \rho_{43} & \rho_{44} & \rho_{45} & \rho_{46} \\ \rho_{51} & \rho_{52} & \rho_{53} & \rho_{54} & \rho_{55} & \rho_{56} \\ \rho_{61} & \rho_{62} & \rho_{63} & \rho_{64} & \rho_{65} & \rho_{66} \end{pmatrix} \quad (10.161)$$

$\downarrow tr_{(A)}$

$$\begin{pmatrix} \rho_{11} + \rho_{44} & \rho_{12} + \rho_{45} & \rho_{13} \\ \rho_{21} + \rho_{54} & \rho_{22} + \rho_{55} + \rho_{66} & \rho_{23} \\ \rho_{31} & \rho_{32} & \rho_{33} \end{pmatrix}.$$

From this, we can understand the action of state-reduction map from the bipartition table:

1. Coherences between basis elements $|e_{i,k}\rangle\langle e_{j,l}|$ in different rows ($i \neq j$) of the bipartition table are discarded. Coherences between basis elements in the same row of the BPT are preserved.
2. For each pair of columns k, l (including $k = l$), the sum of coherences between $|e_{i,k}\rangle\langle e_{i,l}|$ over all rows i is the new coherence term for the reduced element $|\beta_k\rangle\langle\beta_l|$.

The number of matrix elements of ρ which also appear in ρ_B after the state-reduction map is applied depends on the alignment structure of the cells in the BPT. In particular, some elements do not appear in the reduced density matrix. A natural question to ask is what information is preserved by the state-reduction map induced by the partial bipartition. It was shown in [246] that the bipartition operators S_{kl} span the operator subspace of all (and only) the observables whose information is preserved under state reduction. Then we can interpret the reduced state ρ_B as the state that contains all (and only) the information that is accessible with the observables in the operator space $span\{S_{kl}\}$. This naturally reduces to the standard picture in the familiar case of a tensor-product bipartition $\mathcal{H} \cong \mathcal{H}_A \otimes \mathcal{H}_B$, where

the bipartition operators take the form

$$S_{kl} = I_A \otimes |\beta_k\rangle \langle \beta_l|. \tag{10.162}$$

The restricted set of observables $span \{S_{kl}\} = I_A \otimes \mathcal{L}(\mathcal{H}_B)$ imply that the observer can only measure system \mathcal{H}_B .

We can also generalize the partial bipartition structure to include direct-sum sectors thereof, which corresponds to the following decomposition of Hilbert space,

$$\mathcal{H} \cong \bigoplus_q \left(\mathcal{H}_{A_q} \otimes \mathcal{H}_{B_q} \right), \tag{10.163}$$

where each sector q is spanned by the basis elements $|e_{ik}^q\rangle$ of the block q and each sector is further decomposed into a partial bipartition according to the arrangement of elements inside the block. Such a decomposition can be captured as a bipartition table with a block-diagonal arrangement of non-rectangular tables,

$e_{1;1,1}$	$e_{1;1,2}$	\dots													
$e_{1;2,1}$	\ddots														
\vdots															
<table style="border-collapse: collapse;"> <tr> <td style="border: 1px solid black; padding: 5px;">$e_{2;1,1}$</td> <td style="border: 1px solid black; padding: 5px;">$e_{2;1,2}$</td> <td style="border: 1px solid black; padding: 5px;">\dots</td> <td></td> </tr> <tr> <td style="border: 1px solid black; padding: 5px;">$e_{2;2,1}$</td> <td style="border: 1px solid black; padding: 5px;">\ddots</td> <td></td> <td></td> </tr> <tr> <td style="border: 1px solid black; padding: 5px;">\vdots</td> <td></td> <td></td> <td></td> </tr> </table>				$e_{2;1,1}$	$e_{2;1,2}$	\dots		$e_{2;2,1}$	\ddots			\vdots			
$e_{2;1,1}$	$e_{2;1,2}$	\dots													
$e_{2;2,1}$	\ddots														
\vdots															
\ddots															

$\tag{10.164}$

For each sector q , we can define a set of bipartition operators $\{S_{kl}^q\}$ using the basis elements in that sector. By construction, under the state-reduction map specified by such a BPT, coherences between different direct-sum sectors are lost, and the resultant density matrix will be block-diagonal corresponding to different blocks q .

Examples

Let us return to the example of the two spin- $\frac{1}{2}$ particles we raised at the beginning of this section. Again, consider the total spin basis labeled by $\{|S_z, \mu\rangle\}$, where S_z is the total spin-z of the two spins and μ labels the information about the multiplet

nature of the state (with $\mu = s$ for singlet and $\mu = t$ for triplet), which written in terms of the computational tensor product basis $\{|0\rangle, |1\rangle\}^{\otimes 2}$,

$$|1, t\rangle = |1, 1\rangle \quad (10.165)$$

$$|0, s\rangle = \frac{|01\rangle - |10\rangle}{\sqrt{2}} \quad (10.166)$$

$$|0, t\rangle = \frac{|01\rangle + |10\rangle}{\sqrt{2}} \quad (10.167)$$

$$|-1, t\rangle = |00\rangle, \quad (10.168)$$

and a partial bipartition of this Hilbert space,

$$\begin{array}{ccc}
 \boxed{1, t} & \boxed{0, t} & \boxed{-1, t} & \rightarrow & \boxed{\alpha_t} \\
 & \boxed{0, s} & & \rightarrow & \boxed{\alpha_s} \\
 \downarrow & \downarrow & \downarrow & & \\
 \boxed{\beta_{-1}} & \boxed{\beta_0} & \boxed{\beta_1} & & .
 \end{array} \quad (10.169)$$

The degree of freedom fixed by each column is the total spin- z and what varies within the columns is the multiplet (singlet-triplet) label. With the non-rectangular nature of the BPT, the column space \mathcal{H}_B (spanned by $\{|\beta_{-1}\rangle, |\beta_0\rangle, |\beta_1\rangle\}$) forms a partial subsystem which encodes variation of the total spin- z and the row space \mathcal{H}_A (spanned by $\{|\alpha_t\rangle, |\alpha_s\rangle\}$) forms a partial subsystem which encodes variation of multiplet information. We can now define the BPOs labeled by the value of total spin- z from the BPT column structure,

$$\begin{aligned}
 S_{+1,+1} &= |1, t\rangle \langle 1, t| & S_{+1,0} &= |1, t\rangle \langle 0, t| & S_{+1,-1} &= |1, t\rangle \langle -1, t| \\
 & & S_{0,0} &= |0, t\rangle \langle 0, t| + |0, s\rangle \langle 0, s| & S_{0,-1} &= |0, t\rangle \langle -1, t| \\
 & & & & S_{-1,-1} &= |-1, t\rangle \langle -1, t| .
 \end{aligned} \quad (10.170)$$

The other three BPOs can simply be obtained from $S_{kl} = S_{lk}^\dagger$. The state-reduction map induced by this BPT,

$$\rho \mapsto \sum_{k,l=+1,0,-1} \text{tr}(S_{kl}\rho) |l\rangle \langle k| \quad (10.171)$$

can be interpreted as tracing out the multiplet degree of freedom. The resulting state has the degrees of freedom associated with the total spin- z of the original system: that is has the Hilbert space of a single composite particle with this spin. The total spin operators $S_x^{tot}, S_y^{tot}, S_z^{tot}$ on the two particles are in the span of $\{S_{kl}\}$

$$\begin{aligned}
 S_z^{tot} &= S_{+1,+1} - S_{-1,-1} \\
 S_+^{tot} &= S_{+1,0} + S_{0,-1} \\
 S_-^{tot} &= S_{0,+1} + S_{-1,0},
 \end{aligned}$$

where S_x^{tot} and S_y^{tot} can be constructed from the ladder operators S_{\pm}^{tot} . Therefore, the reduced state preserves information about total spin operators $S_x^{tot}, S_y^{tot}, S_z^{tot}$. It should be noted that for such partial bipartitions, the span of $\{S_{kl}\}$ is not necessarily an algebra (it may not be closed under products) so even if we know that the reduced state preserves information about $S_x^{tot}, S_y^{tot}, S_z^{tot}$, it may not retain information about their products which we usually take for granted. Thus, we see a more general picture emerging where we can define partitions of Hilbert space based on a restricted set of observables which need not generate an algebra. Partial bipartitions offer a construction to account for such cases.

This construction easily extends, for example, to an arbitrary number N of spin $\frac{1}{2}$ particles. For even N , the BPT takes the form,

$\frac{N}{2}, +\frac{N}{2}$...	$\frac{N}{2}, +2$	$\frac{N}{2}, +1$	$\frac{N}{2}, 0$	$\frac{N}{2}, -1$	$\frac{N}{2}, -2$...	$\frac{N}{2}, -\frac{N}{2}$
		⋮	⋮	⋮	⋮	⋮		
		2, +2	2, +1	2, 0	2, -1	2, -2		
			1, +1	1, 0	1, -1			
			⋮	⋮	⋮			
			1, +1	1, 0	1, -1			
				0, 0				
				⋮				
				0, 0				

(10.172)

where, for each value of the total spin j , there are multiple equivalent representations that we have stacked on top of each other (suppressing the label for identical representations with the same j). Each row is associated with a specific “copy”

ν of the total spin j representation and the pair j, ν specifies one multiplet (note the different notation used in this table in contrast to the $N = 2$ spin case above for clarity of exposition of the idea). As before, we use the columns to define the BPO $\{S_{kl}\}$ and then the map that traces over the multiplets. The resulting state is associated with a single spin $\frac{N}{2}$ particle that encodes information about the state of the total spin of this system.

We will now use these partial bipartitions in the following Sections 10.7 and 10.8 where we will construct a paradigm to find quasi-classical coarse-grainings of Hilbert space, based on a collective feature of the system compatible with Hamiltonian evolution. Such coarse-grainings will typically not correspond to tensor factorizations of Hilbert space, and hence using this technology of partial bipartitions, we will be able to capture more general partitions suited for the purpose.

10.7 Classicality from Coarse-Grainings using Partial Bipartitions: Variational Approach

As discussed in Section 10.6, partial bipartitions offer a more general way than a standard tensor product structure to decompose Hilbert space into two parts. One particular application of partial bipartitions is to coarse-grain Hilbert space, since, in many situations, the relevant information preserved by the coarse-graining will not correspond to a tensor factor of Hilbert space. In this section, we outline a paradigm to find quasi-classical coarse-grainings of Hilbert space based on Hamiltonian evolution of the system. We call this the *variational* approach since we will iterate/vary over all possible BPTs (in some restricted set) to find the one(s) which demonstrate quasi-classical behavior.

A natural feature of many coarse-grainings is that they focus on collective or average properties of the underlying degrees of freedom and ignore its internal structure; for example, one can, under appropriate circumstances, coarse-grain a rigid-body system of N -particles into its center of mass coordinate, which is a collective feature, while discarding information about the relative locations of the particles, then study how the coarse-grained variable evolves and what characteristics the coarse-graining preserves. We will focus on such coarse-grainings based on a collective property of the system, and their compatibility with dynamics which demonstrate quasi-classical behavior.

Partial Bipartition of Many-body Systems into Collective and Internal Degrees of Freedom

Consider a finite-dimensional Hilbert space of a collection of N underlying degrees of freedom (dofs) specified by a tensor-product structure,

$$\mathcal{H} \cong \bigotimes_{\mu=1}^N \mathcal{H}_{\mu}, \quad (10.173)$$

which evolve under Hamiltonian evolution given by H . We consider these N degrees of freedom to be fixed, specified by the physical system under consideration, e.g. a collection of N particles, etc. It is assumed that the Hamiltonian in general admits interactions between all N dofs, and in case there exist any subsets of these dofs which are decoupled under the action of the Hamiltonian, we consider each such decoupled subspace individually in this prescription. Our goal is to develop a coarse-graining algorithm informed by the Hamiltonian H which chooses a partial bipartition, $\mathcal{H} \cong \mathcal{S}_{\text{collective}} \otimes \mathcal{S}_{\text{internal}}$. The partial subsystem $\mathcal{S}_{\text{collective}}$ is the coarse-grained version of \mathcal{H} we wish to preserve under the coarse-graining/state-reduction map based on a characteristic collective feature of the system (involving all N degrees of freedom) compatible with the Hamiltonian which behaves classically (in a sense we define below) by tracing over the space of internal features $\mathcal{S}_{\text{internal}}$. This will correspond to a BPT of a partial bipartition where the columns will define the coarse-grained subspace $\mathcal{S}_{\text{collective}}$ and the rows will define the $\mathcal{S}_{\text{internal}}$ subspace that will be traced over.

Compatible Collective Observables and Macroscopic Pointer States

Let us define the set of *collective* observables of the full Hilbert space as those that can be written as

$$M_c = \sum_{\mu=1}^N M_{\mu}, \quad (10.174)$$

with,

$$M_{\mu} = \hat{\mathbb{I}}_1 \otimes \hat{\mathbb{I}}_2 \otimes \dots \otimes \hat{\mathbb{I}}_{\mu-1} \otimes m_{\mu} \otimes \hat{\mathbb{I}}_{\mu+1} \otimes \dots \otimes \hat{\mathbb{I}}_N, \quad (10.175)$$

where each M_{μ} acts *non-trivially only* on \mathcal{H}_{μ} whose dimension we take to be $\dim \mathcal{H}_{\mu} = d_{\mu}$. The operator m_{μ} can be parameterized by

$$m_{\mu} = \left(\sum_{a=1}^{d_{\mu}^2-1} c_a^{(\mu)} \Lambda_a^{(\mu)} \right), \quad (10.176)$$

where $\Lambda_a^{(\mu)}$ are the $d_\mu^2 - 1$ Generalized Gell-Mann generators (of $SU(d_\mu)$) which form a complete basis of non-trivial (i.e. without the identity $\hat{\mathbb{1}}_\mu$) operators acting on \mathcal{H}_μ . To ensure that these operators have a non-trivial action on the degree of freedom they act on, we impose the restriction that at least one of the $c_a^{(\mu)} \neq 0$, for each μ . In addition, we will mostly work with normalized operators on $\mathcal{L}(\mathcal{H})$, the space of linear operators on \mathcal{H} , to be able to focus on features true to the structure of different operators, and not explicitly due to difference in overall multiplicative factors. For concreteness, we choose to use the Frobenius norm²² in this paper, under which the collective observable will be normalized, i.e., $\|M_c\|_f = 1$.

Our coarse-graining prescription aims for a collective observable as one of the defining properties of $\mathcal{S}_{\text{collective}}$ which is *most compatible* with—that is, *stationary* with respect to—the Hamiltonian H (we will use a normalized version of the Hamiltonian under the Frobenius norm too). Thus, one can pick out the most compatible collective observable relevant to the coarse-graining by minimizing the norm of the commutator $[H, M_c]$ over all choices of collective observables M_c ,

$$M_c : \min_{\{c_a^{(\mu)}\}} \left\| [H, M_c] \right\|_f. \quad (10.178)$$

This is in close parallel with the ideas of the *predictability sieve* [170] used in the decoherence literature, where one sifts through different states in Hilbert space to determine the set which is most compatible with the Hamiltonian and is used to define pointer states of the system which are classical. One defining feature of classical dynamics is *robustness* of a set of states (the classical ones) reflected in their effective deterministic classical character. Said differently, the pointer states are special low-entropy states which under evolution stay robust to entanglement production: a given classical degree of freedom in the system does not arbitrarily entangle with all other degrees of freedom at short time scales. This is intimately linked to the form of and constraints on the Hamiltonian, such as locality [29]. Beginning with low entropy states is natural given the second law of thermodynamics, and classicality constrains the rate of entanglement growth for classical states. In this sense, eigenstates of the collective observable chosen by the compatibility condition of Eq. (10.178) are classical, macroscopic pointer states which capture an average, collective property of the underlying dofs which is as robust under evolution as possible. Take note

²²The Frobenius norm of a linear operator $A \in \mathcal{L}(\mathcal{H})$, also referred to as the Hilbert-Schmidt norm, is defined as,

$$\|A\|_f = \sqrt{\text{Tr}(A^\dagger A)}. \quad (10.177)$$

that the collective observable *cannot* be the identity operator (which would trivially commute with H) since we are only considering non-trivial observables which have no support on the identity operator. The total freedom in the choice of M_c are the $\sum_{\mu=1}^N (d_{\mu}^2 - 1)$ number of parameters $\{c_a^{(\mu)}\}$. Further restrictions on the set $\{c_a^{(\mu)}\}$ can be imposed by looking at the symmetry structure of the Hamiltonian and the Hilbert space, if any. For example, if \mathcal{H} contains a collection of identical but distinguishable particles on which the Hamiltonian acts symmetrically, then this can be used to constrain the form of M_{μ} to be the same for this collection of particles.

Now, as expected, due to the collective observable containing a slew of identity operators in each term in the sum, M_c will have a high degeneracy in its eigenspectrum; therefore, the distinct eigenvalues of M_c will be used to label distinct columns of the BPT which will define the coarse-graining $\mathcal{S}_{\text{collective}}$. The compatibility condition Eq. (10.178) of the collective observable M_c with the Hamiltonian of Eq. (10.178) will ensure that transition of an eigenstate of M_c (which corresponds to a deterministic value of the collective variable) into other eigenstates will be minimized under time evolution, and hence that the columns of the BPT correspond to robust collective macrostates. Once the collective observable has been selected, it will give us a total of $N_C \leq \dim \mathcal{H}$ distinct eigenvalues and corresponding N_C subspaces $\mathcal{H}_k^{(c)}$ with dimension $\dim \mathcal{H}_k^{(c)} = h_k$ for $k = 1, 2, 3, \dots, N_C$. Each such subspace labels a distinct value of the collective observable, specifying a macroscopic pointer state of the coarse-graining. In addition to the subspace structure determined by specification of the compatible M_c , one can use the tensor product decomposition of Hilbert space into the underlying N dofs of Eq. (10.173) to resolve each of these subspaces $\mathcal{H}_k^{(c)}$ by spanning them with the tensor product eigenbasis of M_c which have the same eigenvalue labeled by k .

Thus, we now have a direct-sum structure to \mathcal{H} ,

$$\mathcal{H} \cong \bigoplus_{k=1}^{N_C} \mathcal{H}_k^{(c)}, \quad (10.179)$$

where each direct-sum subspace is specified by the span of the *tensor product eigenbasis* of M_c with a given distinct eigenvalue, and this direct-sum structure satisfies $\sum_{k=1}^{N_C} h_k = \dim \mathcal{H}$.

Now that we have identified the column structure based on the degeneracy structure of the compatible collective observable M_c and the basis elements which enter the BPT and represent macroscopic pointer states of $\mathcal{S}_{\text{collective}}$, we are left with the the

task of assigning the row structure which will fix the BPT. Here, we have a discrete set of combinatoric choices of row alignments we can do, given the column structure and the specification of the basis elements of the compatible collective observable. For this purpose, we now turn to understanding the conditions under which the coarse-graining is quasi-classical.

Superselection Sectors and Emergent Quasi-Classicality

We can use the transition structure of the Hamiltonian in the tensor product eigenbasis of M_c to further split our partial bipartition into direct-sum sectors which will act as superselection sectors in our coarse-graining scheme. Based on the Hamiltonian expressed in this tensor product M_c basis, one can identify unions of column subspaces, $\tilde{\mathcal{H}}_q \cong \bigoplus_{k_q} \mathcal{H}_{k_q}^{(c)}$ for some $q = 1, 2, \dots, N_{\text{sectors}}$, for which the Hamiltonian has no tunneling terms connecting these subspace unions, such that for all states $|\psi_q\rangle \in \tilde{\mathcal{H}}_q$ and $|\psi_{q'}\rangle \in \tilde{\mathcal{H}}_{q'}$,

$$\langle \psi_q | H | \psi_{q'} \rangle = 0, \quad \text{if } q \neq q'. \quad (10.180)$$

Each such union of sectors represents a superselection sector for our coarse-graining since these different unions do not interact. Each direct-sum sector will be arranged as a distinct block in a BPT of a partial bipartition in the compact form with the row structure yet to be identified based on a criterion of emergent quasi-classicality. Compact form within each sector will allow minimal loss of coherence under the state-reduction map induced by the BPT, so the coarse-graining we find will indeed reflect emergent quasi-classicality from dynamical decoherence and not the mere discarding of quantum coherences by misalignments between basis states in the structure of the BPT. This is already a first step towards emergent quasi-classicality since lack of transitions between sectors of Hilbert space governed by the Hamiltonian identify them as classical. Quantum coherences between such sectors cannot be observed or have any dynamical effect, and this lack of coherence can be enforced by the block diagonal structure of the BPT.

To fix the row structure within each direct-sum superselection sector, we now turn back to the question of emergent quasi-classicality. A feature of our coarse-graining will be that dynamics in the reduced space following the BPT state-reduction map will reflect features of classicality. We have already identified the column structure of our BPT which labels our macroscopic pointer states, based on compatibility of a collective observable with the Hamiltonian. The compact form of our BPTs ensure that minimal coherence between basis states is lost due to the action of the

state-reduction map itself so we can now focus on the action of the Hamiltonian to induce *dynamical* decoherence. In the usual dynamical decoherence understanding, coherences between pointer states in an initial low entropy state are suppressed dynamically by interactions with the auxiliary degrees of freedom. In quasi-classical coarse-grainings, we expect the row alignment of the BPT to allow Hamiltonian evolution to decohere superpositions of our macroscopic pointer states by “interaction” with $\mathcal{S}_{\text{internal}}$. For such quasi-classical BPTs, we can demand the rate at which this dynamical decoherence happens to be fastest and hence, most effective.

We will, for concreteness, focus on small time evolution since classical states, as opposed to non-classical ones, will exhibit decoherence starting at short time scales, and are expected to stay decohered as time progresses. We thus will quantify entropy production by studying the growth rate using the *linear* entanglement entropy²³. While the production of entropy in a partial bipartition is in general an indicator of more generic quantum correlations, we interpret it as an entanglement entropy between $\mathcal{S}_{\text{internal}}$ and $\mathcal{S}_{\text{collective}}$. This is because a BPT offers a generalization of the tensor product structure and interactions between these partial subsystems is expected to lead to dynamical decoherence starting from an initial low entropy state just as in the case of the usual system-environment tensor structure in the standard decoherence literature. Consider a pure state of the full Hilbert space $\rho(t) = |\psi(t)\rangle \langle\psi(t)| \in \mathcal{L}(\mathcal{H})$ evolving under evolution by the Hamiltonian H , and a BPT which induces a state-reduction map $\text{Tr}_{(R)}$ by tracing out the partial subsystem defined by its row subspace. Under this state-reduction map, the pure state ρ gets mapped to

$$\rho_c(t) \equiv \text{Tr}_{(R)} \rho(t) , \quad (10.181)$$

whose entanglement can be quantified by the linear entropy,

$$S_{\text{lin}}(t) = 1 - \text{Tr}(\rho_c^2(t)) . \quad (10.182)$$

It can be shown, as was done in [29], that for initially pure, *unentangled* states, the linear entanglement entropy grows at $\mathcal{O}(t^2)$ to leading order and hence one can quantify the growth rate of entanglement entropy as,

$$\ddot{S}_{\text{lin}}(0) = -\text{Tr}(\rho_c(0)\ddot{\rho}_c(0) + \ddot{\rho}_c(0)\rho_c(0) + 2\dot{\rho}_c(0)) , \quad (10.183)$$

²³One could equally well use von Neumann entanglement entropy too, of which the linear entropy forms the leading order contribution. We focus on the linear entropy to get better analytic tractability.

where a dot over a quantity represents its time derivative and we have,

$$\dot{\rho}_c(0) = \text{Tr}_{(R)} (\dot{\rho}(0)) = \text{Tr}_{(R)} (-i [H, \rho(0)]) , \quad (10.184)$$

$$\ddot{\rho}_c(0) = \text{Tr}_{(R)} (\ddot{\rho}(0)) = \text{Tr}_{(R)} (-[H, [H, \rho(0)])] . \quad (10.185)$$

We now proceed to use this quantifier $\ddot{S}_{\text{lin}}(0)$ of entanglement growth rate to quantify the classicality of a given BPT. The most natural initial states suited for a decoherence analysis offered by a partial bipartition are the ones supported on basis states of a single row in the BPT. In the familiar case of a tensor product structure corresponding to a rectangular BPT, such a state would correspond to an unentangled state – a tensor product of a superposition for the state of the column subsystem \mathcal{H}_A with a single basis state of the row system \mathcal{H}_B . For example, in the decoherence literature, considering a system and environment split $\mathcal{H} \cong \mathcal{H}_S \otimes \mathcal{H}_E$, one considers initial states of the form $|\psi(0)\rangle = (\sum_s c_s |s\rangle) \otimes |E_{\text{ready}}\rangle$ for some ready state on the environment. Thus states supported on a single row of a BPT of a partial bipartition are natural extensions of such initial pure states which are unentangled and therefore are good candidates to measure the dynamical decoherence of. Borrowing intuition and language from the decoherence paradigm, the state first branches, i.e. the environment (the row variable in our BPT) states evolve conditionally depending on the pointer state $|s\rangle$ of the system (corresponding to the columns of the BPT), following which there is dynamic decoherence where these conditional states of environment become orthogonal in time and stay so. We expect a similar situation here where an initial low entropy state, such as the one supported on a single row of the BPT in a superposition of pointer states of $\mathcal{S}_{\text{collective}}$, undergoes entropy production associated with dynamical decoherence that suppresses coherences between the pointer states, leading to classical branches. The branching of such initial states happens at $\mathcal{O}(t)$ following which we expect these conditionally evolved states to decohere, which we can capture by the entanglement growth rate via Eq. (10.183) which grows $\mathcal{O}(t^2)$. Using this understanding, we propose a metric to quantify this dynamic decoherence as a probe of emergent quasi-classicality of a given BPT: One can construct, for each row $i = 1, 2, \dots, N_R$ of the BPT, a *uniform* superposition state over all basis states in that row (each labelling a different macroscopic pointer state),

$$|\phi_i\rangle = \frac{1}{\sqrt{w_i}} \sum_{k \in \{1 \dots w_i\}} |e_{i,k}\rangle , \quad (10.186)$$

where w_i is the number of basis elements in the i -th row of the BPT and k iterates over all such basis elements. For each such uniform superposition state, defined

on each row, we can compute the entanglement growth rate $\ddot{S}_{\text{lin},i}(0)$ as a measure of dynamical decoherence and then quantify the emergent classicality of the BPT, Q_{BPT} as the average of these entanglement growth rates over all rows of the BPT,

$$Q_{\text{BPT}} = \frac{1}{N_R} \sum_{i=1}^{N_R} \ddot{S}_{\text{lin},i}(0). \quad (10.187)$$

The average over all rows can be interpreted as a statistical mixture over different basis states of the partial system (label by the rows), representing a probabilistic treatment of not knowing the state of the partial system which will be traced over. This is one such metric which captures the idea of emergent classicality using a notion of effective dynamical decoherence. We adopt this as a demonstration of principle, but emphasize that, depending on the context of the coarse-graining being constructed, one can come up with more amenable definitions of quantities which capture the emergent quasi-classical nature of the BPT. Given this metric, one can now vary over all possible BPT row arrangements, which are discrete and finite choices of basis element arrangement within each column, and choose the BPT which maximizes Q_{BPT} representing most effective dynamical decoherence and hence, is the most quasi-classical. It should be noted that this prescription may not always yield a unique preferred BPT reflecting a preferred underlying classical partial bipartition $\mathcal{H} \sim \mathcal{S}_{\text{collective}} \otimes \mathcal{S}_{\text{internal}}$, but rather will often select a class of BPTs which have the same classicality quantification based on the metric above. One can interpret this residual freedom as gauge choices of coarse-grainings, which, even though they induce different state-reduction maps based on the BPT, have the same measure of emergent classicality in the reduced subspace of the macroscopic variable based on the chosen metric. Often, this will be intimately tied with some symmetry structure in the Hamiltonian which does not distinguish between the underlying different degrees of freedom and hence leads to a class of BPTs with the same emergent quasi-classical behavior.

The above algorithm just described for obtaining such collective, quasi-classical coarse-grainings can now be summarized as follows:

1. Based on the given microfactorization of Hilbert space into degrees of freedom, find a collective observable M_c which is most compatible with the Hamiltonian as given by Eq. (10.178).
2. Eigenspaces of M_c corresponding to distinct eigenvalues will label different column subspaces of the BPT as macroscopic, collective pointer states ro-

bust under Hamiltonian evolution. These will make up the partial subsystem $\mathcal{S}_{\text{collective}}$ which will be the coarse-graining of \mathcal{H} .

3. Eigenspaces of M_c with distinct eigenvalues, along with the microfactorization, furnish an orthonormal basis for Hilbert space and resolve the column subspaces with tensor product basis elements with distinct eigenvalues.
4. Once the column structure of the BPT is fixed, use the transition structure of the Hamiltonian in this tensor product basis of M_c to identify superselection sectors as done in Eq. (10.180), each of which will form a disjoint block of the BPT. Each block will be arranged in the compact form to minimize loss of coherence due to the action of the state-reduction map induced by the BPT.
5. Now consider dynamical decoherence to fix the remaining freedom in each such block in the compact form to identify the alignment of the rows in the BPT. Iterate over the finite, discrete permutations of row arrangements and select (the class of) BPT(s) which maximize entanglement production as a measure of effective dynamical decoherence as done in Eq. (10.187).

In the next section, using a concrete example of the Ising model, we will demonstrate this algorithm for constructing a quasi-classical coarse-graining based on a collective variable compatible with the Hamiltonian.

10.8 Example of the Variational Approach: Coarse-Graining the Ising Model as a Partial Bipartition

Let us now consider a concrete example where we can apply the coarse-graining scheme developed above. We will focus on the Ising model in 1-D and see how we can capture collective features of the model which are effectively classical. Consider $N \geq 2$ spin- $\frac{1}{2}$ particles described by a tensor-product²⁴ Hilbert space $\mathcal{H} \cong \bigotimes_{\mu=1}^N \mathcal{H}_{\mu}$ on a 1-D lattice evolving under the Ising Hamiltonian,

$$H \sim - \sum_{\mu=1}^{N-1} \left(\sigma_z^{(\mu)} \otimes \sigma_z^{(\mu+1)} \right) - g \sum_{\mu=1}^N \sigma_x^{(\mu)}, \quad (10.188)$$

where $g > 0$ characterizes the strength of the external magnetic field in the x -direction and the symbol \sim in the definition of an operator implies that we will

²⁴For completeness, we mention that while one can study several dual pairs of lattice theories such as the Ising model [22, 255], which differ by global decomposition changes of Hilbert space, in this paper we focus on a fixed micro-decomposition of the underlying degrees of freedom.

normalize it under the Frobenius norm. As usual, $\sigma_z^{(\mu)}$ is the Pauli z-operator on the μ -th spin on the lattice and $\sigma_x^{(\mu)}$ is the Pauli x-operator. Note that our Ising Hamiltonian does *not* have periodic boundary conditions and corresponds to an open chain with N sites. We choose this specific boundary condition since the results in this case are more compact to describe and therefore help in the exposition of the idea. The same analysis could also be implemented for different boundary conditions and the results could be interpreted along similar lines. Our goal is now to look for the collective observable of the N spins most compatible with the Hamiltonian. We model the operator M_μ in Eqs. (10.174) and (10.175) as a unit-normed operator under the Frobenius norm,

$$M_\mu = \sqrt{\frac{2}{1+\alpha^2}} \left(\sigma_z^{(\mu)} + \alpha \sigma_x^{(\mu)} \right), \quad \forall \mu, \quad (10.189)$$

characterized by the parameter $\alpha \geq 0$ quantifying the mix between Pauli x and z operators. As a simplifying assumption, since the Hamiltonian only contains Pauli-x and Pauli-z operators, we do not take support on $\sigma_y^{(\mu)}$ in Eq. (10.189) and only consider mixing between x and z to determine the most compatible collective observable. This assumption could be relaxed to perform a more complete analysis. It should be noted that we take the operator M_μ characterized by the same parameter α for each spin μ . Under the Hamiltonian, all but the edge spins are treated on an equal footing and are indistinguishable from the point of view of dynamics. Hence one should expect a similar parametrization, because in this variational approach, we only have access to the Hamiltonian, and any structure that emerges should respect the underlying symmetry of the dynamics. The edge spins, represented by M_1 and M_N , should in general be treated differently due to non-periodic boundary conditions and while this analysis can be carried out in a straightforward way, we choose to parametrize their contribution to M_c by the same value of α . This can be justified on two grounds. First, there are only 2 edge spins compared to $(N-2)$ bulk ones and for moderately sized chains and larger, any difference due to edge spins will be sub-dominant. Second, choosing the same parametrization for each spin will allow a more elegant understanding of the collective observable M_c as an *average* quantity over the spin chain and a clean interpretation of the coarse-graining scheme where the macroscopic variable will be labeled by distinct values of this average quantity.

We can now compute the Frobenius norm of the commutator of M_c and the Ising

Hamiltonian H parametrized by α , which gives us

$$\left\| [H, M_c] \right\|_f = \frac{(N-1)\alpha^2 + 2Ng^2}{2^{N-3} N (4Ng^2 + N-1)(1+\alpha^2)}. \quad (10.190)$$

Minimization of this norm above with respect to the parameter α will give us a collective observable most compatible with the Hamiltonian. To minimize this norm, we write it in a more suggestive way,

$$\begin{aligned} \left\| [H, M_c] \right\|_f &= \frac{1}{1+(1/\alpha^2)} \left[\left(\frac{1}{2^{N-3}N} \right) \frac{(N-1)}{4Ng^2 + N-1} \right] \\ &+ \frac{1}{1+\alpha^2} \left[\left(\frac{1}{2^{N-3}N} \right) \frac{2Ng^2}{4Ng^2 + N-1} \right], \end{aligned} \quad (10.191)$$

where we have factored out the g dependence in each term in the sum above, which we identify as,

$$\left\| [H, M_c] \right\|_f = \left(\frac{1}{1+(1/\alpha^2)} \right) T_1(g) + \left(\frac{1}{1+\alpha^2} \right) T_2(g). \quad (10.192)$$

We notice a turning point in the g dependence of $T_1(g)$ and $T_2(g)$. We find that this norm is minimized for the following condition depending on the value of g which controls the relative importance of the two different terms in the normalized Ising Hamiltonian. For $g^2 < (N-1)/2N$, we see that $T_1(g) > T_2(g)$ and hence to minimize the norm in Eq. (10.190), the α dependent prefactor of $T_1(g)$ should be minimized which implies $\alpha = 0$. On the other hand, when $g^2 > (N-1)/2N$, we see that $T_2(g) > T_1(g)$ and hence $\alpha = \infty$ ensures minimization of the dominant term and hence the norm itself. One can confirm these results by formally differentiating, and checking for minima conditions in the relations above. Thus, we find that depending on the value of g in the normalized Hamiltonian, the most compatible collective observable corresponds to,

$$\alpha(g) = \begin{cases} 0, & g < g_{\text{crit}} \\ \infty, & g > g_{\text{crit}} \end{cases}, \quad (10.193)$$

where g_{crit} is the critical value²⁵ of g given by

$$g_{\text{crit}} = \sqrt{\frac{N-1}{2N}}, \quad (10.194)$$

²⁵We have derived the value of g_{crit} from the compatibility condition of Eq. (10.178); it should not be confused with the, in general different, value of g where the phase transition in the Ising model takes place.

such that for $g < g_{\text{crit}}$ when the Pauli z-z interaction term dominates, the most compatible collective observable M_c is the average spin-z of the Ising chain (which corresponds to $\alpha = 0$),

$$M_c \sim \sum_{\mu=1}^N \sigma_z^{(\mu)}, \quad g < g_{\text{crit}}, \quad (10.195)$$

and for $g > g_{\text{crit}}$, when the external magnetic field in the x -direction dominates, the collective observable which is most compatible with the Hamiltonian is the average spin-x of the chain (which corresponds to $\alpha = \infty$),

$$M_c \sim \sum_{\mu=1}^N \sigma_x^{(\mu)}, \quad g > g_{\text{crit}}. \quad (10.196)$$

Thus, we see a phenomenon akin to a phase transition where, depending on the dominant term in the Hamiltonian, the most compatible M_c is the one which is commuting with the dominant term.

Once we have obtained the most compatible collective observable M_c , we can immediately use its distinct eigenvalues m_k to label the macroscopic states of our coarse-graining by

$$m_k \in \left\{ -\frac{N}{2}, -\frac{N-2}{2}, \dots, \frac{N-2}{2}, \frac{N}{2} \right\}, \quad (10.197)$$

and these will be used to label distinct columns of the BPT which will specify the coarse-graining. Since the $N + 1$ distinct values of M_c will serve as labels of our macrostates under the coarse-graining prescription, our coarse-grained space will have a dimension $\dim \mathcal{S}_{\text{collective}} = N_C$. Already we see a major benefit of our scheme in dimension reduction: our collective scheme will map our original Hilbert space of $\dim \mathcal{H} = 2^N$ to a reduced, coarse-grained space with $\dim \mathcal{S}_{\text{collective}} = (N + 1)$. The dimension of the k -th collective (macroscopic) subspace corresponding to the M_c eigenvalue $|m_k| = (N - 2(k - 1))/2$ for $k = 1, 2, \dots, \left\lceil \frac{N_C}{2} \right\rceil$ is then the binomial coefficient,

$$\dim \mathcal{H}_k^{(c)} = \binom{N}{k-1}. \quad (10.198)$$

Given that we are working with N underlying spins specified by the tensor decomposition of Eq. (10.173), we can use the natural tensor-product basis of M_c to specify the orthonormal basis which we will be working with to fill the cells of our BPT. When $g < g_{\text{crit}}$, corresponding to M_c being the average spin-z of the lattice, we use the $\{|0\rangle, |1\rangle\}^{\otimes N}$ basis where $\{|0\rangle, |1\rangle\}$ are the eigenstates of σ_z and in the

other case when $g > g_{\text{crit}}$ so that M_c is the average spin-x of the chain, we can use the $\{|+\rangle, |-\rangle\}^{\otimes N}$ where $\{|+\rangle, |-\rangle\}$ are the eigenstates of σ_x . Thus we now have a *fixed* orthonormal basis we will use to construct a BPT for the partial bipartition for the Ising model and a specification of different columns of the BPT labeled by distinct eigenvalues of the compatible collective observable M_c . The only freedom we now have is the choice of row alignments in our BPT for which we will turn to effective dynamical decoherence as a quantifier of quasi-classical behavior of the coarse-graining. We will take each disjoint block in our BPT corresponding to superselection sectors in the partial bipartition to be in compact form to make sure that minimal coherence is lost due to the action of the state reduction itself and any decoherence will be due to Hamiltonian evolution. As we will see, the two cases of $g > g_{\text{crit}}$ and $g < g_{\text{crit}}$ will have very different superselection properties based on the Hamiltonian, hence we will deal with them separately and describe the results for each case in detail.

$g < g_{\text{crit}}$: Average Spin-z as Collective Observable

Let us first focus on the case when $g < g_{\text{crit}}$, so that the $z - z$ interaction term in the Ising Hamiltonian dominates which sets the most compatible collective observable $M_c \sim \sum_{\mu=1}^N \sigma_z^{(\mu)}$, the average spin-z of the Ising chain. As discussed before, this choice of M_c offers us an orthonormal basis of $\{|0\rangle, |1\rangle\}^{\otimes N}$ to work with in the BPT. The action of the Hamiltonian on these tensor product basis furnished from eigenstates of M_c is to *flip single bits* in the $\{|0\rangle, |1\rangle\}$ basis due to the presence of the external magnetic field in the x -direction (in the case when $g > 0$). Due to this transition structure of the Hamiltonian in the M_c basis, bit flips can successively connect each of the N_c column subspaces and hence there is no superselection sector structure in this case.

We illustrate the results for the case of $N = 3$ spins since there the results are tractable and easy to follow to demonstrate the physics behind them²⁶. For $N = 3$, the compatible collective observable M_c has $N_c = 4$ distinct eigenvalues which will label different columns of our BPT. In Table 10.1, we list these eigenstates of M_c arranged in columns by their distinct eigenvalues. This Table 10.1 is not yet a BPT since we have not yet considered row alignments, just a listing of eigenstates arranged by columns labeled by distinct eigenvalues of the compatible M_c . We will now consider

²⁶While for such small number of spins, one might want to treat the edge spins on a different footing than the bulk ones since the edge contribution may not be sub-dominant, we take the same parametrization for each spin as in Eq. (10.189) as a demonstration of principle with the M_c being an average quantity over the entire chain.

M_c value:	$-\frac{3}{2}$	$-\frac{1}{2}$	$\frac{1}{2}$	$\frac{3}{2}$
	$ 000\rangle$	$ 100\rangle$	$ 011\rangle$	$ 111\rangle$
		$ 010\rangle$	$ 101\rangle$	
		$ 001\rangle$	$ 110\rangle$	

Table 10.1: Tensor Product Eigenstates for $M_c = \sum_{\mu=1}^3 \sigma_z^{(\mu)}$ for $N = 3$ spins, arranged in columns labeled by distinct eigenvalues. Note that this is *not* a BPT, just an enumeration of the eigenstates arranged by the column structure governed by the compatible M_c .

different BPTs in compact form by iterating over different row arrangements of the eigenstates within each of the columns fixed by the collective observable M_c . By this token, there will be a total of $\prod_{k=1}^{N_c} (h_k!)$ number of permutations of row arrangements which will be the set of BPTs we will consider. There will, of course, be many redundancies in this way of enumerating different BPTs (such as inconsequential rearrangements differing by row swaps) compatible with the M_c column structure, but we iterate over them anyway to keep the permutations easy to track. In the case of $N = 3$ spins, we will have a total of 36 BPTs to iterate over and for each such BPT, we compute Q_{BPT} , the average entanglement growth rate over pure, uniform states defined on each row as defined in Eq. (10.187), and choose the class of BPTs which maximize this quantifier, representing effective dynamical decoherence as the most classical and compatible coarse-graining given the Hamiltonian. In Figure 10.4, we plot the average entanglement growth rate Q_{BPT} for these 36 BPTs for the case of $N = 3$ spins with the collective observable being $M_c \sim \sum_{\mu} \sigma_z^{(\mu)}$. We notice that these BPTs come in three distinct classes differentiated by entanglement growth rates. The class of BPTs with the maximum entanglement growth rate is selected as the most quasi-classical one and we find that there are six such distinct BPTs belonging to this selected quasi-classical equivalence class. (While the plot in figure 10.4 shows 12 such BPTs with the largest value of Q_{BPT} , as mentioned there are redundancies in our enumeration and only 6 of them are distinct from the perspective of the state-reduction map they induce.) In Fig. 10.6, we display these 6 selected, quasi-classical BPTs.

These selected BPTs have a common transition structure given by the Hamiltonian, which we portray in Fig. 10.5 to better understand these results. The arrows depict transitions between different basis states given by the Hamiltonian. It can be seen that the selected quasi-classical BPTs are ones which induce transitions under the

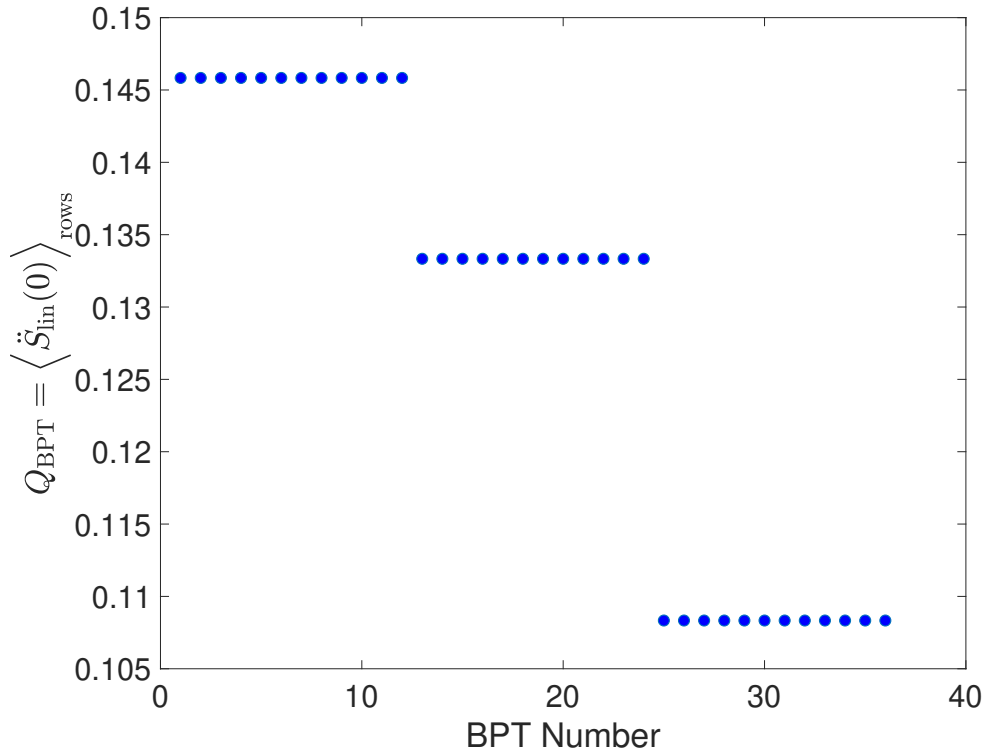


Figure 10.4: Plot of average entanglement growth rate Q_{BPT} over different BPTs (different row arrangements) for $N = 3$ spins with the compatible collective observable $M_c = \sum_{\mu=1}^3 \sigma_z^{(\mu)}$ corresponding to a value of $g = 0.5 < g_{\text{crit}}$.

Hamiltonian by spreading maximally across rows of the BPT. This way, maximum coherence is lost for pure states supported on one row, leading to decoherence of different macroscopic pointer states.

Similar to the $N = 3$ case, one can run an analysis on $N = 4$ spins in which case there will be $N_c = 5$ columns labeled by distinct eigenvalues of M_c . The results we find are very similar to the $N = 3$ spin case. The selected BPTs have row alignments for which the Hamiltonian transitions maximize dynamical decoherence between different macroscopic pointer states under the state-reduction map induced by the BPT. In the table in Fig. 10.7, we show one instance of the class of selected BPTs with the largest Q_{BPT} . Given that the Hamiltonian again induces single bit flips, we see that this BPT has a transition structure to maximize dynamical loss of coherence. In figure 10.8, we plot the average entanglement growth rate Q_{BPT} for all the different row alignments possible given the column structure fixed by the collective M_c . As with the $N = 3$ case, we see different classes of BPTs emerge

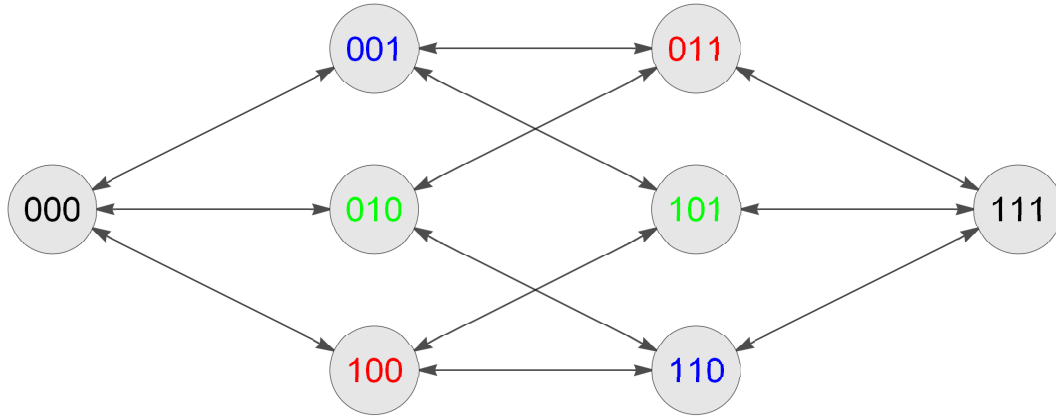


Figure 10.5: Transition structure of the Hamiltonian in the tensor product basis of $M_c = \sum_{\mu=1}^3 \sigma_z^{(\mu)}$ for $N = 3$ spins. It should be noted that this is not a BPT representation, but only illustrates the transition structure of the Hamiltonian in the chosen basis.

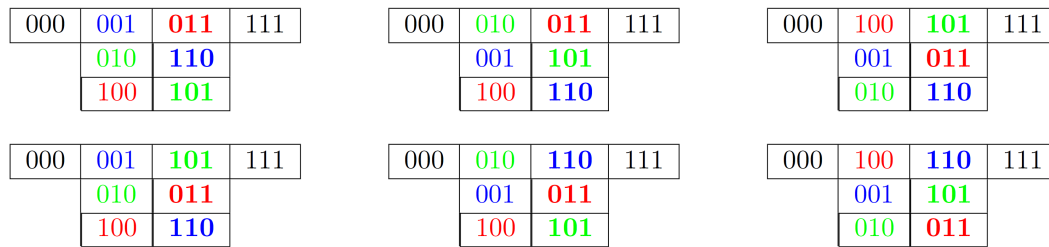


Figure 10.6: (color online) The 6 selected, quasi-classical BPTs which maximize Q_{BPT} as a measure of dynamical coherence for $N = 3$ spins corresponding to the compatible collective observable $M_c = \sum_{\mu=1}^3 \sigma_z^{(\mu)}$. Allowed transitions by the Hamiltonian flip single bits in the $\{|0\rangle, |1\rangle\}$ basis. States in the middle two columns not connected by Hamiltonian transitions are shown by the same color.

which correspond to different entanglement growths. It is interesting to note how distinct the first few classes with the largest entanglement growth rates are which correspond to quasi-classical behavior (as shown in the inset in figure 10.8), in contrast with generic permutations where the entanglement growth varies in a more smooth fashion, representing the generic nature of typical BPTs being away from quasi-classicality.

$g > g_{\text{crit}}$: Average Spin-x as Collective Observable

In the other case when $g > g_{\text{crit}}$, the external magnetic field term along the x -direction in the Ising Hamiltonian dominates which sets the most compatible collective observable to be $M_c \sim \sum_{\mu=1}^N \sigma_x^{(\mu)}$, the average spin-x of the Ising chain. As discussed

0000	1000	1010	1101	1111
	0100	0101	1110	
	0010	0110	1011	
	0001	1001	0111	
		0011		
		1100		

Figure 10.7: One instance of the class of selected quasi-classical BPTs for $N = 4$ spins corresponding to the compatible collective observable $M_c = \sum_{\mu=1}^3 \sigma_z^{(\mu)}$. Allowed transitions by the Hamiltonian flip single bits in the $\{|0\rangle, |1\rangle\}$ basis.

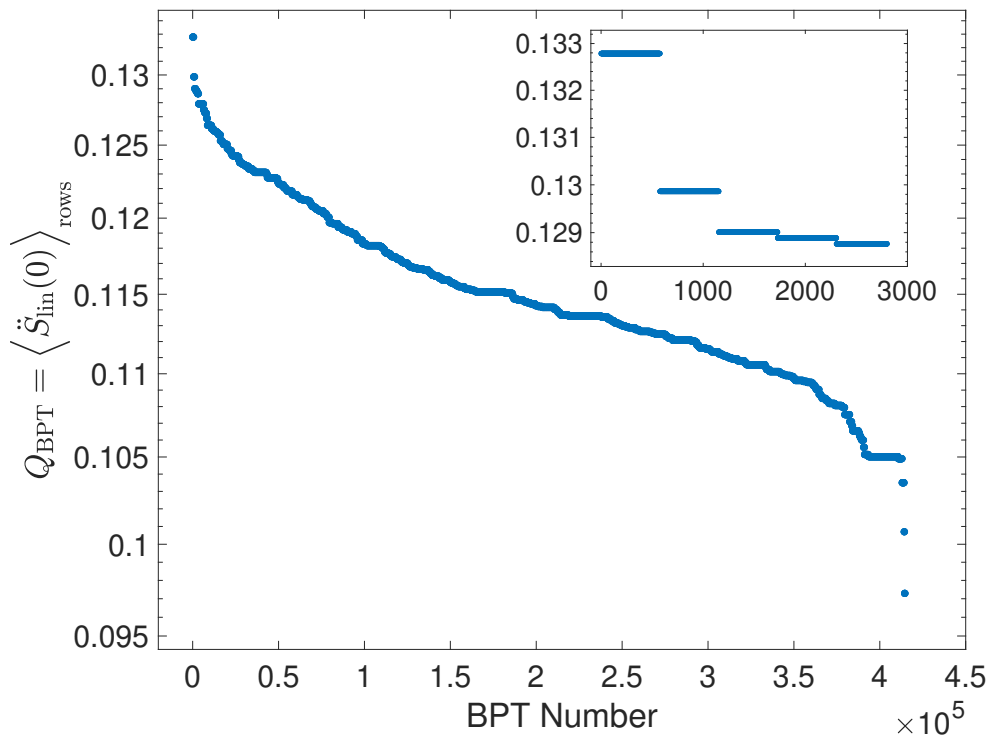


Figure 10.8: Plot of average entanglement growth rate Q_{BPT} over different BPTs (different row arrangements) for $N = 4$ spins with the compatible collective observable $M_c = \sum_{\mu=1}^3 \sigma_z^{(\mu)}$ corresponding to a value of $g = 0.6 < g_{\text{crit}}$. The inset shows the first few classes of BPTs with lowest values of Q_{BPT} .

before, this choice of M_c offers us an orthonormal basis of $\{|+\rangle, |-\rangle\}^{\otimes N}$ to work with in the BPT. The action of the Hamiltonian on these tensor product basis furnished from eigenstates of M_c is to *flip two adjacent bits* in the $\{|+\rangle, |-\rangle\}$ basis due to the presence of the $z - z$ interaction term. Due to this transition structure of the Hamil-

tonian in the M_c basis, bit flips of two adjacent spins *cannot* successively connect each of the N_C column subspaces and hence there will be superselection sectors in this case. Based on this transition structure of the Hamiltonian, we can split the $M_c \sim \sum_{\mu} \sigma_x^{(\mu)}$ basis into superselection sectors and iterate over row arrangements in each sector to maximize dynamical decoherence (by maximizing the average entanglement growth rate Q_{BPT}) to find the most compatible, quasi-classical coarse-graining. In the table in Fig. 10.9, we show the unique selected quasi-classical BPT. The selected BPTs again have the same feature that the transitions by the Hamiltonian are such that there is maximum dynamical decoherence under the state-reduction map induced by the BPT. A detailed analysis of this case of $g > g_{\text{crit}}$ can be done as was done for the $g < g_{\text{crit}}$ case by studying the variation of Q_{BPT} for these BPTs and the Hamiltonian transition structure, but we keep the discussion here brief since the results follow the same physics as described in the previous subsection. We see that depending on the nature of the Hamiltonian, different coarse-grained features can emerge as the ones which qualify as classical. Underlying symmetries of the Hamiltonian are reflected in the class of coarse-grainings which get picked out and reinforce the role played by dynamics in determining the set of quasi-classical variables of a system.

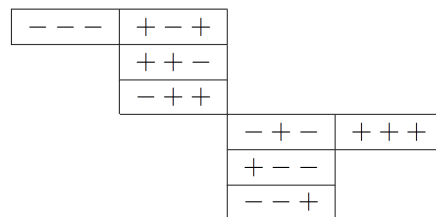


Figure 10.9: The selected, unique quasi-classical BPTs with minimum entanglement growth rate for $N = 3$ spins corresponding to the compatible collective observable $M_c = \sum_{\mu=1}^3 \sigma_x^{(\mu)}$. Allowed transitions by the Hamiltonian flip two adjacent bits in the $\{|+\rangle, |-\rangle\}$ basis which induce the superselection sectors.

We would emphasize that a number of assumptions, albeit physically motivated, went into the formulation of this algorithm and for completeness, we enumerate them here to remind the reader of the context we are focusing on. First, we are working with a fixed microfactorization of Hilbert space into a collection of degrees of freedom which we wish to coarse-grain. We further take this access to the microfactorization

to furnish us a tensor product basis for Hilbert space, in particular for the collective observable M_c . Once we have picked out M_c by the compatibility condition with the Hamiltonian of Eq. (10.178), we focus only on compact BPTs since they minimize loss of coherence due to the action of the state-reduction map itself so we can study the dynamical decoherence which leads to classicality. One could work with more general bipartitions by allowing unitary change of basis which mixes between degrees of freedom and it would be interesting to develop an algorithm, akin to the one of Section 10.4, to construct partial BPTs based on access to a restricted set of observables which do not span an algebra. Such an algorithm would generalize considerations to non-compact form as well as allow for superselection sectors governed by the specifying set of measurements.

To measure the dynamical decoherence induced by the internal subspace $\mathcal{S}_{\text{internal}}$, we used linear entanglement entropy for small times to measure how fast decoherence happens since non-classical states are expected to not decohere as fast on short timescales. Our choice of initial states were uniform superposition states supported on a single row of the BPT, which offered a natural generalization of initial, unentangled states between the system and a ready state for the environment. One can imagine relaxing these assumptions to develop a more generic framework by studying a broader class of initial states, which would reflect more freedom in the ready state of $\mathcal{S}_{\text{internal}}$, or the type of superpositions in $\mathcal{S}_{\text{collective}}$ best suited to physical situations where decoherence is expected to be important. While our choice of linear entanglement entropy was for ease of mathematical manipulation, different measures of decoherence and entanglement such as von Neumann entropy could also be used. One can study the long time behavior where it is expected dynamical decoherence will have picked out the classical pointer basis where the reduced density matrix becomes diagonal and stays so. While more detailed, we expect the basic underlying physics to still be similar to the results described in this paper.

We would also briefly recall some features of the numerics which have gone into figures 10.4 and 10.8. Recall that we are working with a normalized Hamiltonian so as to be able to tune the value of the interaction parameter g which sets the strength of the external magnetic field in the x -direction to be able to toggle between a Hamiltonian with only the $z - z$ interaction ($g = 0$) between neighboring spins to a Hamiltonian with only the external field ($g = \infty$). While this normalization is for us to get a better handle between the interplay of H and M_c , it affects the

rate of entropy production and hence our results here are a proof of principle. Our measure of quasi-classicality of maximizing Q_{BPT} is a suggestive quantifier that captures the qualitative idea that superpositions of classical macroscopic pointer states decohere effectively under evolution. We have focused on small time evolution for concreteness (by probing $\dot{S}_{\text{lin}}(0)$) since we expect that classical states under the quasi-classical BPT will start decohering rather quickly, unlike non-classical ones. The first few classes of BPTs with largest Q_{BPT} are the most quasi-classical compared to generic BPTs. We emphasize that our measure of Eq. (10.187) is a zeroth-order attempt to capture the broad idea of quasi-classicality and depending on the exact application one wishes to have, this quantifier can be more suitably chosen to yield more precise and richer quasi-classical coarse-grainings. The examples illustrated here were for a small number N of spins for ease of tractability of results and we expect these results will become sharper as one goes to higher dimensions, since decoherence is typically aided by having large dimensions of the internal “environment” being traced over.

10.9 Applications and Future Work

In this section we discuss some of the potential applications of generalized and partial bipartitions to extant problems in the literature.

Quantum Information Encoding

It has long been recognized that the irreducible representation (irrep) structure of an operator algebra plays an important role in quantum information. In particular, in the theory of quantum error correction, the generalized bipartition structure is recognized as the fundamental structure behind all quantum error correcting codes [237, 256, 257]. Noiseless subsystems, for example, are identified by the generalized bipartition associated with the commutant algebra generated by the errors [247]. Subsystem codes [236, 237, 258], which generalize the idea of noiseless subsystems, are identified by a generalized bipartition usually associated with a non-abelian group (which also generalizes the construction of stabilizer codes that are associated with abelian groups [259, 260]). Similarly, the idea of quantum state compression with respect to a preferred set of observables [261] relies on the generalized bipartition associated with the algebra of preferred observables; it is conceptually equivalent to the notion of quantum state reductions from a restricted algebra of observables that we discussed in Section 10.3. In such applications, the problem of identifying the generalized bipartition associated with the relevant algebra is fundamental. In

the cases where the relevant algebra is given by a group with a well understood irrep structure, the generalized bipartition is clear. In all other cases, however, the algorithm presented in Section 10.4 can be used as an analytical tool to identify the generalized bipartition.

We may also consider the more general problem of characterizing how the evolution given by a Hamiltonian or a channel acting on the physical system affects the logical degrees of freedom. Such problems are traditionally addressed by looking for symmetries of dynamics that identify the generalized bipartition (i.e. the irrep decomposition) with respect to which the dynamics are restricted to distinct irrep sectors [246]. The main difficulty with this approach is of course in identifying “useful” symmetries. An alternative approach would be to identify an algebra that contains the operator(s) of dynamics directly, without appealing to symmetries. The action of quantum channels, for example, can be restricted to the irrep sectors of the algebra generated by their Kraus operators [262]. Similarly, when dealing with Hamiltonians, even if we cannot find the irrep structure of the algebra generated by the Hamiltonian itself (a task that is equivalent to diagonalizing it), we can consider an irrep structure of some larger algebra that contains the Hamiltonian. This is, in fact, what we achieve by identifying a symmetry: the commutant algebra of the symmetry group is an algebra that contains the Hamiltonian which allows us to restrict its action to the irreps of the group. There are other ways, however, besides symmetries, to identify an algebra that contains the Hamiltonian. For example, if the Hamiltonian is a sum of multiple terms, then it belongs to the algebra generated by those terms. In particular, given a parameterized Hamiltonians as a sum of “tunable” terms whose strength is set by some natural or experimental constraints, the dynamics can be restricted to the irreps of the algebra generated by the tunable terms, independent of the parameters. A prime example of such scenario is the tunable exchange interaction in the Heisenberg spin- $\frac{1}{2}$ chain that implements qubit operations [263]. It would be interesting to see if the algorithm of Section 10.4 can address such problems, especially when the standard symmetry considerations fall short.

Bulk Reconstruction

The AdS/CFT correspondence [1, 264–266] equates the partition function, and thus the Hilbert space, of string theory or M-theory on negatively curved backgrounds and superconformal field theories. In the large N limit, the relation describes a duality between classical (super)gravity in $D + 1$ dimensions with fixed small and negative

cosmological constant and a particular sector of (super)conformal field theories in D dimensions with fixed large central charge. So, in this limit, the correspondence becomes a holographic one in which we can use computations in a CFT living on the boundary of an appropriate spacetime to tell us about gravitational quantities in the bulk of the spacetime, and vice versa. In many cases, we would prefer to treat the bulk as a fixed solution to Einstein's equations sourced by quantum fields—that is, to consider only energy regimes and sets of observables which do not probe stringy or quantum-gravitational degrees of freedom in the bulk. In the language we have used throughout the paper, it is thus natural to think of the classical states as living in a coarse-grained Hilbert space obtained by tracking only a restricted set of observables, namely (low-point) correlation functions of light bulk fields. We can then apply the holographic duality and ask what the coarse-grained Hilbert space looks like from the perspective of the CFT. In particular, we can ask what the holographic duals of classical bulk observables are, or how classical information about the bulk can be “reconstructed” from the CFT state.

In recent years, a holographic error-correcting code approach to bulk reconstruction has been developed along these lines [34, 267–269]. When the bulk dual of a CFT state is captured by a single bulk (Lorentzian) geometry, causality dictates that we should be able to recover all of the information inside a region by considering only its past domain of dependence. Hence we do not require knowledge of the entire coarse-grained CFT boundary state to reconstruct a local correlation function at a particular point in the bulk, but only some smaller region of the boundary at an earlier time. (We cannot directly associate a state to this region of the boundary, since the CFT does not factorize spatially, but we can instead consider the subalgebra of observables supported in the region.) Because multiple possible boundary subregions can be used to redundantly reconstruct the same point in the bulk, the appropriate quantum-mechanical description of the bulk information contained in a given holographic CFT state is a *complementary* error-correcting code, which can be divided into small code subspaces, each of which can be used to reconstruct the appropriate bulk observables.

The methods of this paper apply directly to bulk reconstruction, at least when an appropriate UV cutoff or latticization is provided to render the system finite-dimensional. It would be very interesting to directly construct the generalized bipartition for the classical observables in an explicit tensor network model (see e.g. [270]). To probe the complementary nature of the resulting reduced state, we

could consider, for example, first restricting to all classical observables, then further reducing to the state given only by the observables supported inside a particular lightcone. It would also be interesting to use our state-reduction methods to explicitly construct the set of holographic states by considering both a restricted set of classical bulk observables and a restricted set of boundary observables, which in general we expect to yield two different state-reduction maps, and enumerating the set of states for which their action is identical.

Edge Modes and Gauge Symmetries

In perturbative quantum field theory²⁷, we start from the free-field Hilbert space, which is constructed via a mode expansion in which the degrees of freedom are oscillators with given frequencies. One basis for the Hilbert space is the field-value basis, in which each mode has a definite occupation number. However, this picture runs into difficulties when the theory has (gauge or global) symmetries—that is, constraints, for example a Gauss law, on the allowed set of states in the “gauged” or “physical” Hilbert space. On the level of the mode expansion, these constraints prevent us from treating each mode as independent, meaning that the physical Hilbert space may not factorize into modes at all, and in particular that we might not be able to construct a reduced state by tracing out degrees of freedom in a gauge-invariant way.

As a toy model, for example, we can consider a lattice of 3 qubits with a \mathbb{Z}_2 symmetry, in which we identify a given state with the reversed state created by flipping the spin of each qubit simultaneously across some axis of the Bloch sphere. Without this global symmetry, the Hilbert space is isomorphic to $(\mathbb{C}^2)^{\otimes 3}$, an 8-dimensional Hilbert space which manifestly factorizes into three pieces. However, imposing the symmetry reduces the Hilbert space to a 4-dimensional one in which we can no longer precisely identify individual qubits. On the level of the abstract Hilbert space, to be sure, there was no need to talk about the larger 8-dimensional space at all—we could just have started directly with the 4-dimensional physical Hilbert space.

Although it is not justified from the physical Hilbert space alone, we nevertheless often have in mind a particular “ungauged” Hilbert space that does have nice fac-

²⁷In this motivational description of quantum field theory, we are ignoring many subtleties such as normalization, renormalization, unitary inequivalence, convergence of the perturbative expansion, well-definedness of the theory, loop corrections, IR issues, etc., etc. We invite the reader to consult their favorite QFT textbook and/or keep in mind a lattice regularization which explicitly fixes the Hilbert space of the theory.

torization properties. Then we would like to be able to sensibly construct a reduced state even when the theory has an obstructing symmetry, such as the state of a gauge theory or conformal field theory on an interval, or the state of a spatial subregion in a diffeomorphism-invariant theory like general relativity. Such a construction is provided by the edge modes program [233–235] (see also [271]). On the quantum-mechanical level, one looks for an embedding of the physical Hilbert space, which need not factorize, into a larger Hilbert space with some desired factorization properties, such as the existence of spatial intervals. Given this embedding, we can map the original state to a state in the larger Hilbert space, and then reduce in the usual way. The choice of embedding is not unique, but the edge modes program provides a particularly symmetric choice of embedding which corresponds to summing over all possible representations of matter charged under the symmetry, the eponymous edge modes.

From this description it should be clear that our approach is complementary. The edge modes approach starts with a “small,” physical Hilbert space, chooses a “large,” auxiliary Hilbert space to embed into, and then constructs the reduced states by applying the appropriate partial-trace map on this large Hilbert space. The generalized bipartition approach starts directly with a choice of operators specifying the allowed subregions, and provides a state-reduction map, not necessarily the partial-trace map, which produces the reduced states. If we take the approach of Footnote 2 above and think of the generalized bipartition as a diagonal embedding into a larger bipartite Hilbert space, our approach naturally produces the desired auxiliary, ungauged Hilbert space as well. It would be very interesting to directly compare the state-reduction maps from generalized bipartitions to the edge-modes description in discrete systems such as \mathbb{Z}_n lattice gauge theories. In the context of holography, we might, for example, compute the entropy of a subinterval of a CFT, and compare to the Cardy formula, the replica prescription, the edge modes prescription, and the Ryu-Takayanagi formula, some of which give definite answers and some of which should depend on the particular choice of embedding.

Quantum Gravity

Any realistic theory of quantum gravity must contain states, like our world, which look at low energies and large distances like field-theoretic excitations on top of a fixed spatial background. That is, there should exist some sectors of the quantum gravity Hilbert space that look like QFTs on curved spacetime. If quantum gravity is a *bona fide* quantum-mechanical theory that describes more than a single fixed

metric, it should contain many more states which look nothing like field theories on fixed backgrounds. In ascending order of speculation, the theory should certainly include superpositions of geometries (which can be straightforwardly produced experimentally by placing test masses in superpositions, e.g. [272]), if its UV completion still has a good notion of spatial backgrounds, it should contain heavy or stringy states, and it might contain “spacetime foam”-like states in which the notion of spacetime breaks down entirely. Hence, we should most likely not expect states with good spacetime descriptions to be simple factors of the full QG Hilbert space [273], especially if the UV description of gravity is holographic in the manner of AdS/CFT or de Sitter complementarity [17, 18, 41, 175].

A “space from Hilbert space” picture [17, 23, 65, 172], in which local spatial degrees of freedom are emergent rather than fundamental, would require a detailed picture of exactly how these geometric and field-theoretic degrees of freedom in fact emerge. In this chapter, we have attacked precisely this problem in a quantum-mechanical context. Generalized bipartitions and partial bipartitions are tools for producing reduced states which provide information about degrees of freedom that are not manifest in the full Hilbert space (c.f. [274], which points out that the set of approximately-localized operators in a subregion of a gravitational theory may not comprise an algebra). Interactions between these degrees of freedom and the rest of the theory drive dynamics which may pick out a certain subset as classical observables along the lines of the decoherence program. Because quantum cosmology lacks a fixed separation between system and environment, a variational approach is required to find the “most classical” bipartitions, or to understand what dynamics lead these preferred observables to look like spacetime variables.

Part V

Bibliography

BIBLIOGRAPHY

- [1] J. M. Maldacena, “The Large N limit of superconformal field theories and supergravity,” *Int. J. Theor. Phys.* **38** (1999) 1113–1133, [arXiv:hep-th/9711200](https://arxiv.org/abs/hep-th/9711200) [hep-th].
- [2] F. M. Kronz and T. A. Luper, “Unitarily inequivalent representations in algebraic quantum theory,” *Int. J. Theor. Phys.* **44** no. 8, (Aug, 2005) 1239–1258. <https://doi.org/10.1007/s10773-005-4683-0>.
- [3] R. Haag, “On Quantum Field Theories,” *Matematisk-fysiske Meddelelser* **29** no. 12, (1955) 1–37.
- [4] B. S. DeWitt, “Quantum theory of gravity. 1. The canonical theory,” *Phys. Rev.* **160** (1967) 1113–1148.
- [5] D. N. Page and W. K. Wootters, “Evolution without evolution: Dynamics described by stationary observables,” *Phys. Rev. D* **27** (Jun, 1983) 2885–2892. <https://link.aps.org/doi/10.1103/PhysRevD.27.2885>.
- [6] W. K. Wootters, “Time replaced by quantum correlations,” *Int. J. Theor. Phys.* **23** no. 8, (1984) 701–711.
- [7] D. N. Page, “Time as an inaccessible observable,” Tech. Rep. NSF-ITP-89-18, Calif. Univ. Santa Barbara. Inst. Theor. Phys., Santa Barbara, CA, Feb, 1989. <http://cds.cern.ch/record/195521>.
- [8] V. Giovannetti, S. Lloyd, and L. Maccone, “Quantum time,” *Phys. Rev. D* **92** (Aug, 2015) 045033. <https://link.aps.org/doi/10.1103/PhysRevD.92.045033>.
- [9] R. Jagannathan, “On generalized Clifford algebras and their physical applications,” [arXiv:1005.4300](https://arxiv.org/abs/1005.4300) [math-ph].
- [10] A. Singh and S. M. Carroll, “Modeling position and momentum in finite-dimensional Hilbert spaces via generalized Pauli operators,” [arXiv:1806.10134](https://arxiv.org/abs/1806.10134) [quant-ph].
- [11] N. P. Landsman, “Observation and superselection in quantum mechanics,” *Studies in History and Philosophy of Science Part B: Studies in History and Philosophy of Modern Physics* **26** no. 1, (1995) 45–73.
- [12] H. Reeh and S. Schlieder, “Bemerkungen zur unitäräquivalenz von lorentzinvarianten feldern,” *Il Nuovo Cimento (1955-1965)* **22** no. 5, (Dec, 1961) 1051–1068. <https://doi.org/10.1007/BF02787889>.

- [13] E. Witten, “APS medal for exceptional achievement in research: Invited article on entanglement properties of quantum field theory,” *Rev. Mod. Phys.* **90** no. 4, (2018) 045003, [arXiv:1803.04993 \[hep-th\]](#).
- [14] S. M. Carroll and A. Singh, *Mad-Dog Everettianism: Quantum mechanics at its most minimal*, pp. 95–104. Springer International Publishing, 2019. https://doi.org/10.1007/978-3-030-11301-8_10.
- [15] S. B. Giddings, “Hilbert space structure in quantum gravity: an algebraic perspective,” *J. High Energ. Phys.* **12** (2015) 099, [arXiv:1503.08207 \[hep-th\]](#).
- [16] S. Coleman, “Quantum sine-gordon equation as the massive thirring model,” *Phys. Rev. D* **11** (Apr, 1975) 2088–2097. <http://link.aps.org/doi/10.1103/PhysRevD.11.2088>.
- [17] N. Bao, S. M. Carroll, and A. Singh, “The Hilbert space of quantum gravity is locally finite-dimensional,” *Int. J. Mod. Phys. D* **26** no. 12, (2017) 1743013, [arXiv:1704.00066 \[hep-th\]](#).
- [18] J. D. Bekenstein, “Universal upper bound on the entropy-to-energy ratio for bounded systems,” *Phys. Rev. D* **23** (Jan, 1981) 287–298. <http://link.aps.org/doi/10.1103/PhysRevD.23.287>.
- [19] S. M. Carroll and A. Chatwin-Davies, “Cosmic Equilibration: A Holographic No-Hair Theorem from the Generalized Second Law,” *Phys. Rev. D* **97** no. 4, (2018) 046012, [arXiv:1703.09241 \[hep-th\]](#).
- [20] W. Fischler, “Taking de Sitter seriously.” Talk given at Role of Scaling Laws in Physics and Biology (Celebrating the 60th Birthday of Geoffrey West), Santa Fe, Dec., 2000.
- [21] T. Banks, “QuantuMechanics and CosMology.” Talk given at the festschrift for L. Susskind, Stanford University, May 2000, 2000.
- [22] J. S. Cotler, G. R. Penington, and D. H. Ranard, “Locality from the Spectrum,” *Commun. Math. Phys.* **368** no. 3, (2019) 1267–1296, [arXiv:1702.06142 \[quant-ph\]](#).
- [23] C. Cao, S. M. Carroll, and S. Michalakis, “Space from Hilbert space: Recovering geometry from bulk entanglement,” *Phys. Rev. D* **95** no. 2, (2017) 024031, [arXiv:1606.08444 \[hep-th\]](#).
- [24] C. Cao and S. M. Carroll, “Bulk entanglement gravity without a boundary: Towards finding einstein’s equation in hilbert space,” *Phys. Rev. D* **97** (Apr, 2018) 086003. <https://link.aps.org/doi/10.1103/PhysRevD.97.086003>.

- [25] D. Wallace, “How to prove the Born Rule,” *ArXiv e-prints* (June, 2009) , [arXiv:0906.2718](https://arxiv.org/abs/0906.2718) [quant-ph].
- [26] C. T. Sebens and S. M. Carroll, “Self-locating uncertainty and the origin of probability in Everettian quantum Mechanics,” *Brit. J. Phil. Sci.* (2014) , [arXiv:1405.7577](https://arxiv.org/abs/1405.7577).
- [27] W. H. Zurek, “Pointer Basis of Quantum Apparatus: Into What Mixture Does the Wave Packet Collapse?,” *Phys. Rev.* **D24** (1981) 1516–1525.
- [28] M. Tegmark, “Consciousness as a state of matter,” *Chaos Solitons Fractals* **76** (2015) 238–270, [arXiv:1401.1219](https://arxiv.org/abs/1401.1219) [quant-ph].
- [29] S. M. Carroll and A. Singh, “Quantum Mereology: Factorizing Hilbert Space into Subsystems with Quasi-Classical Dynamics,” [arXiv:2005.12938](https://arxiv.org/abs/2005.12938) [quant-ph].
- [30] T. Jacobson, “Entanglement equilibrium and the Einstein equation,” *Phys. Rev. Lett.* **116** no. 20, (2016) 201101, [arXiv:1505.04753](https://arxiv.org/abs/1505.04753) [gr-qc].
- [31] A. Albrecht and A. Iglesias, “The Clock ambiguity and the emergence of physical laws,” *Phys. Rev.* **D77** (2008) 063506, [arXiv:0708.2743](https://arxiv.org/abs/0708.2743) [hep-th].
- [32] A. Connes and C. Rovelli, “Von Neumann algebra automorphisms and time thermodynamics relation in general covariant quantum theories,” *Class. Quant. Grav.* **11** (1994) 2899–2918, [arXiv:gr-qc/9406019](https://arxiv.org/abs/gr-qc/9406019) [gr-qc].
- [33] S. M. Carroll, “What if Time Really Exists?,” [arXiv:0811.3772](https://arxiv.org/abs/0811.3772) [gr-qc].
- [34] D. Harlow, “The Ryu-Takayanagi formula from quantum error correction,” *Commun. Math. Phys.* **354** no. 3, (2017) 865–912, [arXiv:1607.03901](https://arxiv.org/abs/1607.03901) [hep-th].
- [35] J. D. Bekenstein, “Black holes and entropy,” *Phys. Rev. D* **7** (Apr, 1973) 2333–2346. <http://link.aps.org/doi/10.1103/PhysRevD.7.2333>.
- [36] T. Banks, “Cosmological breaking of supersymmetry?,” *Int. J. Mod. Phys.* **A16** (2001) 910–921, [arXiv:hep-th/0007146](https://arxiv.org/abs/hep-th/0007146) [hep-th].
- [37] E. Witten, “Quantum gravity in de Sitter space,” in *Strings 2001: International Conference Mumbai, India, January 5-10, 2001*. 2001. [arXiv:hep-th/0106109](https://arxiv.org/abs/hep-th/0106109) [hep-th]. <http://alice.cern.ch/format/showfull?sysnb=2259607>.
- [38] L. Dyson, M. Kleban, and L. Susskind, “Disturbing implications of a cosmological constant,” *J. High Energ. Phys.* **10** (2002) 011, [arXiv:hep-th/0208013](https://arxiv.org/abs/hep-th/0208013).

- [39] M. K. Parikh and E. P. Verlinde, “De Sitter holography with a finite number of states,” *J. High Energ. Phys.* **01** (2005) 054, [arXiv:hep-th/0410227 \[hep-th\]](#).
- [40] M. Van Raamsdonk, “Building up spacetime with quantum entanglement,” *Gen. Rel. Grav.* **42** (2010) 2323–2329, [arXiv:1005.3035 \[hep-th\]](#). [Int. J. Mod. Phys.D19,2429(2010)].
- [41] L. Susskind, L. Thorlacius, and J. Uglum, “The stretched horizon and black hole complementarity,” *Phys. Rev.* **D48** (1993) 3743–3761, [arXiv:hep-th/9306069 \[hep-th\]](#).
- [42] R. Bousso, “A covariant entropy conjecture,” *J. High Energ. Phys.* **07** (1999) 004, [arXiv:hep-th/9905177 \[hep-th\]](#).
- [43] H. Casini, M. Huerta, and J. A. Rosabal, “Remarks on entanglement entropy for gauge fields,” *Phys. Rev.* **D89** no. 8, (2014) 085012, [arXiv:1312.1183 \[hep-th\]](#).
- [44] D. Harlow, “Wormholes, emergent gauge fields, and the weak gravity conjecture,” *J. High Energ. Phys.* **01** (2016) 122, [arXiv:1510.07911 \[hep-th\]](#).
- [45] D. Marolf, “Emergent gravity requires kinematic nonlocality,” *Phys. Rev. Lett.* **114** no. 3, (2015) 031104, [arXiv:1409.2509 \[hep-th\]](#).
- [46] W. Donnelly and S. B. Giddings, “Diffeomorphism-invariant observables and their nonlocal algebra,” *Phys. Rev.* **D93** no. 2, (2016) 024030, [arXiv:1507.07921 \[hep-th\]](#). [Erratum: Phys. Rev.D94,no.2,029903(2016)].
- [47] W. Donnelly and S. B. Giddings, “Observables, gravitational dressing, and obstructions to locality and subsystems,” *Phys. Rev.* **D94** no. 10, (2016) 104038, [arXiv:1607.01025 \[hep-th\]](#).
- [48] C. Barceló, R. Carballo-Rubio, F. Di Filippo, and L. J. Garay, “From physical symmetries to emergent gauge symmetries,” *JHEP* **10** (2016) 084, [arXiv:1608.07473 \[gr-qc\]](#).
- [49] D. Mattingly, “Modern tests of Lorentz invariance,” *Living Rev. Rel.* **8** (2005) 5, [arXiv:gr-qc/0502097 \[gr-qc\]](#).
- [50] N. Bao, C. Cao, S. M. Carroll, and L. McAllister, “Quantum circuit cosmology: The expansion of the universe since the first qubit,” [arXiv:1702.06959 \[hep-th\]](#).
- [51] A. Singh, “Quantum space, quantum time, and relativistic quantum mechanics,” [arXiv:2004.09139 \[quant-ph\]](#).

- [52] J. D. Bjorken and S. D. Drell, *Relativistic Quantum Mechanics*. International Series In Pure and Applied Physics. McGraw-Hill, New York, 1965.
- [53] R. Shankar, *Principles of quantum mechanics*. Springer Science & Business Media, 2012.
- [54] M. D. Sanctis, “An introduction to relativistic quantum mechanics. i. from relativity to dirac equation,” [arXiv:0708.0052](https://arxiv.org/abs/0708.0052) [physics.gen-ph].
- [55] C. J. Isham, “Canonical quantum gravity and the problem of time,” [arXiv:gr-qc/9210011](https://arxiv.org/abs/gr-qc/9210011) [gr-qc]. [NATO Sci. Ser. C409,157(1993)].
- [56] E. Anderson, *The Problem of Time: Quantum Mechanics versus General Relativity*. Fundamental Theories of Physics, Vol 190. Springer International Publishing, 2017.
<https://www.springer.com/us/book/9783319588469>.
- [57] K. Kuchař, “Proceedings of the 4th canadian conference on general relativity and relativistic astrophysics,”.
- [58] A. Deriglazov and B. F. Rizzuti, “Reparametrization-invariant formulation of classical mechanics and the schrödinger equation,” *Am. J. Phys.* **79** no. 8, (2011) 882–885. <https://doi.org/10.1119/1.3593270>.
- [59] A. A. Deriglazov and K. E. Evdokimov, “Local symmetries and the nöther identities in the hamiltonian framework,” *Int. J. Mod. Phys. A* **15** no. 25, (2000) 4045–4067. <https://doi.org/10.1142/S0217751X00001890>.
- [60] A. A. Deriglazov, “Improved extended hamiltonian and search for local symmetries,” *J. Math. Phys.* **50** no. 1, (2009) 012907.
<https://doi.org/10.1063/1.3068728>.
- [61] A. A. Deriglazov, “Notes on lagrangean and hamiltonian symmetries,” [arXiv:hep-th/9412244](https://arxiv.org/abs/hep-th/9412244) [hep-th].
- [62] P. A. M. Dirac, “Generalized hamiltonian dynamics,” *Can. J. Math.* **2** (1950) 129–148.
- [63] P. Dirac, *Lectures on Quantum Mechanics*. Belfer Graduate School of Science, monograph series. Dover Publications, 2001.
<https://books.google.com/books?id=GVwzb1rZW9kC>.
- [64] B. S. DeWitt, “Quantum theory of gravity. ii. the manifestly covariant theory,” *Phys. Rev.* **162** (Oct, 1967) 1195–1239.
<https://link.aps.org/doi/10.1103/PhysRev.162.1195>.
- [65] S. M. Carroll and A. Singh, “Mad-Dog Everettianism: Quantum mechanics at its most minimal,” [arXiv:1801.08132](https://arxiv.org/abs/1801.08132) [quant-ph].

- [66] S. B. Giddings, “Quantum gravity: a quantum-first approach,” *Lett. High Energ. Phys.* **1** no. 3, (2018) 1–3, [arXiv:1805.06900](https://arxiv.org/abs/1805.06900) [hep-th].
- [67] S. B. Giddings, “Quantum-first gravity,” *Found. Phys.* **49** no. 3, (2019) 177–190.
- [68] R. Gambini, R. A. Porto, and J. Pullin, “Loss of quantum coherence from discrete quantum gravity,” *Classical and Quantum Gravity* **21** no. 8, (Mar, 2004) L51–L57.
<https://doi.org/10.1088%2F0264-9381%2F21%2F8%2F101>.
- [69] R. Gambini, R. A. Porto, and J. Pullin, “A relational solution to the problem of time in quantum mechanics and quantum gravity: a fundamental mechanism for quantum decoherence,” *New Journal of Physics* **6** (Apr, 2004) 45–45.
<https://doi.org/10.1088%2F1367-2630%2F6%2F1%2F045>.
- [70] R. Gambini, R. A. Porto, J. Pullin, and S. Torterolo, “Conditional probabilities with dirac observables and the problem of time in quantum gravity,” *Phys. Rev. D* **79** (Feb, 2009) 041501.
<https://link.aps.org/doi/10.1103/PhysRevD.79.041501>.
- [71] J. Leon and L. Maccone, “The pauli objection,” *Found. Phys.* **47** no. 12, (2017) 1597–1608.
- [72] L. R. S. Mendes and D. O. Soares-Pinto, “Time as a consequence of internal coherence,” *Proceedings of the Royal Society A: Mathematical, Physical and Engineering Sciences* **475** no. 2231, (2019) 20190470.
<https://royalsocietypublishing.org/doi/abs/10.1098/rspa.2019.0470>.
- [73] A. R. Smith and M. Ahmadi, “Relativistic quantum clocks observe classical and quantum time dilation,” [arXiv:1904.12390](https://arxiv.org/abs/1904.12390) [quant-ph].
- [74] A. R. H. Smith and M. Ahmadi, “Quantizing time: Interacting clocks and systems,” *Quantum* **3** (July, 2019) 160.
<https://doi.org/10.22331/q-2019-07-08-160>.
- [75] P. B. Pal, “Dirac, Majorana and Weyl fermions,” *Am. J. Phys.* **79** (2011) 485–498, [arXiv:1006.1718](https://arxiv.org/abs/1006.1718) [hep-ph].
- [76] Santhanam, T. S., and Tekumalla, A. R., “Quantum Mechanics in Finite Dimensions,” *Found. Phys.* **6** no. 5, (1976) 583–587.
- [77] H. Weyl, *The Theory of Groups and Quantum Mechanics*. Dover Books on Mathematics. Dover Publications, 1950.
<https://books.google.com/books?id=jQbEcDDqGb8C>.

- [78] G. 't Hooft, “Dimensional reduction in quantum gravity,” in *Salamfest 1993:0284-296*, pp. 0284–296. 1993. [arXiv:gr-qc/9310026](#) [gr-qc].
- [79] L. Susskind, “The World as a hologram,” *J. Math. Phys.* **36** (1995) 6377–6396, [arXiv:hep-th/9409089](#) [hep-th].
- [80] A. Albrecht, “The theory of everything vs the theory of anything,” [arXiv:gr-qc/9408023](#) [gr-qc]. [Lect. Notes Phys.455,321(1995)].
- [81] A. Albrecht and A. Iglesias, “The Clock Ambiguity: Implications and new developments,” *Fund. Theor. Phys.* **172** (2012) 53–68.
- [82] C. Marletto and V. Vedral, “Evolution without evolution and without ambiguities,” *Phys. Rev. D* **95** (Feb, 2017) 043510. <https://link.aps.org/doi/10.1103/PhysRevD.95.043510>.
- [83] T. Martinelli and D. O. Soares-Pinto, “Quantifying quantum reference frames in composed systems: Local, global, and mutual asymmetries,” *Phys. Rev. A* **99** (Apr, 2019) 042124. <https://link.aps.org/doi/10.1103/PhysRevA.99.042124>.
- [84] P. A. Höhn and A. Vanrietvelde, “How to switch between relational quantum clocks,” [arXiv:1810.04153](#) [gr-qc].
- [85] A. Vanrietvelde, P. A. Höhn, F. Giacomini, and E. Castro-Ruiz, “A change of perspective: switching quantum reference frames via a perspective-neutral framework,” *Quantum* **4** (Jan., 2020) 225. <https://doi.org/10.22331/q-2020-01-27-225>.
- [86] P. A. Höhn, “Switching Internal Times and a New Perspective on the ‘Wave Function of the Universe’,” *Universe* **5** no. 5, (2019) 116, [arXiv:1811.00611](#) [gr-qc].
- [87] A. Vanrietvelde, P. A. Höhn, and F. Giacomini, “Switching quantum reference frames in the n-body problem and the absence of global relational perspectives,” [arXiv:1809.05093](#) [quant-ph].
- [88] C. Rovelli, “‘Forget time’,” *Found. Phys.* **41** (2011) 1475–1490, [arXiv:0903.3832](#) [gr-qc].
- [89] J. D. Bekenstein, “Entropy bounds and black hole remnants,” *Phys. Rev. D* **49** (Feb, 1994) 1912–1921, <https://arxiv.org/abs/gr-qc/9307035>. <http://link.aps.org/doi/10.1103/PhysRevD.49.1912>.
- [90] R. Jagannathan, T. S. Santhanam, and R. Vasudevan, “Finite-dimensional quantum mechanics of a particle,” *Int. J. Theor. Phys.* **20** no. 10, (Oct, 1981) 755–773. <https://doi.org/10.1007/BF00674253>.
- [91] R. Jagannathan and T. S. Santhanam, “Finite dimensional quantum mechanics of a particle. 2.,” *Int. J. Theor. Phys.* **21** (1982) 351.

- [92] J. J. Sylvester and H. F. Baker, “The collected mathematical papers of james joseph sylvester,”.
- [93] J. v. Neumann, “Die eindeutigkeit der schrödingerschen operatoren,” *Mathematische Annalen* **104** (1931) 570–578.
<http://eudml.org/doc/159483>.
- [94] J. Schwinger, “Unitary operator bases,” *Proceedings of the National Academy of Sciences* **46** no. 4, (1960) 570–579.
<http://www.pnas.org/content/46/4/570>.
- [95] J. Schwinger, *Quantum Mechanics*. Springer-Verlag Berlin Heidelberg, 2001.
- [96] A. C. de la Torre and D. Goyeneche, “Quantum mechanics in finite-dimensional hilbert space,” *Am. J. Phys.* **71** no. 1, (2003) 49–54.
<https://doi.org/10.1119/1.1514208>.
- [97] A. Vourdas, “Quantum systems with finite hilbert space: Galois fields in quantum mechanics,” *Journal of Physics A: Mathematical and Theoretical* **40** no. 33, (2007) R285.
<http://stacks.iop.org/1751-8121/40/i=33/a=R01>.
- [98] A. Granik and M. Ross, *On a New Basis for a Generalized Clifford Algebra and its Application to Quantum Mechanics*, pp. 101–110. Birkhäuser Boston, Boston, MA, 1996.
https://doi.org/10.1007/978-1-4615-8157-4_6.
- [99] G. Landi, F. Lizzi, and R. J. Szabo, “From large N matrices to the noncommutative torus,” *Commun. Math. Phys.* **217** (2001) 181–201,
[arXiv:hep-th/9912130](https://arxiv.org/abs/hep-th/9912130) [hep-th].
- [100] R. Jagannathan, “Finite-dimensional quantum mechanics of a particle. iii. the weylian quantum mechanics of confined quarks,” *Int. J. Theor. Phys.* **22** no. 12, (Dec, 1983) 1105–1121.
<https://doi.org/10.1007/BF02080317>.
- [101] J. Tolar, “A classification of finite quantum kinematics,” *Journal of Physics: Conference Series* **538** no. 1, (2014) 012020.
<http://stacks.iop.org/1742-6596/538/i=1/a=012020>.
- [102] V. S. Varadarajan, “Variations on a theme of schwinger and weyl,” *Lett. Math. Phys.* **34** no. 3, (Jul, 1995) 319–326.
<https://doi.org/10.1007/BF01872785>.
- [103] T. Digernes, E. Husstad, and V. S. Varadarajan, “Finite approximation of weyl systems,” *Mathematica Scandinavica* **84** no. 2, (Jun., 1999) 261–283.
<https://www.mscaand.dk/article/view/13879>.

- [104] T. Digernes, V. S. Varadarajan, and S. R. S. Varadhan, “Finite approximations to quantum systems,” *Rev. Math. Phys.* **06** no. 04, (1994) 621–648. <https://doi.org/10.1142/S0129055X94000213>.
- [105] P. Stovicek and J. Tolar, “Quantum mechanics in a discrete space-time,” *Rep. Math. Phys.* **20** no. 2, (1984) 157 – 170. <http://www.sciencedirect.com/science/article/pii/0034487784900302>.
- [106] S. Albeverio, E. I. Gordon, and A. Y. Khrennikov, “Finite-dimensional approximations of operators in the hilbert spaces of functions on locally compact abelian groups,” *Acta Applicandae Mathematica* **64** no. 1, (Oct, 2000) 33–73. <https://doi.org/10.1023/A:1006457731833>.
- [107] M. Marchioli and M. Ruzzi, “Theoretical formulation of finite-dimensional discrete phase spaces: I. algebraic structures and uncertainty principles,” *Annals of Physics* **327** no. 6, (2012) 1538 – 1561. <http://www.sciencedirect.com/science/article/pii/S0003491612000334>.
- [108] M. A. Marchioli and P. E. M. F. Mendonca, “Theoretical formulation of finite-dimensional discrete phase spaces: II. On the uncertainty principle for Schwinger unitary operators,” *Annals Phys.* **336** (2013) 76–97, [arXiv:1304.0253](https://arxiv.org/abs/1304.0253) [quant-ph].
- [109] K. Thas, “The geometry of generalized pauli operators of n-qudit hilbert space, and an application to mubs,” *Europhys. Lett.* **86** no. 6, (2009) 60005. <http://stacks.iop.org/0295-5075/86/i=6/a=60005>.
- [110] Bandyopadhyay, Boykin, Roychowdhury, and Vatan, “A new proof for the existence of mutually unbiased bases,” *Algorithmica* **34** no. 4, (Nov, 2002) 512–528. <https://doi.org/10.1007/s00453-002-0980-7>.
- [111] A. O. Pittenger and M. H. Rubin, “Mutually unbiased bases, generalized spin matrices and separability,” *Linear Algebra and its Applications* **390** (2004) 255 – 278. <http://www.sciencedirect.com/science/article/pii/S0024379504002125>.
- [112] E. R. Livine, “Notes on qubit phase space and discrete symplectic structures,” *Journal of Physics A: Mathematical and Theoretical* **43** no. 7, (2010) 075303. <http://stacks.iop.org/1751-8121/43/i=7/a=075303>.
- [113] H. Heydari, “Geometric formulation of quantum mechanics,” [arXiv:1503.00238](https://arxiv.org/abs/1503.00238) [quant-ph].
- [114] F. Piazza, “Glimmers of a pre-geometric perspective,” *Found. Phys.* **40** (2010) 239–266, [arXiv:hep-th/0506124](https://arxiv.org/abs/hep-th/0506124) [hep-th].

- [115] F. Dowker and A. Kent, “On the consistent histories approach to quantum mechanics,” *J. Statist. Phys.* **82** (1996) 1575–1646, [arXiv:gr-qc/9412067](https://arxiv.org/abs/gr-qc/9412067) [gr-qc].
- [116] R. Haag, *Local Quantum Physics*. Springer-Verlag Berlin Heidelberg, 1966.
- [117] V. Pestun *et al.*, “Localization techniques in quantum field theories,” *J. Phys.* **A50** no. 44, (2017) 440301, [arXiv:1608.02952](https://arxiv.org/abs/1608.02952) [hep-th].
- [118] T. D. Newton and E. P. Wigner, “Localized states for elementary systems,” *Rev. Mod. Phys.* **21** (Jul, 1949) 400–406. <https://link.aps.org/doi/10.1103/RevModPhys.21.400>.
- [119] L. O. Herrmann, “Localization in relativistic quantum theories,” June, 2010. <http://philsci-archive.pitt.edu/5427/>.
- [120] G. N. Fleming, “Reeh-schlieder meets newton-wigner,” 1998. <http://philsci-archive.pitt.edu/649/>.
- [121] H. Halvorson, “Reeh-Schlieder defeats Newton-Wigner: On alternative localization schemes in relativistic quantum field theory,” *Phil. Sci.* **68** (2001) 111–133, [arXiv:quant-ph/0007060](https://arxiv.org/abs/quant-ph/0007060) [quant-ph].
- [122] W. Donnelly, “Quantum gravity tomography,” [arXiv:1806.05643](https://arxiv.org/abs/1806.05643) [hep-th].
- [123] S. Banerjee, J.-W. Bryan, K. Papadodimas, and S. Raju, “A toy model of black hole complementarity,” *JHEP* **05** (2016) 004, [arXiv:1603.02812](https://arxiv.org/abs/1603.02812) [hep-th].
- [124] K. S. Gibbons, M. J. Hoffman, and W. K. Wootters, “Discrete phase space based on finite fields,” *Phys. Rev. A* **70** (Dec, 2004) 062101. <https://link.aps.org/doi/10.1103/PhysRevA.70.062101>.
- [125] W. K. Wootters, “A wigner-function formulation of finite-state quantum mechanics,” *Annals of Physics* **176** no. 1, (1987) 1 – 21. <http://www.sciencedirect.com/science/article/pii/000349168790176X>.
- [126] A. Luis, “Quantum phase space points for wigner functions in finite-dimensional spaces,” *Phys. Rev. A* **69** (May, 2004) 052112. <https://link.aps.org/doi/10.1103/PhysRevA.69.052112>.
- [127] V. V. Albert, S. Pascazio, and M. H. Devoret, “General phase spaces: From discrete variables to rotor and continuum limits,” *Journal of Physics A: Mathematical and Theoretical* **50** no. 50, (2017) 504002. <http://stacks.iop.org/1751-8121/50/i=50/a=504002>.
- [128] R. F. Werner, “Uncertainty relations for general phase spaces,” *Frontiers of Physics* **11** no. 3, (Apr, 2016) 110305. <https://doi.org/10.1007/s11467-016-0558-5>.

- [129] M. Ruzzi and D. Galetti, “Quantum discrete phase space dynamics and its continuous limit,” *Journal of Physics A: Mathematical and General* **33** no. 5, (2000) 1065.
<http://stacks.iop.org/0305-4470/33/i=5/a=317>.
- [130] T. Hakioglu and E. Tepedelenlioglu, “The action-angle wigner function: a discrete, finite and algebraic phase space formalism,” *Journal of Physics A: Mathematical and General* **33** no. 36, (2000) 6357.
<http://stacks.iop.org/0305-4470/33/i=36/a=307>.
- [131] T. Hakioglu, “Finite-dimensional schwinger basis, deformed symmetries, wigner function, and an algebraic approach to quantum phase,” *Journal of Physics A: Mathematical and General* **31** no. 33, (1998) 6975.
<http://stacks.iop.org/0305-4470/31/i=33/a=008>.
- [132] M. Ligabò, “Torus as phase space: Weyl quantization, dequantization, and wigner formalism,” *J. Math. Phys.* **57** no. 8, (2016) 082110.
<https://doi.org/10.1063/1.4961325>.
- [133] M. Maggiore, “The algebraic structure of the generalized uncertainty principle,” *Phys. Lett.* **B319** (1993) 83–86, [arXiv:hep-th/9309034](https://arxiv.org/abs/hep-th/9309034) [hep-th].
- [134] M. Maggiore, “A generalized uncertainty principle in quantum gravity,” *Phys. Lett.* **B304** (1993) 65–69, [arXiv:hep-th/9301067](https://arxiv.org/abs/hep-th/9301067) [hep-th].
- [135] P. Bosso, *Generalized Uncertainty Principle and Quantum Gravity Phenomenology*. PhD thesis, Lethbridge U., 2017. [arXiv:1709.04947](https://arxiv.org/abs/1709.04947) [gr-qc].
<https://inspirehep.net/record/1623894/files/arXiv:1709.04947.pdf>.
- [136] K. Abdelkhalek, W. Chemissany, L. Fiedler, G. Mangano, and R. Schwonnek, “Optimal uncertainty relations in a modified heisenberg algebra,” *Phys. Rev. D* **94** (Dec, 2016) 123505.
<https://link.aps.org/doi/10.1103/PhysRevD.94.123505>.
- [137] D. Gottesman, A. Kitaev, and J. Preskill, “Encoding a qubit in an oscillator,” *Phys. Rev.* **A64** (2001) 012310, [arXiv:quant-ph/0008040](https://arxiv.org/abs/quant-ph/0008040) [quant-ph].
- [138] J. Maldacena, S. H. Shenker, and D. Stanford, “A bound on chaos,” *J. High Energ. Phys.* **08** (2016) 106, [arXiv:1503.01409](https://arxiv.org/abs/1503.01409) [hep-th].
- [139] C. Cao, A. Chatwin-Davies, and A. Singh, “How low can vacuum energy go when your fields are finite-dimensional?,” *Int. J. Mod. Phys. D* **28** no. 14, (2019) 1944006, [arXiv:1905.11199](https://arxiv.org/abs/1905.11199) [hep-th].

- [140] A. G. Cohen, D. B. Kaplan, and A. E. Nelson, “Effective field theory, black holes, and the cosmological constant,” *Phys. Rev. Lett.* **82** (1999) 4971–4974, [arXiv:hep-th/9803132](#) [hep-th].
- [141] T. Banks, “SUSY breaking, cosmology, vacuum selection and the cosmological constant in string theory,” in *ITP Workshop on SUSY Phenomena and SUSY GUTS, Santa Barbara, California, December 7-9, 1995*. 1995. [arXiv:hep-th/9601151](#) [hep-th].
- [142] P. Horava, “M theory as a holographic field theory,” *Phys. Rev.* **D59** (1999) 046004, [arXiv:hep-th/9712130](#) [hep-th].
- [143] P. Horava and D. Minic, “Probable values of the cosmological constant in a holographic theory,” *Phys. Rev. Lett.* **85** (2000) 1610–1613, [arXiv:hep-th/0001145](#) [hep-th].
- [144] A. Horn, “Eigenvalues of sums of hermitian matrices.,” *Pacific J. Math.* **12** no. 1, (1962) 225–241.
<https://projecteuclid.org:443/euclid.pjm/1103036720>.
- [145] A. Knutson and T. Tao, “The honeycomb model of $GL(n)$ tensor products I: Proof of the saturation conjecture,” *arXiv Mathematics e-prints* (Jul, 1998) math/9807160, [arXiv:math/9807160](#) [math.RT].
- [146] **Supernova Cosmology Project** Collaboration, S. Perlmutter *et al.*, “Measurements of Omega and Lambda from 42 High-Redshift Supernovae,” *Astrophys. J.* **517** (1999) 565–586, [arXiv:astro-ph/9812133](#).
- [147] **Supernova Search Team** Collaboration, A. G. Riess *et al.*, “Observational Evidence from Supernovae for an Accelerating Universe and a Cosmological Constant,” *Astron. J.* **116** (1998) 1009–1038, [arXiv:astro-ph/9805201](#).
- [148] U. Yurtsever, “The Holographic entropy bound and local quantum field theory,” *Phys. Rev. Lett.* **91** (2003) 041302, [arXiv:gr-qc/0303023](#) [gr-qc].
- [149] A. Aste, “Holographic entropy bound from gravitational Fock space truncation,” *Europhys. Lett.* **69** (2005) 36–40, [arXiv:hep-th/0409046](#) [hep-th].
- [150] T. A. Brun and J. B. Hartle, “Classical dynamics of the quantum harmonic chain,” *Phys. Rev. D* **60** (Nov, 1999) 123503.
<http://link.aps.org/doi/10.1103/PhysRevD.60.123503>.
- [151] M. Gell-Mann and J. B. Hartle, “Alternative decohering histories in quantum mechanics,” [arXiv:1905.05859](#) [quant-ph].

- [152] A. Kent, “Quantum histories,” *Physica Scripta* **1998** no. T76, (1998) 78.
- [153] C. Jess Riedel, W. H. Zurek, and M. Zwolak, “The rise and fall of redundancy in decoherence and quantum Darwinism,” *New J. Phys.* **14** no. 8, (Aug, 2012) 083010, [arXiv:1205.3197 \[quant-ph\]](#).
- [154] R. B. Griffiths, “Consistent histories and the interpretation of quantum mechanics,” *J. Statist. Phys.* **36** (1984) 219.
- [155] J. P. Paz and W. H. Zurek, “Environment-induced decoherence, classicality, and consistency of quantum histories,” *Phys. Rev. D* **48** (Sep, 1993) 2728–2738.
<https://link.aps.org/doi/10.1103/PhysRevD.48.2728>.
- [156] P. Zanardi, “Virtual quantum subsystems,” *Phys. Rev. Lett.* **87** (2001) 077901, [arXiv:quant-ph/0103030 \[quant-ph\]](#).
- [157] P. Zanardi, D. A. Lidar, and S. Lloyd, “Quantum tensor product structures are observable induced,” *Phys. Rev. Lett.* **92** (2004) 060402, [arXiv:quant-ph/0308043 \[quant-ph\]](#).
- [158] O. Kabernik, J. Pollack, and A. Singh, “Quantum state reduction: Generalized bipartitions from algebras of observables,” *Phys. Rev. A* **101** no. 3, (2020) 032303, [arXiv:1909.12851 \[quant-ph\]](#).
- [159] M. Castagnino and O. Lombardi, “Self-induced decoherence: A new approach,” *Studies in the History and Philosophy of Modern Physics* **35** no. 1, (Jan, 2004) 73–107.
- [160] M. Castagnino, S. Fortin, O. Lombardi, and R. Laura, “A general theoretical framework for decoherence in open and closed systems,” *Class. Quant. Grav.* **25** (2008) 154002, [arXiv:0907.1337 \[quant-ph\]](#).
- [161] O. Lombardi, S. Fortin, and M. Castagnino, “The problem of identifying the system and the environment in the phenomenon of decoherence,” in *EPSA Philosophy of Science: Amsterdam 2009*, H. W. de Regt, S. Hartmann, and S. Okasha, eds., pp. 161–174. Springer Netherlands, Dordrecht, 2012.
- [162] S. Fortin, O. Lombardi, and M. Castagnino, “Decoherence: A Closed-System Approach,” *Braz. J. Phys.* **44** no. 1, (Feb, 2014) 138–153, [arXiv:1402.3525 \[quant-ph\]](#).
- [163] M. Schlosshauer, “Self-induced decoherence approach: Strong limitations on its validity in a simple spin bath model and on its general physical relevance,” *Phys. Rev. A* **72** no. 1, (Jul, 2005) 012109, [arXiv:quant-ph/0501138 \[quant-ph\]](#).

- [164] J. Kofler and Č. Brukner, “Classical world arising out of quantum physics under the restriction of coarse-grained measurements,” *Phys. Rev. Lett.* **99** no. 18, (Nov, 2007) 180403, [arXiv:quant-ph/0609079](#) [quant-ph].
- [165] R. Penrose, “Singularities and time-asymmetry,” in *General Relativity: An Einstein Centenary Survey*, S. Hawking and W. Israel, eds. Cambridge University Press, 1979.
- [166] D. Albert, *Time and Chance*. Harvard University Press, 2003.
- [167] H. Everett, “Relative state formulation of quantum mechanics,” *Rev. Mod. Phys.* **29** (1957) 454–462.
- [168] M. Schlosshauer, *Decoherence and the Quantum-to-Classical Transition*. 2007.
- [169] E. Joos and H. D. Zeh, “The emergence of classical properties through interaction with the environment,” *Zeitschrift für Physik B Condensed Matter* **59** no. 2, (1985) 223–243.
- [170] W. H. Zurek, “Preferred observables, predictability, classicality, and the environment induced decoherence,” [arXiv:gr-qc/9402011](#) [gr-qc].
- [171] C. F. Van Loan and N. Pitsianis, “Approximation with kronecker products,” in *Linear algebra for large scale and real-time applications*, pp. 293–314. Springer, 1993.
- [172] J. Pollack and A. Singh, “Towards space from Hilbert space: finding lattice structure in finite-dimensional quantum systems,” *Quant. Stud. Math. Found.* **6** no. 2, (2019) 181–200, [arXiv:1801.10168](#) [quant-ph].
- [173] H. D. Zeh, “On the interpretation of measurement in quantum theory,” *Found. Phys.* **1** (1970) 69.
- [174] E. Joos and H. D. Zeh, “The emergence of classical properties through interaction with the environment,” *Z. Phys. B* **59** (1985) 223.
- [175] M. Srednicki, “Entropy and area,” *Phys. Rev. Lett.* **71** (1993) 666–669, [arXiv:hep-th/9303048](#) [hep-th].
- [176] G. H. Hardy and S. Ramanujan, “The normal number of prime factors of a number n ,” *Quart. J.* **48** (1917) 76–92.
- [177] P. Erdős, “Note on the number of prime divisors of integers,” *Journal of the London Mathematical Society* **s1-12** no. 4, (1937) 308–314. <http://dx.doi.org/10.1112/jlms/s1-12.48.308>.
- [178] J. Garriga and A. Vilenkin, “Recycling universe,” *Phys.Rev.* **D57** (1998) 2230–2244, [arXiv:astro-ph/9707292](#) [astro-ph].

- [179] S. Kachru, R. Kallosh, A. Linde, and S. P. Trivedi, “De Sitter vacua in string theory,” *Phys. Rev.* **D68** (2003) 046005, [arXiv:hep-th/0301240](#).
- [180] R. Bousso and J. Polchinski, “Quantization of four form fluxes and dynamical neutralization of the cosmological constant,” *J. High Energ. Phys.* **06** (2000) 006, [arXiv:hep-th/0004134](#) [hep-th].
- [181] Y. Nomura, “Physical theories, eternal inflation, and quantum universe,” *J. High Energ. Phys.* **11** (2011) 063, [arXiv:1104.2324](#) [hep-th].
- [182] Y. Nomura, “Quantum Mechanics, Spacetime Locality, and Gravity,” *Found. Phys.* **43** (2013) 978–1007, [arXiv:1110.4630](#) [hep-th].
- [183] K. K. Boddy, S. M. Carroll, and J. Pollack, “De Sitter Space Without Dynamical Quantum Fluctuations,” *Found. Phys.* **46** no. 6, (2016) 702–735, [arXiv:1405.0298](#) [hep-th].
- [184] W. Donnelly and L. Freidel, “Local subsystems in gauge theory and gravity,” *J. High Energ. Phys.* **09** (2016) 102, [arXiv:1601.04744](#) [hep-th].
- [185] A. J. Speranza, “Local phase space and edge modes for diffeomorphism-invariant theories,” [arXiv:1706.05061](#) [hep-th].
- [186] E. Witten, “Symmetry and emergence,” [arXiv:1710.01791](#) [hep-th].
- [187] A. Singh and S. M. Carroll, “Quantum decimation in Hilbert space: Coarse-graining without structure,” *Phys. Rev.* **A97** no. 3, (2018) 032111, [arXiv:1709.01066](#) [quant-ph].
- [188] L. Kadanoff, W. Gotze, D. Hamblen, R. Hecht, E. Lewis, V. V. Palciauskas, M. Rayl, J. Swift, D. Aspnes, and J. Kane, “Static phenomena near critical points: theory and experiment,” *Rev. Mod. Phys.* **39** (1967) 395–431.
- [189] M. E. Fisher, “Renormalization group theory: Its basis and formulation in statistical physics,” *Rev. Mod. Phys.* **70** (1998) 653–681.
- [190] K. G. Wilson, “The Renormalization Group: Critical phenomena and the Kondo problem,” *Rev. Mod. Phys.* **47** (1975) 773.
- [191] M. E. Fisher, “The renormalization group in the theory of critical behavior,” *Rev. Mod. Phys.* **46** (1974) 597–616. [Erratum: *Rev. Mod. Phys.* **47**, 543 (1975)].
- [192] J. L. Cardy, “Scaling and renormalization in statistical physics,” *Cambridge, UK: Univ. Pr. (1996) 238 p. (Cambridge lecture notes in physics: 3)* (1996)

- [193] H. J. Maris and L. P. Kadanoff, “Teaching the renormalization group,” *American Journal of Physics* **46** no. 6, (1978) 652–657. <http://dx.doi.org/10.1119/1.11224>.
- [194] A. A. Migdal, “Gauge transitions in gauge and spin lattice systems,” *Sov. Phys. JETP* **42** (1975) 743. [*Zh. Eksp. Teor. Fiz.*69,1457(1975)].
- [195] B. Schumacher, “Quantum coding,” *Phys. Rev. A* **51** (Apr, 1995) 2738–2747. <https://link.aps.org/doi/10.1103/PhysRevA.51.2738>.
- [196] N. Datta, J. M. Renes, R. Renner, and M. M. Wilde, “One-shot lossy quantum data compression,” *IEEE Transactions on Information Theory* **59** no. 12, (Dec, 2013) 8057–8076.
- [197] W. B. Johnson and J. Lindenstrauss, “Extensions of lipschitz mappings into a hilbert space,” *Conference on Modern Analysis and Probability* **26** (1984) 189–206. <http://dx.doi.org/10.1090/conm/026/737400>.
- [198] S. Dasgupta and A. Gupta, “An elementary proof of a theorem of johnson and lindenstrauss,” *Random Structures and Algorithms* **22** no. 1, (2003) 60–65. <http://dx.doi.org/10.1002/rsa.10073>.
- [199] A. W. Harrow, A. Montanaro, and A. J. Short, “Limitations on quantum dimensionality reduction,” in *Automata, Languages and Programming*, L. Aceto, M. Henzinger, and J. Sgall, eds., pp. 86–97. Springer Berlin Heidelberg, Berlin, Heidelberg, 2011.
- [200] M. Plesch and V. Bužek, “Efficient compression of quantum information,” *Phys. Rev. A* **81** (Mar, 2010) 032317. <https://link.aps.org/doi/10.1103/PhysRevA.81.032317>.
- [201] R. Chao, B. W. Reichardt, C. Sutherland, and T. Vidick, “Overlapping qubits,” *ArXiv e-prints* (Jan., 2017), [arXiv:1701.01062](https://arxiv.org/abs/1701.01062) [quant-ph].
- [202] L. A. Rozema, D. H. Mahler, A. Hayat, P. S. Turner, and A. M. Steinberg, “Quantum data compression of a qubit ensemble,” *Phys. Rev. Lett.* **113** (Oct, 2014) 160504. <https://link.aps.org/doi/10.1103/PhysRevLett.113.160504>.
- [203] J. A. Vaccaro, Y. Mitsumori, S. M. Barnett, E. Andersson, A. Hasegawa, M. Takeoka, and M. Sasaki, “Quantum data compression,” in *Stochastic Algorithms: Foundations and Applications*, A. Albrecht and K. Steinhöfel, eds., pp. 98–107. Springer Berlin Heidelberg, Berlin, Heidelberg, 2003.
- [204] J. Shlens, “A tutorial on principle component analysis: Derivation, discussion and singular value decomposition,”. https://www.cs.princeton.edu/picasso/mats/PCA-Tutorial-Intuition_jp.pdf.

- [205] C. Xi-Yao and G. F. Tuthill, “Quantum decimation for spin-(1/2) chains in a magnetic field,” *Phys. Rev. B* **32** (Dec, 1985) 7280–7289.
<http://link.aps.org/doi/10.1103/PhysRevB.32.7280>.
- [206] C. Castellani, C. Di Castro, and J. Ranninger, “Decimation approach in quantum systems,” *Nucl. Phys.* **B200** (1982) 45–60.
- [207] T. Matsubara, C. Totsuji, and C. J. Thompson, “Quantum cluster decimation,” *Journal of Physics A: Mathematical and General* **24** no. 19, (1991) 4599. <http://stacks.iop.org/0305-4470/24/i=19/a=023>.
- [208] S. R. White, “Density matrix formulation for quantum renormalization groups,” *Phys. Rev. Lett.* **69** (1992) 2863–2866.
- [209] G. Vidal, “Entanglement Renormalization,” *Phys. Rev. Lett.* **99** no. 22, (2007) 220405, [arXiv:cond-mat/0512165](https://arxiv.org/abs/cond-mat/0512165) [cond-mat].
- [210] O. Di Matteo, L. L. Sánchez-Soto, G. Leuchs, and M. Grassl, “Coarse graining the phase space of N qubits,” *Phys. Rev. A* **95** no. 2, (Feb, 2017) 022340, [arXiv:1701.08630](https://arxiv.org/abs/1701.08630) [quant-ph].
- [211] P. Busch and R. Quadt, “Concepts of coarse graining in quantum mechanics,” *Int. J. Theor. Phys.* **32** no. 12, (1993) 2261–2269.
<http://dx.doi.org/10.1007/BF00672998>.
- [212] R. Quadt and P. Busch, “Coarse graining and the quantum—classical connection,” *Open Systems & Information Dynamics* **2** no. 2, (1994) 129–155. <http://dx.doi.org/10.1007/BF02228961>.
- [213] P. Faist, “Quantum coarse-graining: An information-theoretic approach to thermodynamics,” <https://arxiv.org/abs/1607.03104>.
- [214] Y. S. Teo, J. Řeháček, and Z. c. v. Hradil, “Coarse-grained quantum state estimation for noisy measurements,” *Phys. Rev. A* **88** (Aug, 2013) 022111.
<http://link.aps.org/doi/10.1103/PhysRevA.88.022111>.
- [215] C. Agon, V. Balasubramanian, S. Kasko, and A. Lawrence, “Coarse grained quantum dynamics,” [arXiv:1412.3148](https://arxiv.org/abs/1412.3148) [hep-th].
- [216] U. Schollwock, “The density-matrix renormalization group,” *Rev. Mod. Phys.* **77** (2005) 259–315.
- [217] S. R. White, “Density-matrix algorithms for quantum renormalization groups,” *Phys. Rev.* **B48** (1993) 10345–10356.
- [218] S. R. White and D. J. Scalapino, “Density matrix renormalization group study of the striped phase in the 2d $t - J$ model,” *Phys. Rev. Lett.* **80** (Feb, 1998) 1272–1275.
<http://link.aps.org/doi/10.1103/PhysRevLett.80.1272>.

- [219] S. R. White and D. J. Scalapino, “Energetics of domain walls in the 2d $t - J$ model,” *Phys. Rev. Lett.* **81** (Oct, 1998) 3227–3230.
<http://link.aps.org/doi/10.1103/PhysRevLett.81.3227>.
- [220] G. Vidal, “Class of quantum many-body states that can be efficiently simulated,” *Phys. Rev. Lett.* **101** (2008) 110501.
- [221] G. Vidal, *Understanding quantum phase transitions*, ch. Entanglement renormalization: An introduction. Taylor and Francis, 2010.
<http://www.arxiv.org/abs/0912.1651>.
- [222] J. C. Gaiete, “Angular quantization and the density matrix renormalization group,” *Mod. Phys. Lett. A* **16** (2001) 1109–1116,
[arXiv:cond-mat/0106049](https://arxiv.org/abs/cond-mat/0106049) [cond-mat].
- [223] J. C. Gaiete, “Entanglement entropy and the density matrix renormalization group,” <https://arxiv.org/abs/quant-ph/0301120>.
- [224] J. I. Latorre, E. Rico, and G. Vidal, “Ground state entanglement in quantum spin chains,” *Quant. Inf. Comput.* **4** (2004) 48–92,
[arXiv:quant-ph/0304098](https://arxiv.org/abs/quant-ph/0304098) [quant-ph].
- [225] T. J. Osborne and M. A. Nielsen, “Entanglement, quantum phase transitions, and density matrix renormalization,” *Quantum Information Processing* **1** no. 1, (2002) 45–53.
<http://dx.doi.org/10.1023/A:1019601218492>.
- [226] C. Jarzynski, “Nonequilibrium equality for free energy differences,” *Phys. Rev. Lett.* **78** no. 14, (1997) 2690–2693, [arXiv:cond-mat/9610209](https://arxiv.org/abs/cond-mat/9610209) [cond-mat.stat-mech].
- [227] G. E. Crooks, “Nonequilibrium measurements of free energy differences for microscopically reversible Markovian systems,” *J. Stat. Phys.* **90** no. 5-6, (Mar, 1998) 1481–1487.
- [228] A. Bartolotta, S. M. Carroll, S. Leichenauer, and J. Pollack, “Bayesian second law of thermodynamics,” *Phys. Rev.* **E94** no. 2, (2016) 022102,
[arXiv:1508.02421](https://arxiv.org/abs/1508.02421) [cond-mat.stat-mech].
- [229] M. Schlosshauer, “Decoherence, the measurement problem, and interpretations of quantum mechanics,” *Rev. Mod. Phys.* **76** (2004) 1267,
[arXiv:quant-ph/0312059](https://arxiv.org/abs/quant-ph/0312059).
- [230] H. Araki, “Relative entropy of states of von Neumann algebras,” *Publ. Res. Inst. Math. Sci. Kyoto* **1976** (1976) 809–833.
- [231] R. Haag, *Local quantum physics: Fields, particles, algebras*. 1992.
- [232] N. Lashkari, “Constraining quantum fields using modular theory,” *J. High Energ. Phys.* **01** (2019) 059, [arXiv:1810.09306](https://arxiv.org/abs/1810.09306) [hep-th].

- [233] W. Donnelly, “Entanglement entropy and nonabelian gauge symmetry,” *Class. Quant. Grav.* **31** no. 21, (2014) 214003, [arXiv:1406.7304 \[hep-th\]](#).
- [234] W. Donnelly and A. C. Wall, “Entanglement entropy of electromagnetic edge modes,” *Phys. Rev. Lett.* **114** no. 11, (2015) 111603, [arXiv:1412.1895 \[hep-th\]](#).
- [235] J. Lin and D. Radicevic, “Comments on defining entanglement entropy,” [arXiv:1808.05939 \[hep-th\]](#).
- [236] D. Kribs and D. Poulin, “Operator quantum error correction,” *Quantum Error Correction* 163–180. <http://dx.doi.org/10.1017/CB09781139034807.008>.
- [237] D. Kribs, R. Laflamme, and D. Poulin, “Unified and generalized approach to quantum error correction,” *Phys. Rev. Lett.* **94** (May, 2005) 180501. <https://link.aps.org/doi/10.1103/PhysRevLett.94.180501>.
- [238] F. Benatti, R. Floreanini, and U. Marzolino, “Entanglement robustness and geometry in systems of identical particles,” *Phys. Rev. A* **85** (Apr, 2012) 042329.
- [239] A. P. Balachandran, T. R. Govindarajan, A. R. de Queiroz, and A. F. Reyes-Lega, “Entanglement and particle identity: A unifying approach,” *Phys. Rev. Lett.* **110** (Feb, 2013) 080503.
- [240] H. Barnum, E. Knill, G. Ortiz, R. Somma, and L. Viola, “A subsystem-independent generalization of entanglement,” *Phys. Rev. Lett.* **92** (Mar, 2004) 107902. <https://link.aps.org/doi/10.1103/PhysRevLett.92.107902>.
- [241] L. Viola, H. Barnum, E. Knill, G. Ortiz, and R. Somma, “Entanglement beyond subsystems,” *Contemporary Mathematics* (2005) 117–130. <http://dx.doi.org/10.1090/conm/381/07095>.
- [242] K. Murota, Y. Kanno, M. Kojima, and S. Kojima, “A numerical algorithm for block-diagonal decomposition of matrix *-algebras with application to semidefinite programming,” *Japan Journal of Industrial and Applied Mathematics* **27** no. 1, (Jun, 2010) 125–160. <https://doi.org/10.1007/s13160-010-0006-9>.
- [243] X. Wang, M. Byrd, and K. Jacobs, “Numerical method for finding decoherence-free subspaces and its applications,” *Phys. Rev. A* **87** (Jan, 2013) 012338. <https://link.aps.org/doi/10.1103/PhysRevA.87.012338>.

- [244] J. A. Holbrook, D. W. Kribs, and R. Laflamme, “Noiseless subsystems and the structure of the commutant in quantum error correction,” *Quant. Info. Proc.* **2** no. 5, (2003) 381–419.
- [245] C. Duarte, G. D. Carvalho, N. K. Bernardes, and F. de Melo, “Emerging dynamics arising from coarse-grained quantum systems,” *Phys. Rev. A* **96** (Sep, 2017) 032113.
<https://link.aps.org/doi/10.1103/PhysRevA.96.032113>.
- [246] O. Kabernik, “Quantum coarse graining, symmetries, and reducibility of dynamics,” *Phys. Rev. A* **97** no. 5, (May, 2018) 052130,
[arXiv:1801.09770](https://arxiv.org/abs/1801.09770) [quant-ph].
- [247] D. A. Lidar, “Review of decoherence free subspaces, noiseless subsystems, and dynamical decoupling,” *Adv. Chem. Phys.* **154** (2014) 295–354.
- [248] C. Bény and F. Richter, “Algebraic approach to quantum theory: a finite-dimensional guide,” [arXiv:1505.03106](https://arxiv.org/abs/1505.03106) [quant-ph].
- [249] D. R. Farenick, *Algebras of linear transformations*. Springer Science & Business Media, 2012.
- [250] J. H. M. Wedderburn, *Lectures on matrices*, vol. 17. Am. Math. Soc., 1934.
- [251] A. Elby and J. Bub, “Triorthogonal uniqueness theorem and its relevance to the interpretation of quantum mechanics,” *Phys. Rev.* **A49** (1994) 4213.
- [252] J. J. Halliwell, “Somewhere in the universe: Where is the information stored when histories decohere?,” *Phys. Rev.* **D60** (1999) 105031,
[arXiv:quant-ph/9902008](https://arxiv.org/abs/quant-ph/9902008) [quant-ph].
- [253] W. H. Zurek, “Decoherence, einselection, and the quantum origins of the classical,” *Rev. Mod. Phys.* **75** (May, 2003) 715–775.
<https://link.aps.org/doi/10.1103/RevModPhys.75.715>.
- [254] M. E. Rose, *Elementary theory of angular momentum*. Courier Corporation, 1995.
- [255] D. Radicevic, “Entanglement entropy and duality,” *J. High Energ. Phys.* **11** (2016) 130, [arXiv:1605.09396](https://arxiv.org/abs/1605.09396) [hep-th].
- [256] R. Blume-Kohout, H. K. Ng, D. Poulin, and L. Viola, “Characterizing the structure of preserved information in quantum processes,” *Phys. Rev. Lett.* **100** (Jan, 2008) 030501.
<https://link.aps.org/doi/10.1103/PhysRevLett.100.030501>.
- [257] E. Knill, R. Laflamme, and L. Viola, “Theory of quantum error correction for general noise,” *Phys. Rev. Lett.* **84** (Mar, 2000) 2525–2528.
<https://link.aps.org/doi/10.1103/PhysRevLett.84.2525>.

- [258] D. Bacon, “Operator quantum error-correcting subsystems for self-correcting quantum memories,” *Phys. Rev. A* **73** (Jan, 2006) 012340. <https://link.aps.org/doi/10.1103/PhysRevA.73.012340>.
- [259] D. Poulin, “Stabilizer formalism for operator quantum error correction,” *Phys. Rev. Lett.* **95** (Dec, 2005) 230504. <https://link.aps.org/doi/10.1103/PhysRevLett.95.230504>.
- [260] N. Johnston, D. W. Kribs, and C.-W. Teng, “Operator algebraic formulation of the stabilizer formalism for quantum error correction,” *Acta applicandae mathematicae* **108** no. 3, (2009) 687.
- [261] A. Bluhm, L. Rauber, and M. M. Wolf, “Quantum compression relative to a set of measurements,” *Annales Henri Poincaré acute*; **19** no. 6, (Jun, 2018) 1891–1937, [arXiv:1708.04898](https://arxiv.org/abs/1708.04898) [quant-ph].
- [262] P. Zanardi, “Stabilizing quantum information,” *Phys. Rev. A* **63** (Dec, 2000) 012301. <https://link.aps.org/doi/10.1103/PhysRevA.63.012301>.
- [263] D. P. DiVincenzo, D. Bacon, J. Kempe, G. Burkard, and K. B. Whaley, “Universal quantum computation with the exchange interaction,” *Nature* **408** no. 6810, (2000) 339.
- [264] S. S. Gubser, I. R. Klebanov, and A. M. Polyakov, “Gauge theory correlators from noncritical string theory,” *Phys. Lett.* **B428** (1998) 105, [arXiv:hep-th/9802109](https://arxiv.org/abs/hep-th/9802109) [hep-th].
- [265] E. Witten, “Anti-de Sitter space and holography,” *Adv. Theor. Math. Phys.* **2** (1998) 253, [arXiv:hep-th/9802150](https://arxiv.org/abs/hep-th/9802150) [hep-th].
- [266] O. Aharony, S. S. Gubser, J. Maldacena, H. Ooguri, and Y. Oz, “Large N field theories, string theory and gravity,” *Phys. Rept.* **323** (2000) 183, [arXiv:hep-th/9905111](https://arxiv.org/abs/hep-th/9905111) [hep-th].
- [267] A. Almheiri, X. Dong, and D. Harlow, “Bulk locality and quantum error correction in AdS/CFT,” *J. High Energ. Phys.* **04** (2015) 163, [arXiv:1411.7041](https://arxiv.org/abs/1411.7041) [hep-th].
- [268] X. Dong, D. Harlow, and A. C. Wall, “Reconstruction of bulk operators within the entanglement wedge in gauge-gravity duality,” *Phys. Rev. Lett.* **117** no. 2, (2016) 021601, [arXiv:1601.05416](https://arxiv.org/abs/1601.05416) [hep-th].
- [269] J. Cotler, P. Hayden, G. Penington, G. Salton, B. Swingle, and M. Walter, “Entanglement wedge reconstruction via universal recovery channels,” *Phys. Rev.* **X9** no. 3, (2019) 031011, [arXiv:1704.05839](https://arxiv.org/abs/1704.05839) [hep-th].
- [270] N. Bao, G. Penington, J. Sorce, and A. C. Wall, “Beyond toy models: Distilling tensor networks in full AdS/CFT,” [arXiv:1812.01171](https://arxiv.org/abs/1812.01171) [hep-th].

- [271] H. Casini, M. Huerta, J. M. Magán, and D. Pontello, “Entanglement entropy and superselection sectors I. Global symmetries,” [arXiv:1905.10487 \[hep-th\]](#).
- [272] D. N. Page and C. D. Geilker, “Indirect evidence for quantum gravity,” *Phys. Rev. Lett.* **47** (1981) 979–982.
- [273] N. Bao, S. M. Carroll, A. Chatwin-Davies, J. Pollack, and G. N. Remmen, “Branches of the black hole wave function need not contain firewalls,” *Phys. Rev.* **D97** no. 12, (2018) 126014, [arXiv:1712.04955 \[hep-th\]](#).
- [274] S. Ghosh and S. Raju, “Quantum information measures for restricted sets of observables,” *Phys. Rev.* **D98** no. 4, (2018) 046005, [arXiv:1712.09365 \[hep-th\]](#).